NASA Technical Memorandum 100545

AVSCOM
Technical Memorandum TM-88-B-008

INFLOW MEASUREMENT MADE WITH A LASER VELOCIMETER ON A HELICOPTER MODEL IN FORWARD FLIGHT

Volume V TAPERED PLANFORM BLADES AT AN ADVANCE RATIO OF 0.23

Susan L. Althoff and Joe W. Elliott
Aerostructures Directorate
USAARTA-AVSCOM
Langley Research Center
Hampton, Virginia

Richard H. Sailey
PRC Kentron Inc.
Aerospace Technologies Division
Hampton, Virginia

April 1988

(NASA-TM-100545) INFLOW MEASUREMENT MADE WITH A LASER VELOCIMETER ON A HELICOPTER MODEL IN FORWARD FLIGHT. VOLUME 5: TAPERED PLANFORM BLADES AT AN ADVANCE RATIO OF 0.23 (NASA) 355 p CSCL 01A G3/02

N88-23755

Unclas
0146956

National Aeronautics and Space Administration

Langley Research Center
Hampton, Virginia 23665-5225

SUMMARY

An experimental investigation was conducted in the 14- by 22-Foot Subsonic Tunnel at NASA Langley Research Center to measure the inflow into a scale model helicopter rotor in forward flight (μ_∞ = 0.23). The measurements were made with a two-component Laser Velocimeter (LV) one chord above the plane formed by the path of the rotor tips (tip path plane). A conditional sampling technique was employed to determine the position of the rotor at the time that each velocity measurement was made so that the azimuthal fluctuations in velocity could be determined. Measurements were made at a total of 168 separate locations in order to clearly define the inflow character. This data is presented herein without analysis. In order to increase the availability of the resulting data, both the mean and azimuthally dependent values are included as part of this report on two 5.25 inch floppy disks in Microsoft Corporation MS-DOS format.

INTRODUCTION

One of the problems confronting the helicopter industry is the lack of detailed information about the velocity fluctuations around and through rotating blades. This information is needed for two reasons: to ensure a more complete understanding of the flowfield environment associated with a thrusting rotor and to provide data for the validation of rapidly emerging computational codes. One explanation for the lack of available data is the absence, until recent years, of a suitable device for making such measurements. Making measurements of the velocity around a system of rotating blades requires an accurate, nonintrusive measurement capability that presents a minimum risk to the systems involved. The Laser Velocimeter (LV), which uses high energy light beams to measure velocities, is ideally suited to this task.

The Laser Velocimeter has been successfully used to measure specific areas and localized phenomena within the rotor disk (refs. 1 through 3). In addition, the hotwire anemometer and pressure probes, both having directional measuring limitations, have been employed in similar programs (refs. 4 and 5). This is, however, the first time that a comprehensive program has been undertaken to map the flow into the complete rotor disk. This investigation has been conducted to measure the flow into a representative rotor system as a function of azimuth using a two-component (streamwise and vertical direction) LV system.

NOTATION

A_0 constant term in Fourier series of blade feathering (collective) at r/R = 0.75, deg

A_1 coefficient of cosine term in Fourier series of blade feathering, deg

B_1 coefficient of sine term in Fourier series of blade feathering, deg

C_D rotor drag coefficient, $D/\rho\ \pi R^2\ V_{tip}^2$

C_Q rotor torque coefficient, $Q/\rho\ \pi R^3\ V_{tip}^2$

C_T rotor thrust coefficient, $T/\rho\ \pi R^2\ V_{tip}^2$

D	rotor drag, positive to the rear, lbf
q	dynamic pressure, lbf/ft^2
Q	rotor torque, in-lbf
r	local radius of the rotor system, ft
R	rotor radius, ft
T	thrust produced by the rotor, lbf
U_∞	tunnel freestream velocity, positive downstream ft/sec
U	free-stream component of velocity, positive downstream, ft/sec
u_i	induced component of velocity parallel to the tip path plane (positive flow downstream), ft/sec
V	vertical component of velocity, positive up, ft/sec
v_i	induced component of velocity normal to the tip path plane (positive flow up), ft/sec
V_{tip}	rotor blade tip velocity (ΩR), ft/sec

Greek

α	angle between rotor disk and free-stream velocity (positive nose up), deg
λ	inflow ratio normal to tip path plane (positive up), $(U_\infty \sin(\alpha) + v_i)/V_{tip}$
λ_i	induced inflow ratio normal to tip path plane (positive up), v_i/V_{tip}
μ_∞	rotor advance ratio, $U_\infty \cos(\alpha)/V_{tip}$
μ	inflow ratio parallel to tip path plane (positive downstream), $(U_\infty \cos(\alpha) + u_i)/V_{tip}$
μ_i	induced inflow ratio parallel to tip path plane (positive downstream) u_i/V_{tip}
Ω	rotor rotational speed, radians/sec
ψ	rotor azimuth measured from downstream position, positive counterclockwise, as viewed from above, deg
ρ	air density, $slugs/ft^3$
θ	blade pitch angle at a specific azimuth (positive nose up), deg, $\theta = A_0 - A_1 \cos\psi - B_1 \sin\psi$
$\overline{xx}$	mean value

EXPERIMENTAL APPARATUS

The experimental apparatus used in this investigation included the NASA Langley Research Center 14- by 22-Foot Subsonic Tunnel, the 2-Meter Rotor Test System (2MRTS), and a two-component laser velocimeter system.

The 14- by 22-Foot Subsonic Tunnel is an atmospheric, closed-circuit wind tunnel of conventional design with enhancements for the testing of powered and high-lift configurations (ref. 6). The tunnel is shown in figure 1. When the tunnel is operated in the open configuration, the walls and ceiling of the test section are lifted out of the flow, leaving only a solid floor and a flow collector. In this configuration, the tunnel can be driven to about 170 knots. This investigation was conducted with the tunnel in the open configuration to allow complete optical access to the rotor flowfield.

The 2MRTS is a general purpose rotorcraft model testing system which was mounted on a strut in the forward part of the test section (see fig. 2). The system consists of a 29-horsepower electric drive motor and 90° speed-reducing transmission, a blade pitch remote control system, and two six-component strain gage balances used for measuring forces and moments on the rotor system and fuselage shell. The four-bladed rotor hub is fully articulated with viscous dampers for lead-lag motion and coincident flap and lag hinges. A more detailed description of the 2MRTS can be found in reference 7. The fuselage which was used for this test was a generic high-speed helicopter configuration. The characteristics of the tapered rotor blades used during this investigation can be found in table 1. The rotor blade planform is shown in figure 3. No attempt was made to dynamically scale the rotor blades; rather, they were very rigid to provide a general research capability.

The LV system used in this investigation was designed to measure the instantaneous components of velocity in the longitudinal (free stream) and vertical directions. The LV system is described in reference 8. The system is comprised of four subsystems: optics, traverse, data acquisition, and seeding. The optics subsystem, which is shown in figure 4, operates in backscatter mode and at high power (4 watts in all lines) in order to accommodate the long focal lengths needed to scan the wide test section. The transmitting and receiving optics packages are augmented by a zoom lens system consisting of a 3-in. clear aperture negative lens and a 12-in. clear aperture positive lens. Bragg cells in each of the optical paths provide a directional measurement capability. The velocity measurements are made at a point in space where the four beams cross, called the sample volume. The length of the sample volume (transverse to the flow direction) increases as the sample volume is moved away from the optics assembly. The sample volume length, over the 10- to 20-foot focal length of the system, is less than 1 cm and has a constant diameter of 0.2 mm.

The traverse subsystem provides five degrees of freedom in positioning the sample volume and is controlled by the same computer that is used for data acquisition. Translation of the sample volume in the horizontal and vertical direction is accomplished by displacing the entire optics platform. Translation along the lateral axes is accomplished by displacing the negative lens located in the zoom lens assembly, thus refocusing the sample volume along the axes of optical transmission. The other two degrees of freedom, pan and tilt, are implemented by rotating the final mirror about its vertical and horizontal axes in order to change the direction of optical transmission. The total range of the traversing system is 7 ft vertically, 6 ft streamwise, 16.5 ft laterally, and 10° in both pan and tilt. Measurements can be made outside of this envelope by repositioning the optics platform, which is mounted on wheels to facilitate such relocations. For this study the traversing system was

positioned to the left of the test section when looking downstream as shown in figure 5.

The data acquisition subsystem is shown schematically in figure 6 and interfaces with the optical signal processing equipment to receive two channels of raw LV data and up to five channels of auxiliary data. In this investigation, four of the auxiliary channels were used for the acquisition of data relative to blade position. Two of the channels (one each for the U and V components) measured the azimuthal position of the rotor shaft and the other two measured the lead/lag and flapping motion. The system converts the raw LV data to engineering units and determines the statistical characteristics of the acquired data so that the test results can be evaluated during the acquisition process. The raw data, the data which have been converted to engineering units, and 64 parameters from the tunnel static data acquisition system are written to magnetic tape for later analysis. The final function performed by the data system is to control the five degree-of-freedom scan system.

The seeding subsystem, shown schematically in figure 7, is a solid particle, liquid dispensing system (ref. 9). Polystyrene latex microspheres are suspended in a mixture containing, by volume, 50 percent water and 50 percent ethyl alcohol. The advantages of the polystyrene particles are their low density, high reflectivity, and precise particle size. The particles used in this investigation were 1.7 microns in diameter with a standard deviation of 0.0239 microns. The particle mixture is pumped to an array of 32 nozzles where compressed air is used to atomize the mixture. These nozzles are mounted on a frame 8 feet wide by 6 feet high which is suspended on cables in the settling chamber of the tunnel. The low vapor pressure of water/alcohol mixture allows it to evaporate as it travels the 85 feet from the settling chamber to the test section. This process provides isolated single particles in the flowfield whose velocities are measured as they pass through the sample volume. The local fluid velocity is inferred from the seed particle velocity.

ERROR ANALYSIS

The overall LV system error is obtained by summing the error of all of the components that contribute to an error in the velocity measurement. The error sources are summarized in the table below, and are defined in references 10 and 11. The resulting total bias error of -0.81 to 1.82 percent is obtained by adding the percents contributed by each error source. The total random error of 1.12 percent is obtained by taking the square root of the sum of the squared percents of the random sources. Taking the square root of the sum of the squares of the random and bias errors gives a total system error of 1.38 percent to 2.14 percent.

Error source	Bias error	Random error
Cross beam angle measurement	±0.81	N/A
Diverging fringes	A	A
Time jitter	N/A	N/A
Clock synchronization	0.51	±0.51
Quantization	A	±1.00
Velocity bias	B	B
Bragg bias	B	B
Velocity gradient	B	B
Particle lag	±0.50	B
Total error	-0.81 to 1.82	1.12

A Not measured
B Negligible
N/A Not applicable

TEST PROCEDURES

In all cases, measurements were made at azimuthal increments of 30° from $\psi = 0$, at 3.0 in. (approximately one chord) above the plane formed by the tips of the blades. Measurements were made from a radial location of $r/R = 0.2$ to $r/R = 1.12$, with the majority of the measurement locations concentrated toward the outboard portion of the disk. Figure 8 shows the measurement locations superimposed on the rotor disk. During the test, the rotor tip path plane was maintained at -3° relative to the free stream by zeroing the blade flapping relative to the shaft and setting the shaft angle to -3°. The operating tip speed for the test was held at 624 ft/sec (2200 rpm), the nominal tunnel speed was 144 ft/sec ($\mu_\infty = 0.23$), and the nominal rotor thrust coefficient was 0.0065. Table 2 lists the nominal test conditions and selected test parameters. The LV data acquisition process consisted of placing the sample volume at the measurement location and acquiring data for a period of 1 minute or until 4096 velocity measurements were made in either the longitudinal or the vertical component. During this process, conditional sampling techniques were employed to permanently associate each measured velocity with the location of the rotor blades at the time when the measurement was made. At the conclusion of the process, the measurement location was changed and the acquisition process was repeated.

DATA REDUCTION

Independent velocity measurements in the free stream and vertical direction were made at each measurement location. At the same instant in time that a velocity measurement was made, the location of the blades was recorded for that velocity component. The maximum time required to acquire these data was 1 minute (2200 rotor

ORIGINAL PAGE IS
OF POOR QUALITY

revolutions for this test) and the minimum approximately 20 sec. These data, collected over many revolutions, were sorted into 128 equally spaced azimuth segments (2.81° wide) that are representative of blade position and include corrections for blade lead/lag motion. The velocity value assigned to each interval at a measurement location is the arithmetic mean of all the measurements that were taken in the respective 2.81° wide azimuthal range. The results of this sorting process provide the azimuthally dependent velocity data. The "mean velocity" value refers to the velocity calculated from the arithmetic mean of all the measurements made at a single measurement location.

EXPERIMENTAL RESULTS

Table 3 lists the measurement locations, the mean and standard deviation of the two components of induced inflow velocity, and the number of measurements in each of the measured components (U and V). In figure 9 the mean longitudinal induced component of velocity, μ_i, with a band of ± one standard deviation is plotted vs. blade radius for each radial scan. The standard deviation represents the fluctuation in velocity at a given measurement location; it is not an indication of the error in the mean measurements. The size of the symbols used for plotting the mean velocity values is an approximation of the calculated error in the measurements. Figure 10 presents in the same format the mean normal induced component of velocity, λ_i. The same data without the ± one standard deviation is presented in a contour plot format in figures 11 and 12 in order to show more clearly the interactions over the whole disk (viewed from above). The format of each of the figures (13 through 180) is the induced velocity vs. azimuth at the top of the figure, the number of measurements that went into determining the velocity value for each azimuth segment in the center, and an order ratio analysis of the azimuthal variation at the bottom of the figure. The figure numbers for the azimuthal and radial measurement locations are indicated below.

ORIGINAL PAGE IS
OF POOR QUALITY

Azimuth / r/R	0	30	60	90	120	150	180	210	240	270	300	330
0.20	13	22	37	51	62	77	92	107	122	136	151	166
0.40	14	23	--	52	63	78	93	108	123	137	152	167
0.50	15	24	38	53	64	79	94	109	124	138	153	168
0.60	16	25	39	--	65	80	95	110	125	139	154	169
0.70	17	26	40	54	66	81	96	111	126	140	155	170
0.74	--	27	41	55	67	82	97	112	127	141	156	171
0.78	--	28	42	56	68	83	98	113	128	142	157	172
0.82	--	29	43	57	69	84	99	114	129	143	158	173
0.86	--	30	44	58	70	85	100	115	130	144	159	174
0.90	--	31	45	59	71	86	101	116	131	145	160	175
0.94	--	32	46	60	72*	87	102	117	132	146	161	176
0.98	18*	33	47	61	73*	88	103	118	133	147	162	177
1.02	19*	34	48	--	74*	89	104	119	134	148	163	178
1.04	20*	35	49	--	75*	90	105	120	135	149	164	179
1.10	21	36	50	--	--	--	--	--	--	--	165	180
1.12	--	--	--	--	76*	91	106	121	--	150	--	--

*λ_i data only
-- no data

The mean and standard deviation of the induced inflow velocities (table 3) and the azimuthally dependent induced inflow velocities (figs. 13 through 180) are included on 5.25 flexible disk in the pocket on the inside of the rear cover of this report. The details of the data format and the file structure are located in the file "README.DOC". The disk format is 360 kbyte double-sided, written using the Microsoft Corporation MS-DOS operating system.

CONCLUDING REMARKS

The Laser Velocimeter provides an effective system for making measurements in the dynamic environment associated with rotor blades. It has been used on numerous occasions to measure the localized flow phenomena encountered in such flows. This investigation demonstrates the use of a matured LV system to map the flow into a representative rotor in forward flight by making velocity measurements at 168 locations above the rotor disk. These measurements provide both the mean and azimuthally dependent velocity values, and they provide a detailed look at the nature of this flow.

ORIGINAL PAGE IS
OF POOR QUALITY

REFERENCES

1. Landgrebe, A. J.; and Johnson, B. V.: Measurement of Model Helicopter Rotor Flow Velocities With a Laser Doppler Velocimeter. American Helicopter Society Journal, Vol. 19, July 1974, pp. 39-43.

2. Biggers, J. C.; and Orloff, K. L.: Laser Velocimeter Measurements of the Helicopter Rotor-Induced Flowfield. American Helicopter Society, Annual National V/STOL Forum, 30th, Washington, D.C., May 7-9, 1974.

3. Owen, F. K.; and Taubert, M. E.: Measurement and Prediction of Model-Rotor Flowfields. AIAA 18th Fluid Dynamics, Plasmadynamics and Laser Conference, Cincinnati, Ohio, July 16-18, 1985.

4. Tangler, J. L.; Wohlfeld, R. M.; and Miley, S. J.: An Experimental Investigation of Vortex Stability, Tip Shapes, Compressibility and Noise for Hovering Models. NASA CR-2305, September 1973.

5. Junker, B.: Investigations of Blade-Vortices in the Rotor Downwash. Twelfth European Rotorcraft Forum, Garmish-Partenkirchen, Federal Republic of Germany, September 22-25, 1986.

6. Applin, Z. T.: Flow Improvements in the Circuit of the Langley 4- by 7-Meter Tunnel. NASA TM-85662, December 1983.

7. Phelps, A. E., III; and Berry, J. D.: Description of the U.S. Army 2-Meter Rotor Test System. NASA TM-87762, AVSCOM TM 86-B-4, January 1987.

8. Sellers, W. L.; and Elliott, J. W.: Applications of a Laser Velocimeter in the Langley 4- by 7-Meter Tunnel. Proceedings of the Workshop on Flow Visualization and Laser Velocimetry for Wind Tunnels. NASA CP-2243, March 1982, pp. 283-293.

9. Elliott, J. E.; and Nichols, C. E.: Seeding Systems for Use With a Laser Velocimeter in Large Scale Wind Tunnels. Proceedings of the Workshop on Wind Tunnel Seeding Systems for Laser Velocimeters, NASA CP-2393, March 1985, pp. 93-103.

10. Young, W. H.; Meyers, J. F.; and Hepner, T. E.: Laser Velocimeter Systems Analysis to a Flow Survey Above a Stalled Wing. NASA TN D-8408, August 1977.

11. Dring, R. P.: Sizing Criteria for Laser Anemometry Particles. Journal of Fluid Engineering, Vol. 104, March 1982, pp. 15-17.

TABLE 1.- 2MRTS ROTOR AND BLADE CHARACTERISTICS

Hub type	Fully articulated
Number of blades	4
Airfoil section	NACA 0012
Hinge offset, in., r/R	2.00,0.06
Root cutout, in., r/R	8.25,0.24
Pitch-flap coupling angle, deg	0.0
Twist linear, deg	-13.0
Radius, R, in.	32.50
Rotor solidity, bc/πR	0.0977
Blade stiffness	
Flapwise, lb-in^2	13000
Torsional, lb-in^2	12750
Blade weight, grams	222.0
Lead/lag damping, in-lb/deg/sec	182.4

TABLE 2.- NOMINAL ROTOR CONTROL AND PERFORMANCE PARAMETERS

C_T	0.0065
C_Q	0.000381
C_D	0.00
α, deg	-3.05
Coning, deg	1.8
A_0, deg	7.1
A_1, deg	-0.40
B_1, deg	5.1
μ_∞	0.23
U, ft/sec	144.0
V_{tip}, ft/sec	624.0
Lag, deg	0.90

TABLE 3.- INFLOW VELOCITY SUMMARY

		μ_1			λ_1		
ψ	r/R	Mean	Standard deviation	# measurements	Mean	Standard deviation	# measurements
0	.20	.0143	.0175	157	-.0138	.0129	547
0	.40	.0107	.0172	168	-.0252	.0102	623
0	.50	.0108	.0163	171	-.0273	.0104	536
0	.60	.0074	.0190	121	-.0310	.0107	499
0	.70	.0060	.0165	114	-.0321	.0117	388
0	.98	--	--	0	-.0491	.0246	379
0	1.02	--	--	0	-.0519	.9188	416
0	1.04	--	--	0	-.0531	.0236	570
0	1.10	.0067	.0242	789	-.0548	.0189	843
0	.20	.0249	.0213	1352	-.0083	.0127	3901
0	.40	.0210	.0232	1202	-.0282	.0076	2596
30	.50	.0190	.0212	543	-.0316	.0086	1085
30	.60	.0151	.0182	422	-.0355	.0092	660
30	.70	.0089	.0168	284	-.0383	.0088	388
30	.74	.0091	.0197	178	-.0403	.0084	294
30	.78	.0056	.0203	1064	-.0444	.0086	1670
30	.82	.0057	.0210	755	-.0438	.0081	1095
30	.86	.0035	.0220	600	-.0425	.0073	883
30	.90	.0035	.0220	544	-.0420	.0066	748
30	.94	.0028	.0220	381	-.0409	.0054	535
30	.98	0.0000	.0211	288	-.0403	.0044	427
30	1.02	-.0026	.0231	324	-.0377	.0036	464
30	1.04	-.0023	.0243	306	-.0370	.0035	463
30	1.10	-.0013	.0216	316	-.0345	.0036	553
60	.20	-.0245	.0222	204	-.0059	.0064	457
60	.50	.0148	.0232	330	-.0292	.0084	559
60	.60	.0119	.0223	253	-.0294	.0093	362
60	.70	.0095	.0165	140	-.0269	.0084	224
60	.74	.0085	.0158	174	-.0255	.0084	276
60	.78	.0081	.0278	282	-.0246	.0079	367
60	.82	.0071	.0234	156	-.0264	.0077	325
60	.86	.0054	.0218	280	-.0223	.0065	483
60	.90	.0038	.0201	348	-.0179	.0058	686
60	.94	.0062	.0208	407	-.0133	.0047	690
60	.98	.0050	.0261	483	-.0070	.0045	598
60	1.02	.0048	.0288	1232	-.0037	.0057	2337
90	1.04	.0064	.0301	1252	-.0035	.0055	1951
90	1.10	.0067	.0302	1977	-.0256	.0051	1696
90	.20	.0154	.0162	756	-.0051	.0058	1506
90	.40	.0142	.0162	1186	-.0250	.0073	3312
90	.50	.0159	.0207	933	-.0236	.0086	2104
90	.70	.0138	.0208	1259	-.0134	.0095	1361
90	.74	.0121	.0228	1090	-.0096	.0098	1231
90	.78	.0102	.0211	947	-.0038	.0090	941
90	.82	.0075	.0190	788	.0009	.0090	660

ORIGINAL PAGE IS
OF POOR QUALITY

TABLE 3.- Continued

		μ_1			λ_1		
ψ	r/R	Mean	Standard deviation	# measurements	Mean	Standard deviation	# measurements
90	.86	.0055	.0194	489	.0074	.0080	436
90	.90	.0035	.0184	303	.0134	.0048	292
90	.94	-.0012	.0182	161	.0167	.0050	126
90	.98	-.0007	.0216	173	.0192	.0034	120
120	.20	.0042	.0197	352	.0008	.0065	1261
120	.40	.0047	.0190	550	-.0144	.0077	3054
120	.50	.0070	.0179	442	-.0131	.0083	2619
120	.60	.0037	.0190	597	.0079	.0098	3504
120	.70	.0014	.0185	543	-.0008	.0113	2852
120	.74	.0008	.0189	585	.0035	.0105	2362
120	.78	.0002	.0176	458	.0074	.0090	1666
120	.82	-.0017	.0179	287	.0098	.0074	1138
120	.86	-.0024	.0178	172	.0105	.0069	859
120	.90	-.0039	.0155	104	.0118	.0053	673
120	.94	--	--	0	.0119	.0051	580
120	.98	--	--	0	.0108	.0039	379
120	1.02	--	--	0	.0090	.0053	917
120	1.04	--	--	0	.0089	.0049	825
120	1.12	--	--	0	.0070	.0044	460
150	.20	-.0053	.0148	1166	.0019	.0074	925
150	.40	.0061	.0144	1202	-.0093	.0099	1260
150	.50	.0075	.0143	1186	-.0057	.0116	1199
150	.60	.0074	.0143	948	-.0017	.0131	977
150	.70	.0043	.0136	1185	.0051	.0114	1049
150	.74	.0030	.0146	1321	.0094	.0091	892
150	.78	.0020	.0141	1308	.0105	.0088	961
150	.82	-.0011	.0151	1497	.0116	.0074	1021
150	.86	-.0011	.0163	495	.0131	.0066	2347
150	.90	-.0028	.0156	424	.0128	.0056	2337
150	.94	-.0044	.0211	325	.0121	.0046	2343
150	.98	-.0062	.0197	277	.0110	.0044	2058
150	1.02	-.0080	.0194	268	.0098	.0041	1978
150	1.04	-.0082	.0175	105	.0090	.0039	486
150	1.12	-.0086	.0181	152	.0068	.0043	527
180	.20	-.0018	.0192	480	-.0001	.0049	2089
180	.40	.0018	.0192	418	-.0076	.0097	2244
180	.50	.0036	.0198	403	-.0057	.0115	1896
180	.60	.0066	.0210	353	.0009	.0103	1670
180	.70	.0047	.0210	321	.0049	.0131	1532
180	.74	.0016	.0200	308	.0076	.0130	1439
180	.78	-.0012	.0194	304	.0096	.0122	1308
180	.82	-.0001	.0192	260	.0109	.0100	1311
180	.86	-.0020	.0174	312	.0118	.0090	1177
180	.90	-.0048	.0203	283	.0129	.0068	1125
180	.94	-.0052	.0181	246	.0122	.0057	1191

TABLE 3.- Continued

		μ_1			λ_1		
ψ	r/R	Mean	Standard deviation	# measurements	Mean	Standard deviation	# measurements
180	.98	-.0040	.0181	259	.0119	.0046	1184
180	1.02	-.0052	.0172	246	.0110	.0045	1194
180	1.04	-.0046	.0192	246	.0102	.0046	1076
180	1.12	-.0065	.0172	223	.0075	.0049	1051
210	.20	-.0011	.0145	1290	.0008	.0067	2803
210	.40	.0026	.0156	1150	-.0072	.0085	3403
210	.50	.0034	.0159	1164	-.0074	.0097	3471
210	.60	.0042	.0157	1128	-.0035	.0102	3365
210	.70	.0016	.0186	1305	.0015	.0122	2898
210	.74	.0032	.0150	555	.0025	.0125	1036
210	.78	.0008	.0159	788	.0040	.0123	1520
210	.82	.0009	.0162	1711	.0052	.0116	3058
210	.86	-.0011	.0164	1626	.0074	.0096	3044
210	.90	-.0017	.0157	1713	.0097	.0076	2824
210	.94	-.0048	.0161	1787	.0096	.0073	2793
210	.98	-.0045	.0153	1846	.0089	.0064	2667
210	1.02	-.0046	.0155	1932	.0083	.0083	2677
210	1.04	-.0049	.0161	1732	.0080	.0063	2610
210	1.12	-.0057	.0160	1840	.0065	.0063	2633
240	.20	.0020	.0154	3104	0.0000	.0066	2509
240	.40	.0009	.0170	3010	-.0072	.0079	3022
240	.50	.0030	.0170	2909	-.0084	.0090	3164
240	.60	.0053	.0179	2846	-.0212	.0096	2826
240	.70	.0039	.0178	2348	-.0035	.0106	2364
240	.74	.0042	.0171	2516	-.0028	.0106	2535
240	.78	.0036	.0183	2638	-.0018	.0136	2501
240	.82	.0028	.0183	2601	.0001	.0117	2303
240	.86	.0030	.0181	2747	.0010	.0115	2348
240	.90	.0016	.0177	2790	.0052	.0106	2230
240	.94	.0009	.0169	2784	.0072	.0074	1789
240	.98	.0002	.0171	2865	.0080	.0071	1968
240	1.02	-.0007	.0169	2831	.0085	.0067	1834
240	1.04	-.0021	.0169	2849	.0081	.0066	1911
270	.20	.0054	.0173	2048	-.0019	.0062	2815
270	.40	.0042	.0179	2041	-.0094	.0078	3050
270	.50	.0046	.0188	1867	-.0126	.0078	2814
270	.60	.0046	.0191	1795	-.0135	.0089	2349
270	.70	.0036	.0210	1755	-.0151	.0108	2330
270	.74	.0036	.0194	1742	-.0149	.0108	2236
270	.78	.0040	.0207	1945	-.0149	.0106	2406
270	.82	.0024	.0208	1908	-.0136	.0109	2365
270	.86	.0012	.1241	2106	-.0105	.0112	2368
270	.90	-.0002	.0240	2054	-.0072	.0111	2014
270	.94	-.0002	.0237	2137	-.0014	.0120	1938
270	.98	-.0008	.0233	2124	.0050	.0114	1824

ORIGINAL PAGE IS
OF POOR QUALITY

TABLE 3.- Concluded

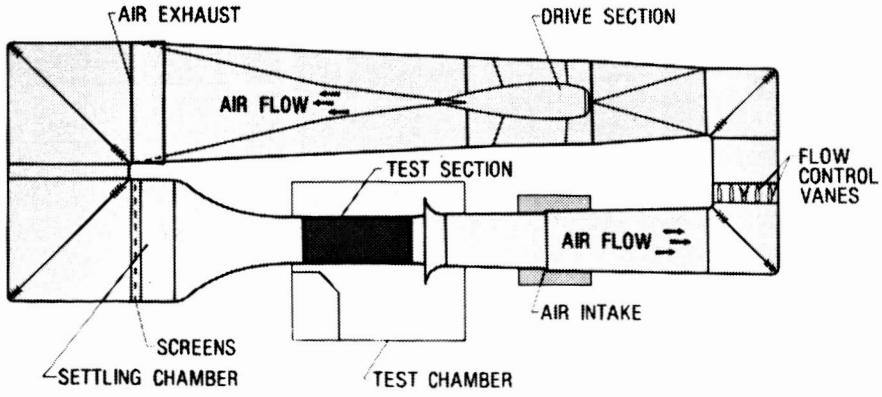
ORIGINAL PAGE IS OF POOR QUALITY

		μ_1			λ_1		
ψ	r/R	Mean	Standard deviation	# measurements	Mean	Standard deviation	# measurements
270	1.02	-.0024	.0231	1888	-.0128	.0076	1125
270	1.04	-.0050	.0234	1072	-.0160	.0066	644
270	1.12	-.0045	.0239	311	-.0154	.0066	174
300	.20	.0056	.0213	124	-.0026	.0061	359
300	.40	.0063	.0201	104	-.0081	.0064	349
300	.50	.0038	.0202	519	-.0135	.0070	2879
300	.60	.0034	.0220	311	-.0173	.0084	1678
300	.70	.0074	.0223	145	-.0214	.0094	739
300	.74	.0037	.0230	104	-.0232	.0098	521
300	.78	--	--	0	-.0267	.0095	225
300	.82	--	--	0	-.0249	.0095	221
300	.86	--	--	0	-.0254	.0085	199
300	.90	-.0005	.0236	2213	-.0255	.0092	3342
300	.94	-.0025	.0227	2205	-.0258	.0089	3525
300	.98	-.0024	.0219	1484	-.0247	.0080	2317
300	1.02	-.0030	.0221	1052	-.0230	.0076	1613
300	1.04	-.0049	.0207	854	-.0219	.0063	1253
300	1.10	-.0067	.0212	422	-.0123	.0066	546
330	.20	.0072	.0209	221	-.0057	.0076	502
330	.40	.0069	.0208	262	-.0088	.0070	557
330	.50	.0038	.0177	215	-.0123	.0089	590
330	.60	.0071	.0191	189	-.0161	.0106	598
330	.70	.0049	.0185	198	-.0193	.0113	484
330	.74	.0030	.0210	182	-.0203	.0111	452
330	.78	.0020	.0225	175	-.0223	.0106	413
330	.82	.0018	.0203	138	-.0250	.0107	313
330	.86	.0018	.0201	111	-.0261	.0092	233
330	.90	-.0003	.0176	106	-.0270	.0111	227
330	.94	0.0000	.0171	973	-.0293	.0079	3010
330	.98	-.0057	.0215	863	-.0295	.0068	2253
330	1.02	-.0057	.0208	703	-.0287	.0063	2055

ORIGINAL PAGE IS
OF POOR QUALITY



(a) Aerial view



(b) Schematic

Figure 1.- 14 × 22 Foot Subsonic Tunnel.

PRECEDING PAGE BLANK NOT FILMED

PAGE 14 INTENTIONALLY BLANK

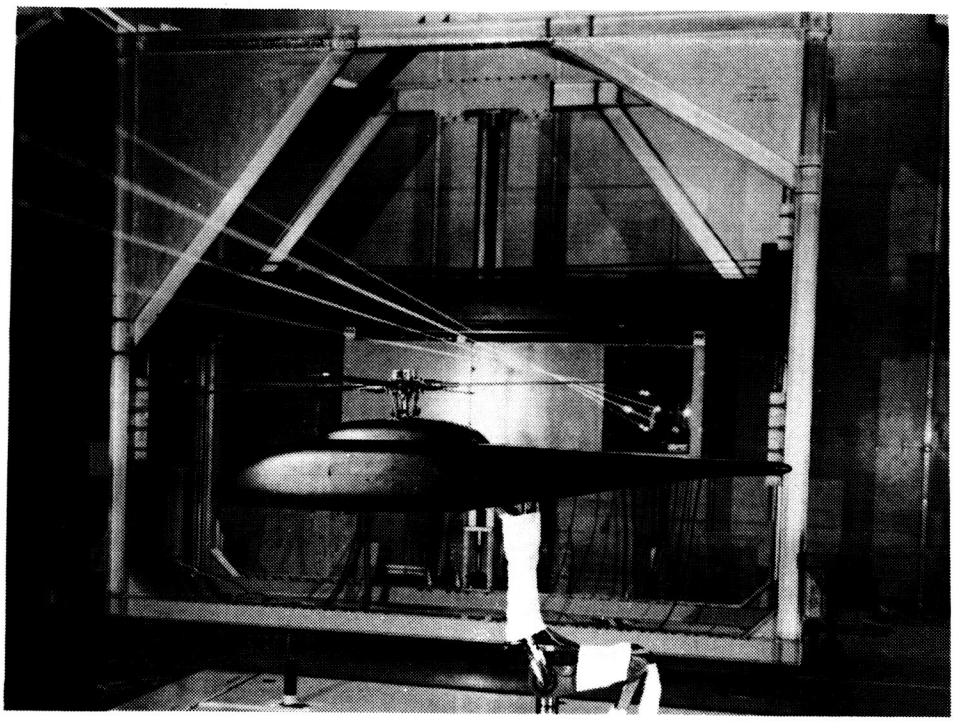


Figure 2.- 2MRTS mounted in forward bay of the test section

ORIGINAL PAGE IS
OF POOR QUALITY

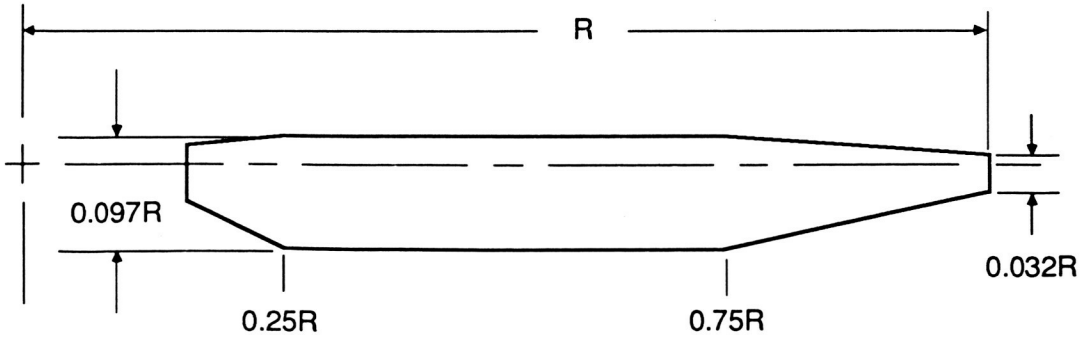


Figure 3.- Rotor blade planform. R = 32.5 inches.

ORIGINAL PAGE IS
OF POOR QUALITY

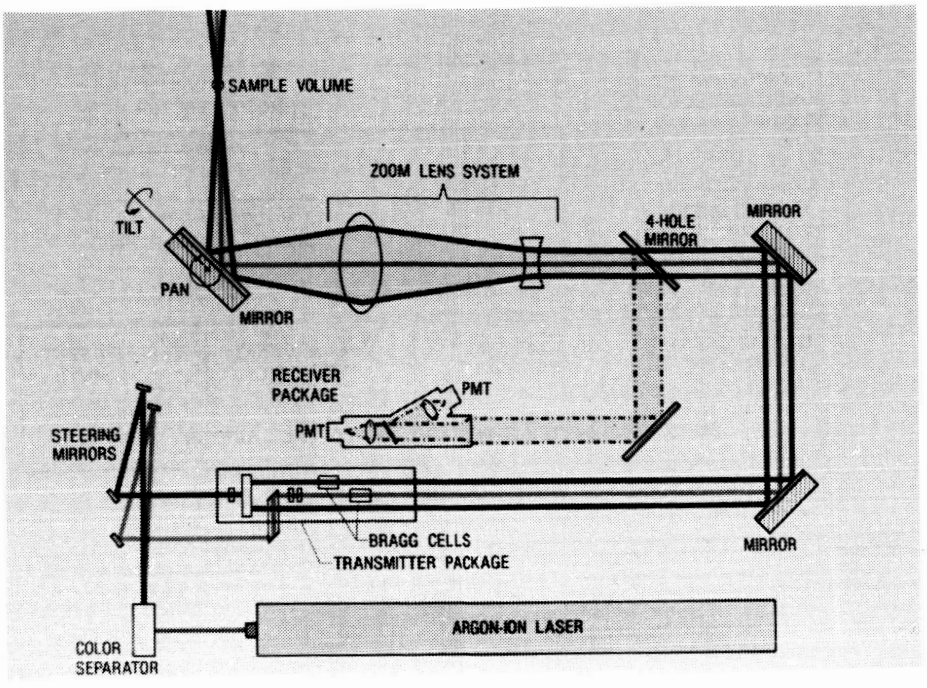


Figure 4.- Schematic diagram of Laser Velocimeter Optics Subsystem.

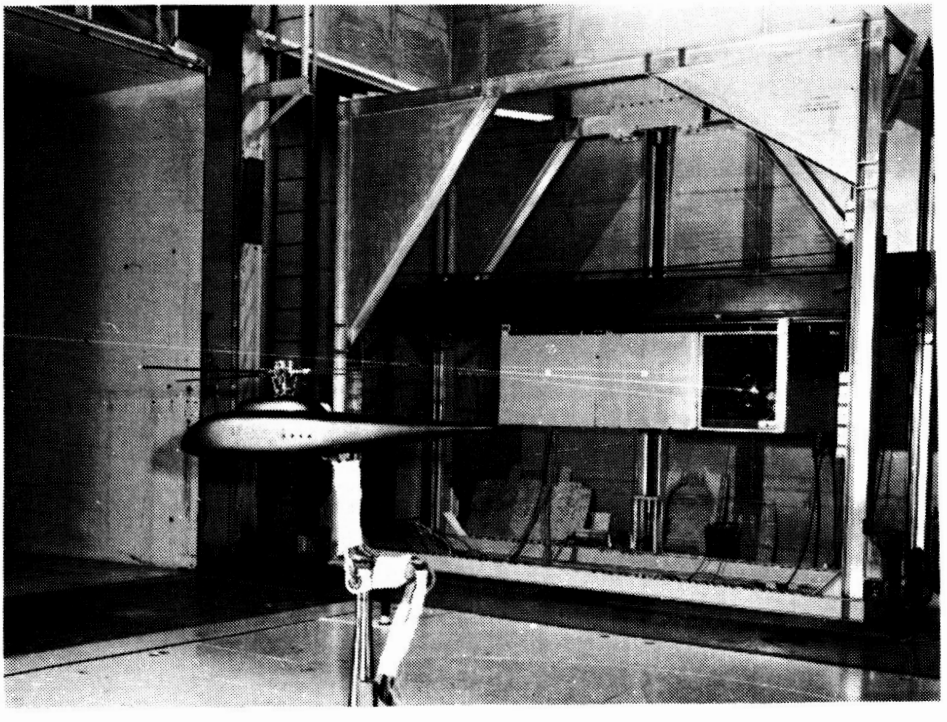


Figure 5.- Laser Velocimeter positioned in test chamber.

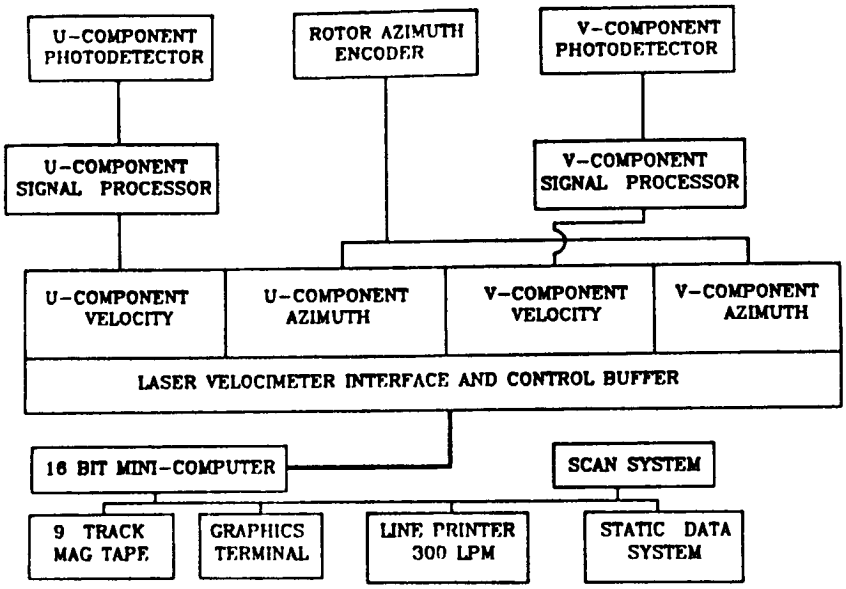


Figure 6.- Schematic view of data aquisition and control subsystem.

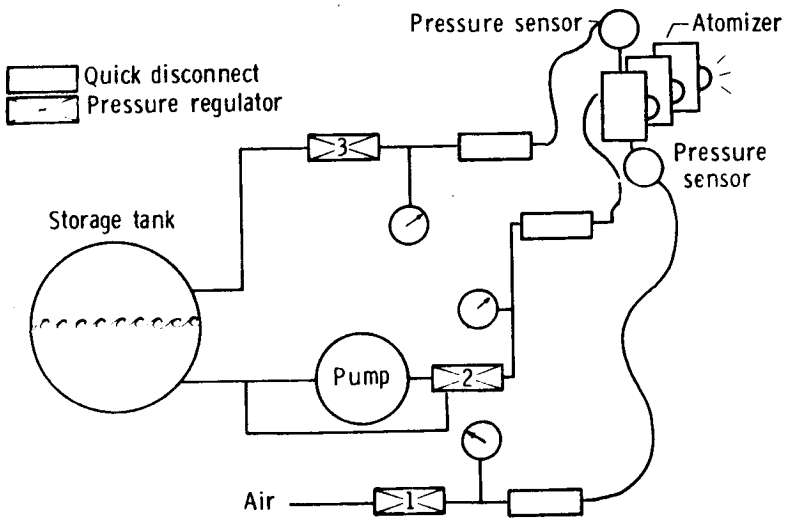


Figure 7.- Schematic of Seeding system.

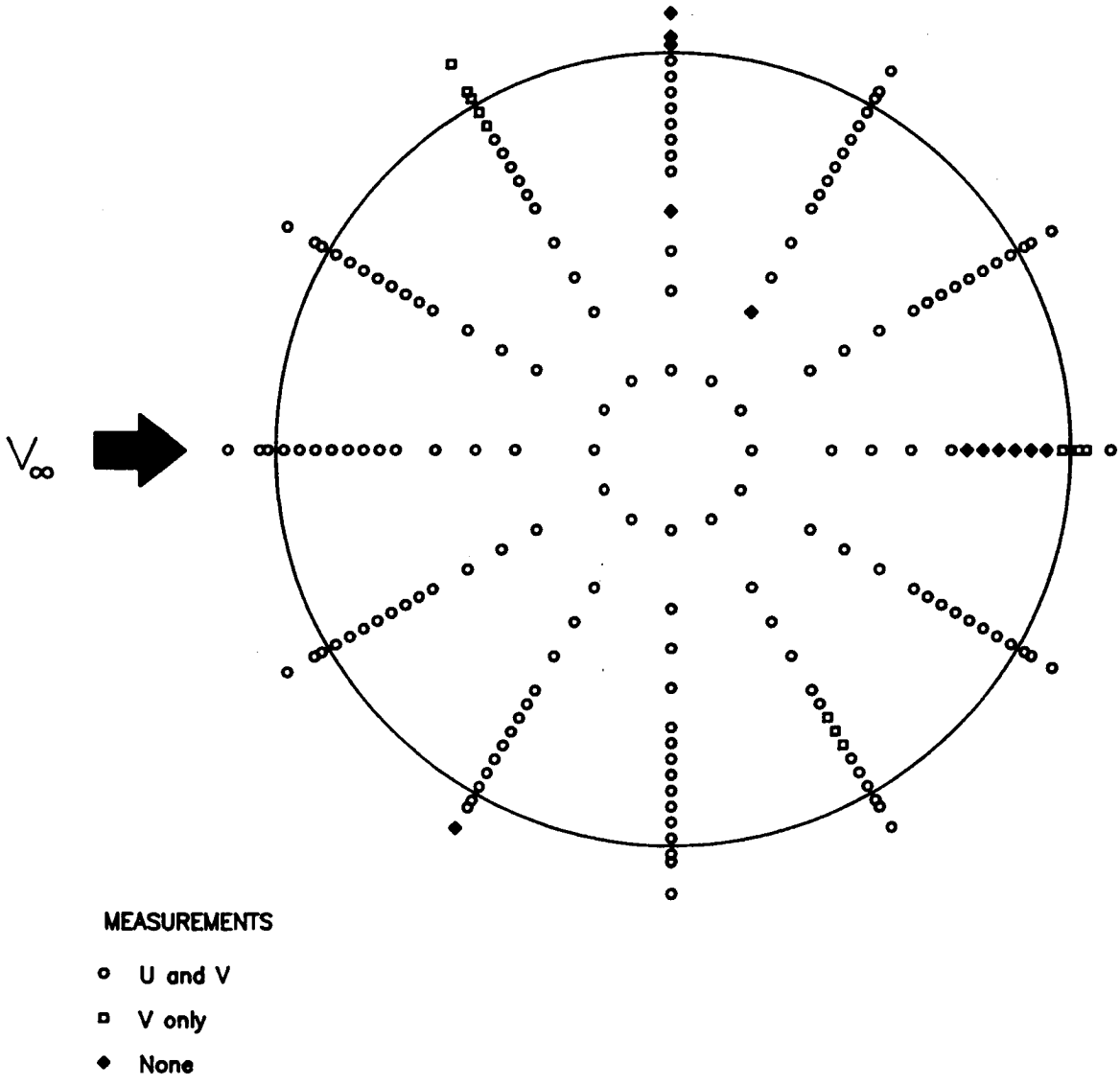


Figure 8.– Locations of velocity measurements, 3.0 inches above rotor tip path plane.

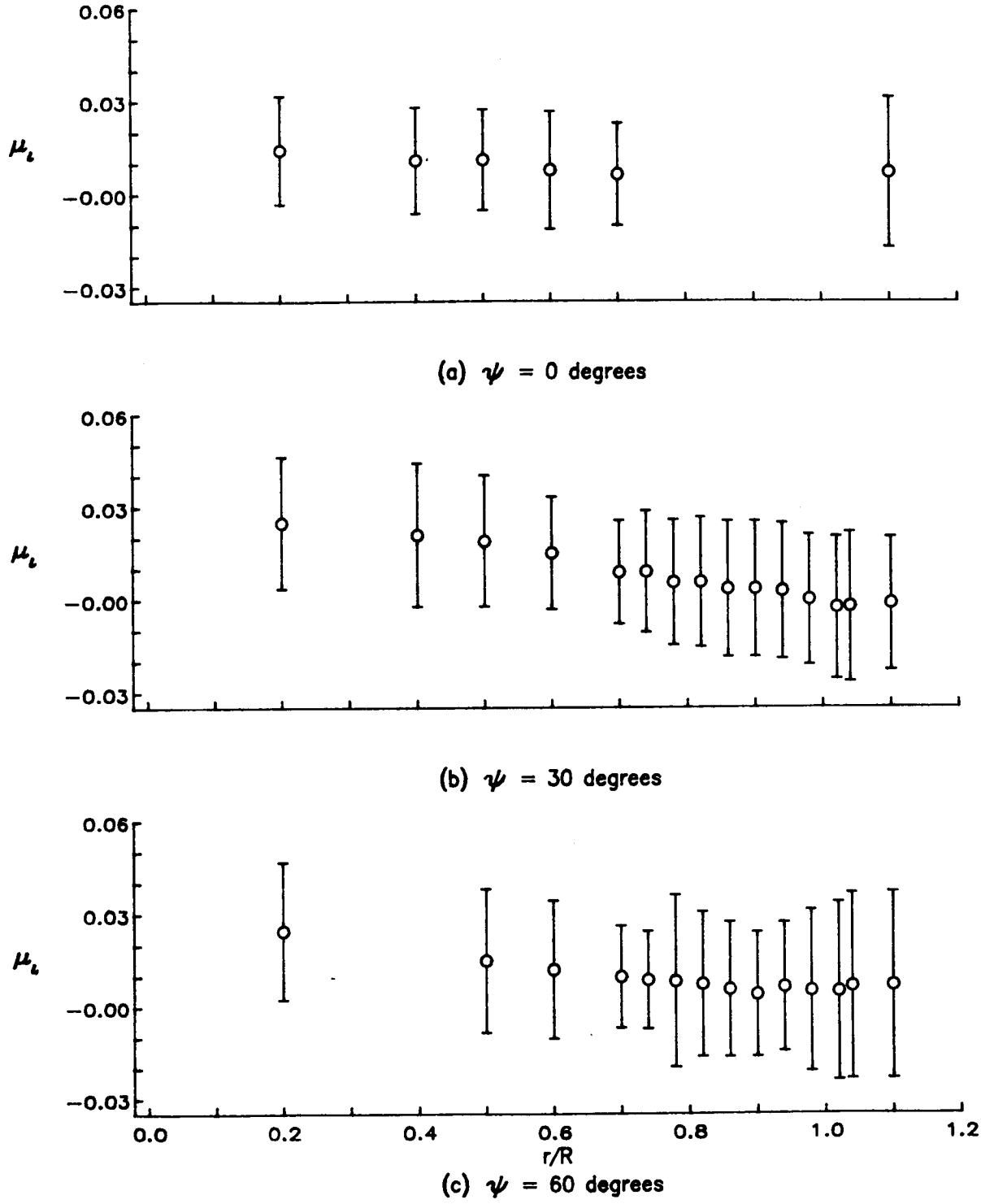
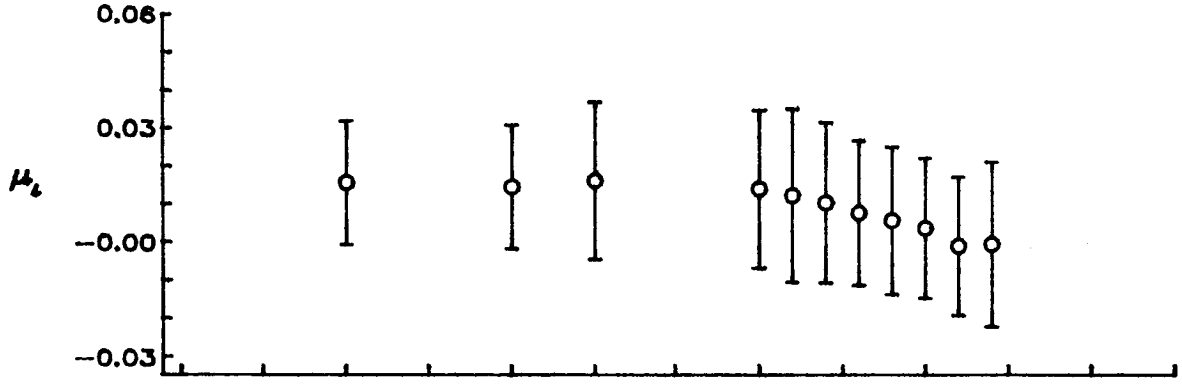
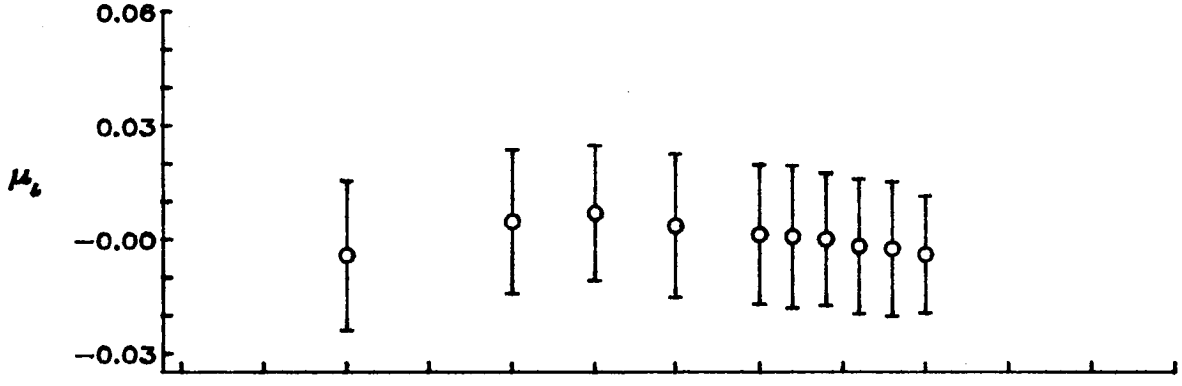


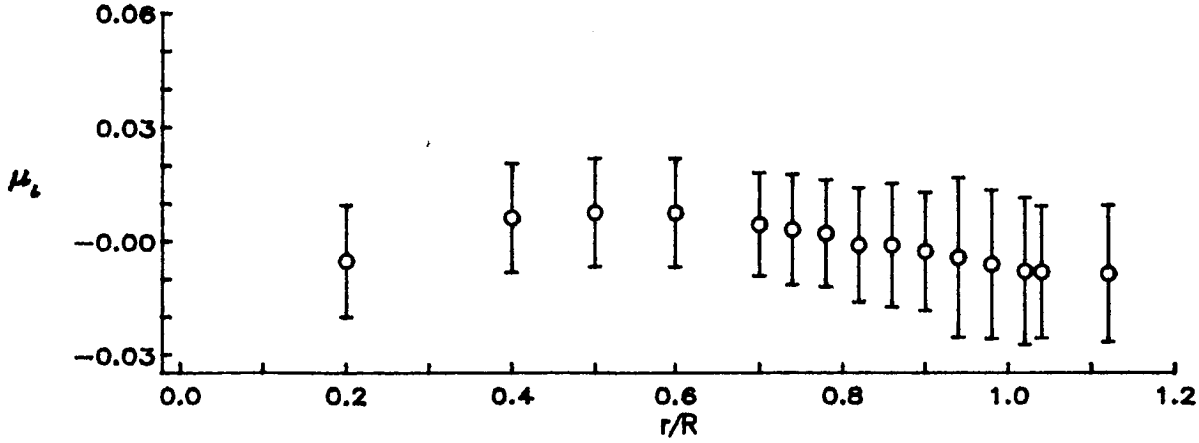
Figure 9.– Radial distribution of mean induced inflow ratio (μ_i).



(d) ψ = 90 degrees

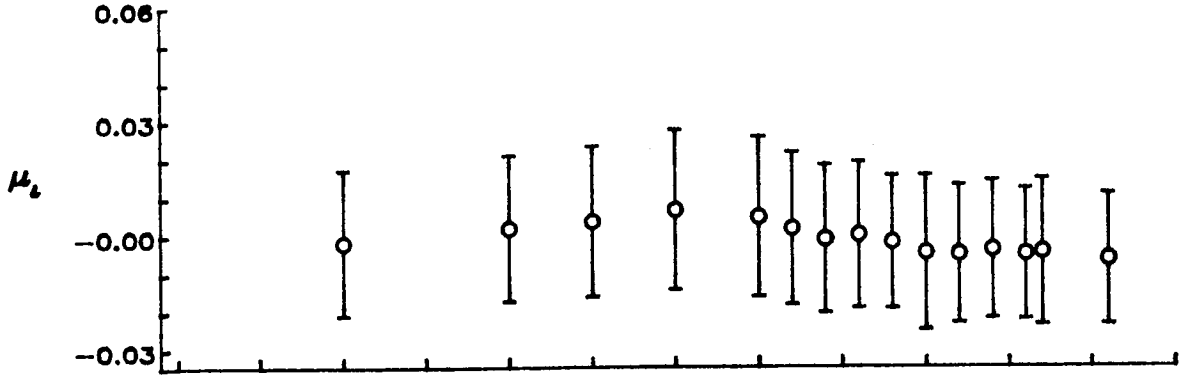


(e) ψ = 120 degrees

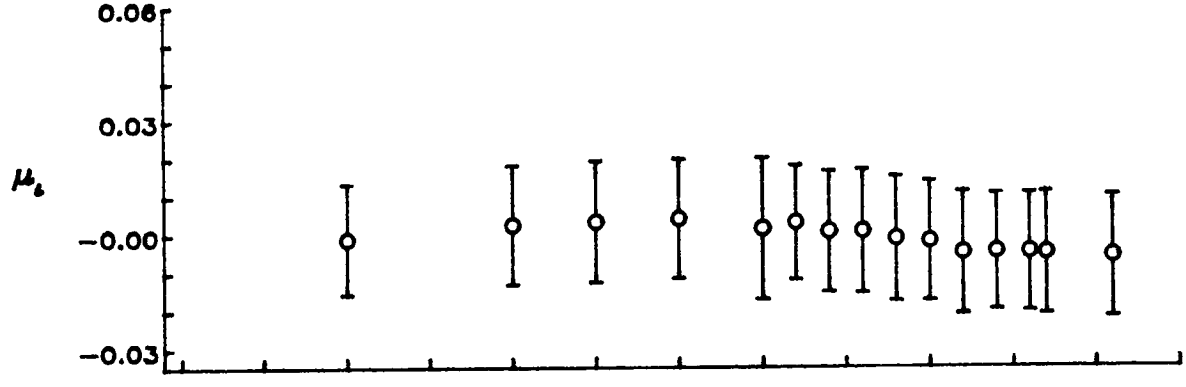


(f) ψ = 150 degrees

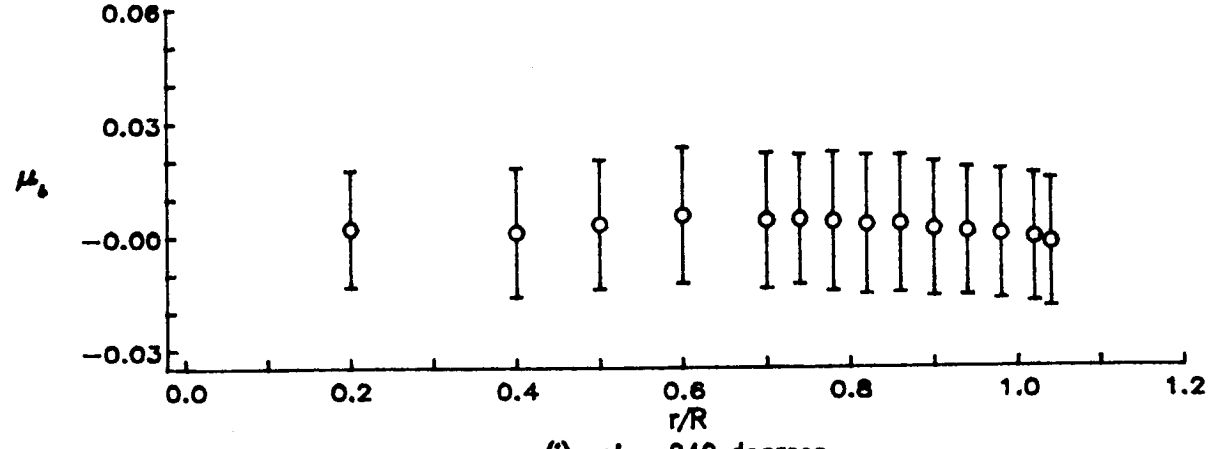
Figure 9.– Continued.



(g) ψ = 180 degrees

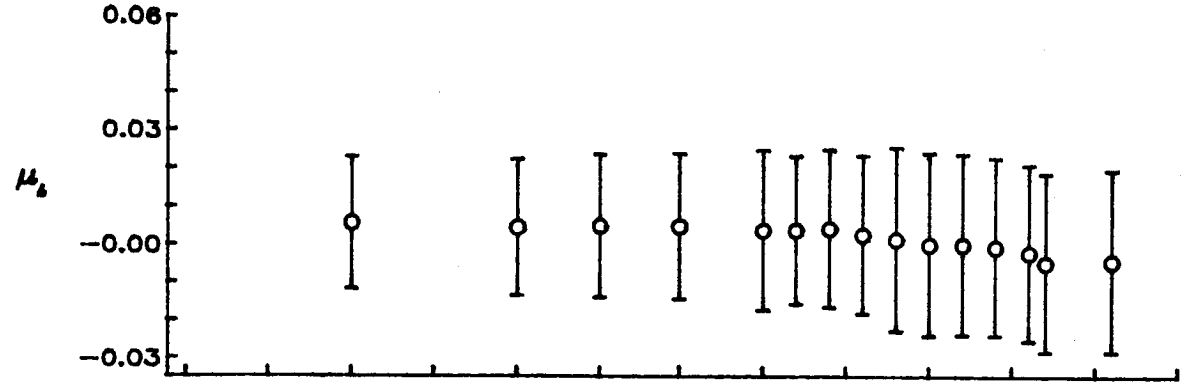


(h) ψ = 210 degrees

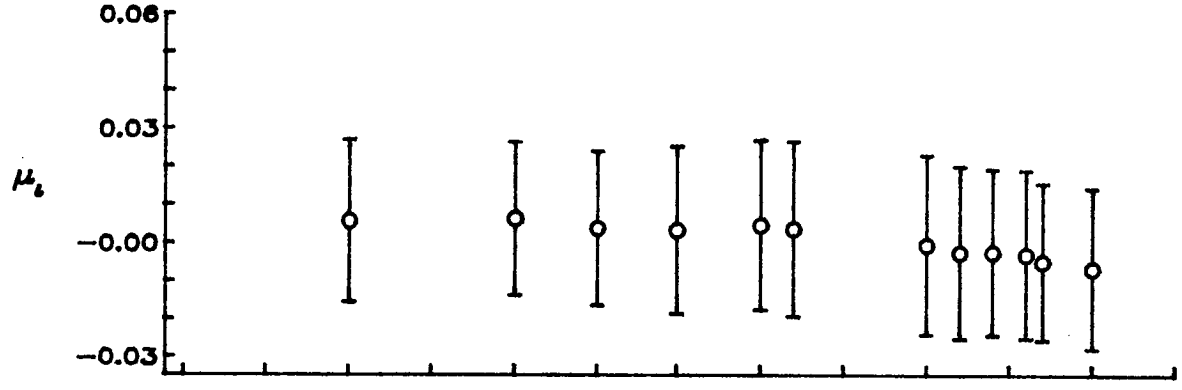


(i) ψ = 240 degrees

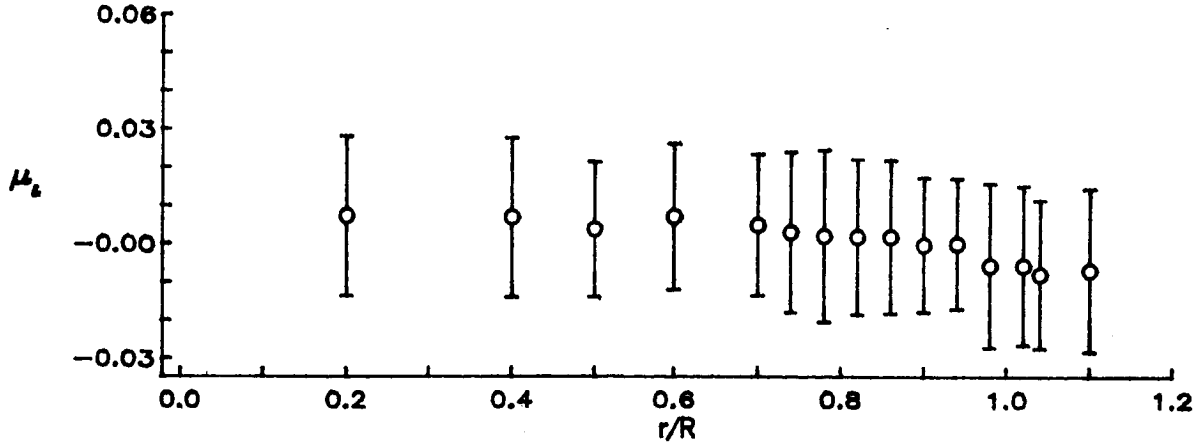
Figure 9.– Continued.



(j) ψ = 270 degrees

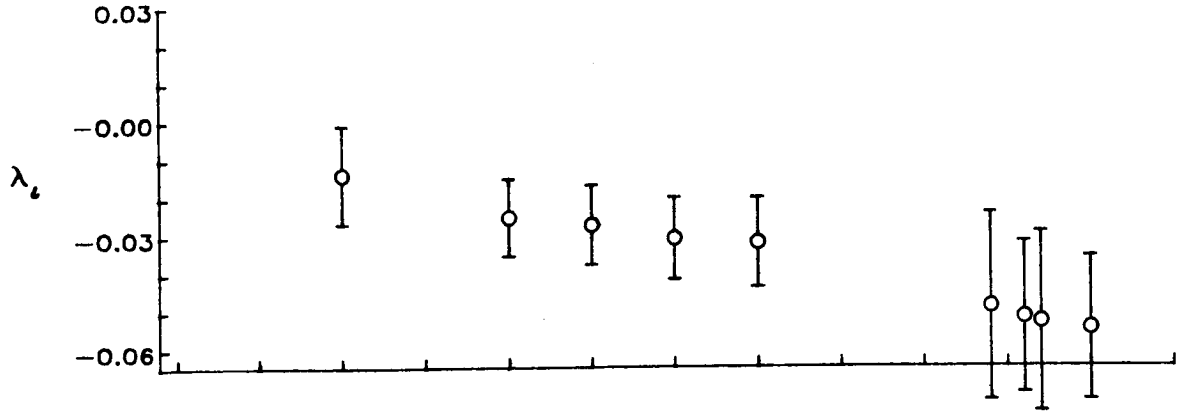


(k) ψ = 300 degrees

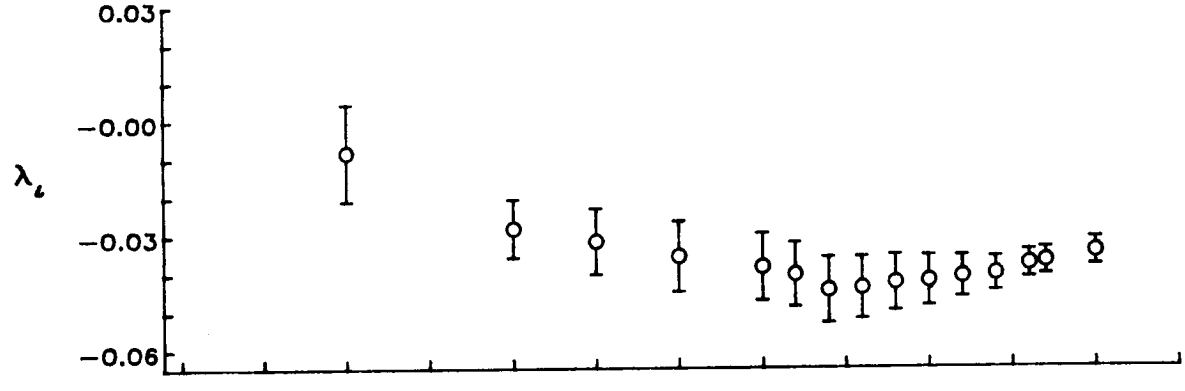


(l) ψ = 330 degrees

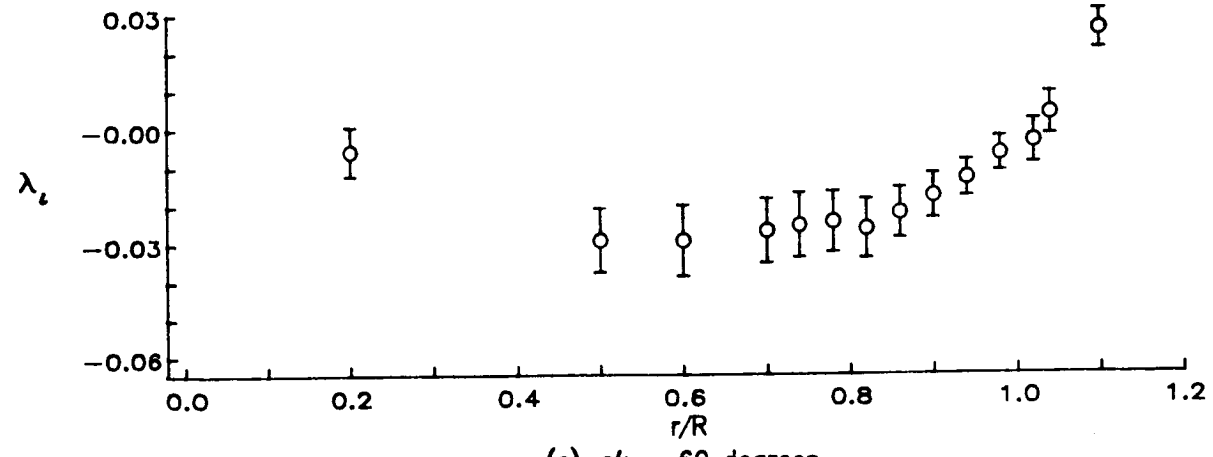
Figure 9.– Concluded.



(a) ψ = 0 degrees

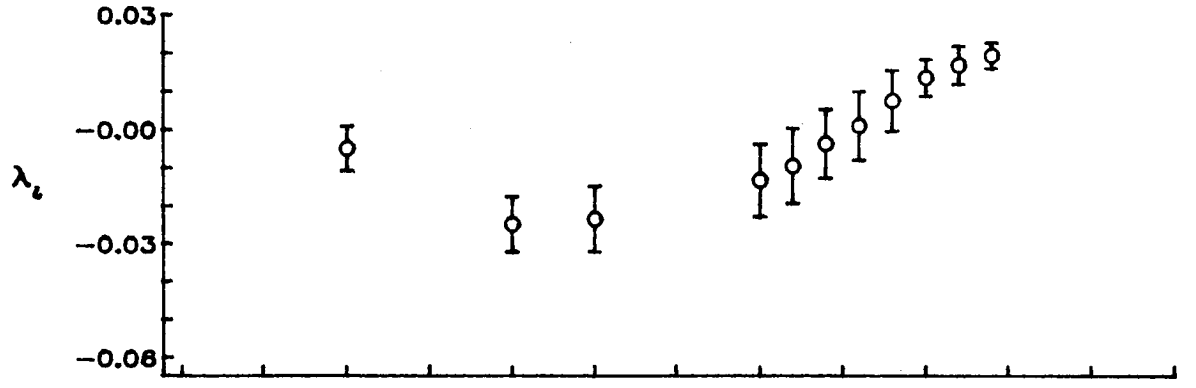


(b) ψ = 30 degrees

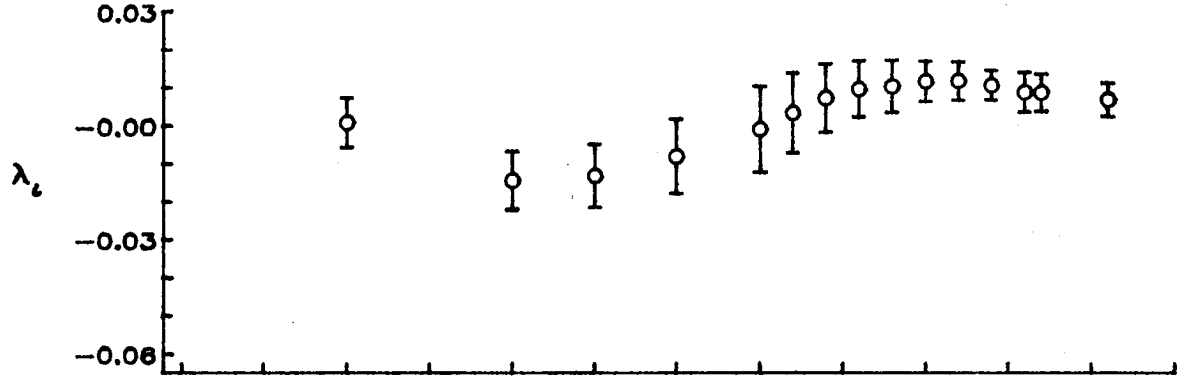


(c) ψ = 60 degrees

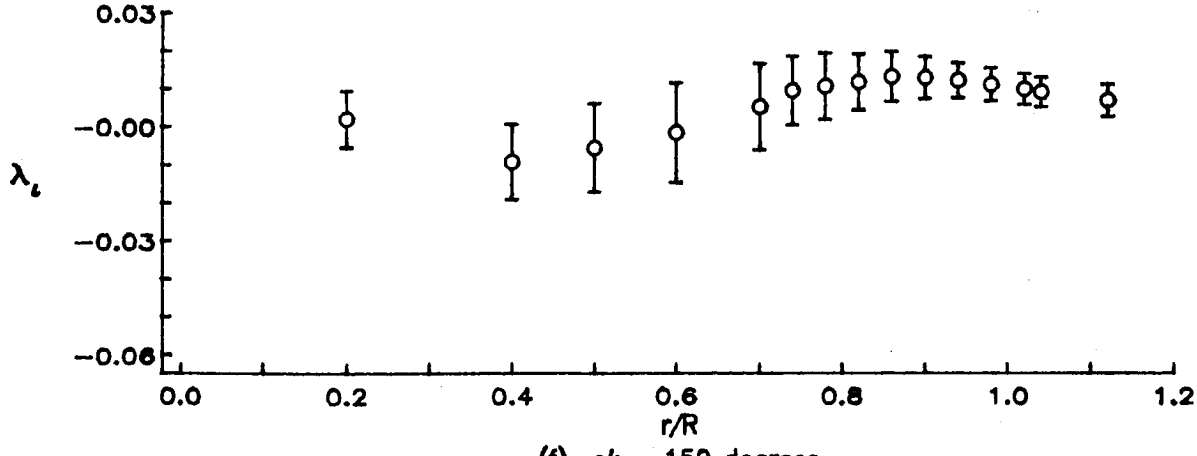
Figure 10.– Radial distribution of mean induced inflow ratio (λ_i).



(d) ψ = 90 degrees

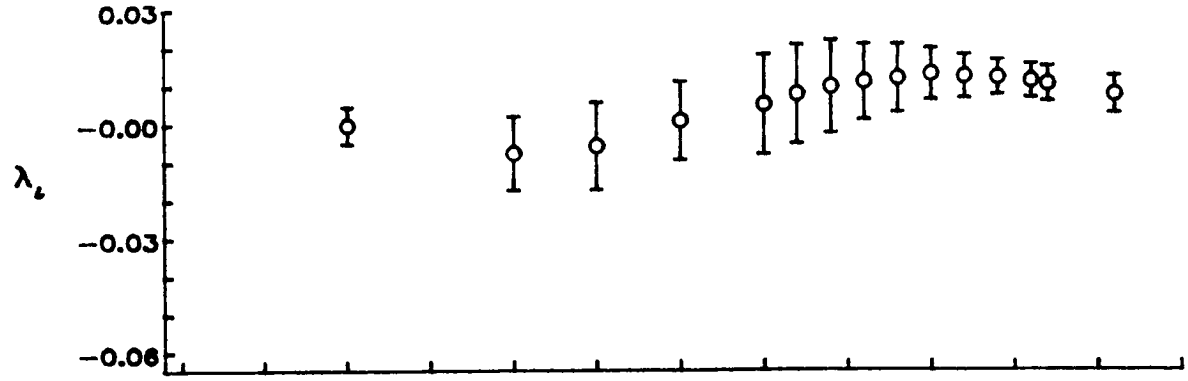


(e) ψ = 120 degrees

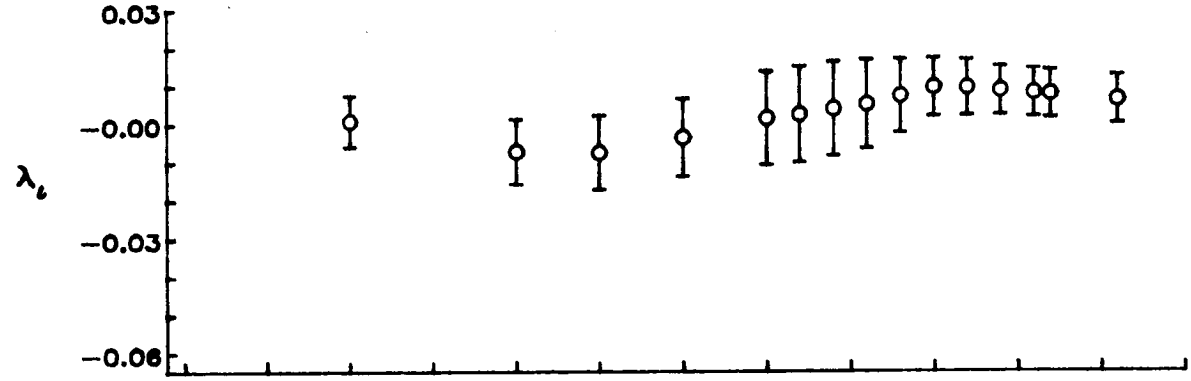


(f) ψ = 150 degrees

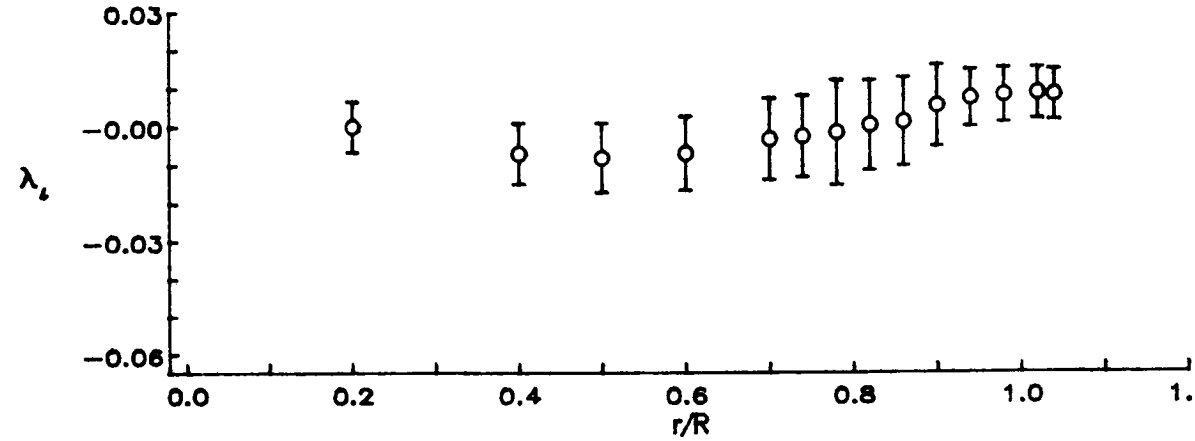
Figure 10.– Continued.



(g) ψ = 180 degrees

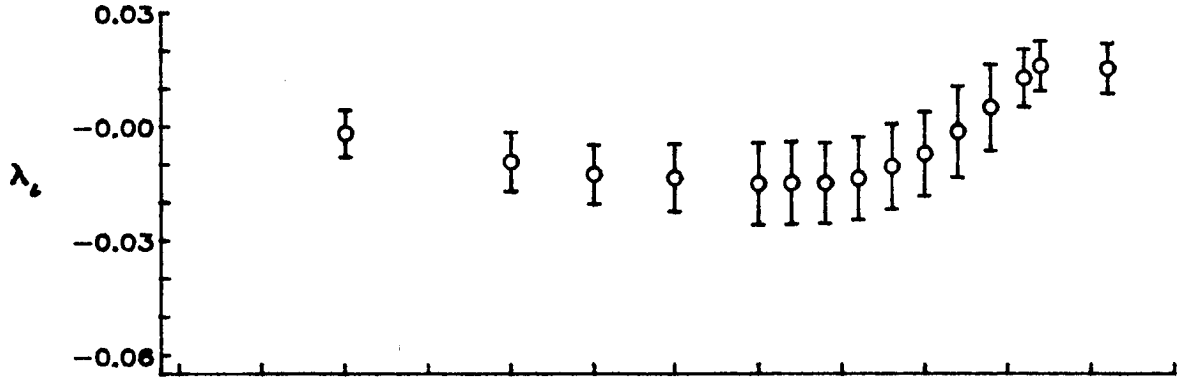


(h) ψ = 210 degrees

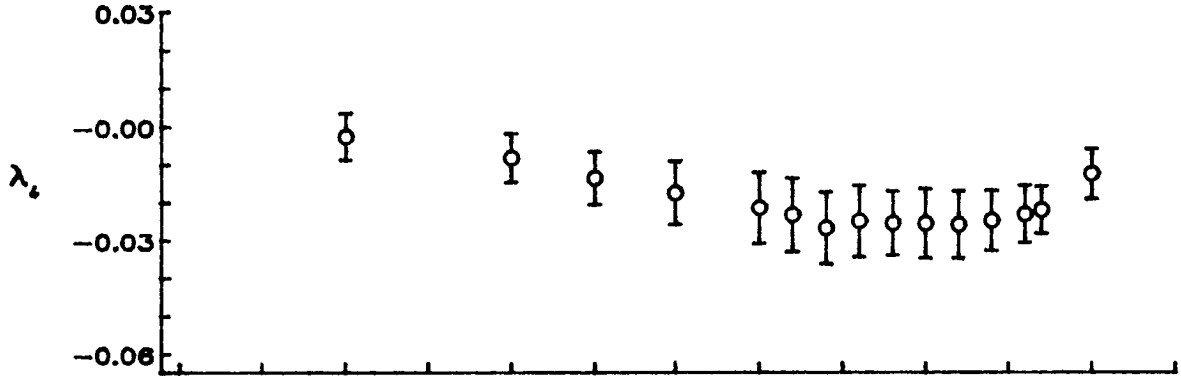


(i) ψ = 240 degrees

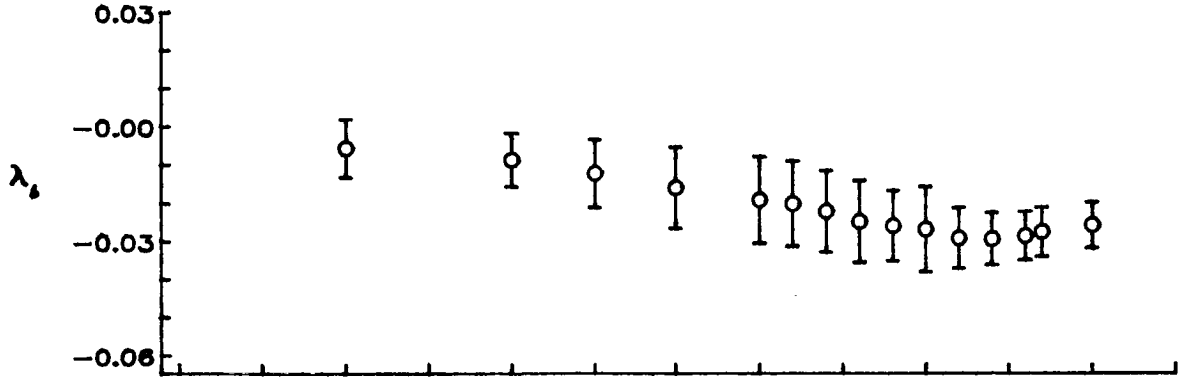
Figure 10.– Continued.



(j) ψ = 270 degrees

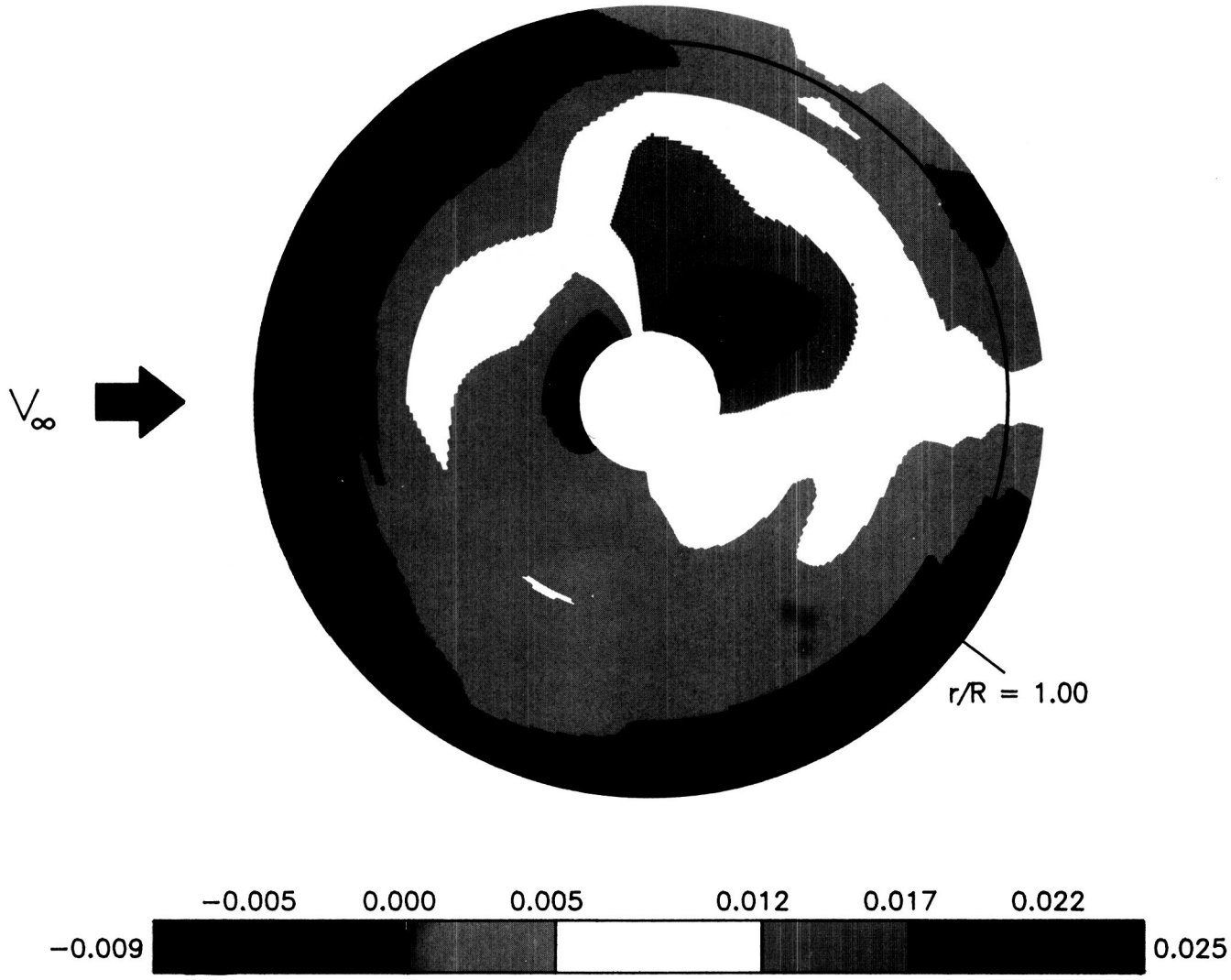


(k) ψ = 300 degrees



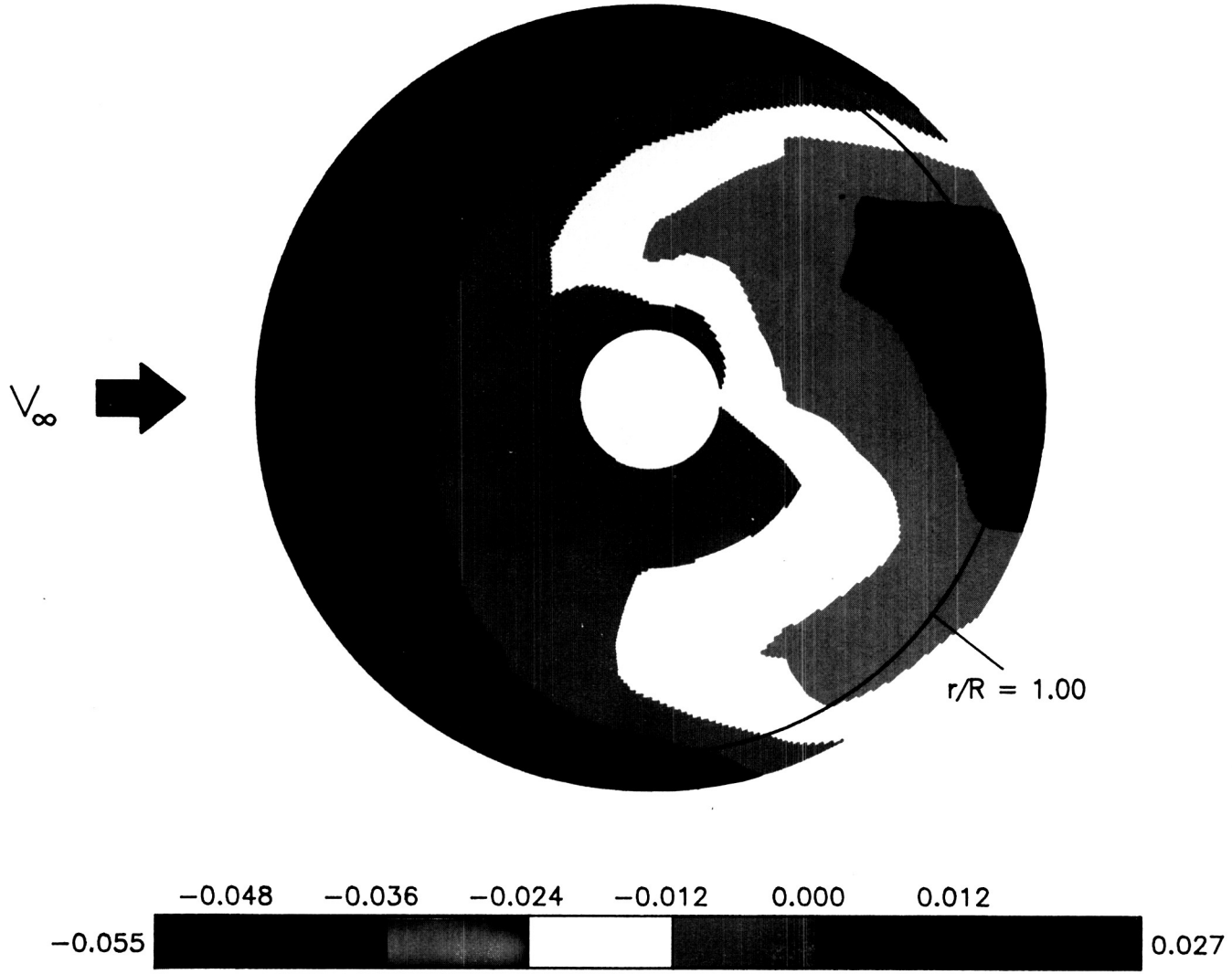
(l) ψ = 330 degrees

Figure 10.– Concluded.



ORIGINAL PAGE
COLOR PHOTOGRAPH

Figure 11.– Contour plot of mean induced inflow ratio (μ_i).



ORIGINAL PAGE
COLOR PHOTOGRAPH

Figure 12.– Contour plot of mean induced inflow ratio (λ_i).

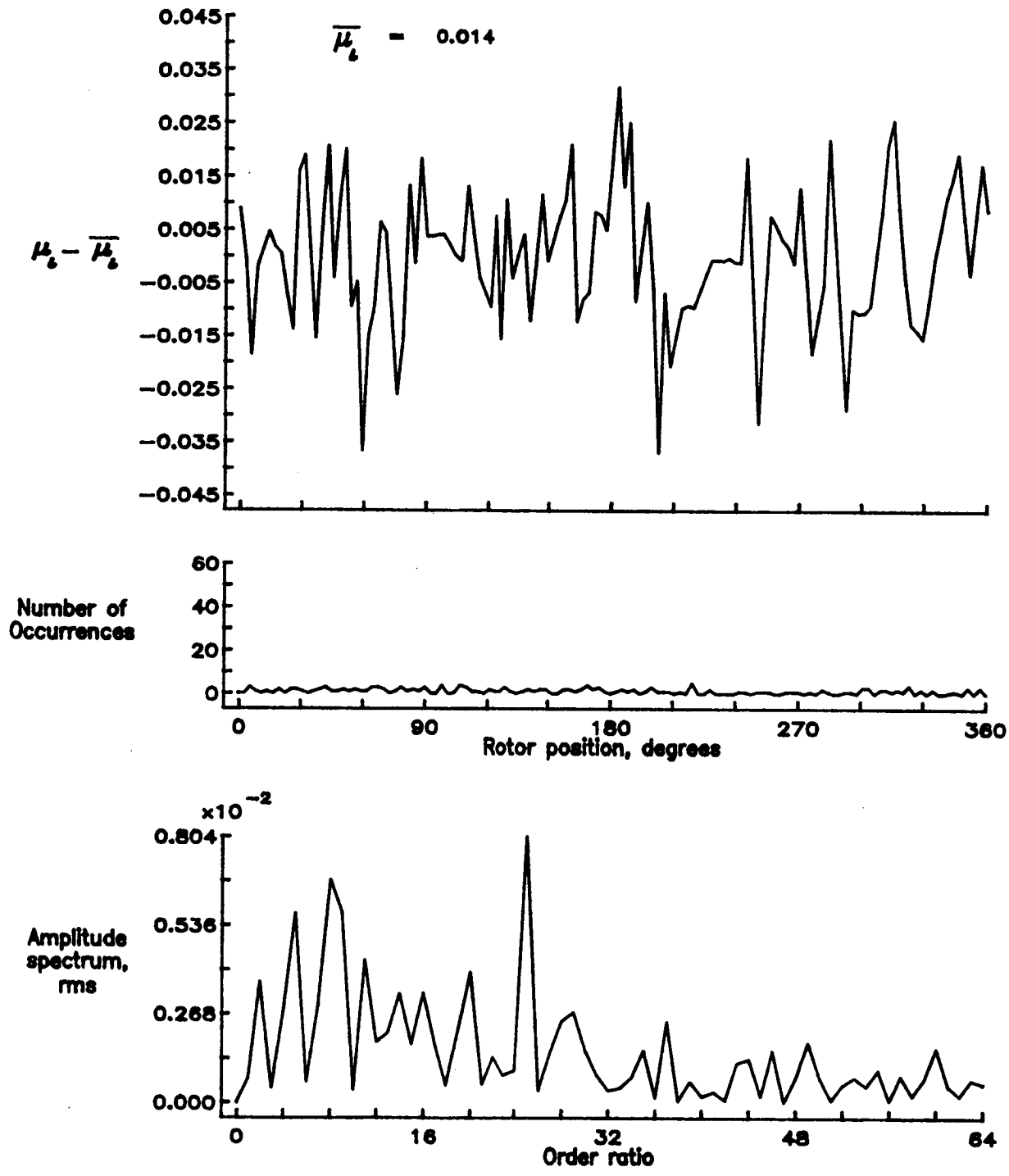


Figure 13.– Induced inflow velocity measured at 0 degrees and r/R of 0.20.

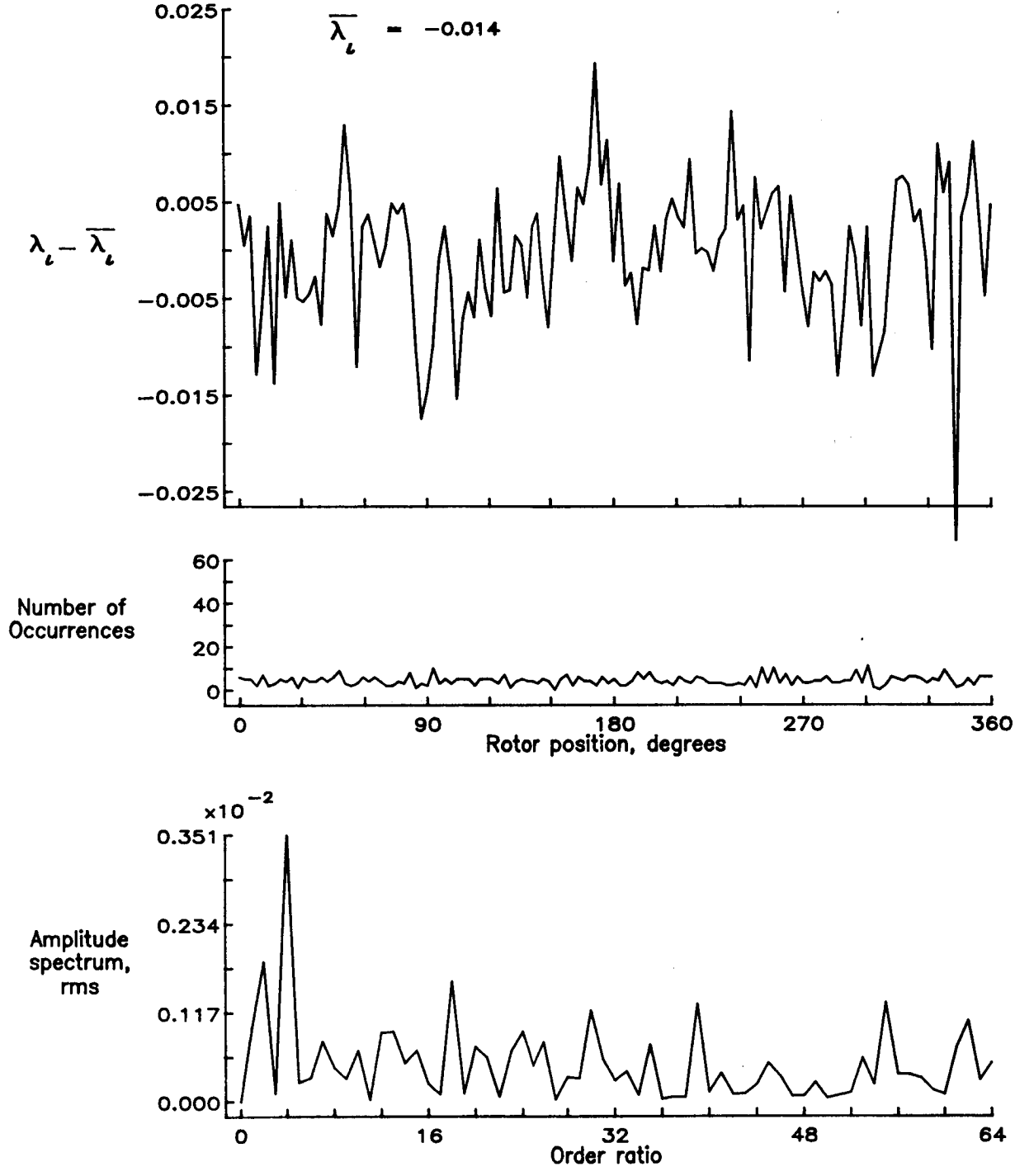


Figure 13.– Concluded.

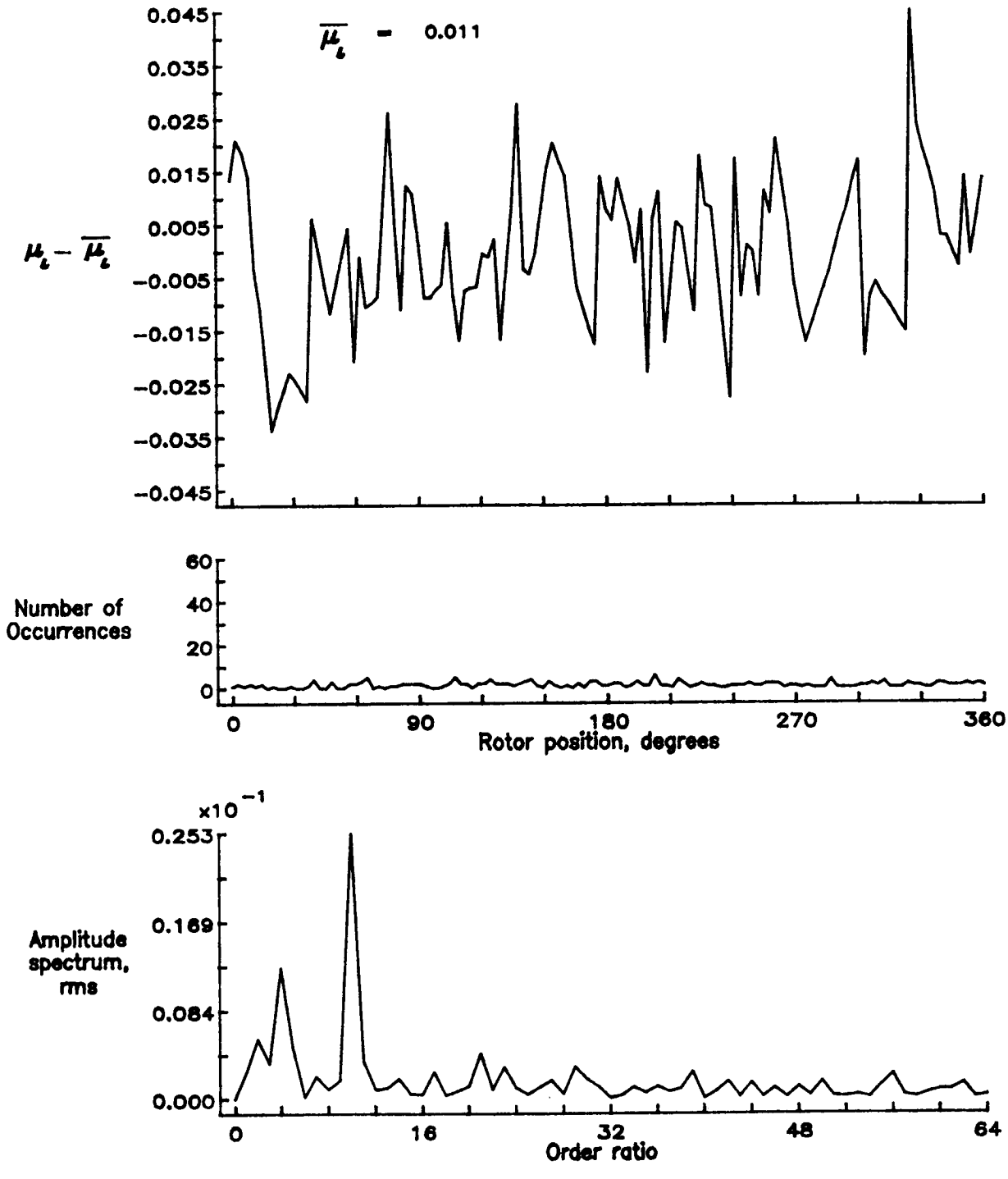


Figure 14.– Induced inflow velocity measured at 0 degrees and r/R of 0.40.

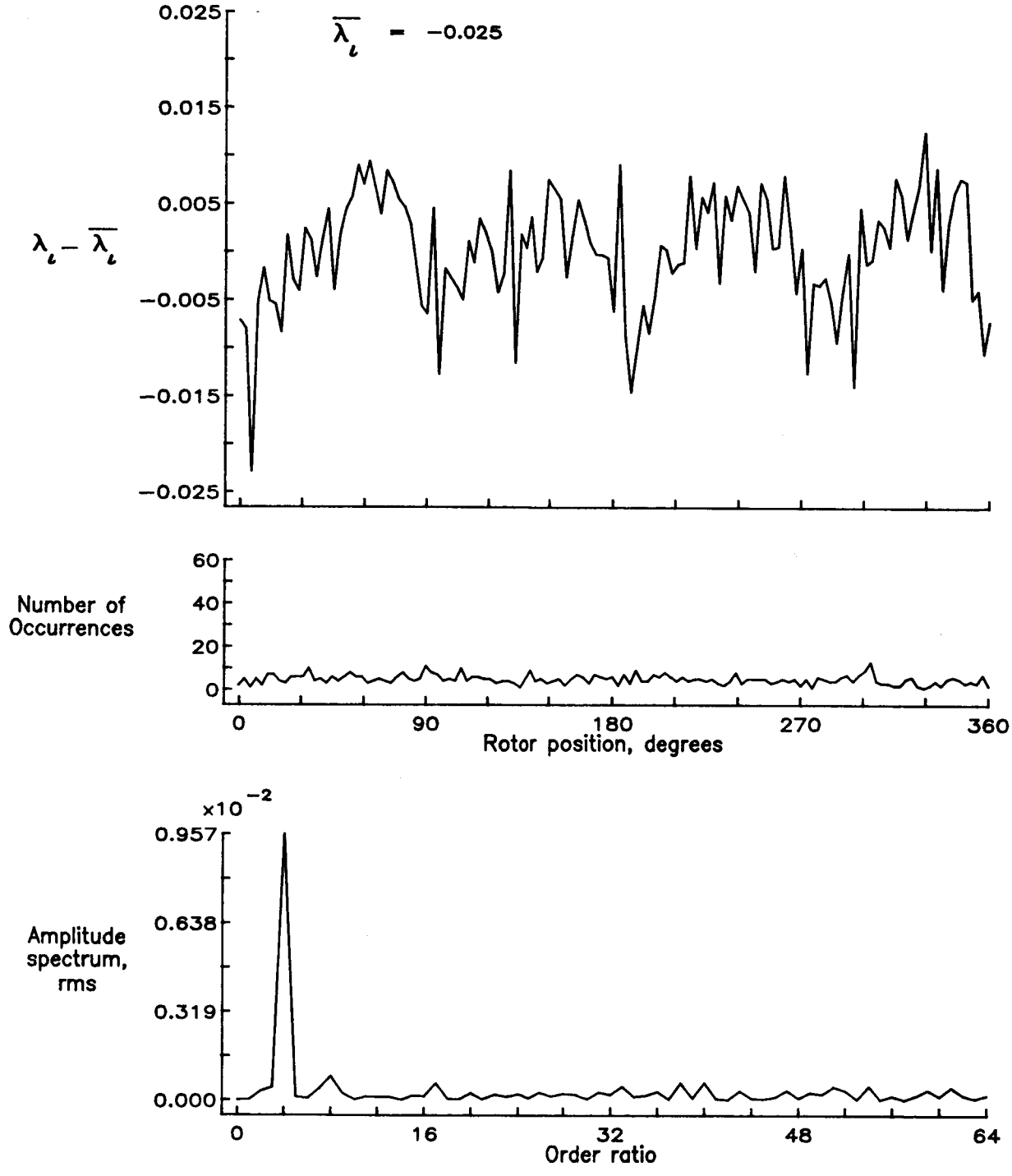


Figure 14.— Concluded.

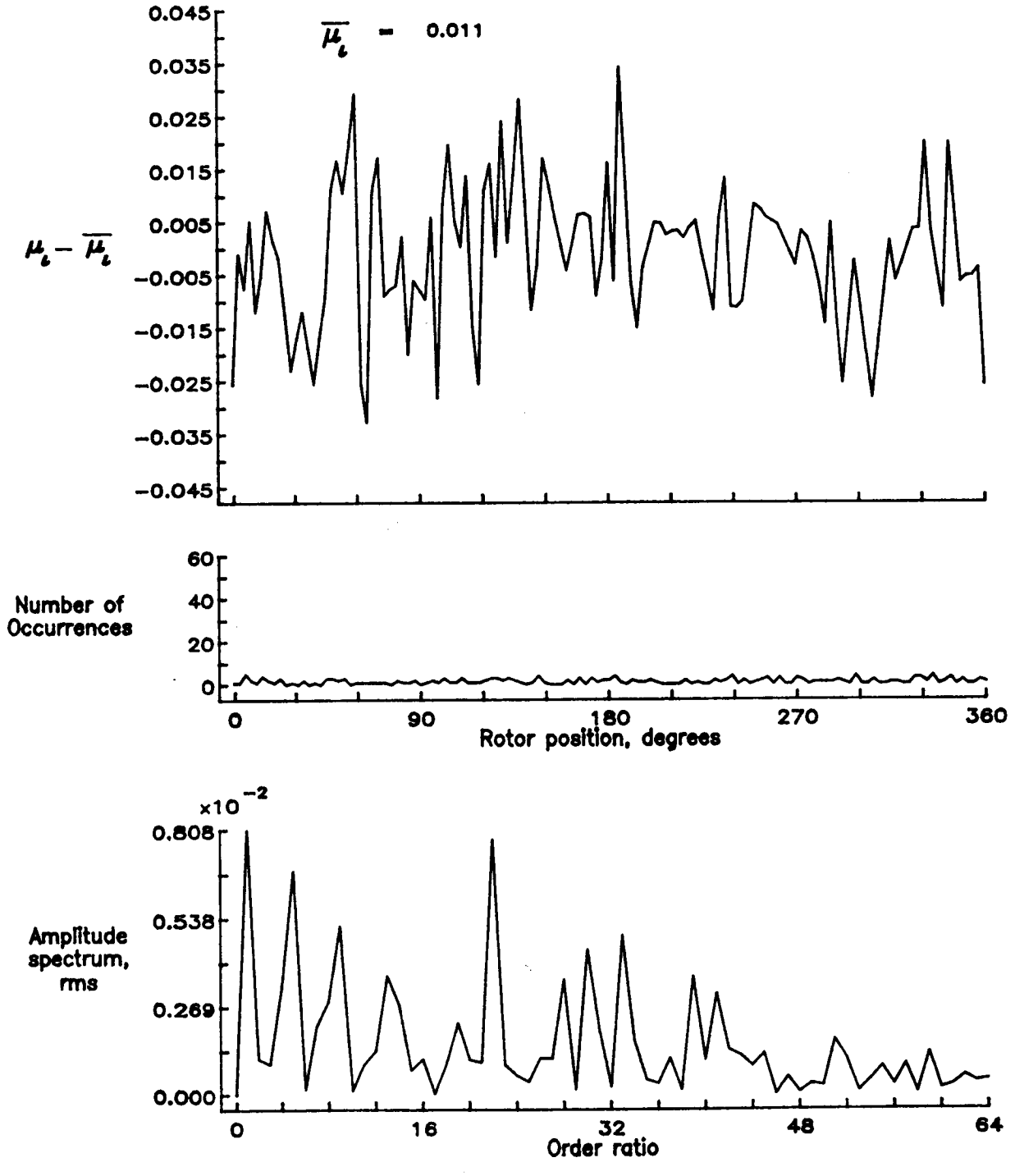


Figure 15.– Induced inflow velocity measured at 0 degrees and r/R of 0.50.

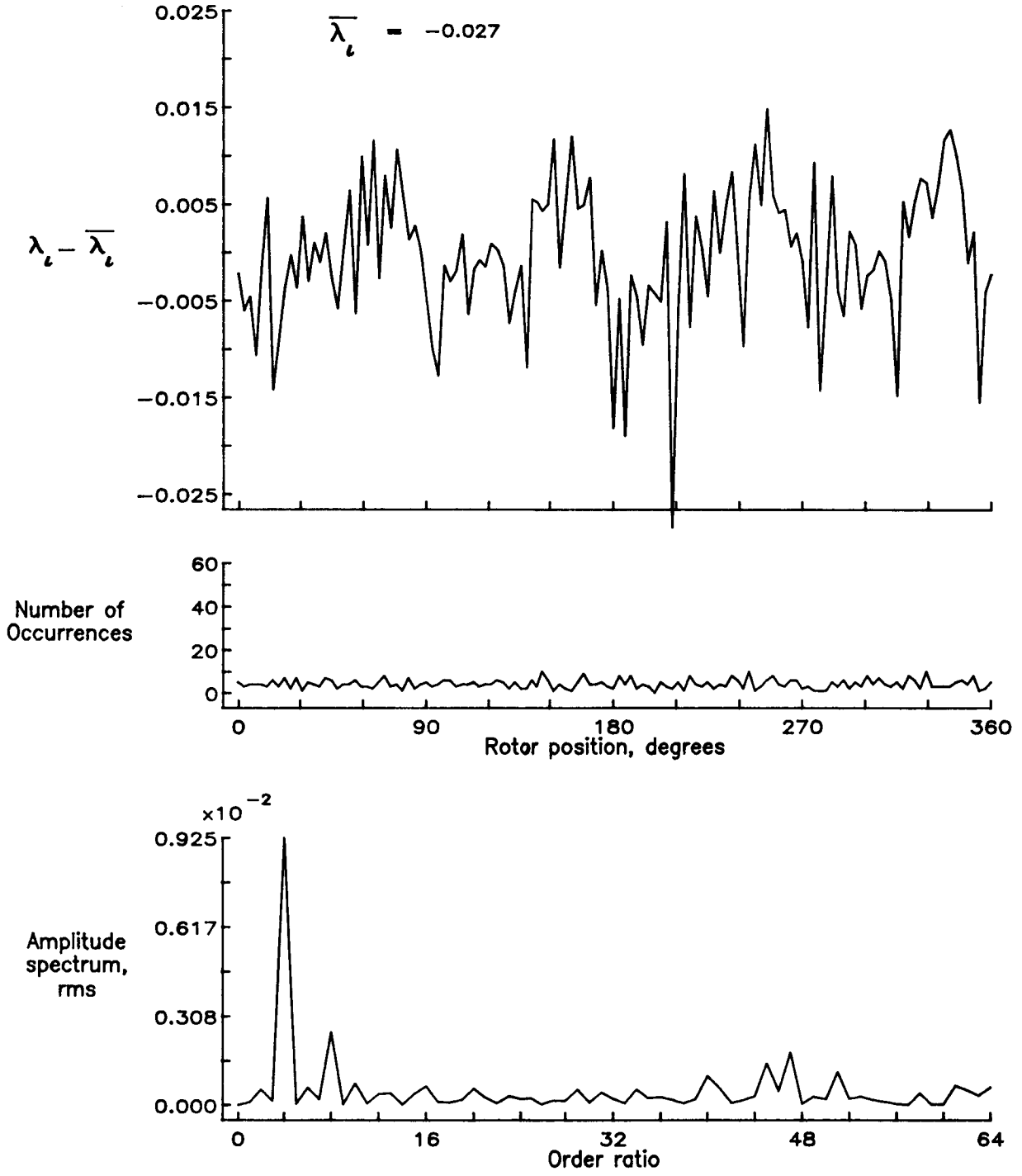


Figure 15.– Concluded.

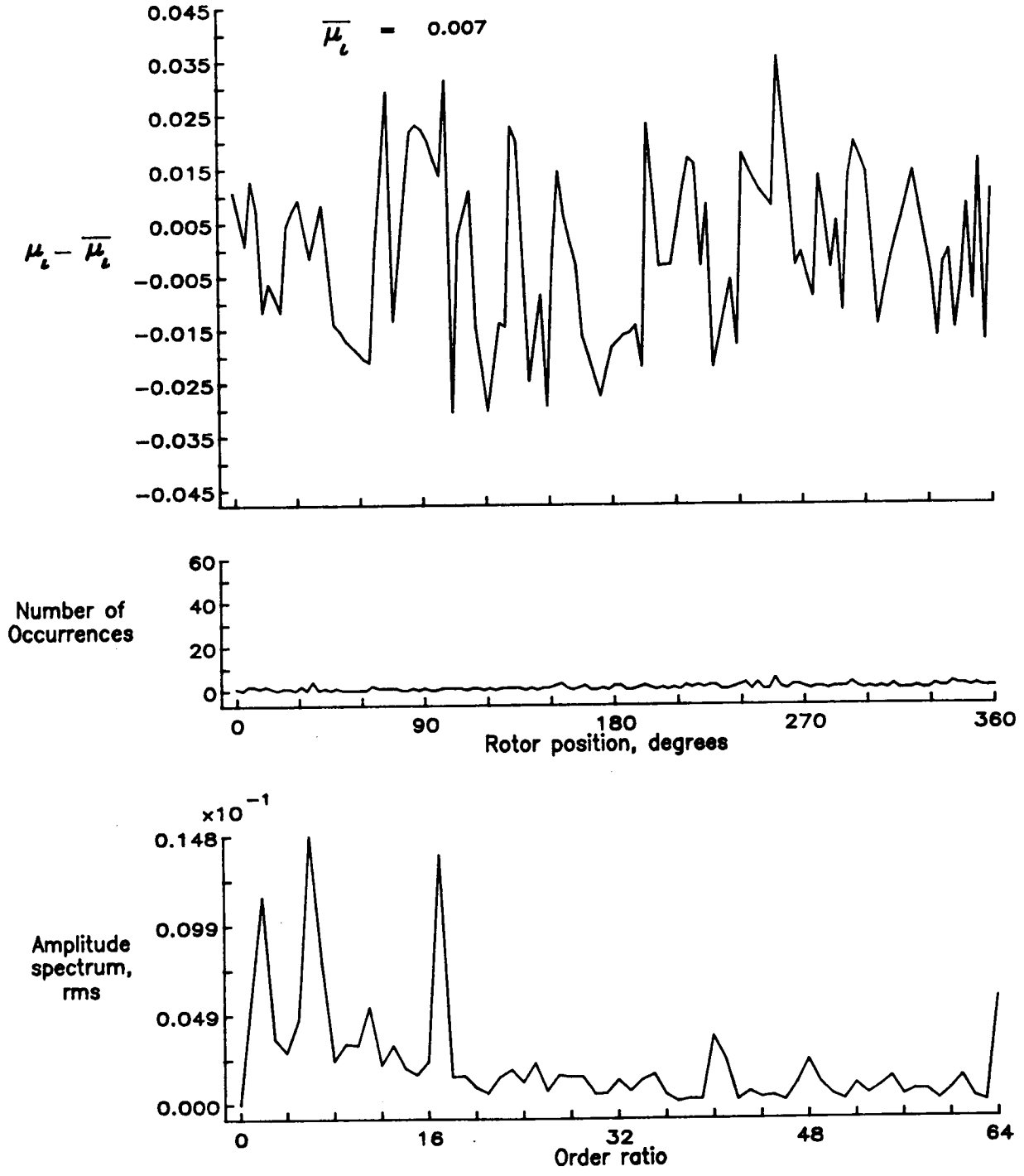


Figure 16.– Induced inflow velocity measured at 0 degrees and r/R of 0.60.

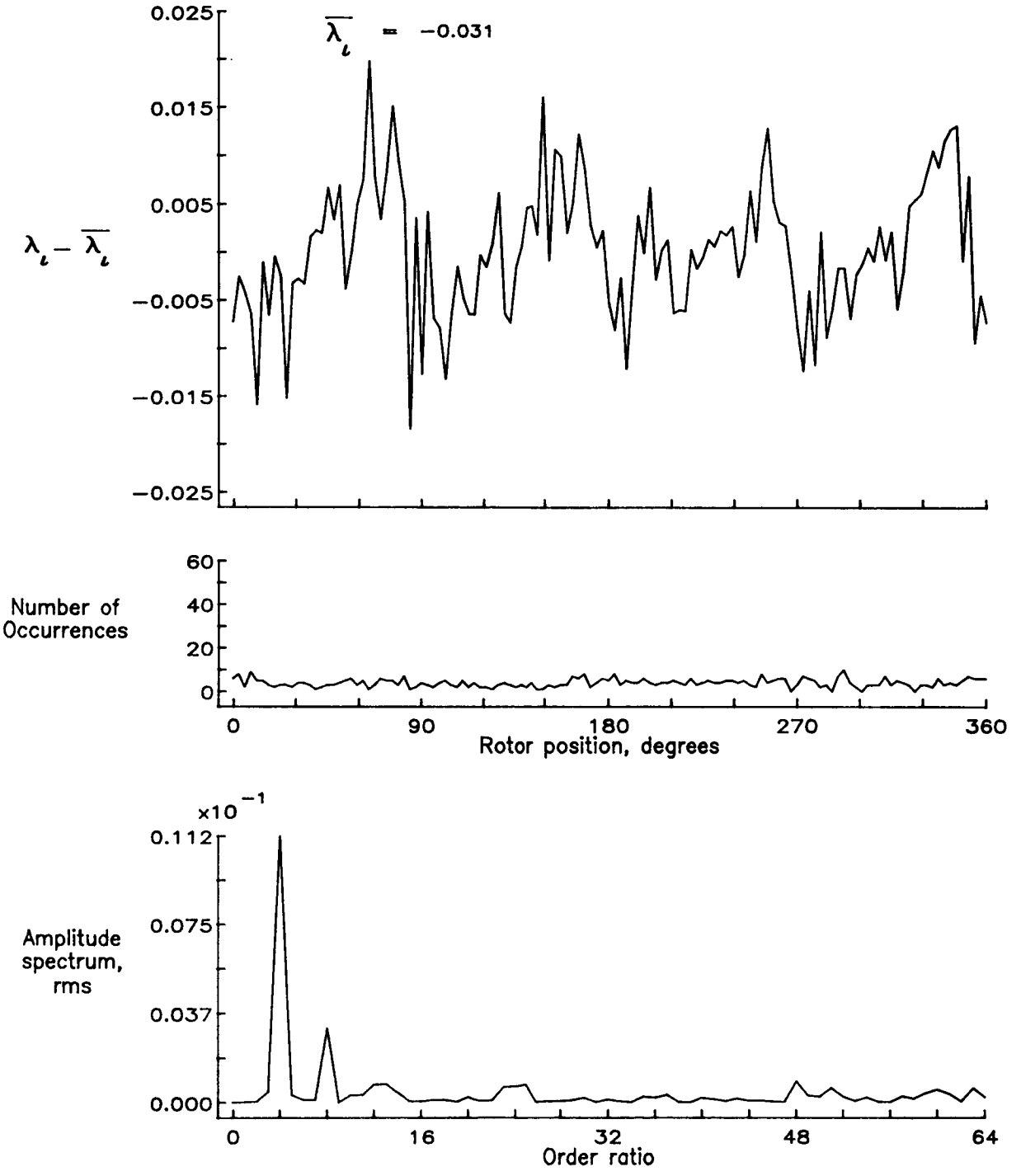


Figure 16.– Concluded.

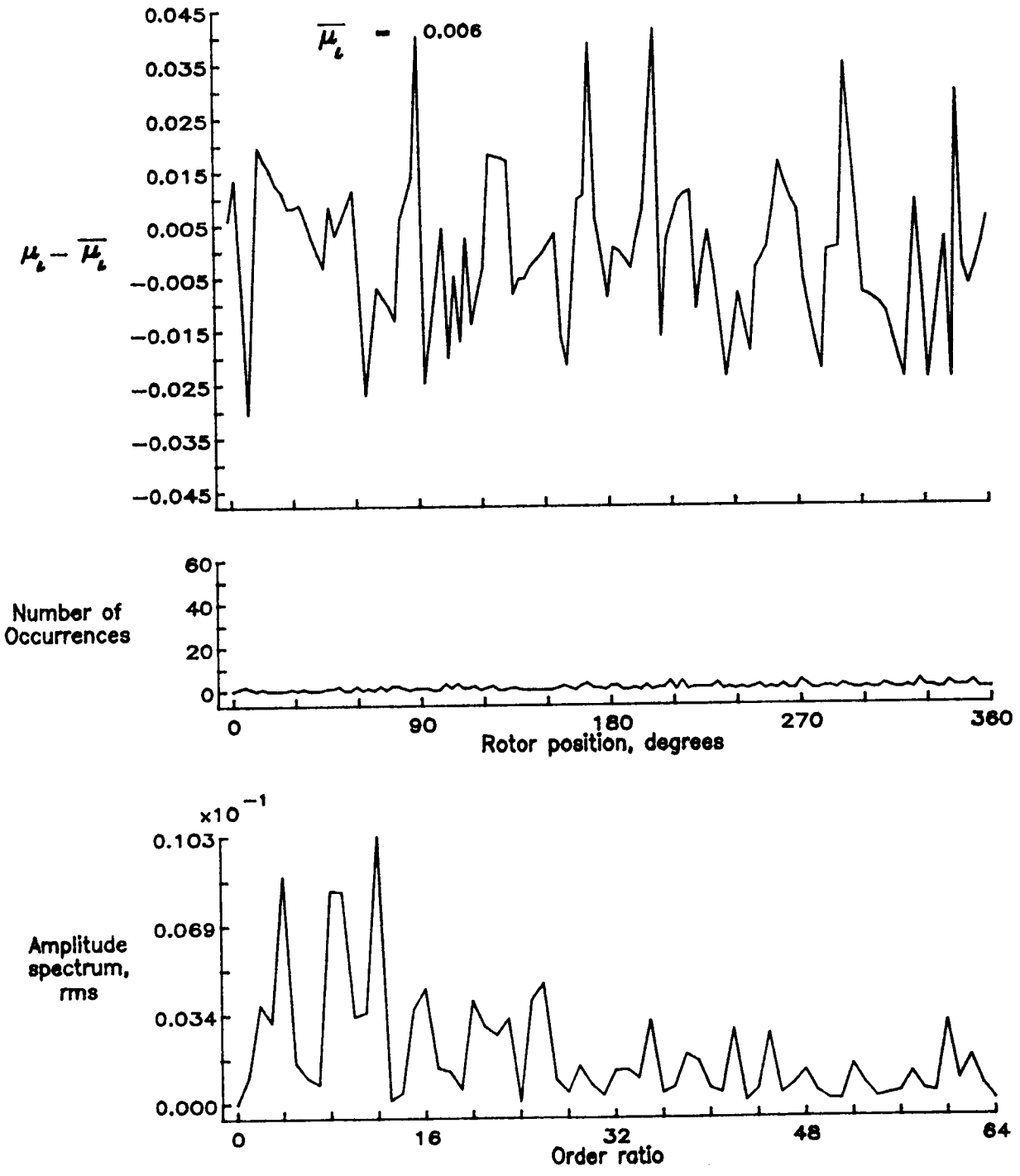


Figure 17.– Induced inflow velocity measured at 0 degrees and r/R of 0.70.

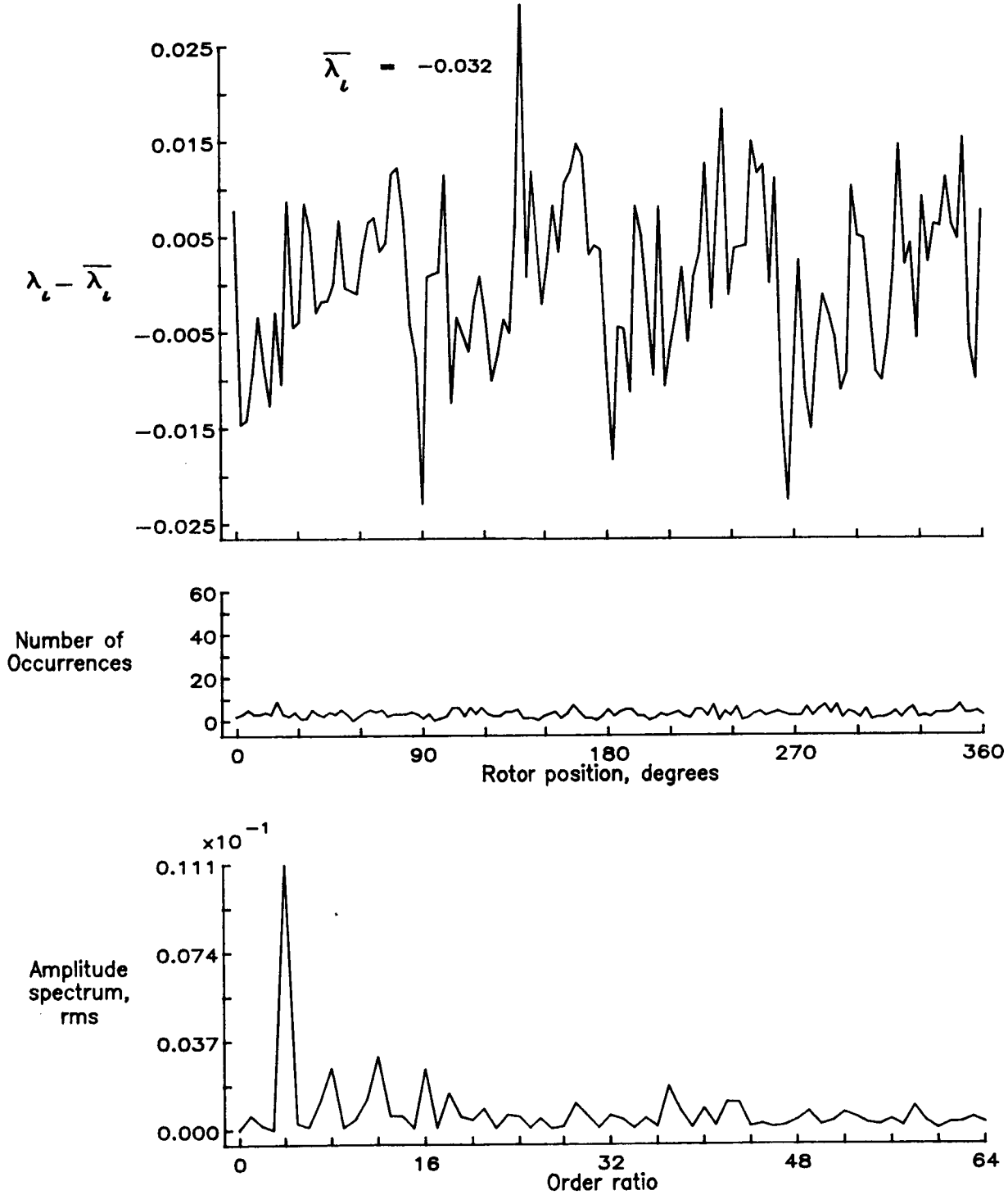


Figure 17.– Concluded.

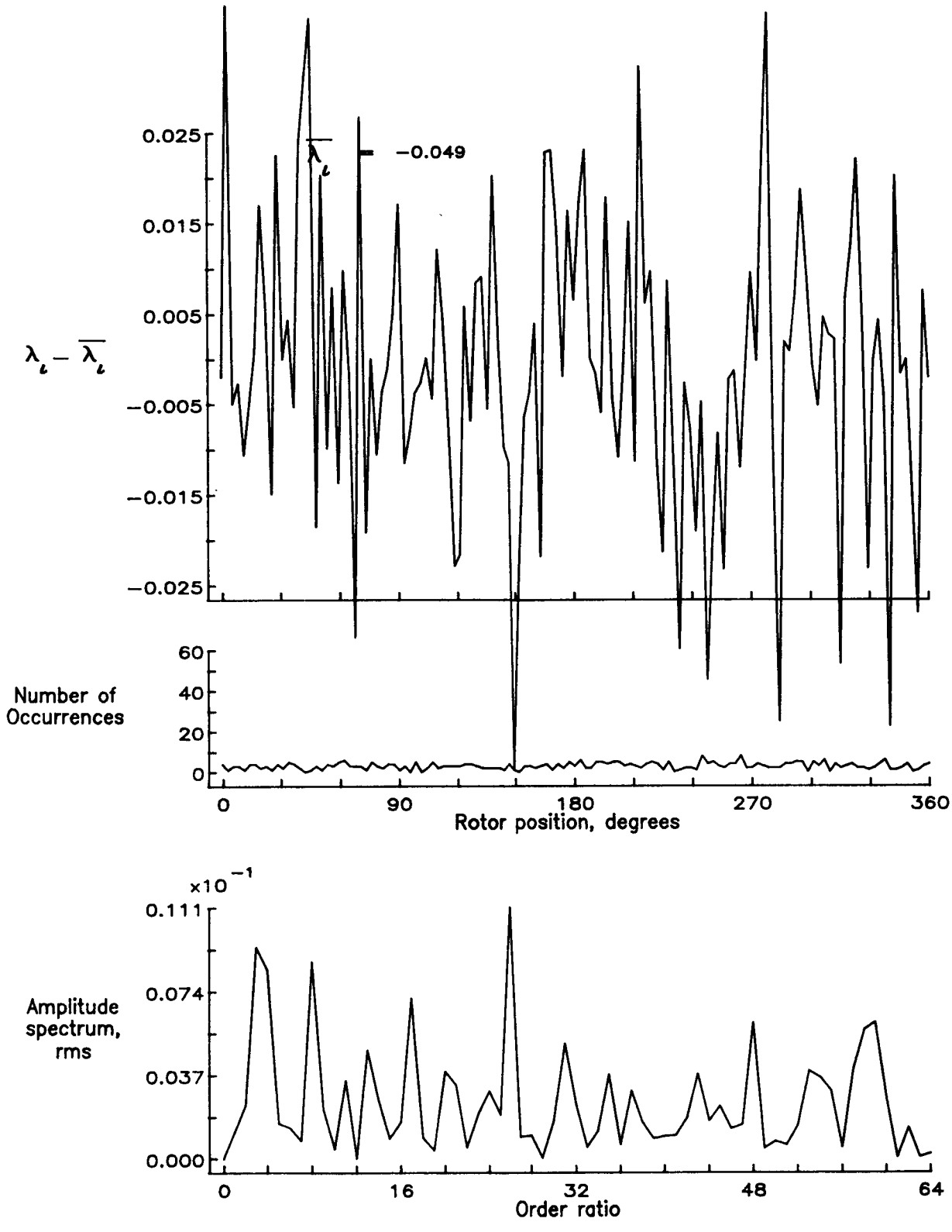


Figure 18.– Induced inflow velocity measured at 0 degrees and r/R of 0.98.

PRECEDING PAGE BLANK NOT FILMED

PAGE 40 INTENTIONALLY BLANK

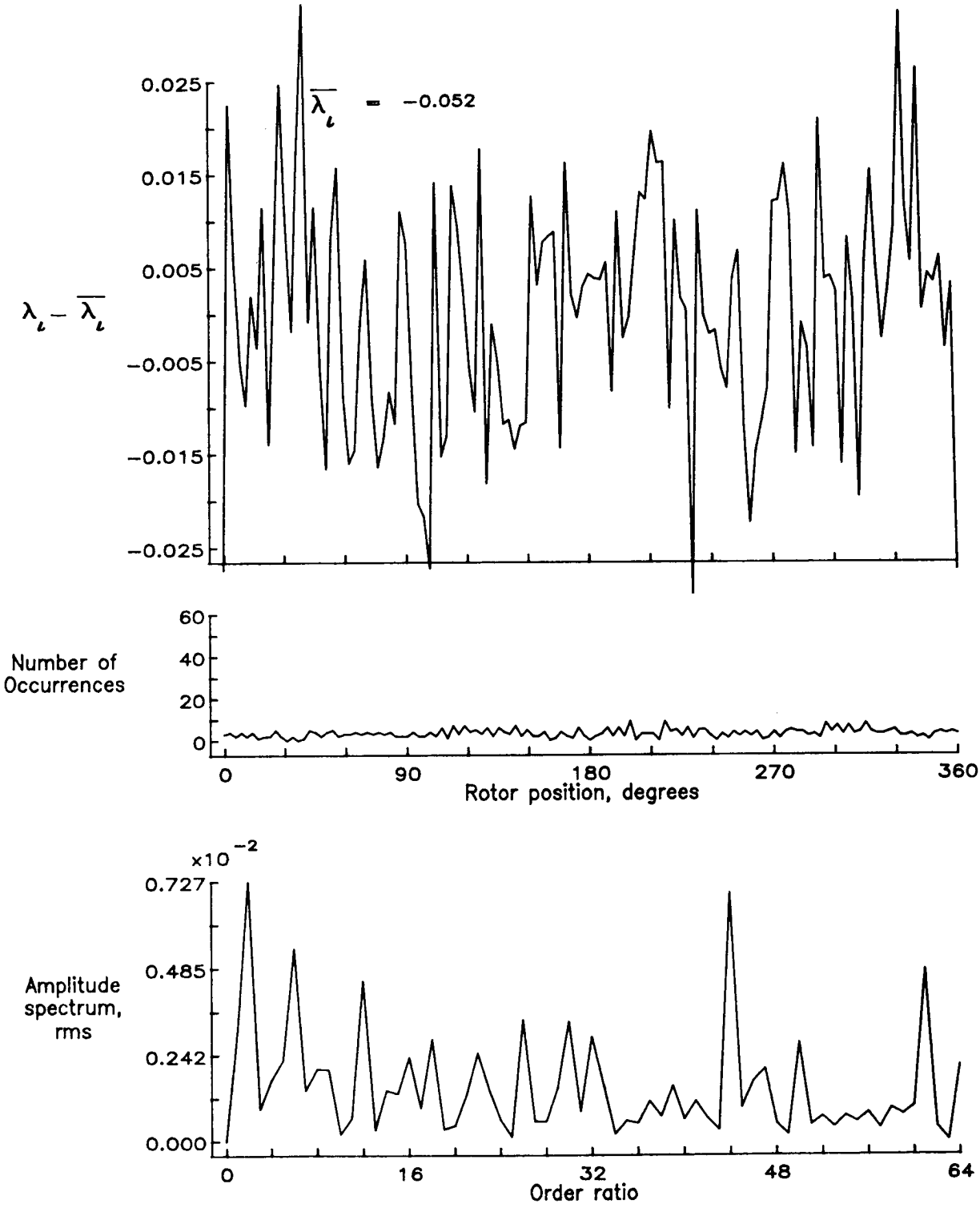


Figure 19.– Induced inflow velocity measured at 0 degrees and r/R of 1.02.

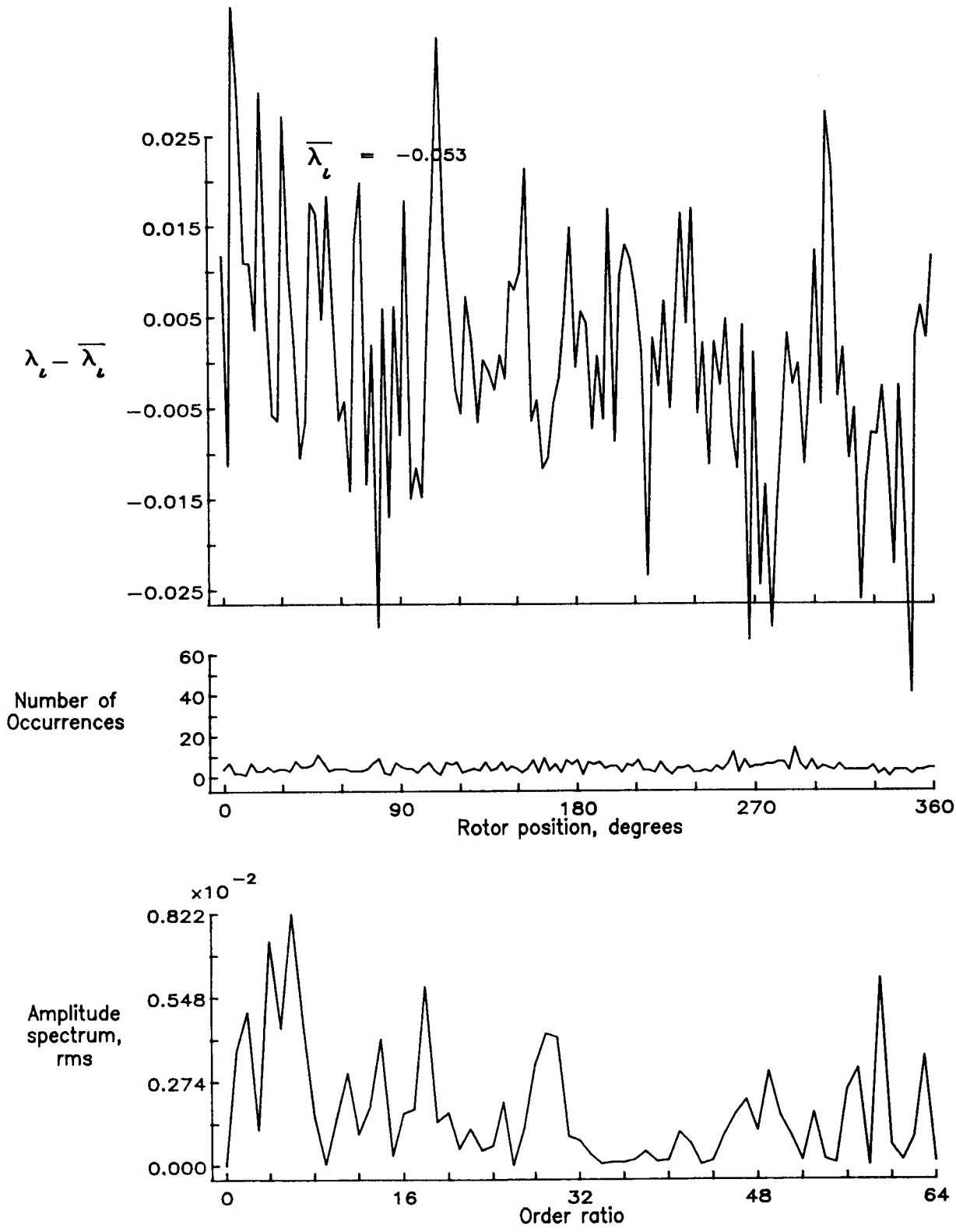


Figure 20.– Induced inflow velocity measured at 0 degrees and r/R of 1.04.

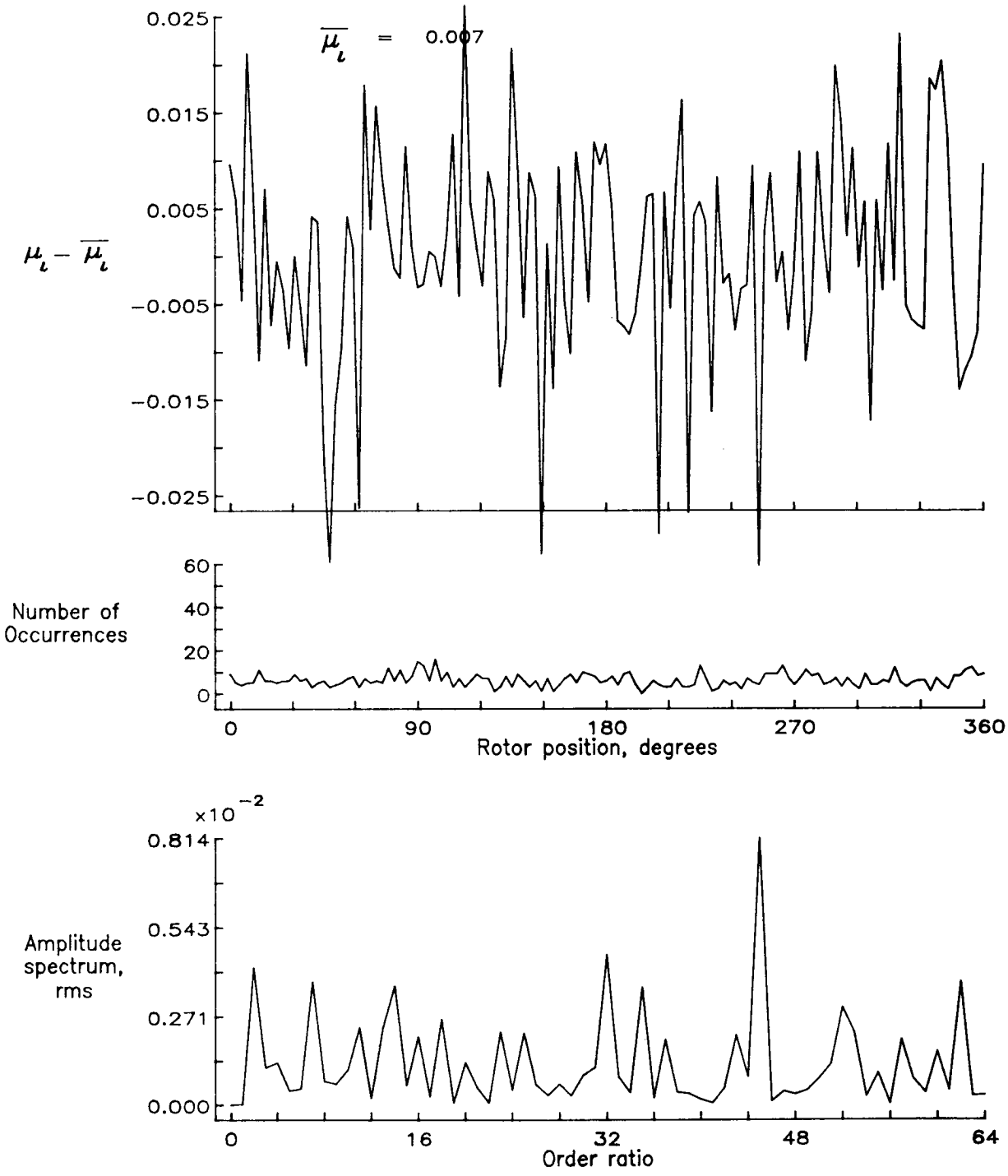


Figure 21.– Induced inflow velocity measured at 0 degrees and r/R of 1.10.

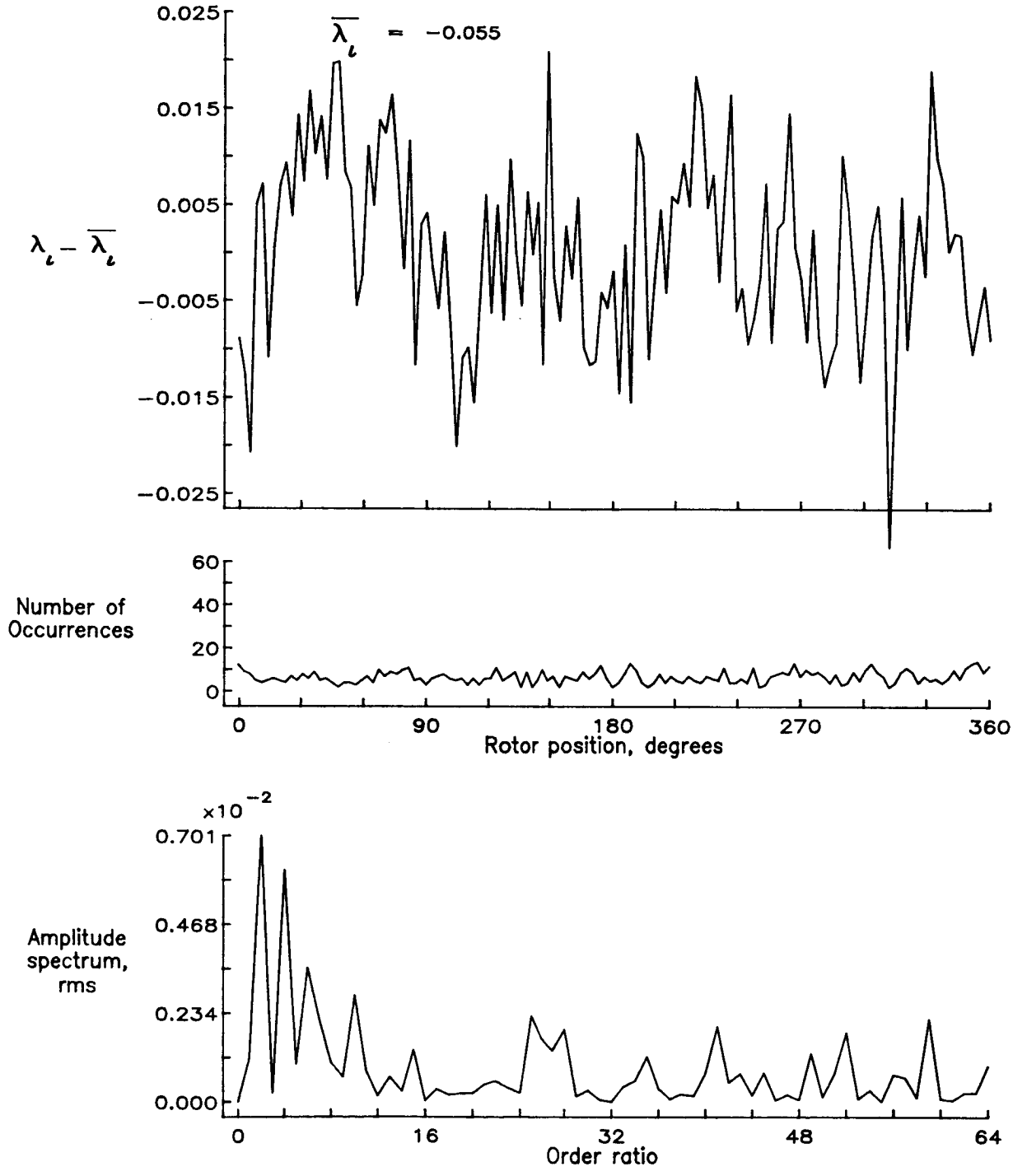


Figure 21.– Concluded.

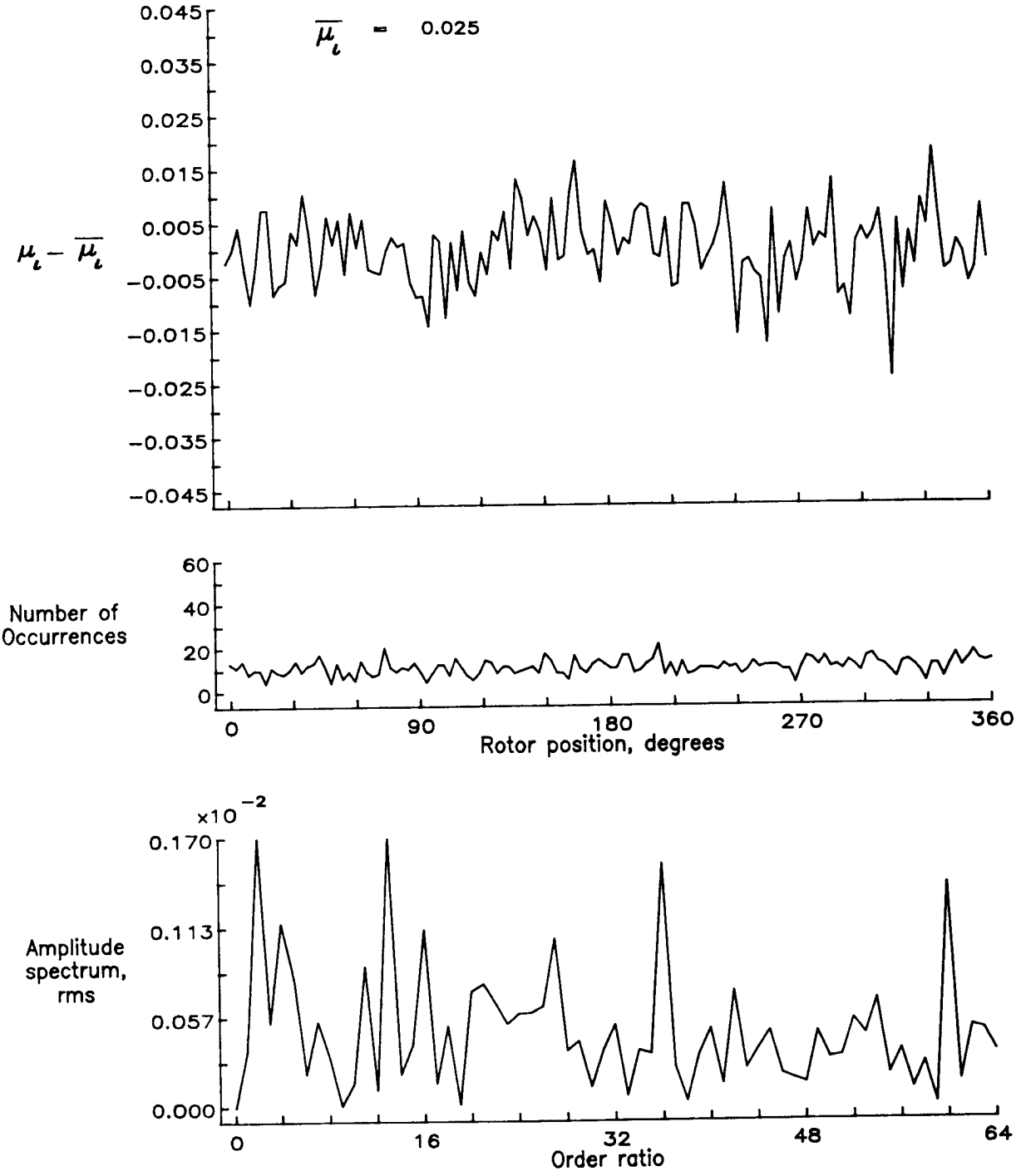


Figure 22.– Induced inflow velocity measured at 30 degrees and r/R of 0.20.

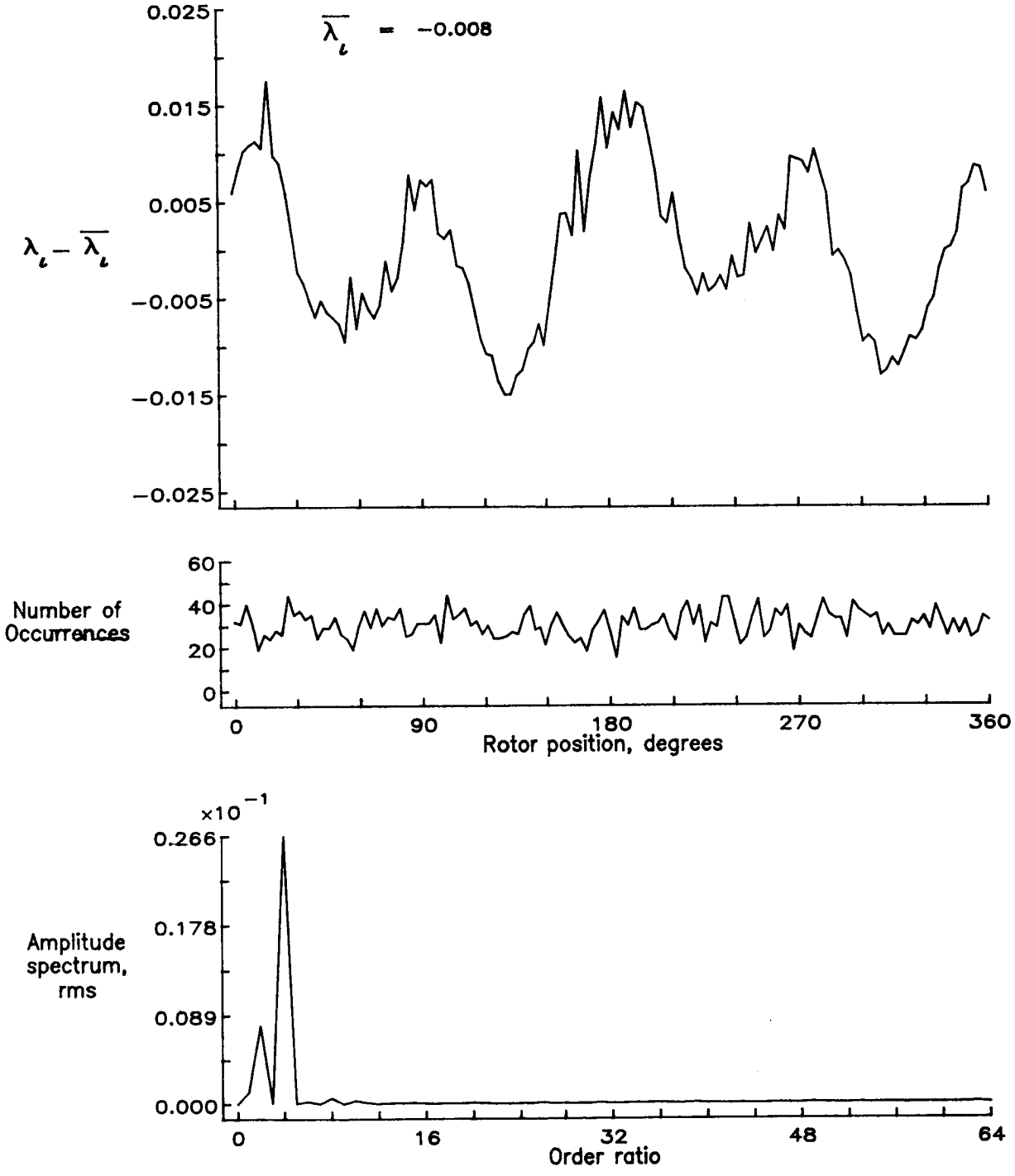


Figure 22.– Concluded.

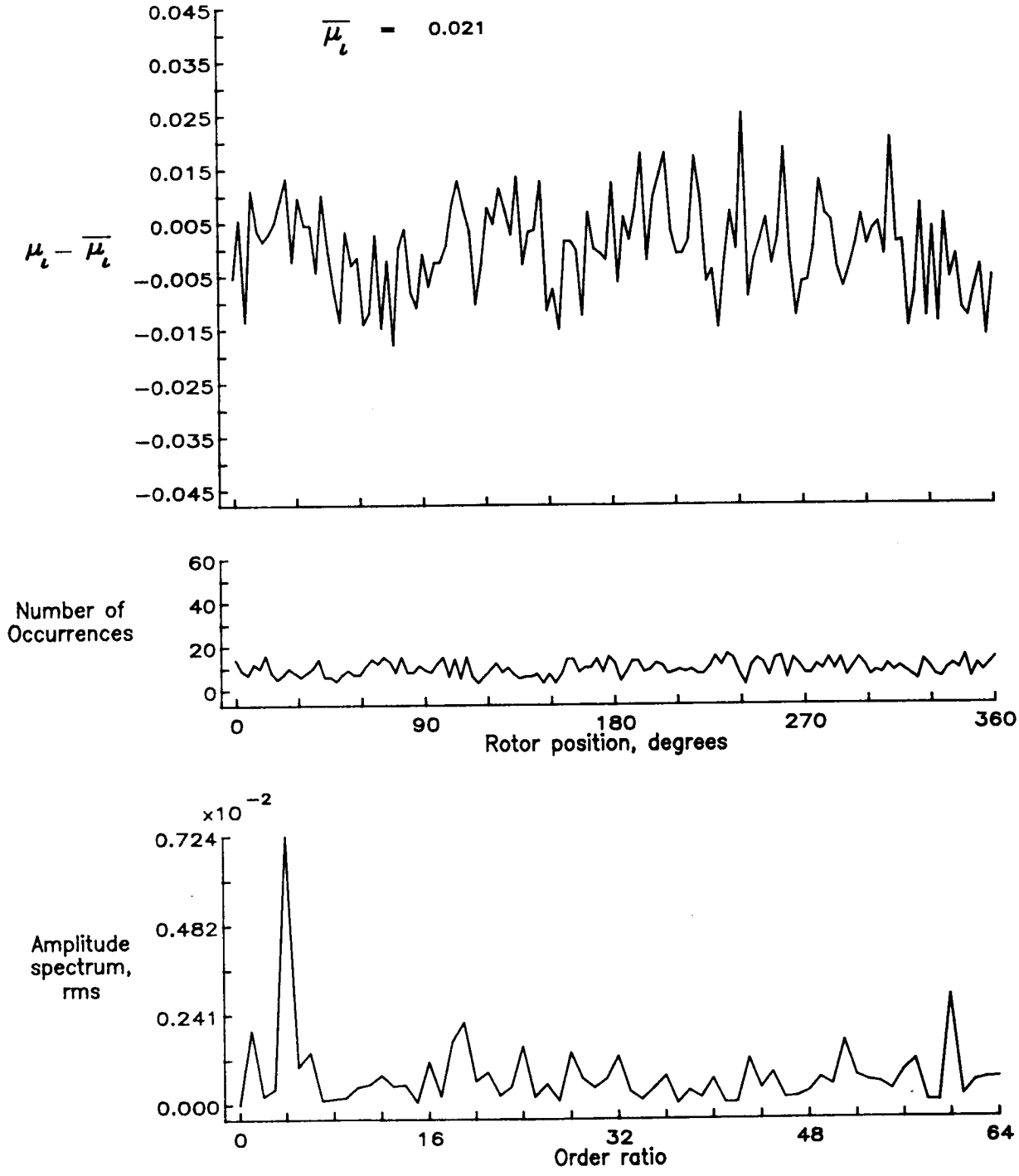


Figure 23.– Induced inflow velocity measured at 30 degrees and r/R of 0.40.

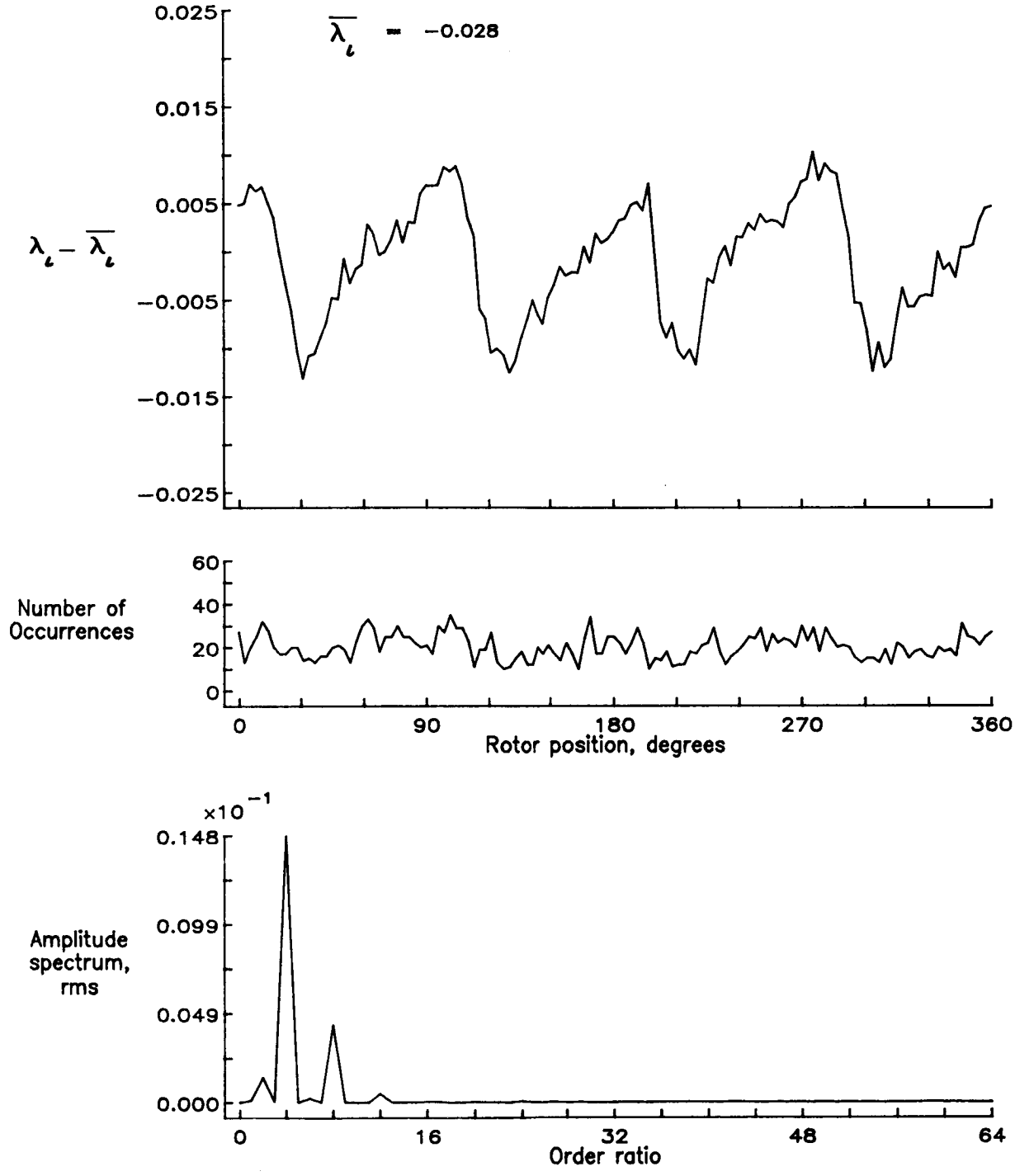


Figure 23.– Concluded.

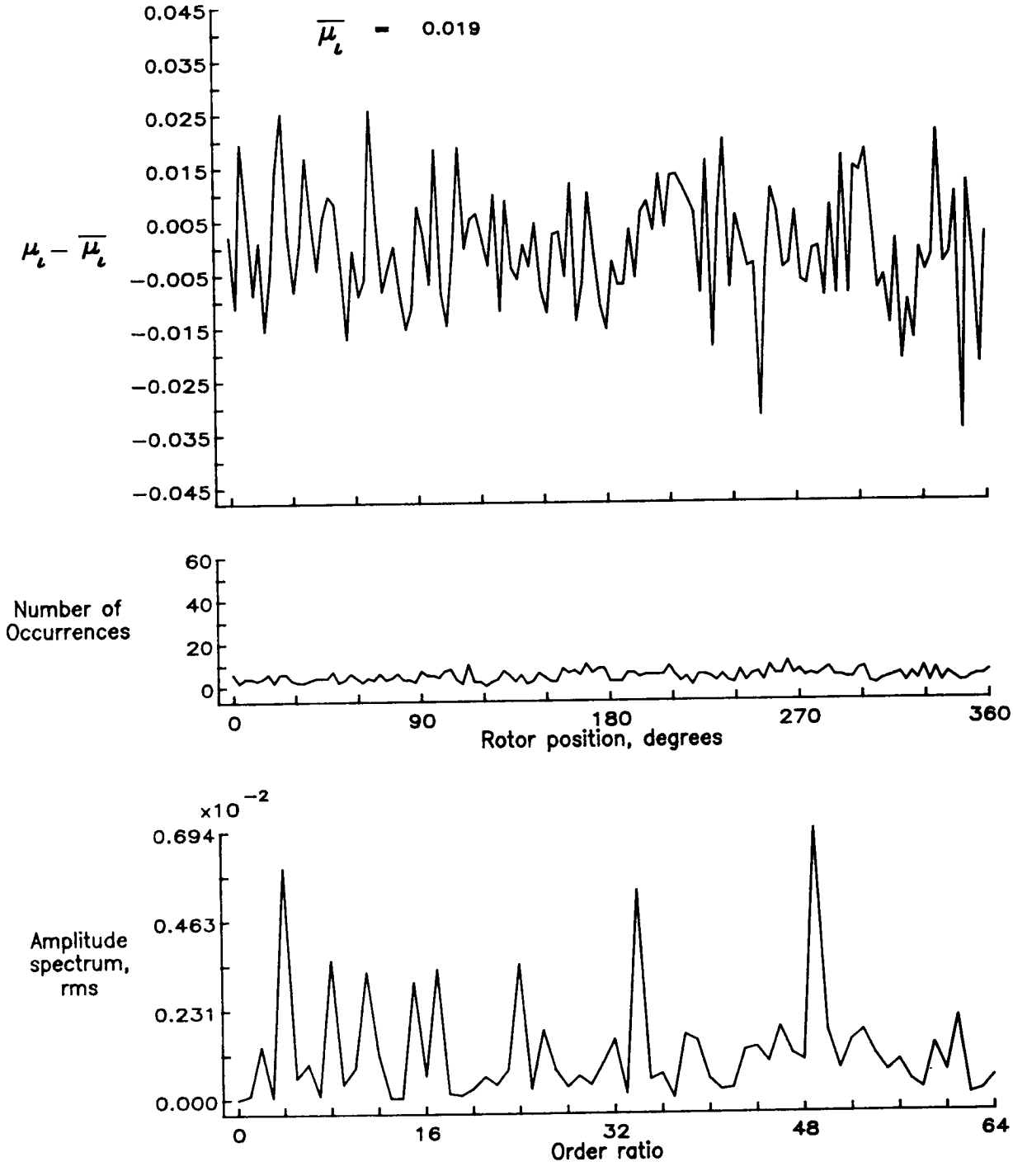


Figure 24.– Induced inflow velocity measured at 30 degrees and r/R of 0.50.

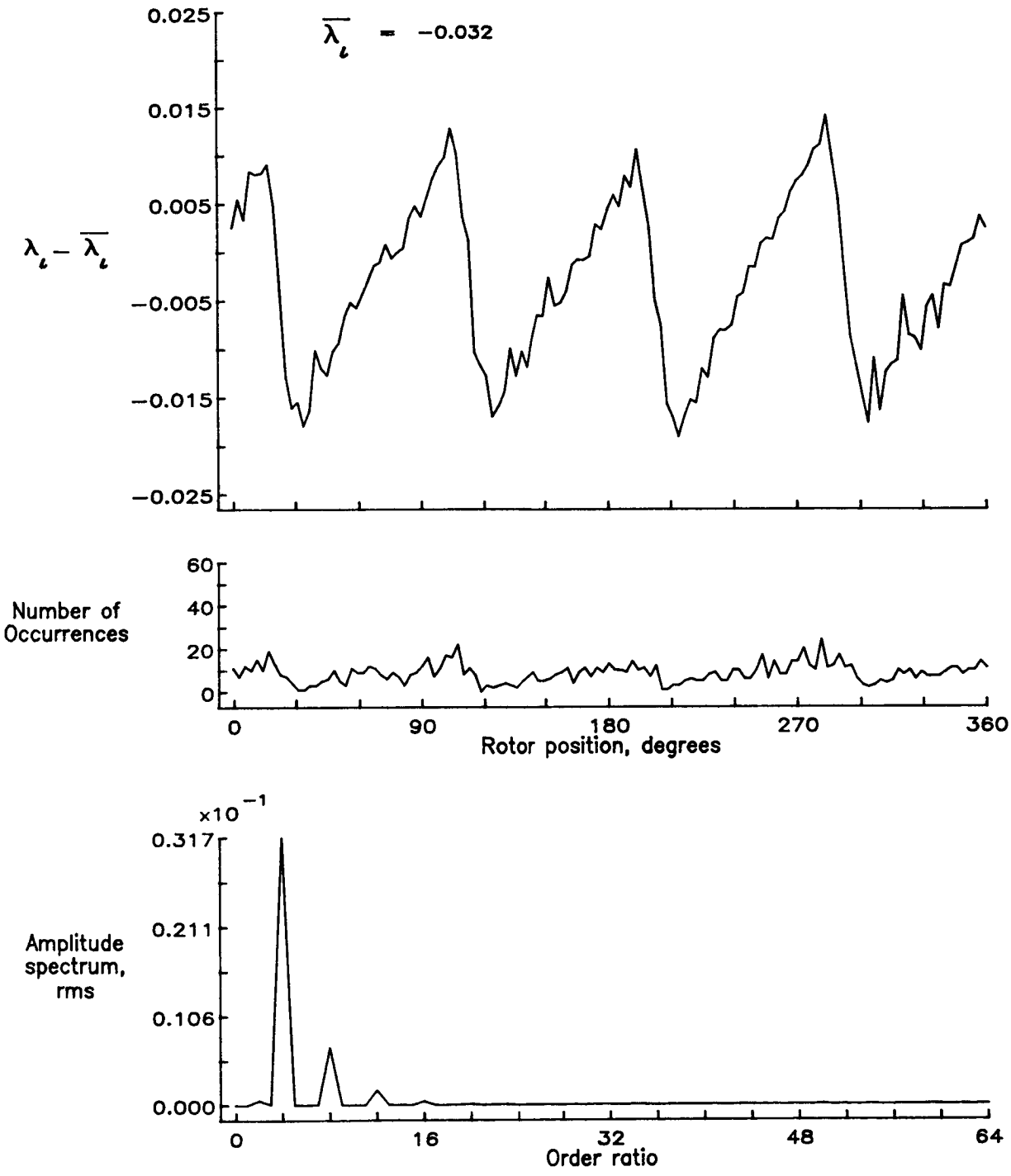


Figure 24.– Concluded.

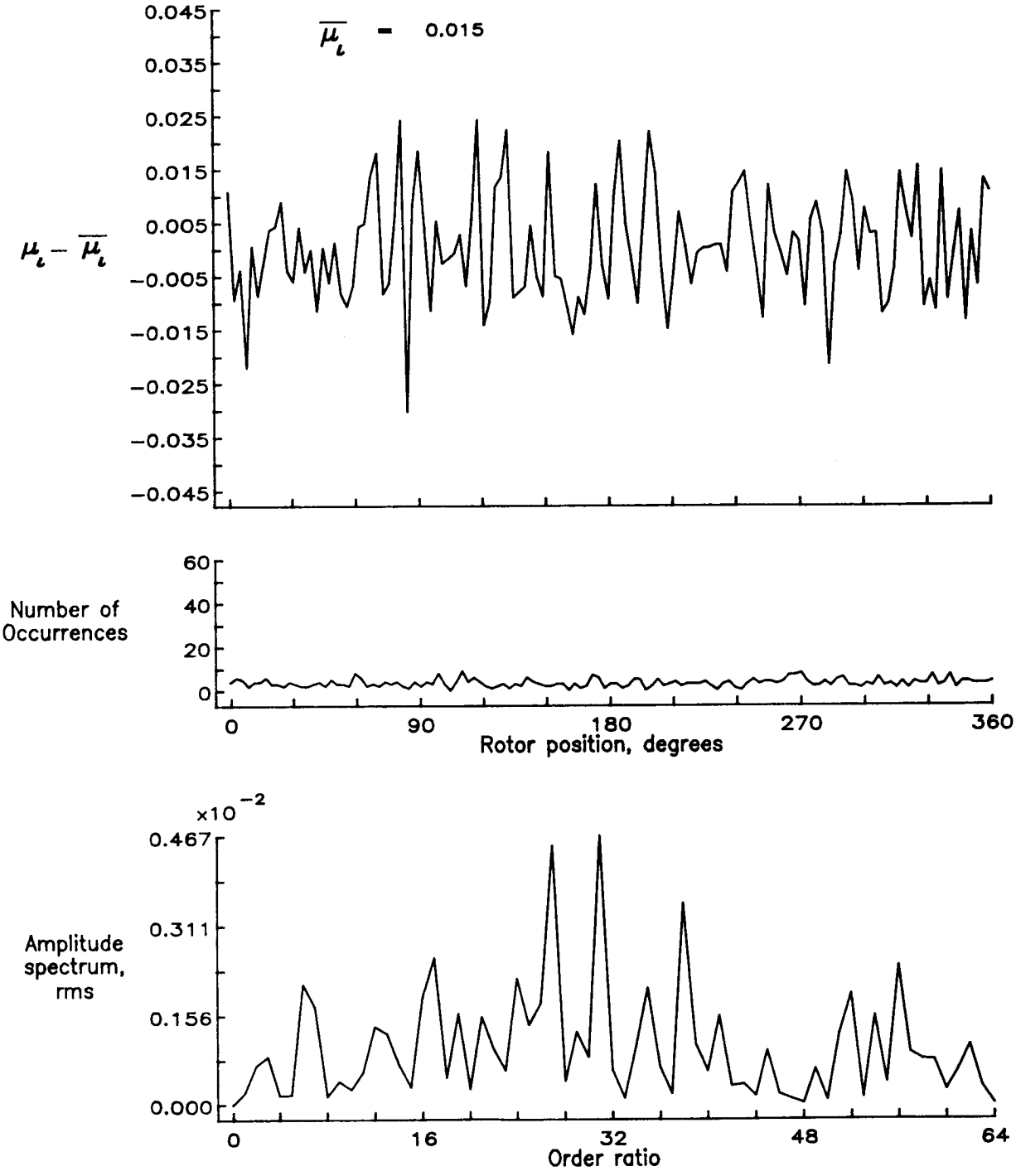


Figure 25.– Induced inflow velocity measured at 30 degrees and r/R of 0.60.

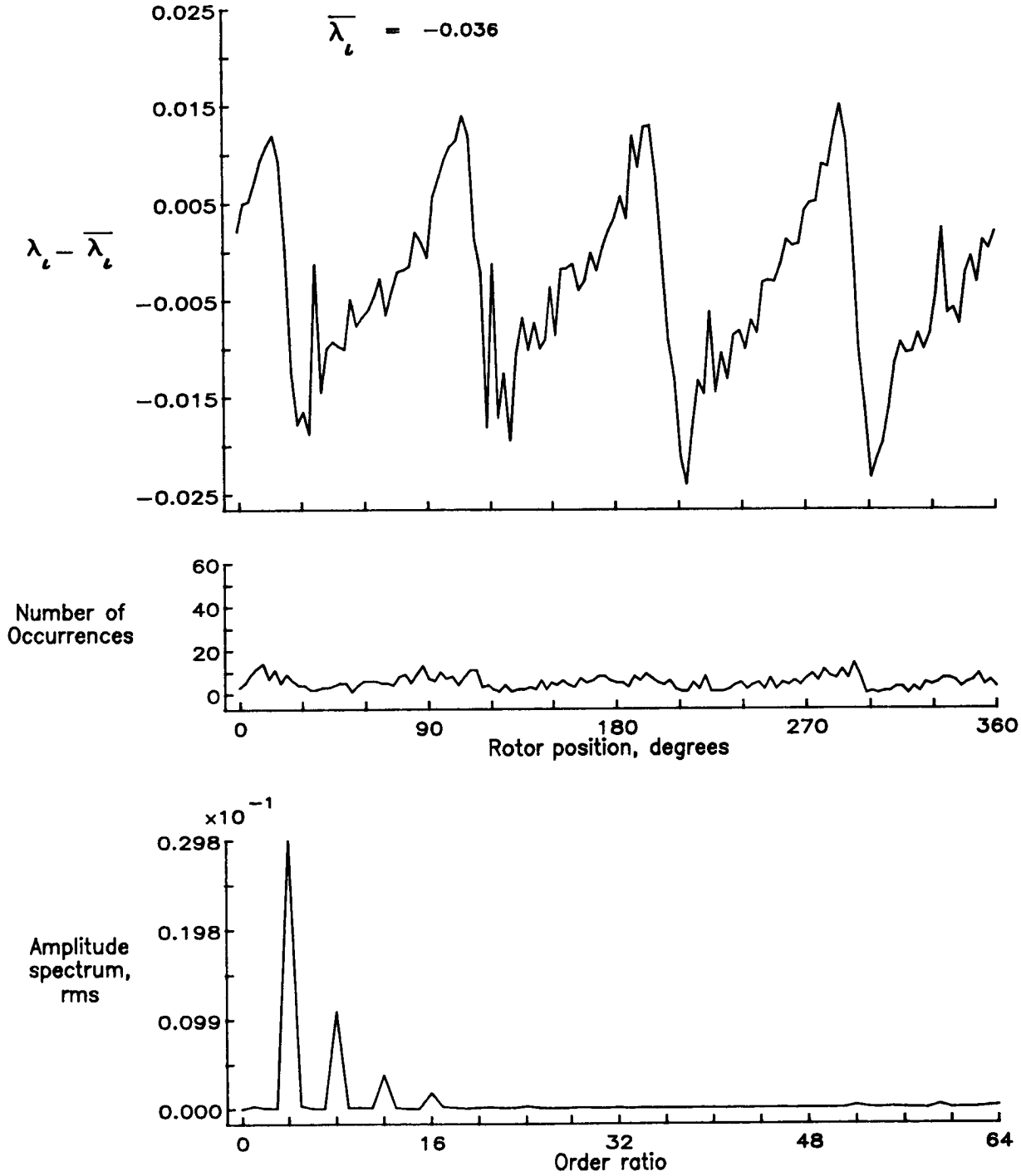


Figure 25.– Concluded.

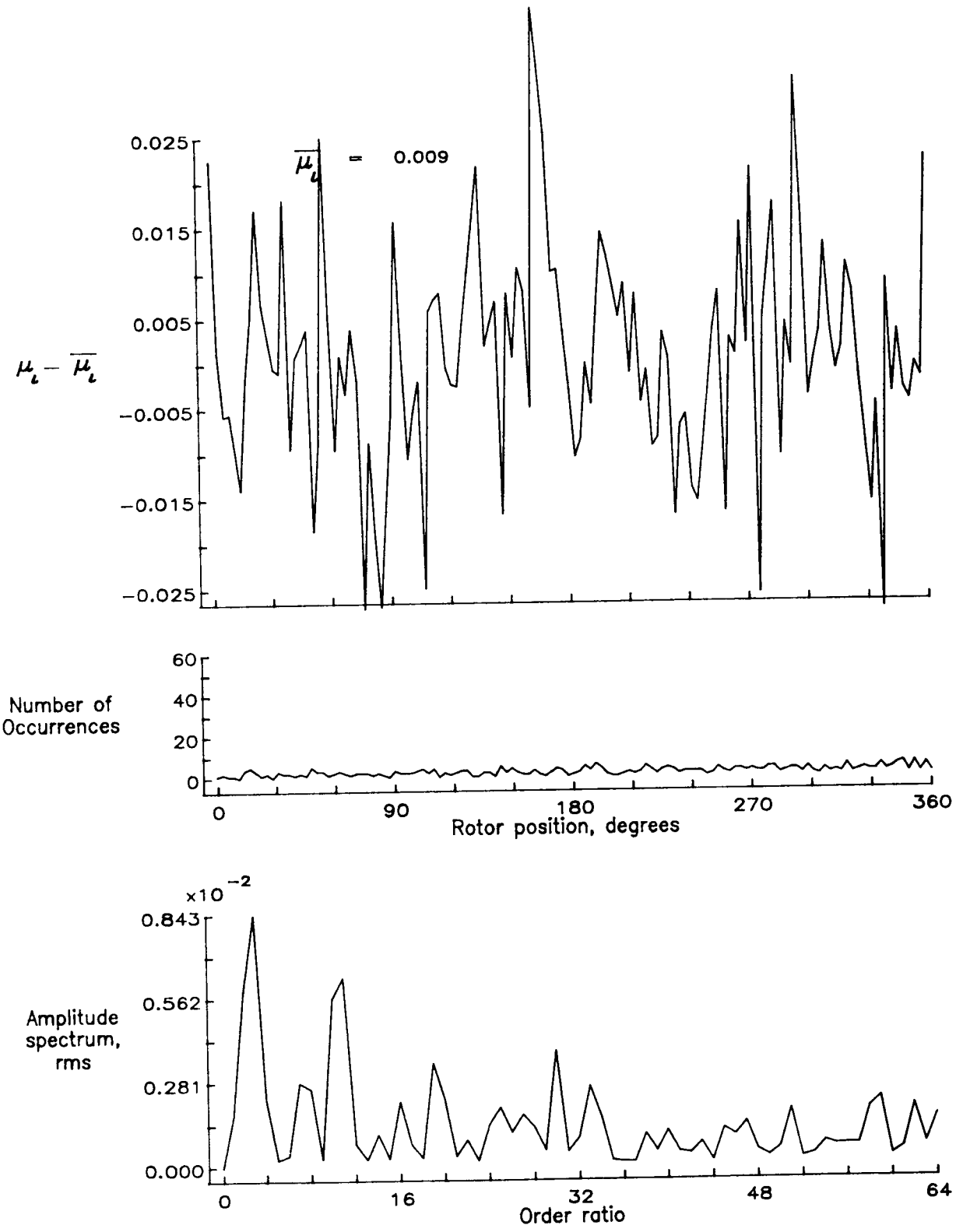


Figure 26.– Induced inflow velocity measured at 30 degrees and r/R of 0.70.

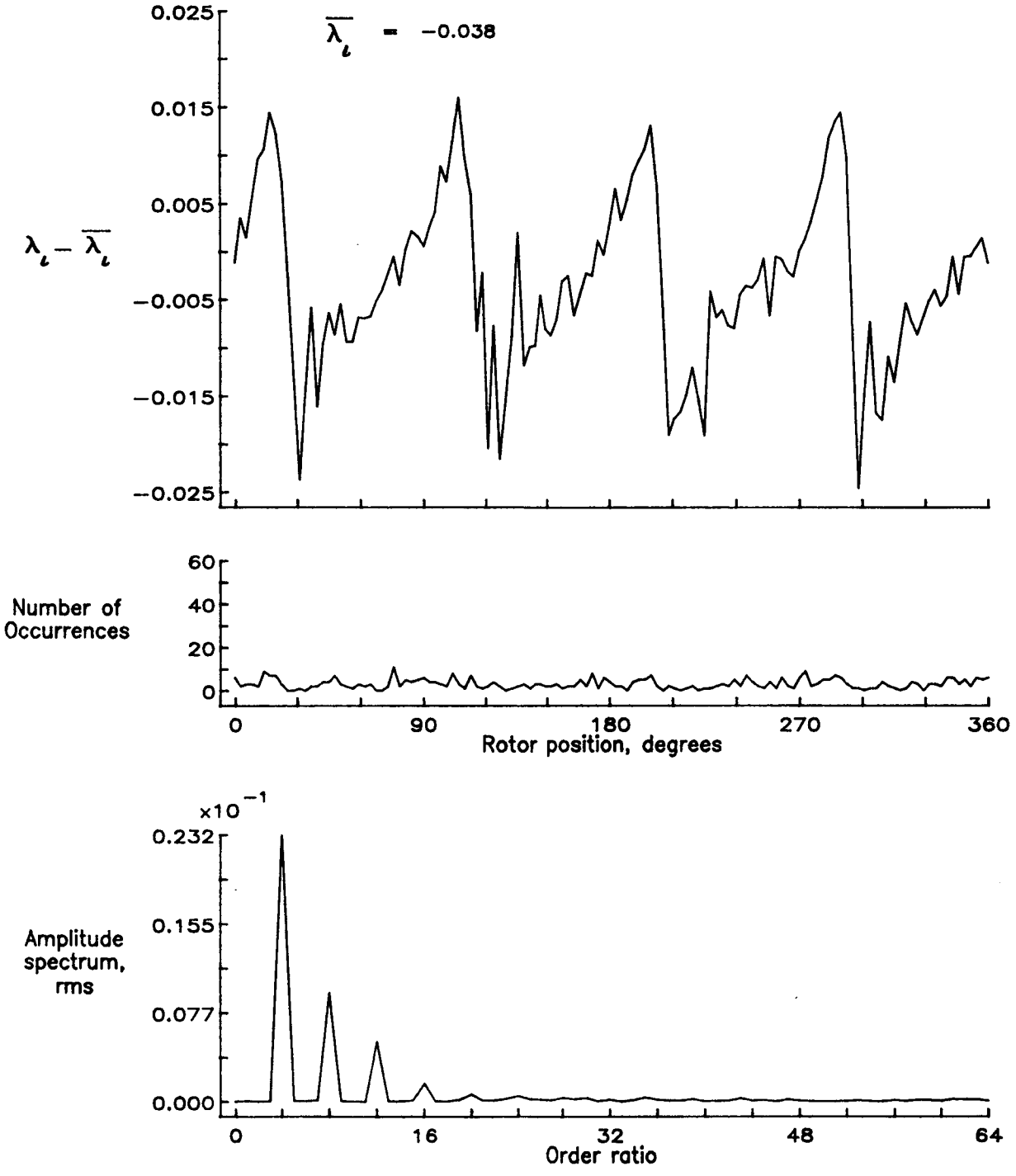


Figure 26.– Concluded.

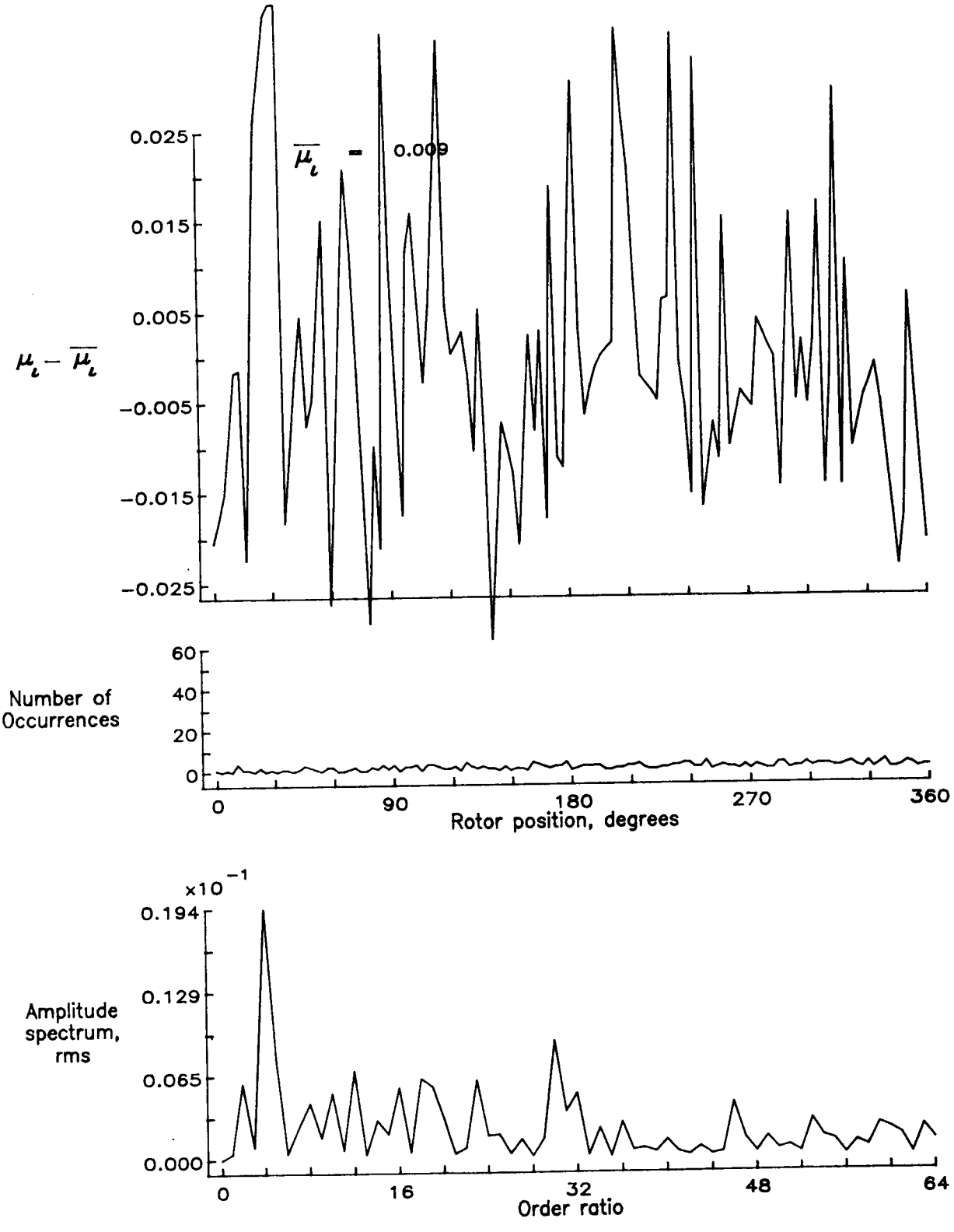


Figure 27.– Induced inflow velocity measured at 30 degrees and r/R of 0.74.

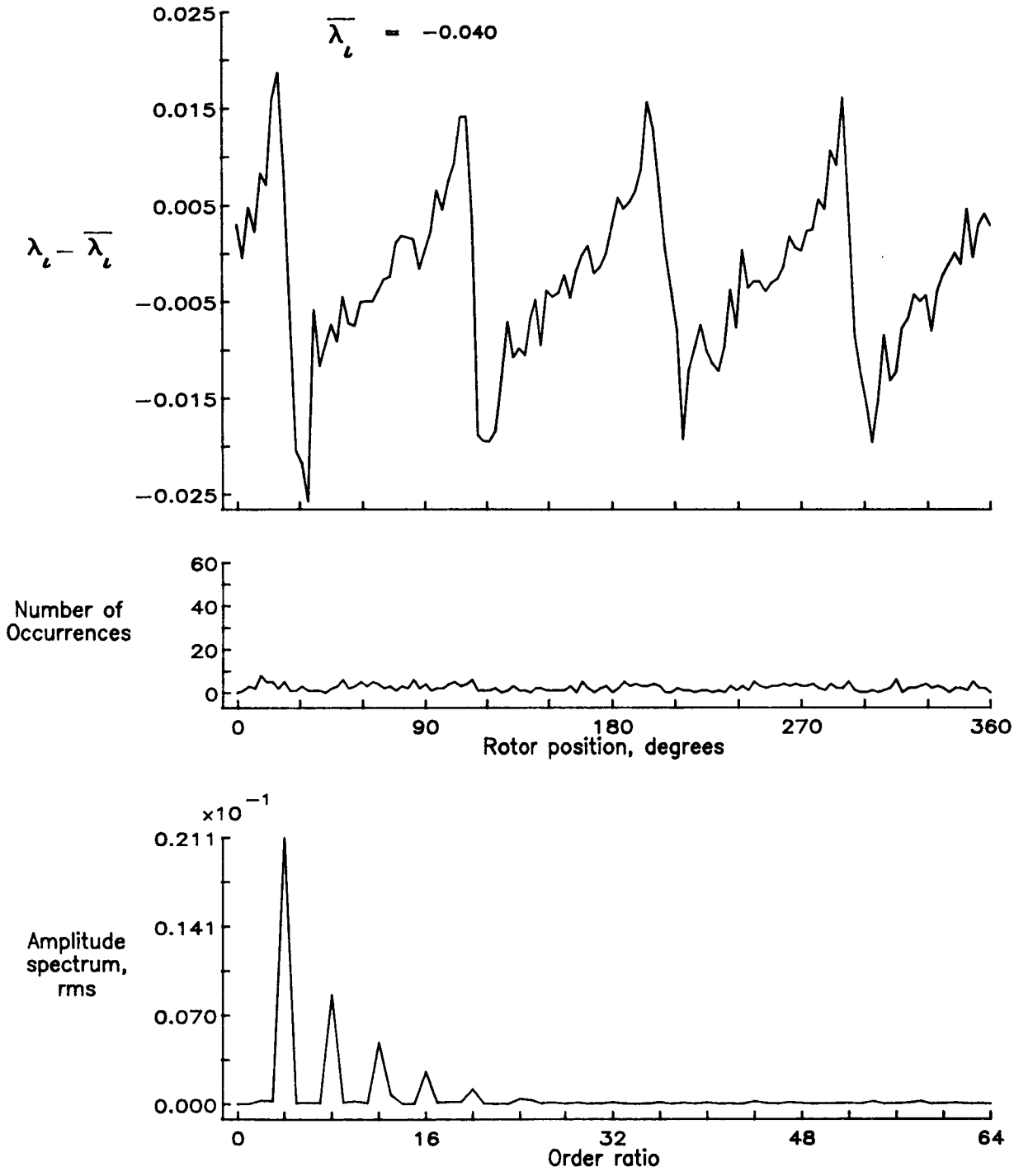


Figure 27.– Concluded.

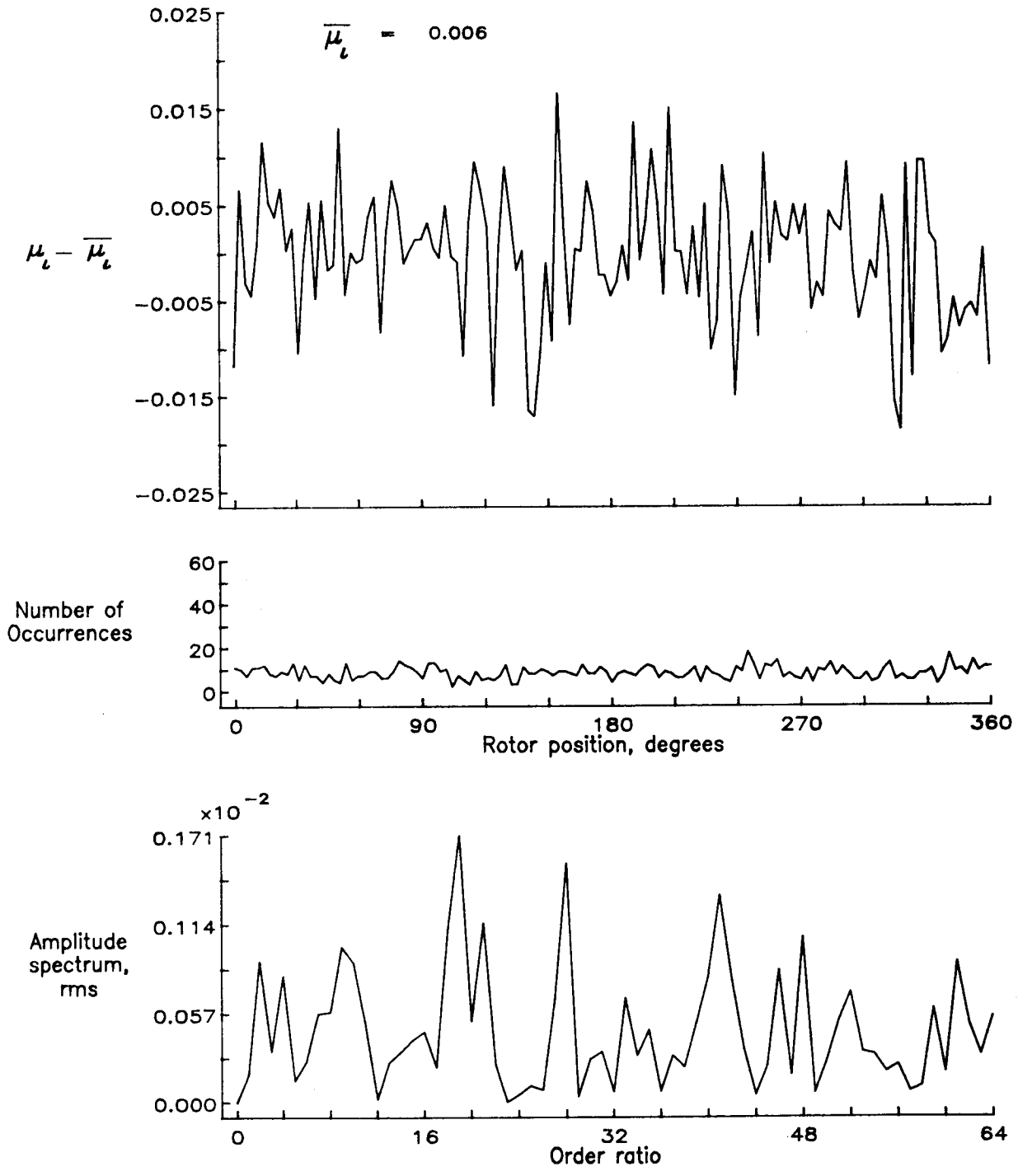


Figure 28.– Induced inflow velocity measured at 30 degrees and r/R of 0.78.

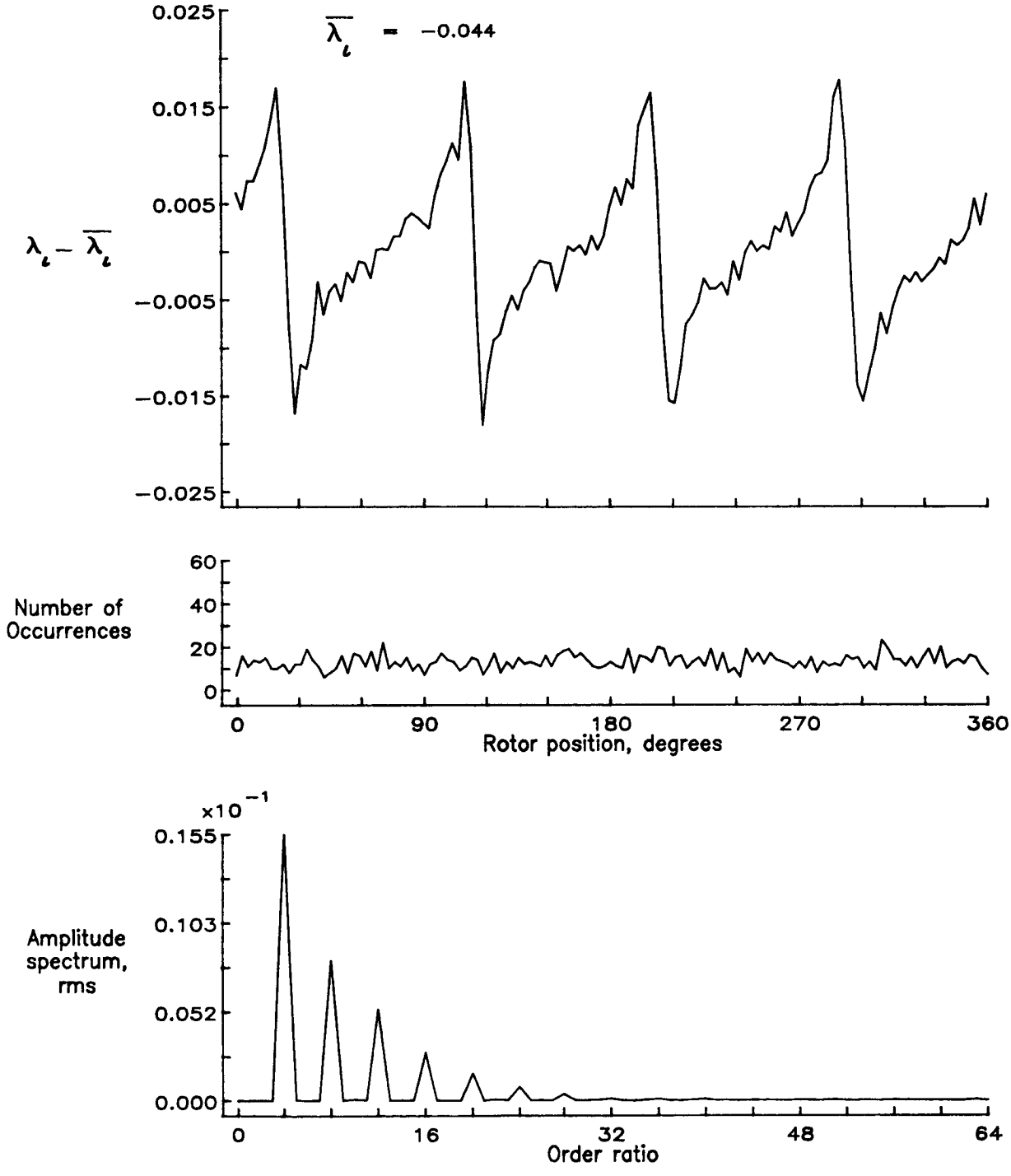


Figure 28.– Concluded.

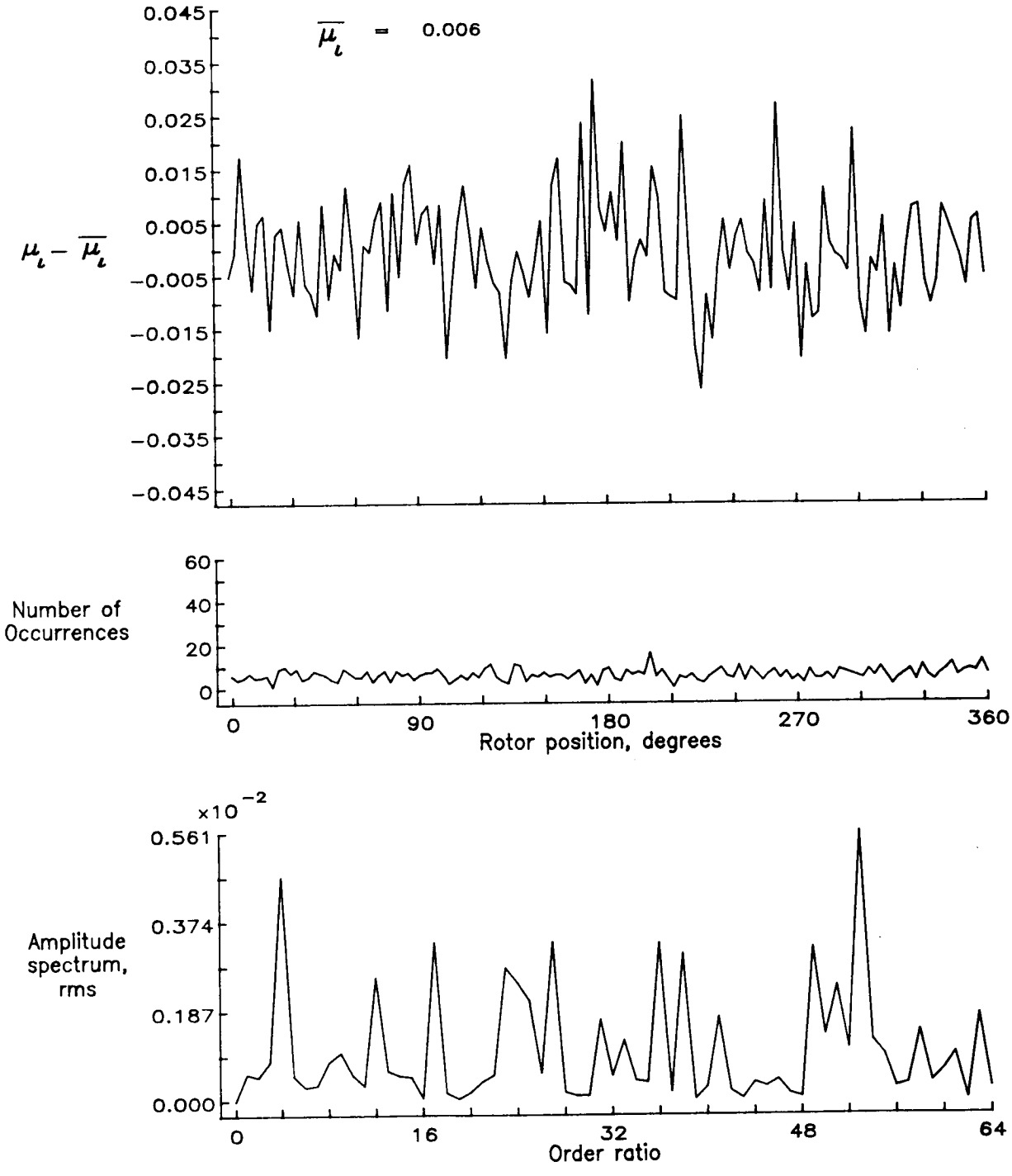


Figure 29.– Induced inflow velocity measured at 30 degrees and r/R of 0.82.

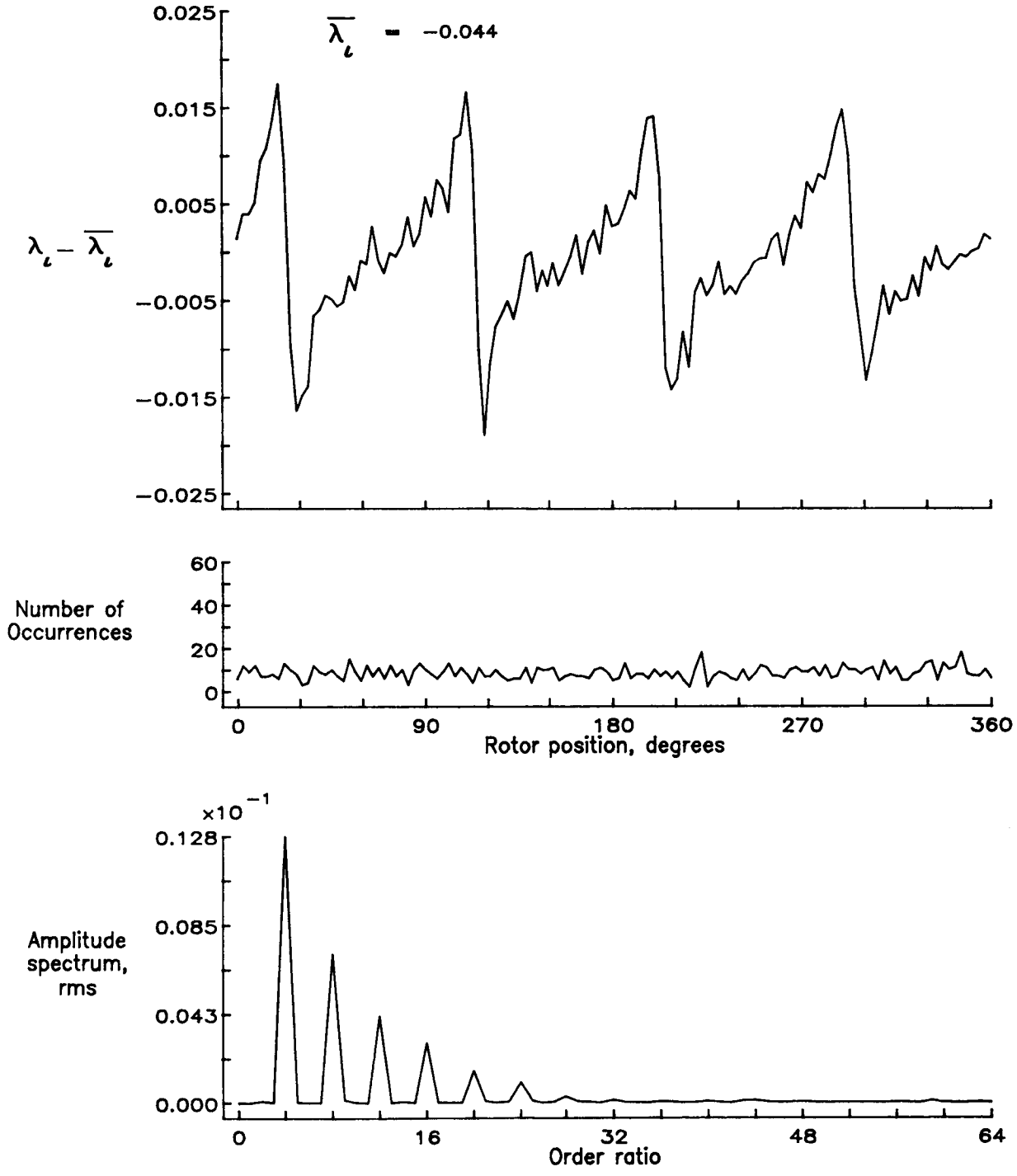


Figure 29.– Concluded.

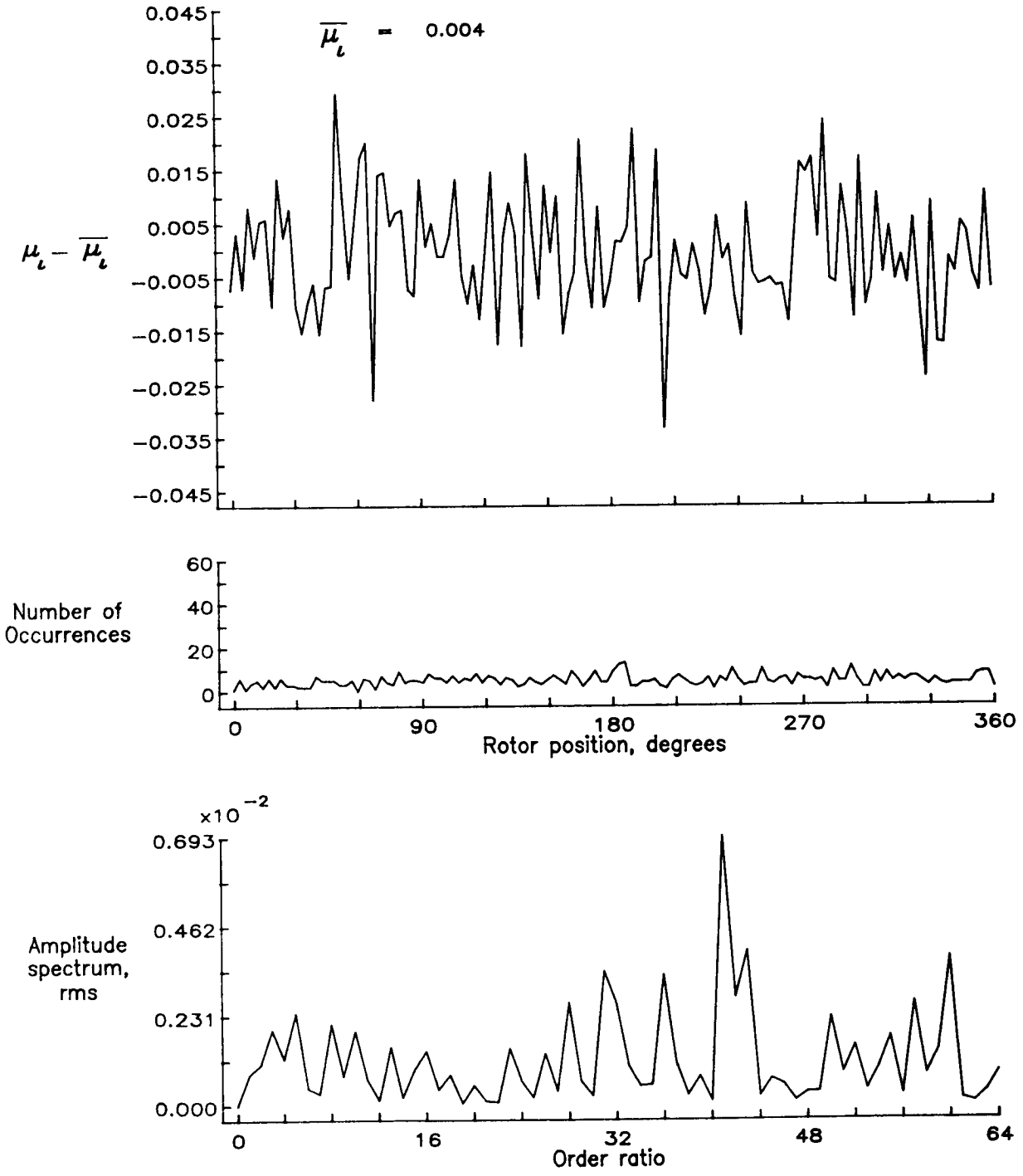


Figure 30.– Induced inflow velocity measured at 30 degrees and r/R of 0.86.

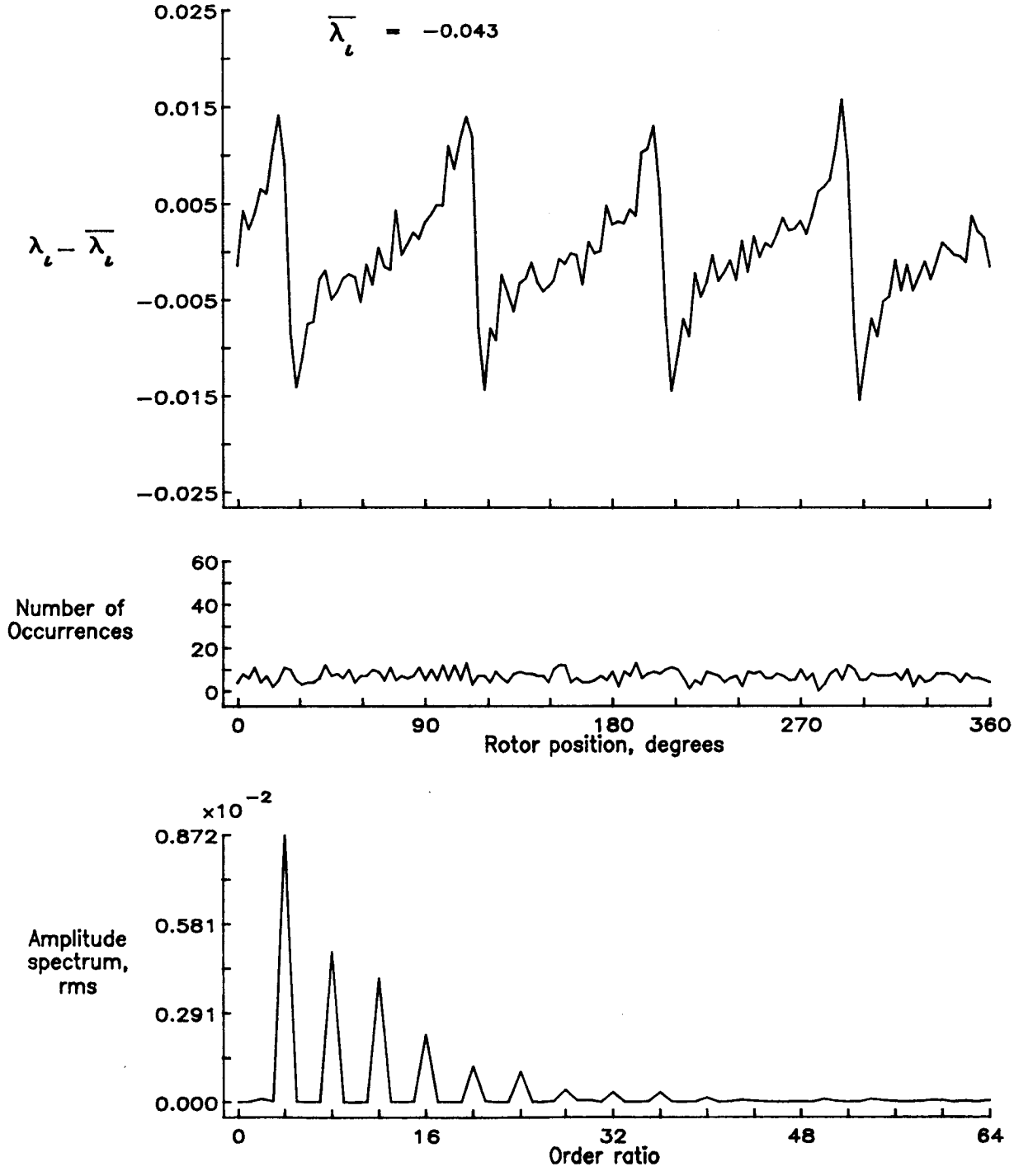


Figure 30.– Concluded.

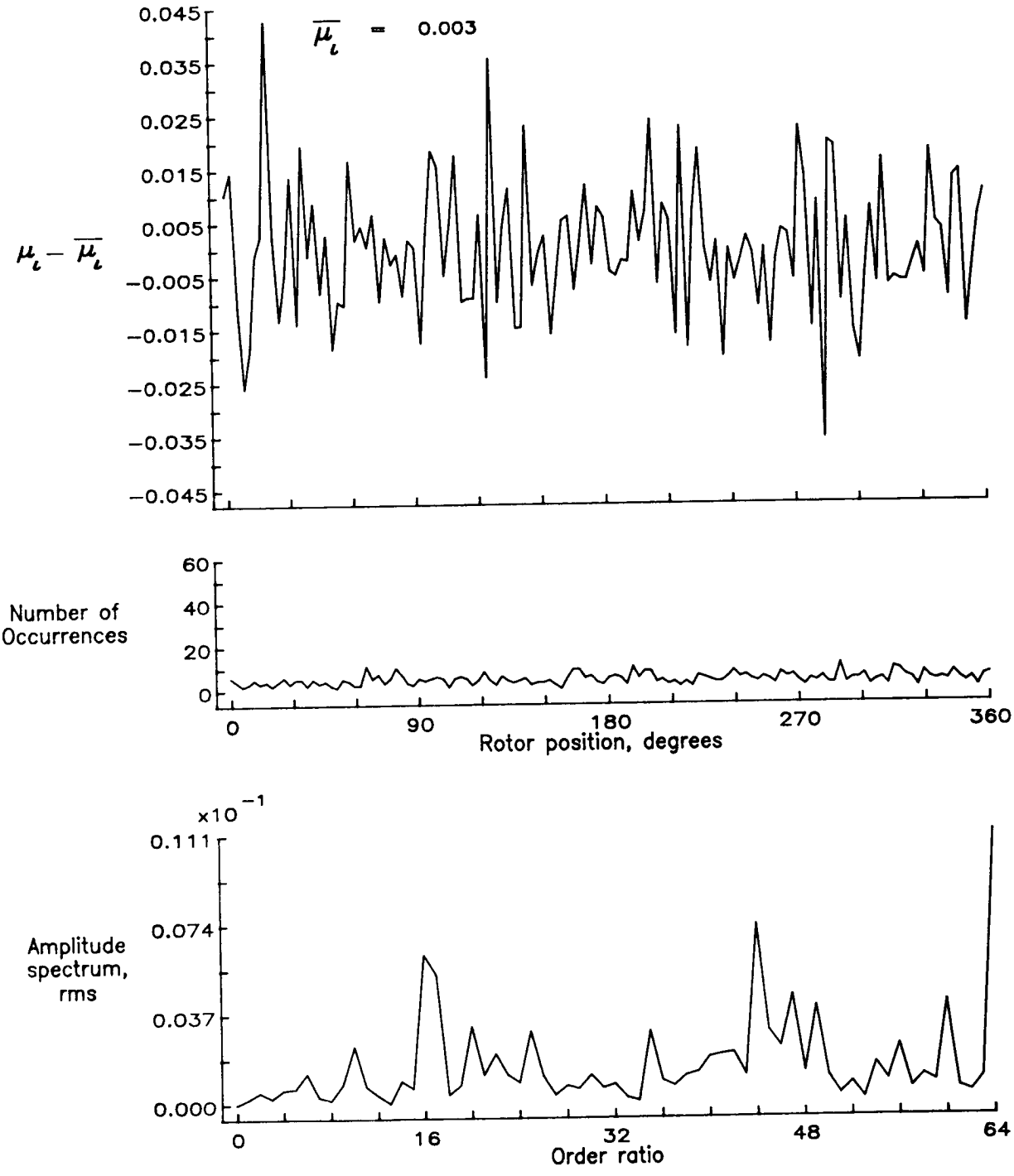


Figure 31.– Induced inflow velocity measured at 30 degrees and r/R of 0.90.

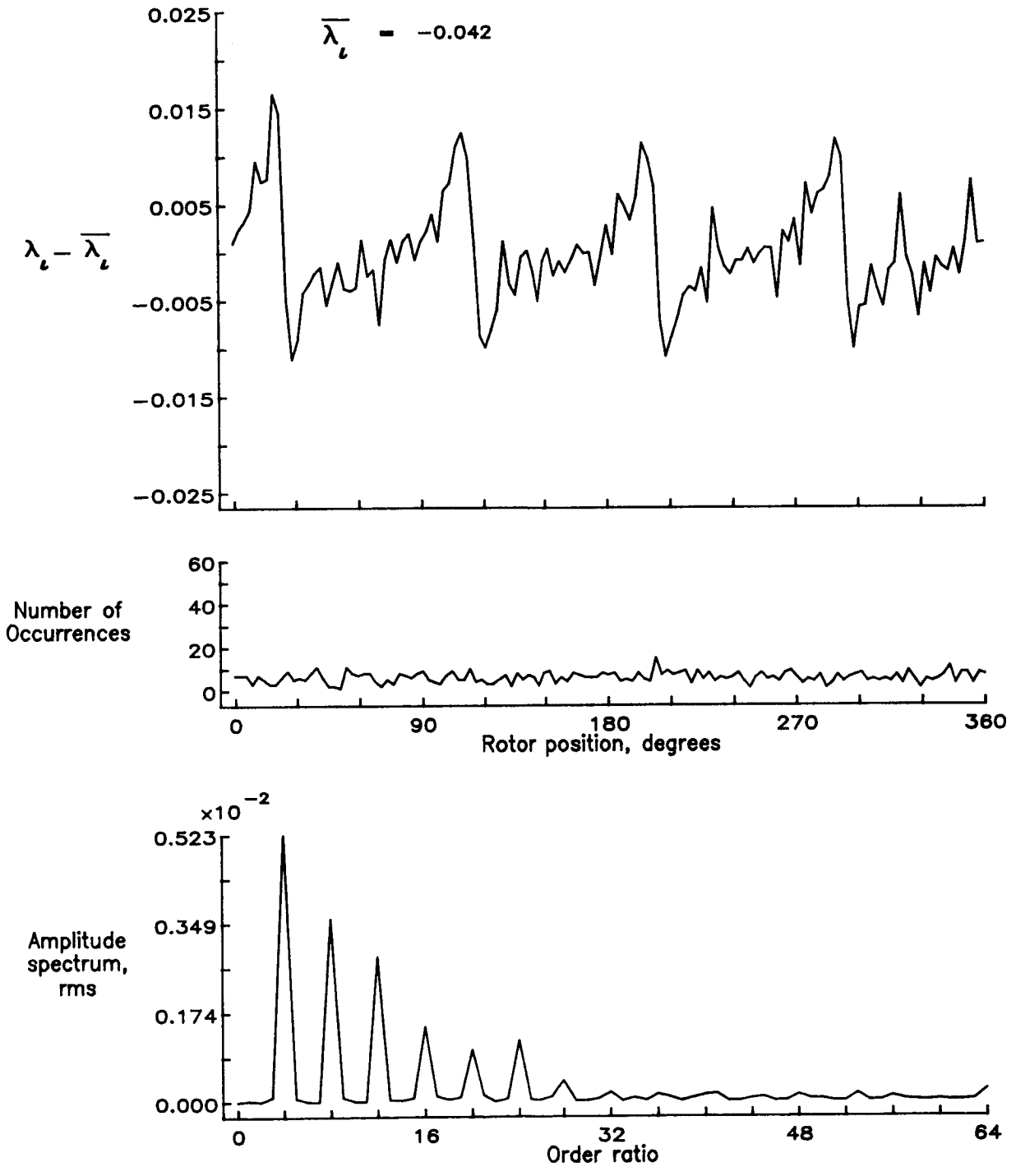


Figure 31.– Concluded.

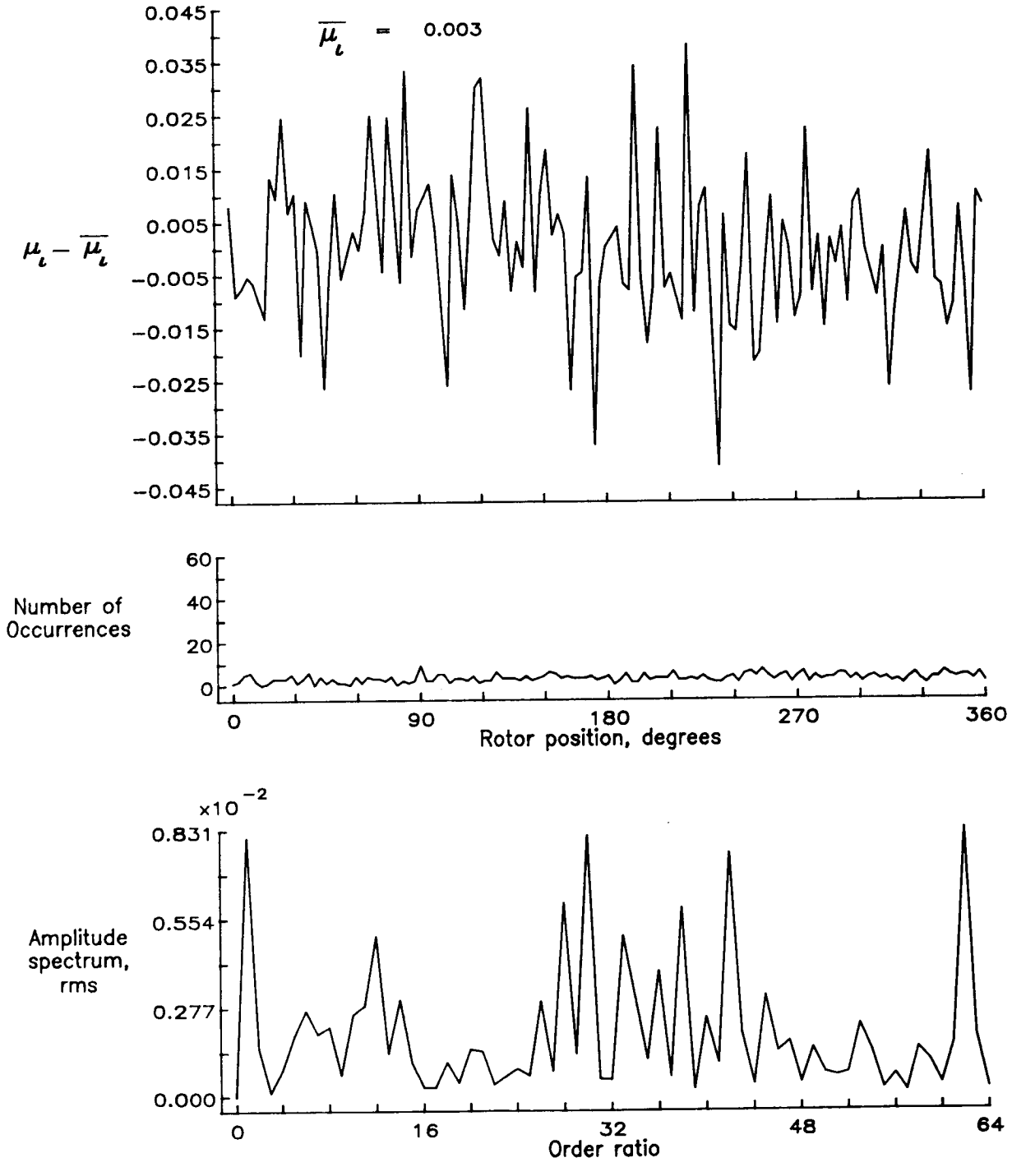


Figure 32.– Induced inflow velocity measured at 30 degrees and r/R of 0.94.

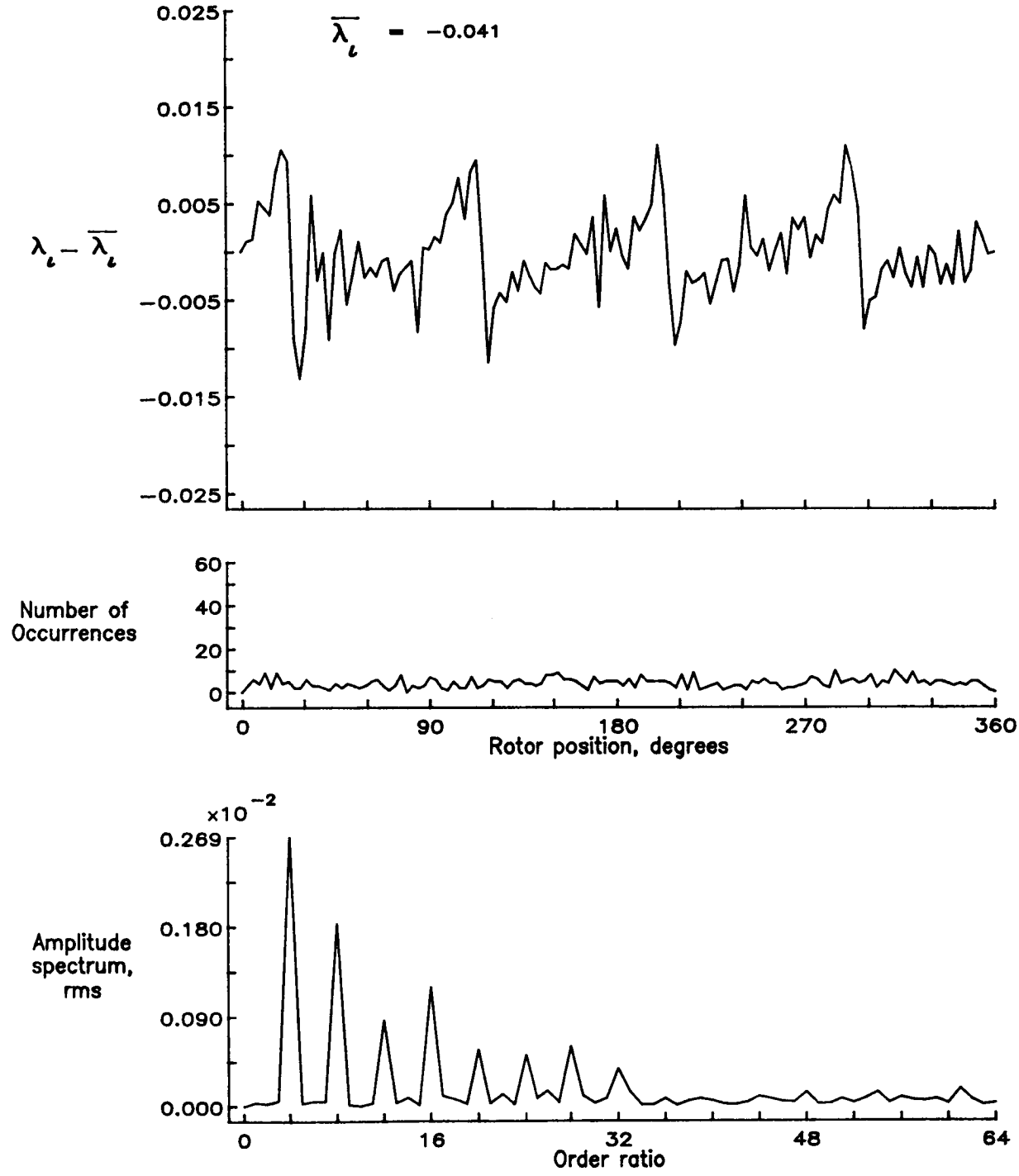


Figure 32.– Concluded.

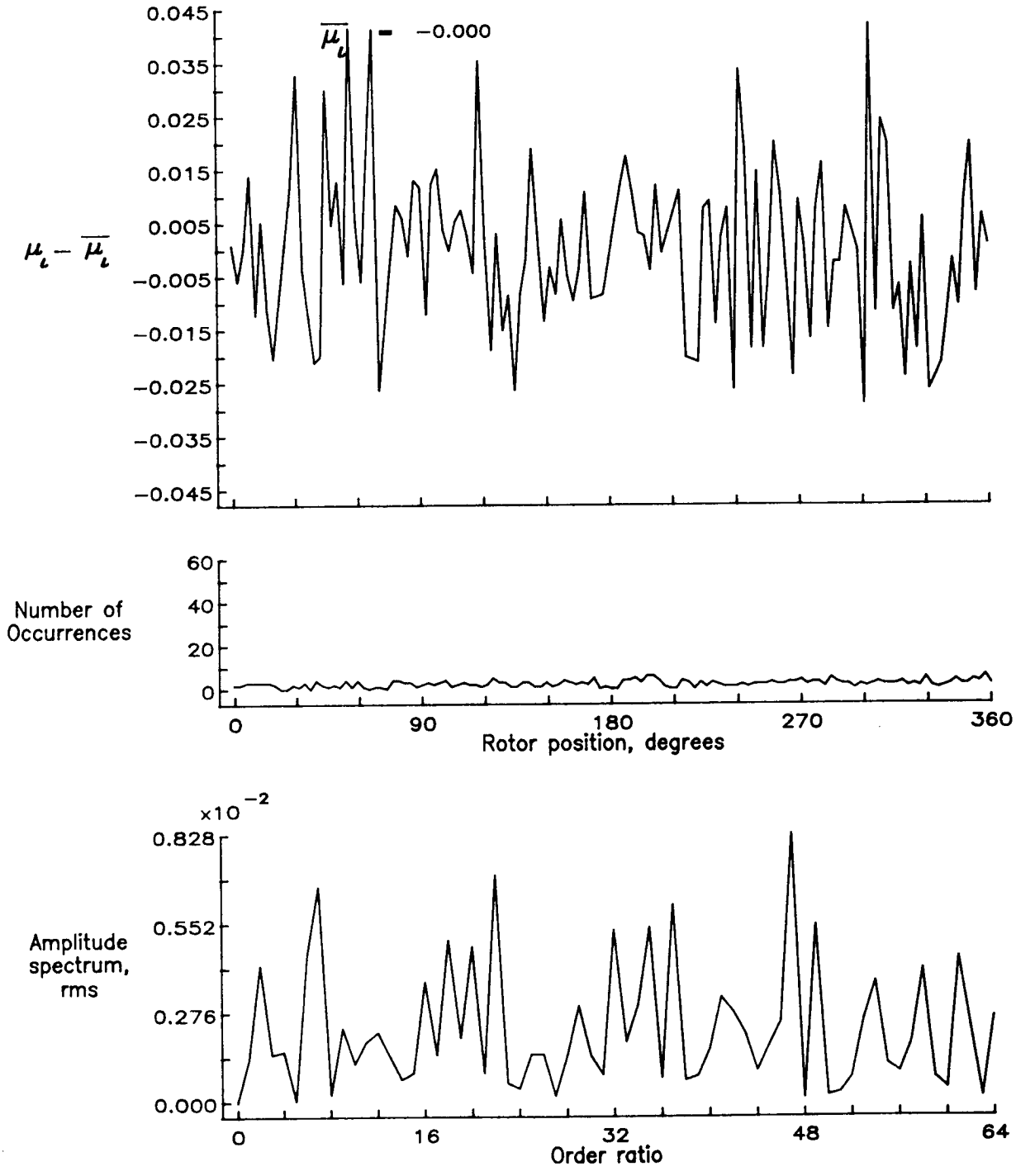


Figure 33.– Induced inflow velocity measured at 30 degrees and r/R of 0.98.

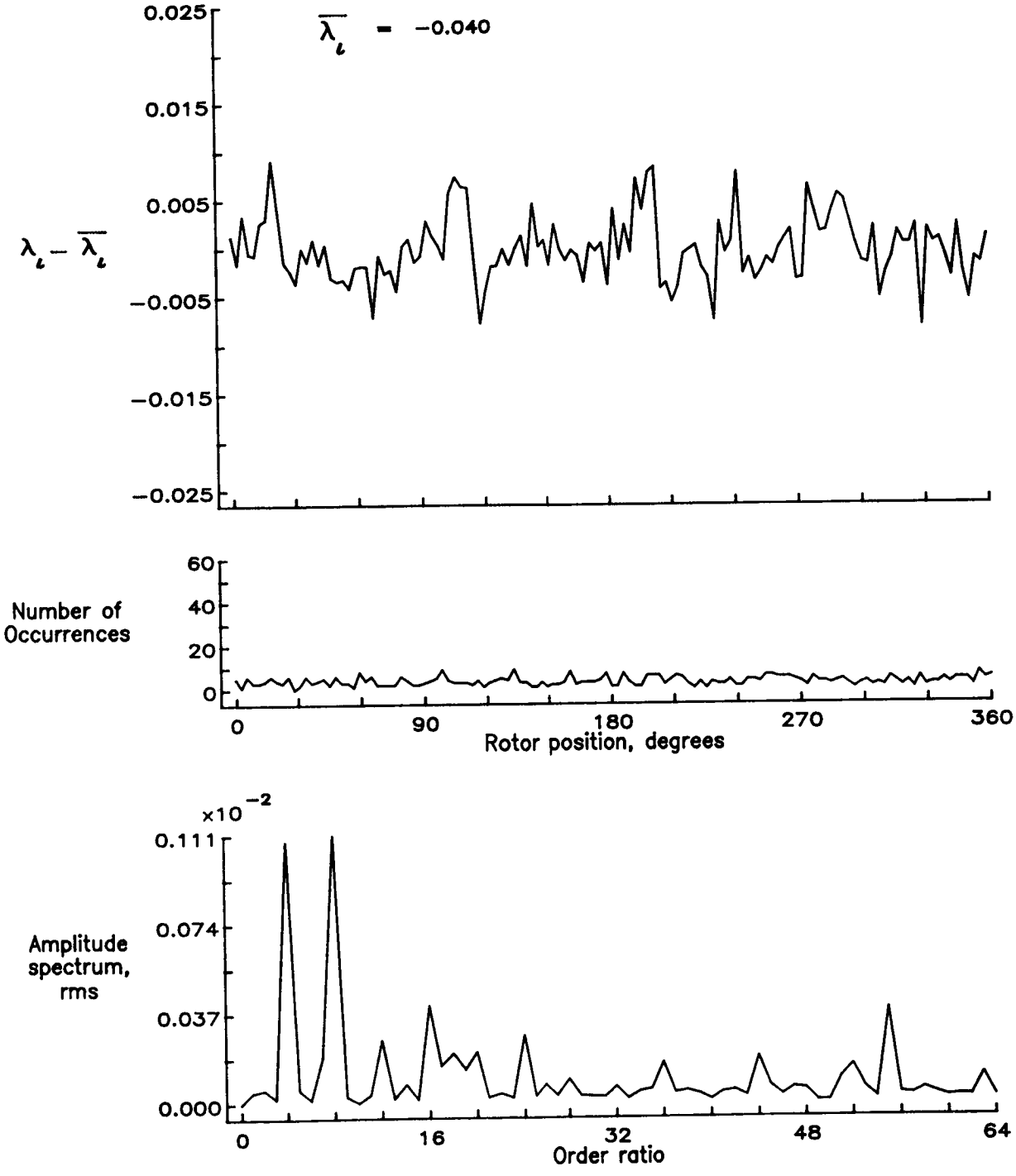


Figure 33.– Concluded.

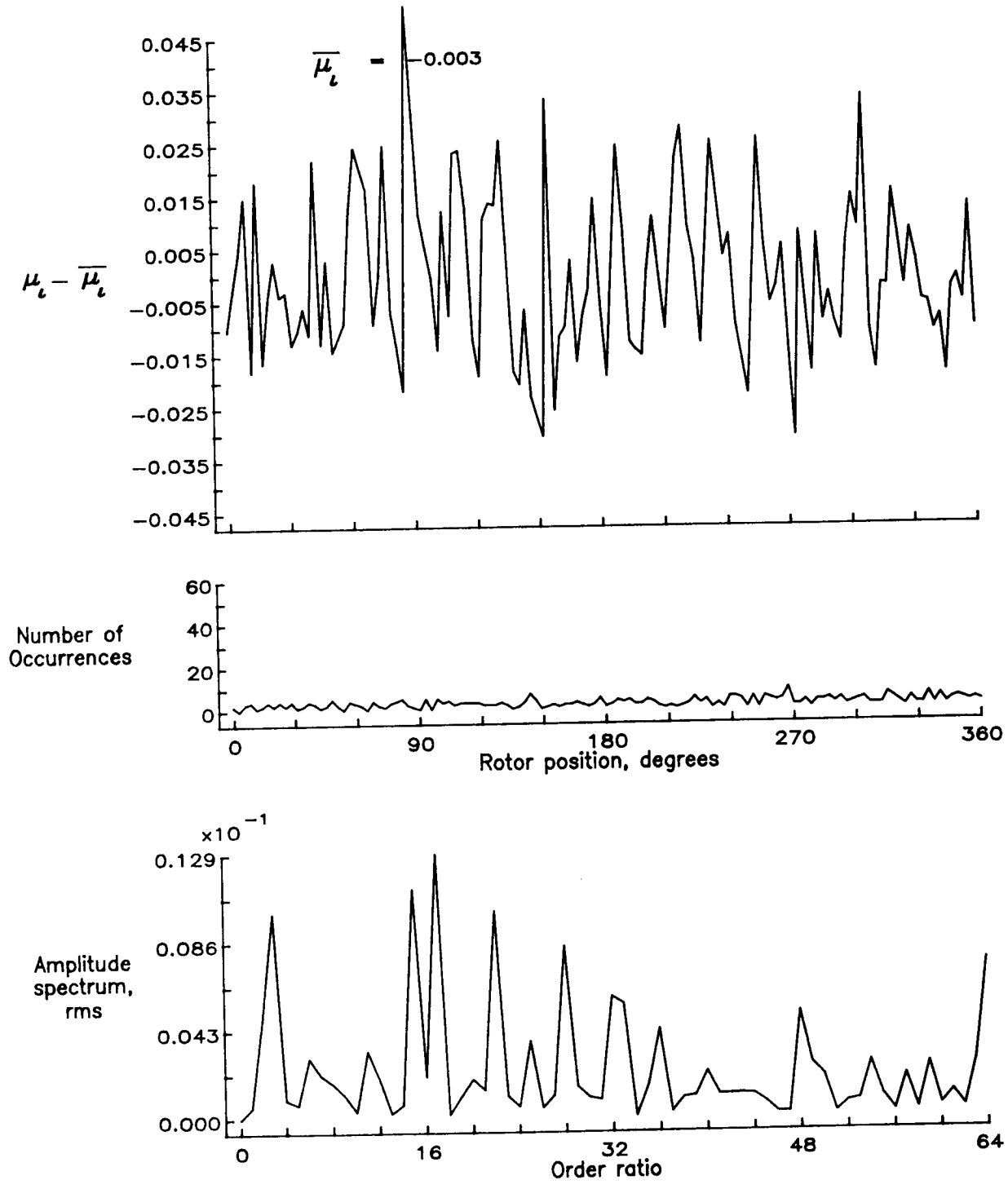


Figure 34.– Induced inflow velocity measured at 30 degrees and r/R of 1.02.

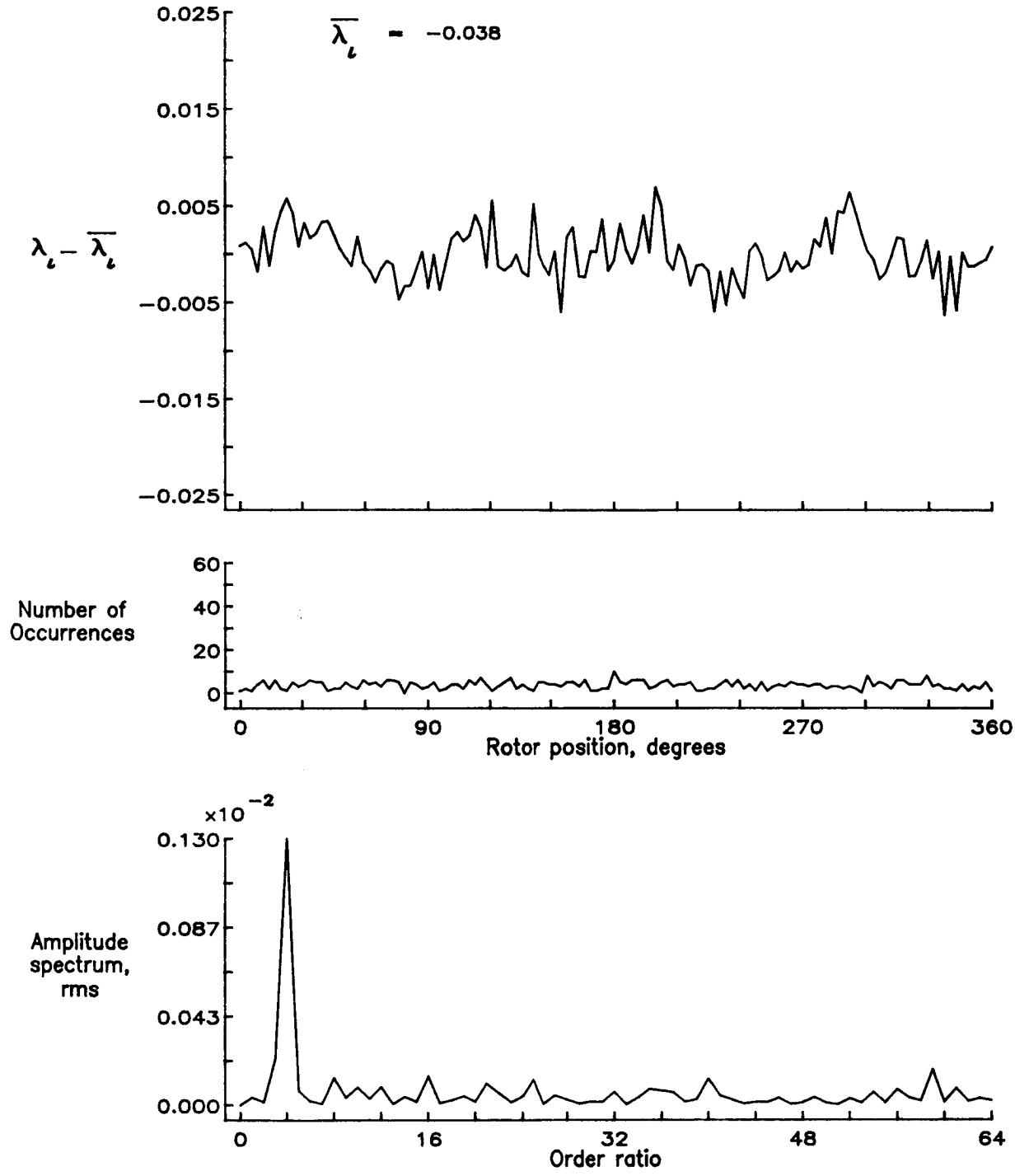


Figure 34.– Concluded.

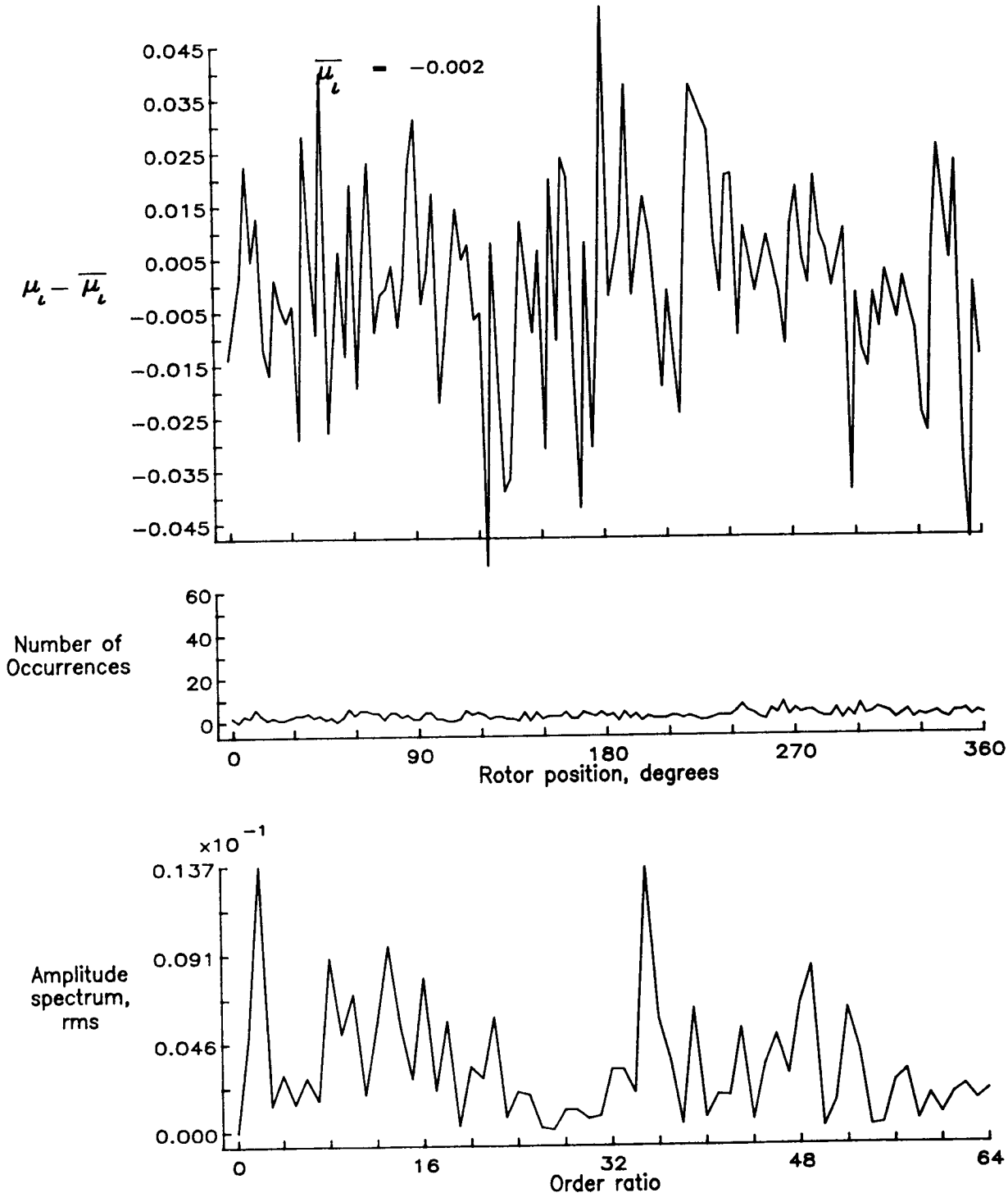


Figure 35.– Induced inflow velocity measured at 30 degrees and r/R of 1.04.

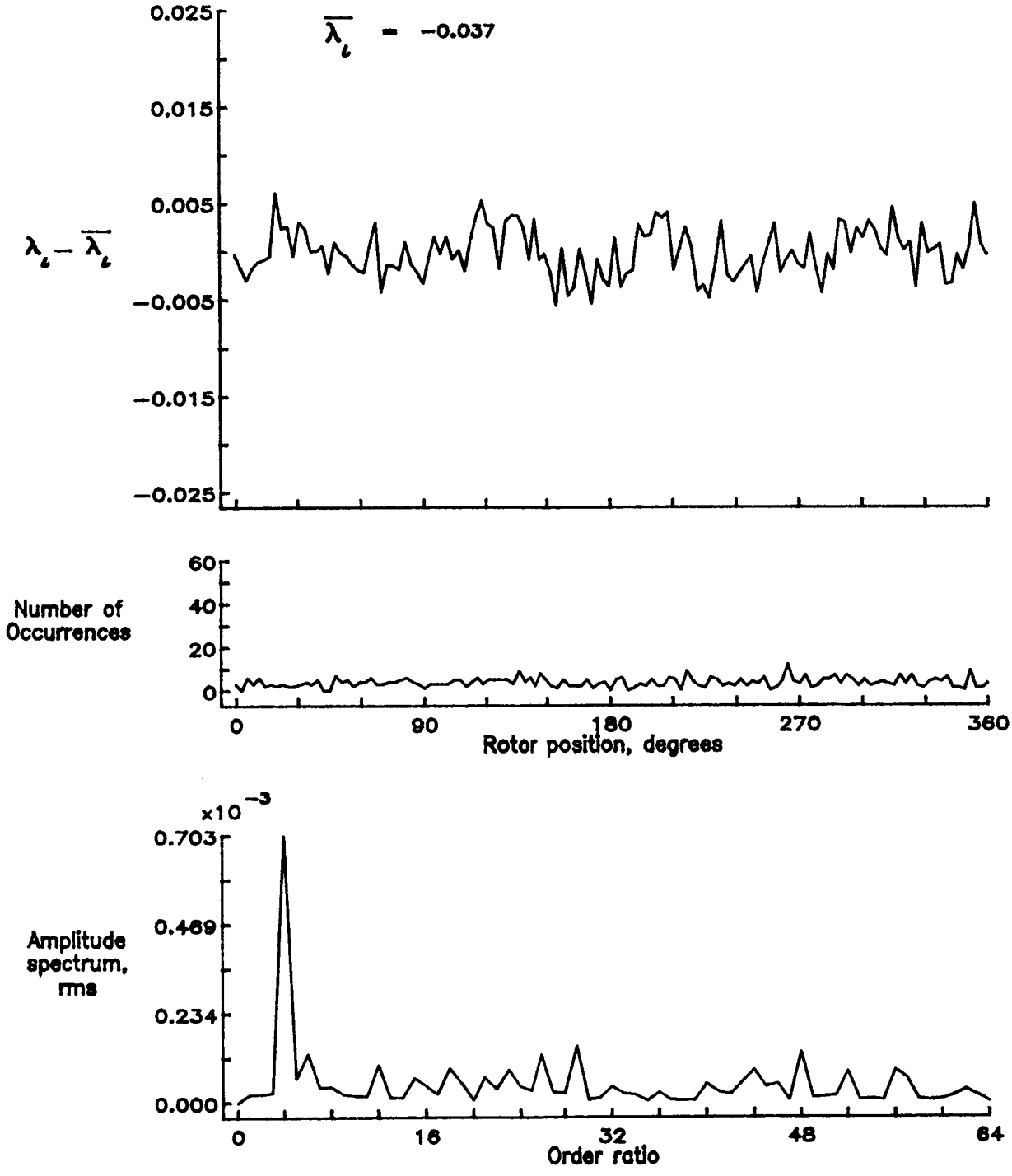


Figure 35.– Concluded.

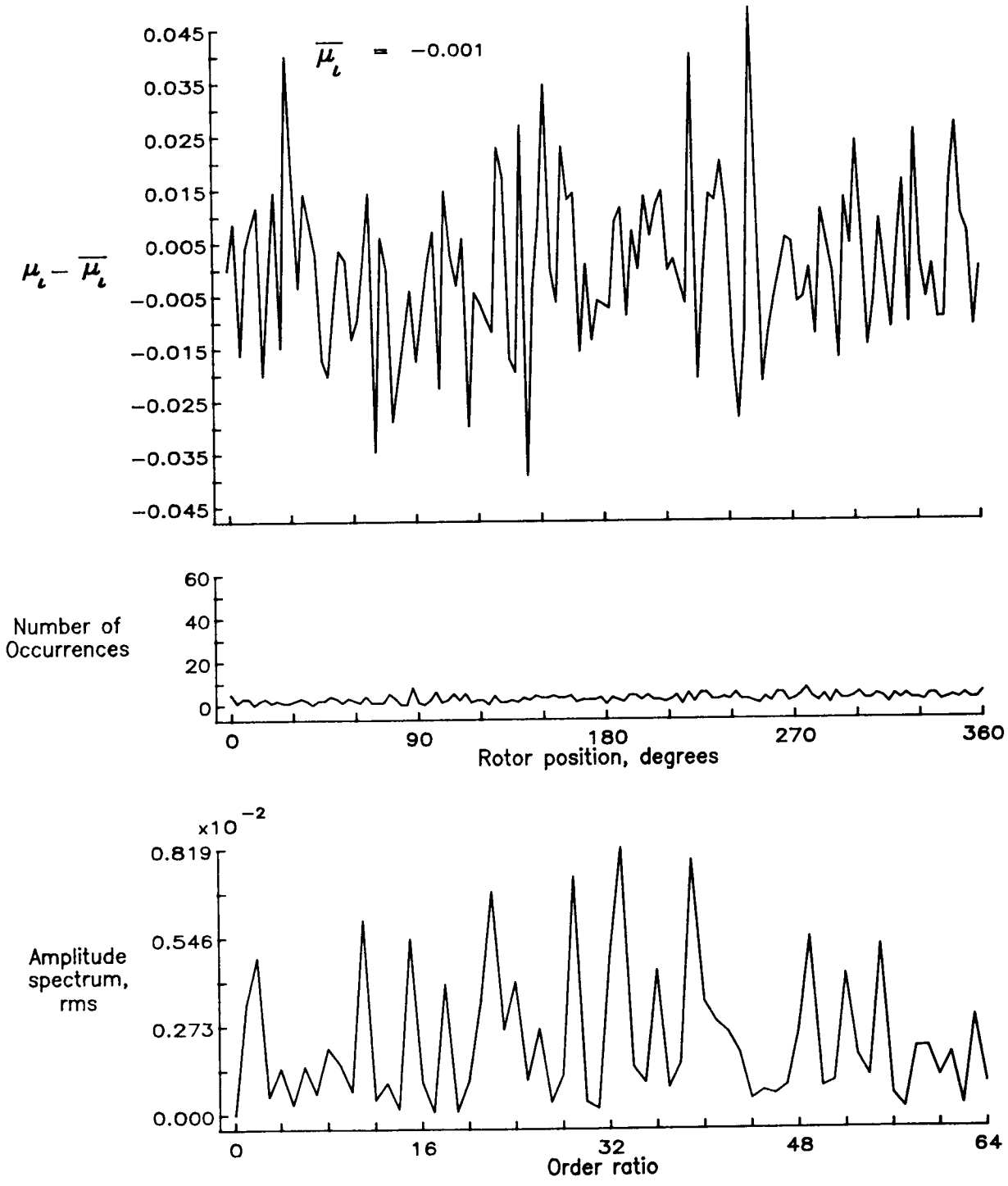


Figure 36.– Induced inflow velocity measured at 30 degrees and r/R of 1.10.

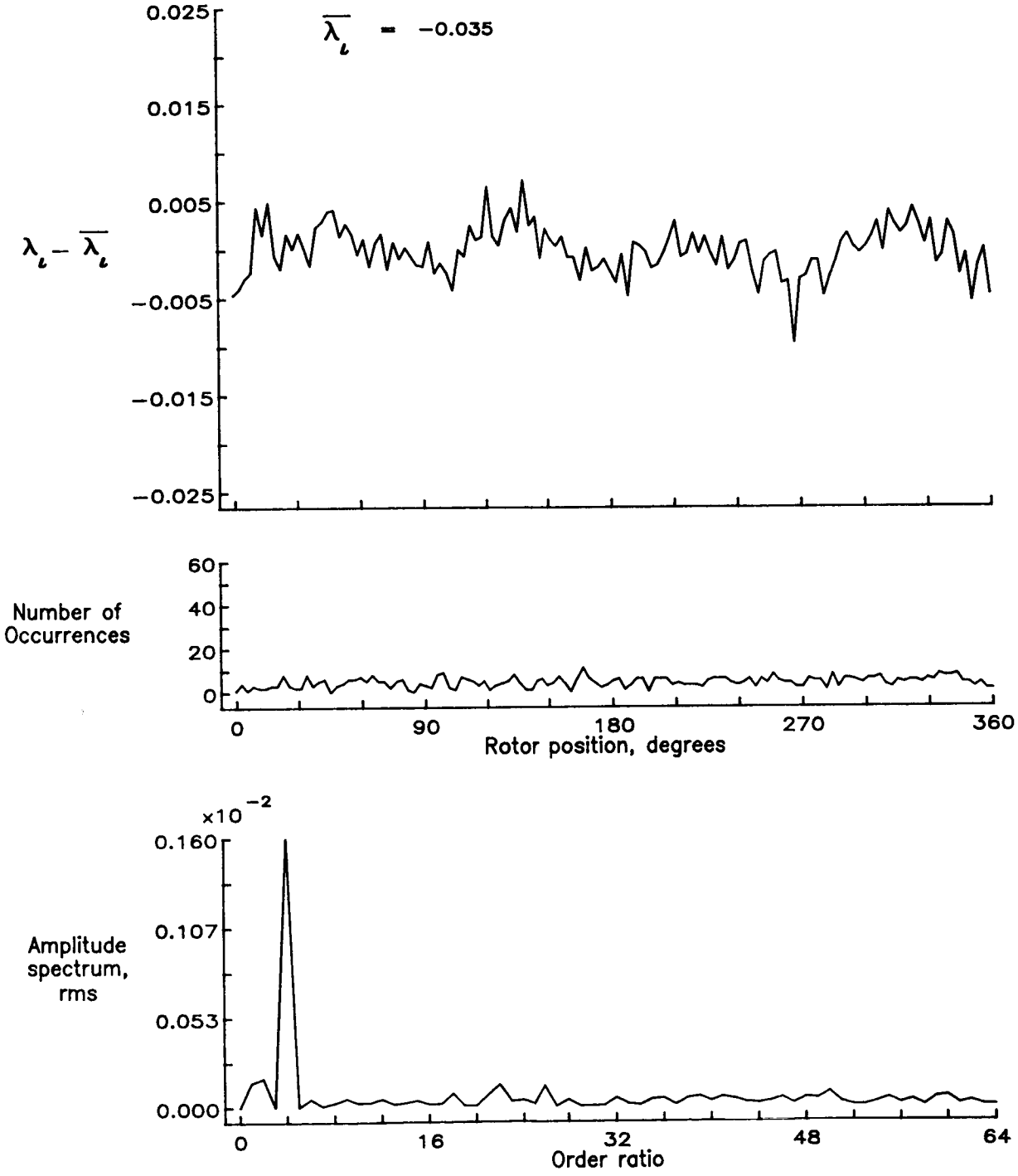


Figure 36.– Concluded.

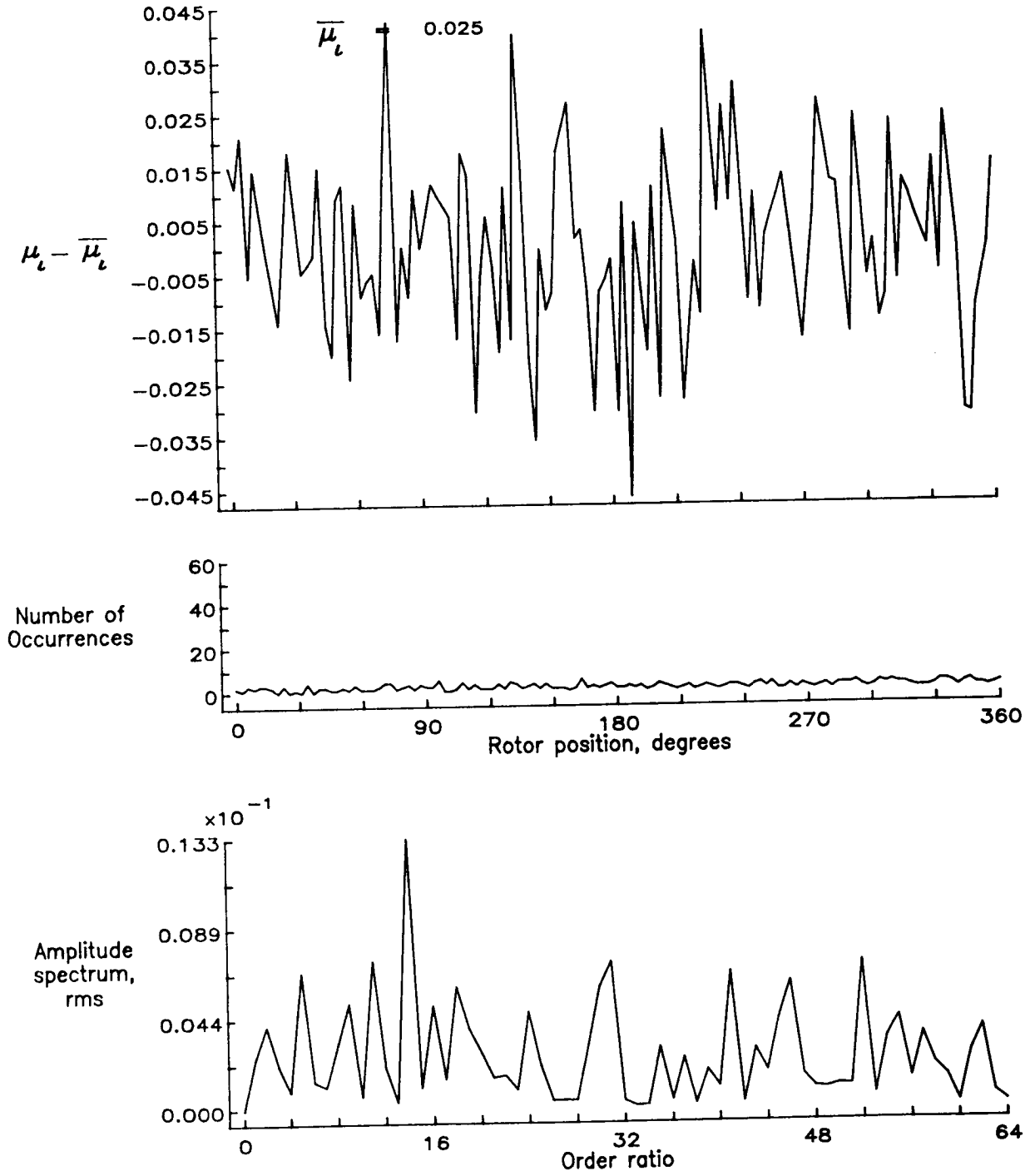


Figure 37.– Induced inflow velocity measured at 60 degrees and r/R of 0.20.

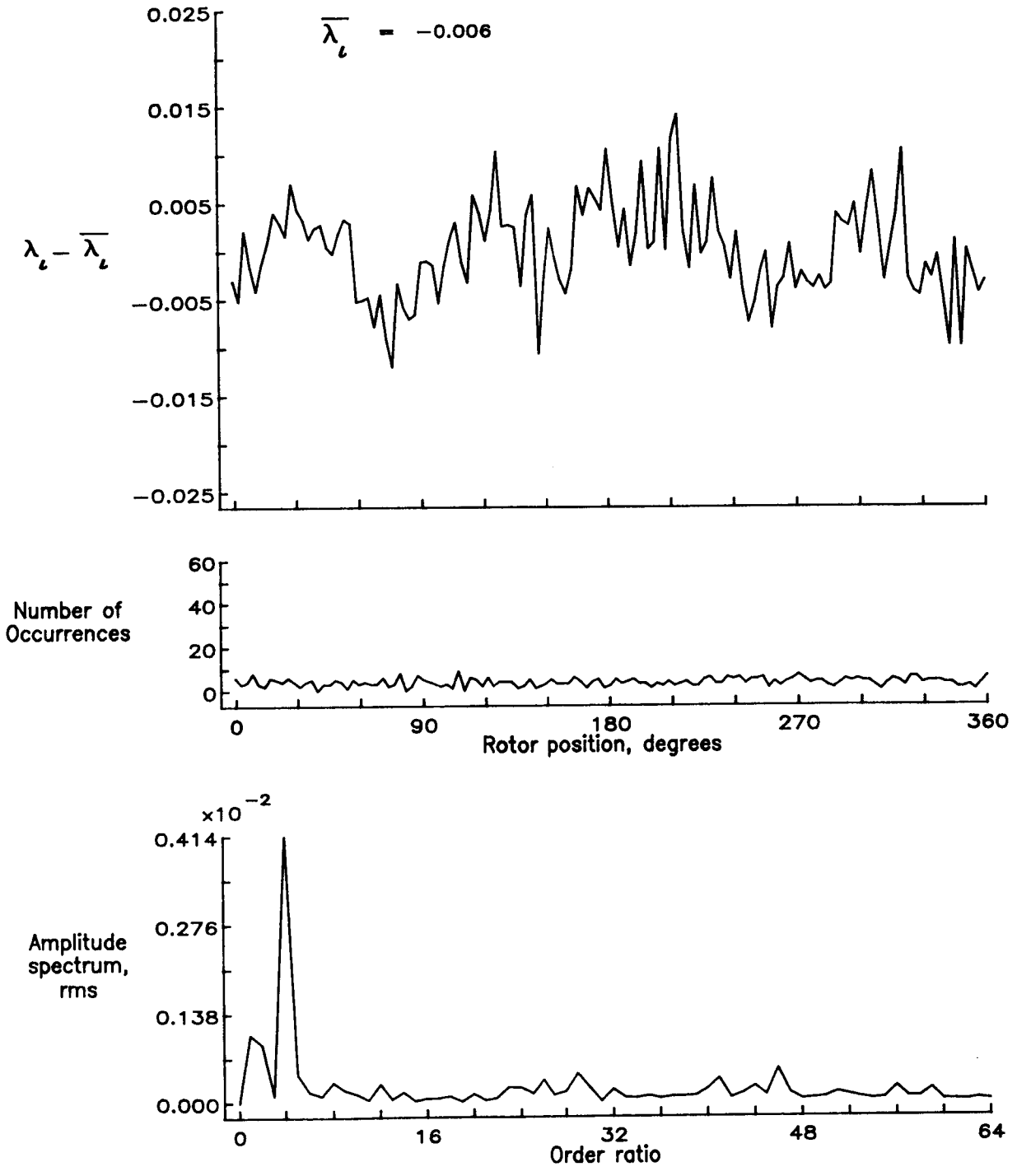


Figure 37.– Concluded.

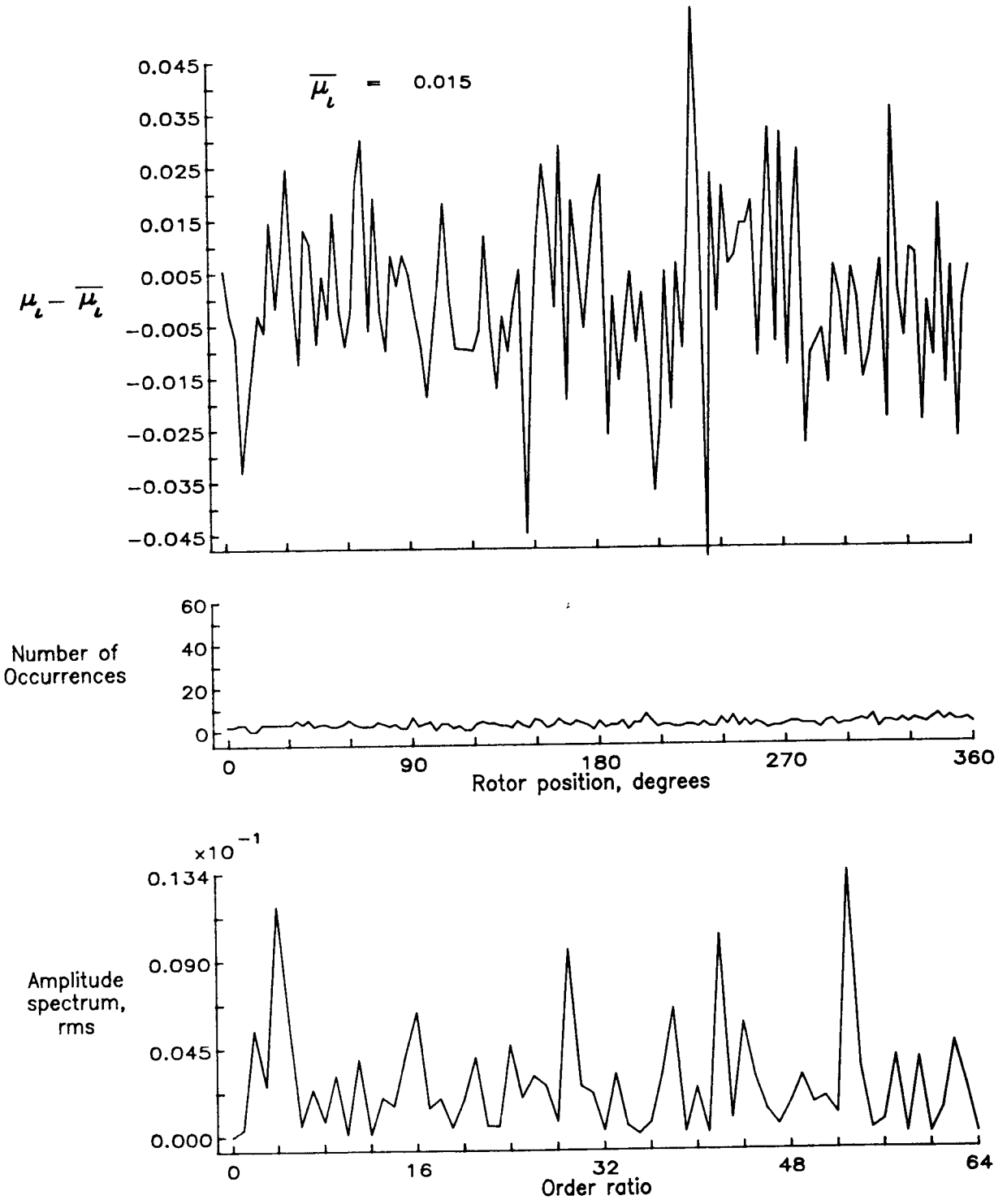


Figure 38.– Induced inflow velocity measured at 60 degrees and r/R of 0.50.

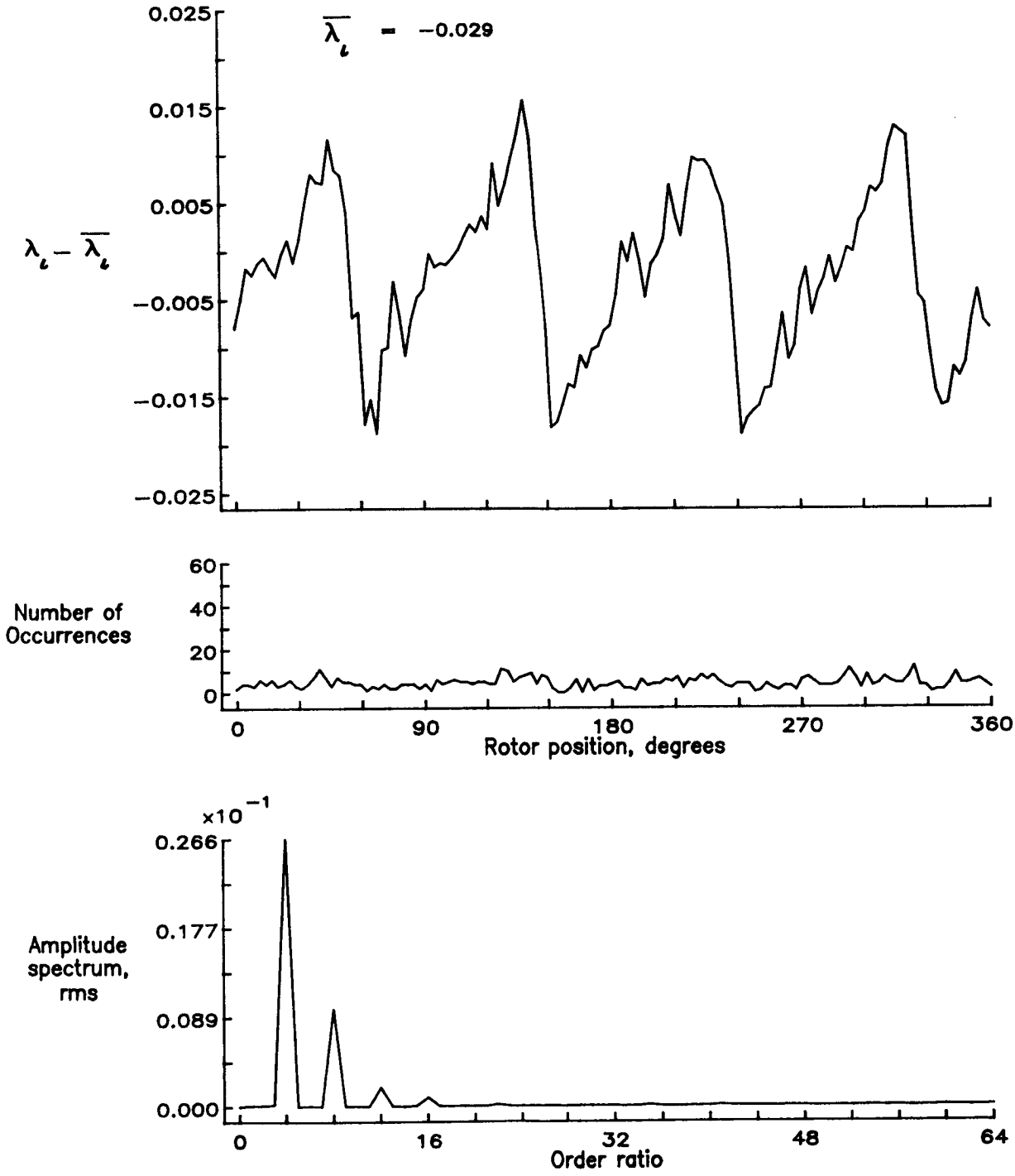


Figure 38.– Concluded.

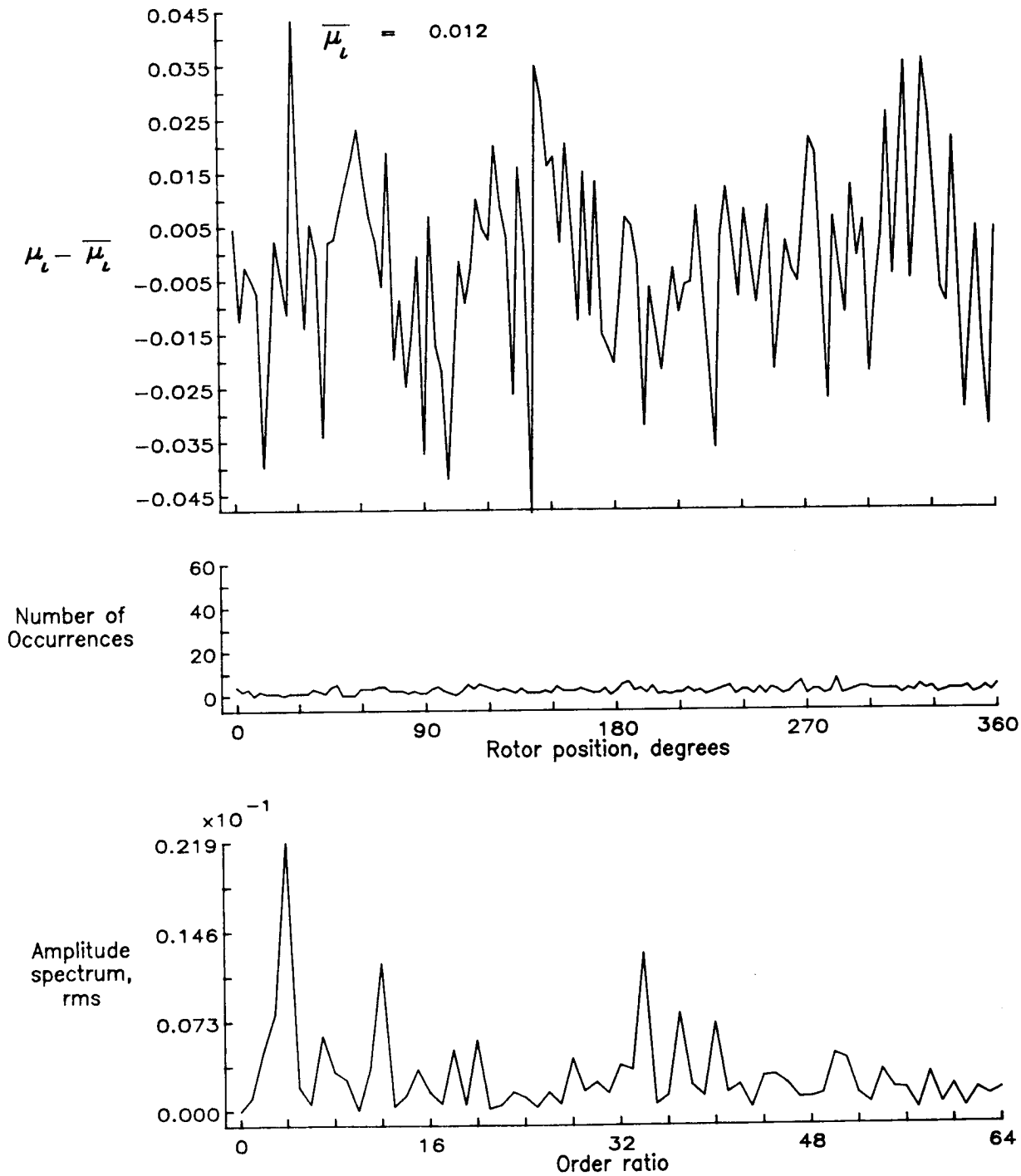


Figure 39.– Induced inflow velocity measured at 60 degrees and r/R of 0.60.

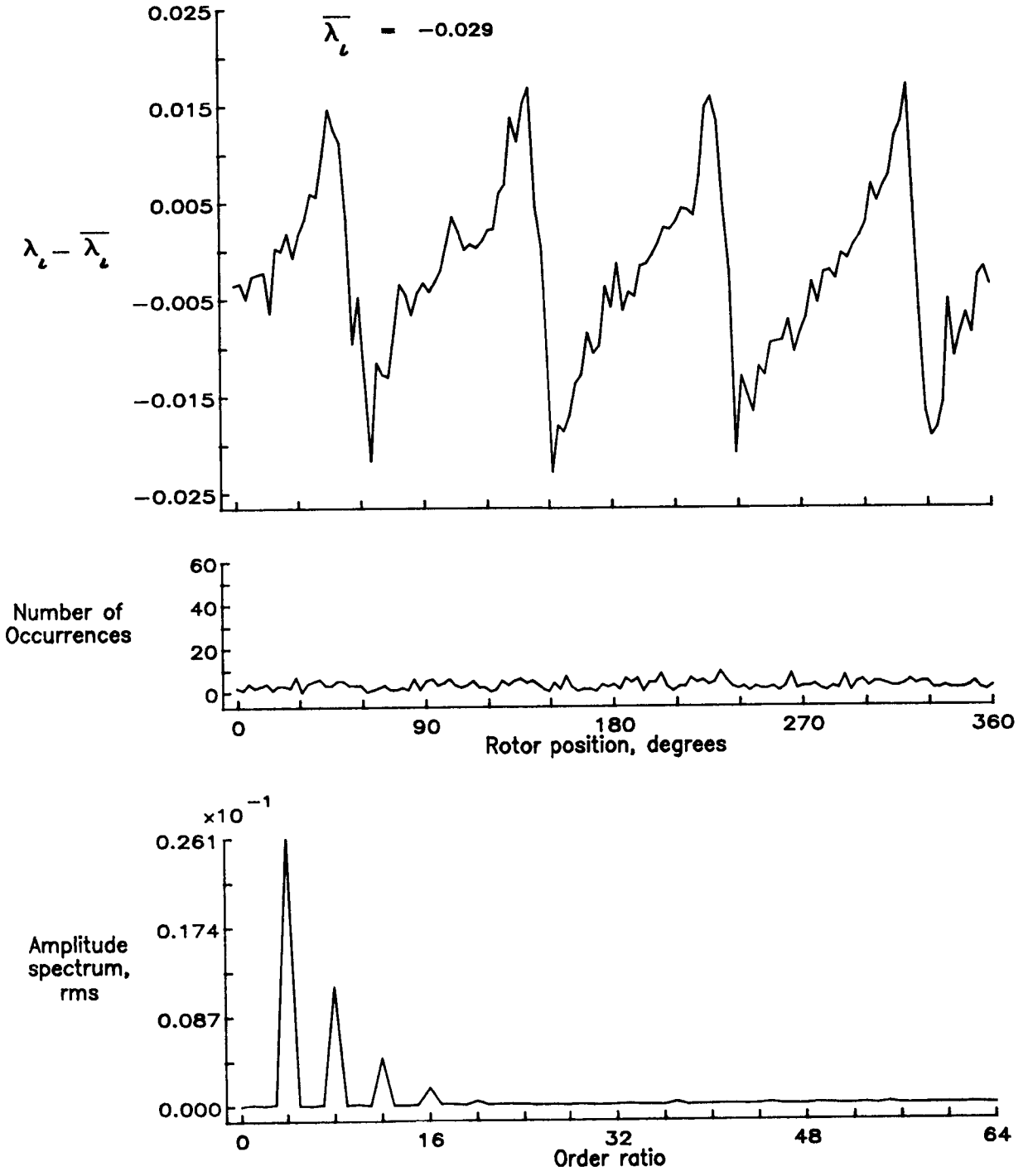


Figure 39.– Concluded.

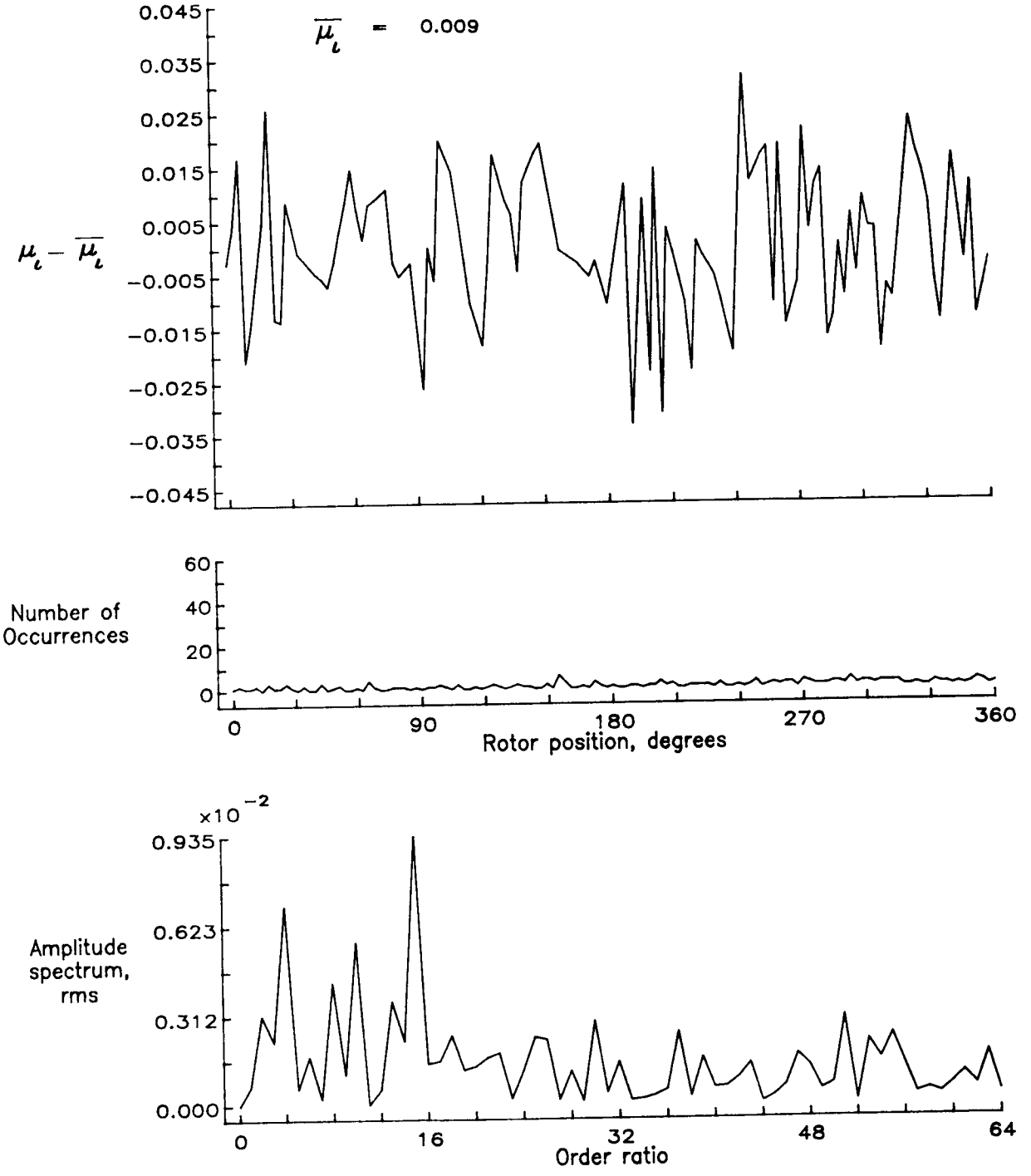


Figure 40.– Induced inflow velocity measured at 60 degrees and r/R of 0.70.

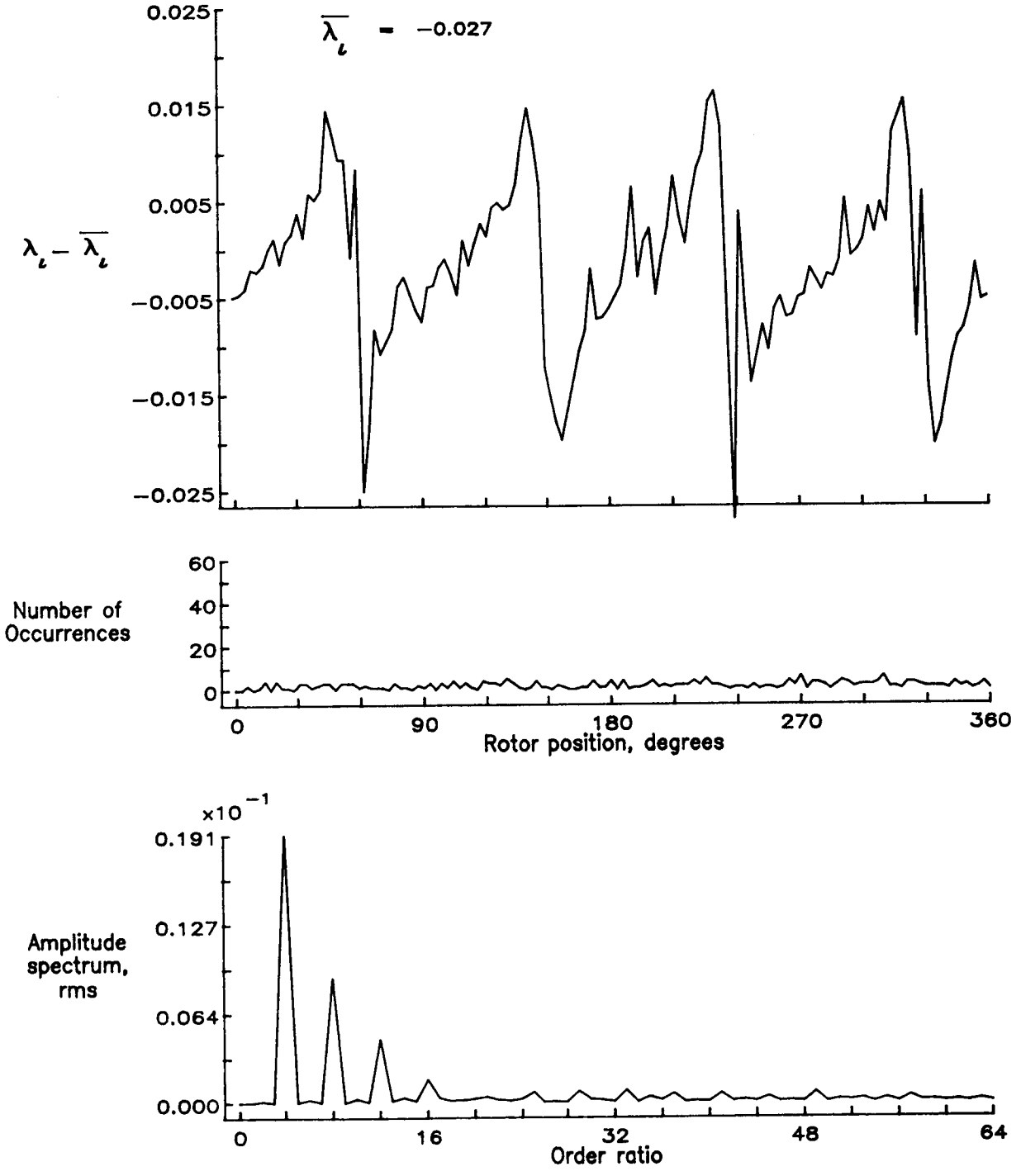


Figure 40.– Concluded.

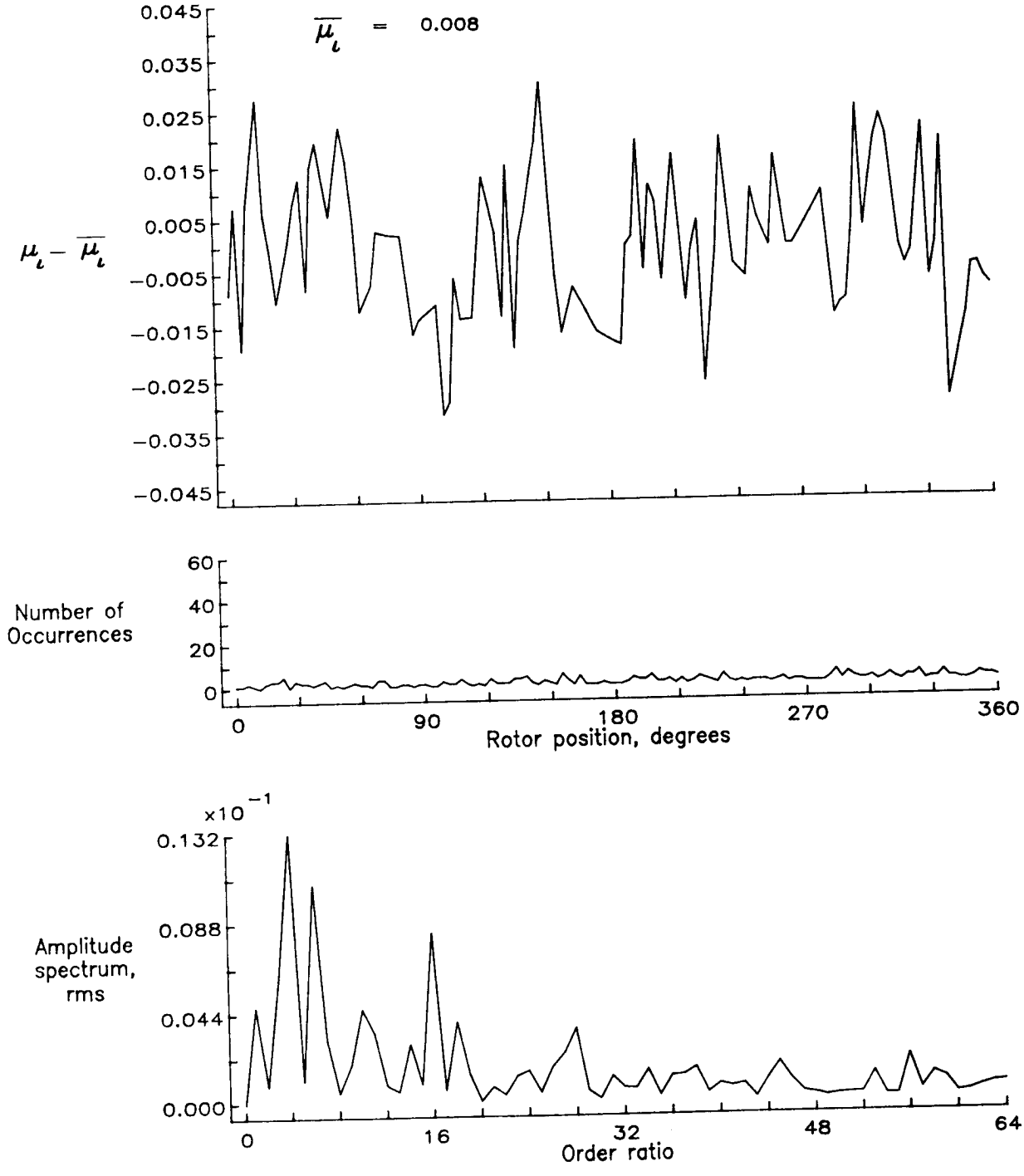


Figure 41.– Induced inflow velocity measured at 60 degrees and r/R of 0.74.

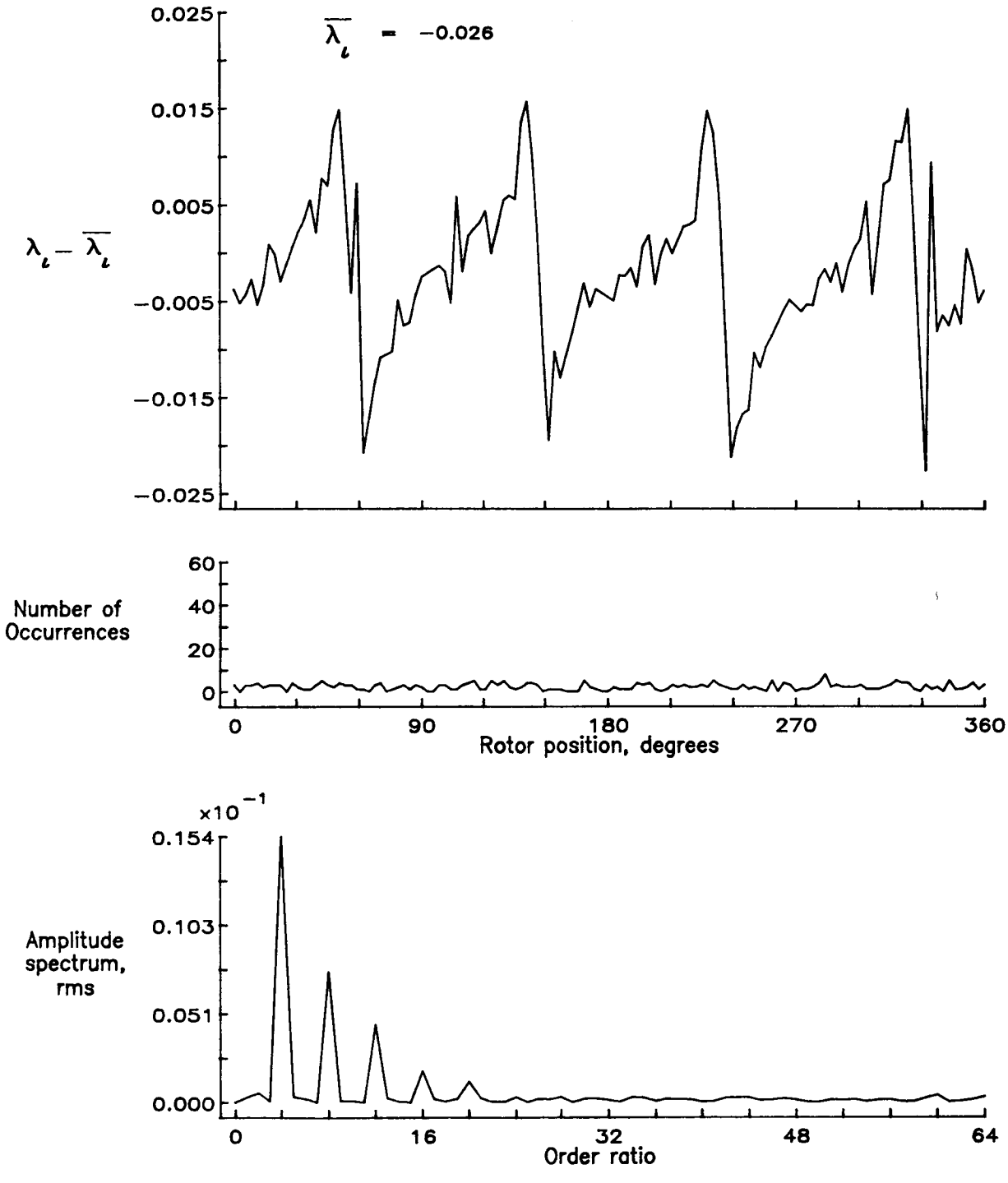


Figure 41.– Concluded.

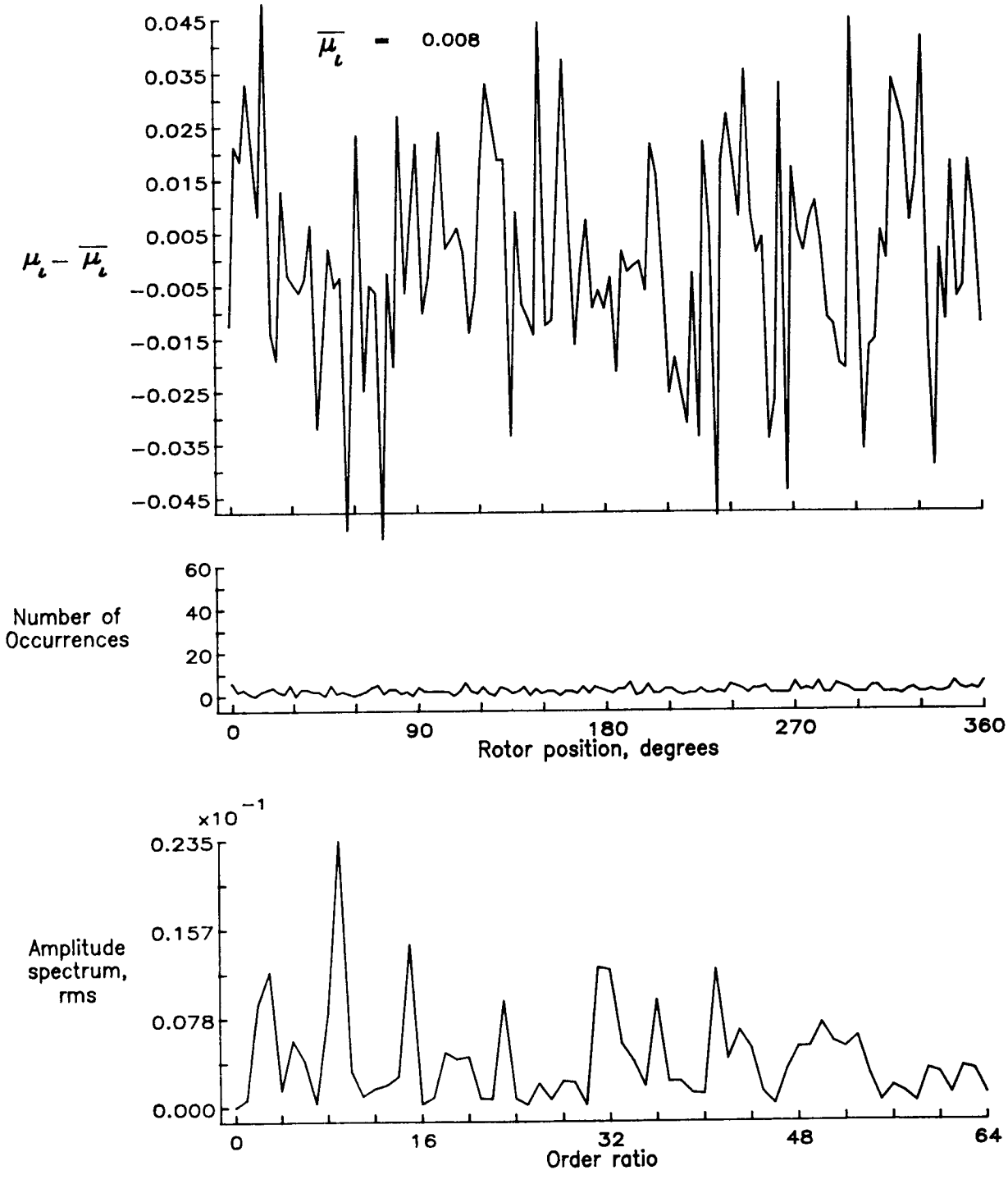


Figure 42.– Induced inflow velocity measured at 60 degrees and r/R of 0.78.

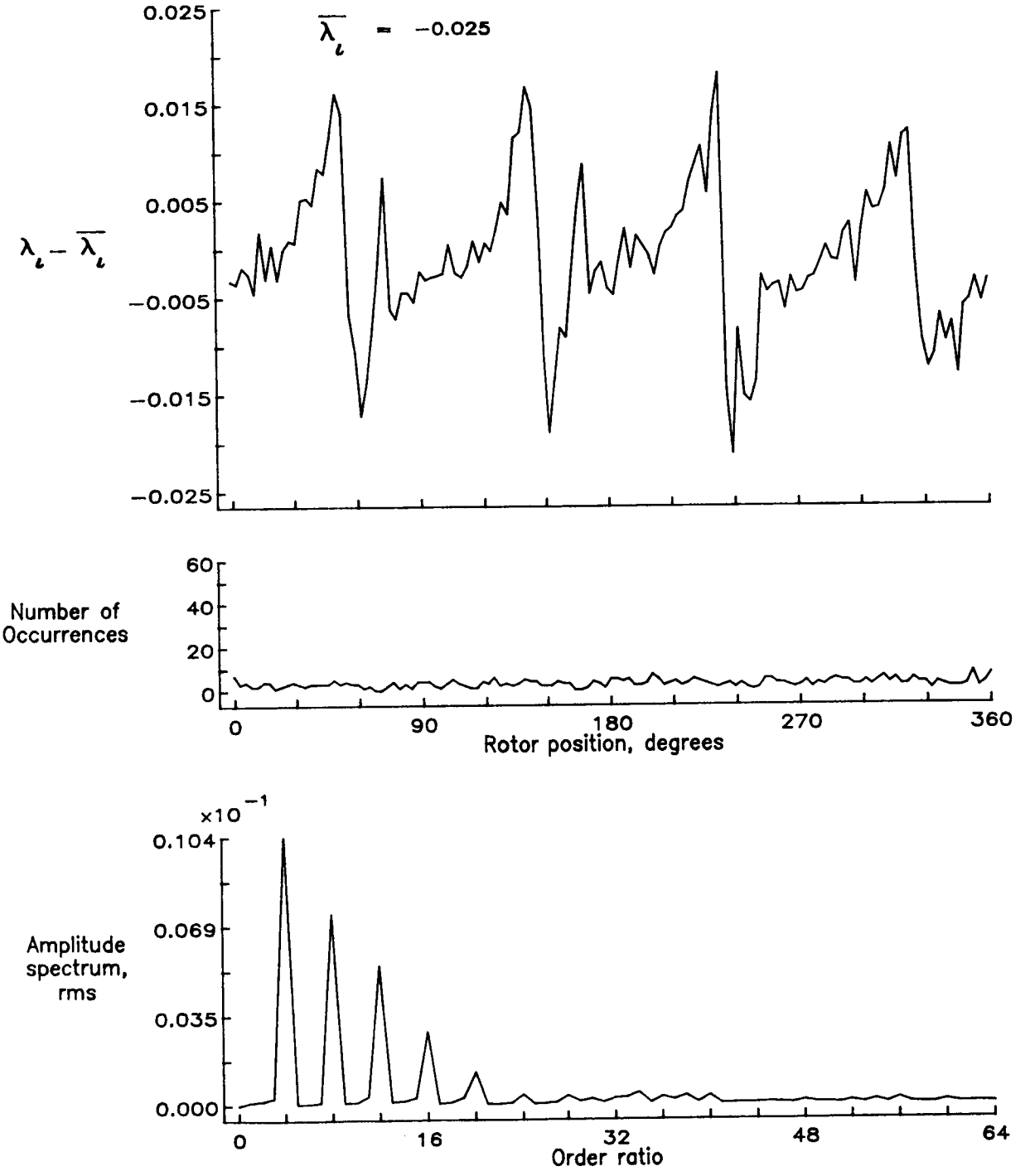


Figure 42.– Concluded.

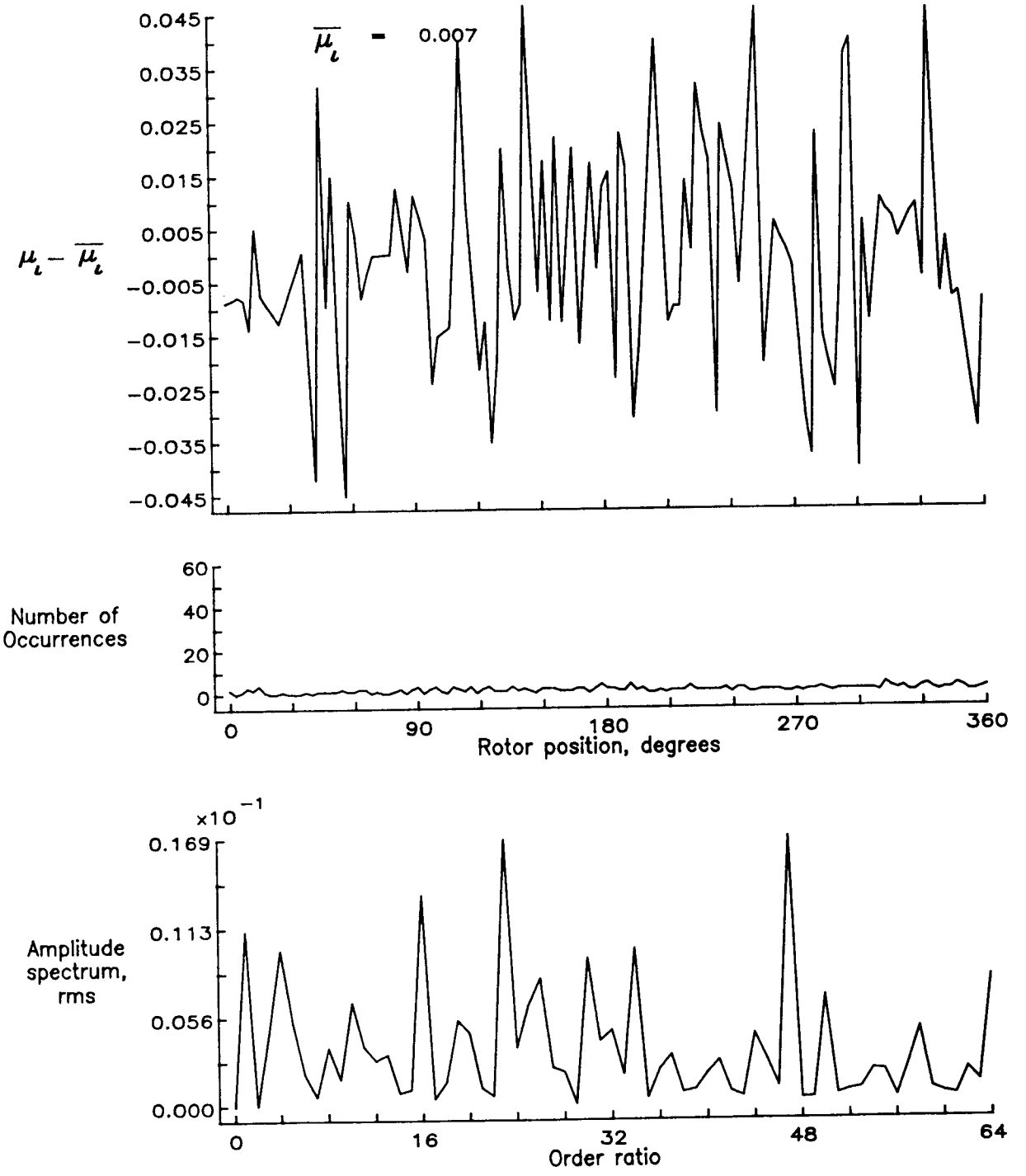


Figure 43.– Induced inflow velocity measured at 60 degrees and r/R of 0.82.

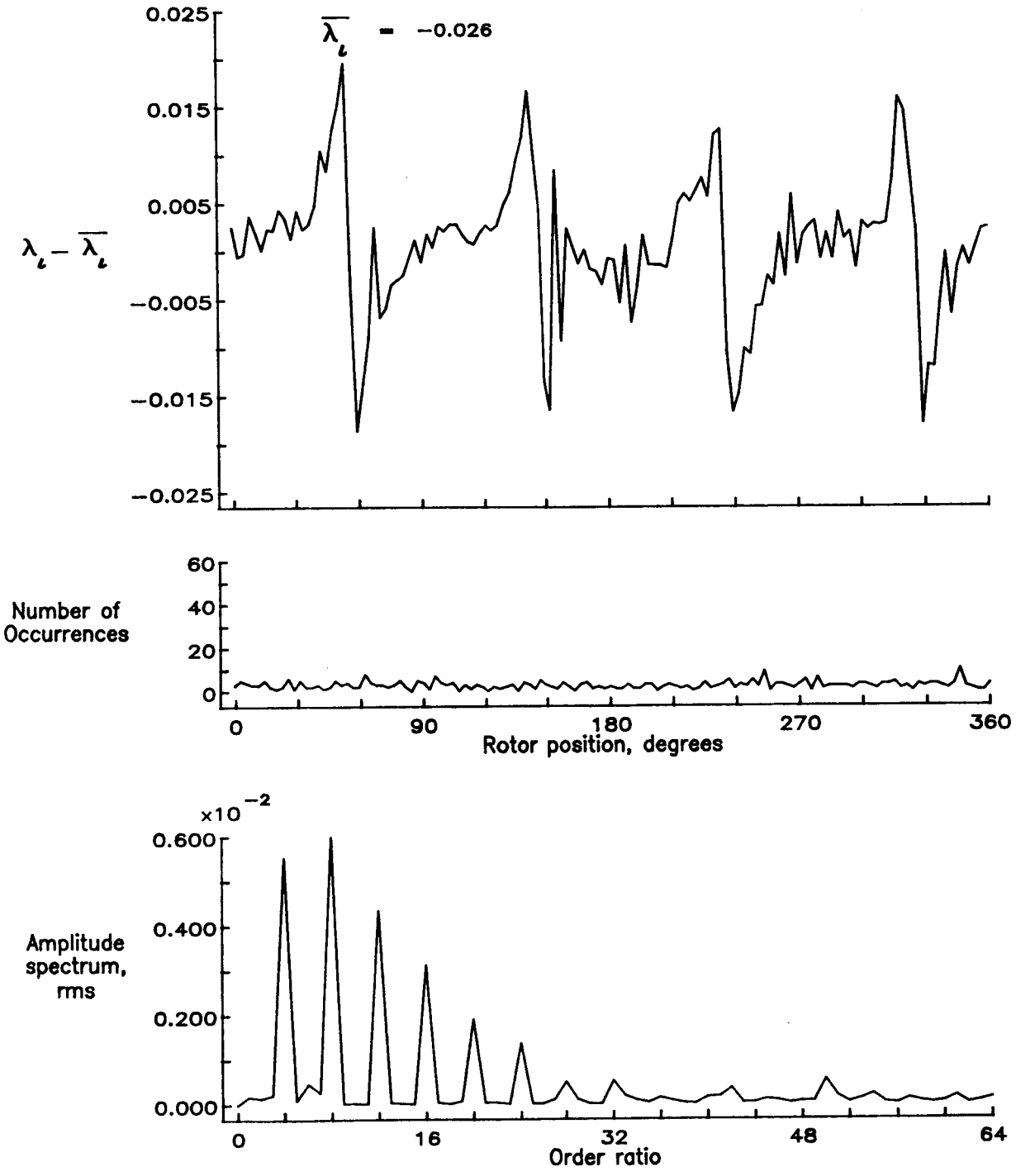


Figure 43.– Concluded.

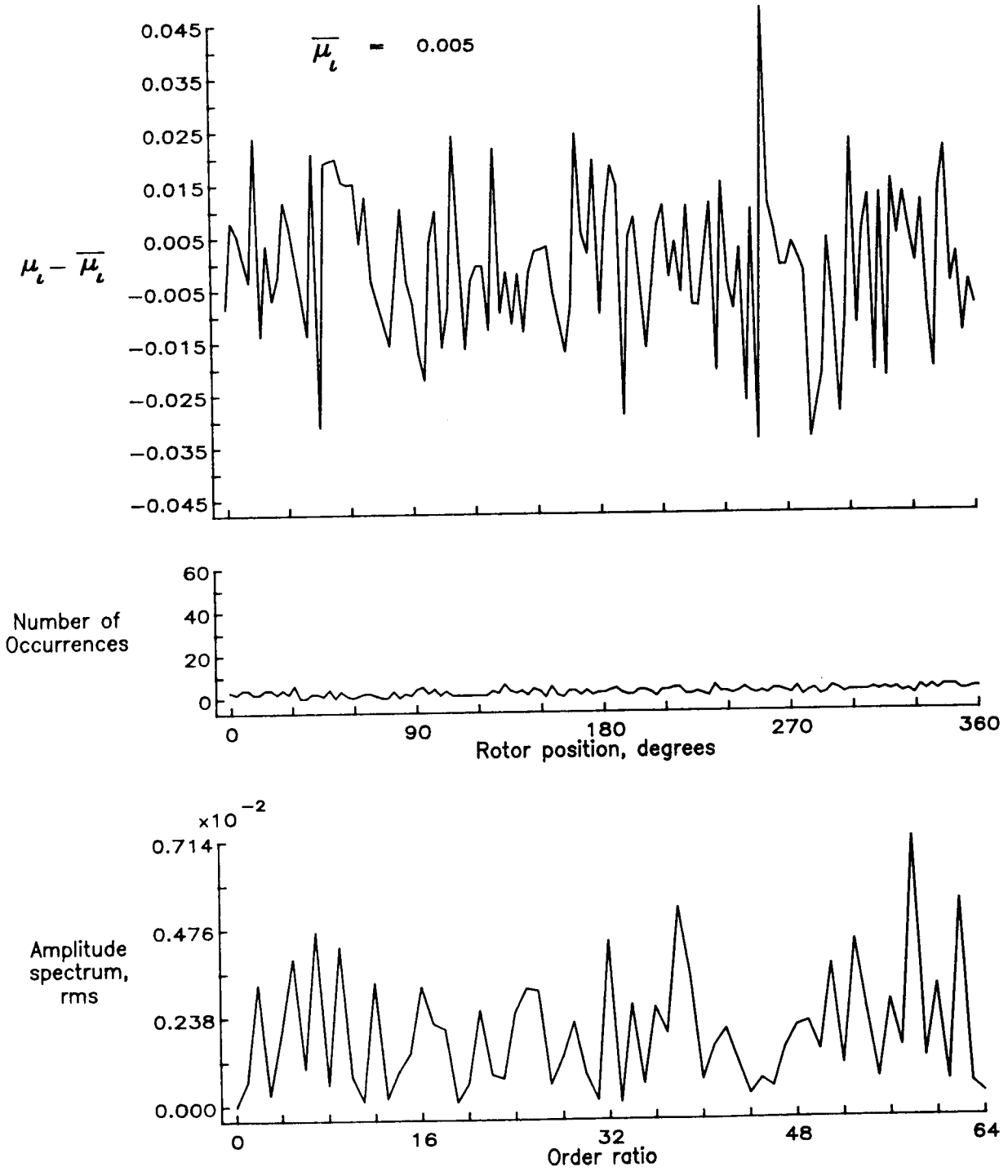


Figure 44.– Induced inflow velocity measured at 60 degrees and r/R of 0.86.

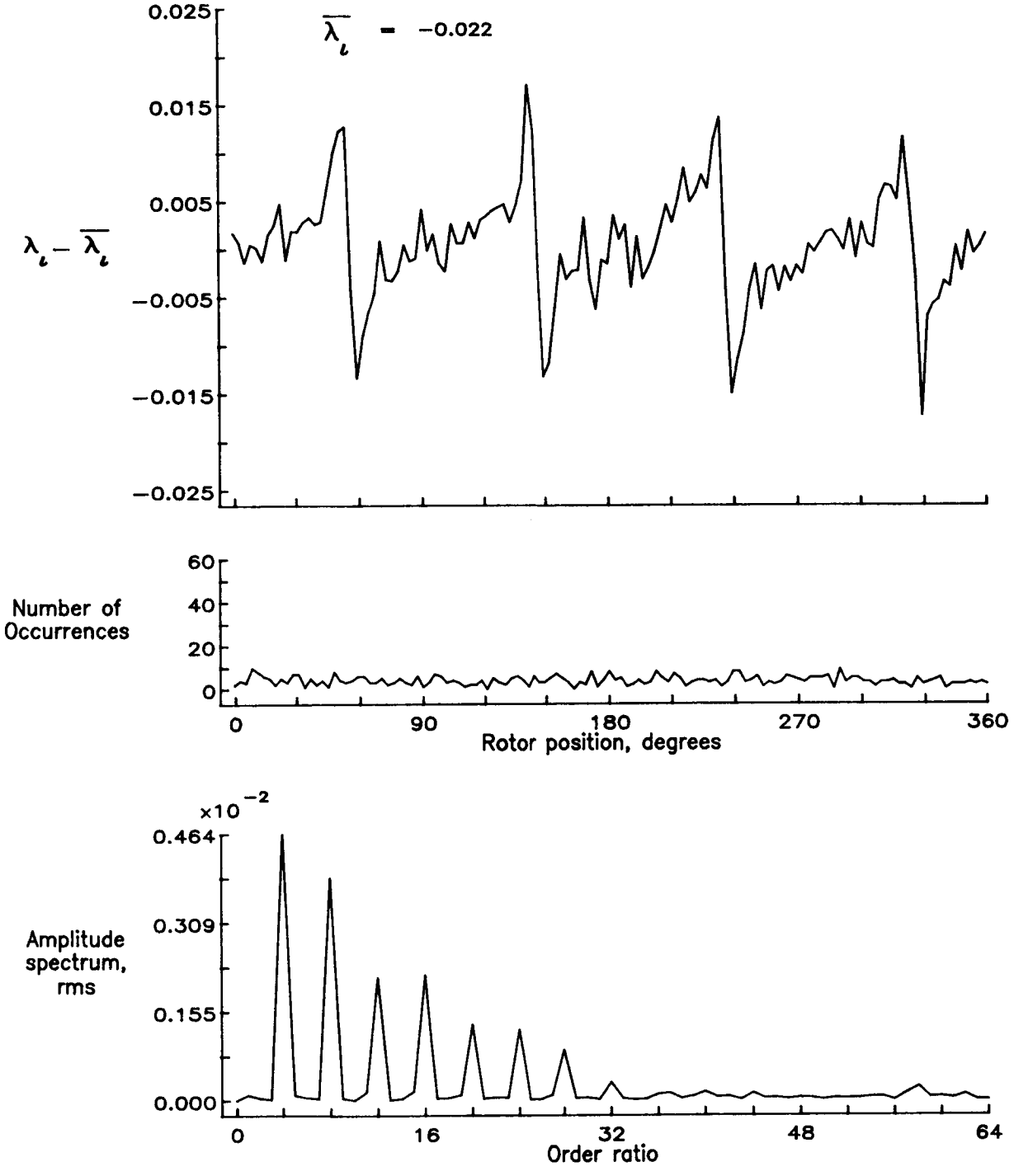


Figure 44.– Concluded.

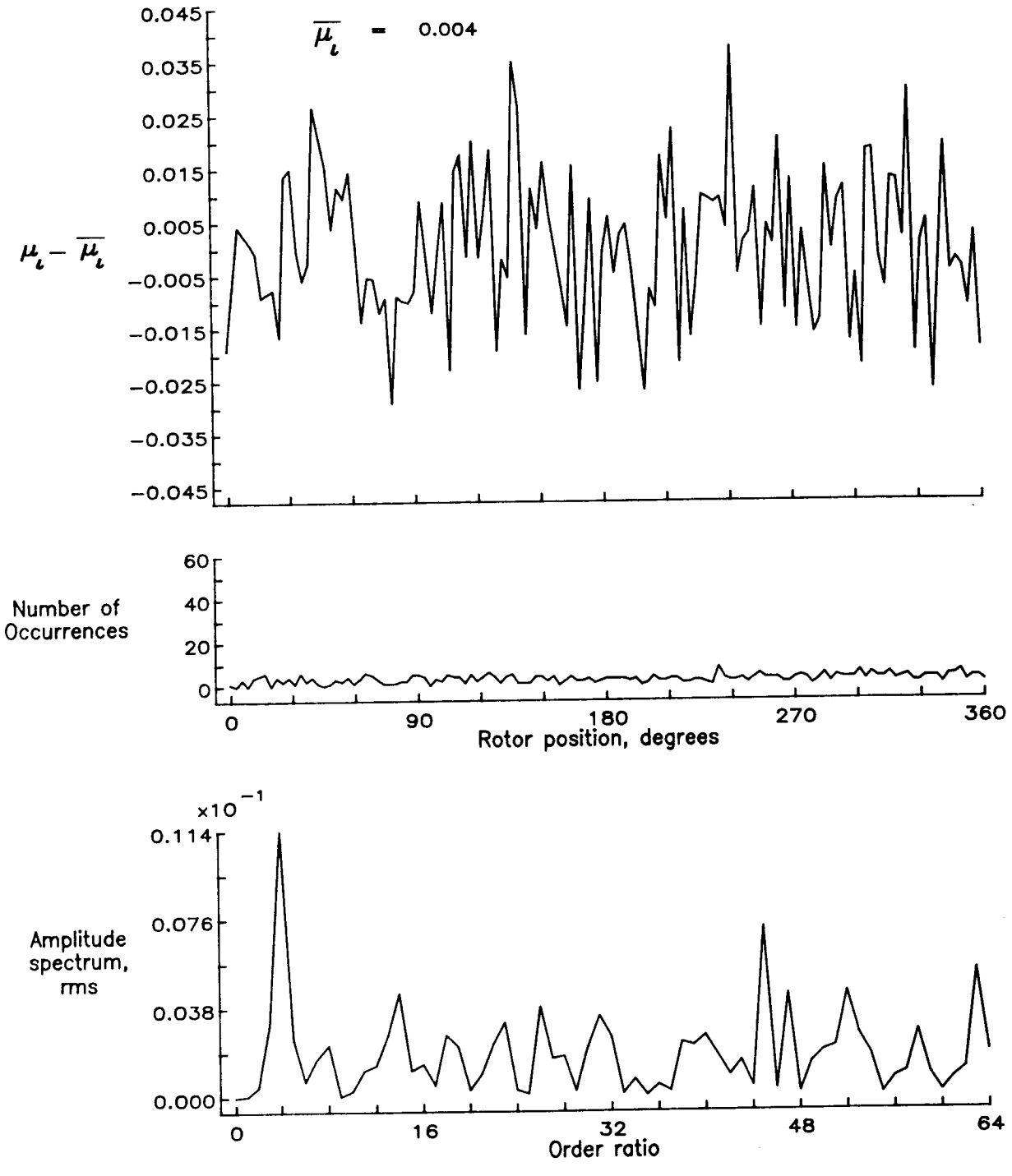


Figure 45.– Induced inflow velocity measured at 60 degrees and r/R of 0.90.

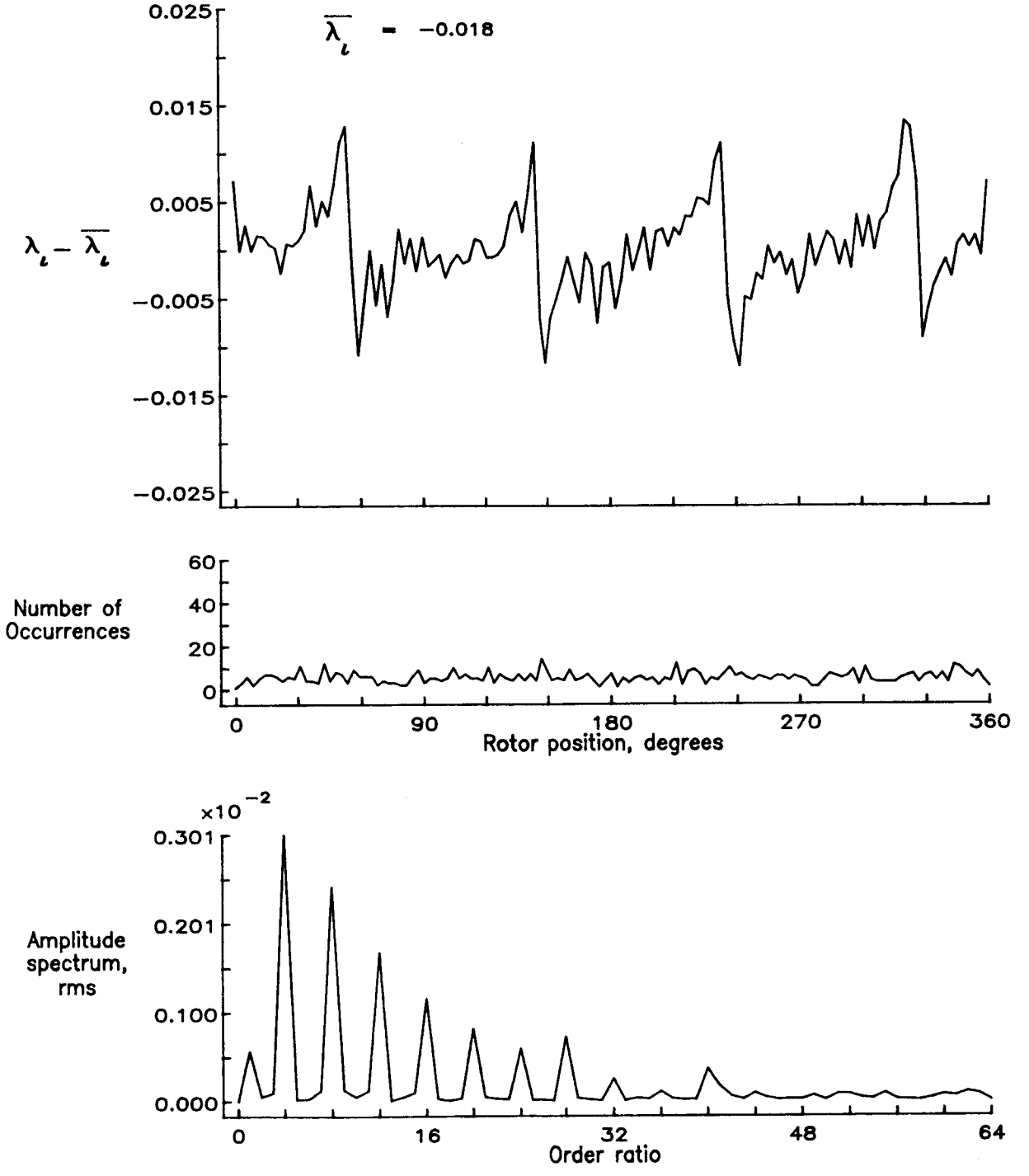


Figure 45.– Concluded.

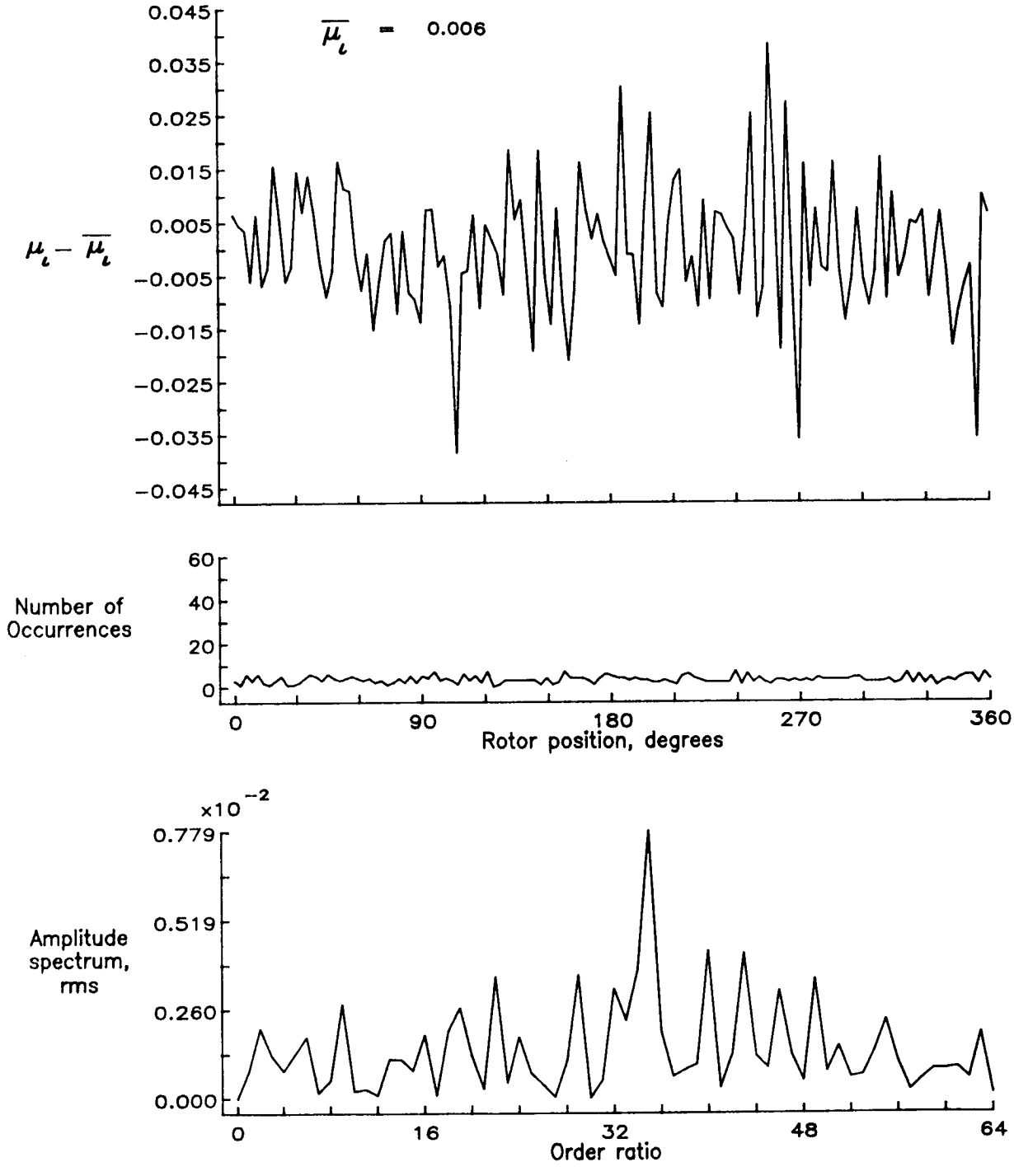


Figure 46.– Induced inflow velocity measured at 60 degrees and r/R of 0.94.

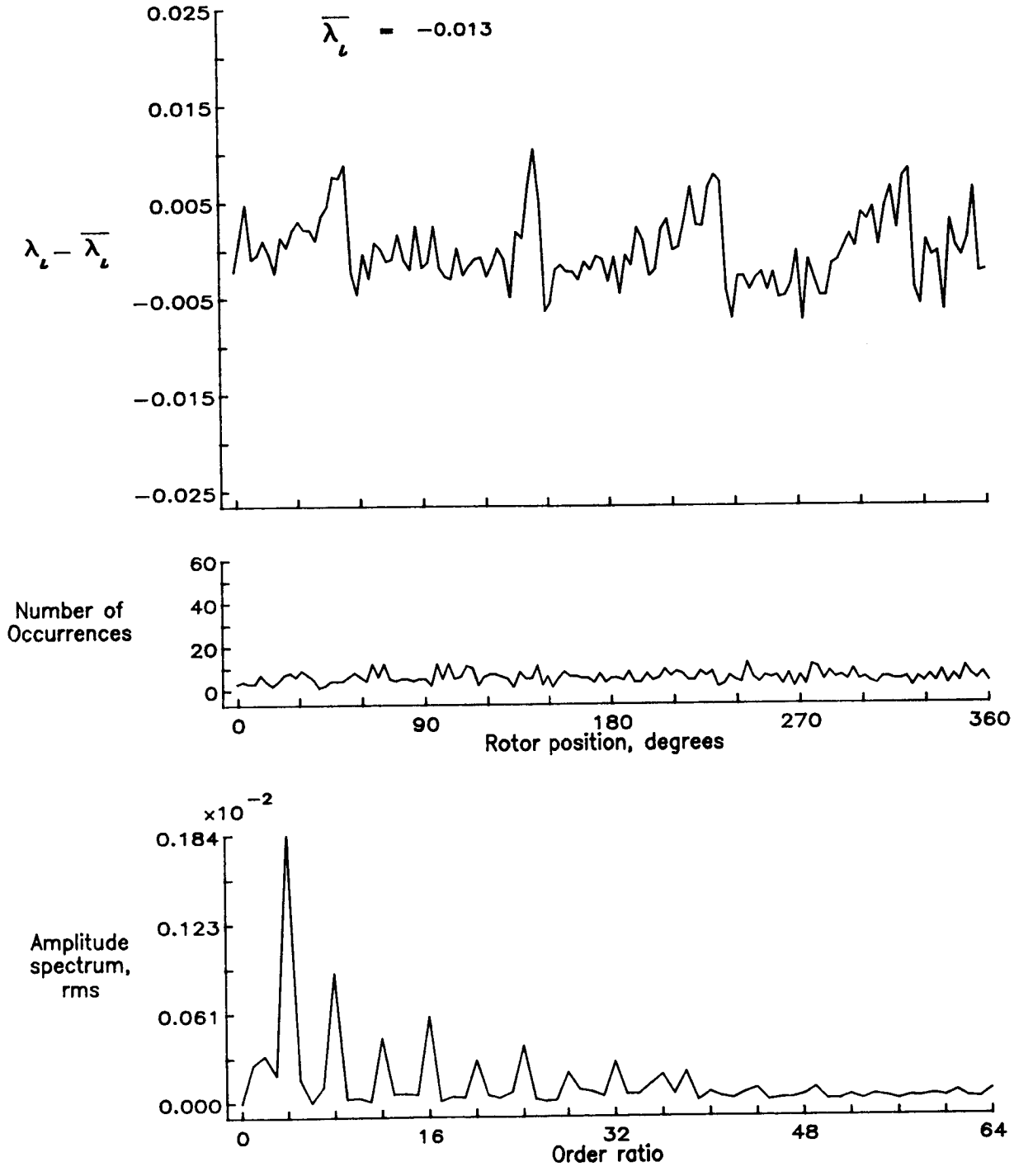


Figure 46.– Concluded.

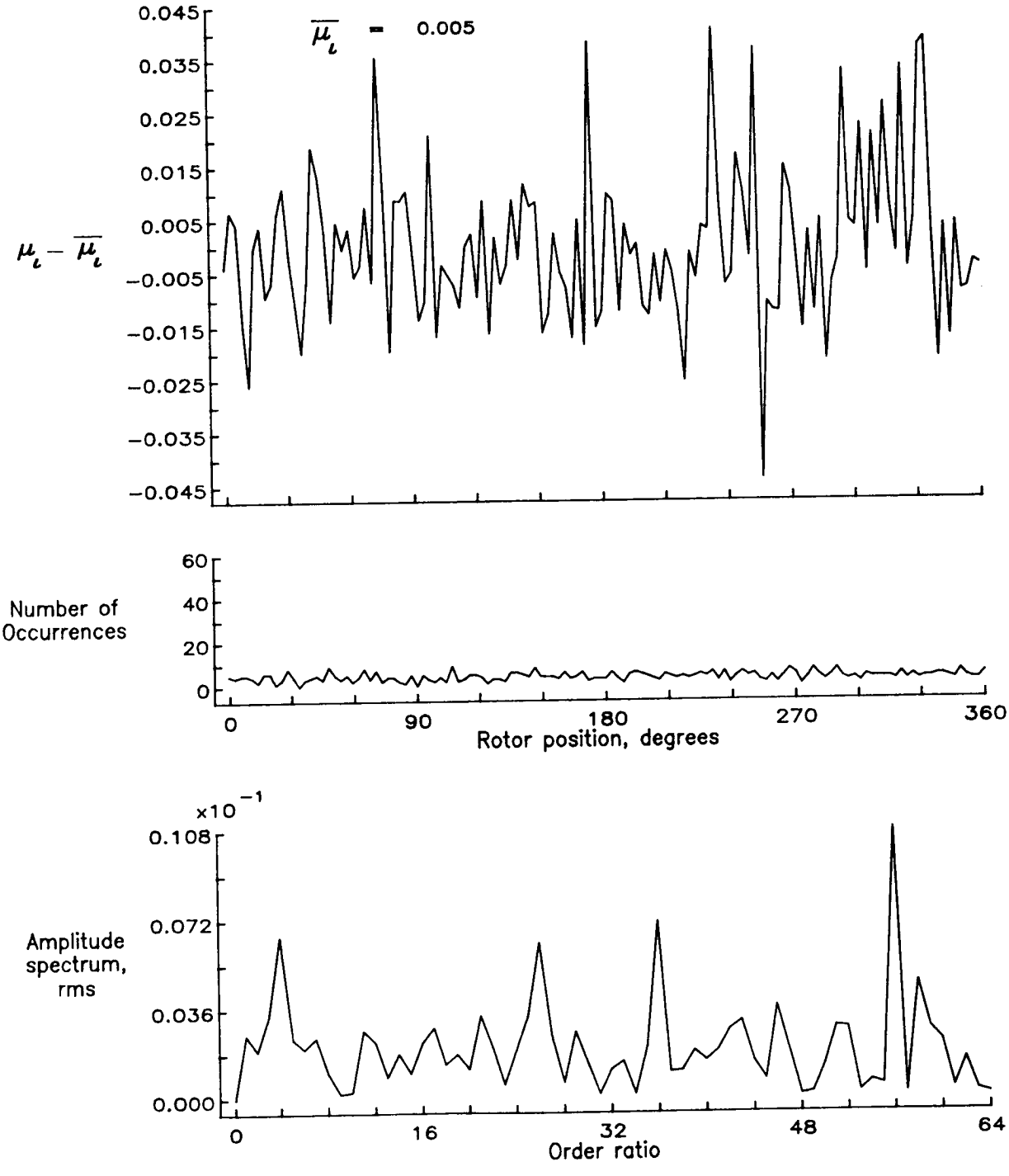


Figure 47.– Induced inflow velocity measured at 60 degrees and r/R of 0.98.

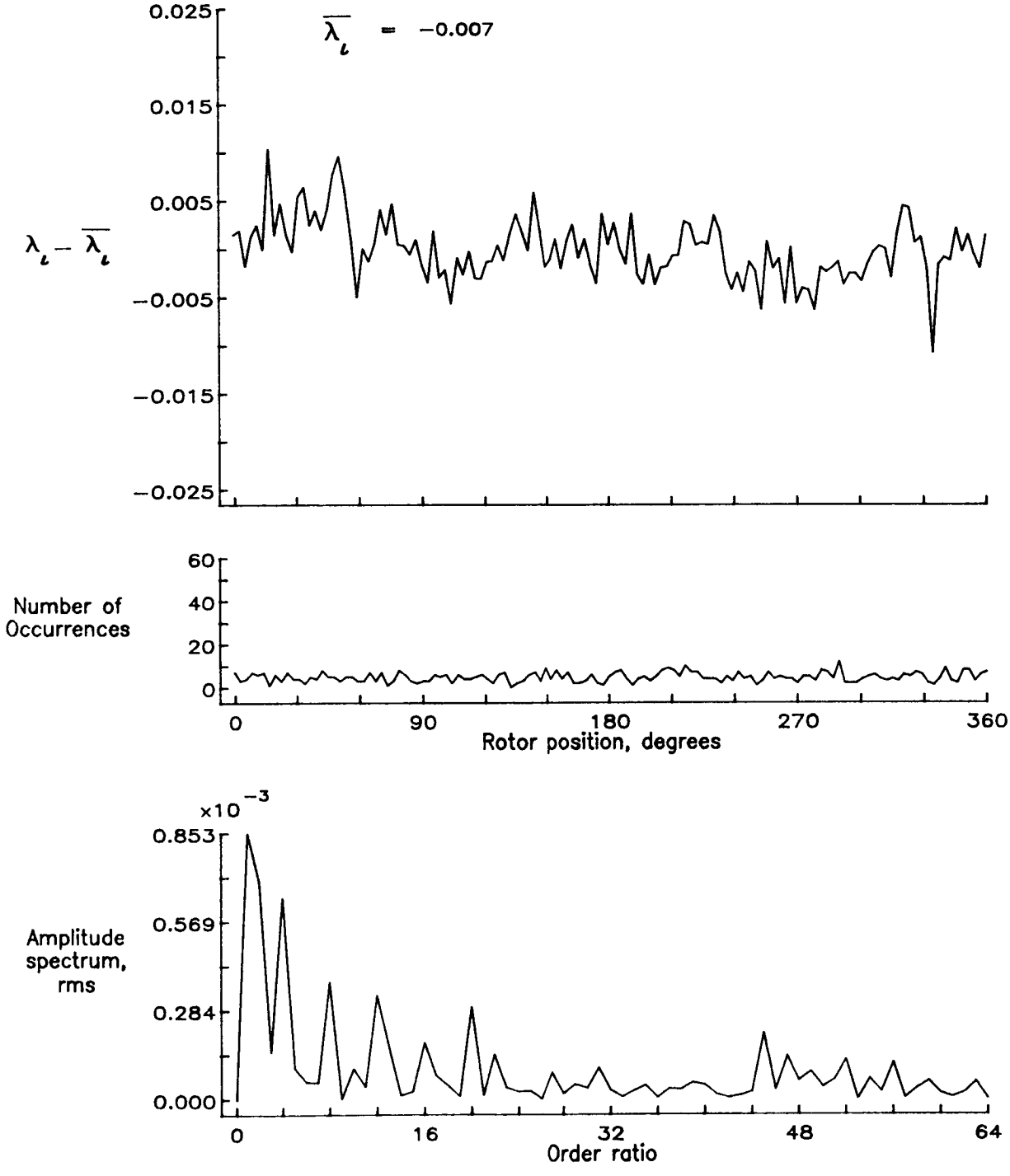


Figure 47.– Concluded.

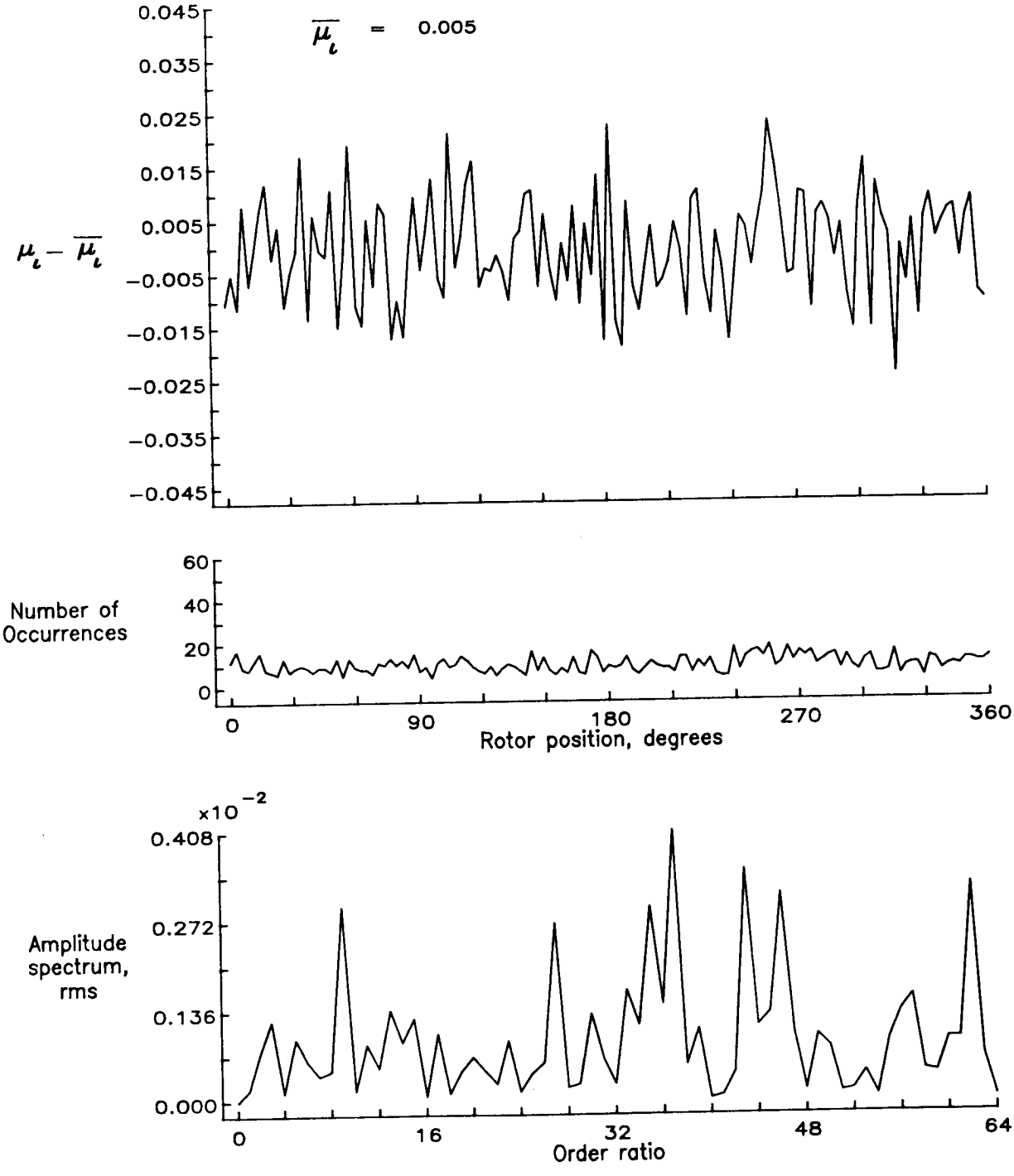


Figure 48.– Induced inflow velocity measured at 60 degrees and r/R of 1.02.

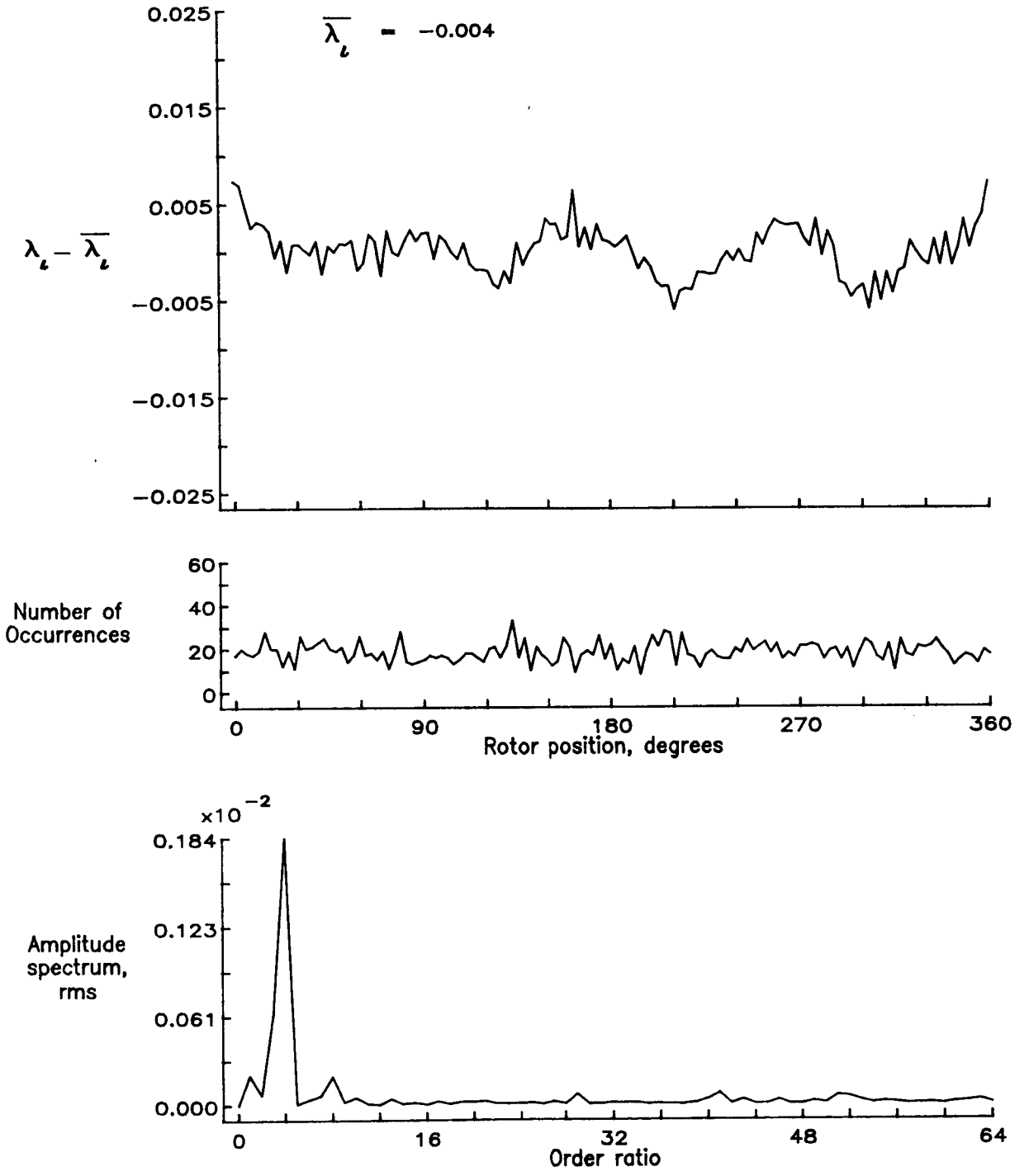


Figure 48.– Concluded.

C-2

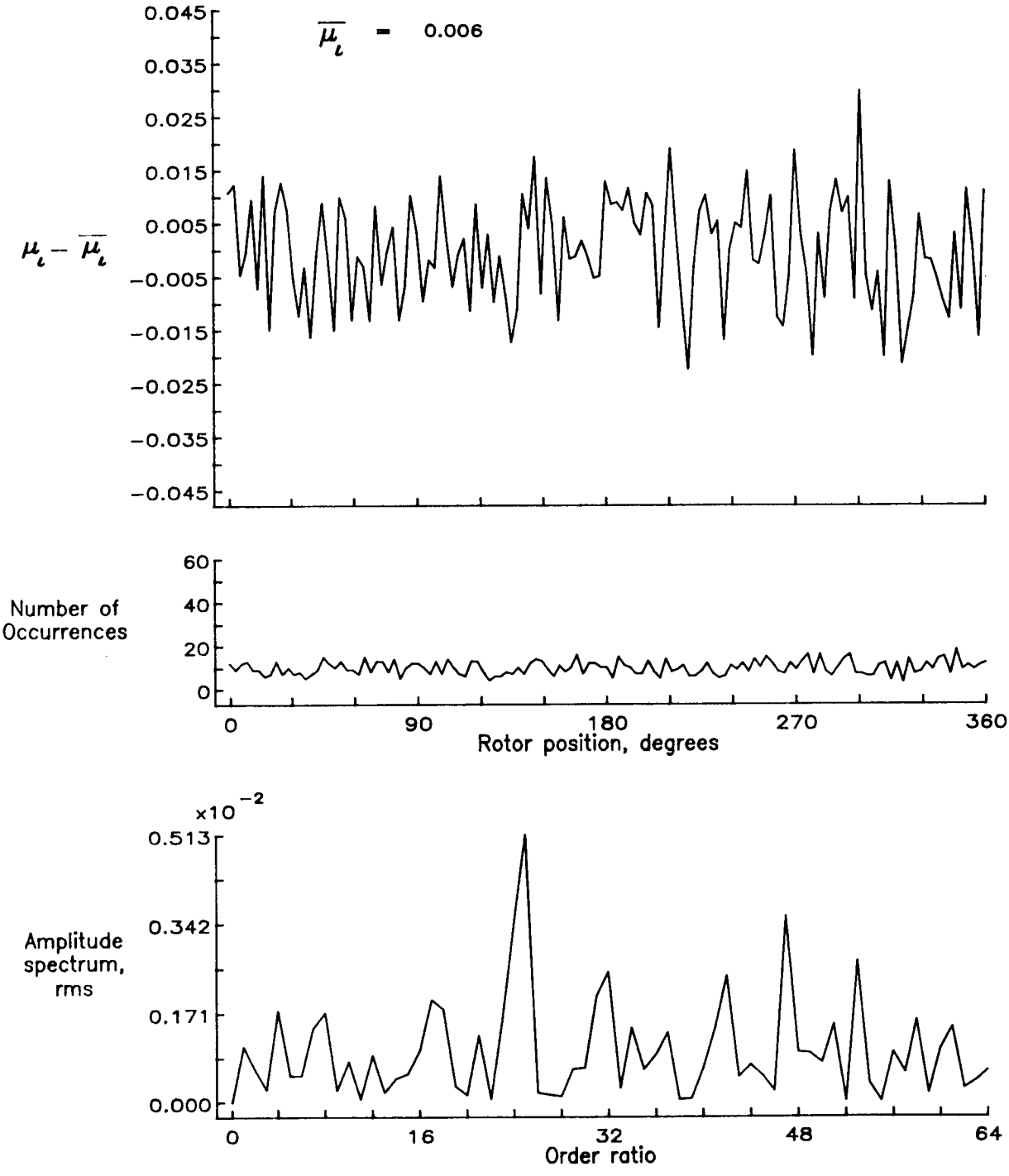


Figure 49.– Induced inflow velocity measured at 60 degrees and r/R of 1.04.

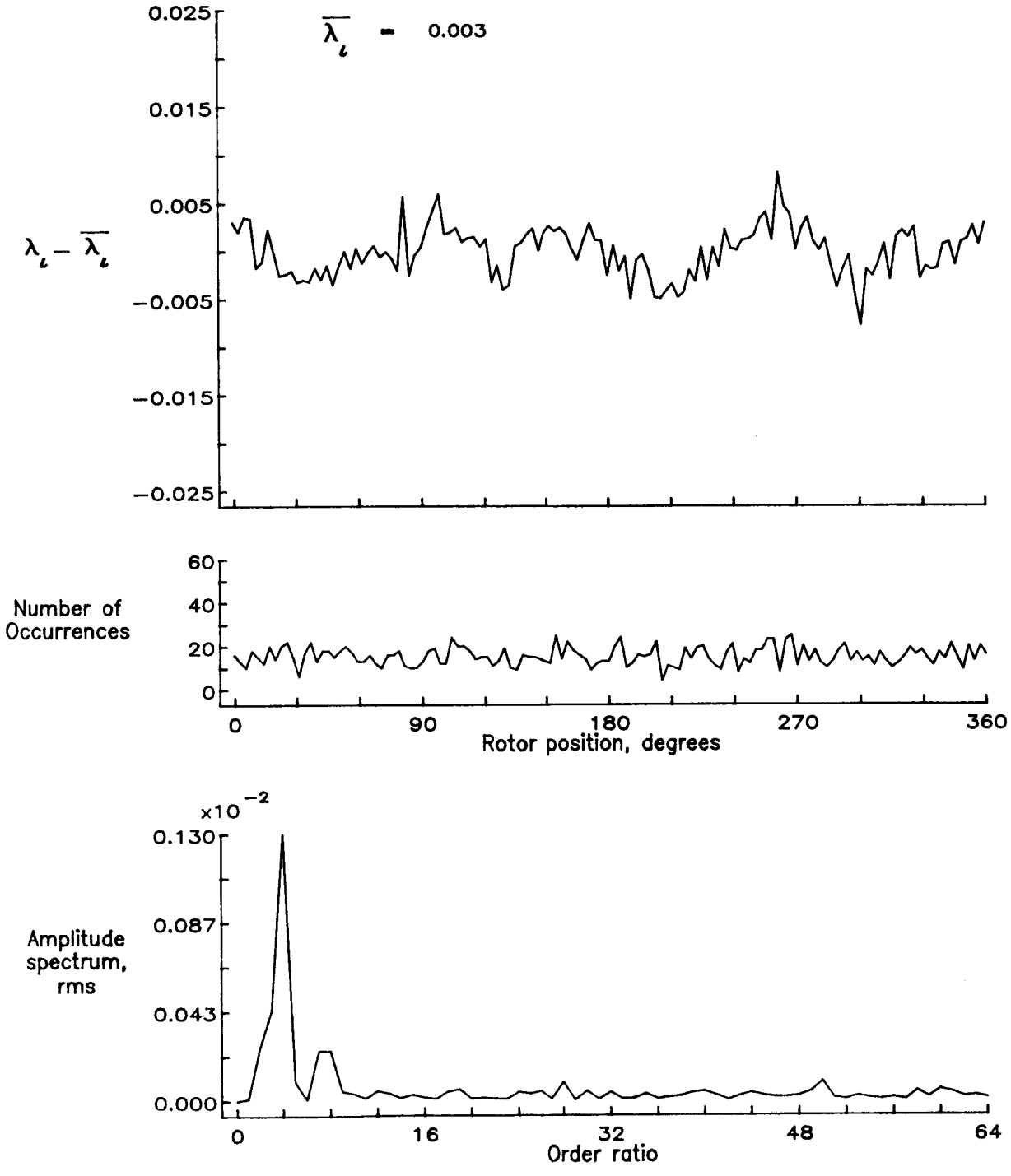


Figure 49.– Concluded.

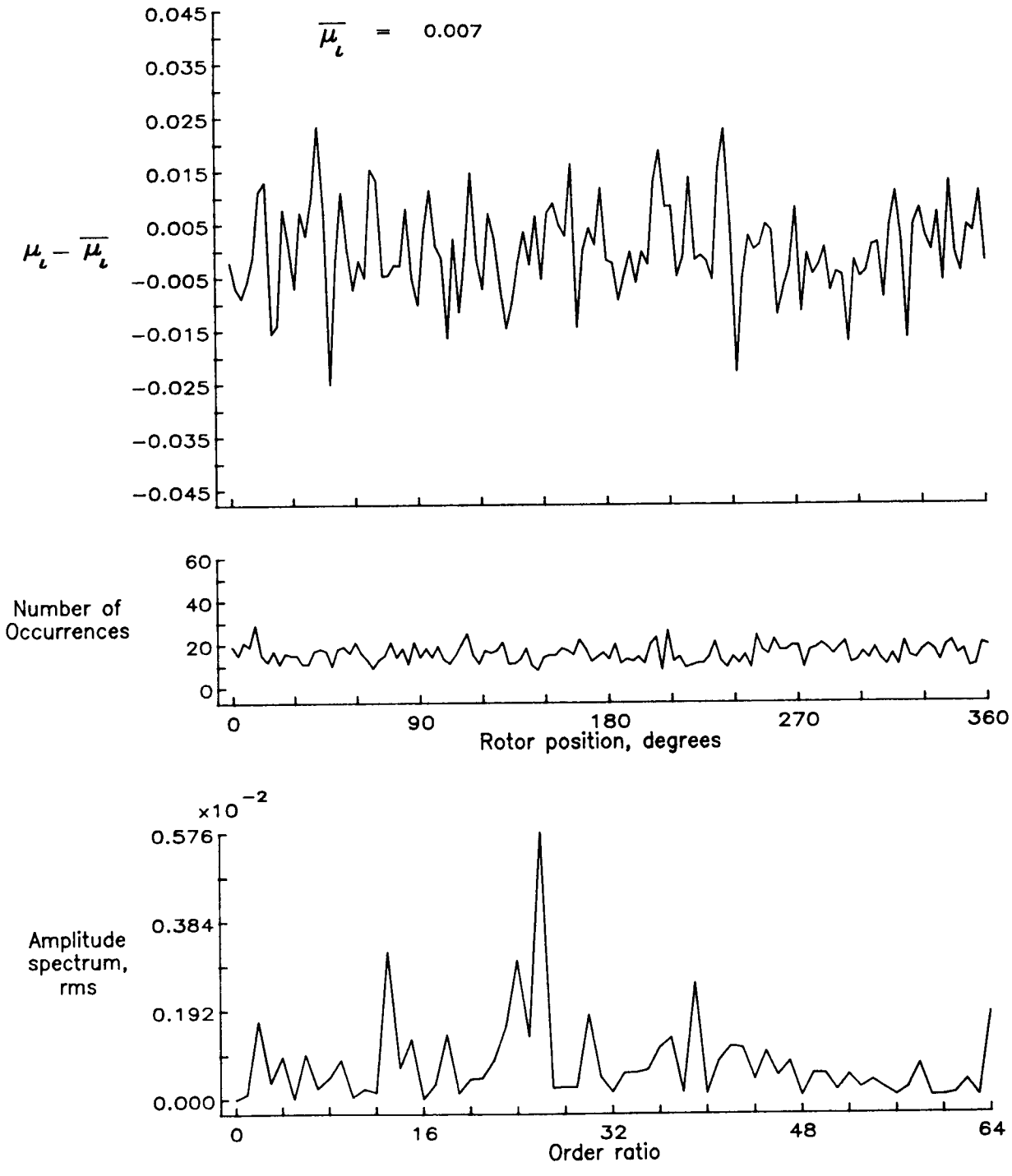


Figure 50.– Induced inflow velocity measured at 60 degrees and r/R of 1.10.

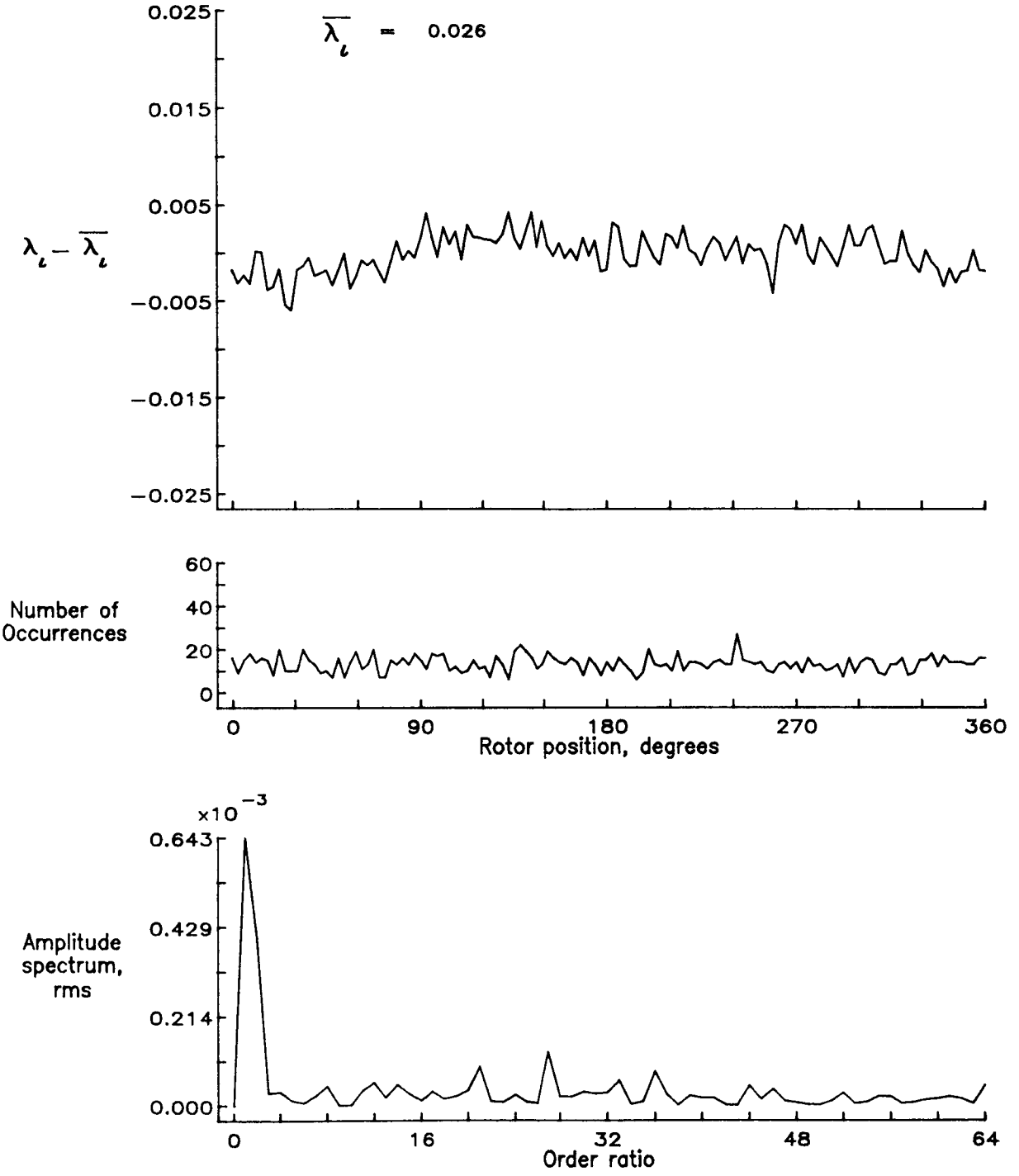


Figure 50.– Concluded.

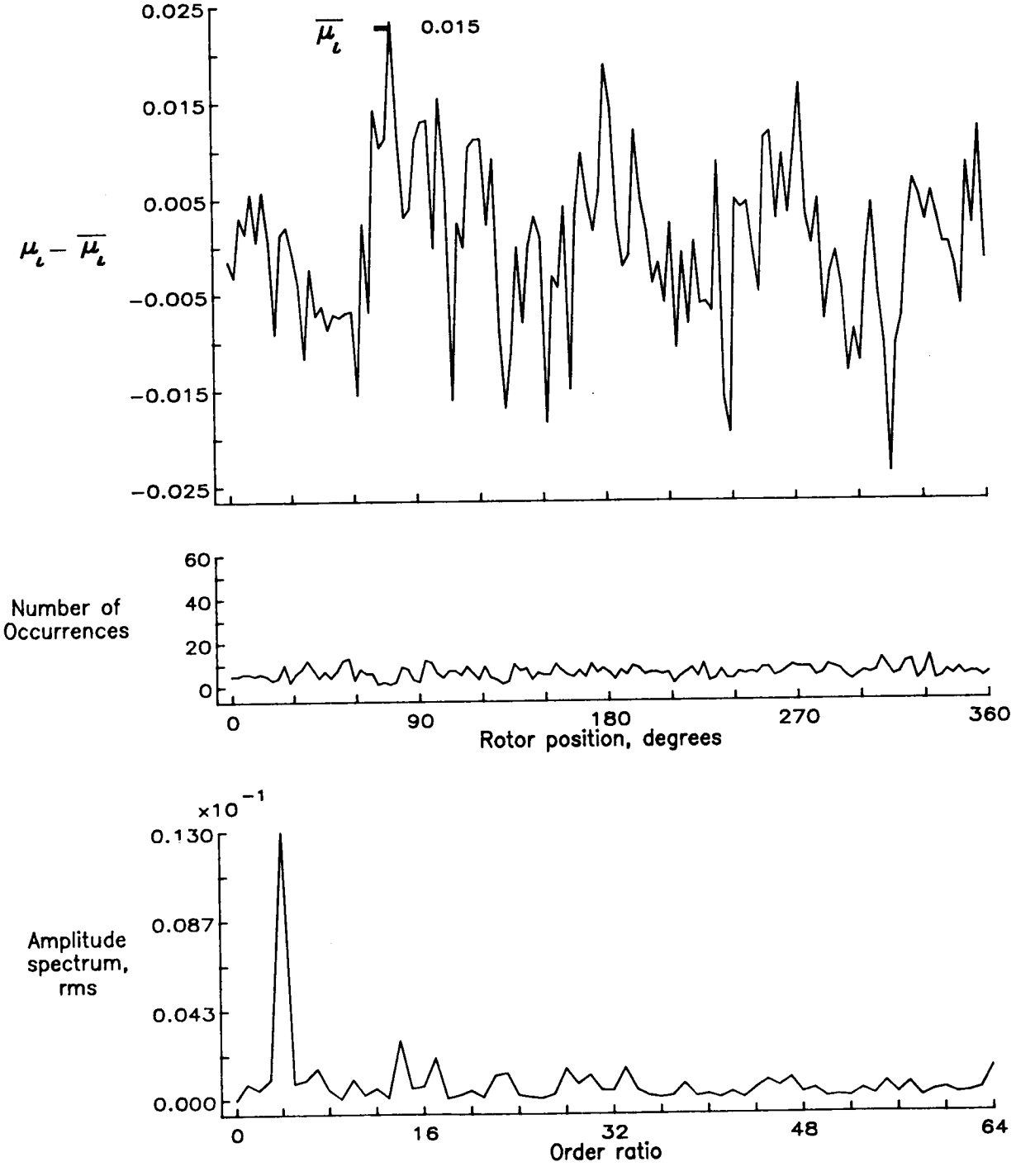


Figure 51.– Induced inflow velocity measured at 90 degrees and r/R of 0.20.

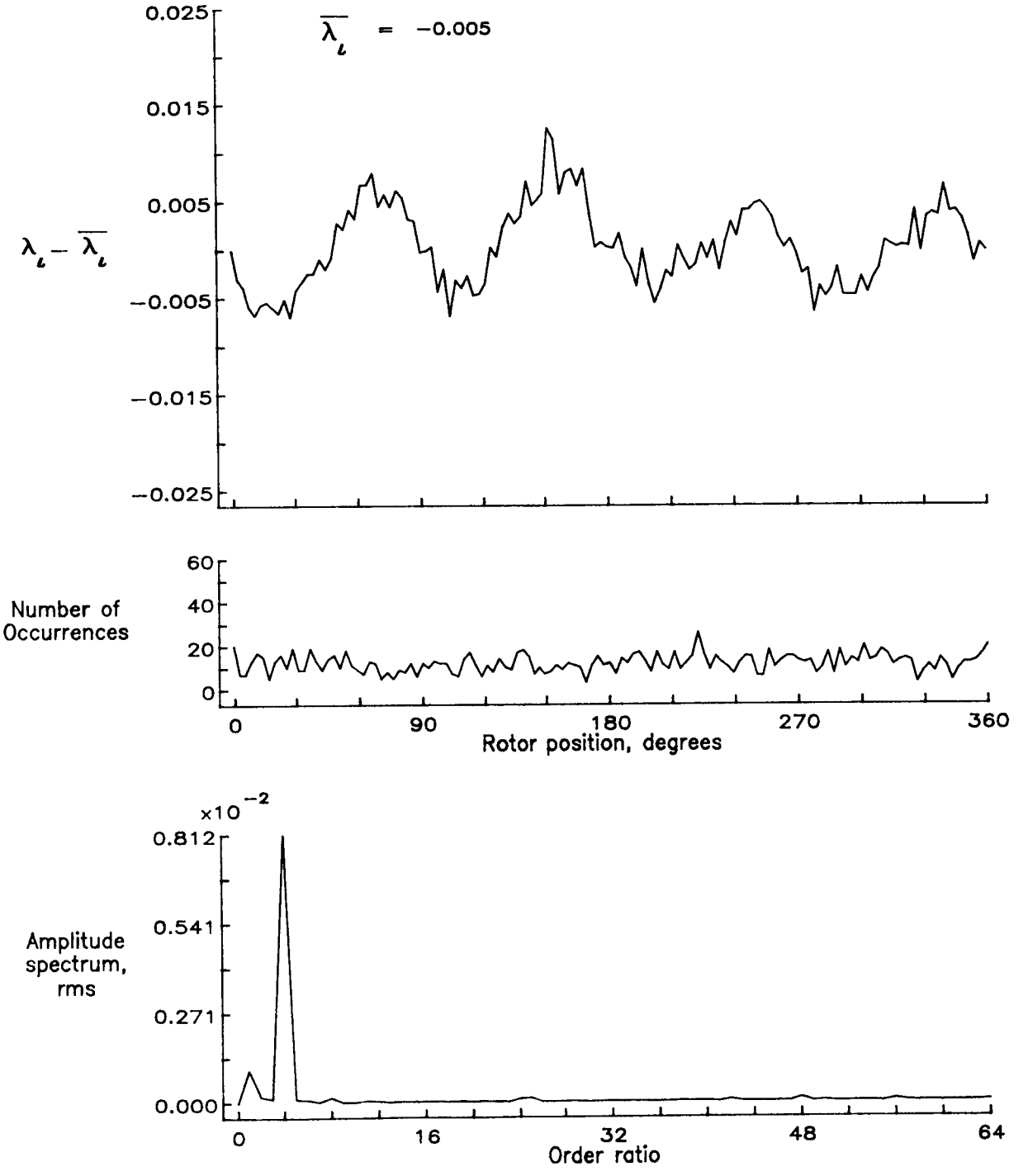


Figure 51.– Concluded.

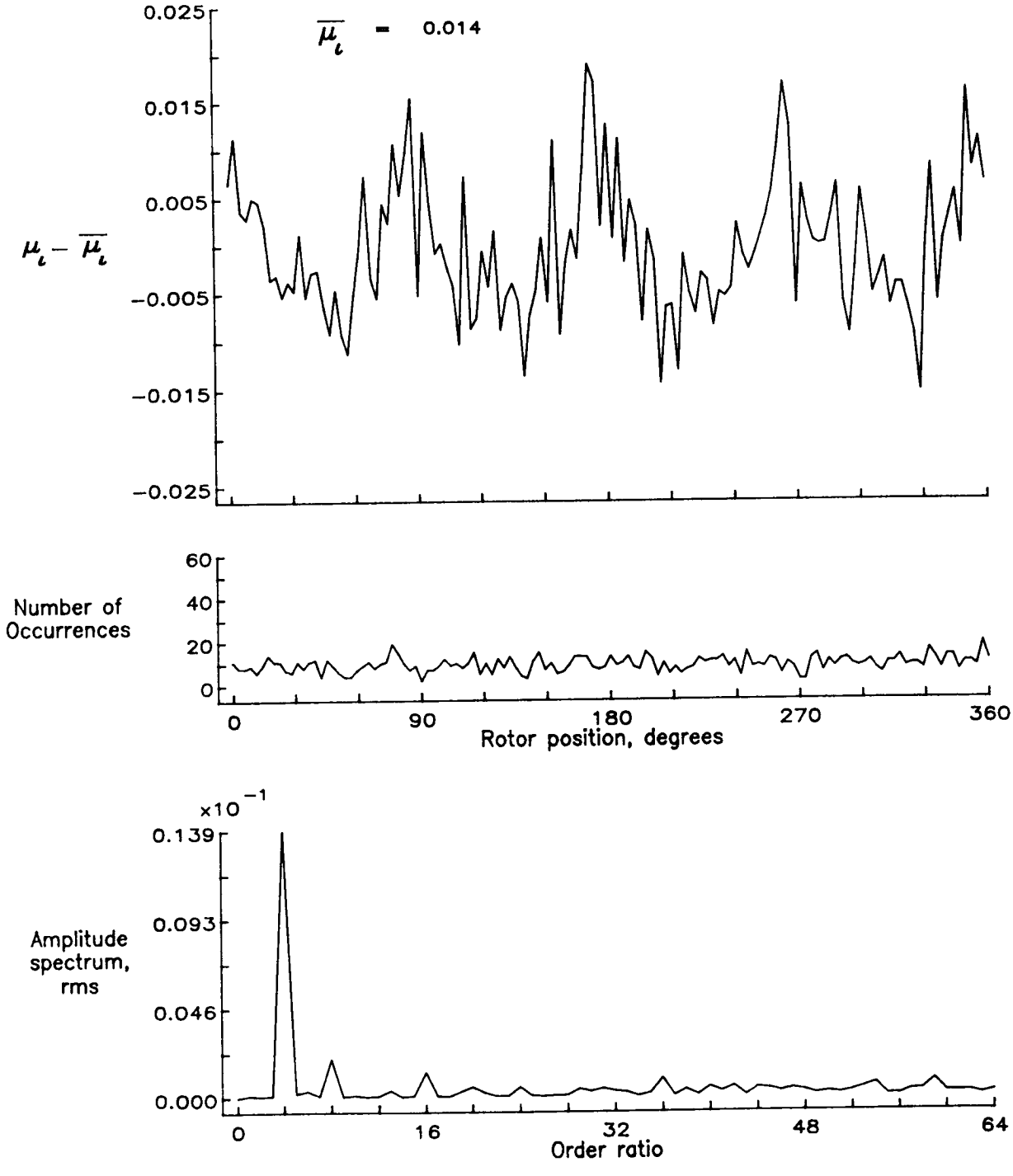


Figure 52.– Induced inflow velocity measured at 90 degrees and r/R of 0.40.

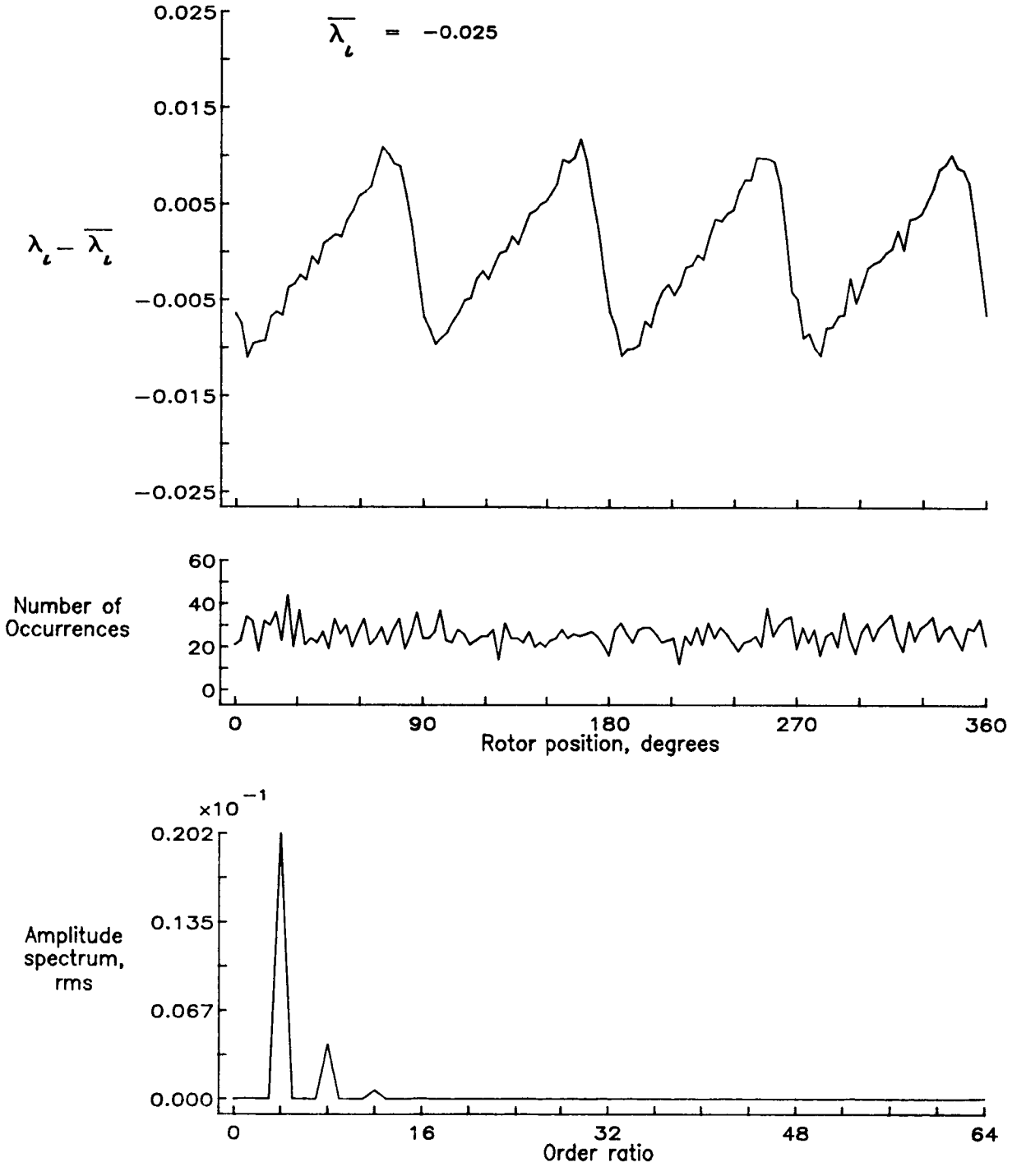


Figure 52.– Concluded.

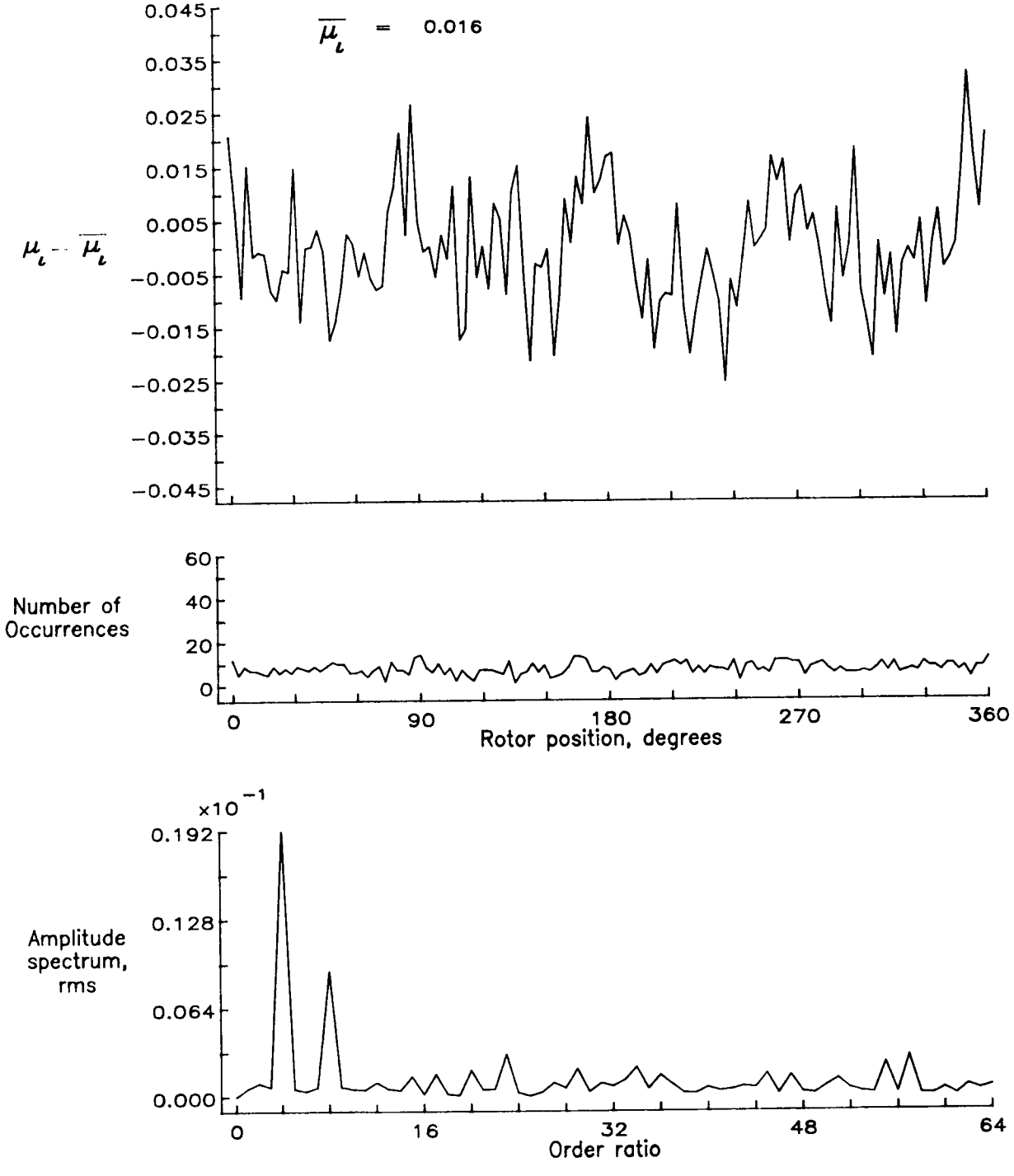


Figure 53.– Induced inflow velocity measured at 90 degrees and r/R of 0.50.

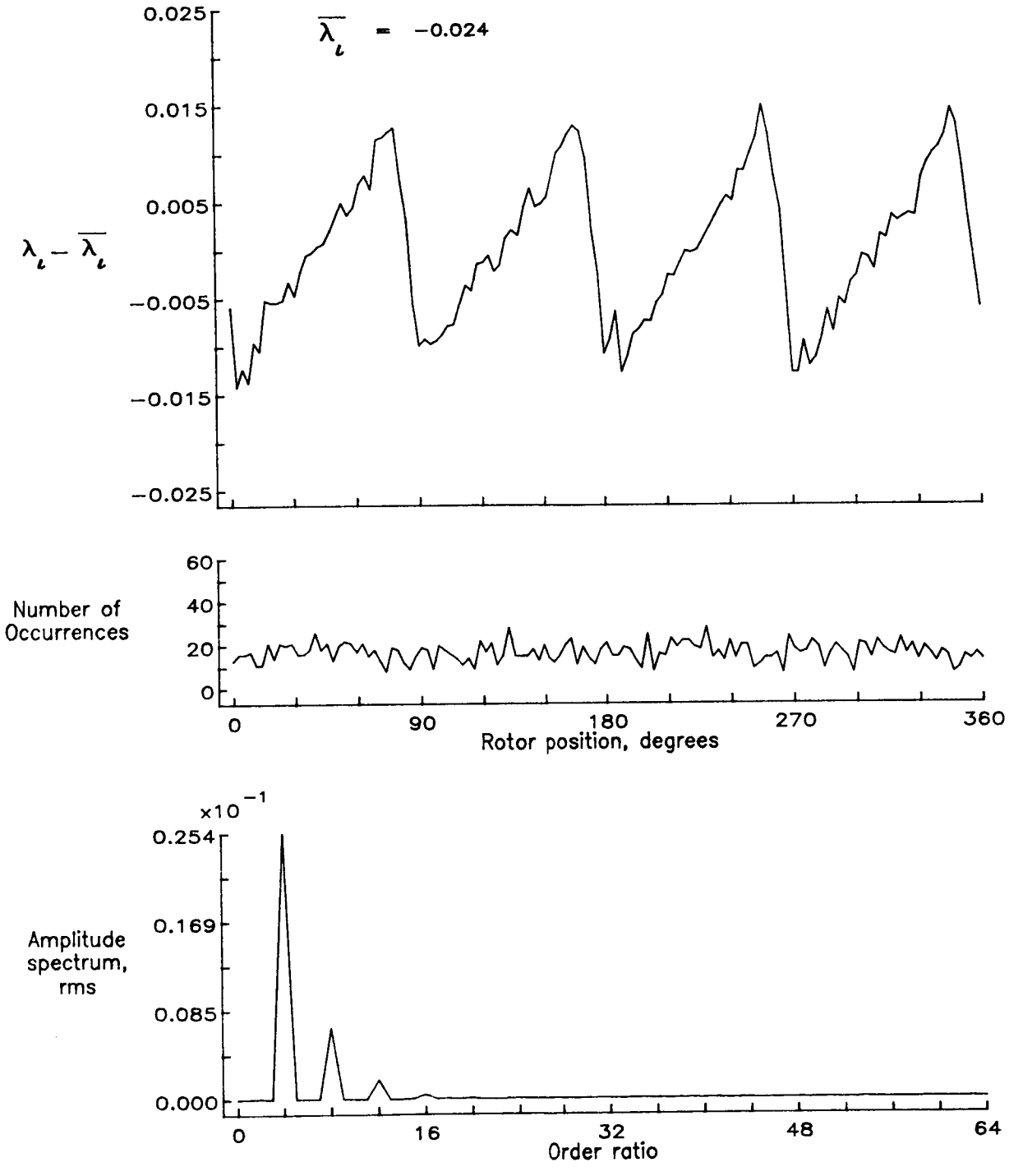


Figure 53.– Concluded.

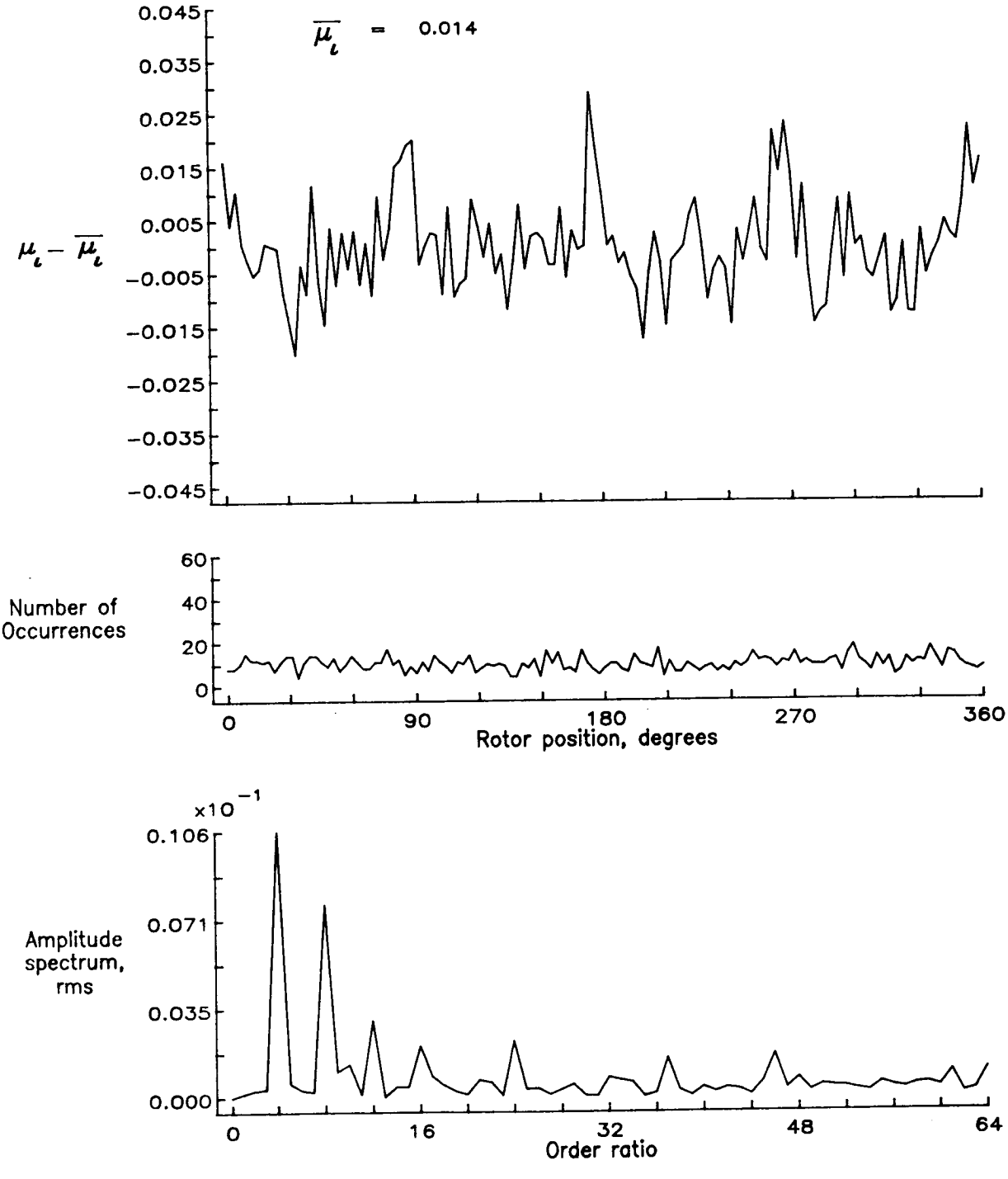


Figure 54.– Induced inflow velocity measured at 90 degrees and r/R of 0.70.

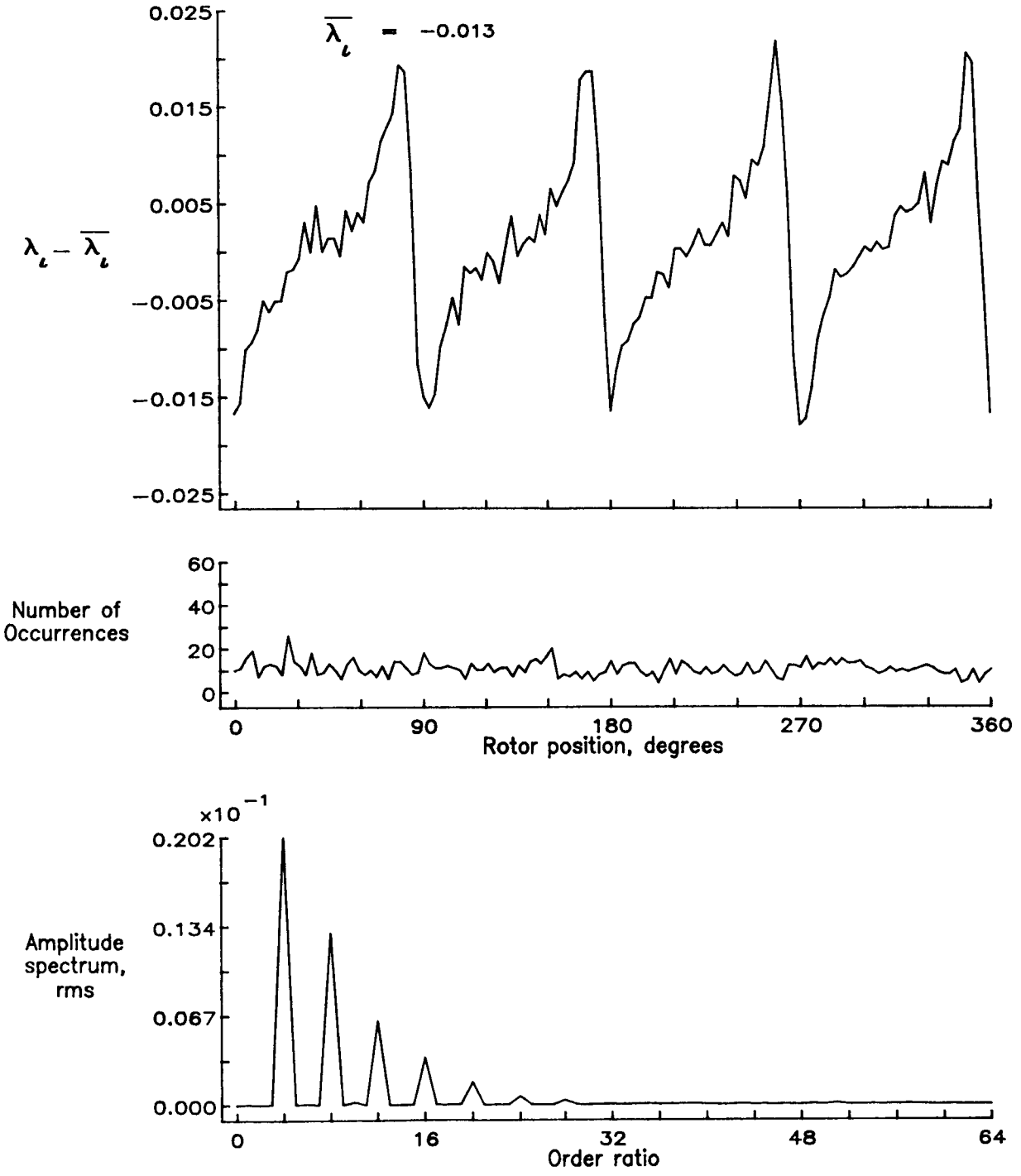


Figure 54.— Concluded.

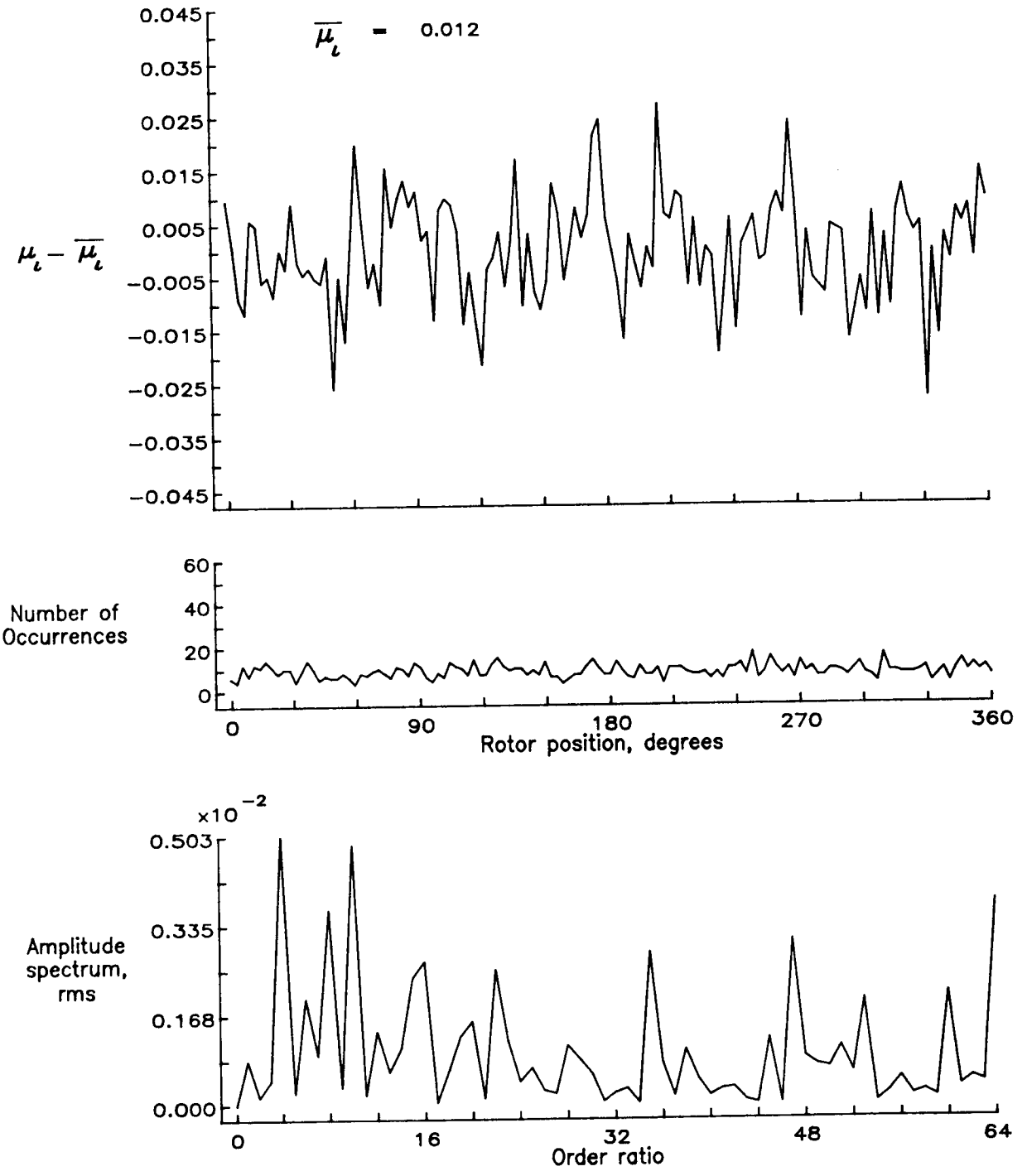


Figure 55.– Induced inflow velocity measured at 90 degrees and r/R of 0.74.

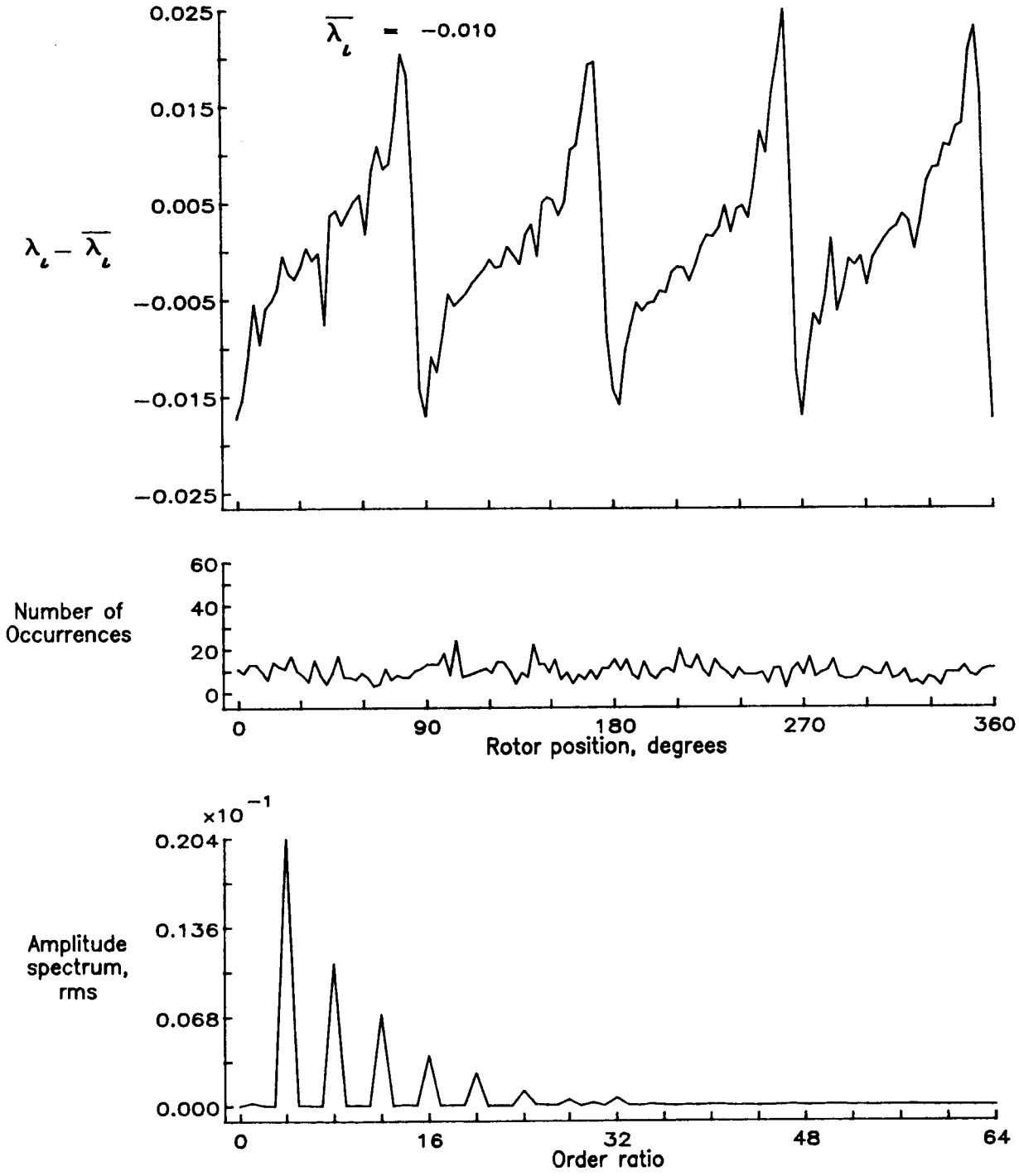


Figure 55.– Concluded.

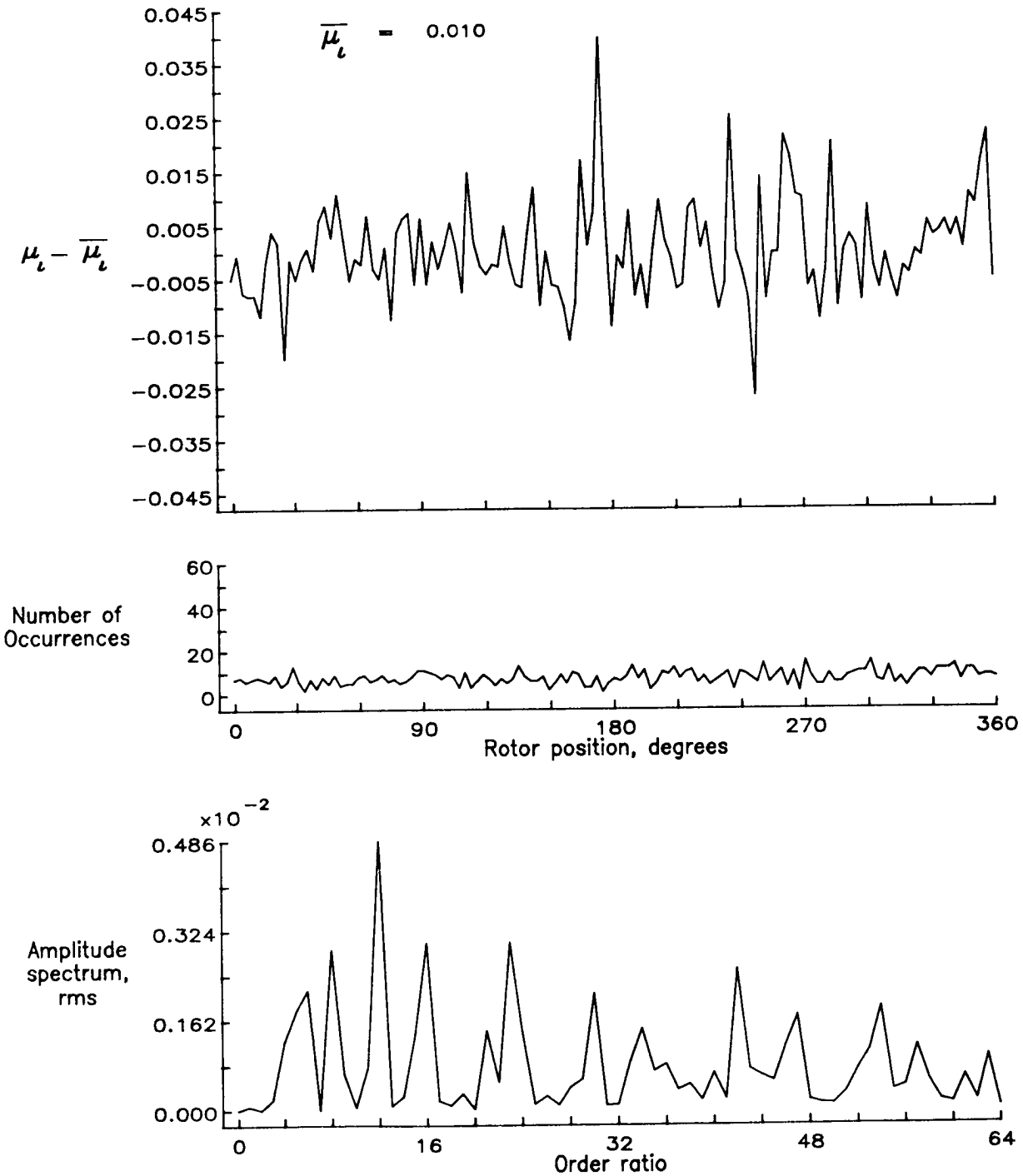


Figure 56.– Induced inflow velocity measured at 90 degrees and r/R of 0.78.

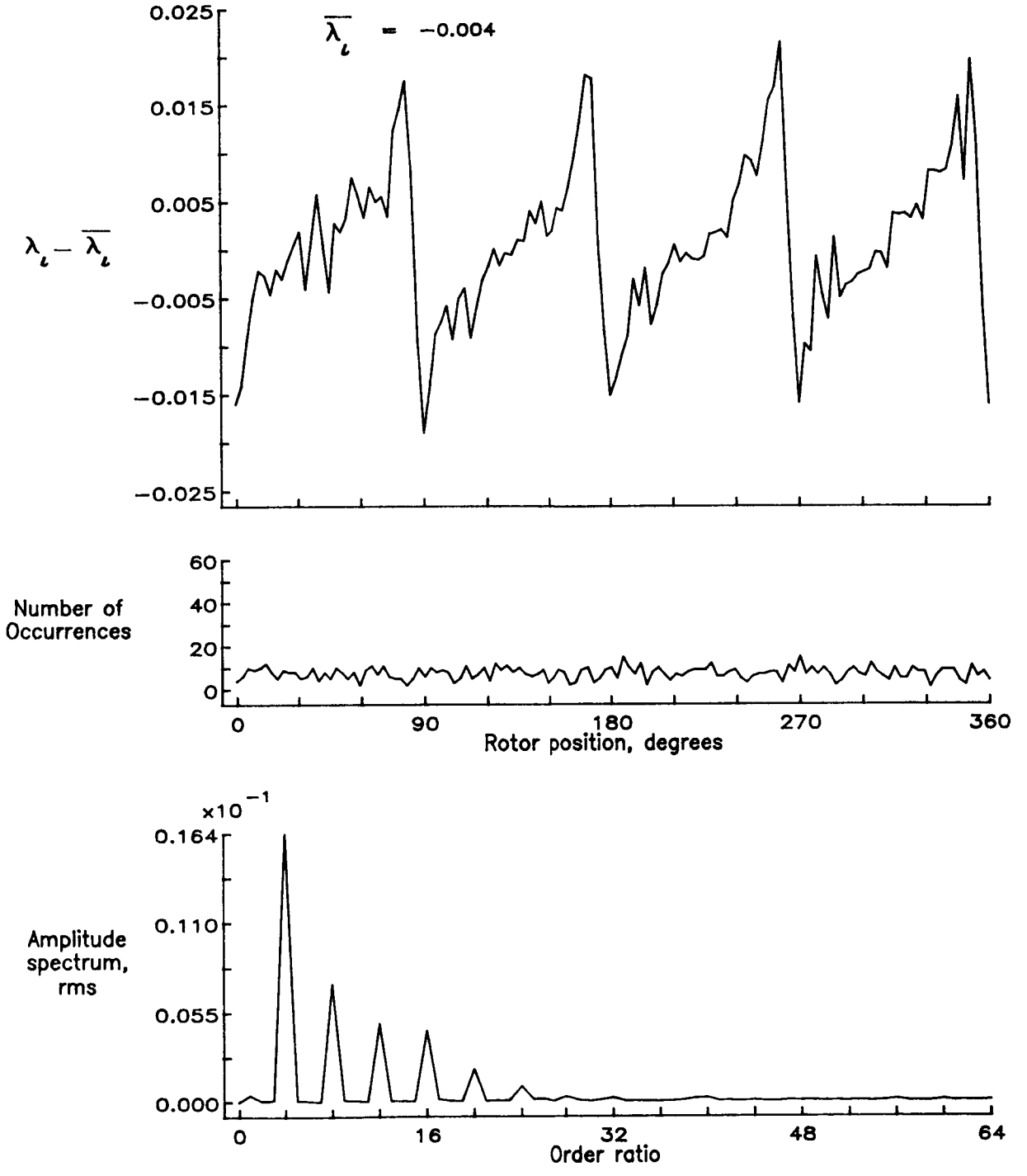


Figure 56.– Concluded.

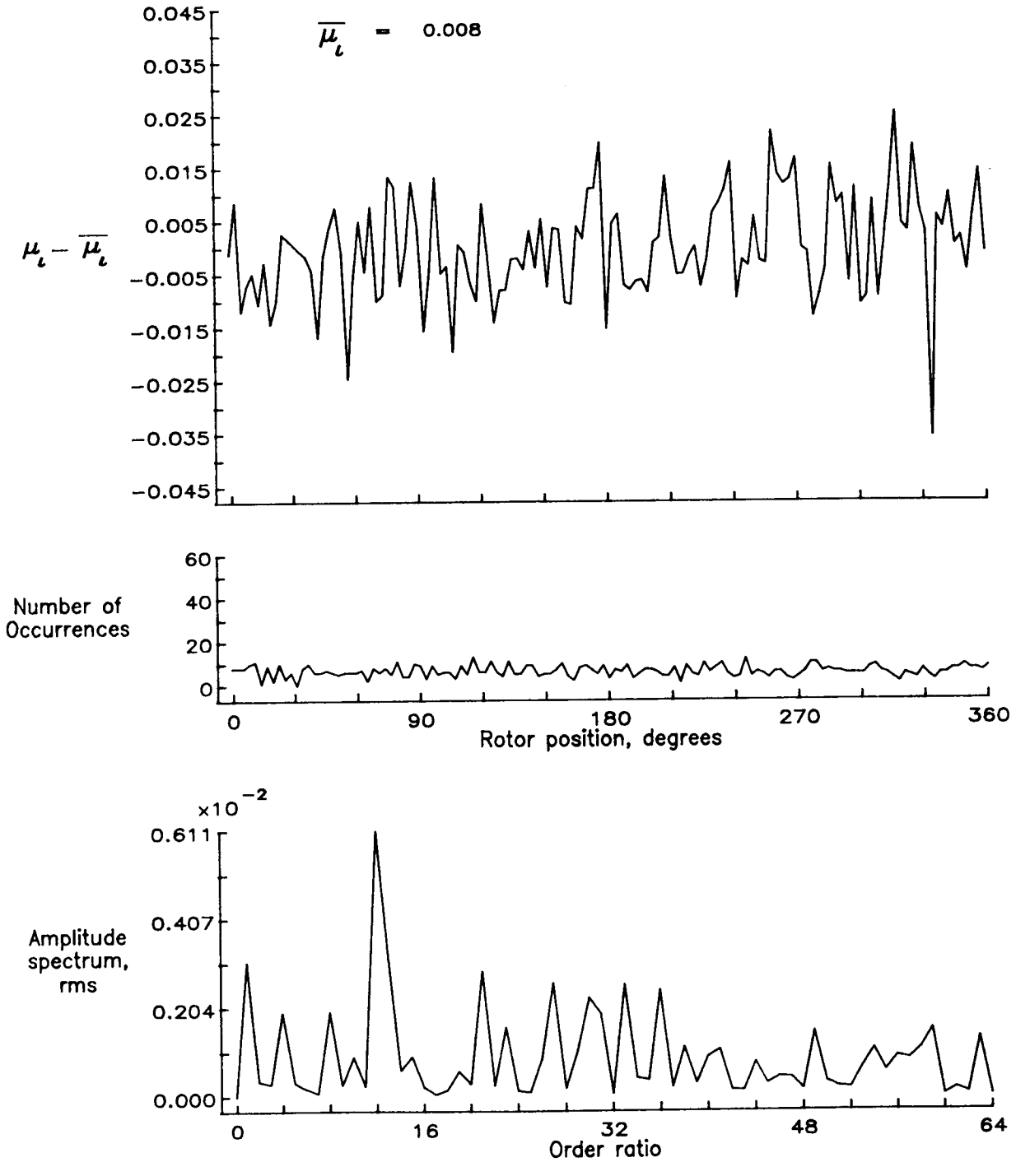


Figure 57.– Induced inflow velocity measured at 90 degrees and r/R of 0.82.

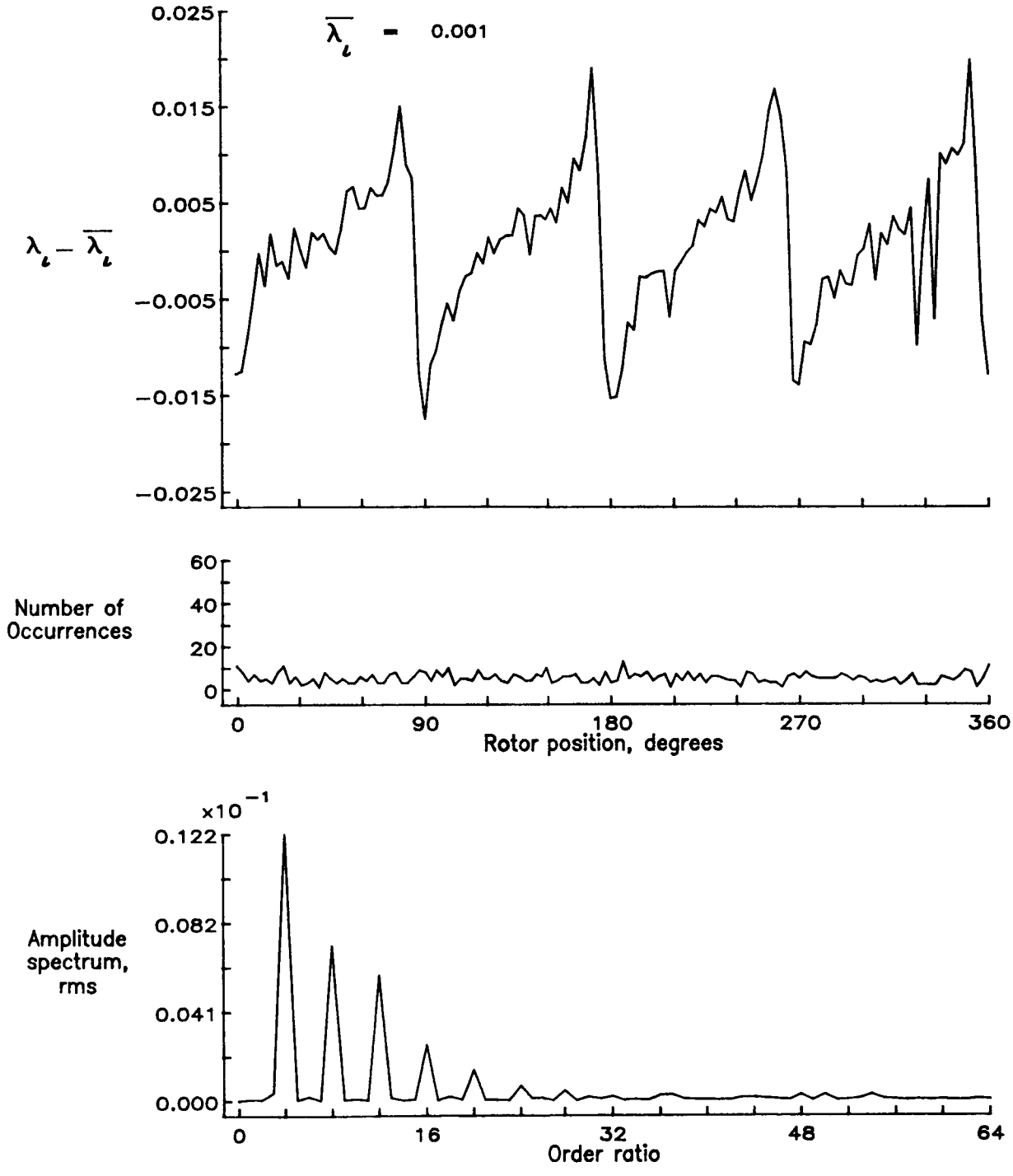


Figure 57.– Concluded.

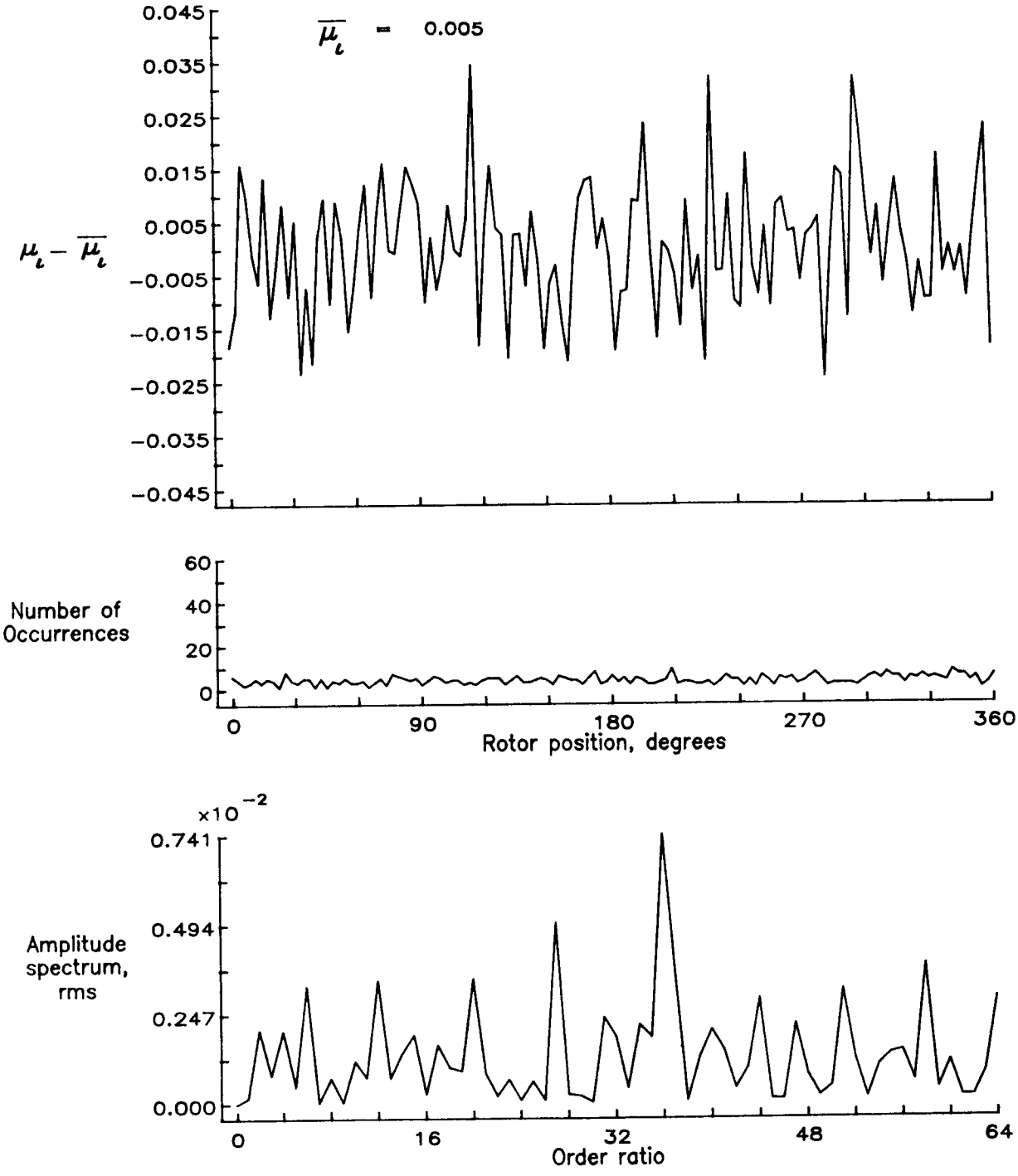


Figure 58.– Induced inflow velocity measured at 90 degrees and r/R of 0.86.

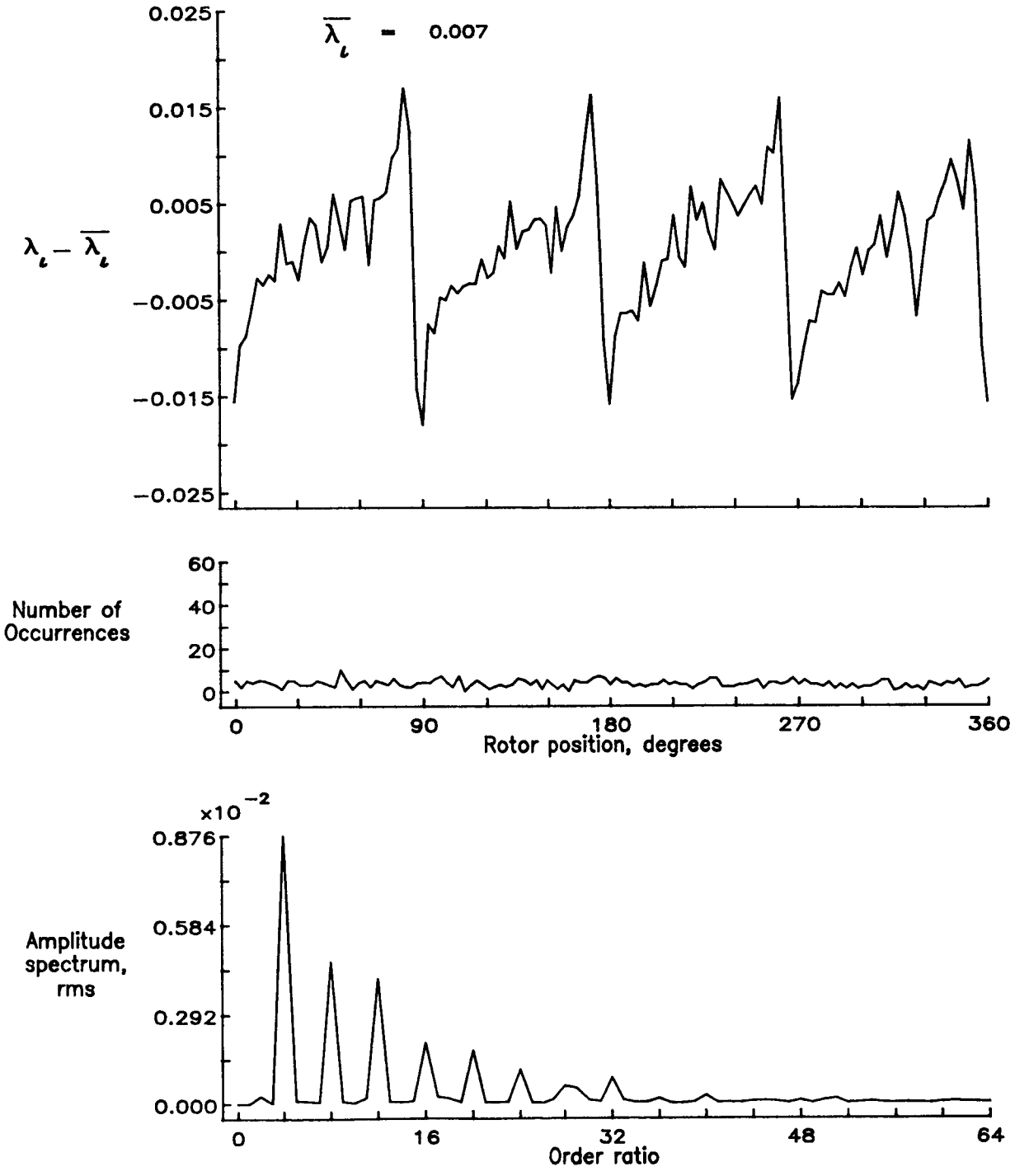


Figure 58.– Concluded.

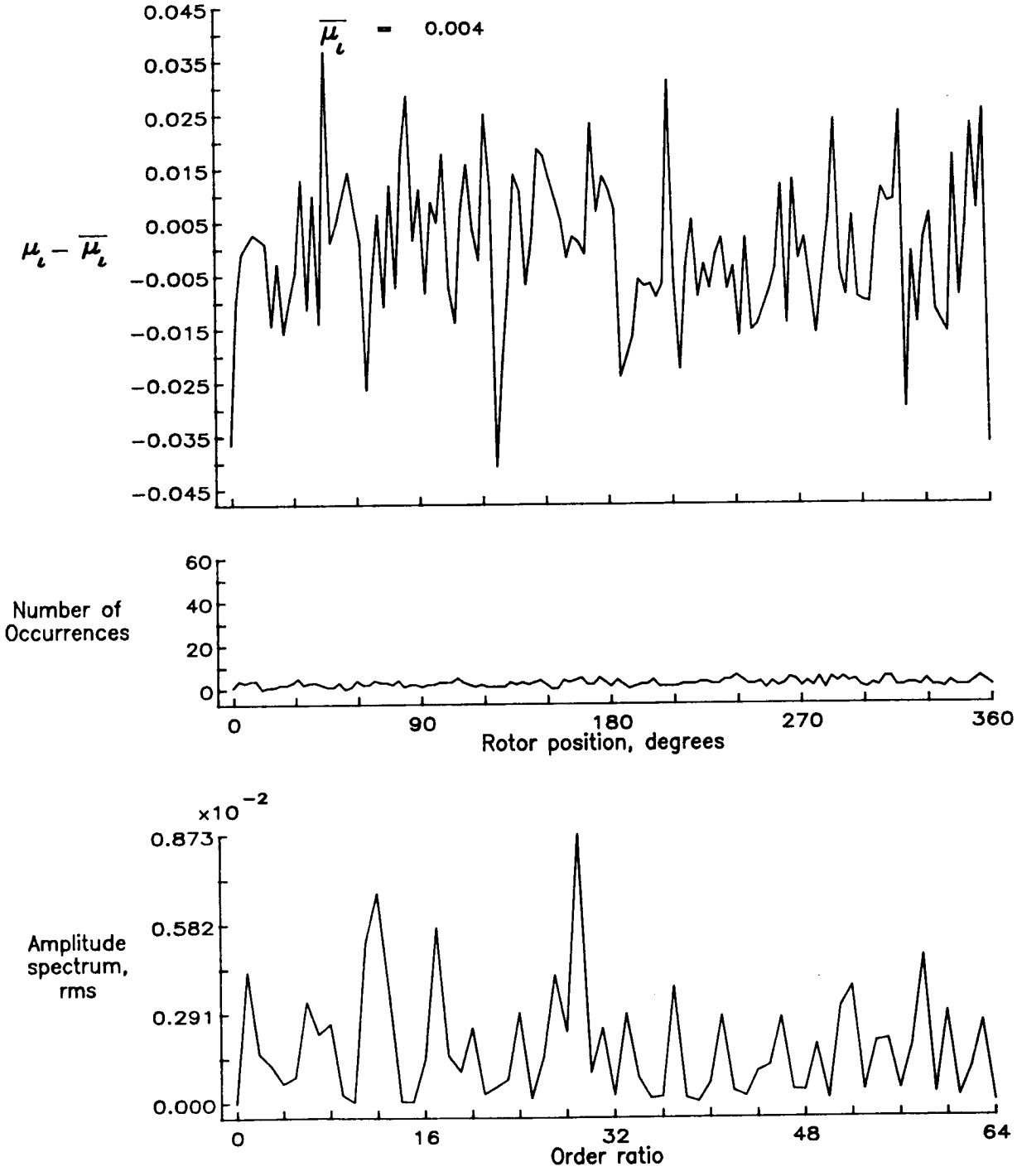


Figure 59.– Induced inflow velocity measured at 90 degrees and r/R of 0.90.

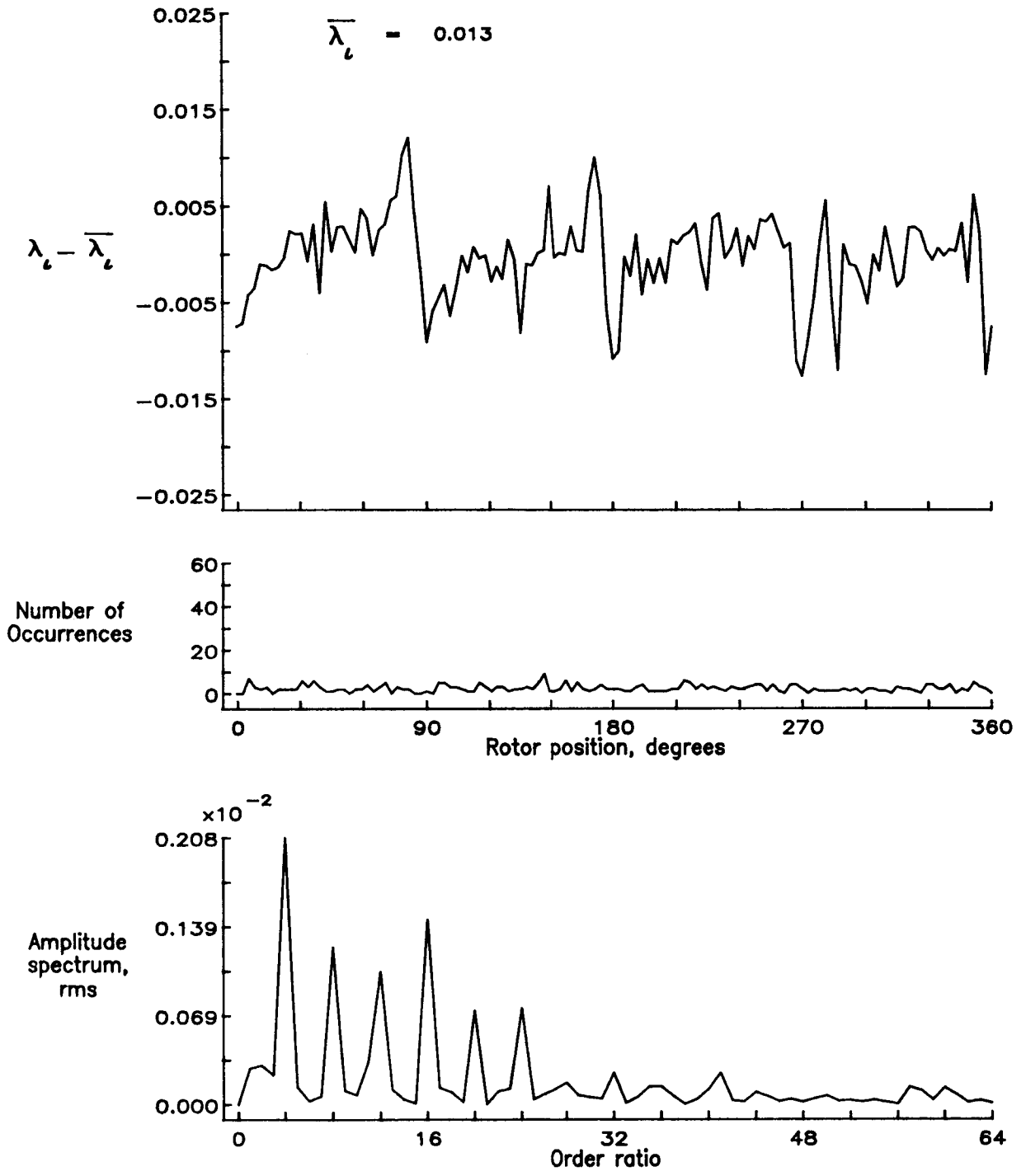


Figure 59.– Concluded.

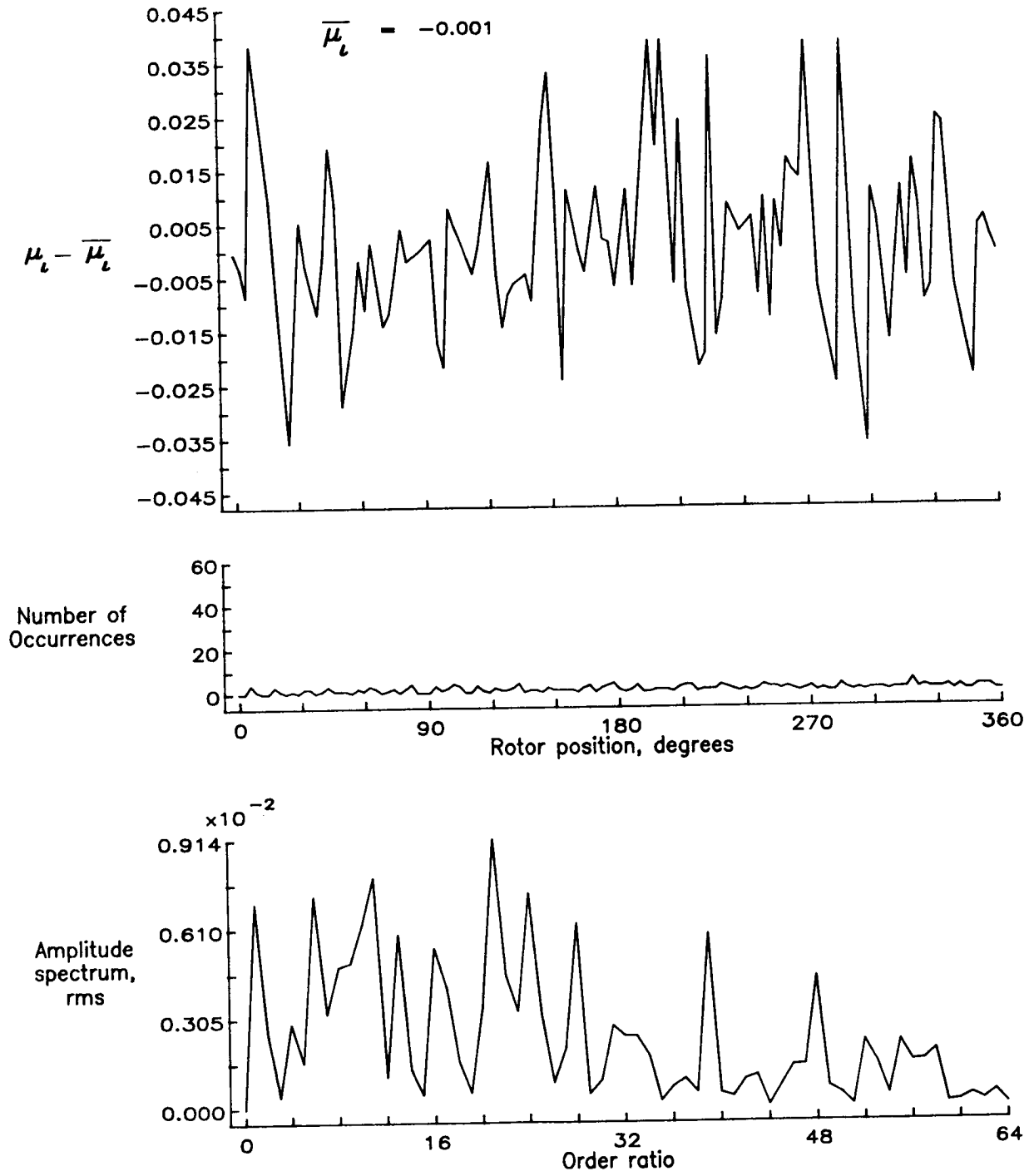


Figure 60.– Induced inflow velocity measured at 90 degrees and r/R of 0.94.

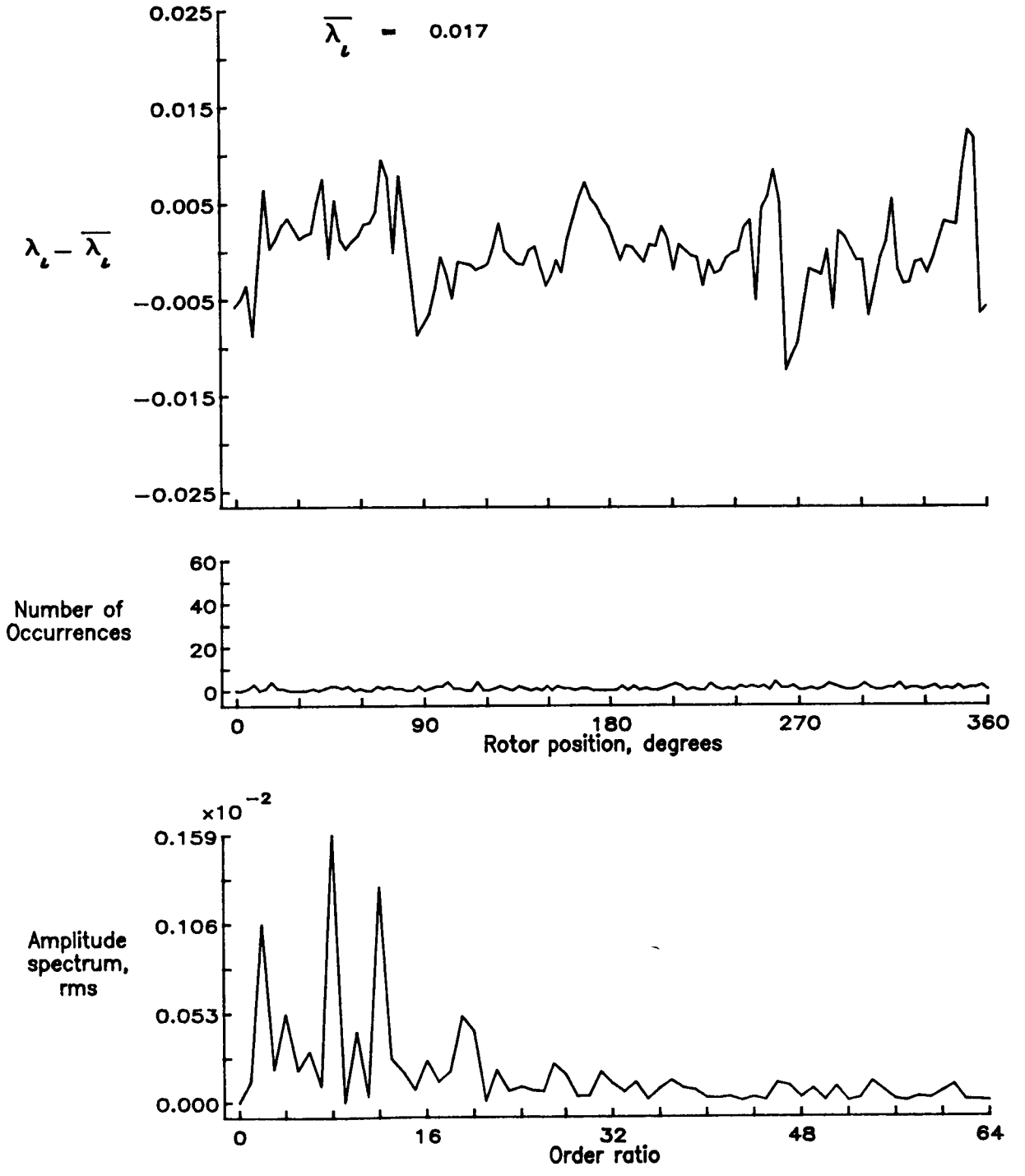


Figure 60.– Concluded.

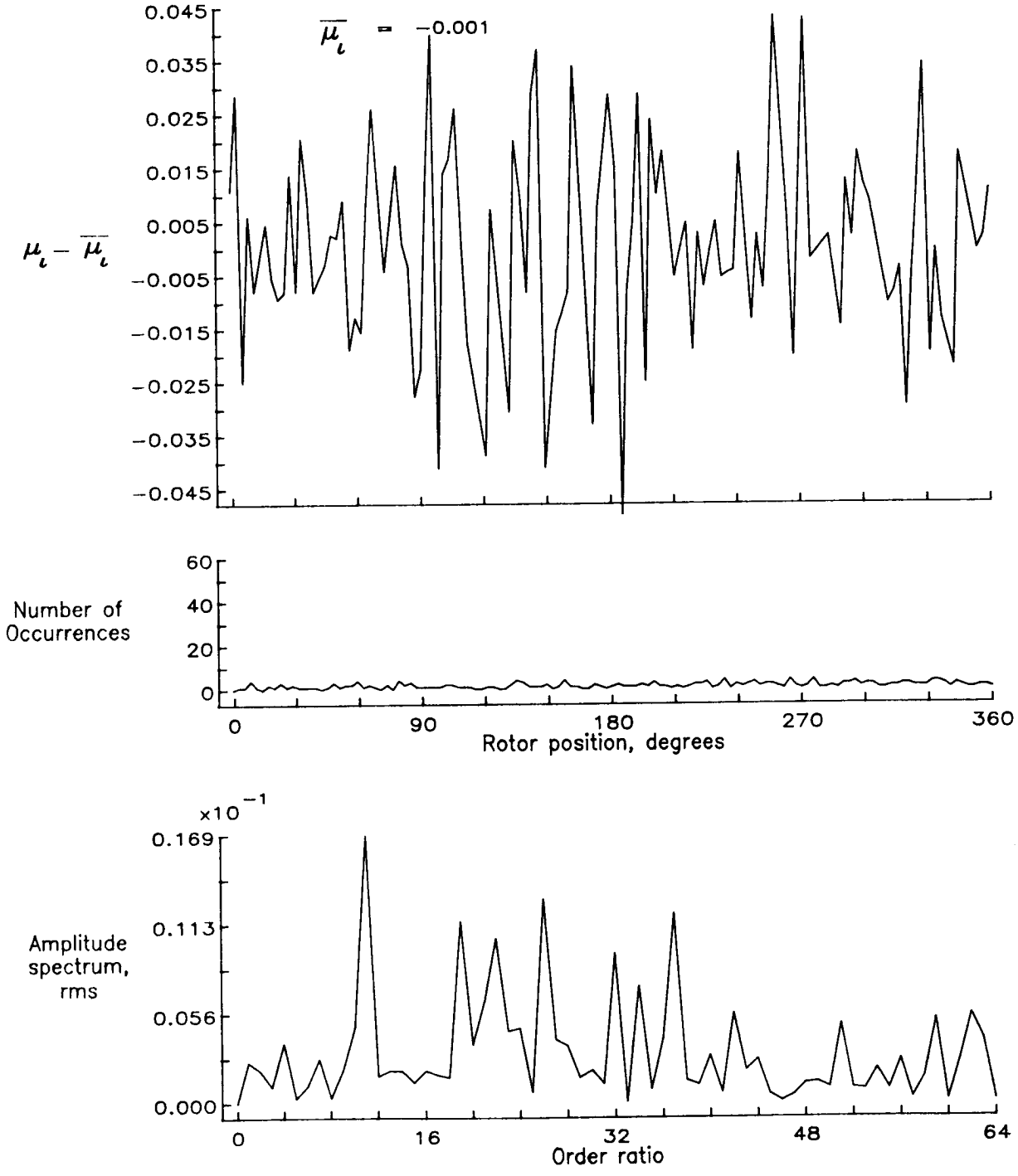


Figure 61.– Induced inflow velocity measured at 90 degrees and r/R of 0.98.

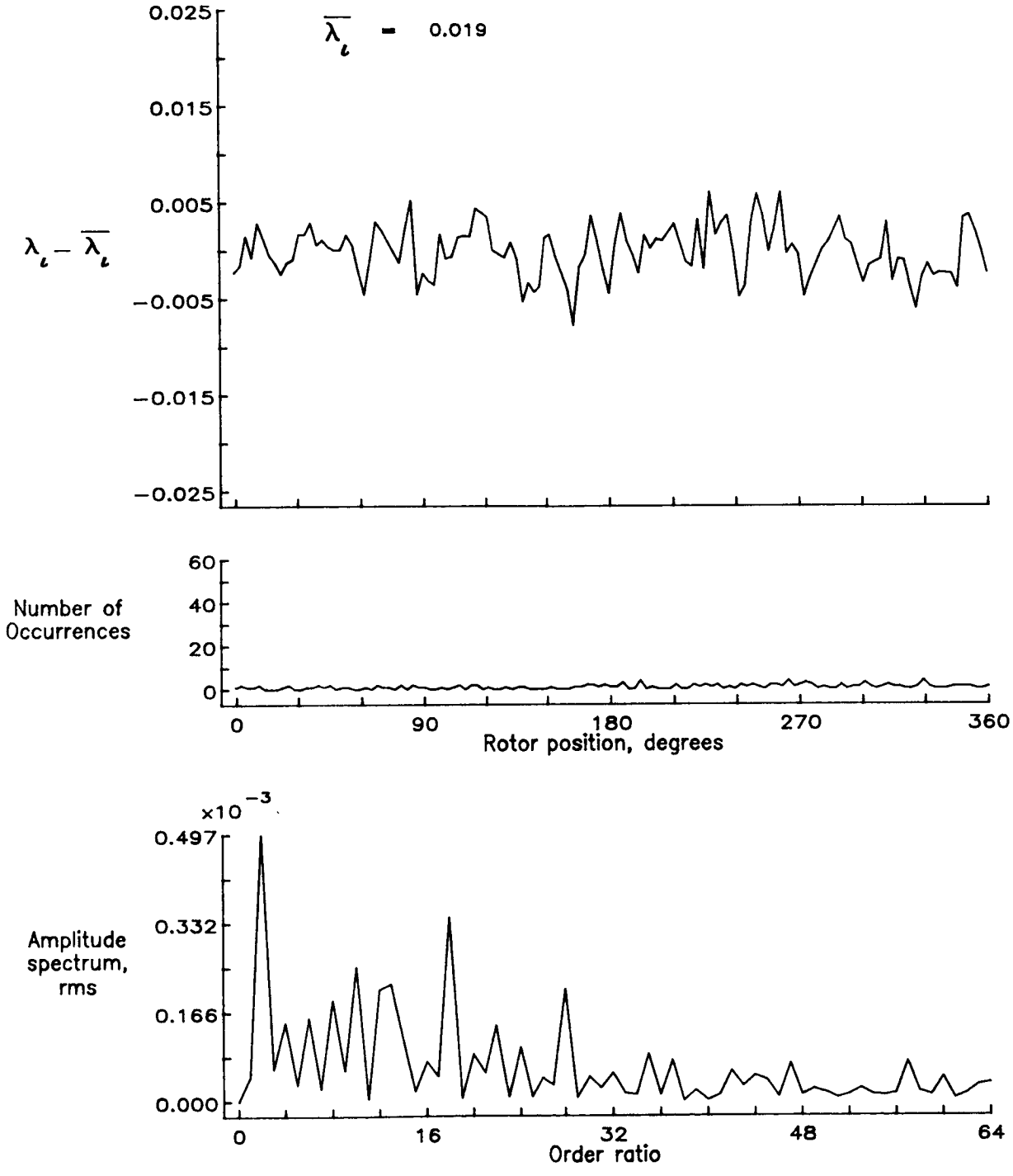


Figure 61.– Concluded.

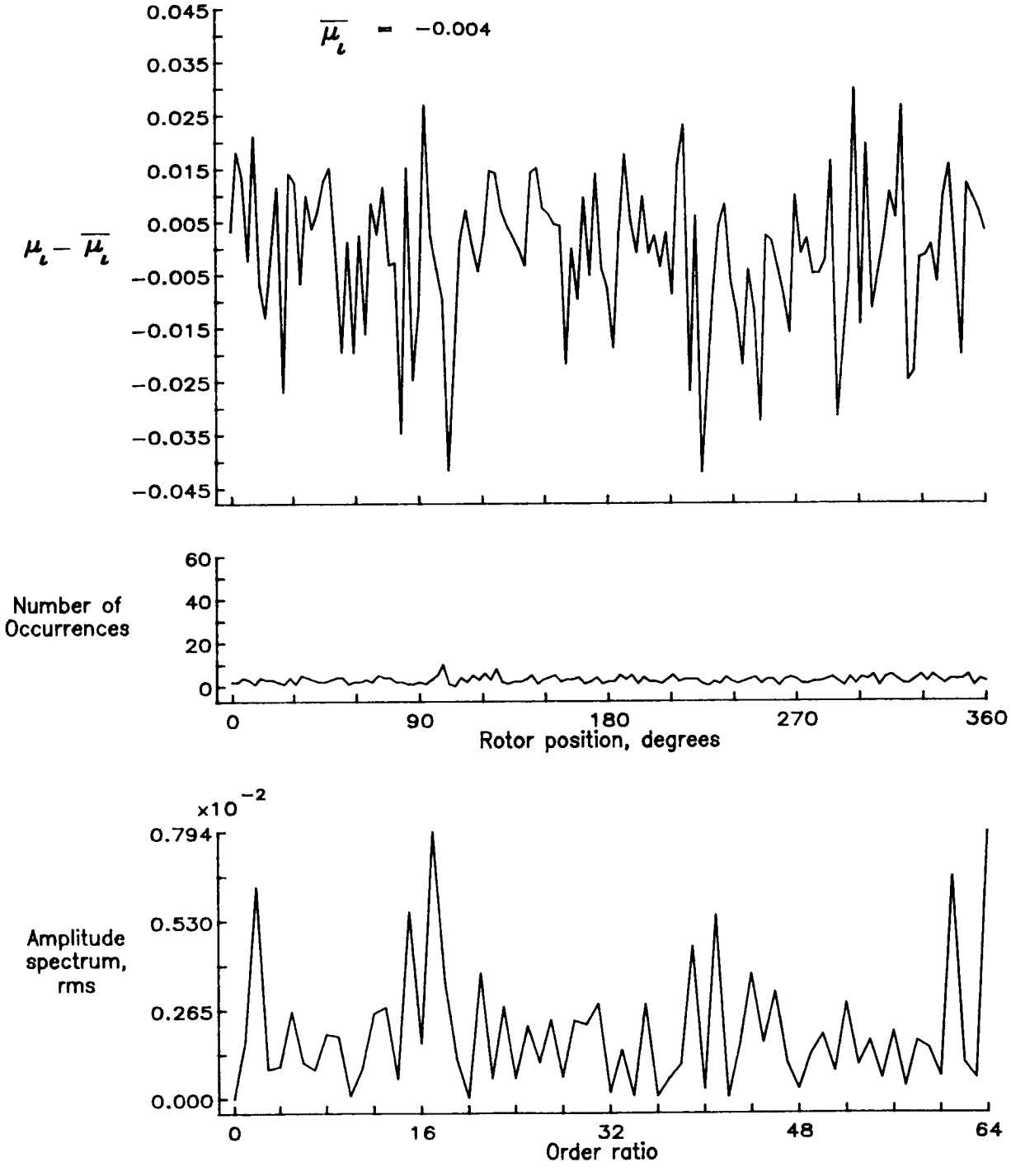


Figure 62.– Induced inflow velocity measured at 120 degrees and r/R of 0.20.

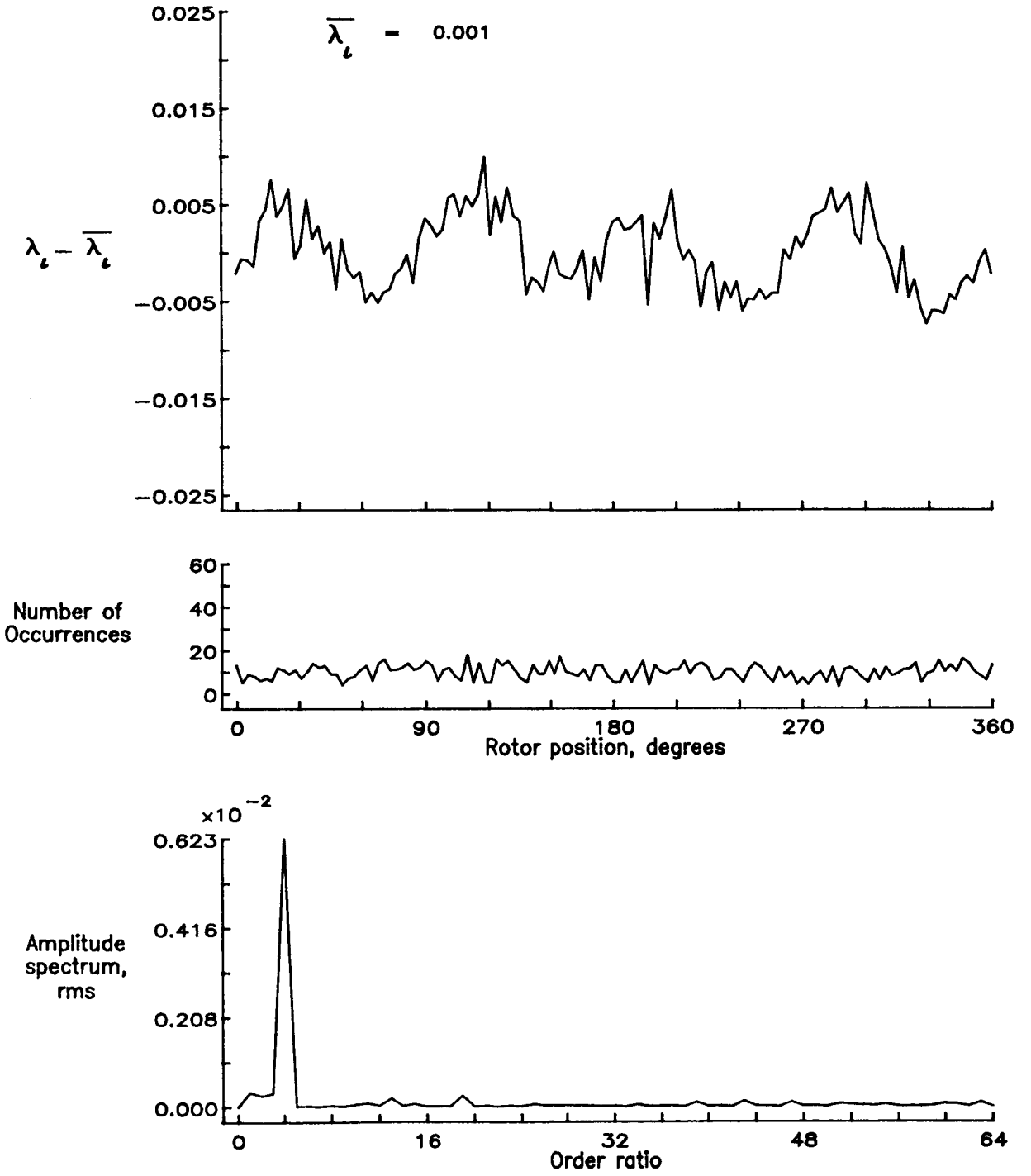


Figure 62.– Concluded.

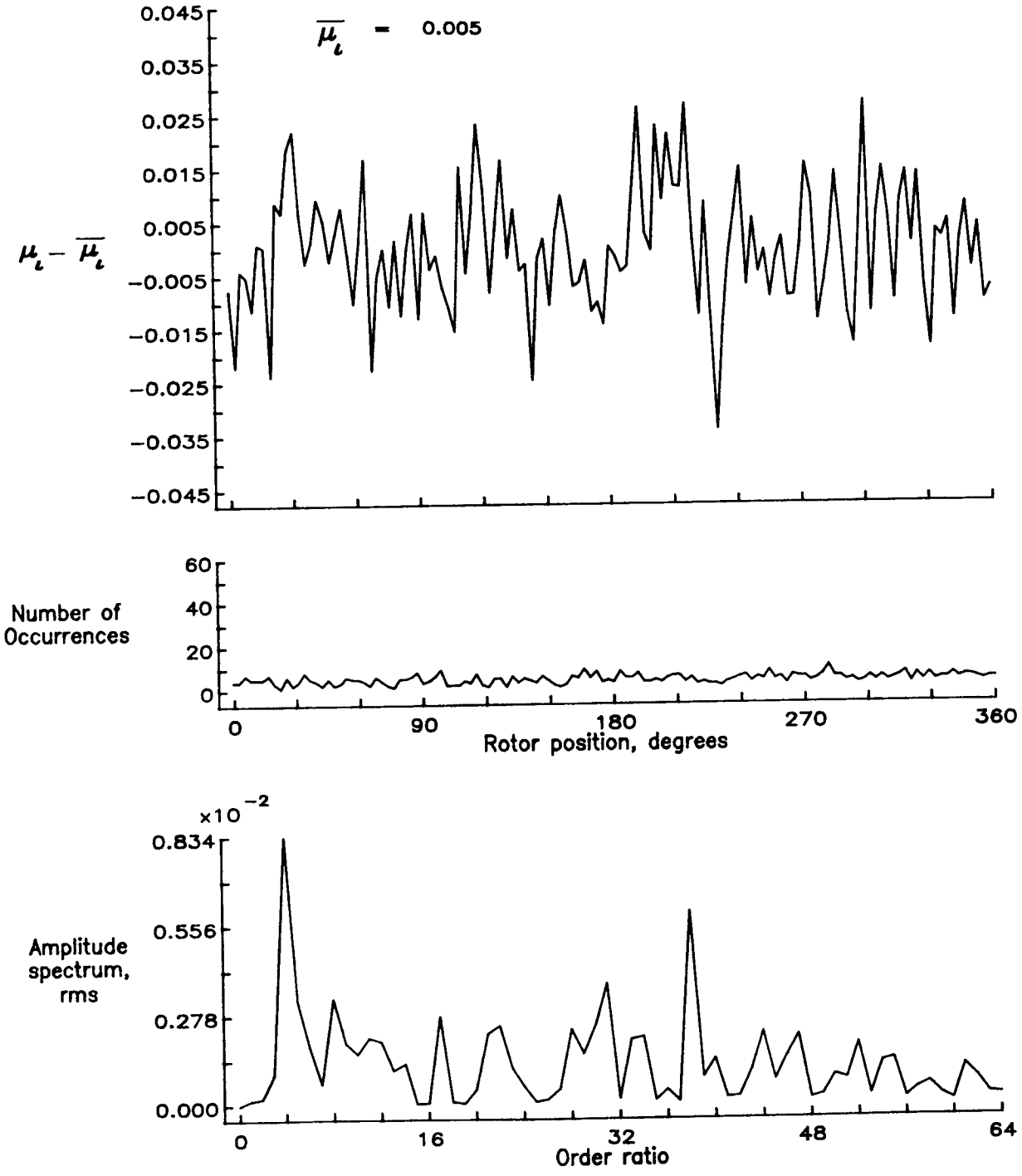


Figure 63.– Induced inflow velocity measured at 120 degrees and r/R of 0.40.

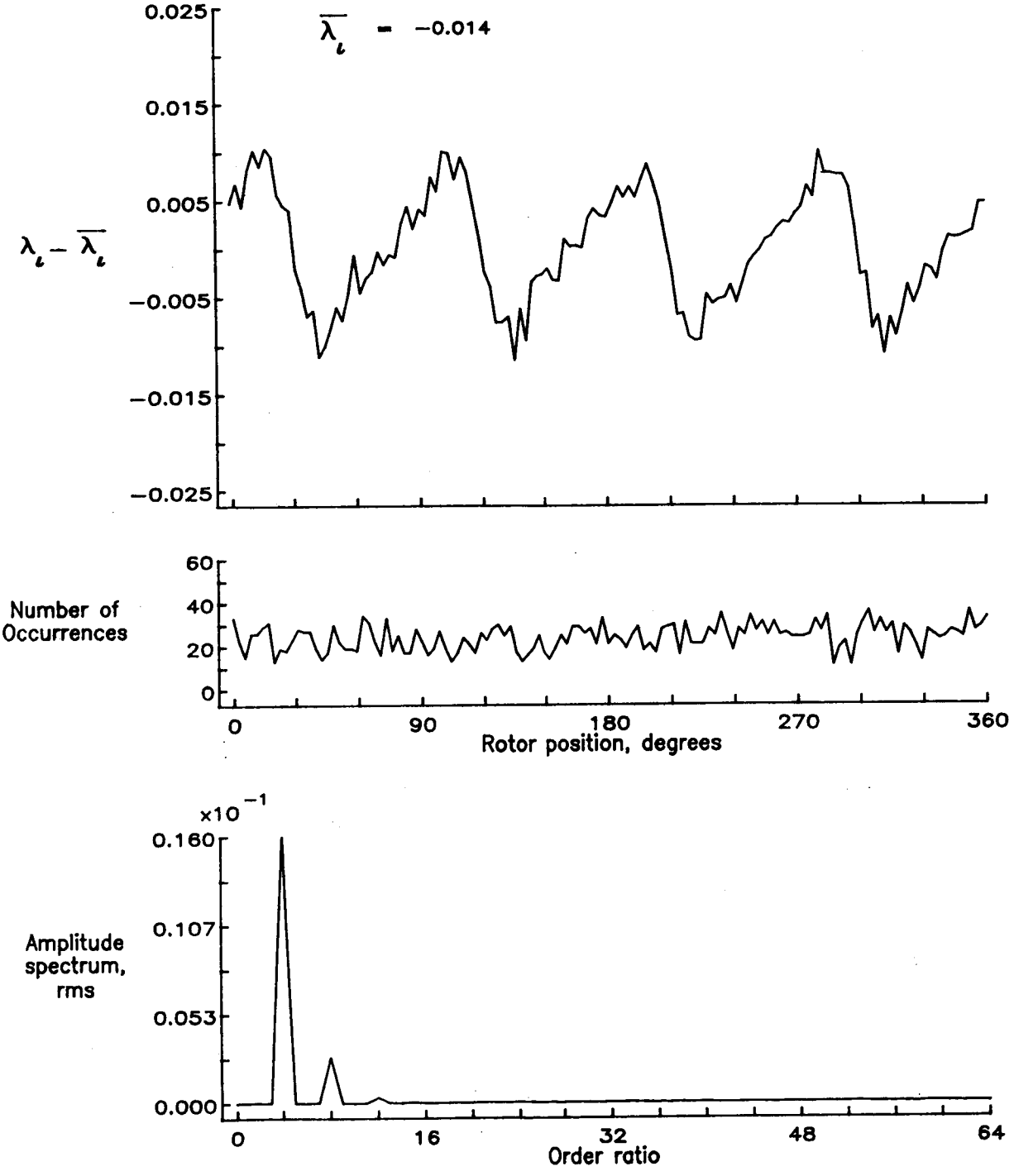


Figure 63.– Concluded.

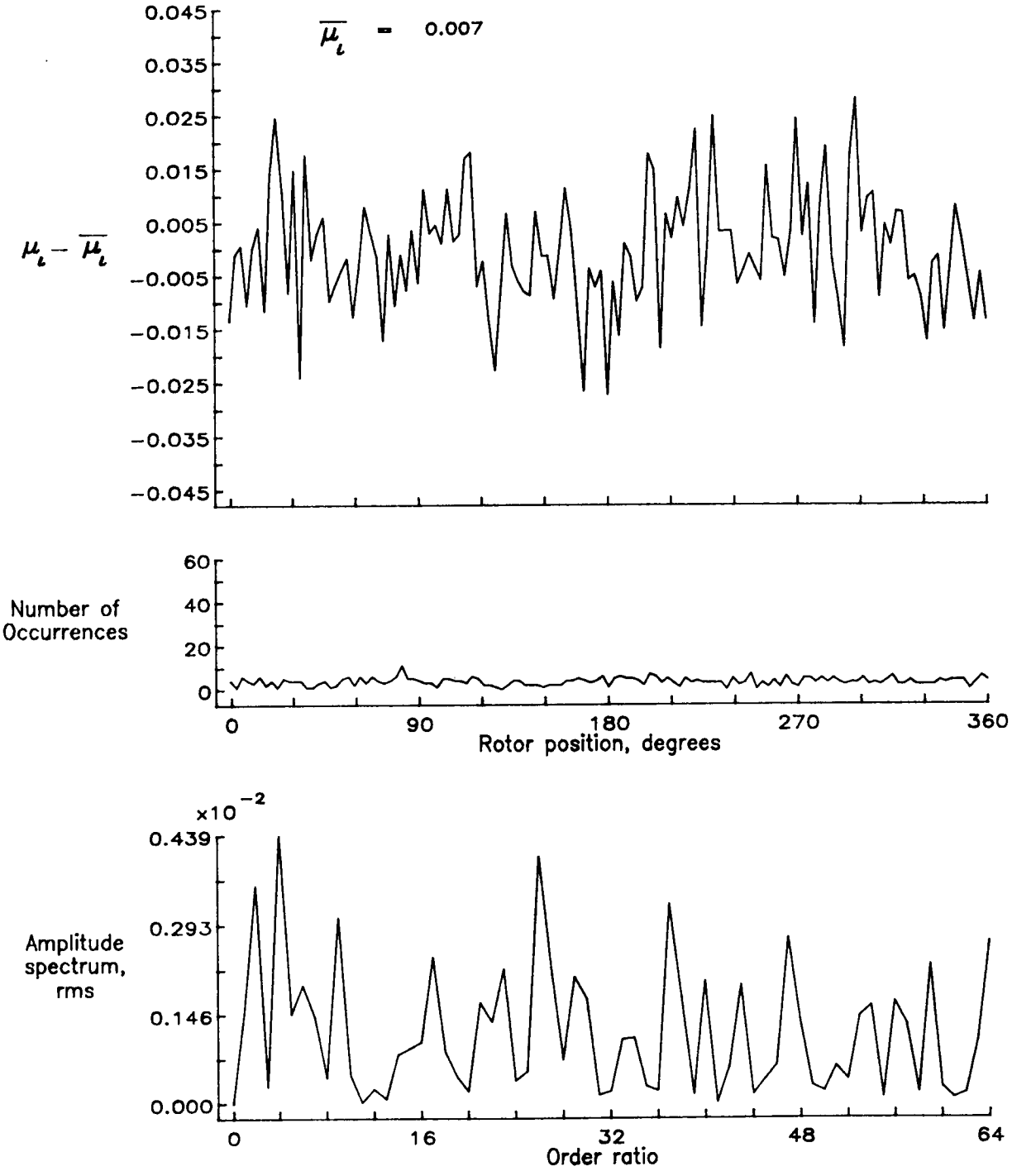


Figure 64.– Induced inflow velocity measured at 120 degrees and r/R of 0.50.

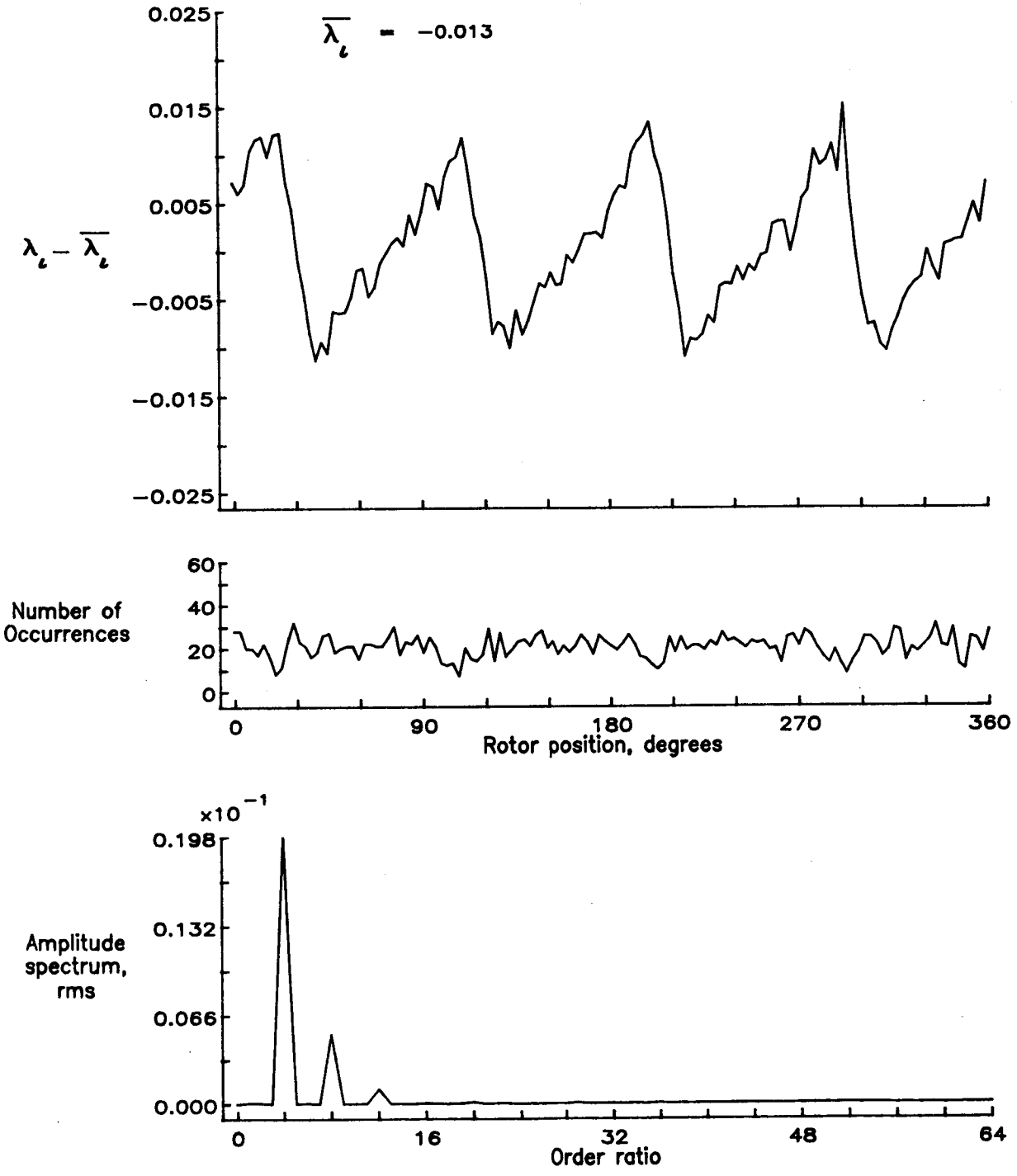


Figure 64.– Concluded.

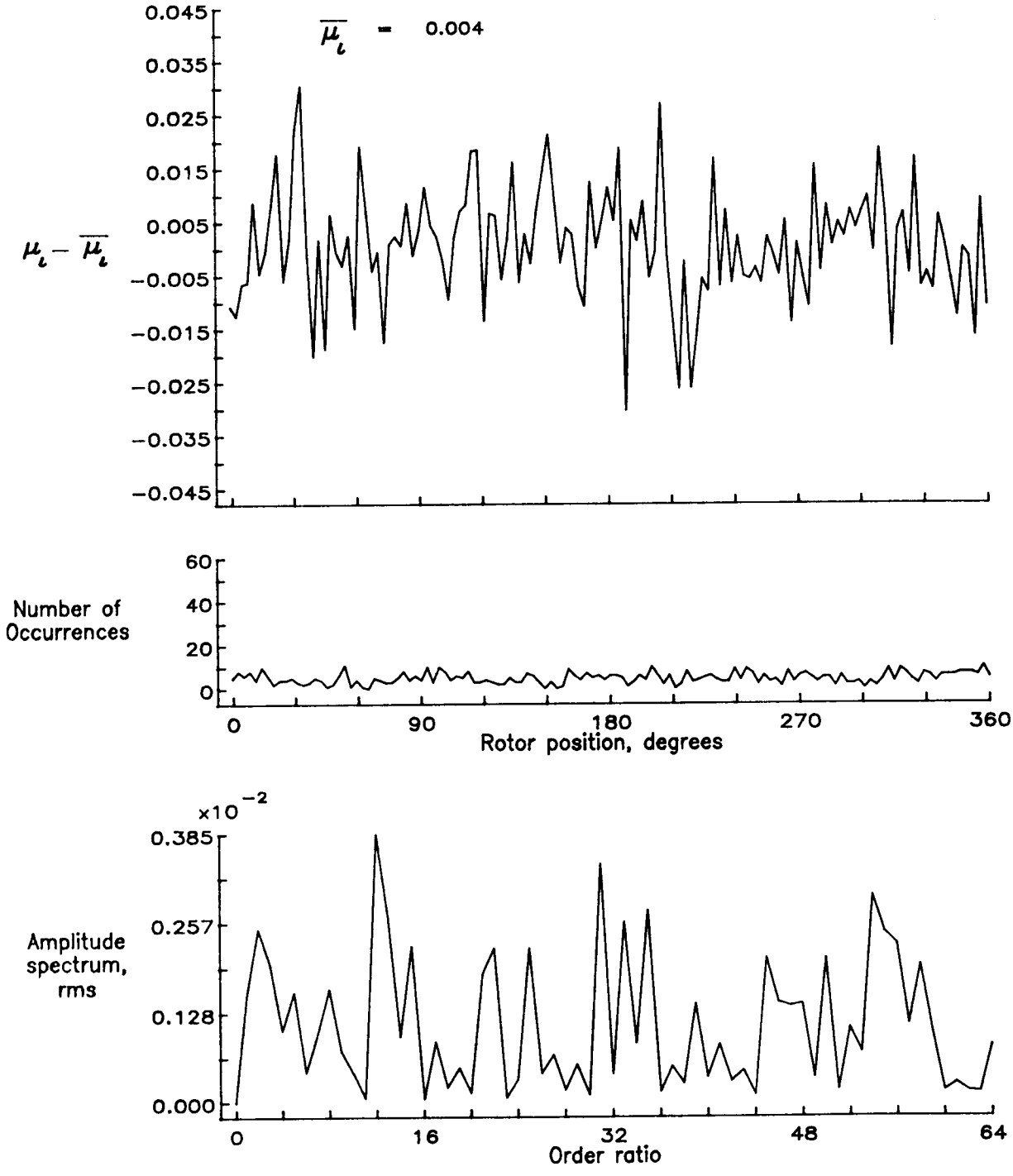


Figure 65.– Induced inflow velocity measured at 120 degrees and r/R of 0.60.

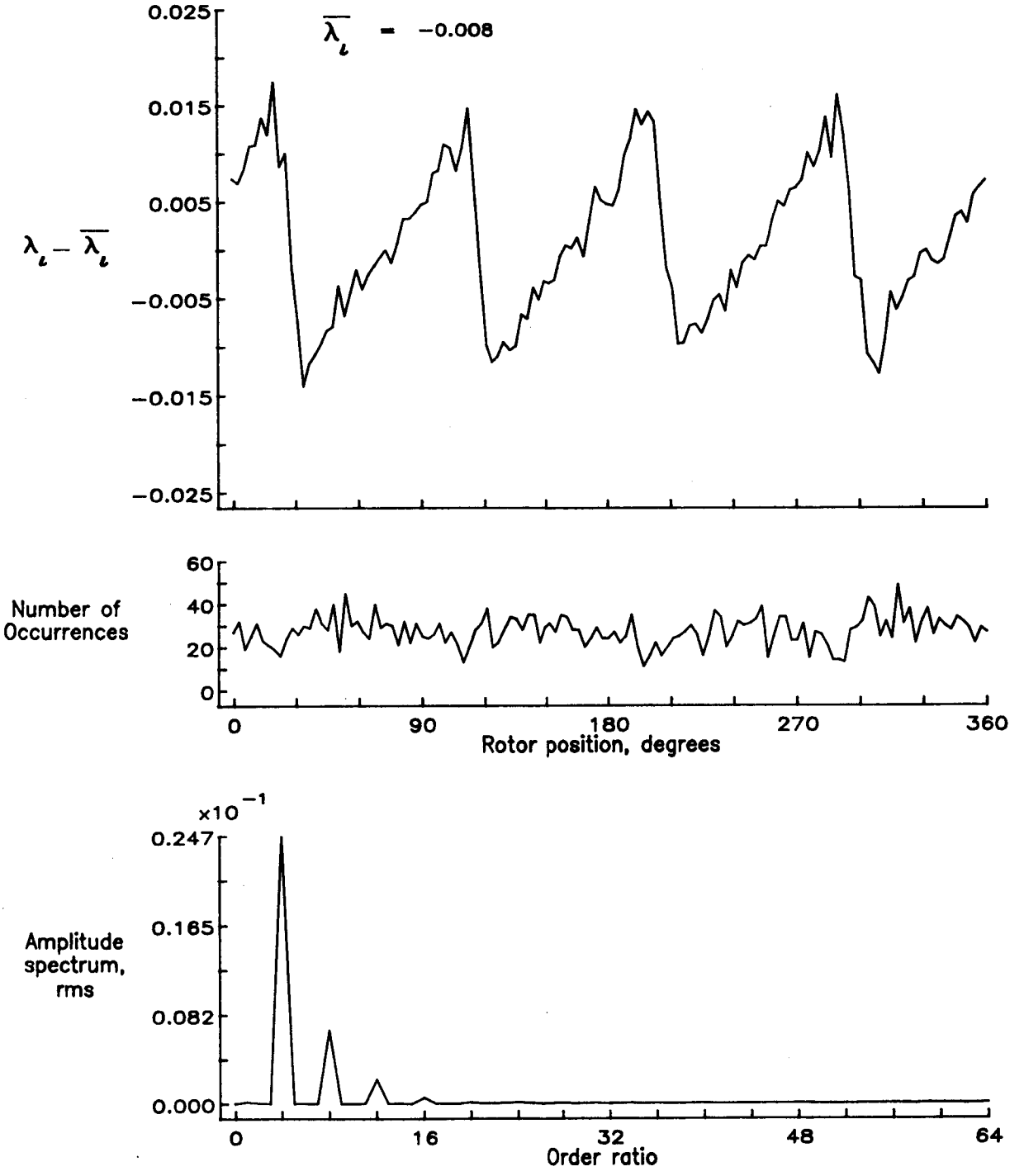


Figure 65.– Concluded.

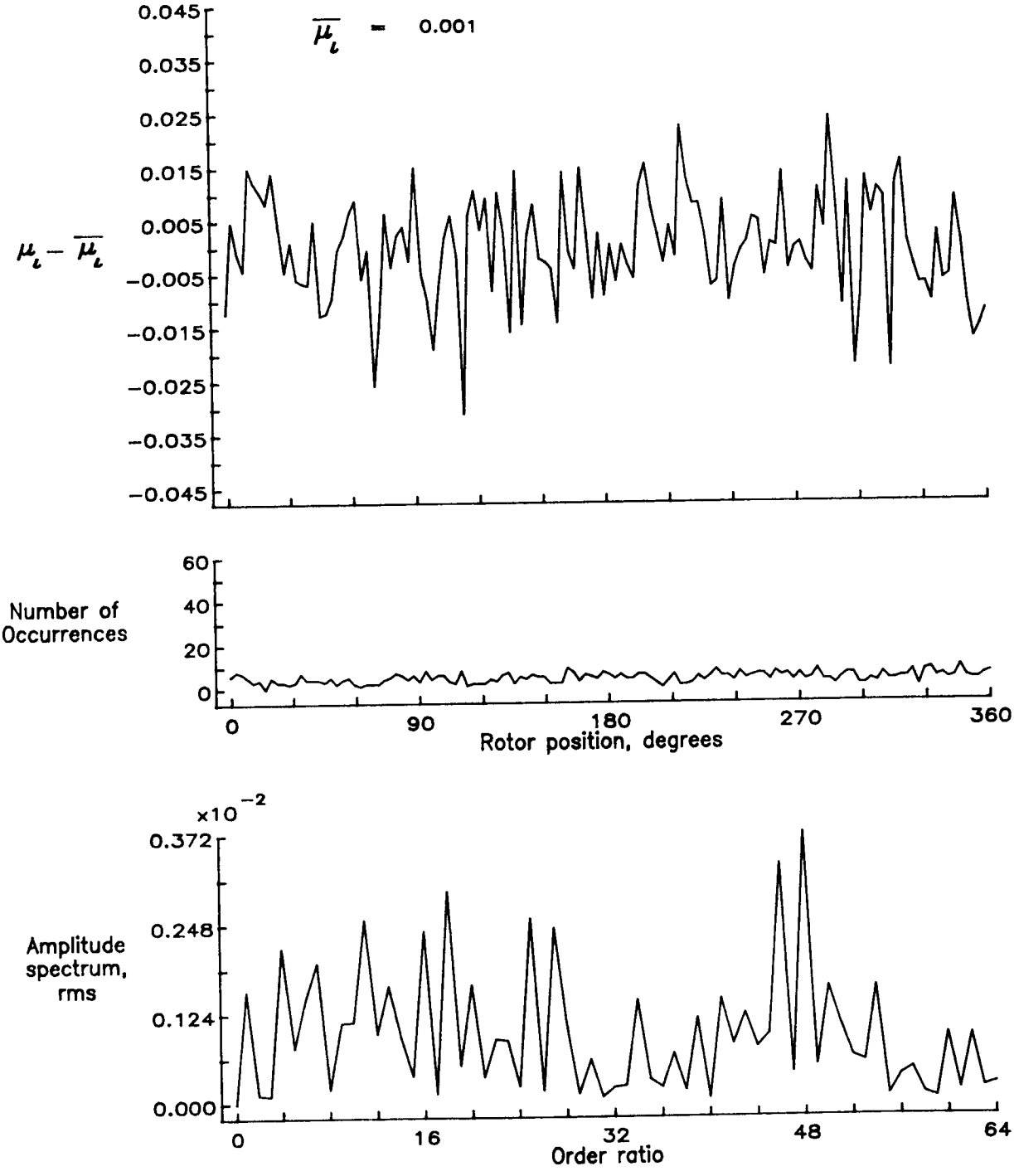


Figure 66.– Induced inflow velocity measured at 120 degrees and r/R of 0.70.

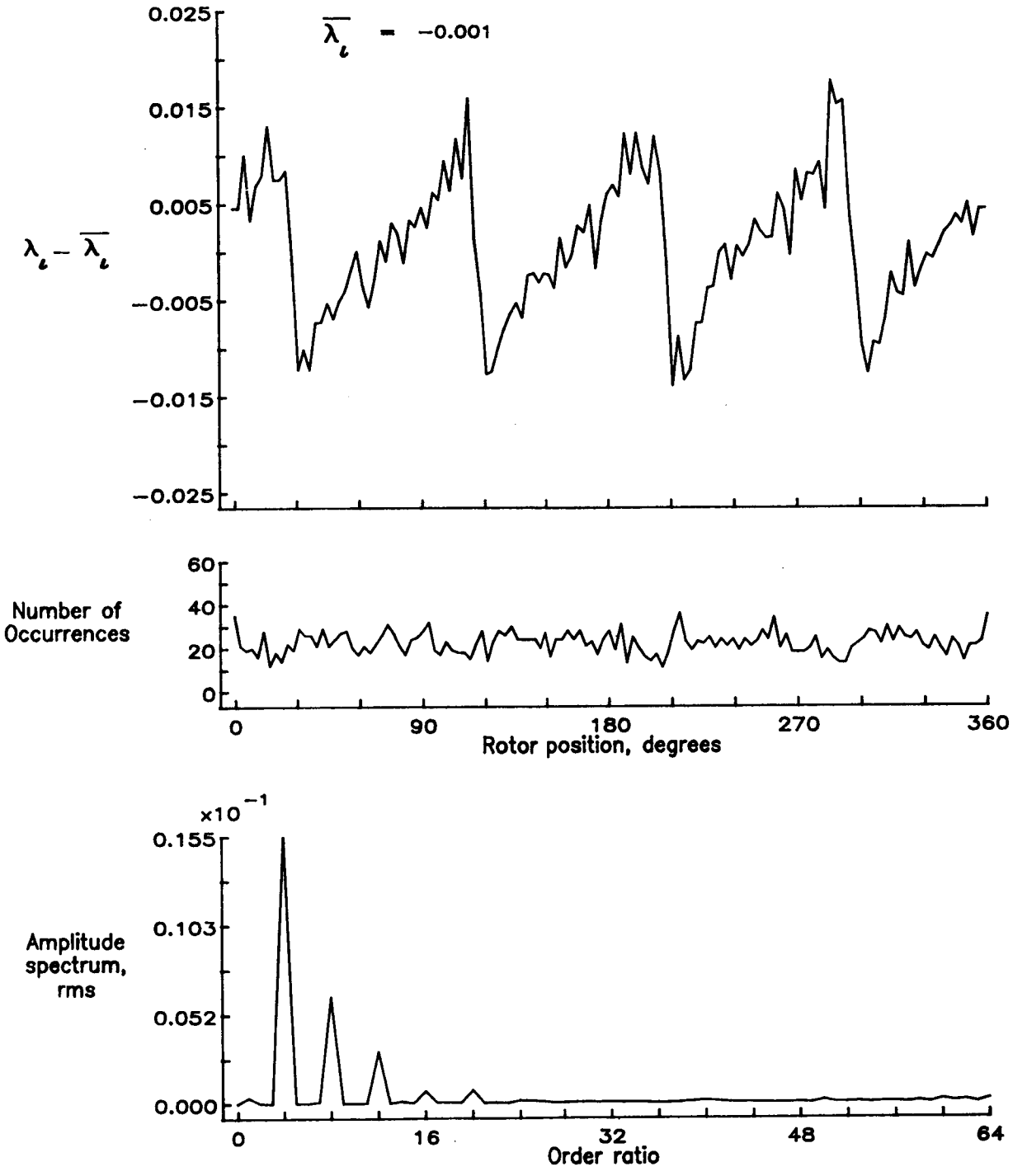


Figure 66.– Concluded.

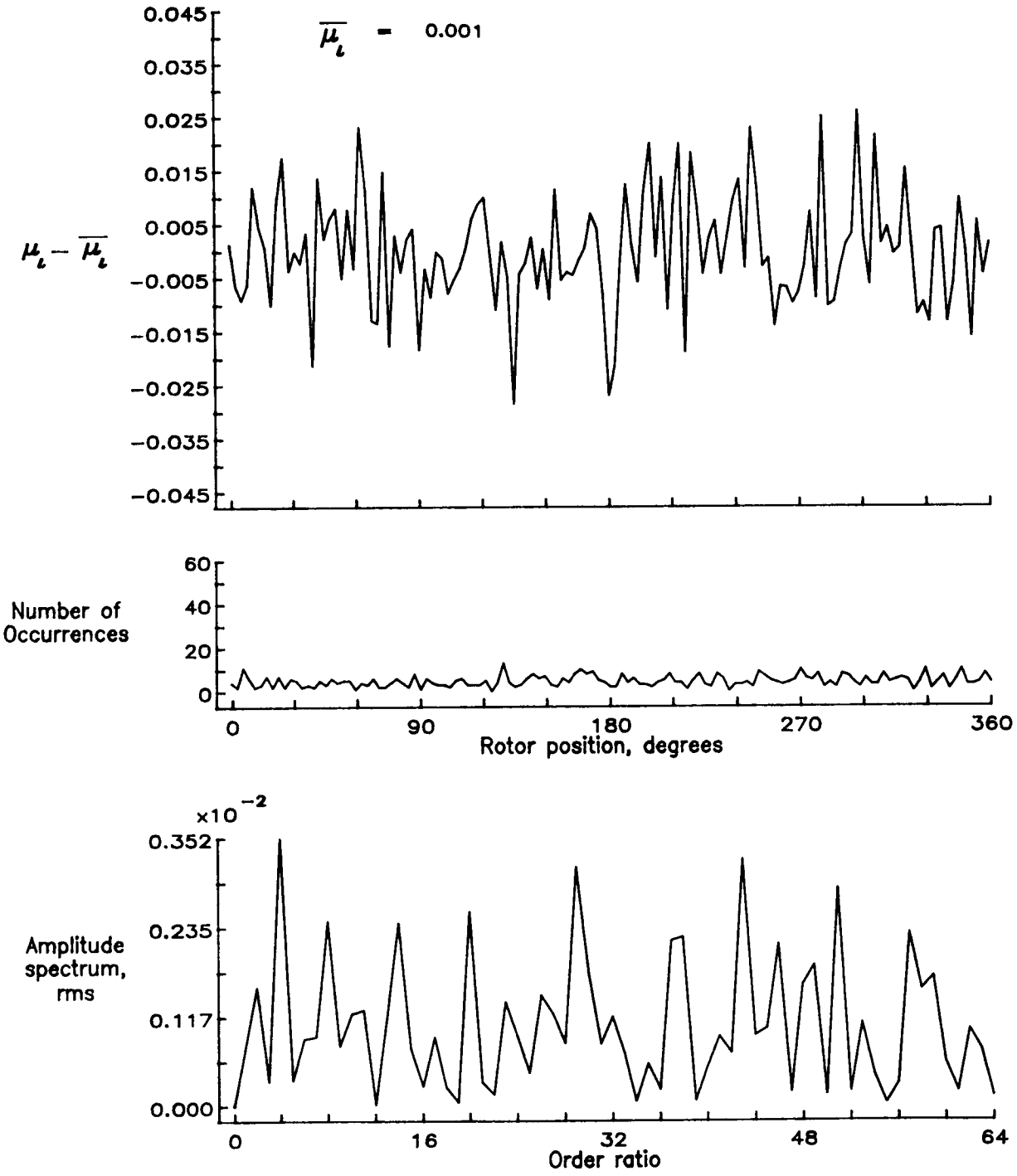


Figure 67.– Induced inflow velocity measured at 120 degrees and r/R of 0.74.

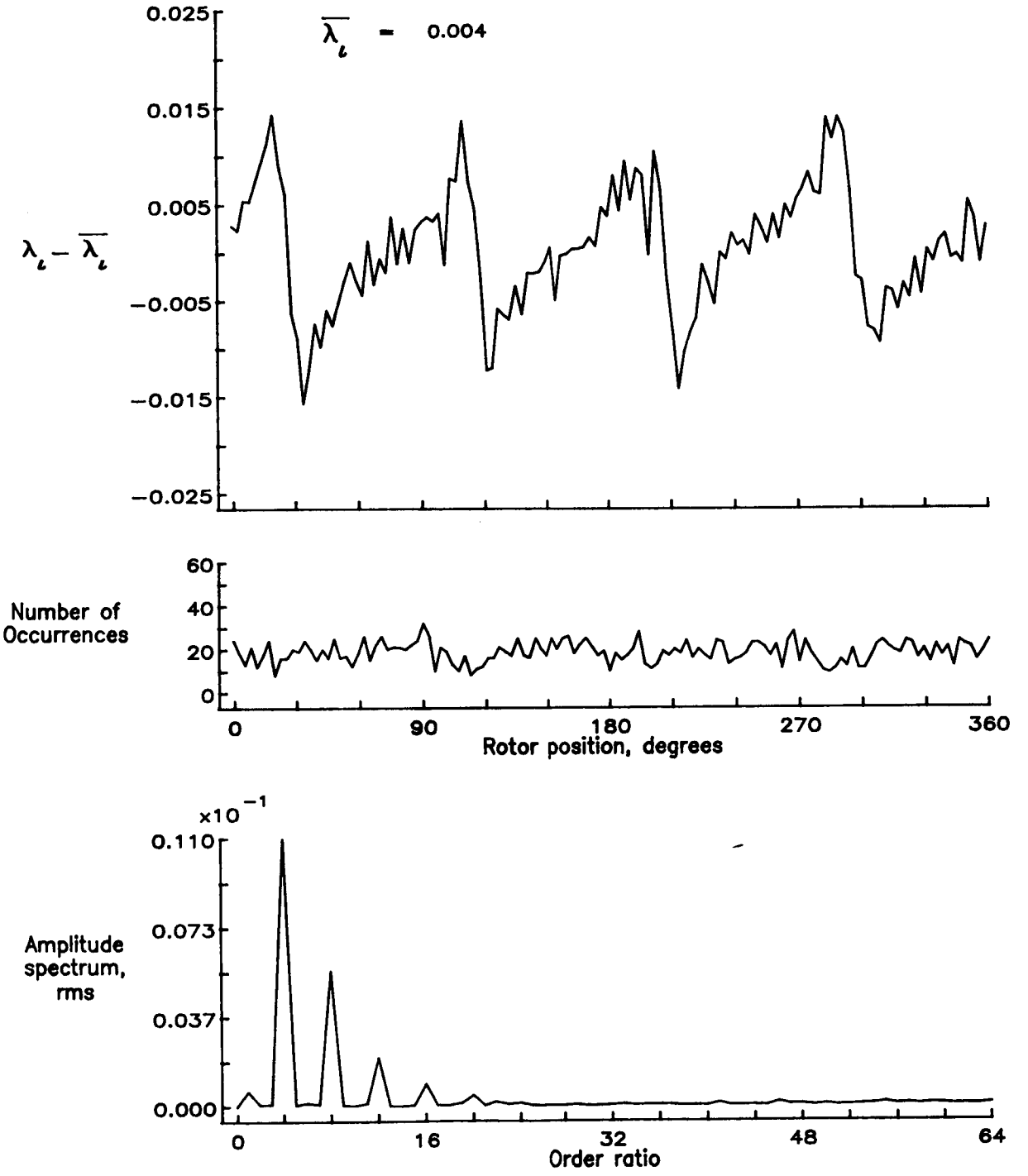


Figure 67.– Concluded.

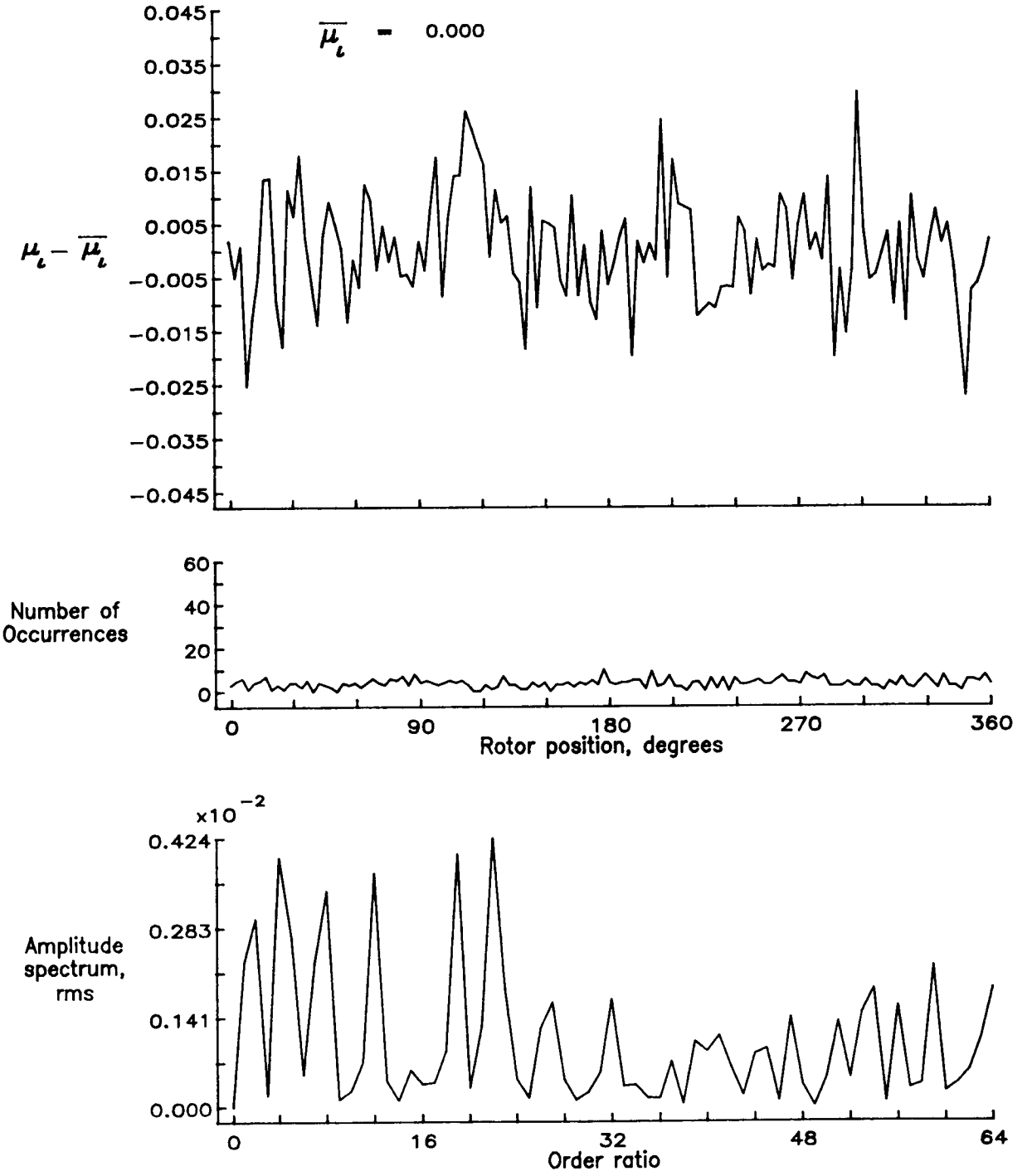


Figure 68.– Induced inflow velocity measured at 120 degrees and r/R of 0.78.

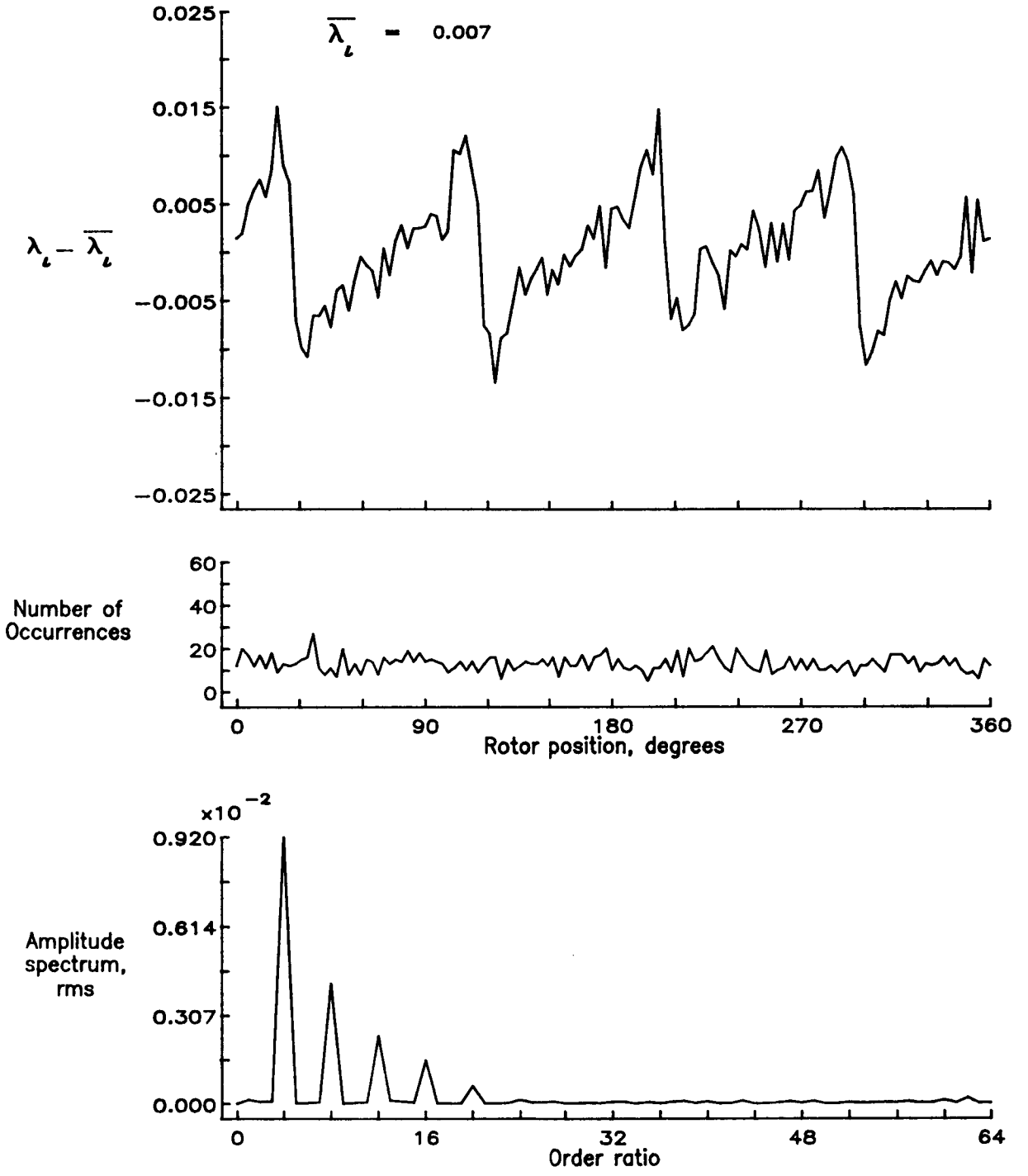


Figure 68.– Concluded.

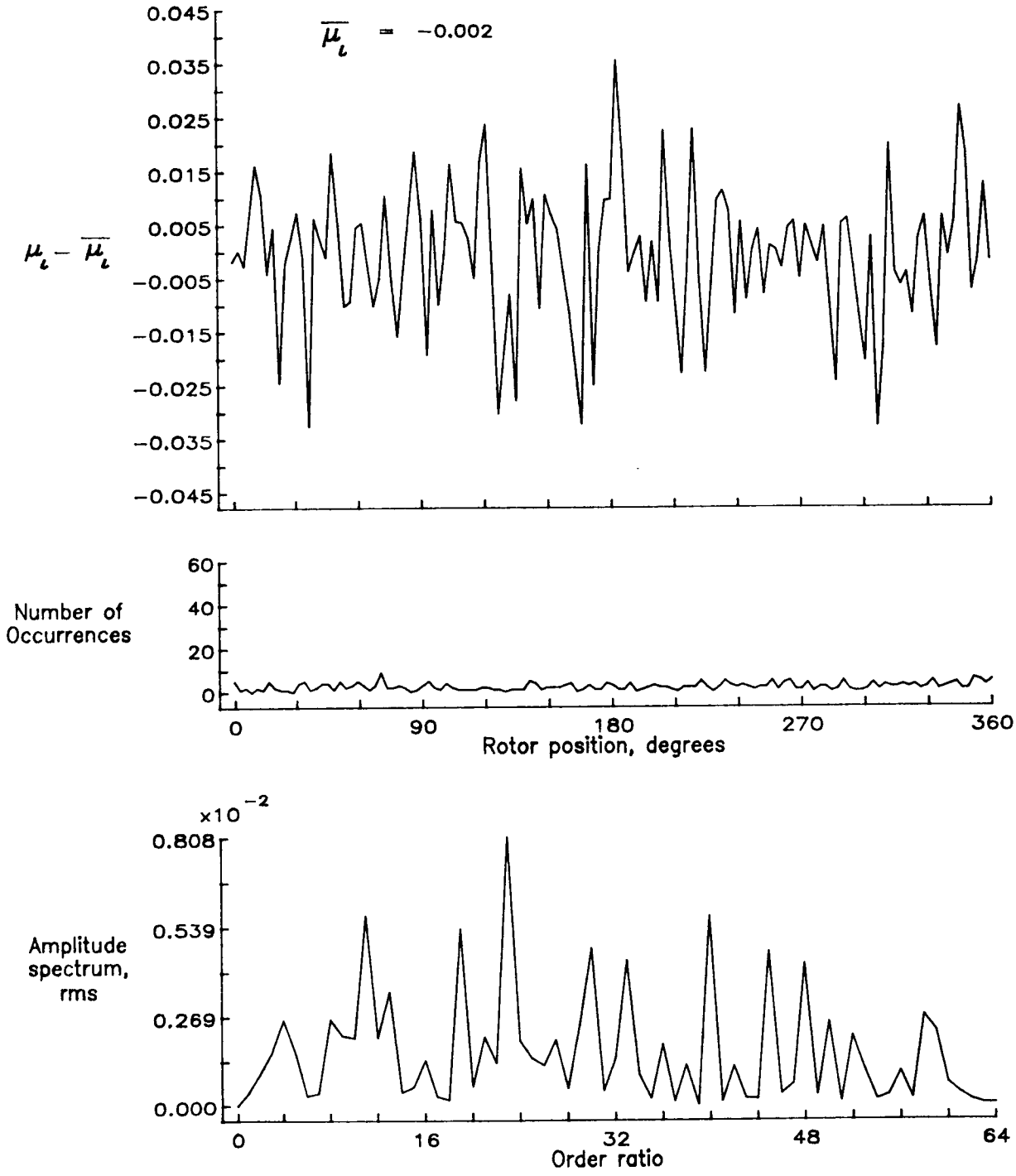


Figure 69.– Induced inflow velocity measured at 120 degrees and r/R of 0.82.

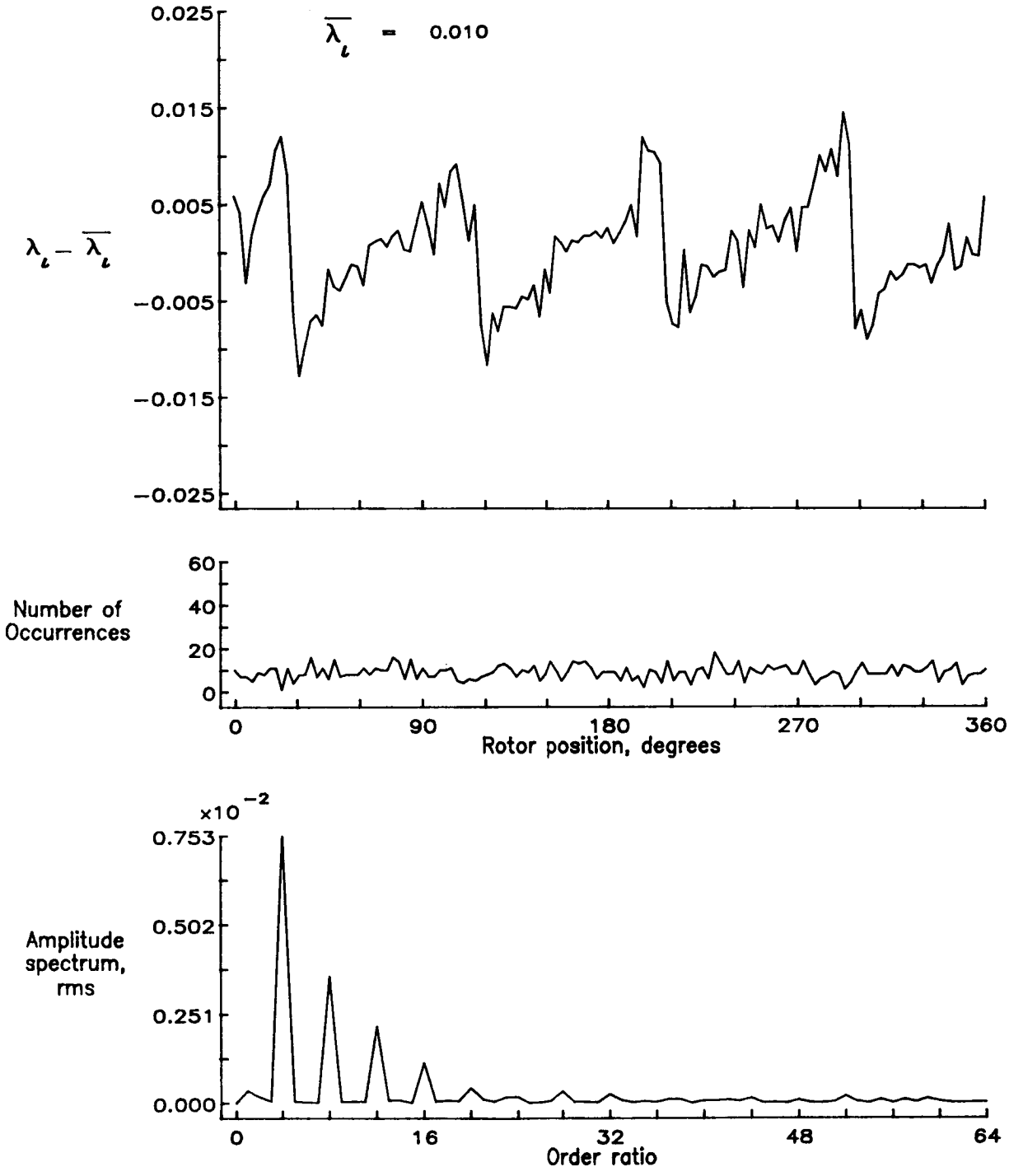


Figure 69.– Concluded.

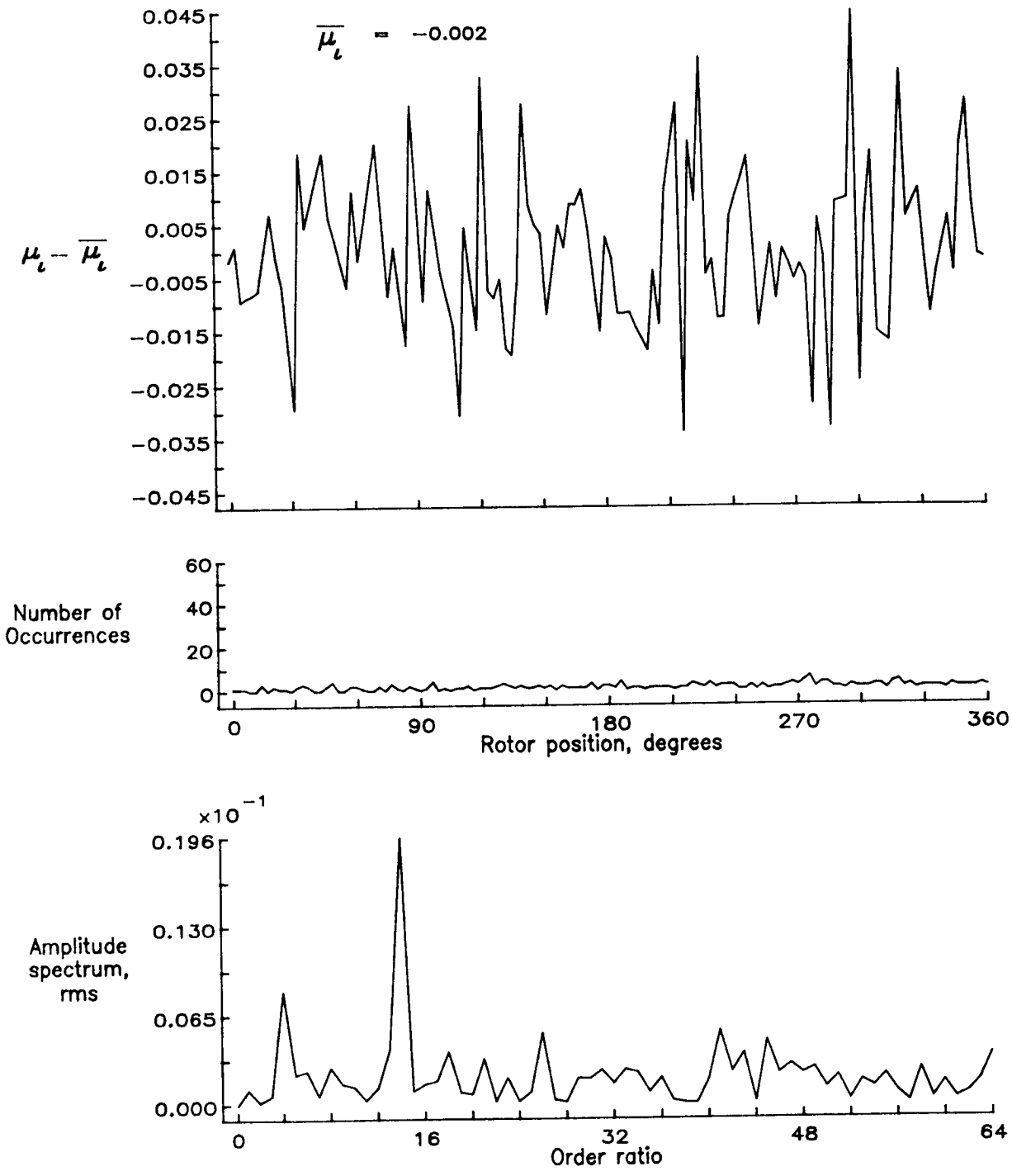


Figure 70.– Induced inflow velocity measured at 120 degrees and r/R of 0.86.

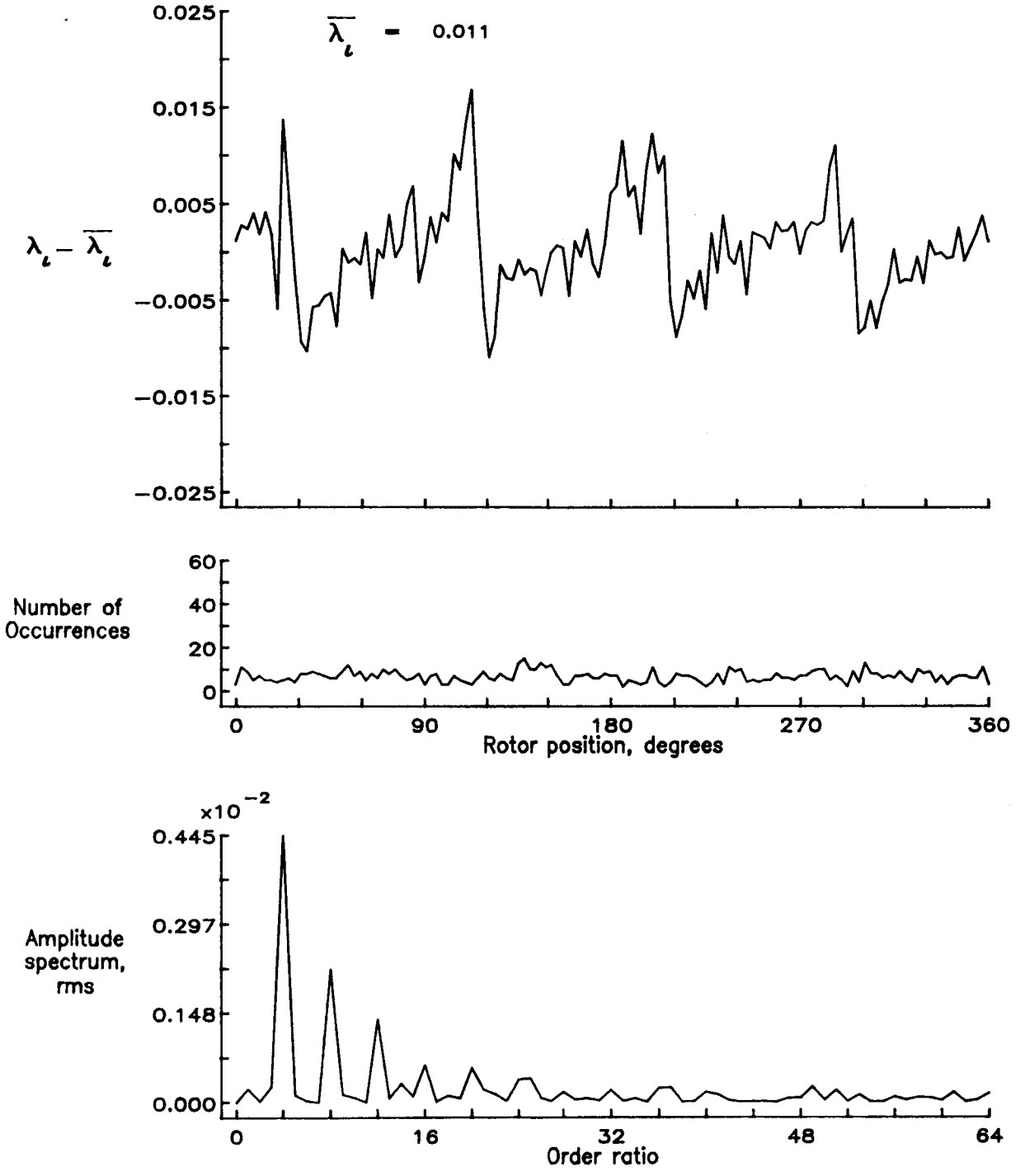


Figure 70.– Concluded.

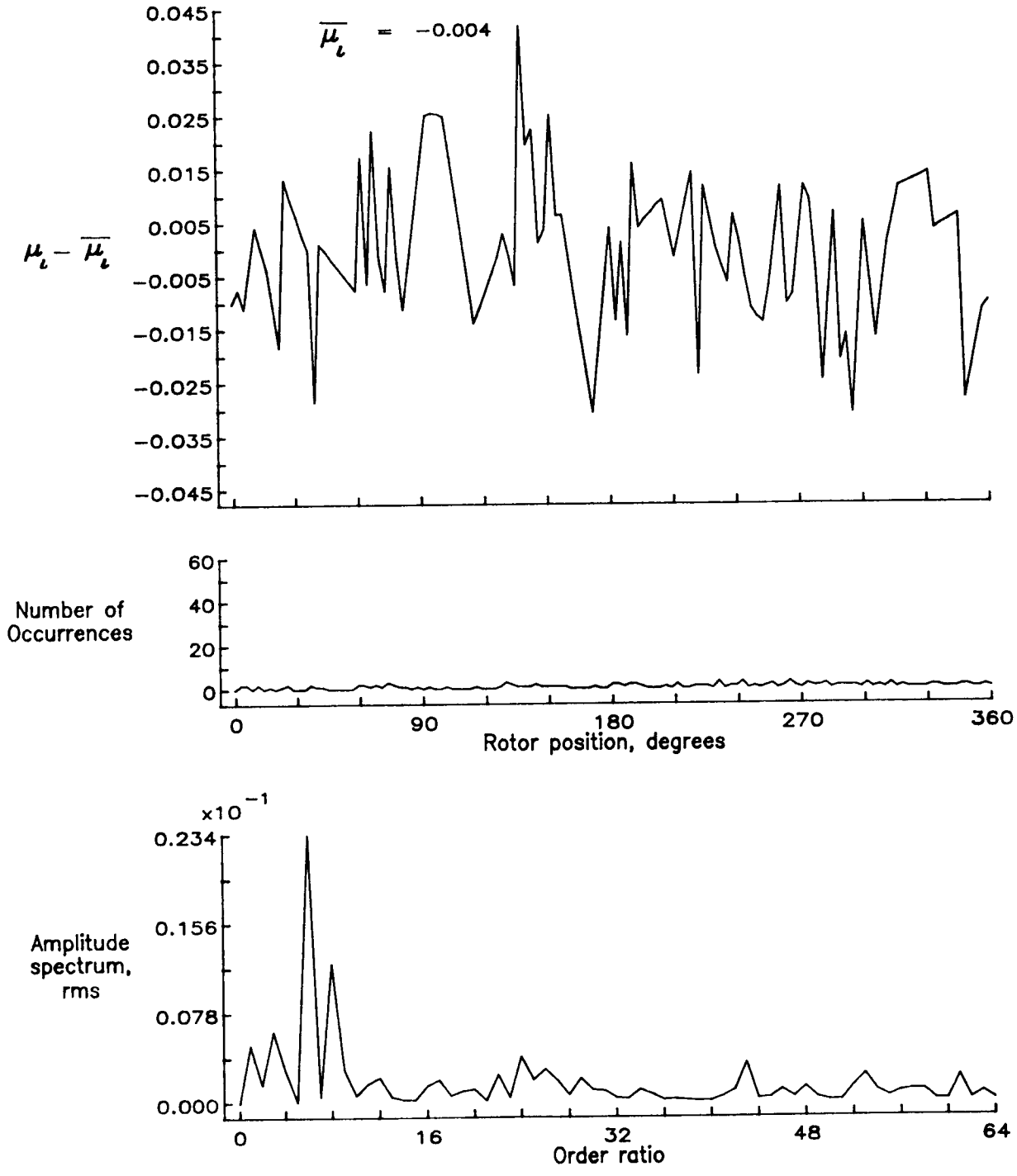


Figure 71.– Induced inflow velocity measured at 120 degrees and r/R of 0.90.

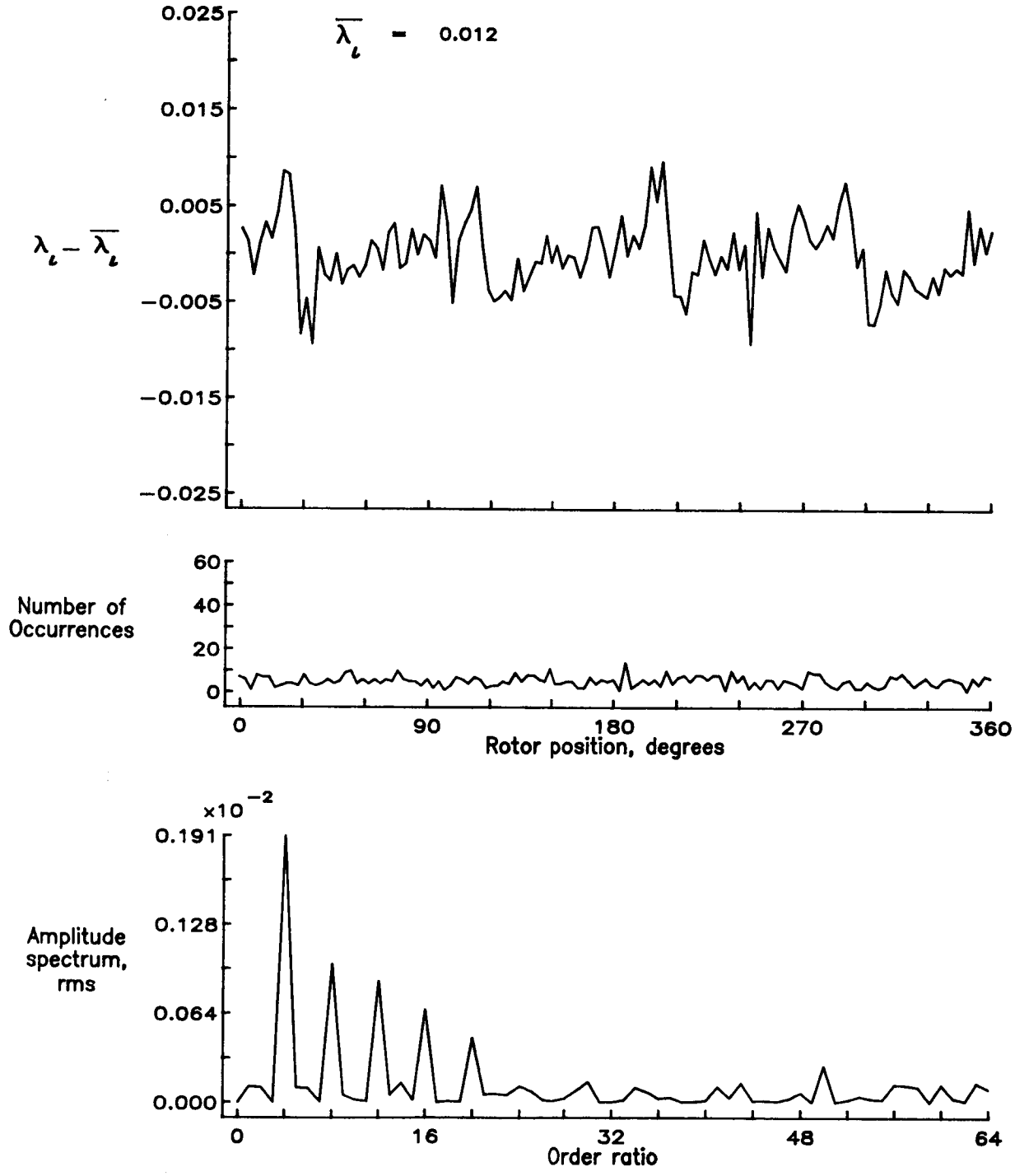


Figure 71.– Concluded.

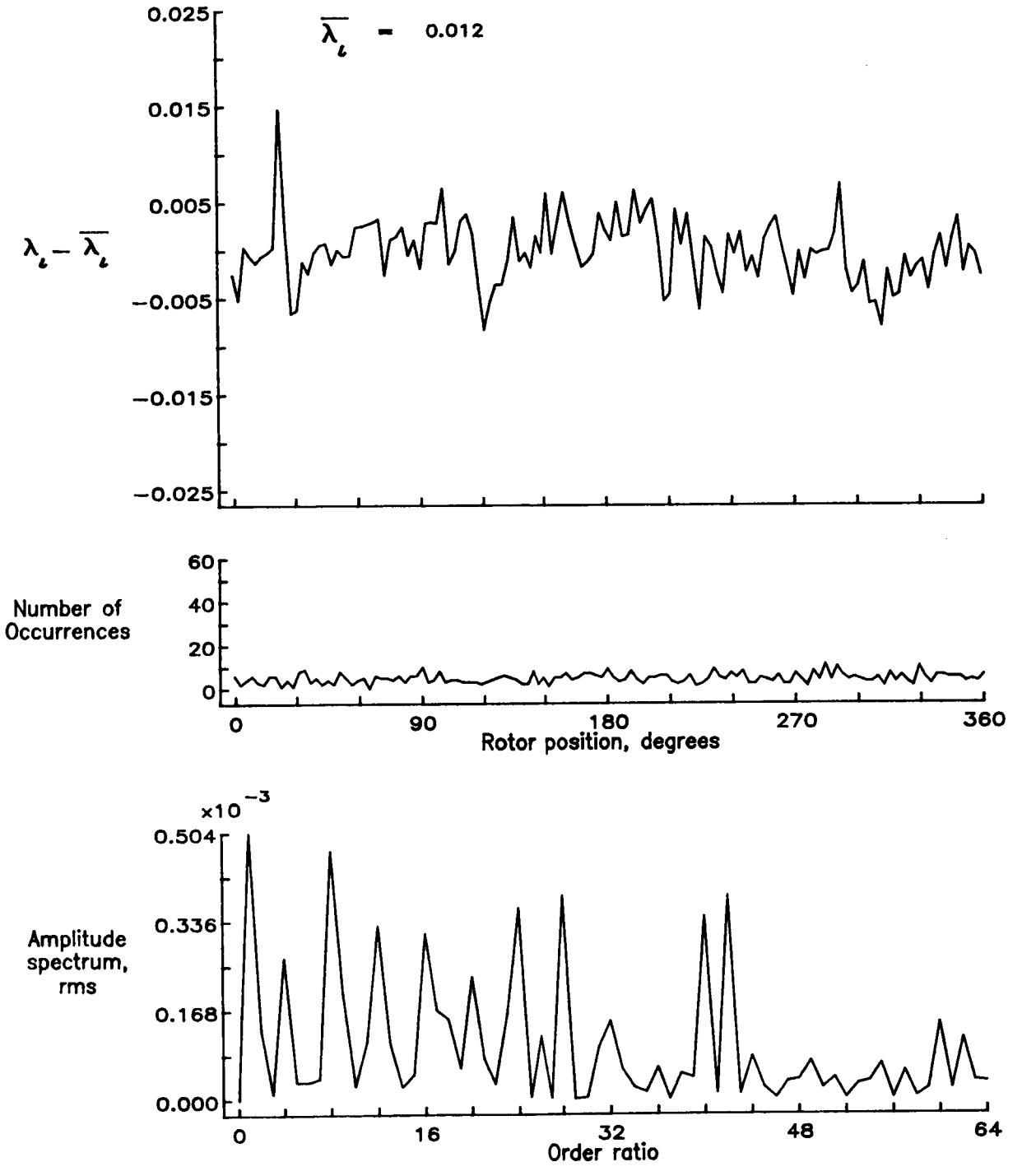


Figure 72.– Induced inflow velocity measured at 120 degrees and r/R of 0.94.

PRECEDING PAGE BLANK NOT FILMED

PAGE 146 INTENTIONALLY BLANK

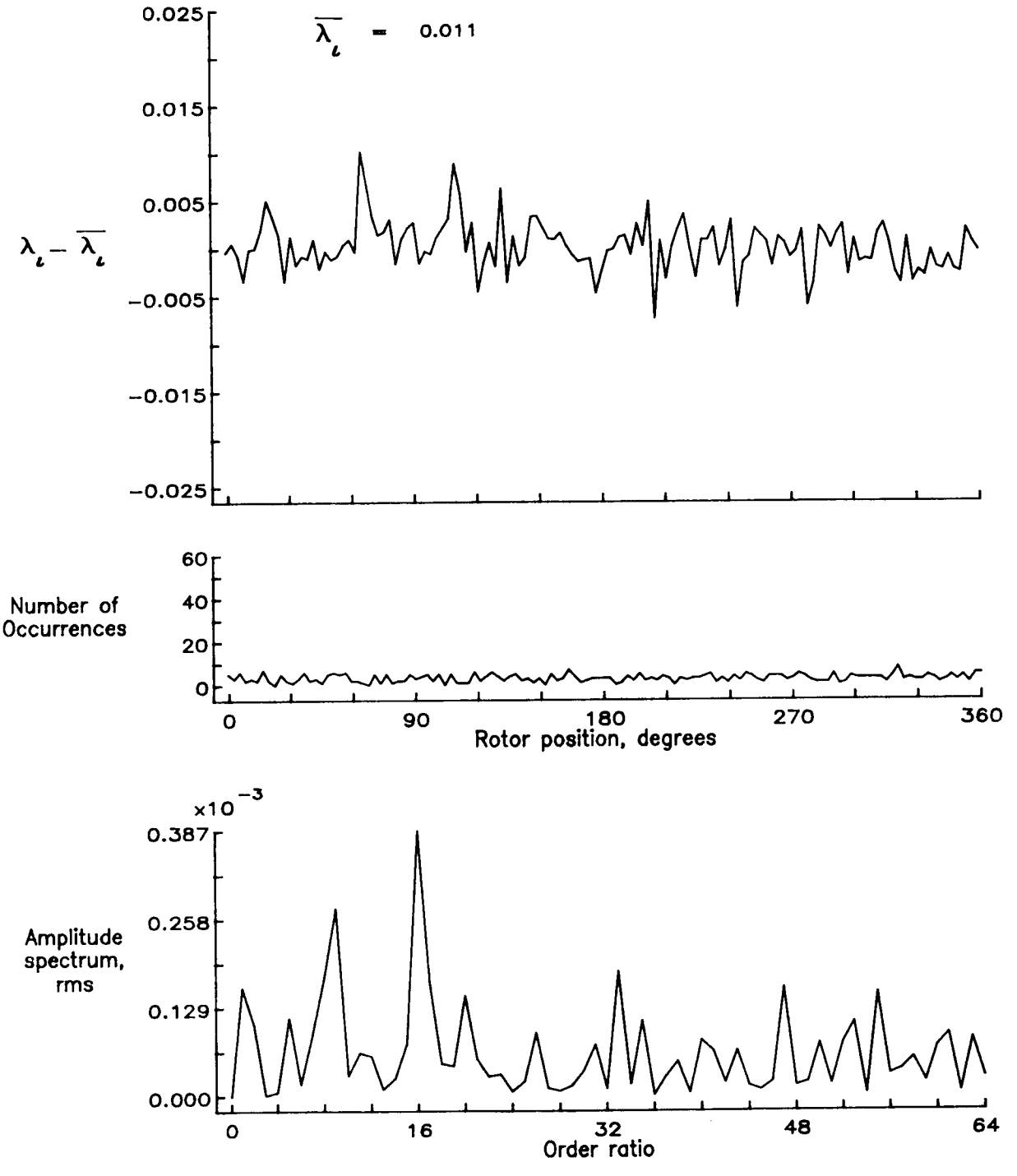


Figure 73.– Induced inflow velocity measured at 120 degrees and r/R of 0.98.

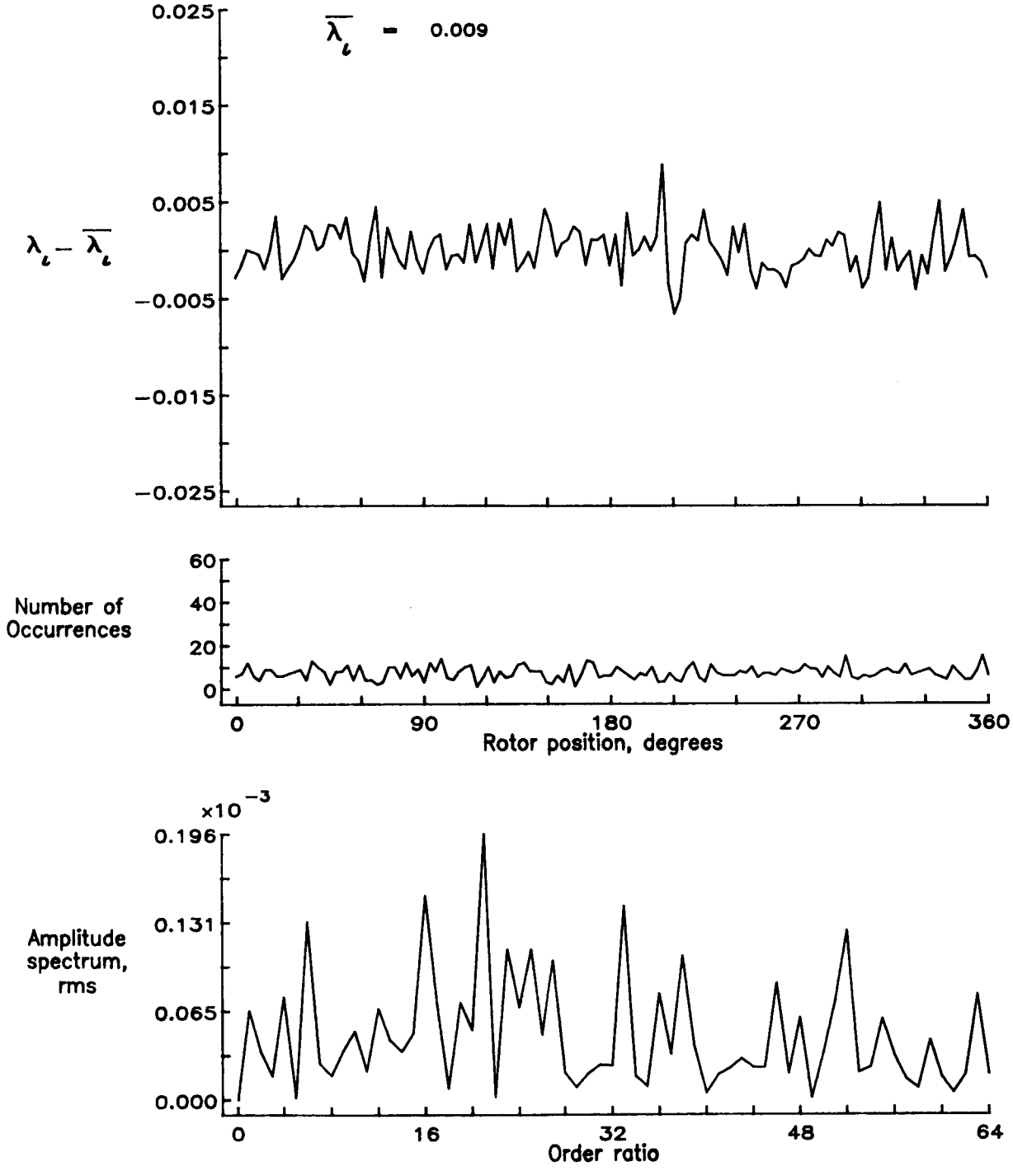


Figure 74.– Induced inflow velocity measured at 120 degrees and r/R of 1.02.

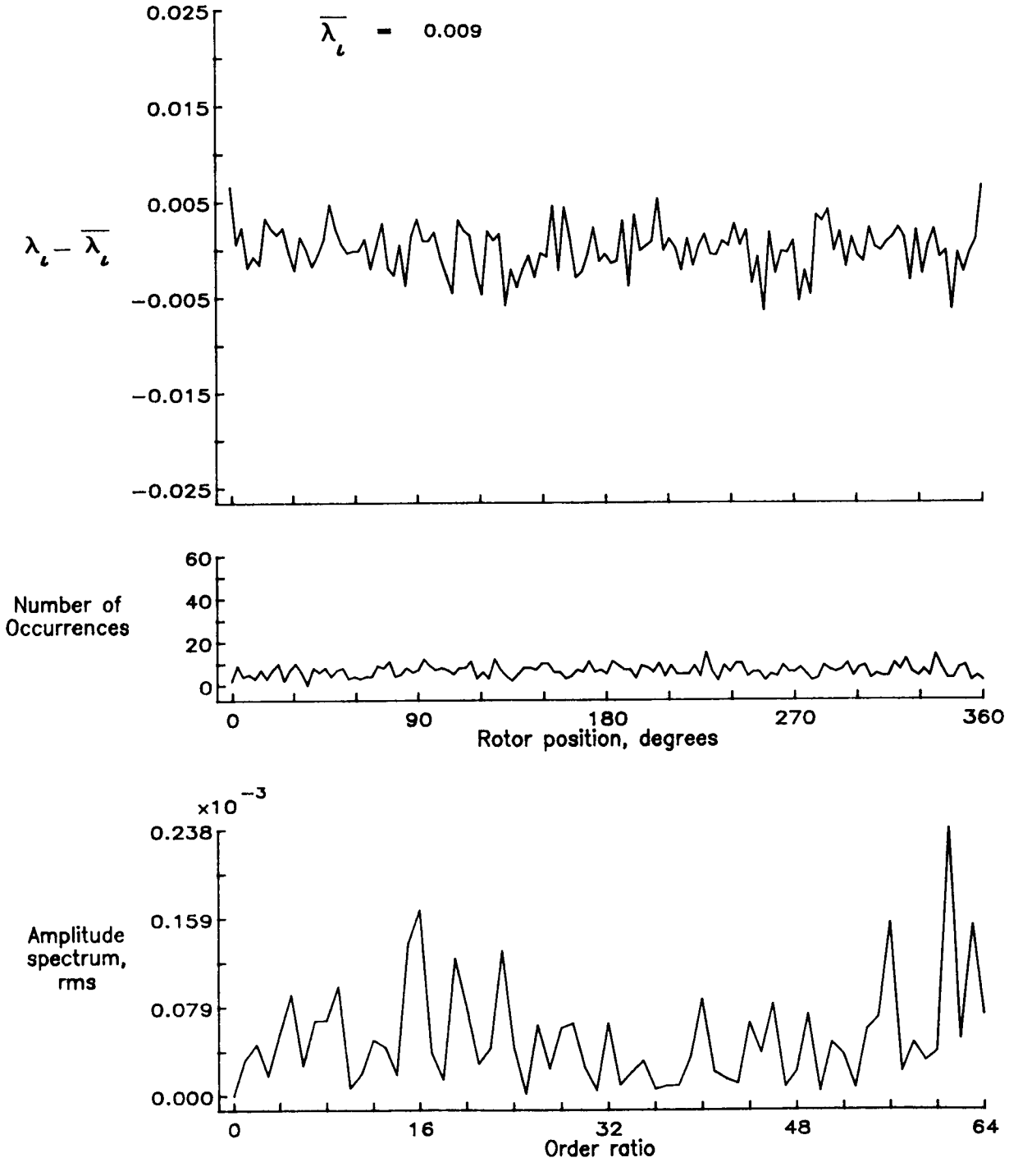


Figure 75.– Induced inflow velocity measured at 120 degrees and r/R of 1.04.

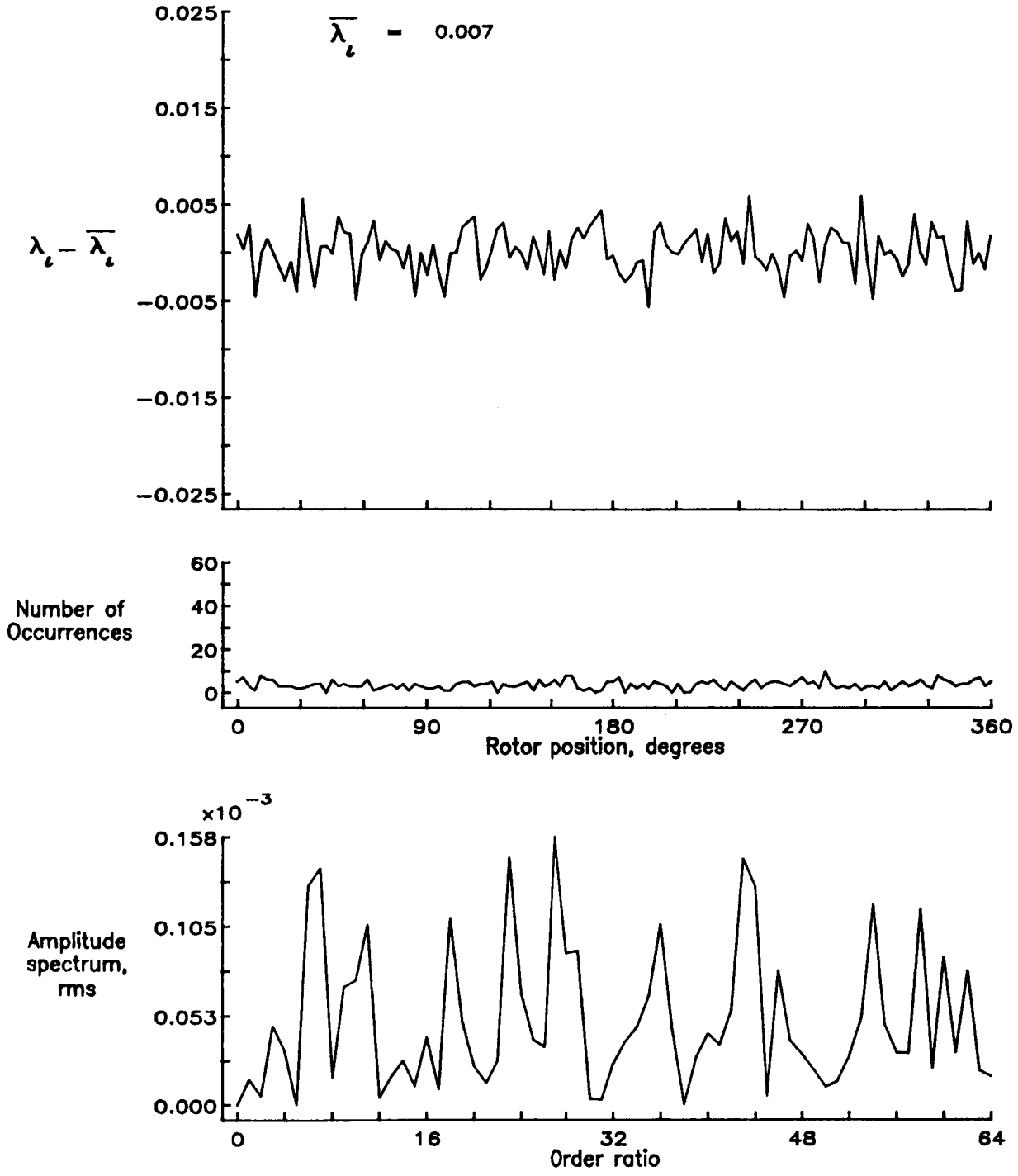


Figure 76.– Induced inflow velocity measured at 120 degrees and r/R of 1.12.

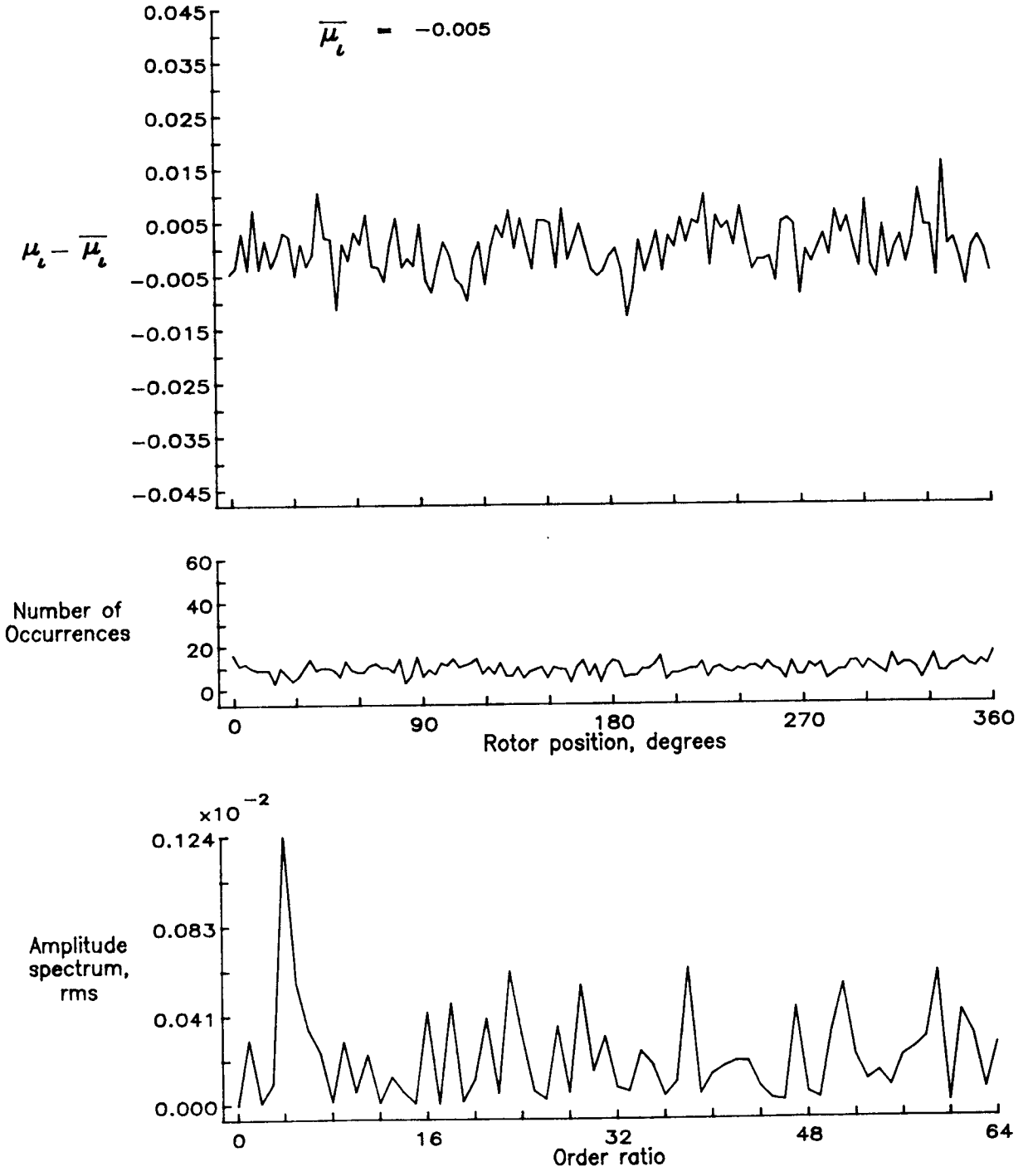


Figure 77.– Induced inflow velocity measured at 150 degrees and r/R of 0.20.

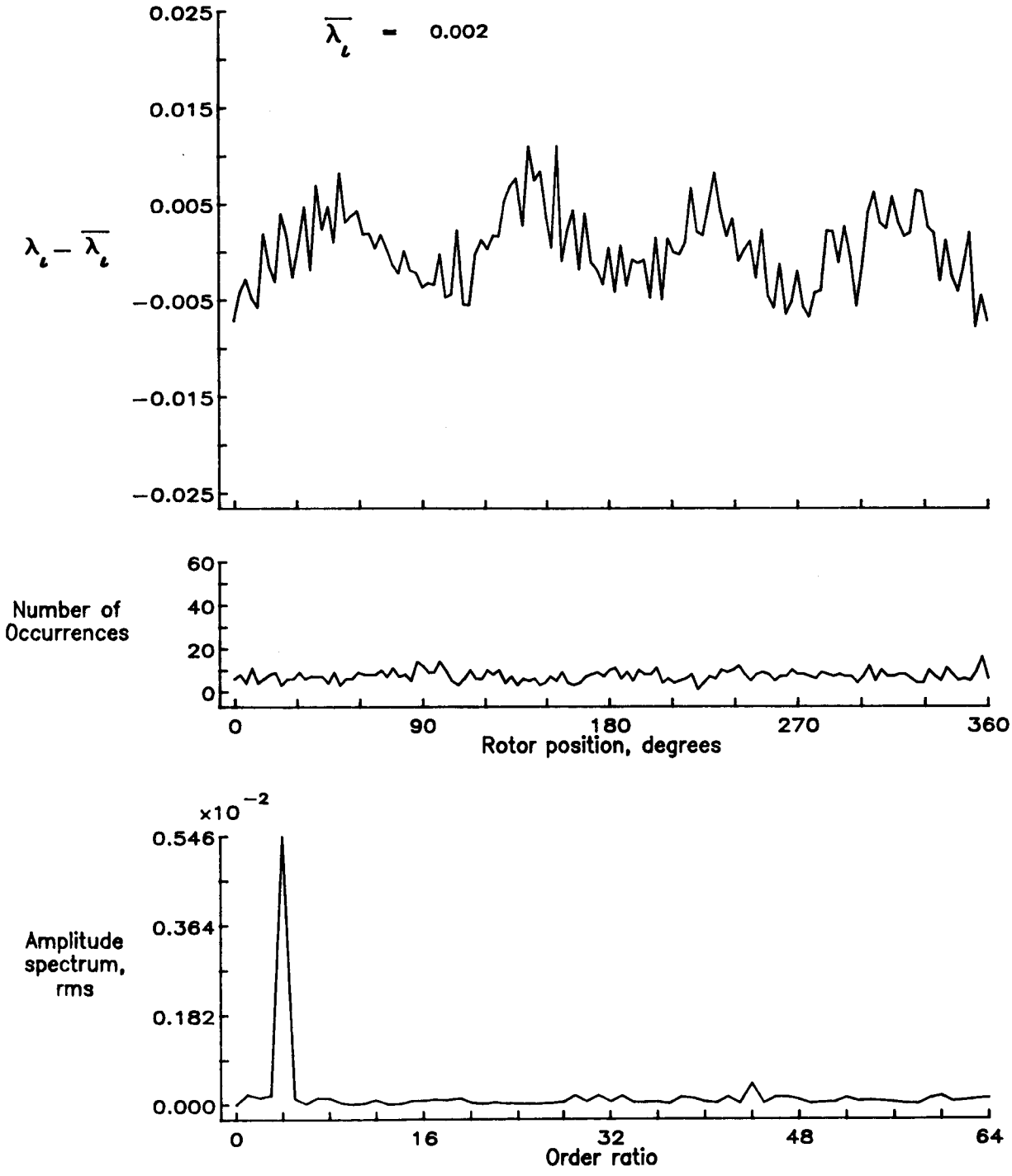


Figure 77.– Concluded.

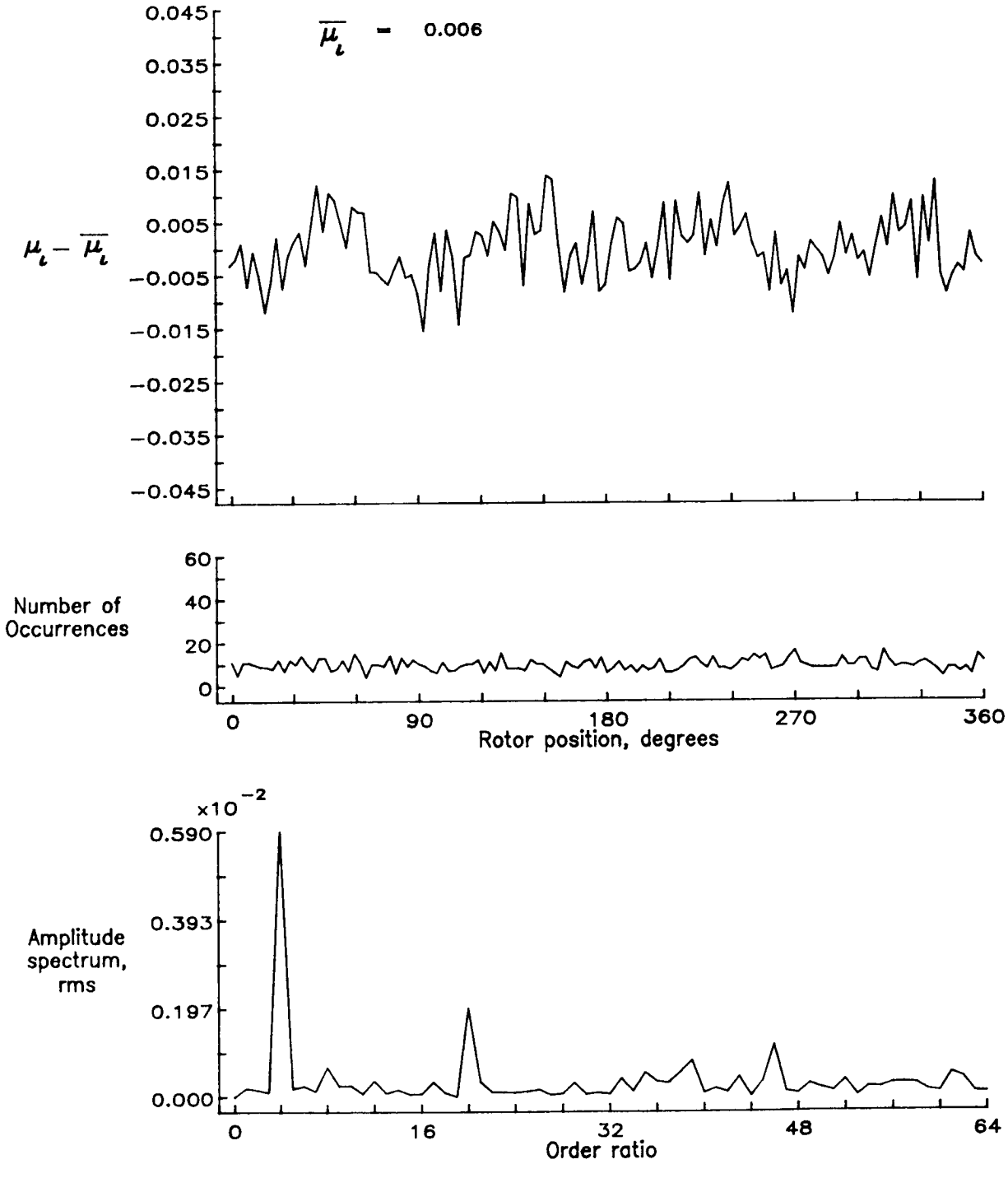


Figure 78.– Induced inflow velocity measured at 150 degrees and r/R of 0.40.

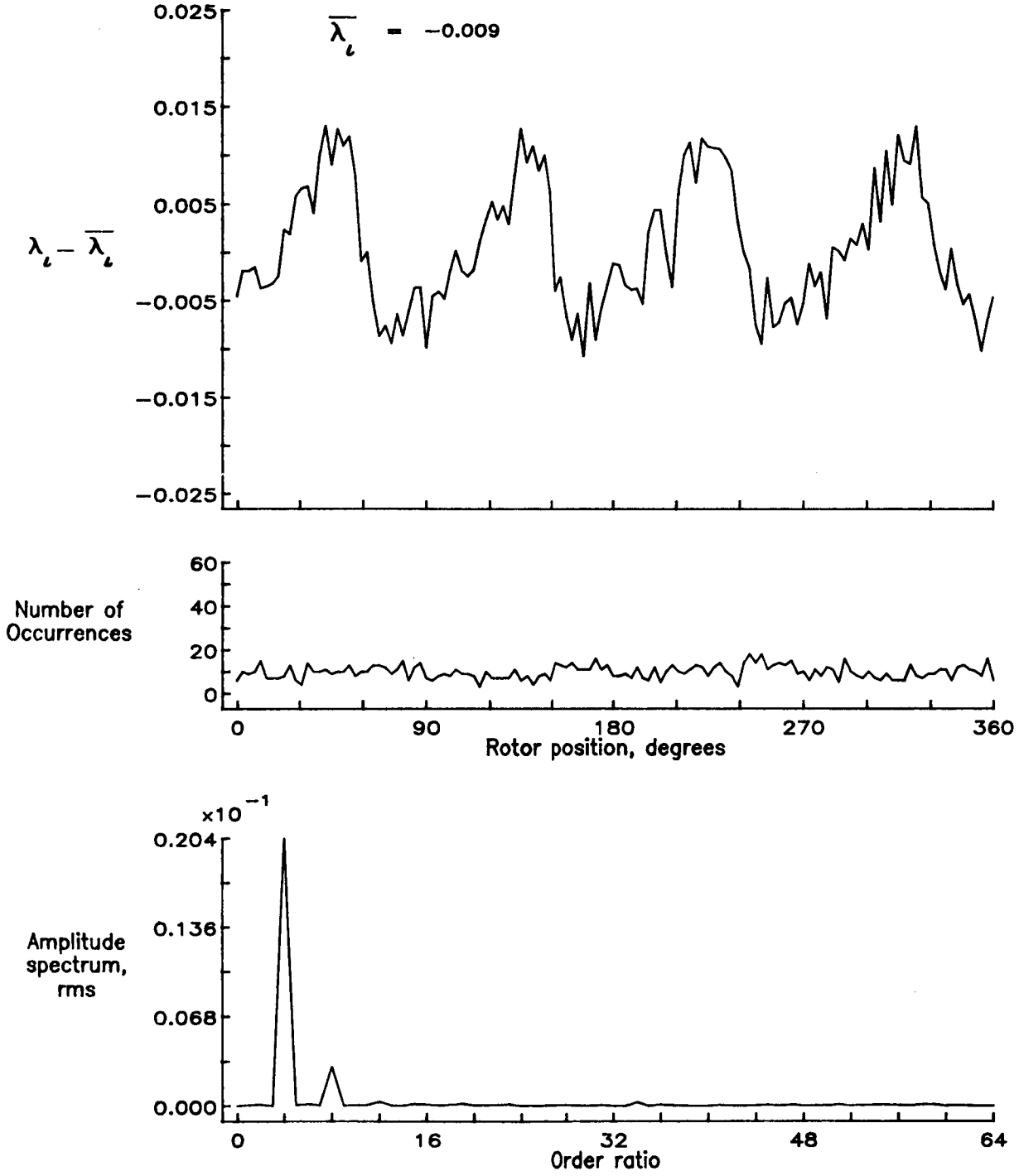


Figure 78.– Concluded.

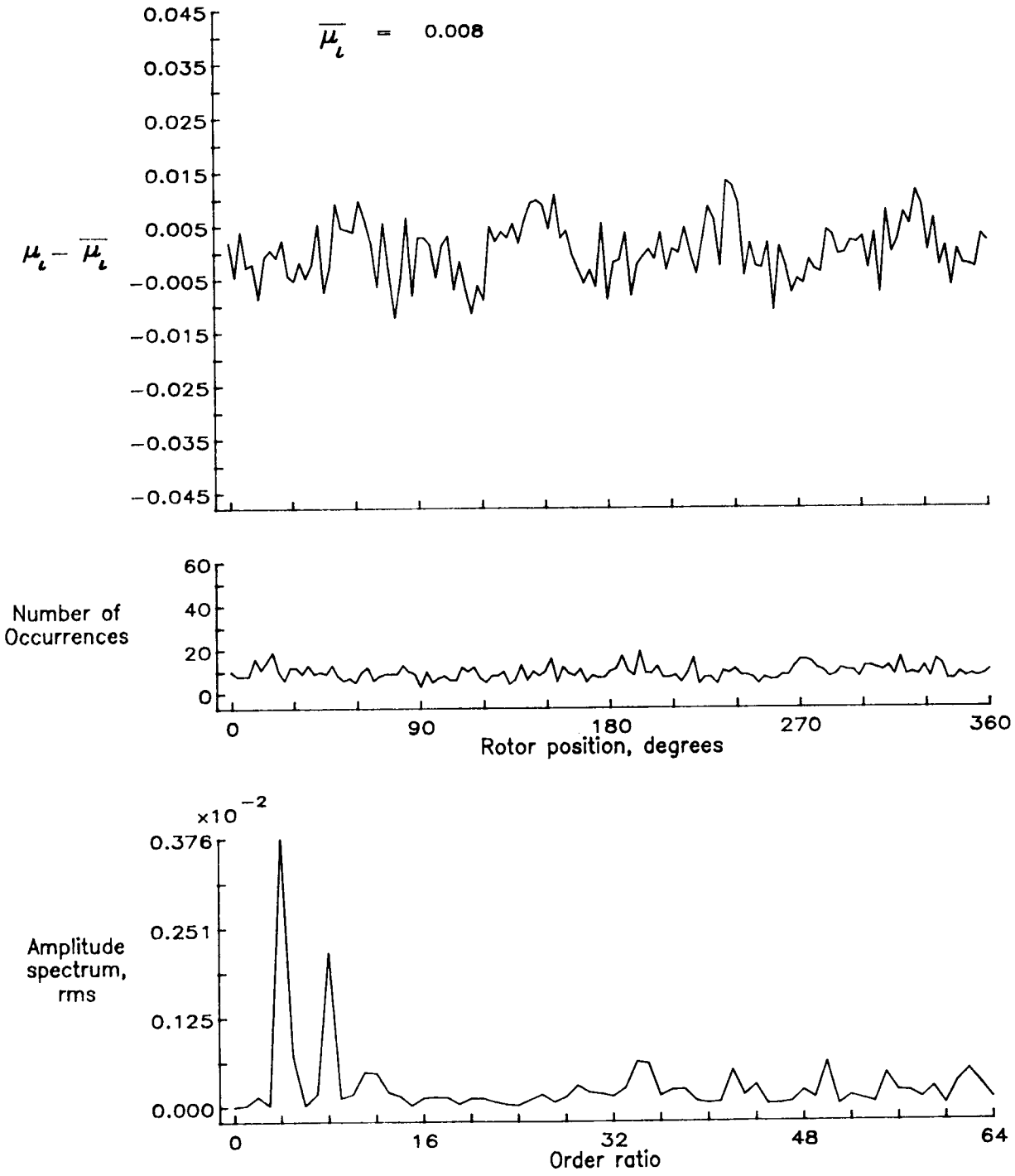


Figure 79.– Induced inflow velocity measured at 150 degrees and r/R of 0.50.

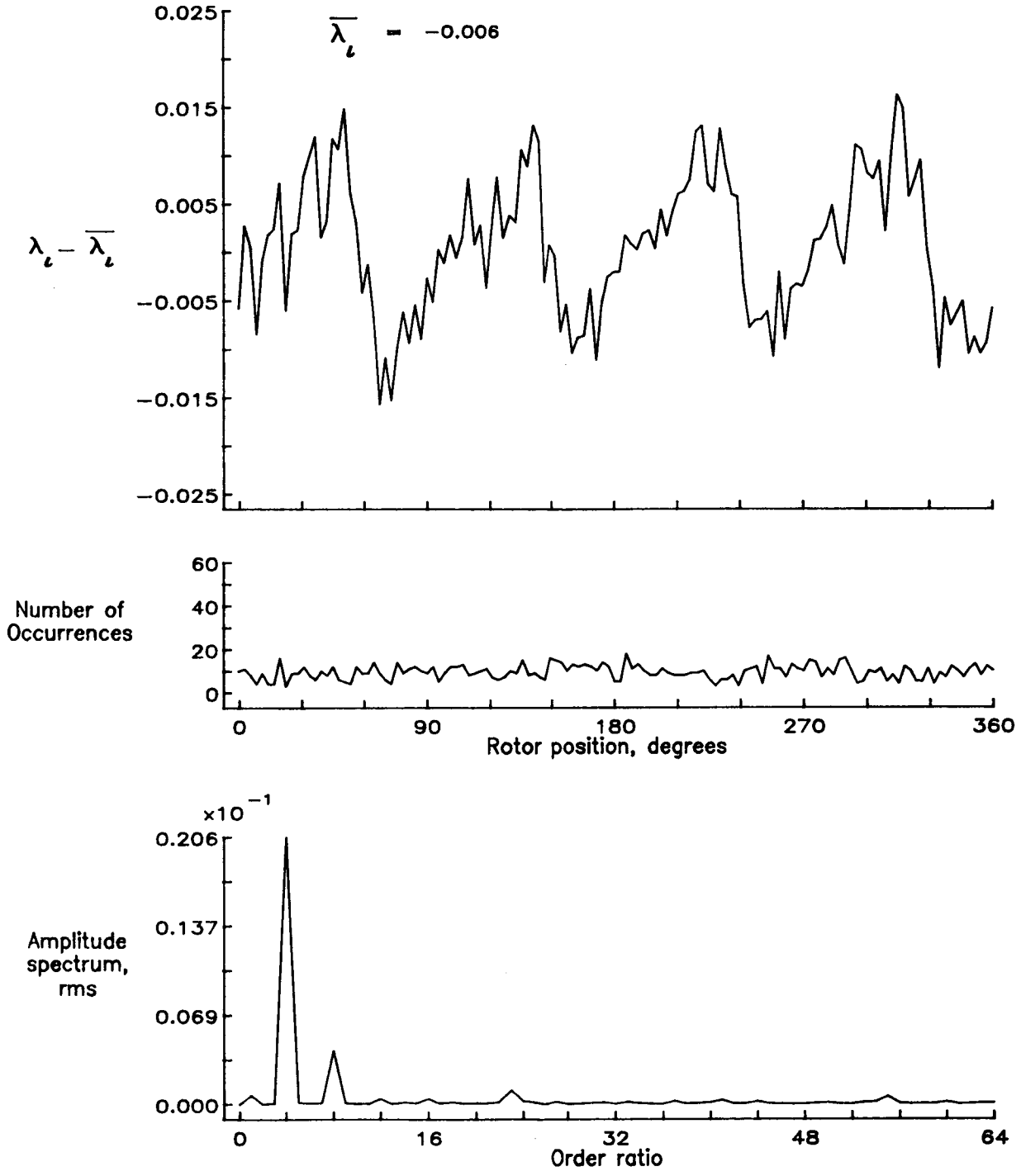


Figure 79.– Concluded.

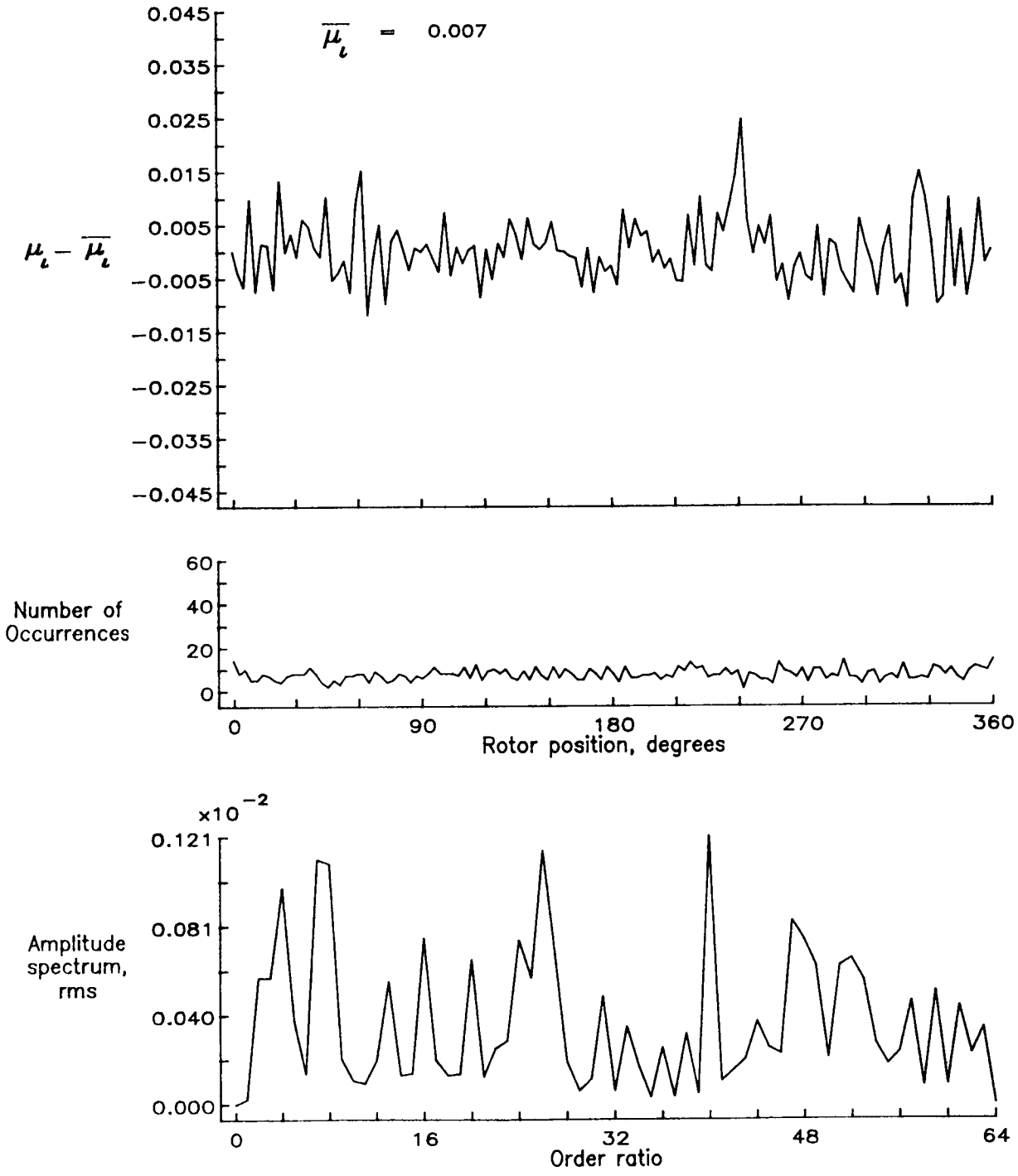


Figure 80.– Induced inflow velocity measured at 150 degrees and r/R of 0.60.

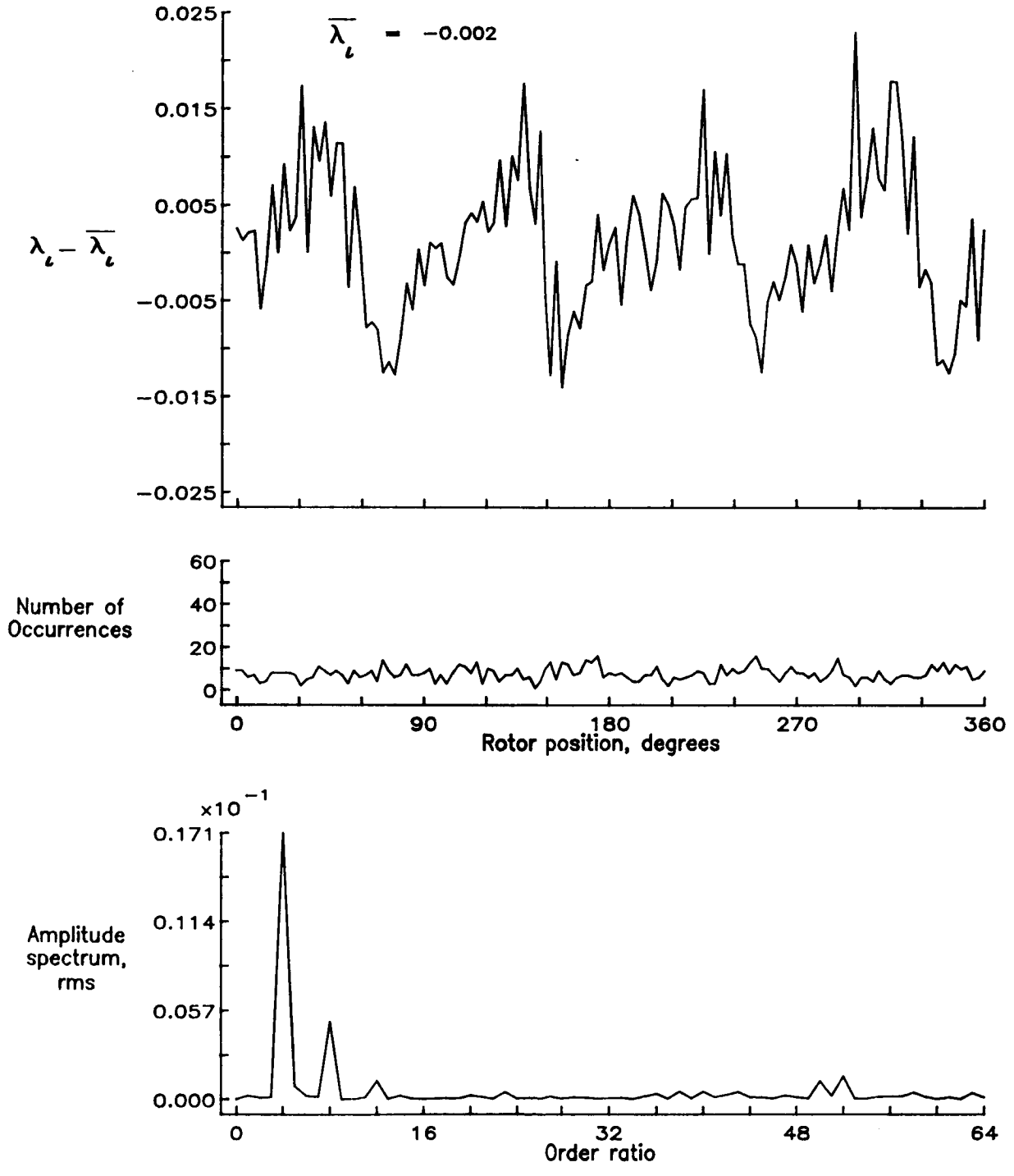


Figure 80.– Concluded.

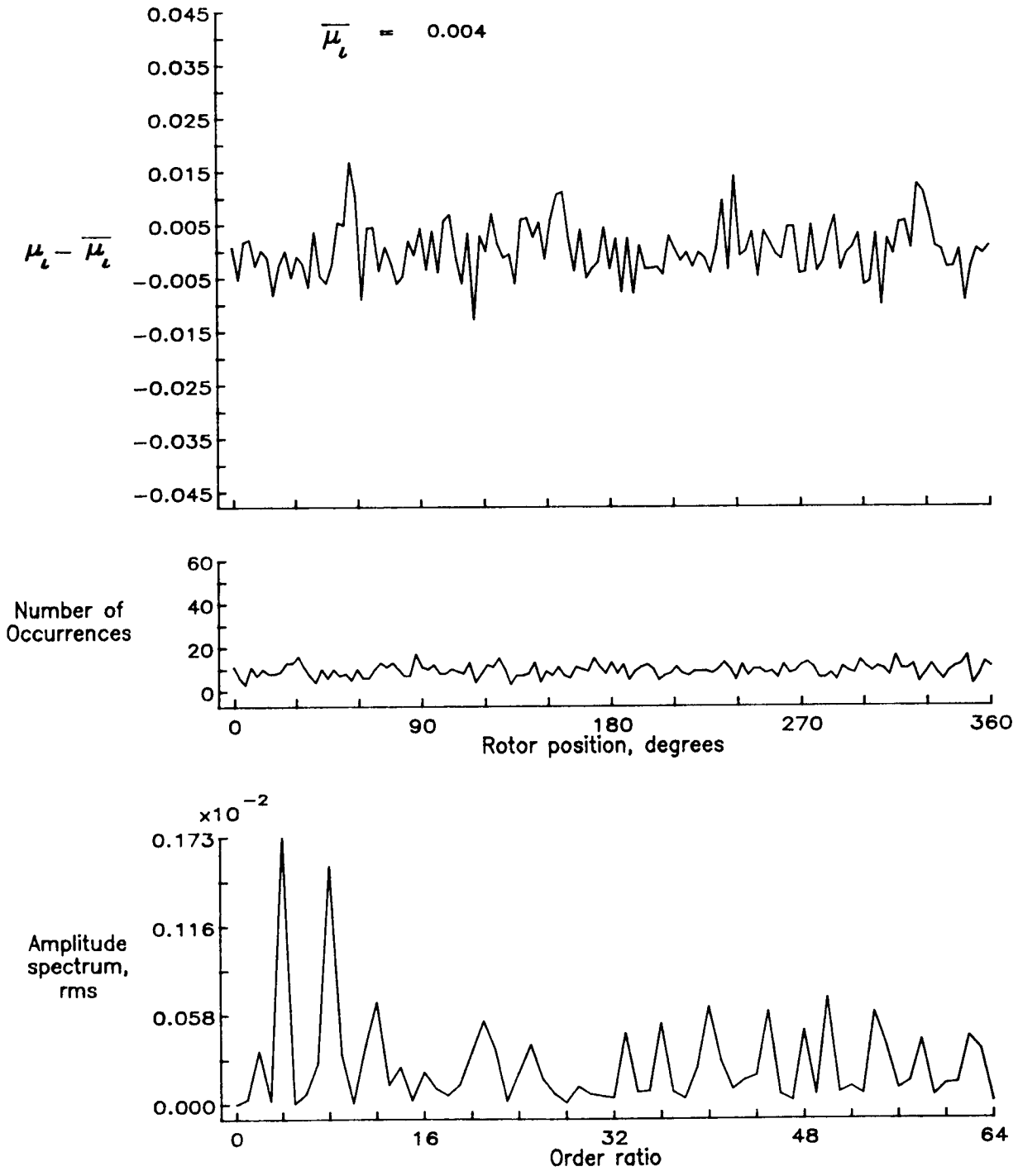


Figure 81.– Induced inflow velocity measured at 150 degrees and r/R of 0.70.

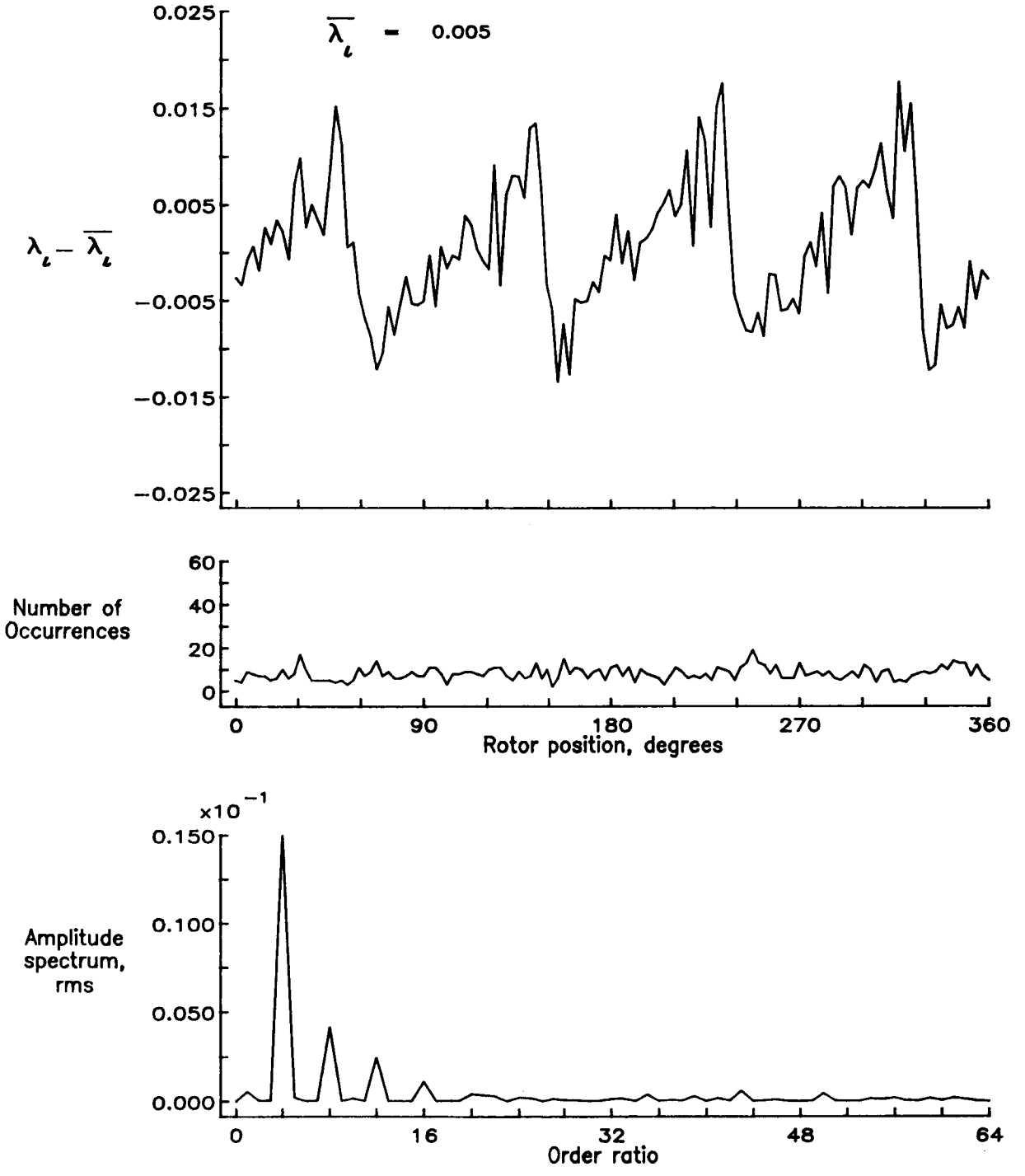


Figure 81.– Concluded.

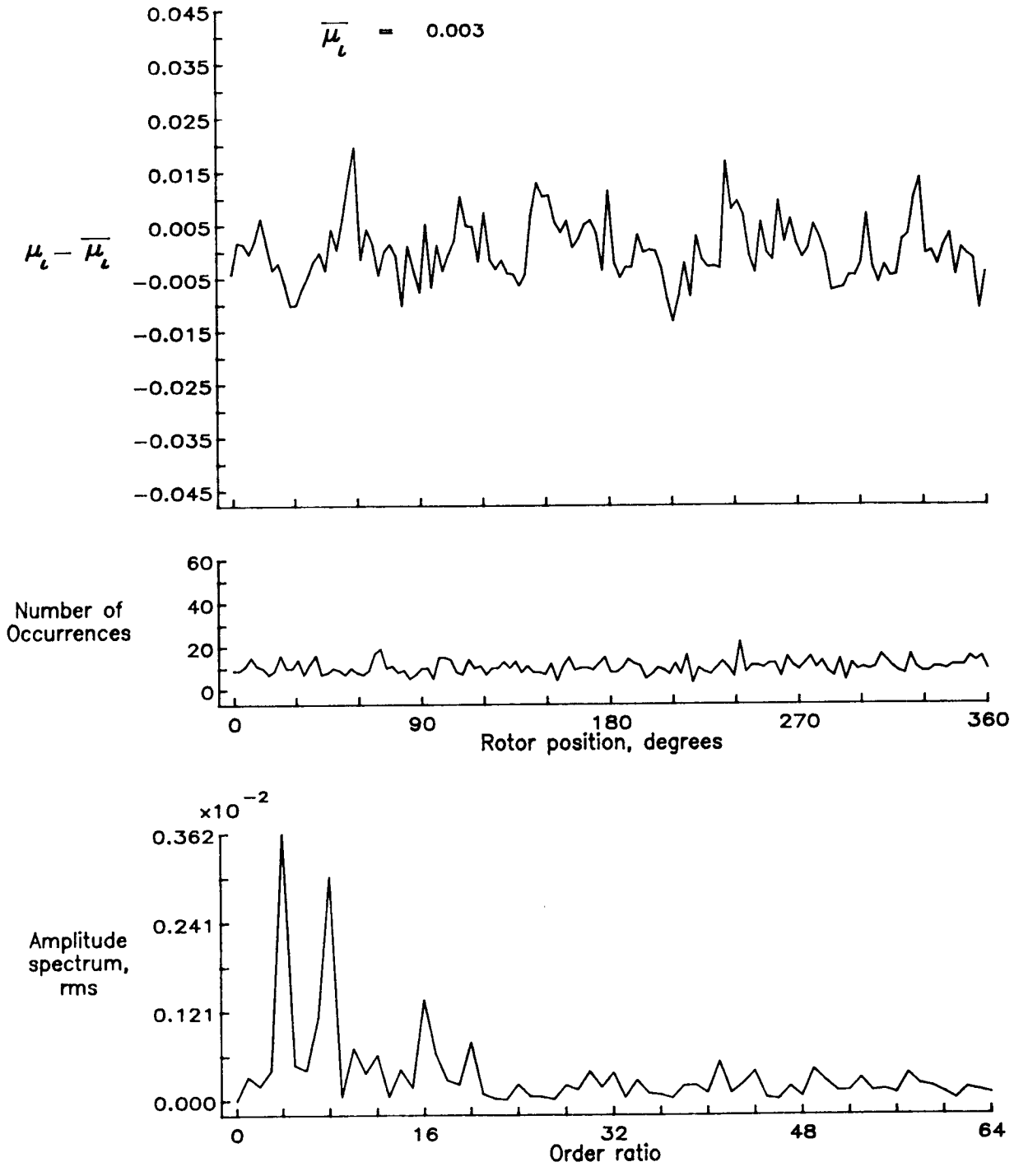


Figure 82.– Induced inflow velocity measured at 150 degrees and r/R of 0.74.

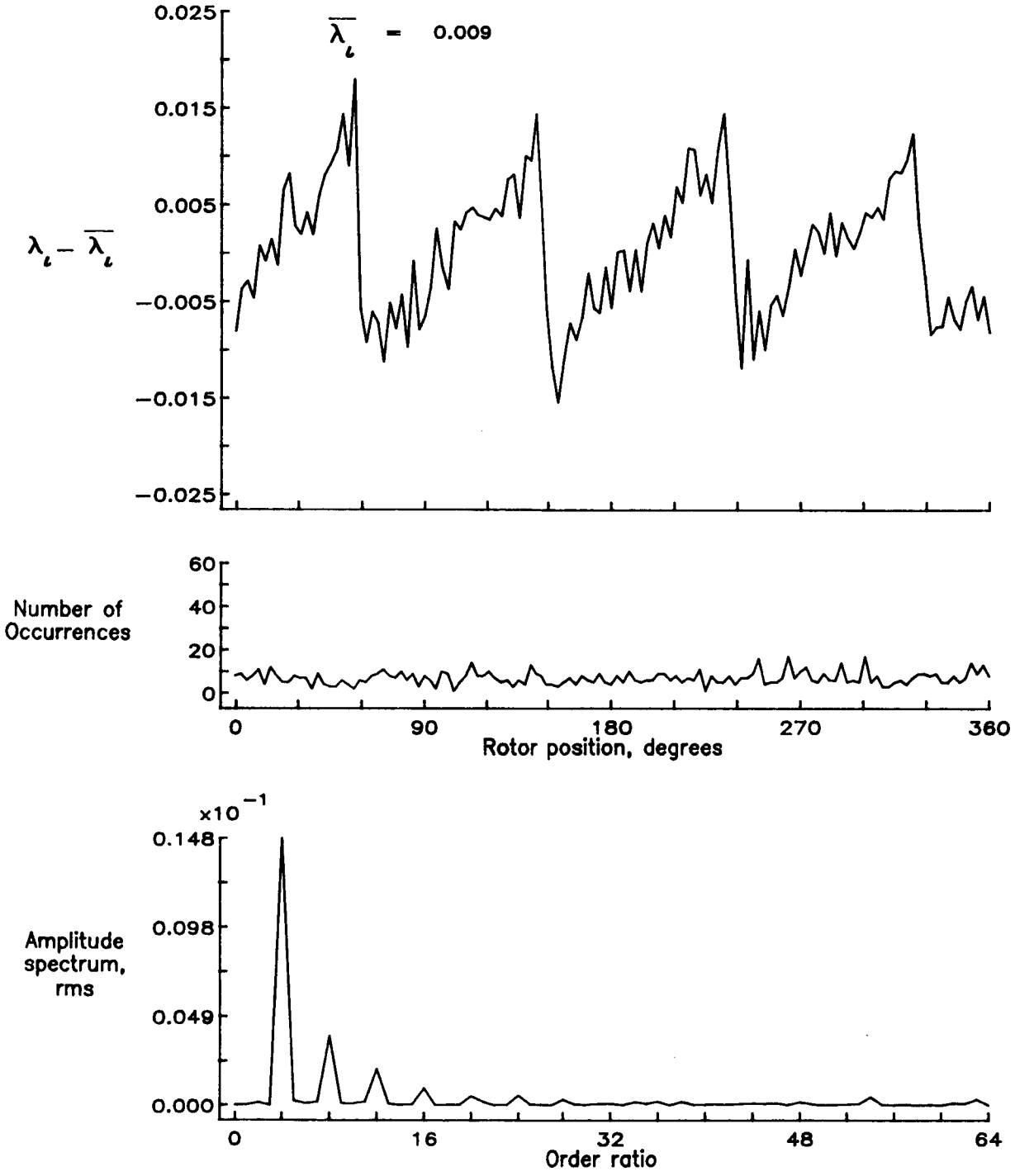


Figure 82.– Concluded.

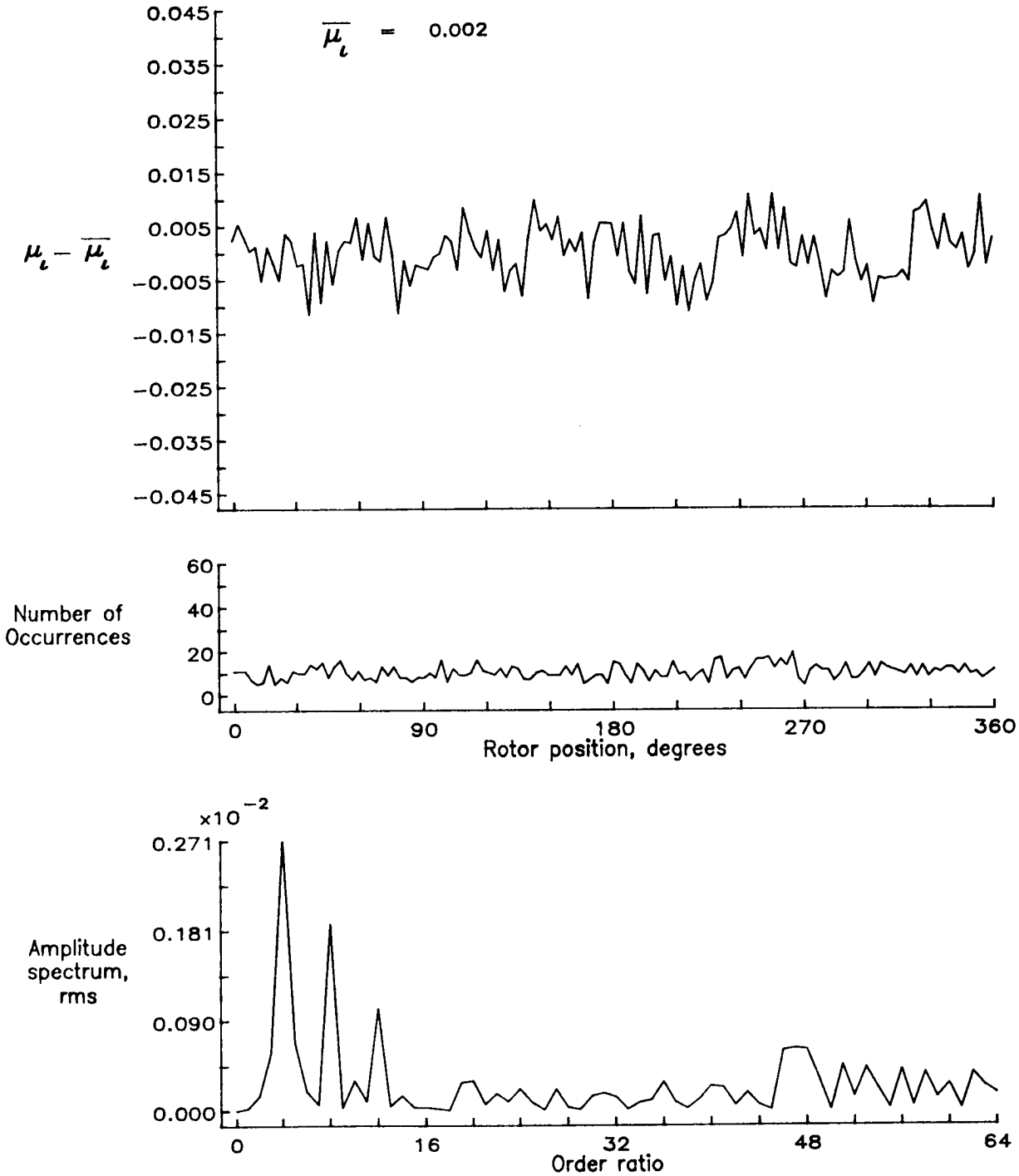


Figure 83.– Induced inflow velocity measured at 150 degrees and r/R of 0.78.

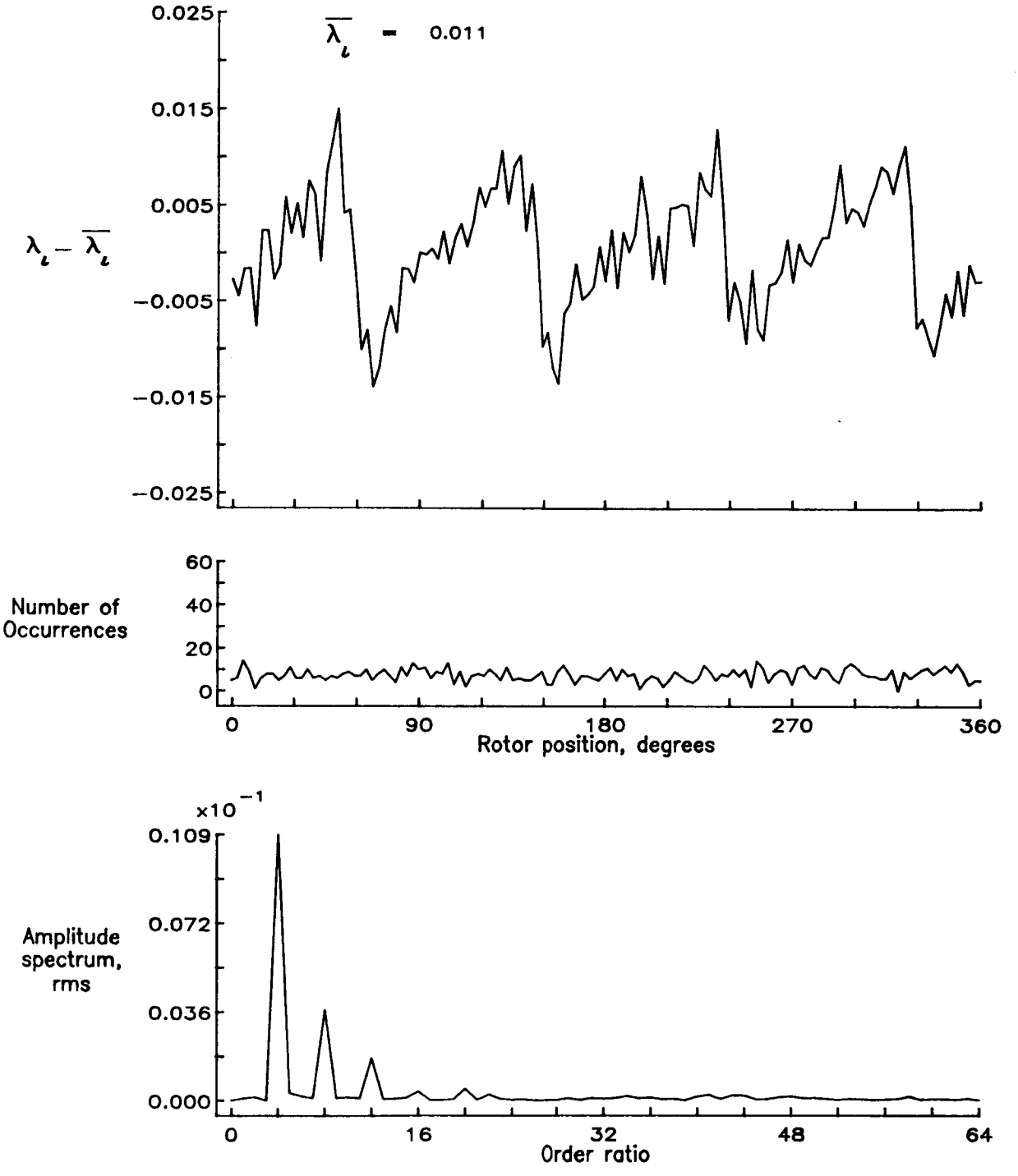


Figure 83.– Concluded.

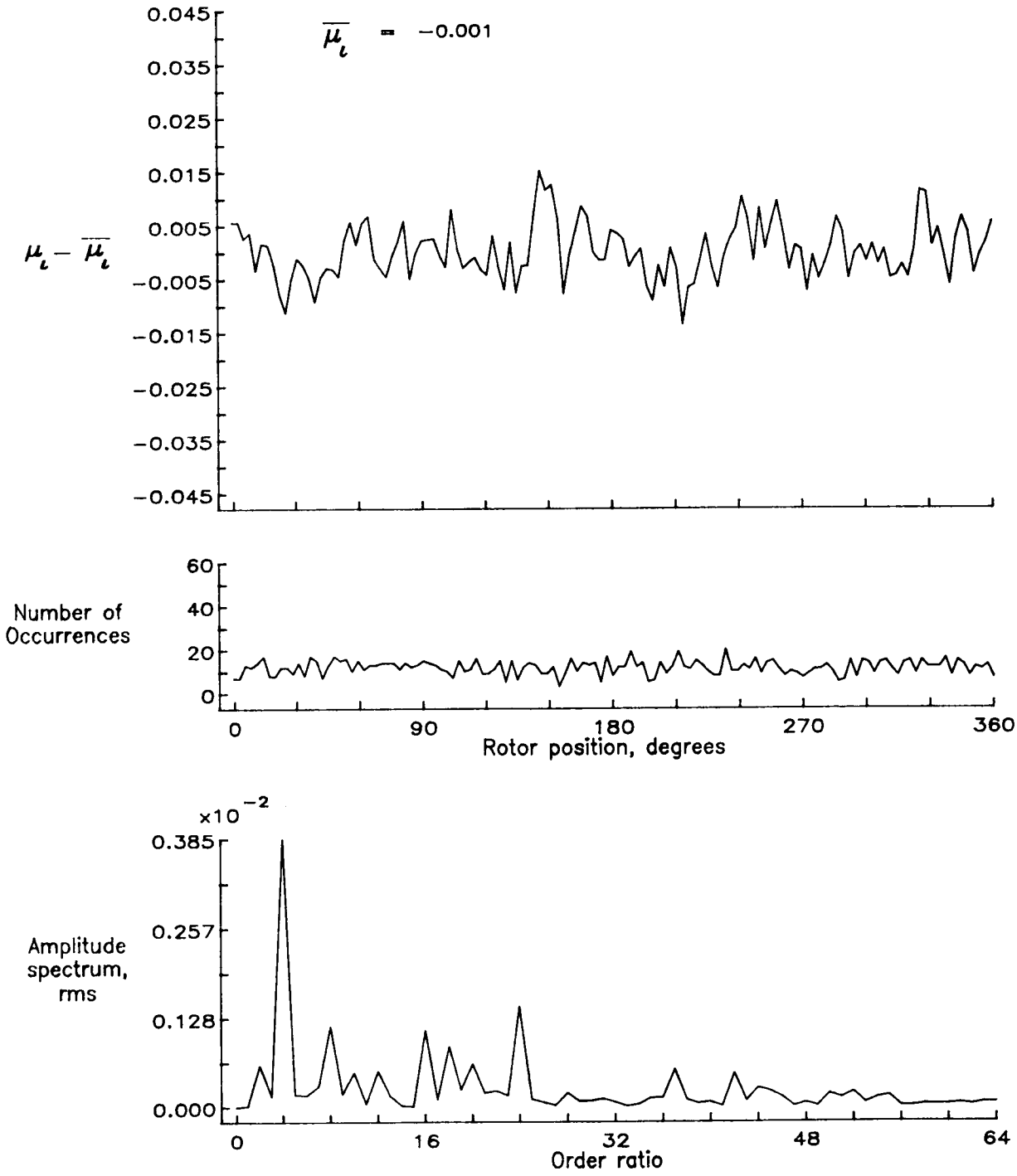


Figure 84.– Induced inflow velocity measured at 150 degrees and r/R of 0.82.

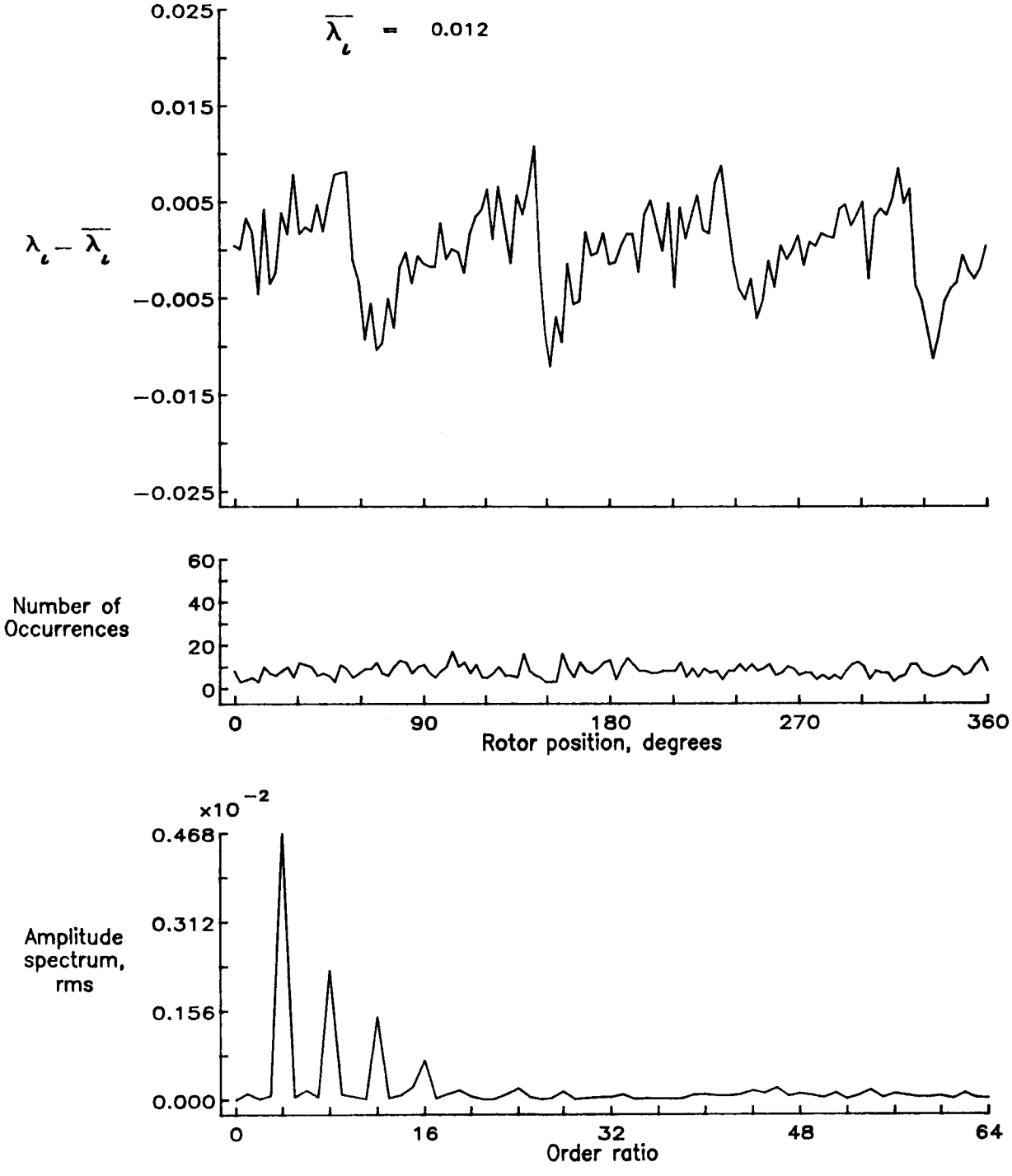


Figure 84.– Concluded.

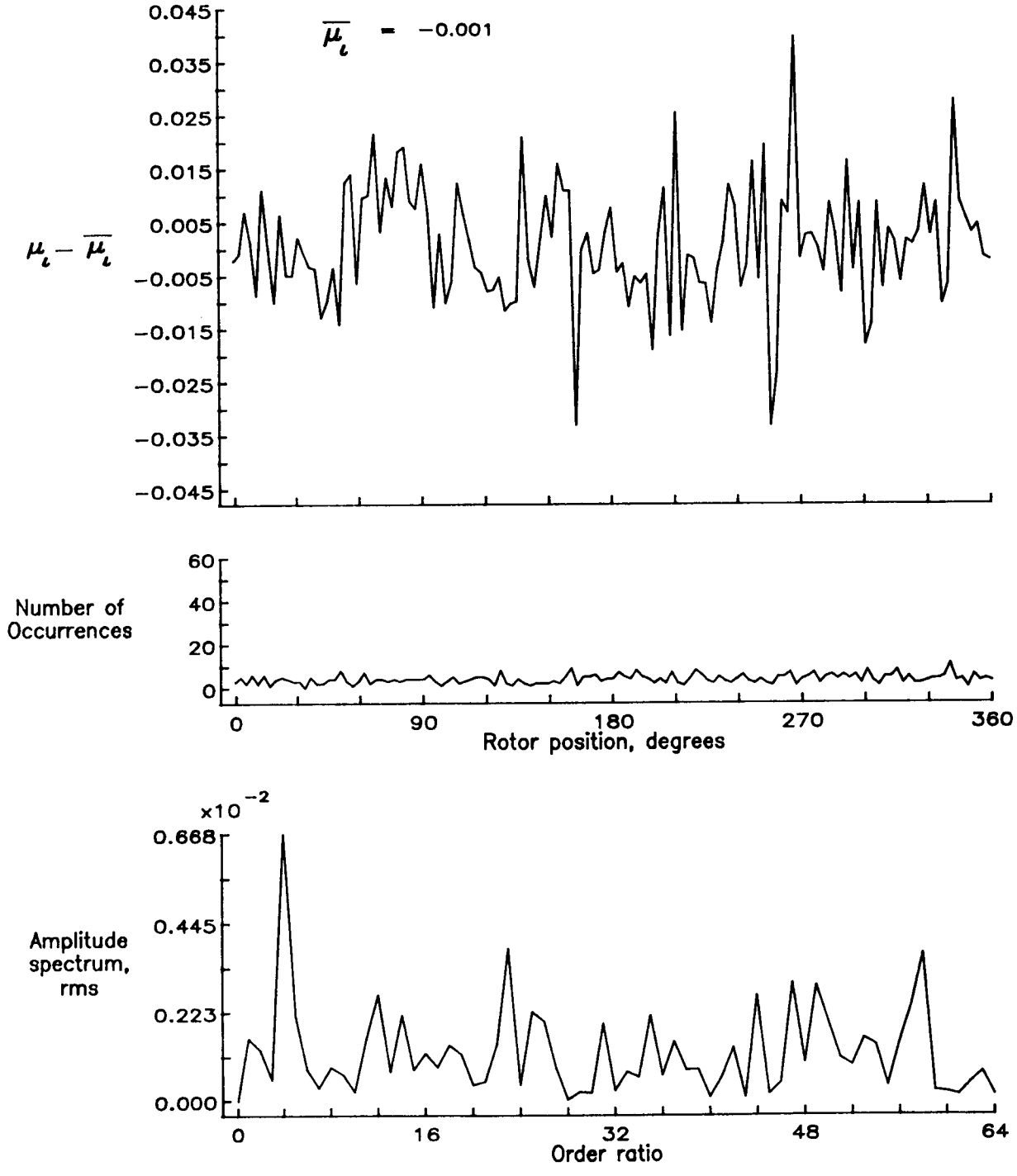


Figure 85.– Induced inflow velocity measured at 150 degrees and r/R of 0.86.

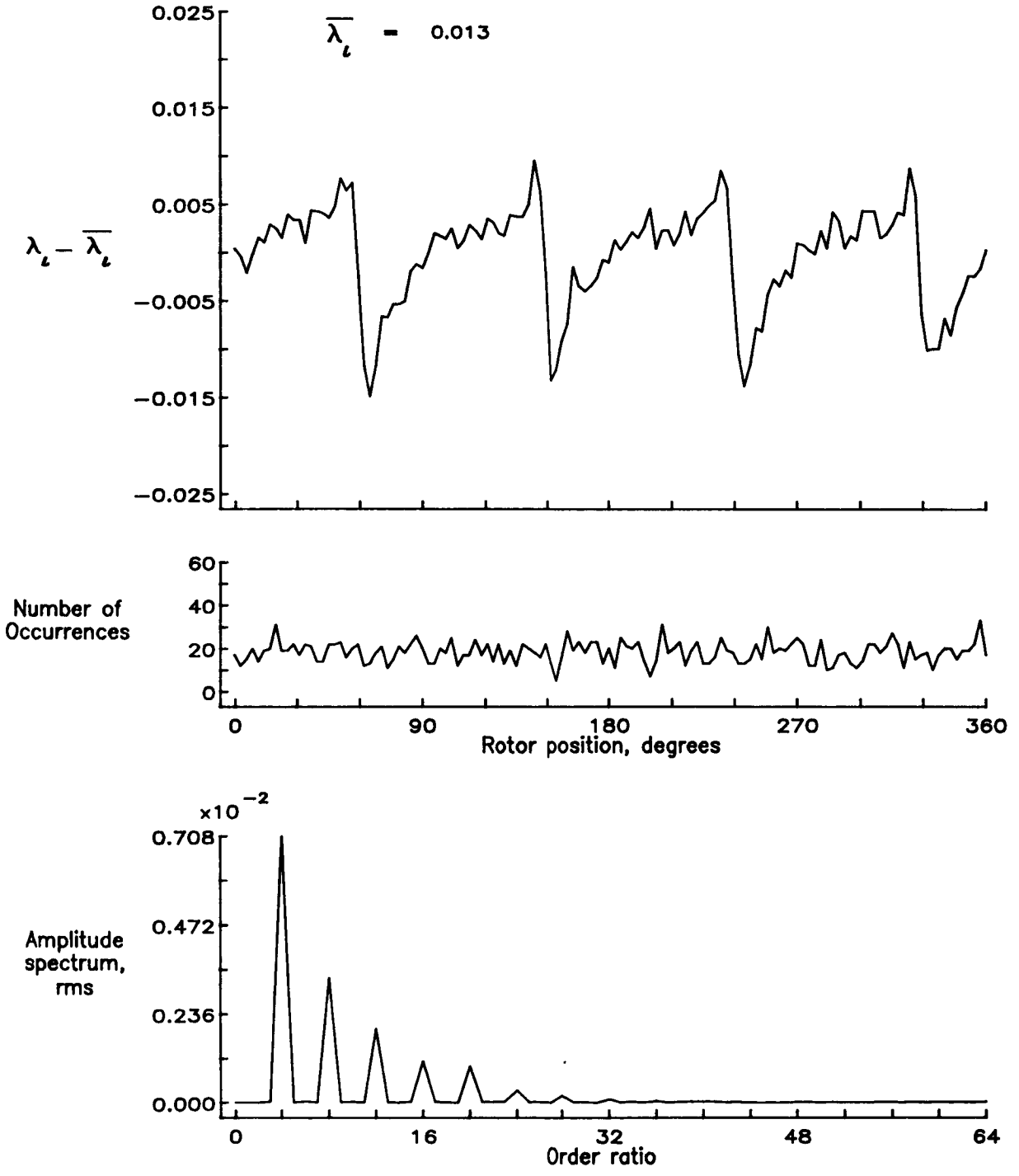


Figure 85.– Concluded.

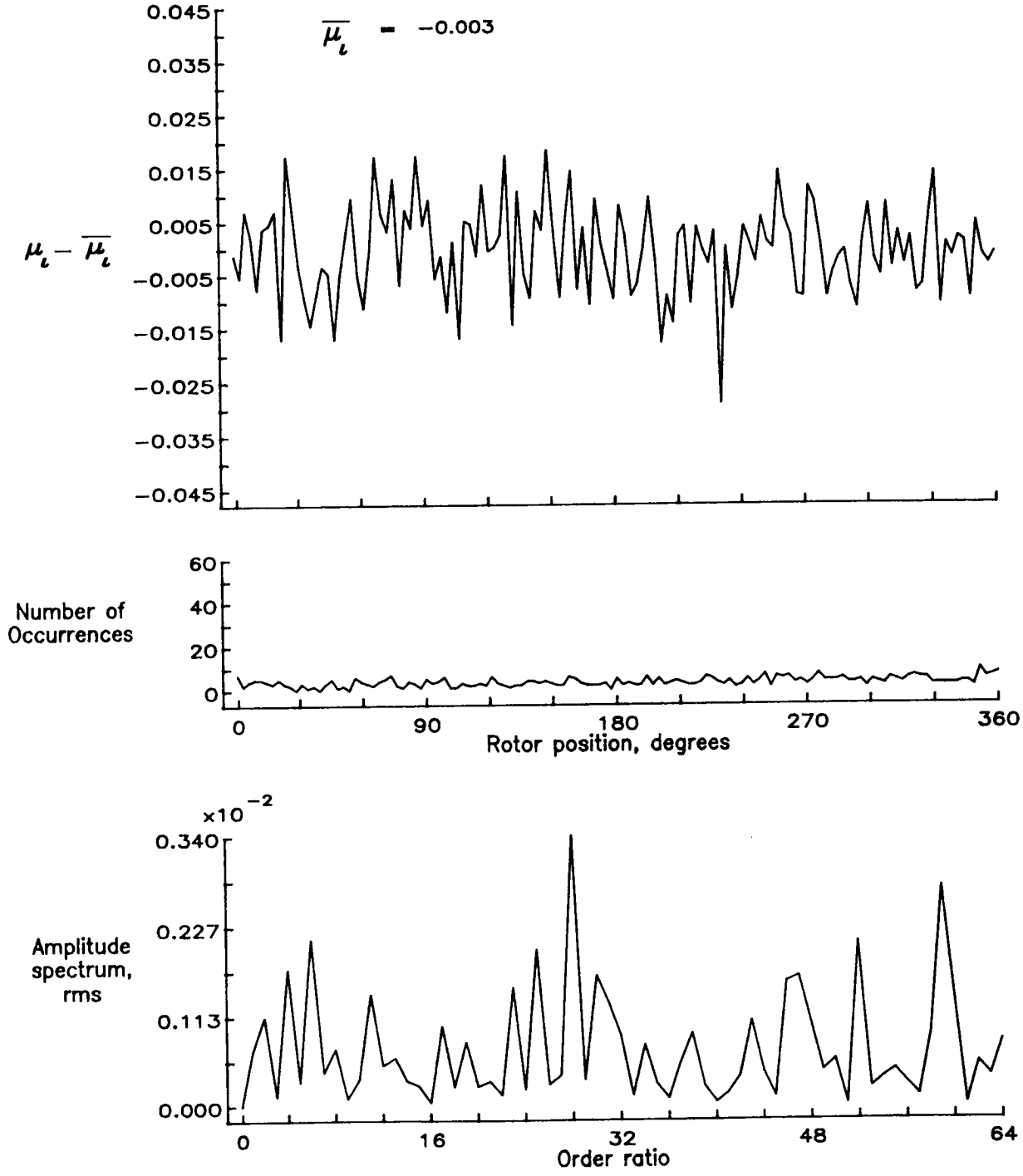


Figure 86.– Induced inflow velocity measured at 150 degrees and r/R of 0.90.

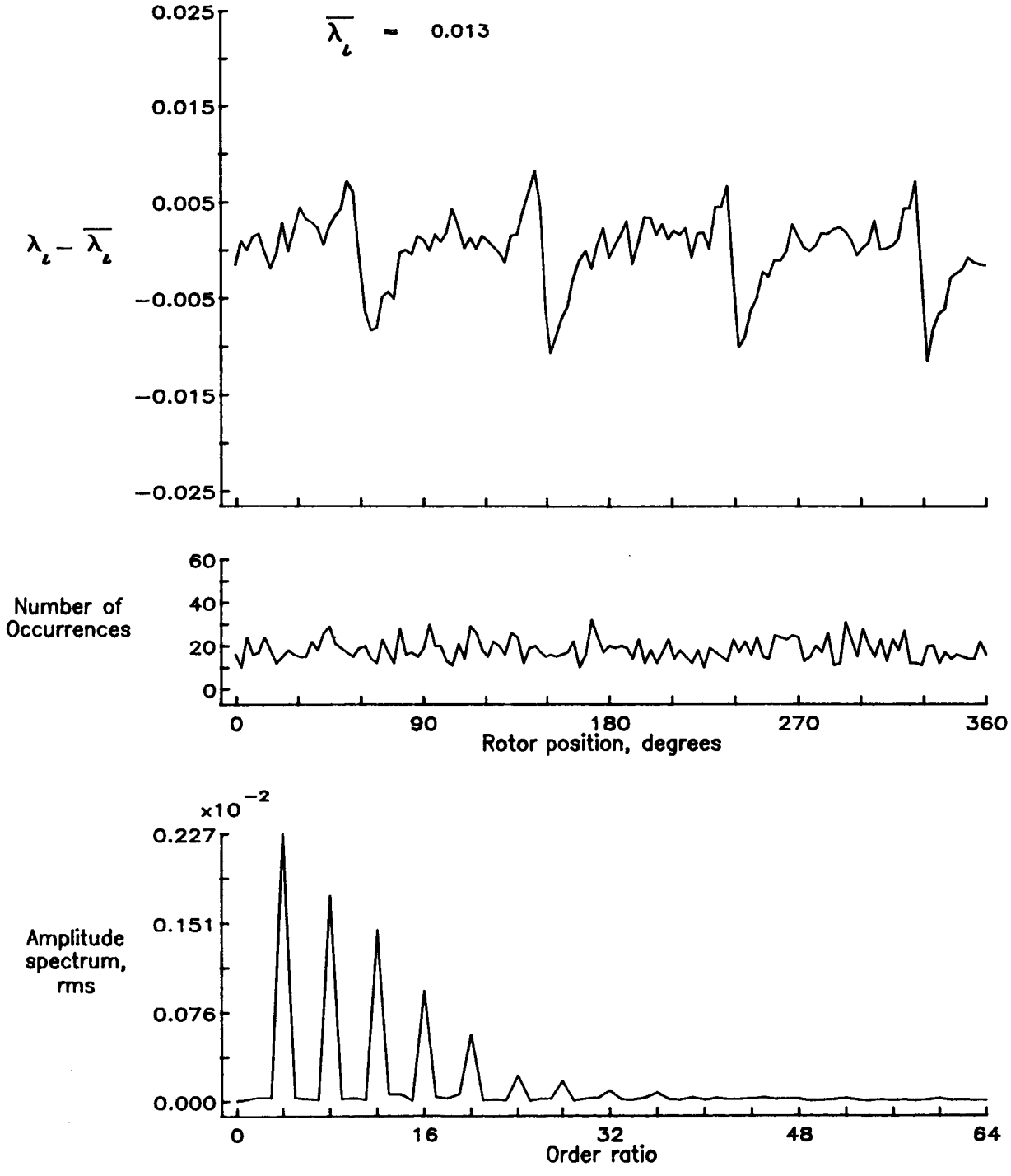


Figure 86.– Concluded.

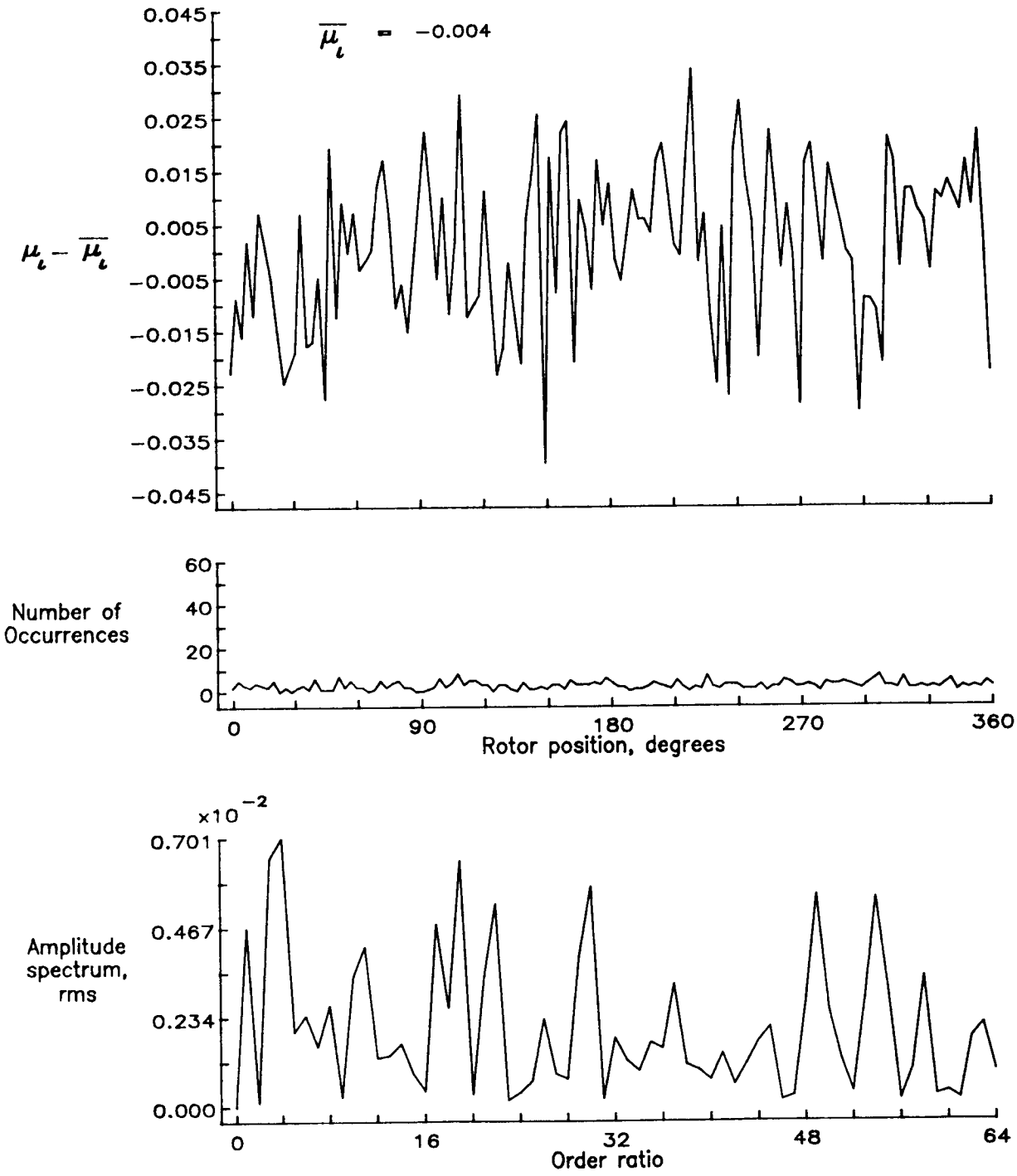


Figure 87.– Induced inflow velocity measured at 150 degrees and r/R of 0.94.

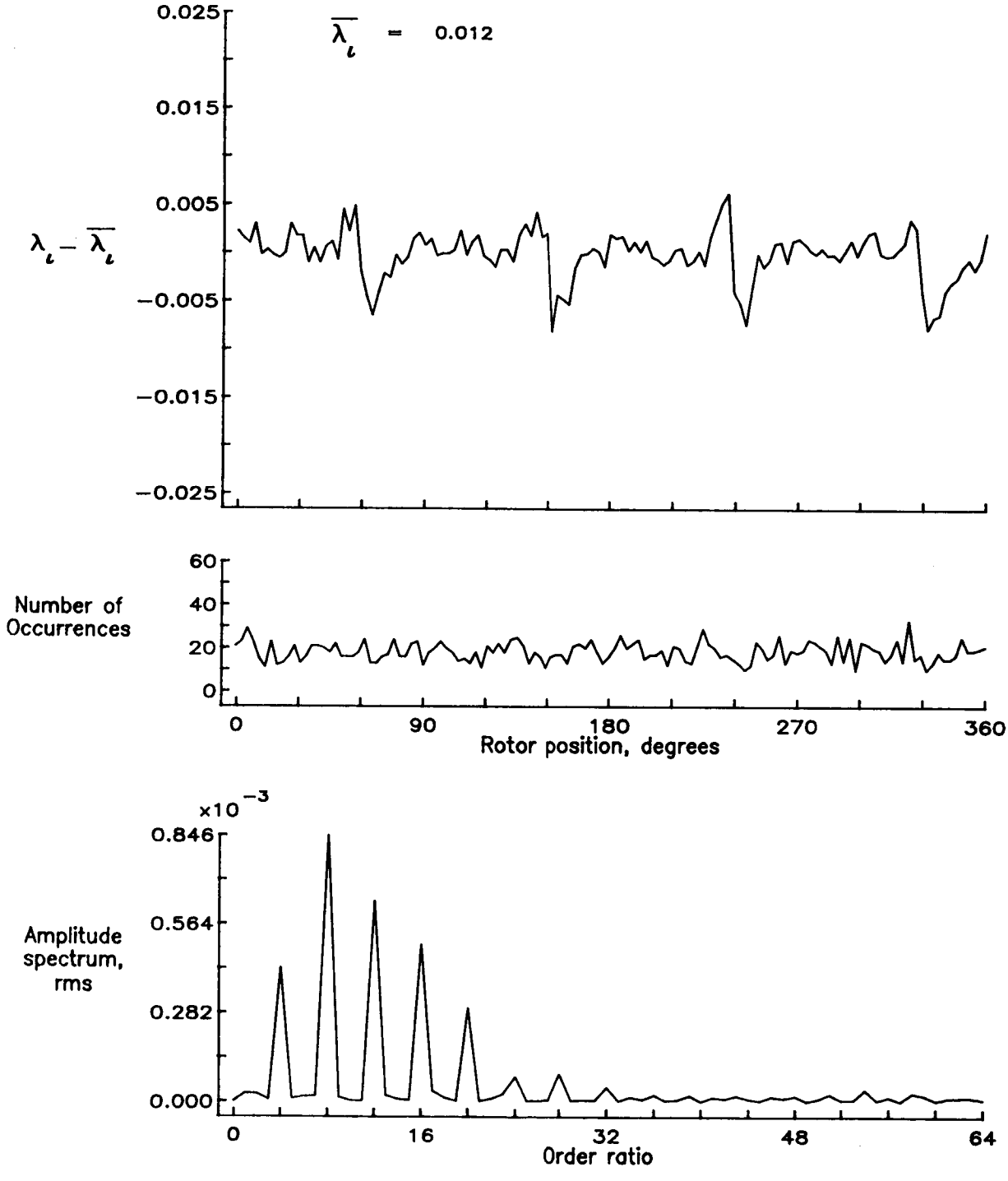


Figure 87.– Concluded.

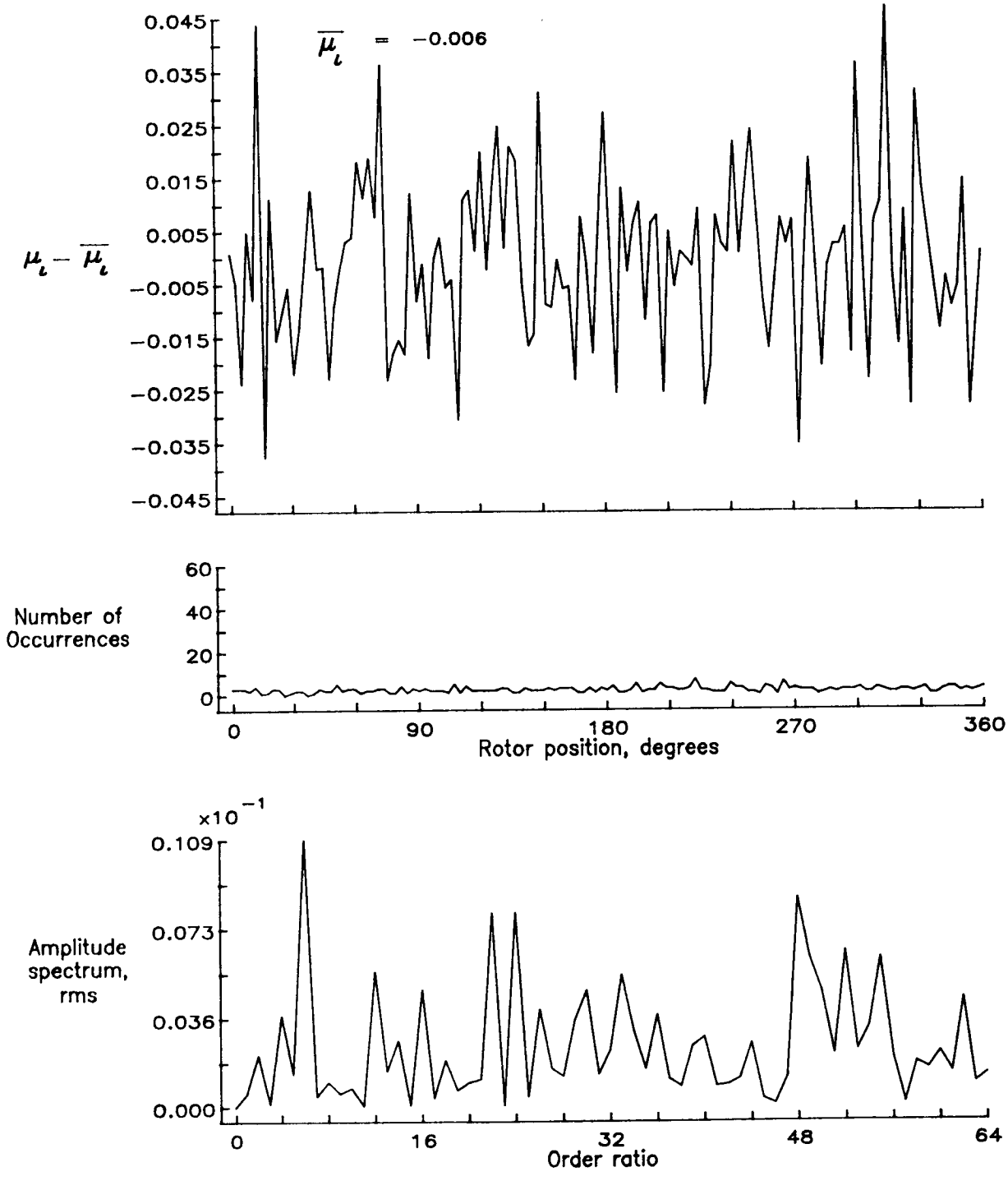


Figure 88.– Induced inflow velocity measured at 150 degrees and r/R of 0.98.

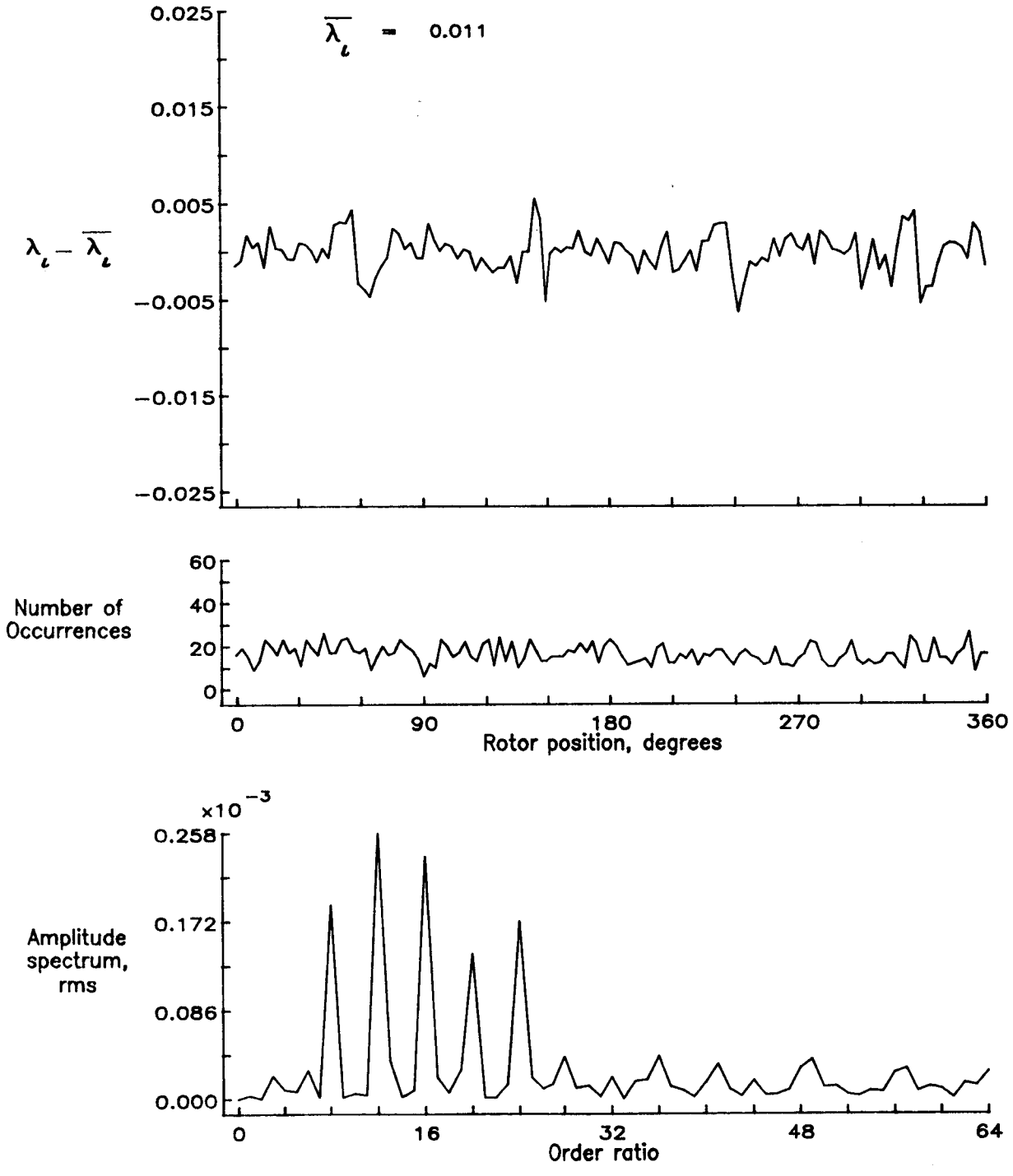


Figure 88.– Concluded.

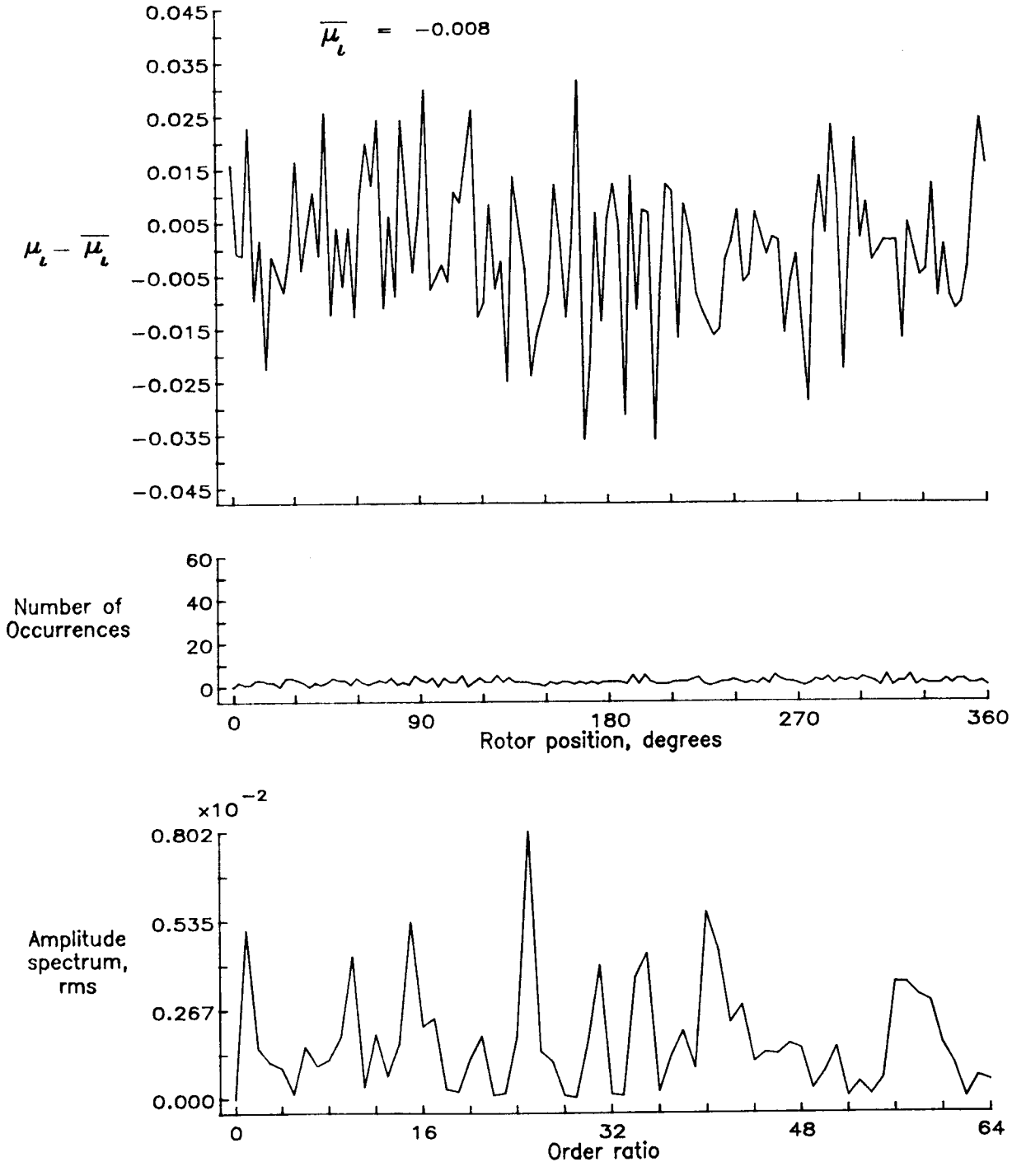


Figure 89.– Induced inflow velocity measured at 150 degrees and r/R of 1.02.

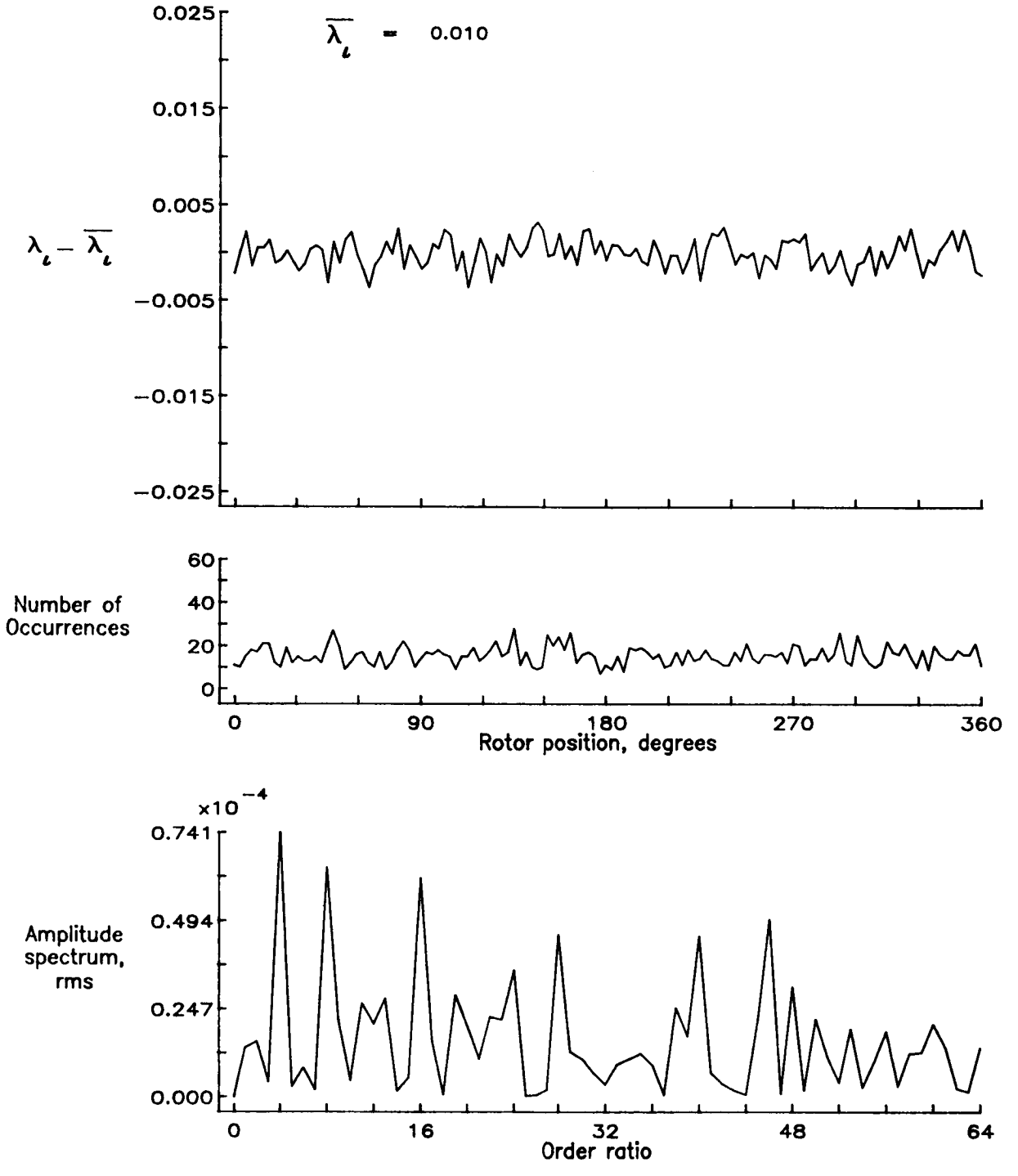


Figure 89.– Concluded.

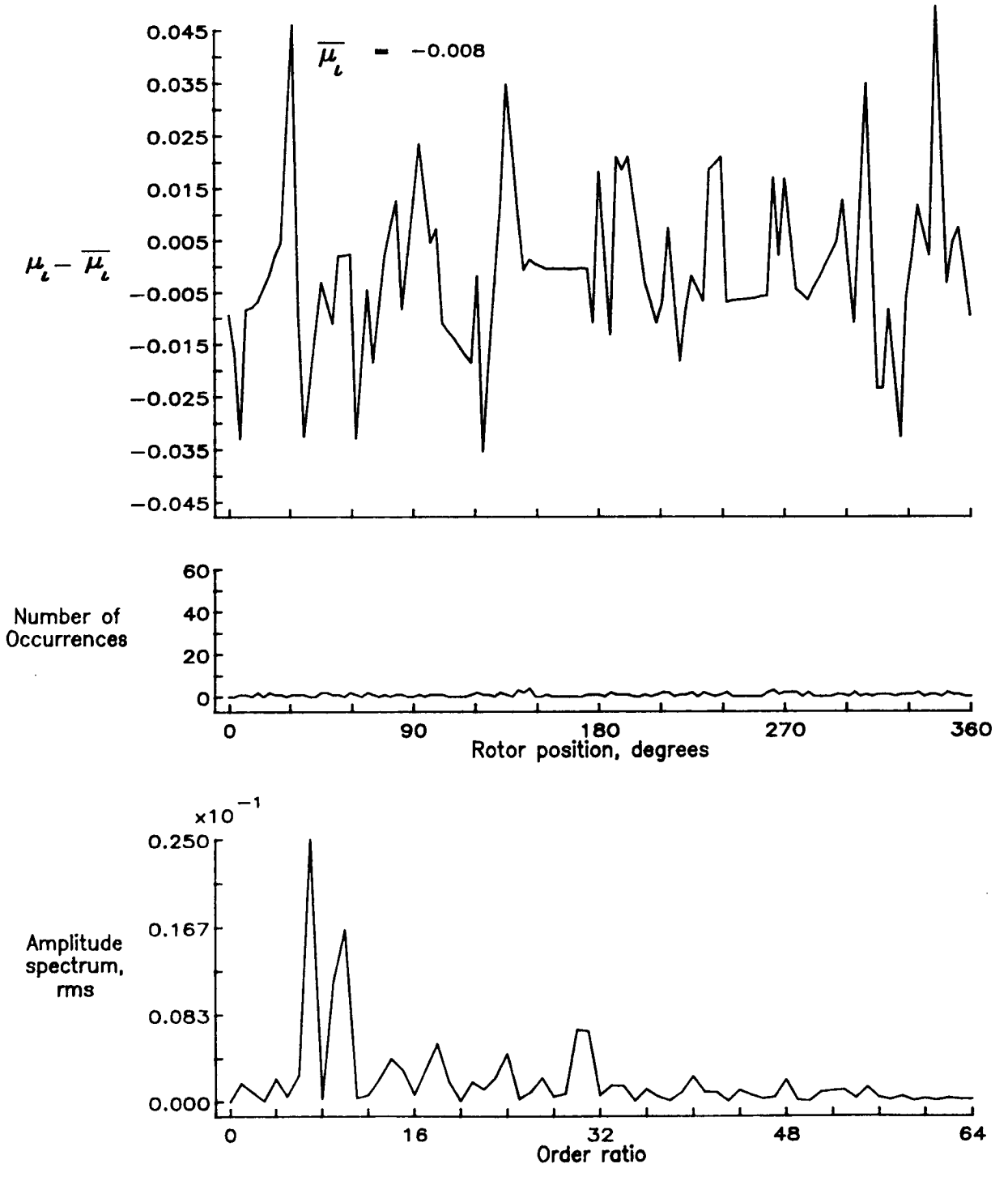


Figure 90.– Induced inflow velocity measured at 150 degrees and r/R of 1.04.

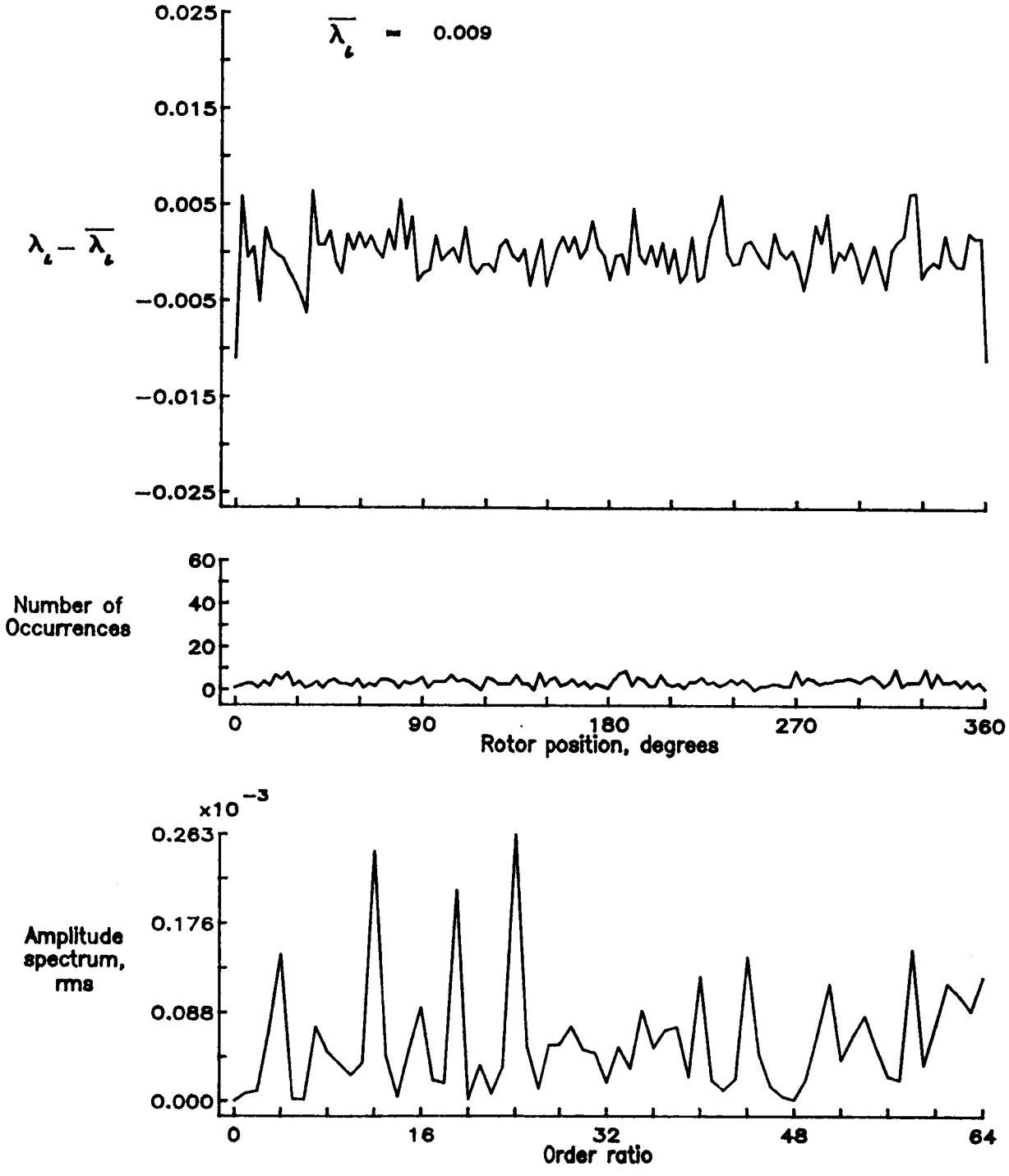


Figure 90.– Concluded.

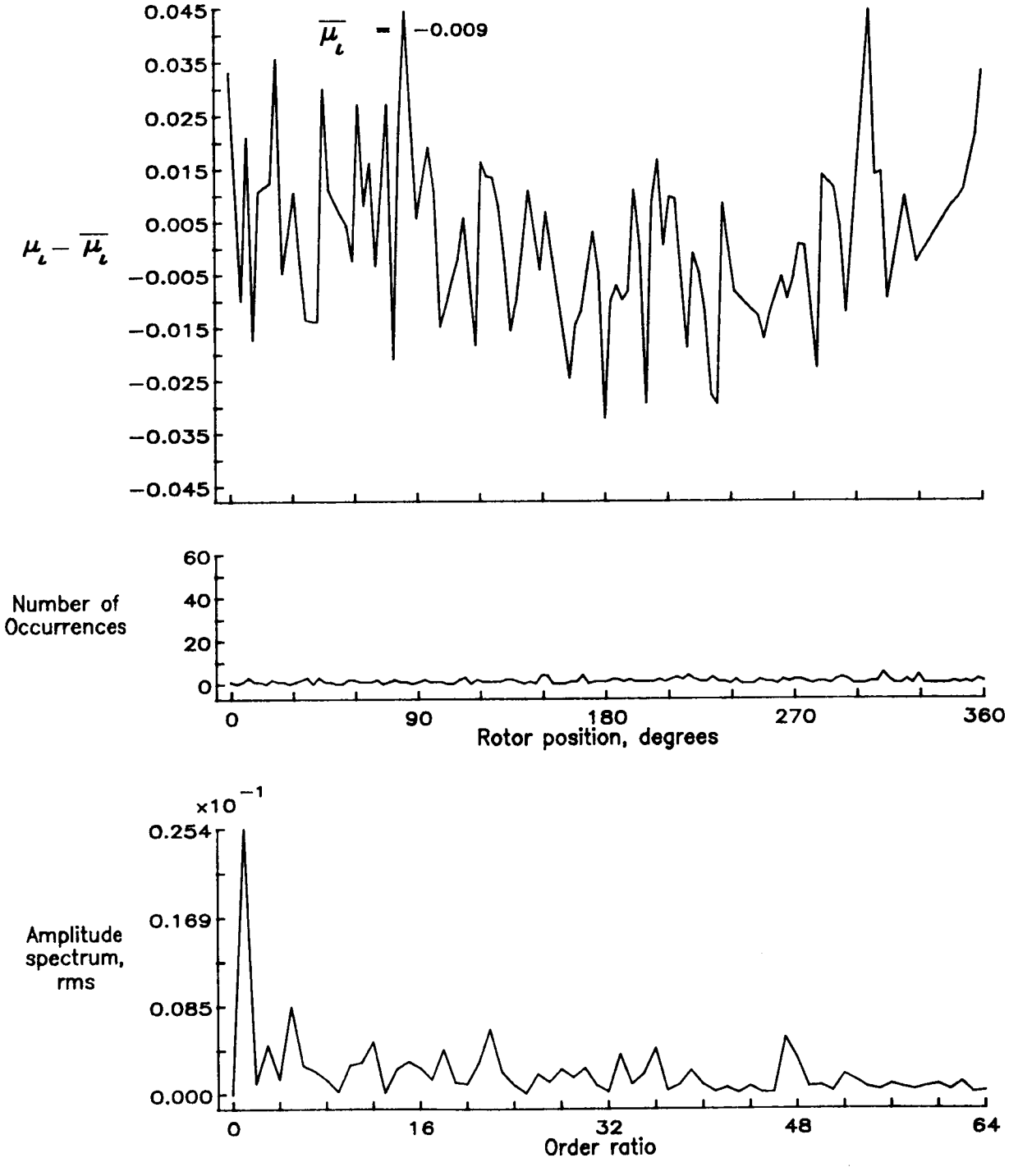


Figure 91.– Induced inflow velocity measured at 150 degrees and r/R of 1.12.

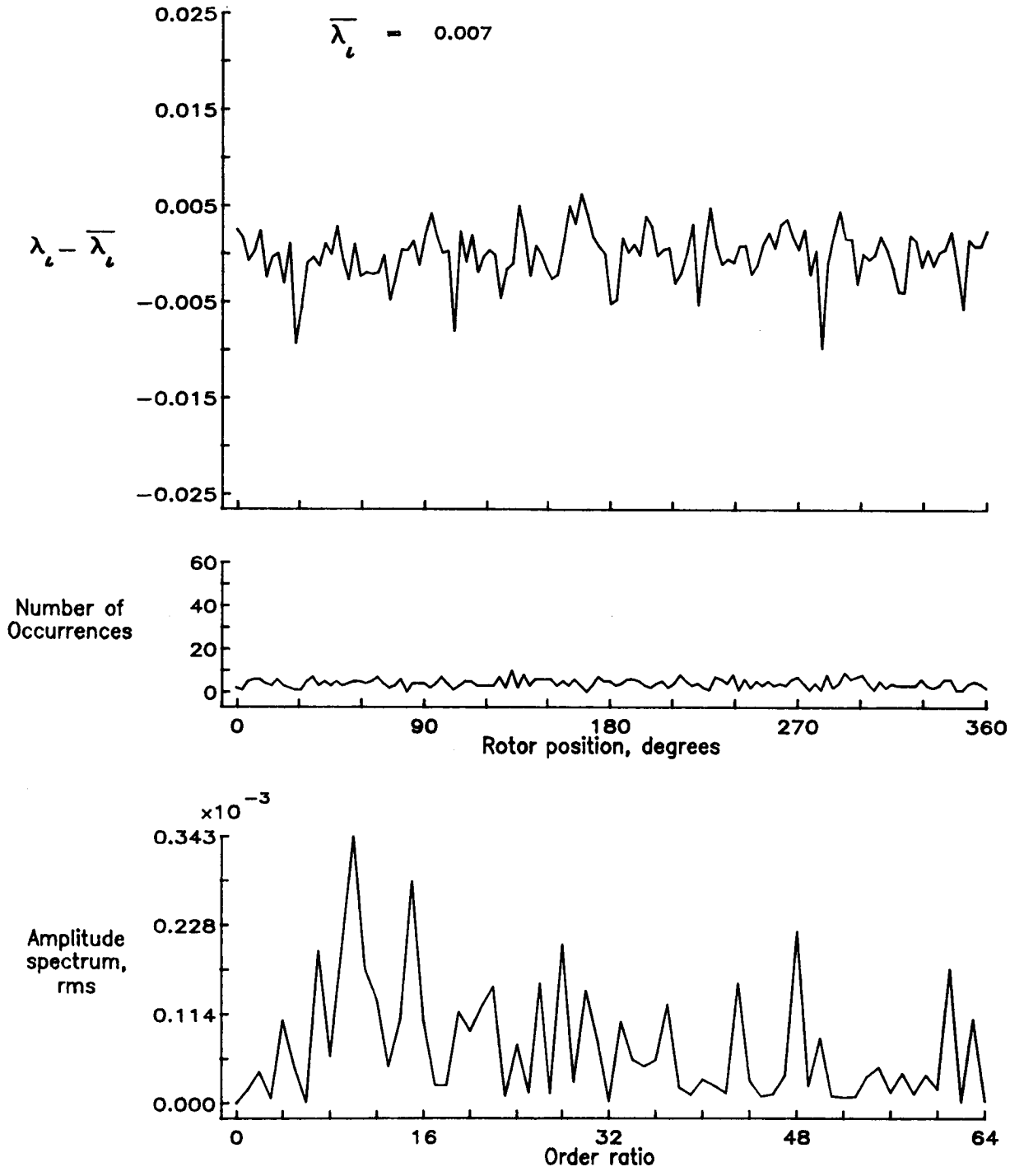


Figure 91.– Concluded.

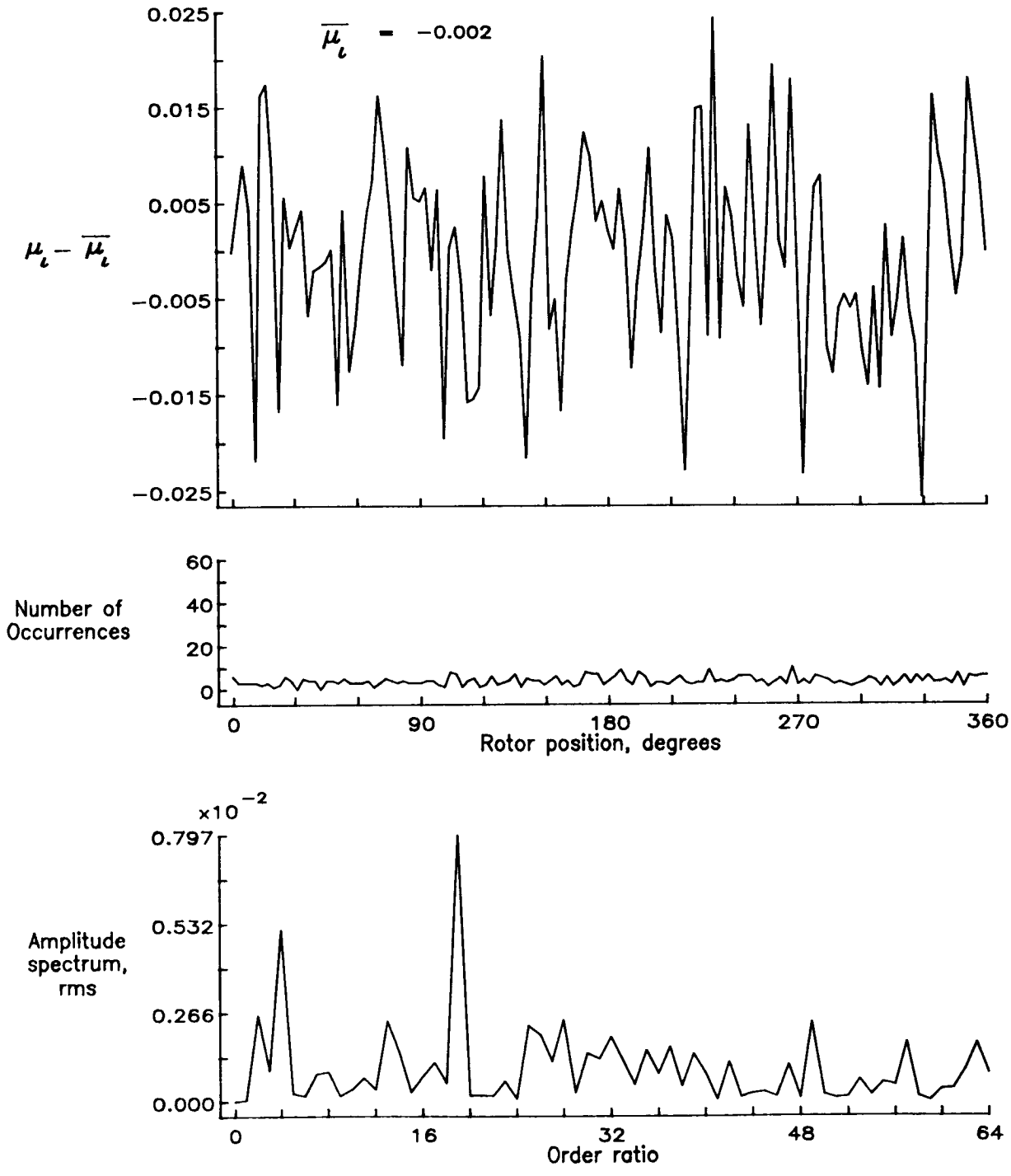


Figure 92.– Induced inflow velocity measured at 180 degrees and r/R of 0.20.

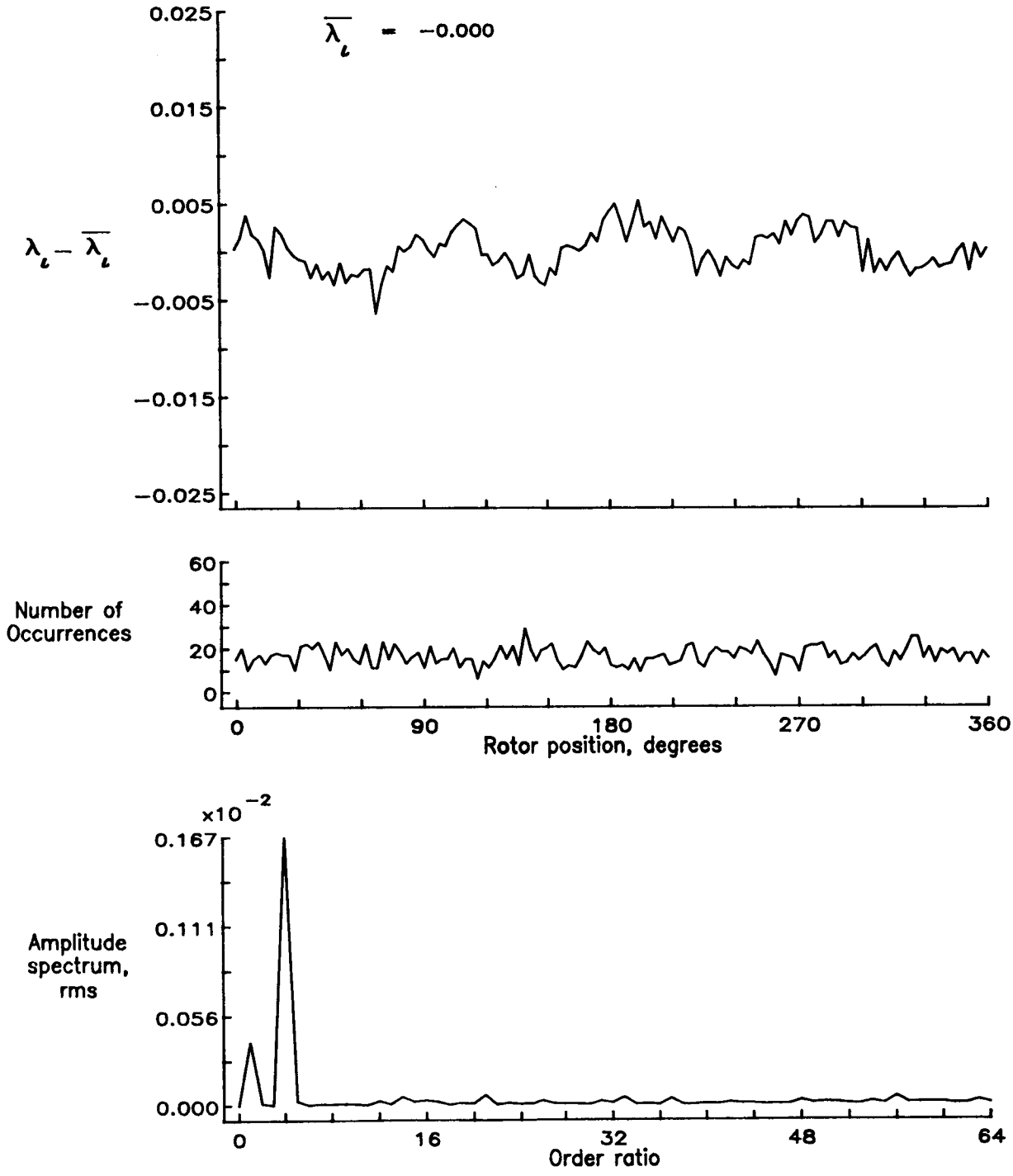


Figure 92.– Concluded.

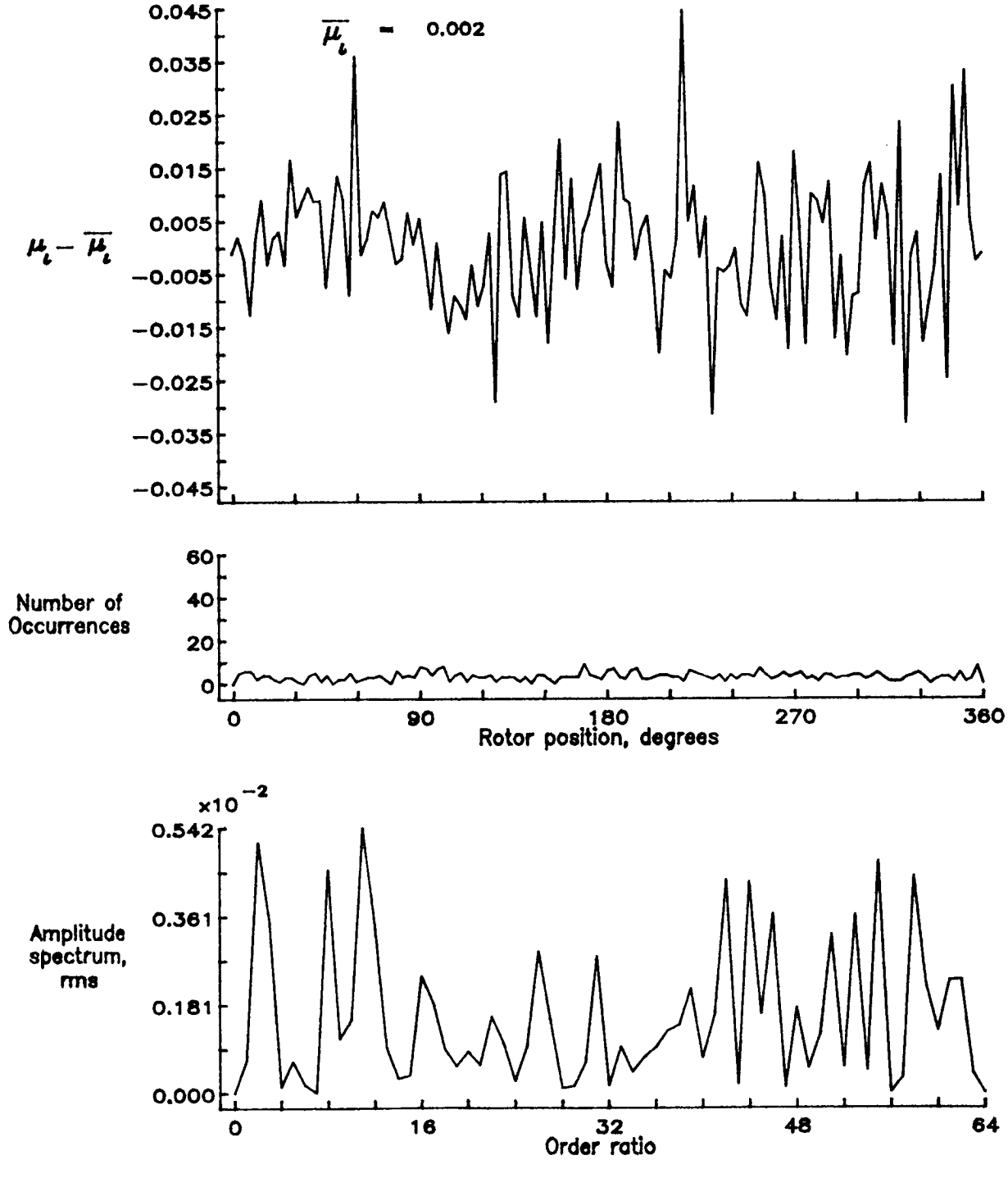


Figure 93.– Induced inflow velocity measured at 180 degrees and r/R of 0.40.

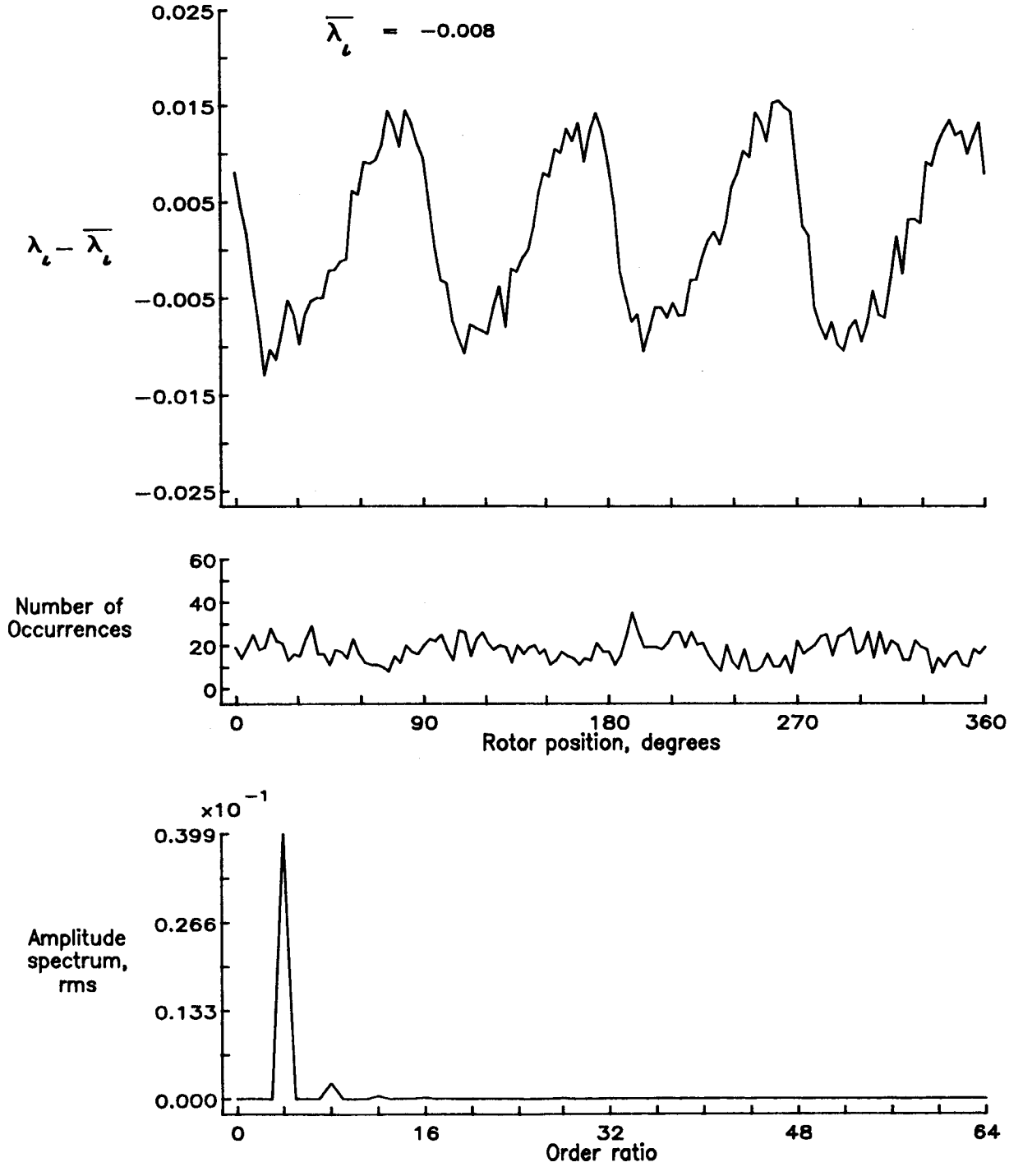


Figure 93.– Concluded.

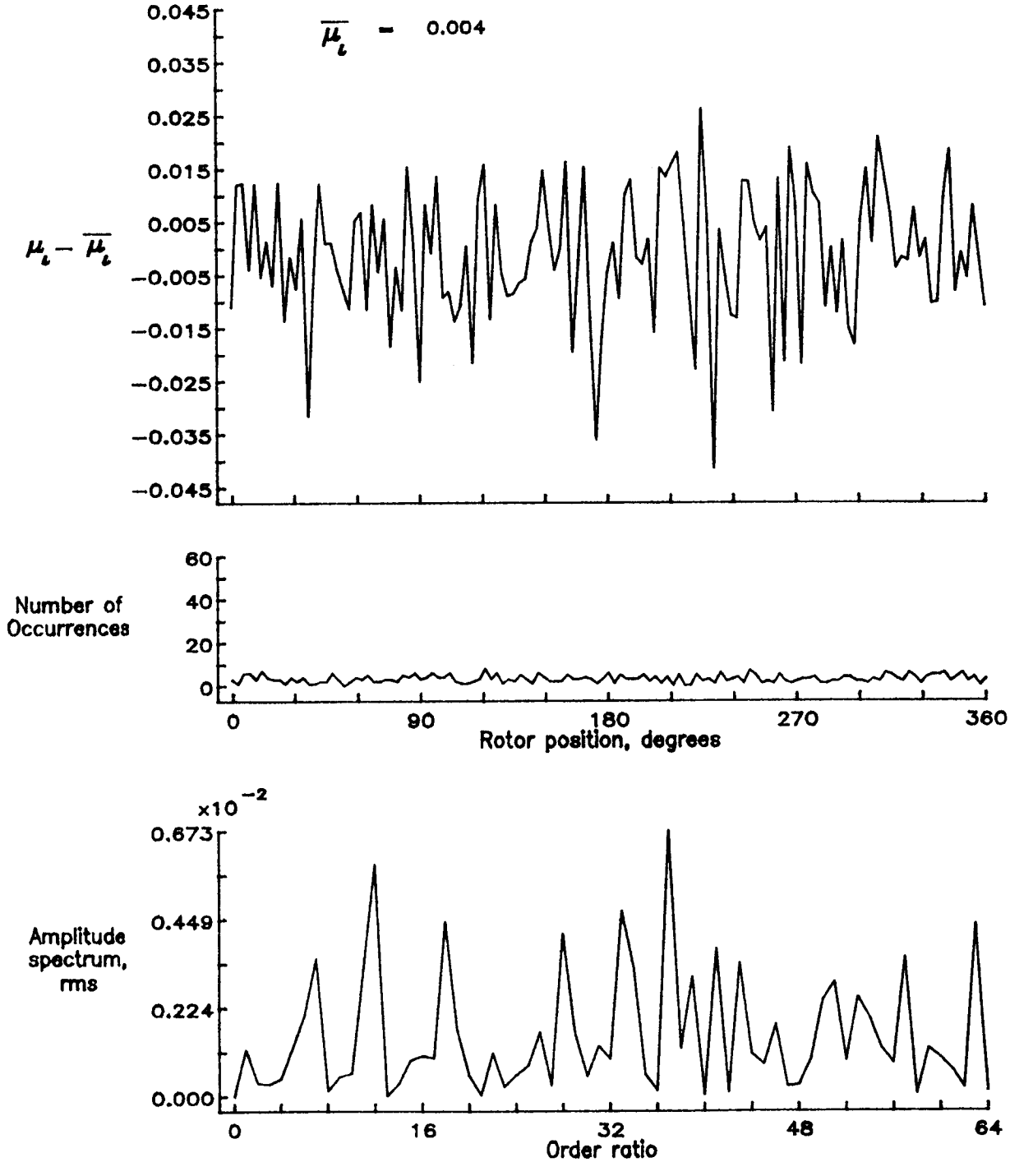


Figure 94.– Induced inflow velocity measured at 180 degrees and r/R of 0.50.

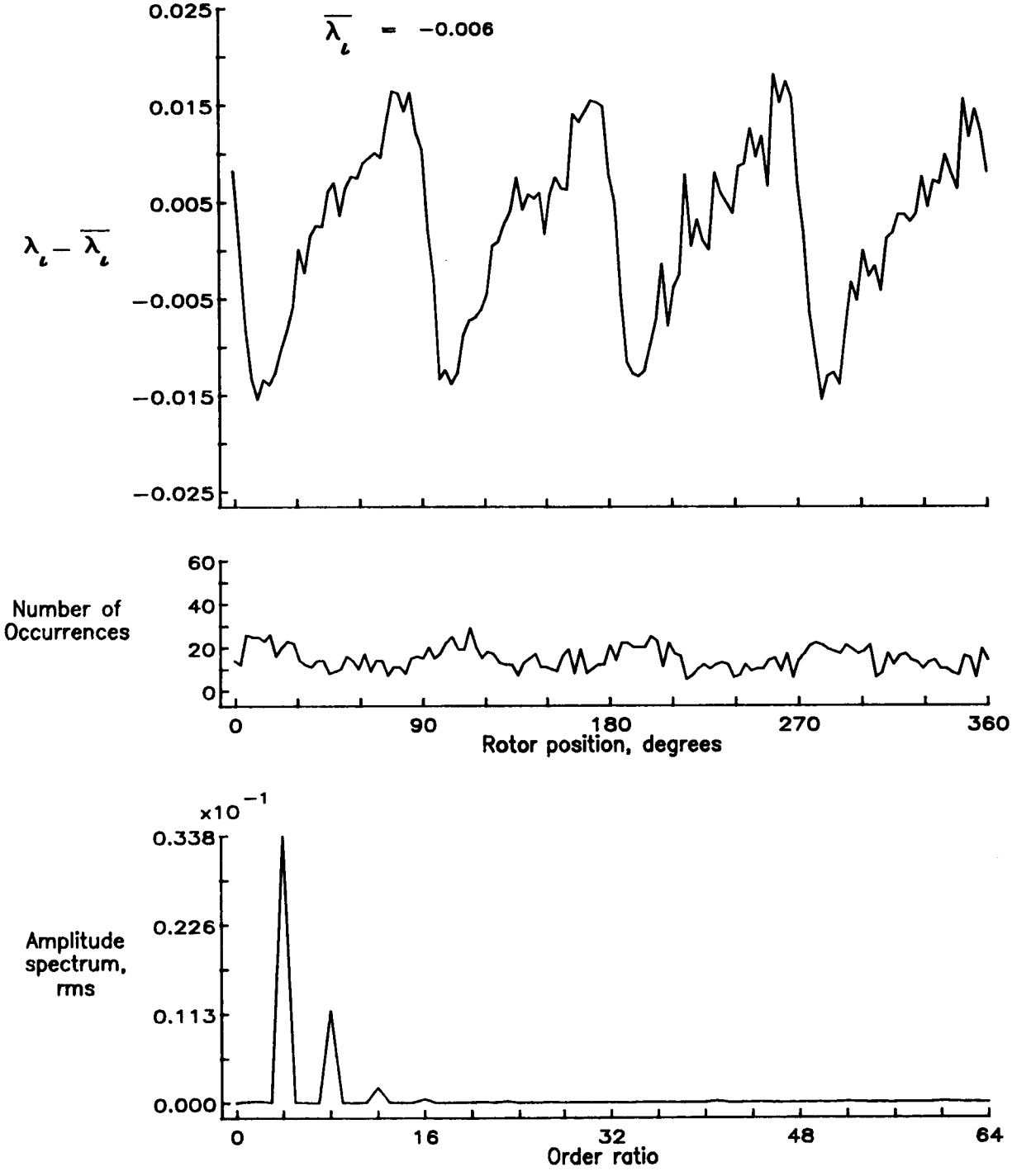


Figure 94.– Concluded.

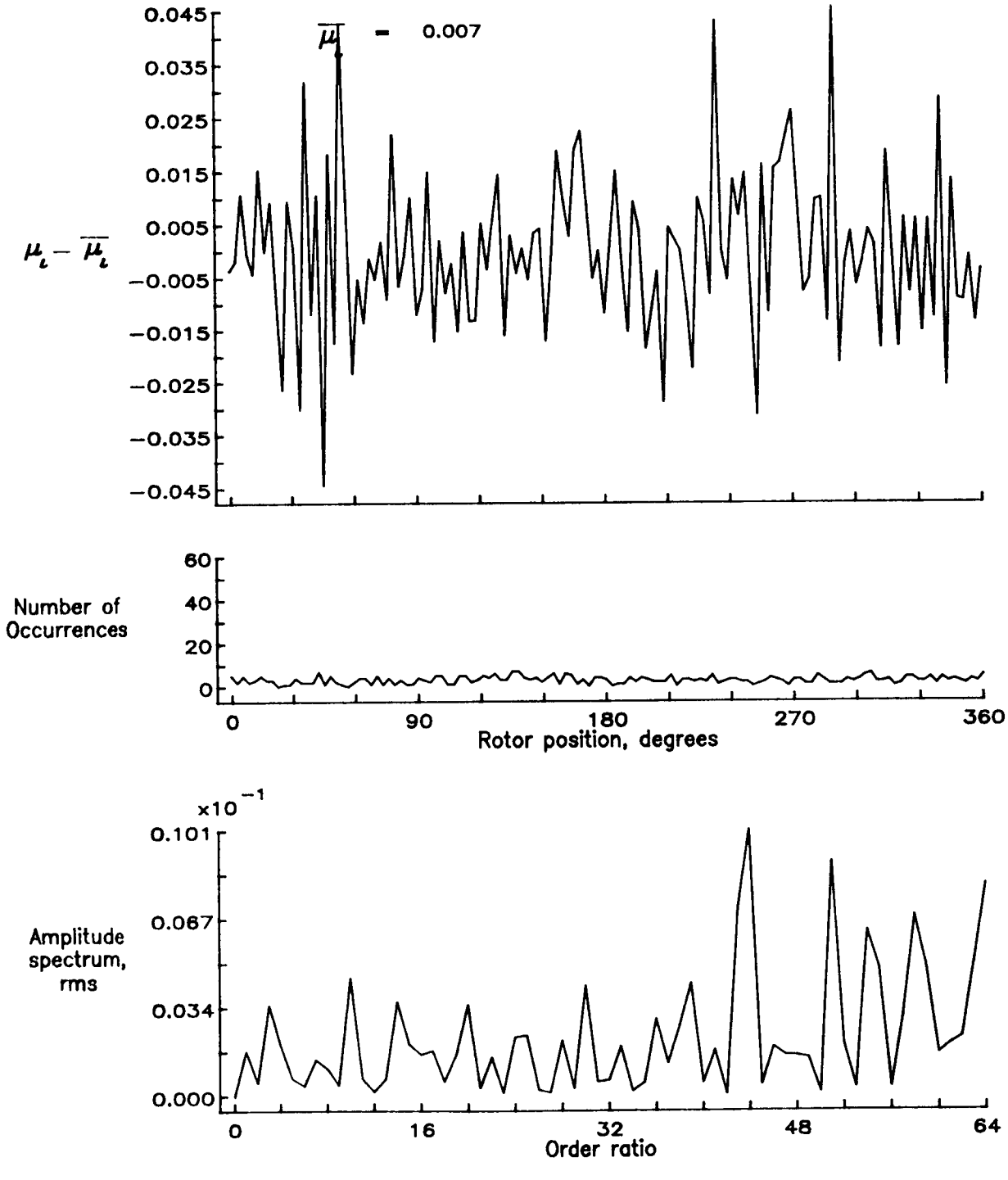


Figure 95.– Induced inflow velocity measured at 180 degrees and r/R of 0.60.

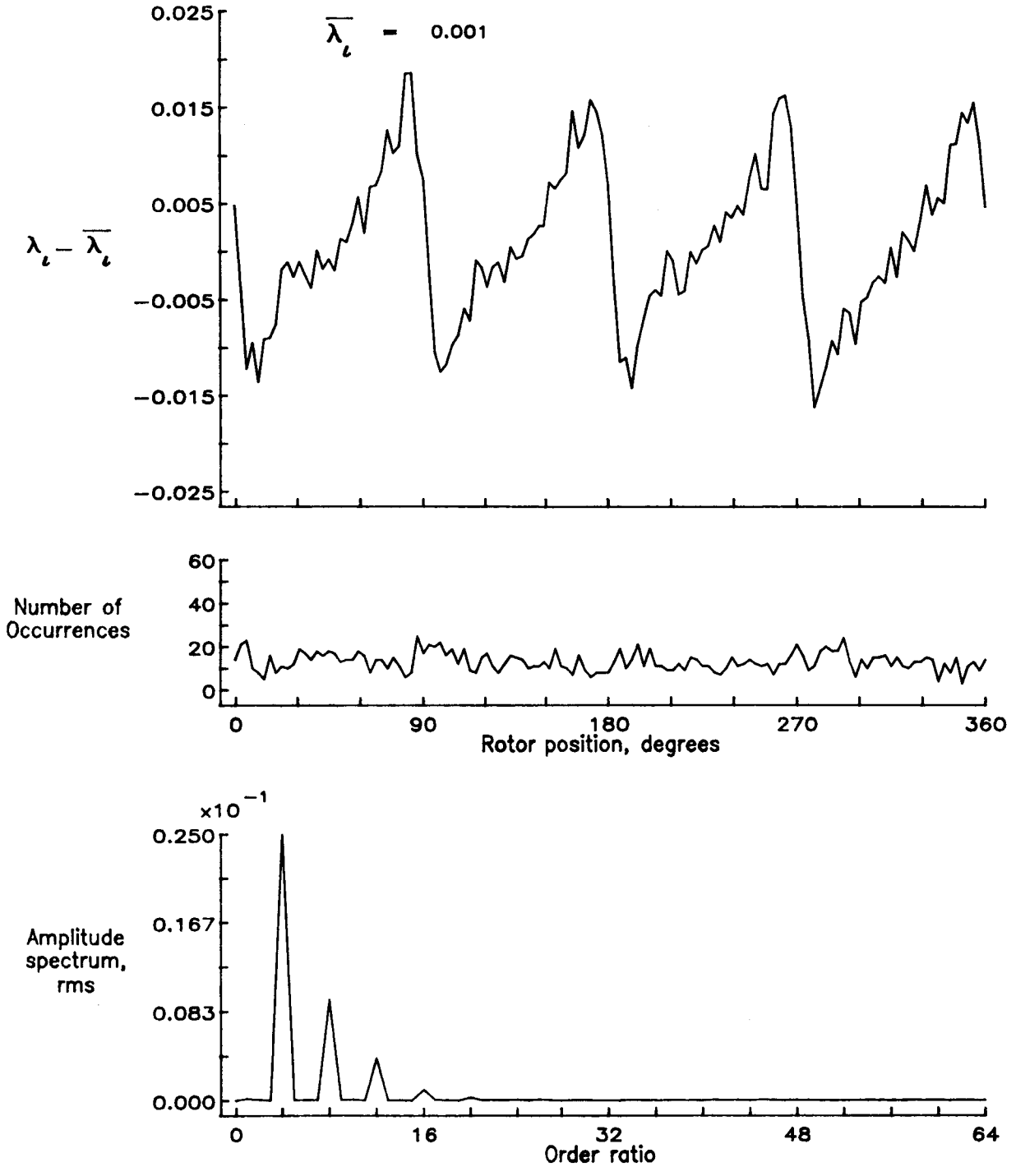


Figure 95.– Concluded.

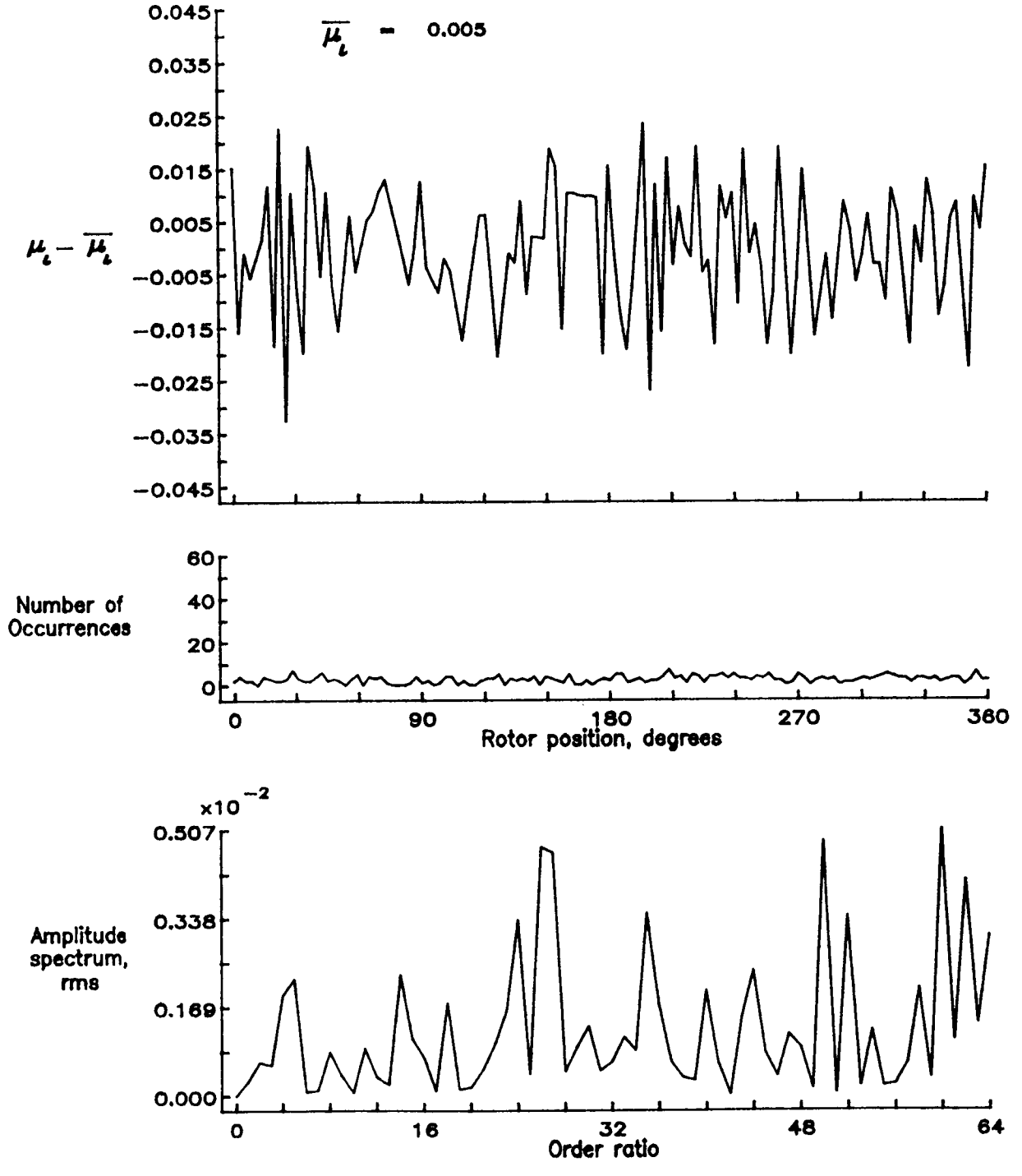


Figure 96.– Induced inflow velocity measured at 180 degrees and r/R of 0.70.

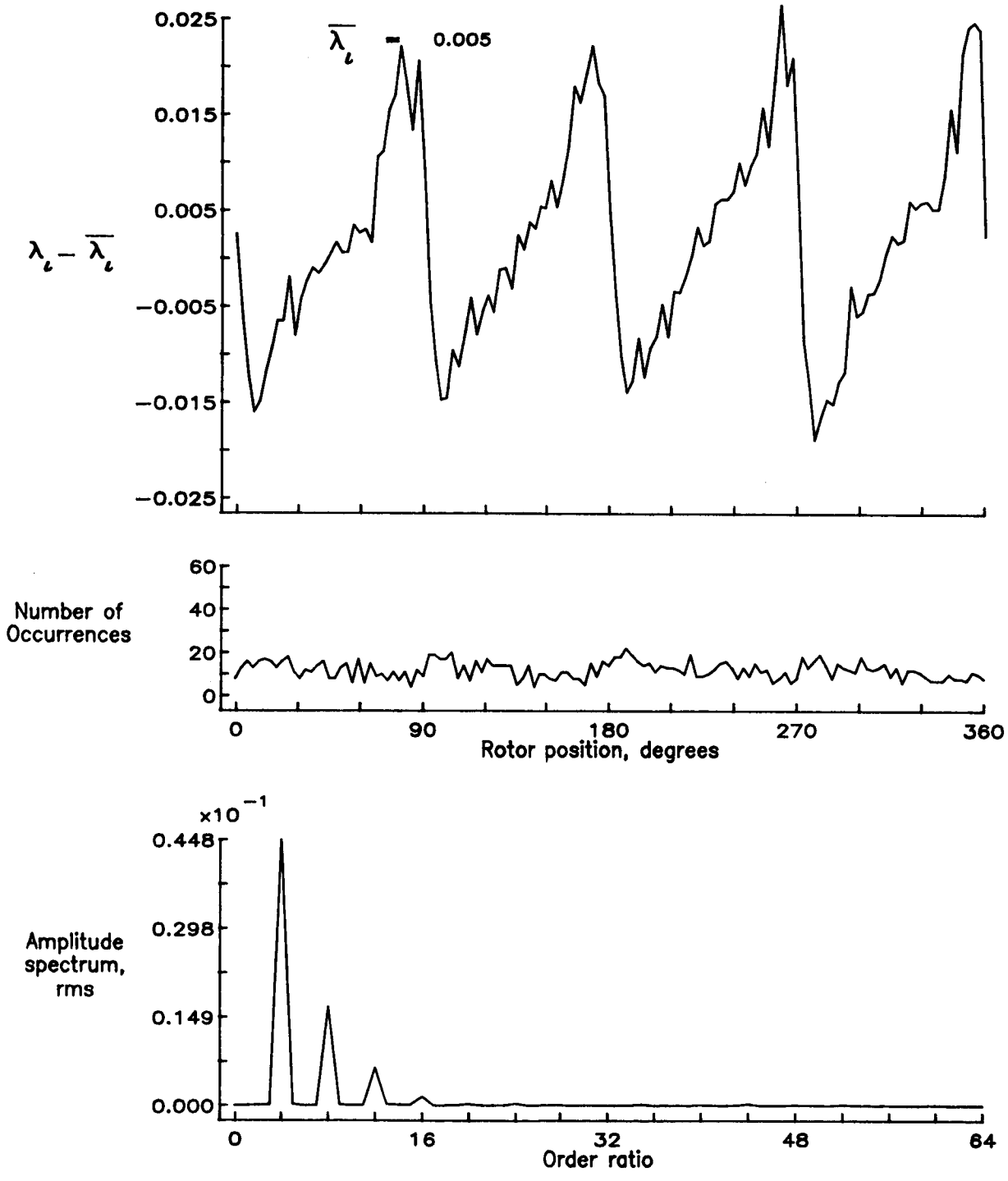


Figure 96.– Concluded.

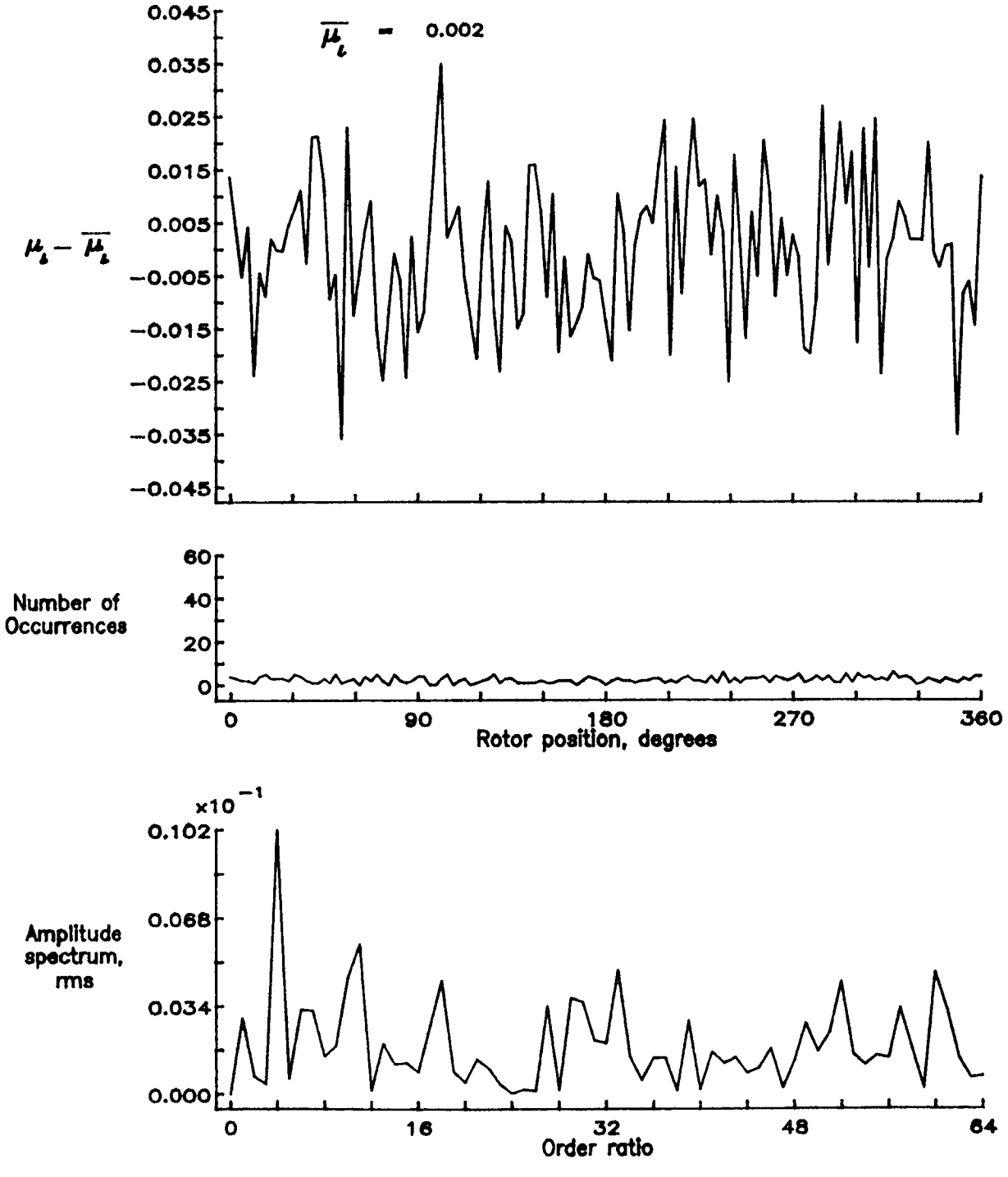


Figure 97.– Induced inflow velocity measured at 180 degrees and r/R of 0.74.

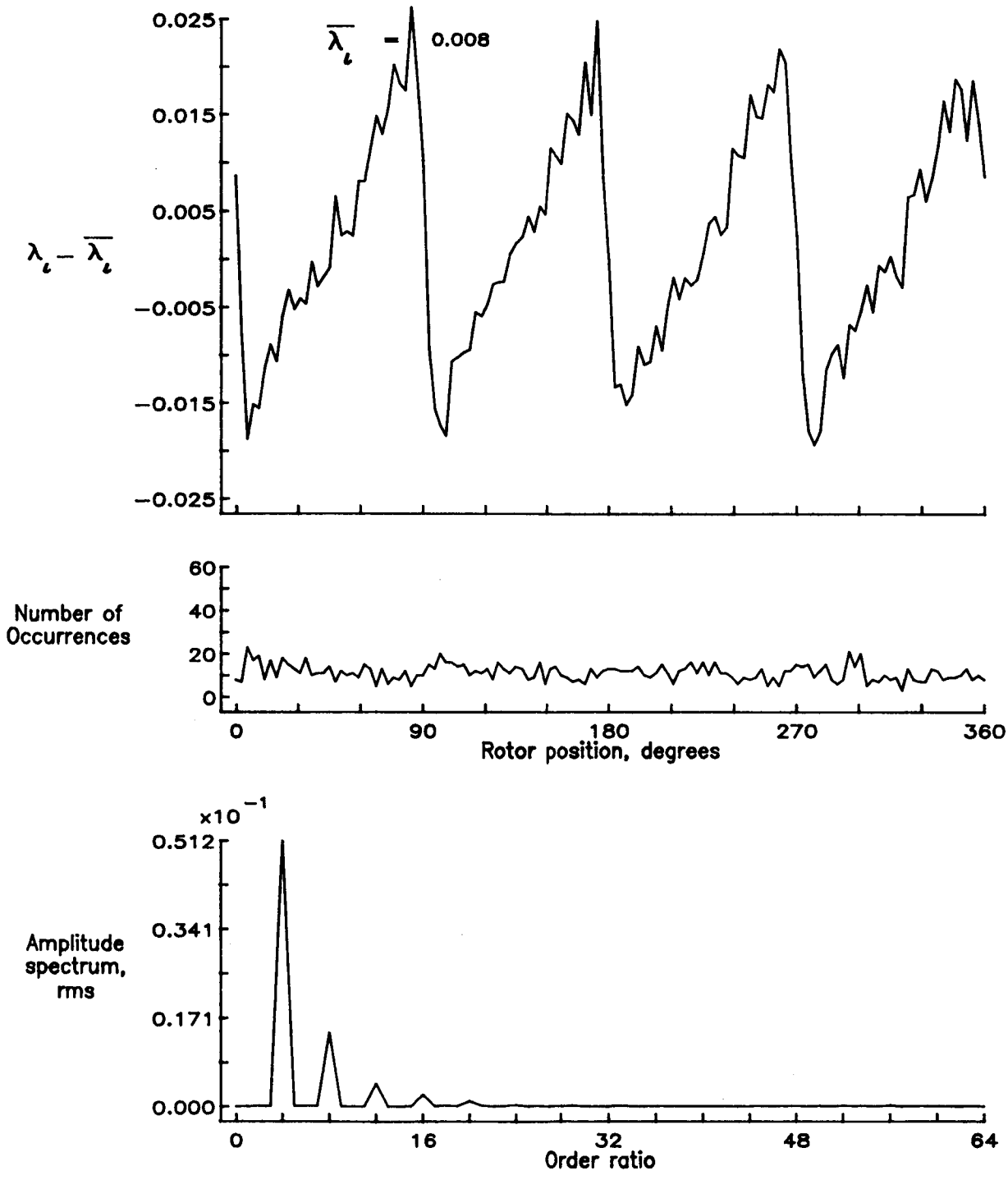


Figure 97.– Concluded.

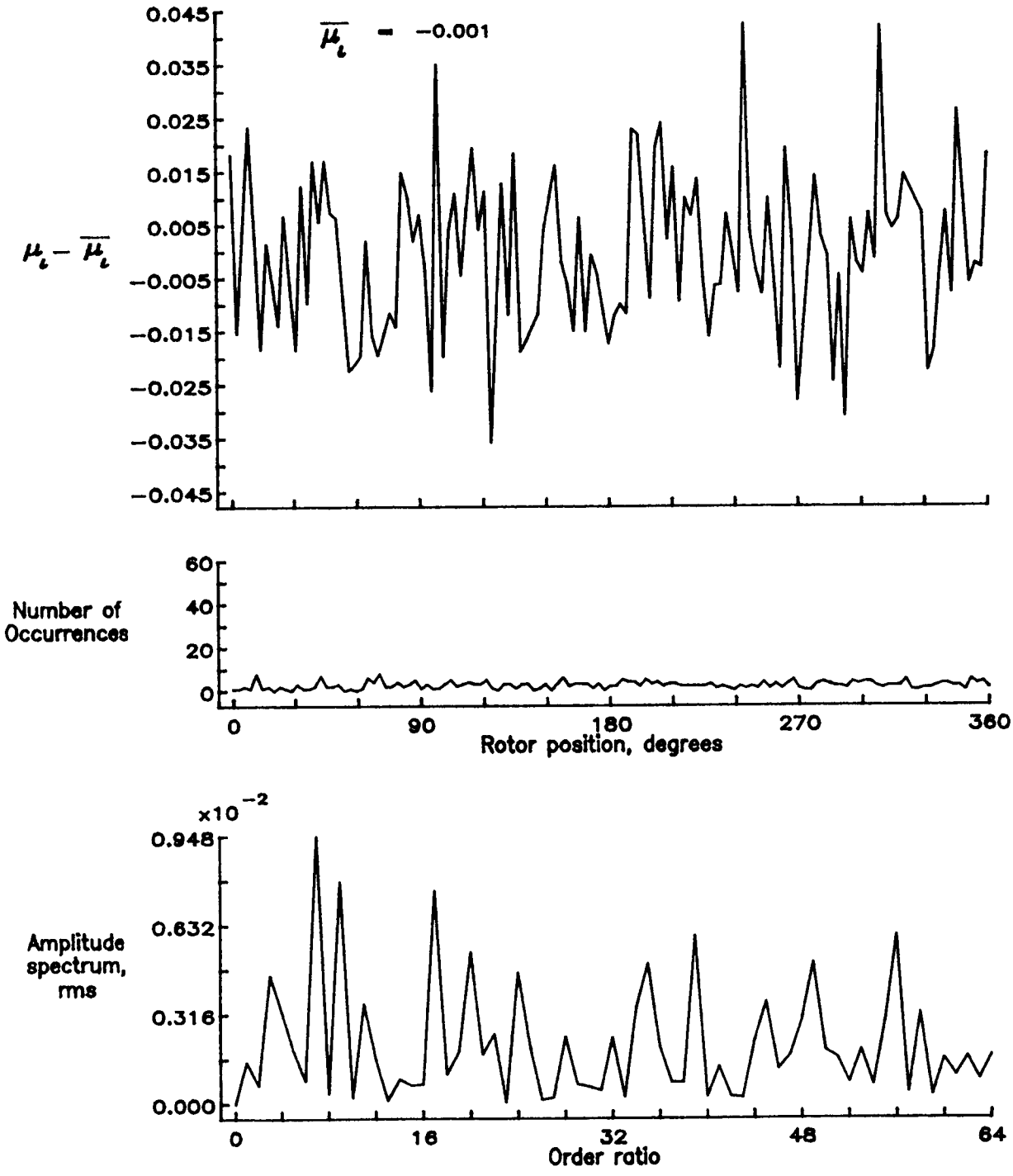


Figure 98.– Induced inflow velocity measured at 180 degrees and r/R of 0.78.

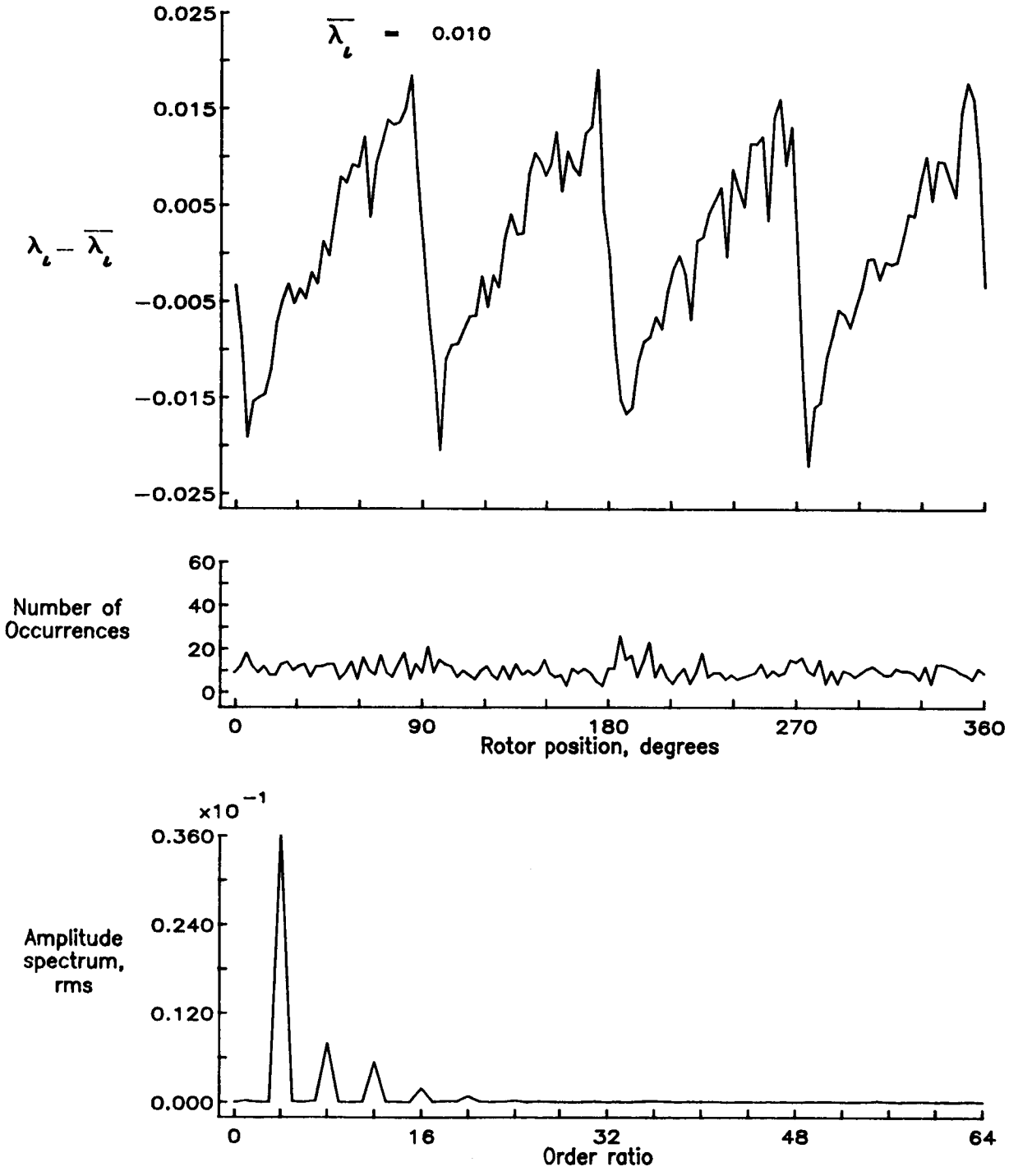


Figure 98.– Concluded.

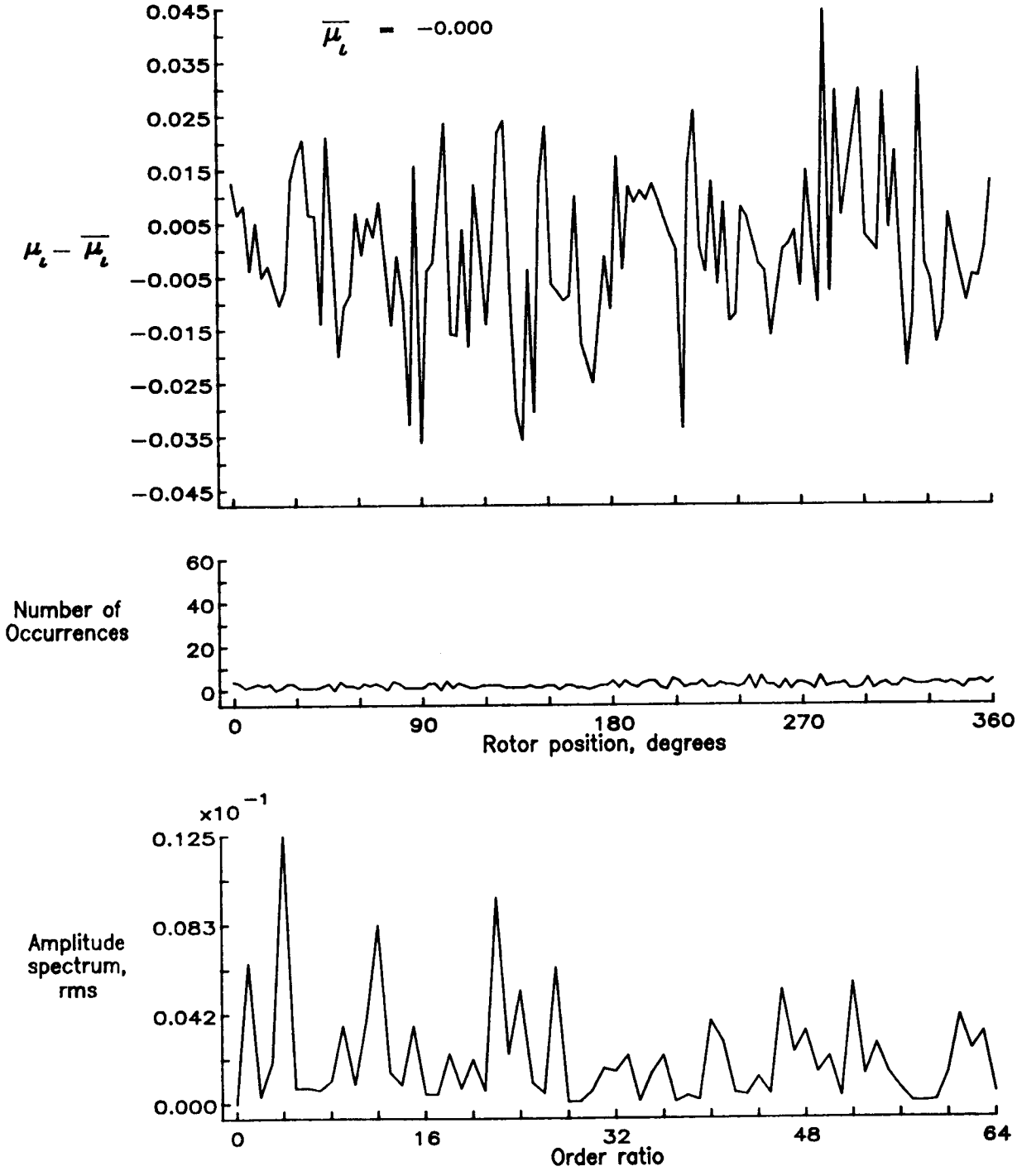


Figure 99.– Induced inflow velocity measured at 180 degrees and r/R of 0.82.

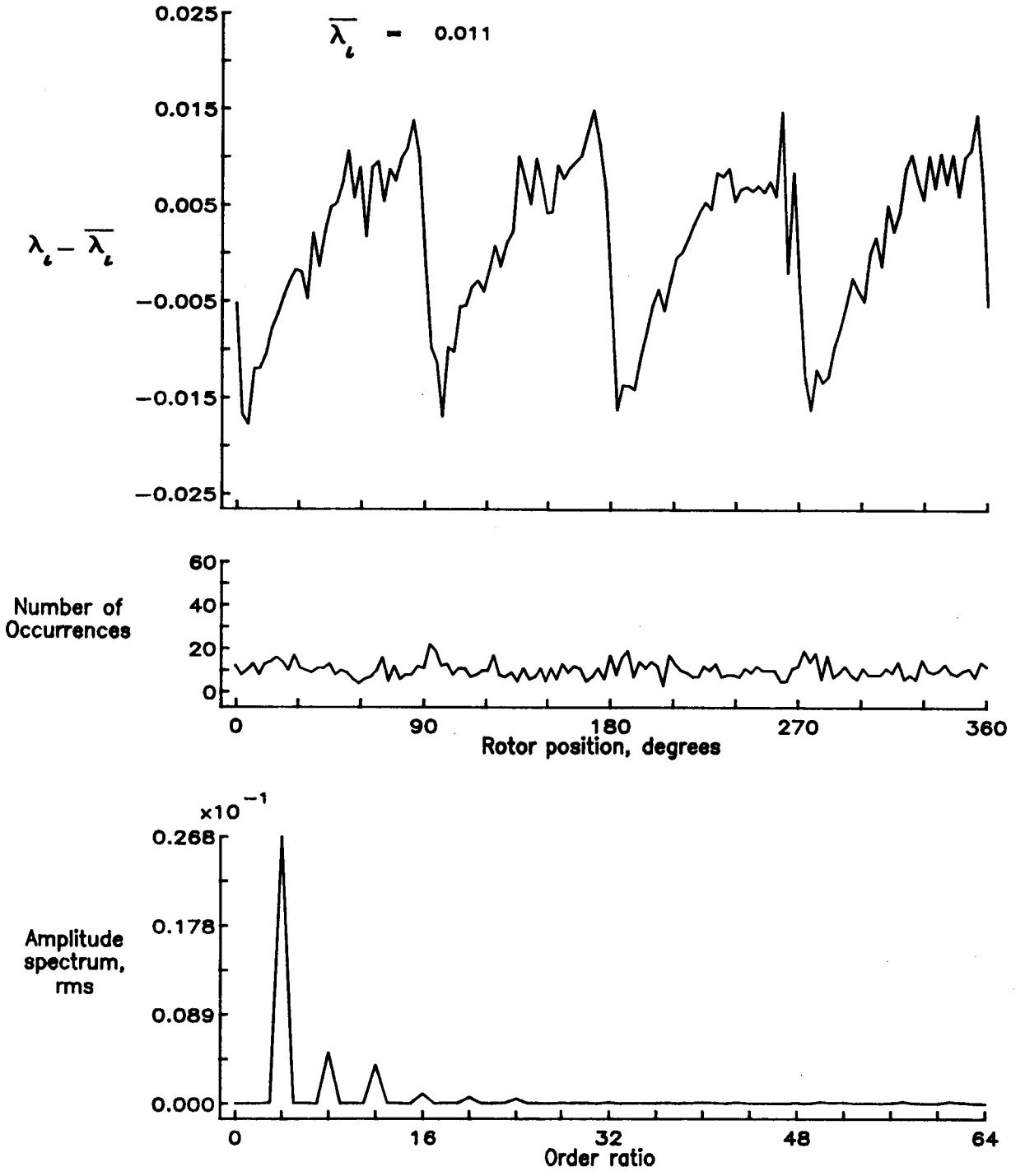


Figure 99.– Concluded.

C-3

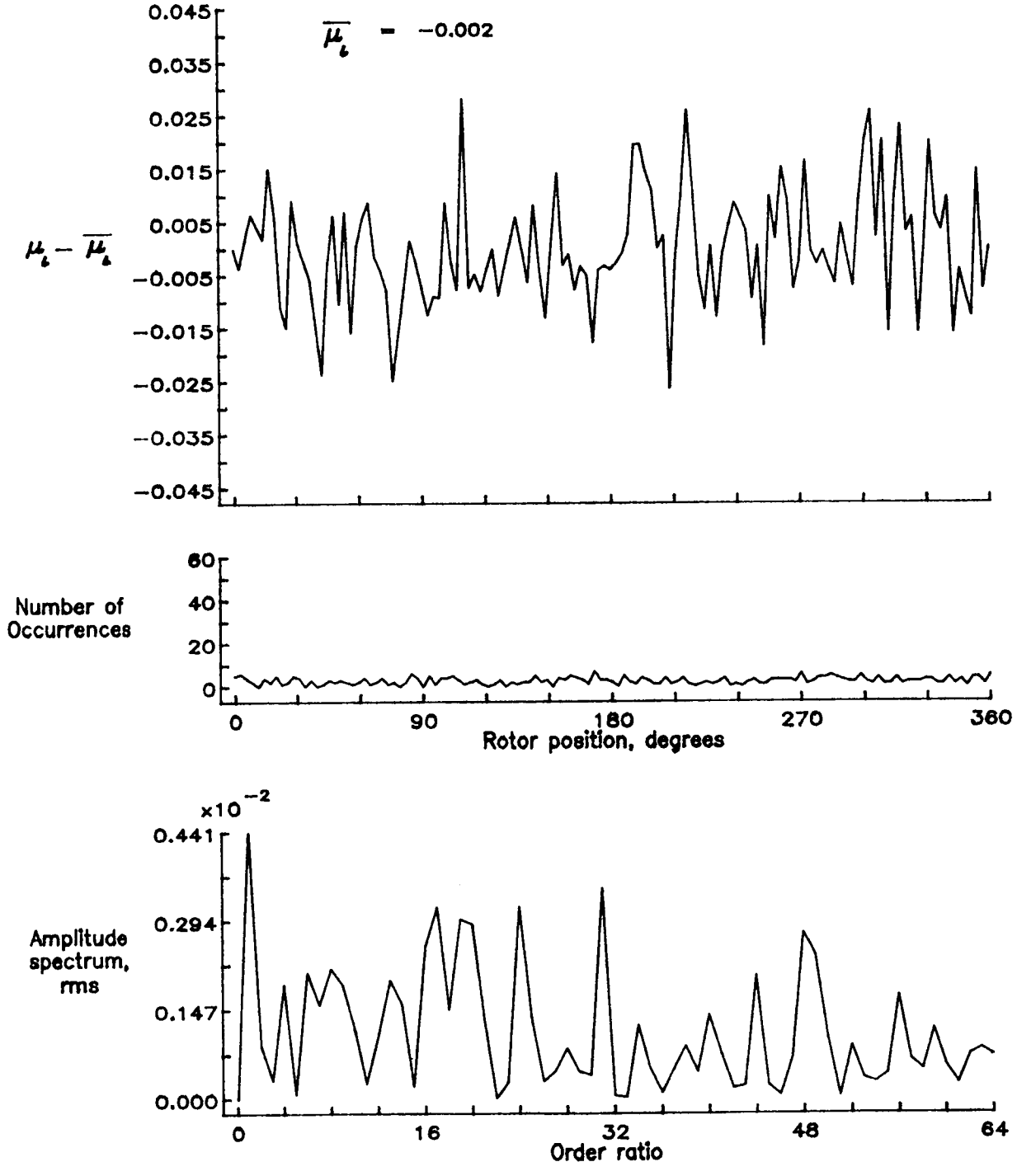


Figure 100.– Induced inflow velocity measured at 180 degrees and r/R of 0.86.

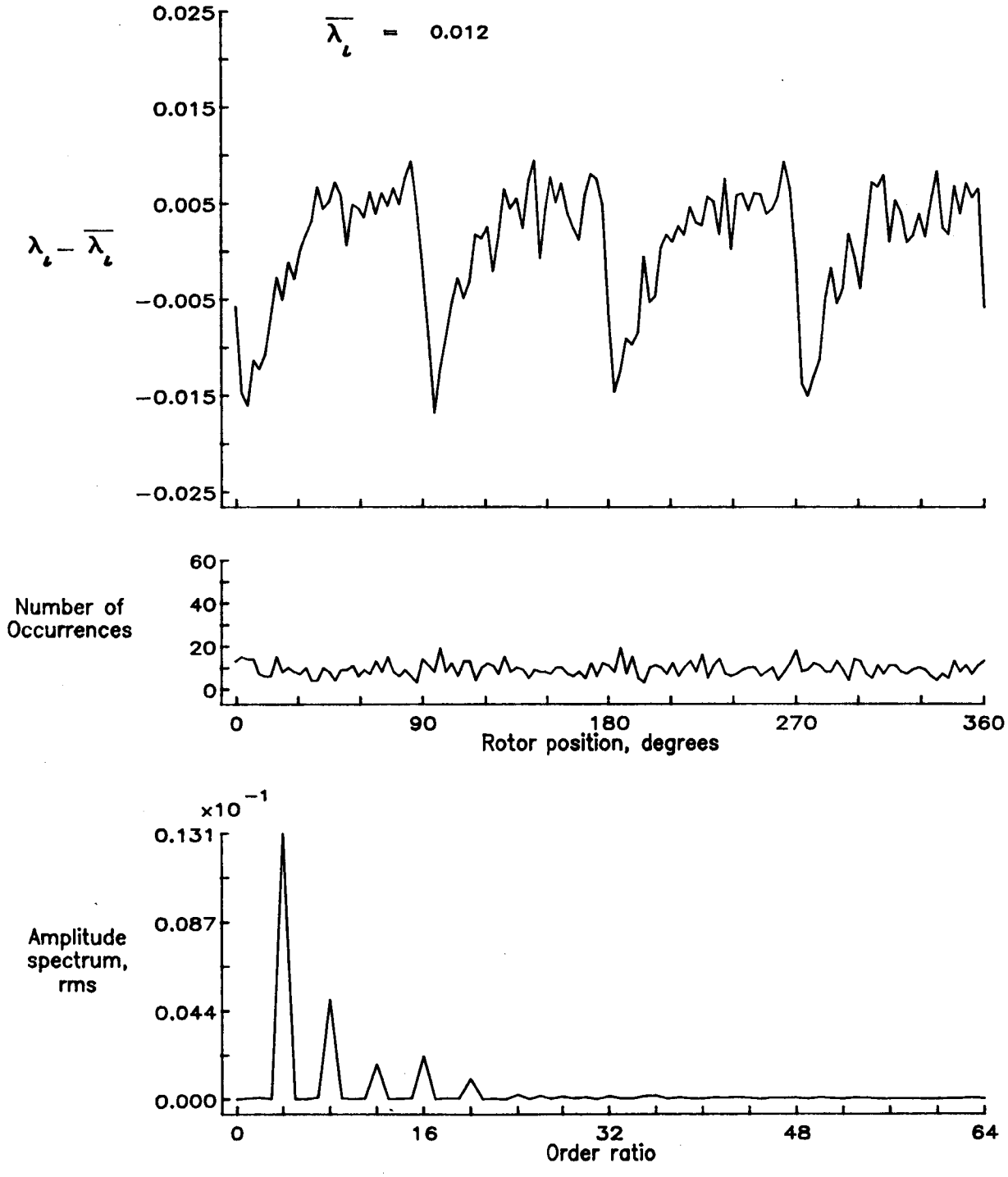


Figure 100.– Concluded.

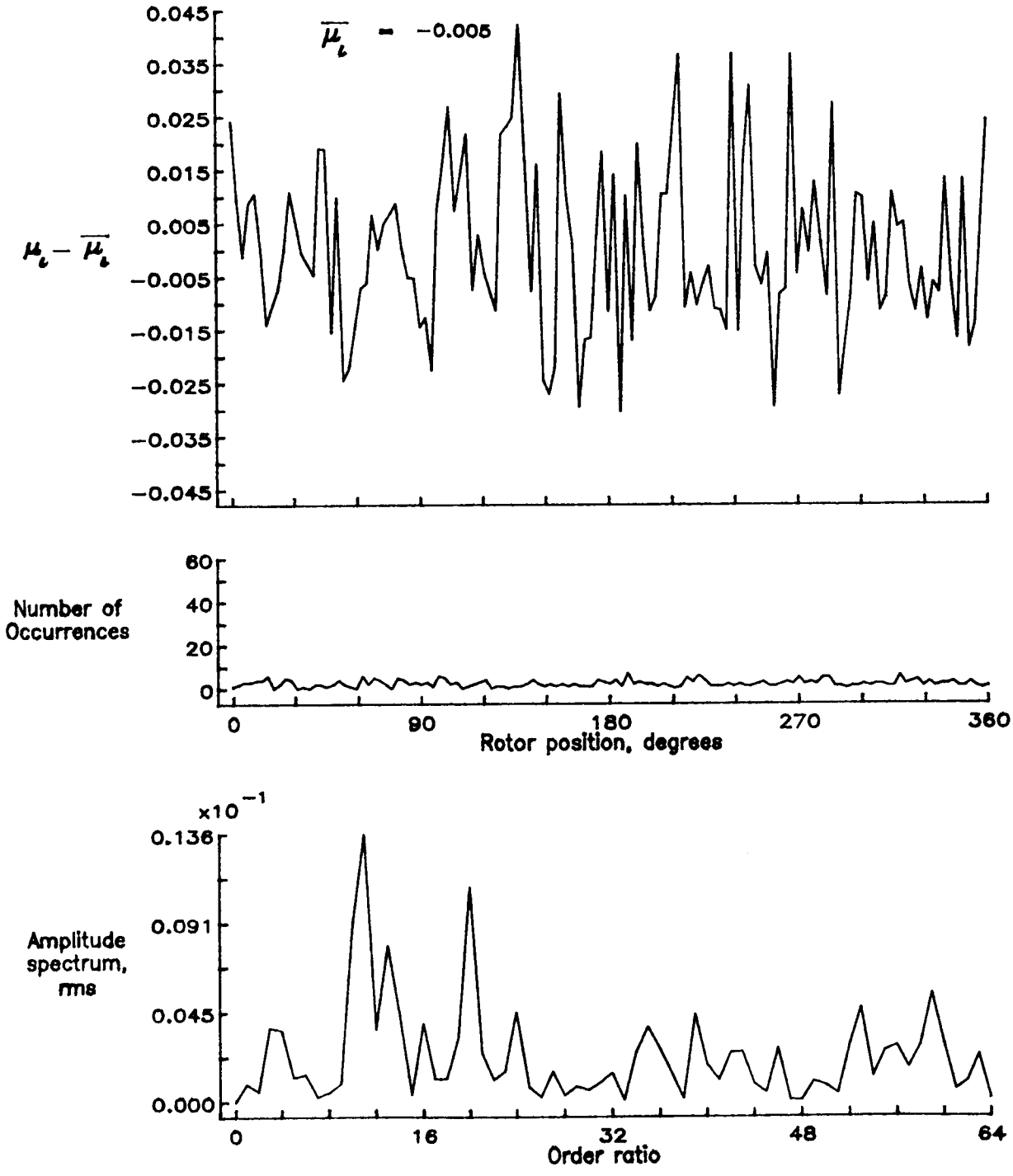


Figure 101.– Induced inflow velocity measured at 180 degrees and r/R of 0.90.

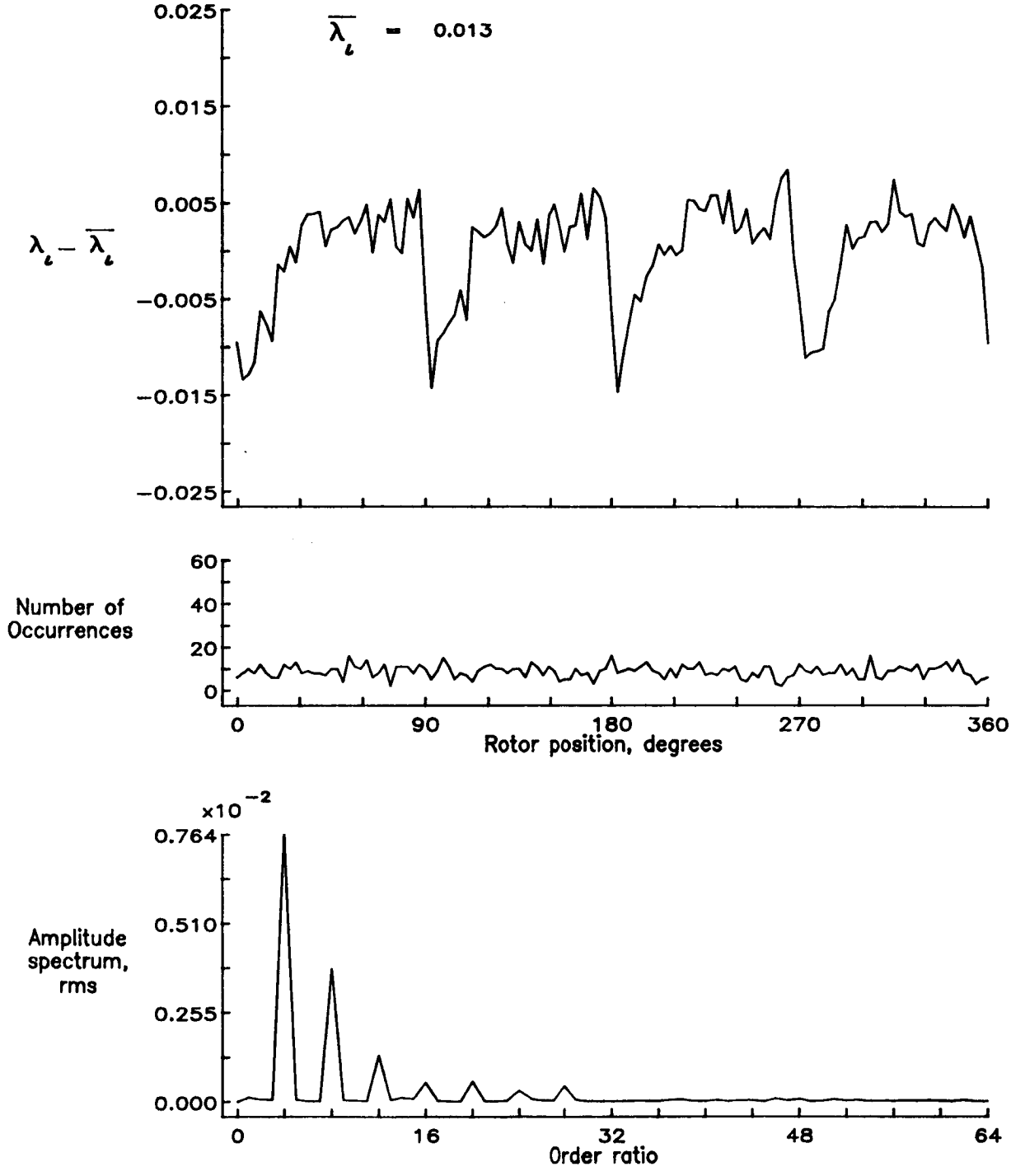


Figure 101.– Concluded.

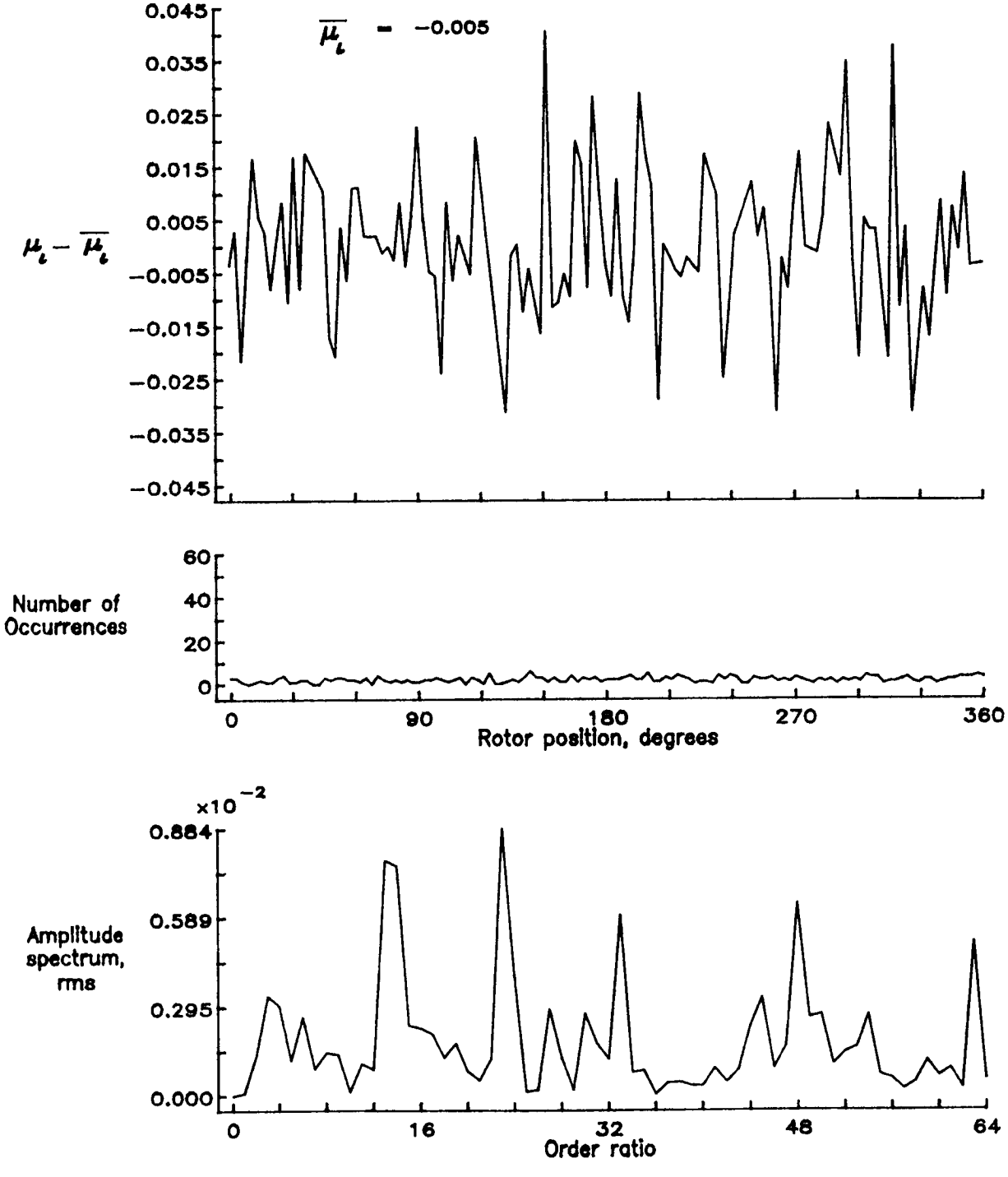


Figure 102.– Induced inflow velocity measured at 180 degrees and r/R of 0.94.

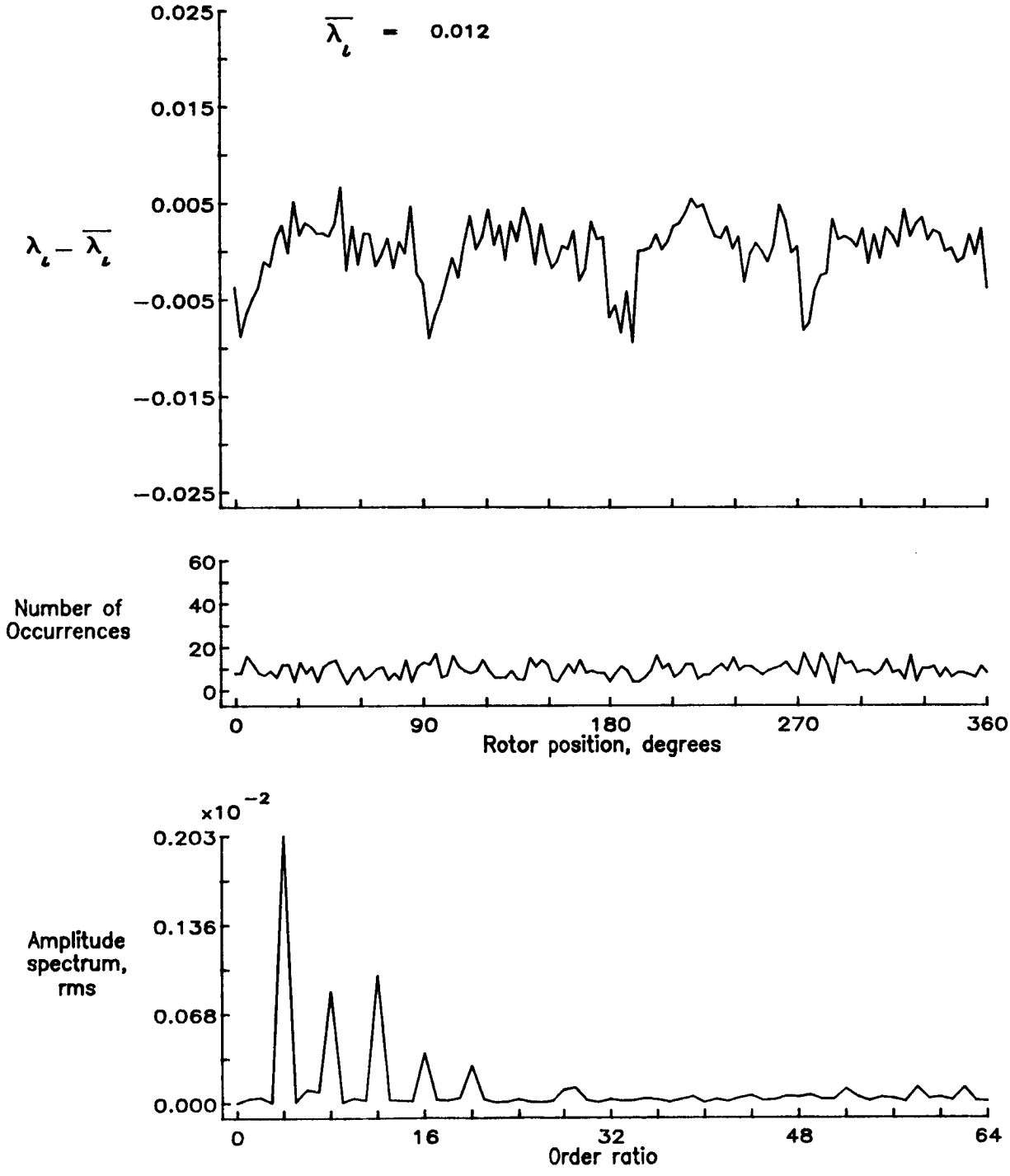


Figure 102.– Concluded.

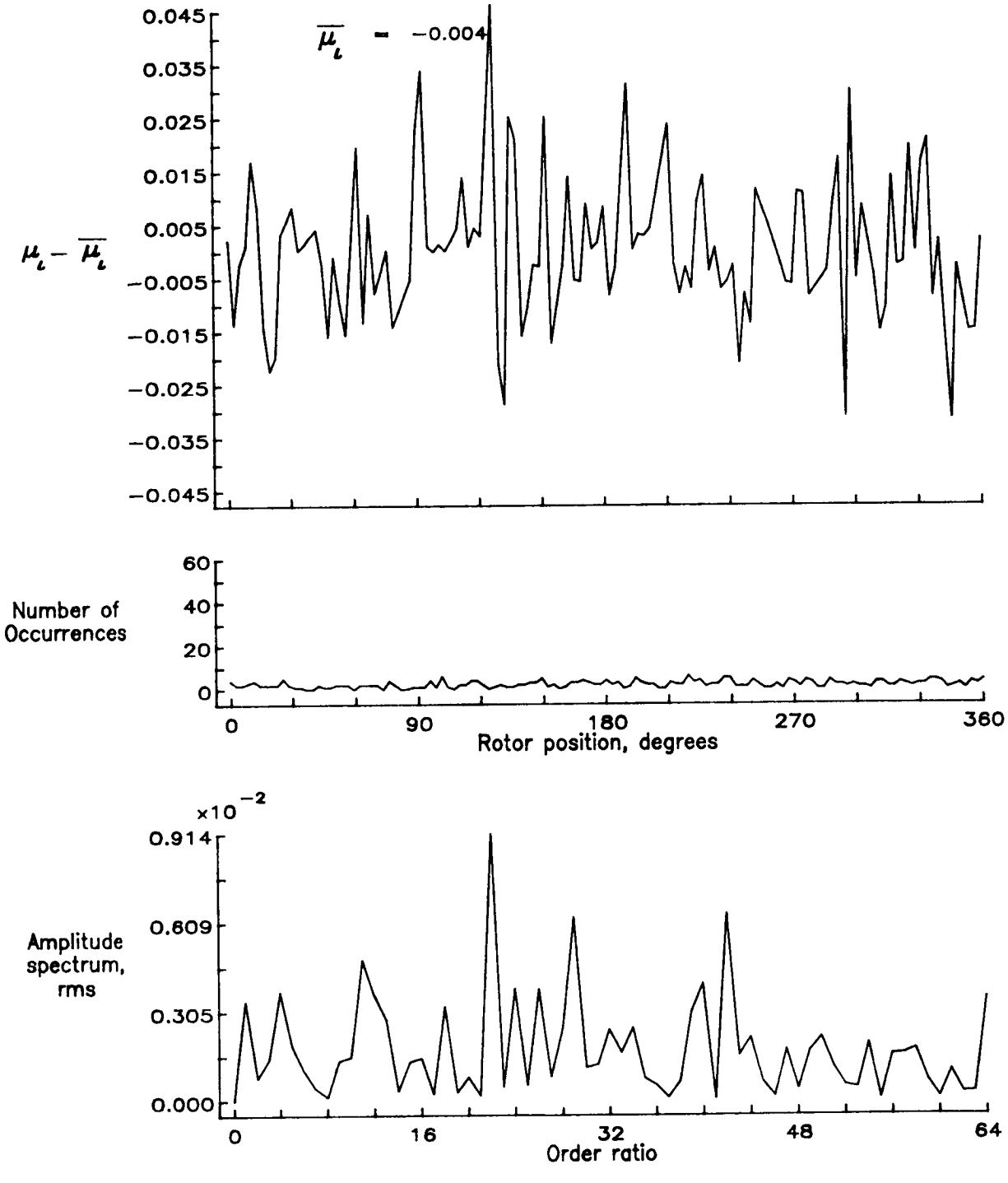


Figure 103.– Induced inflow velocity measured at 180 degrees and r/R of 0.98.

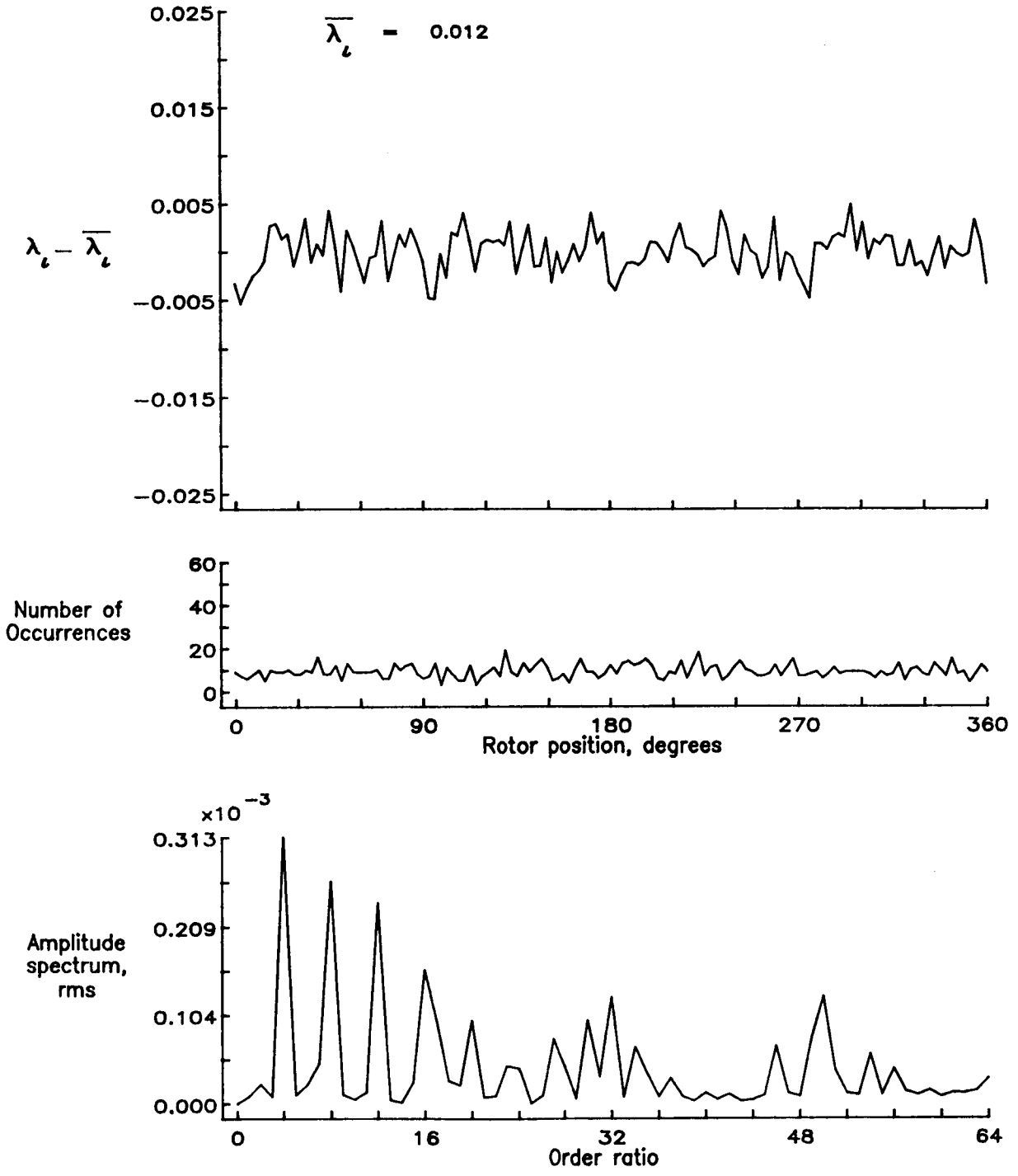


Figure 103.– Concluded.

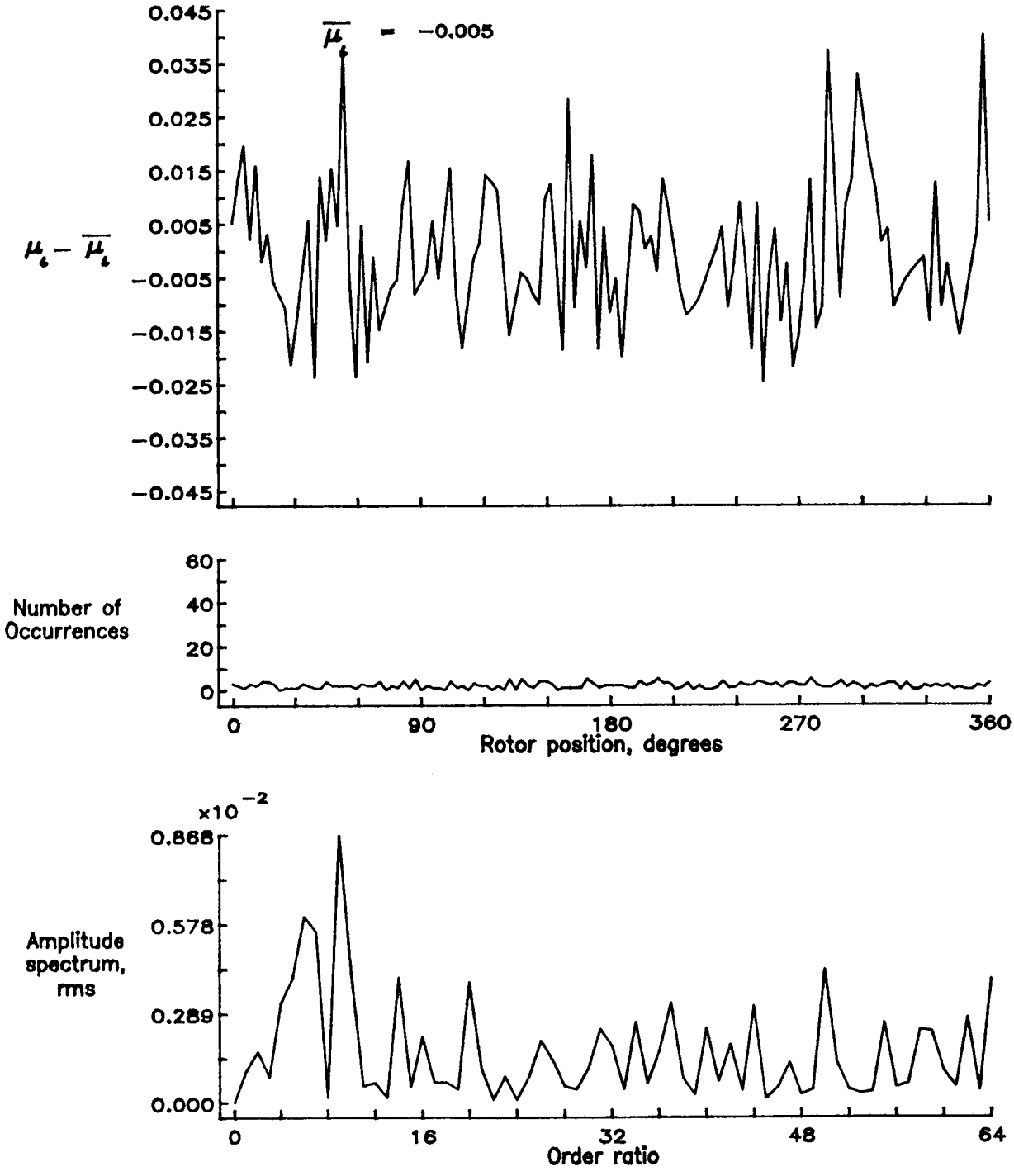


Figure 104.– Induced inflow velocity measured at 180 degrees and r/R of 1.02.

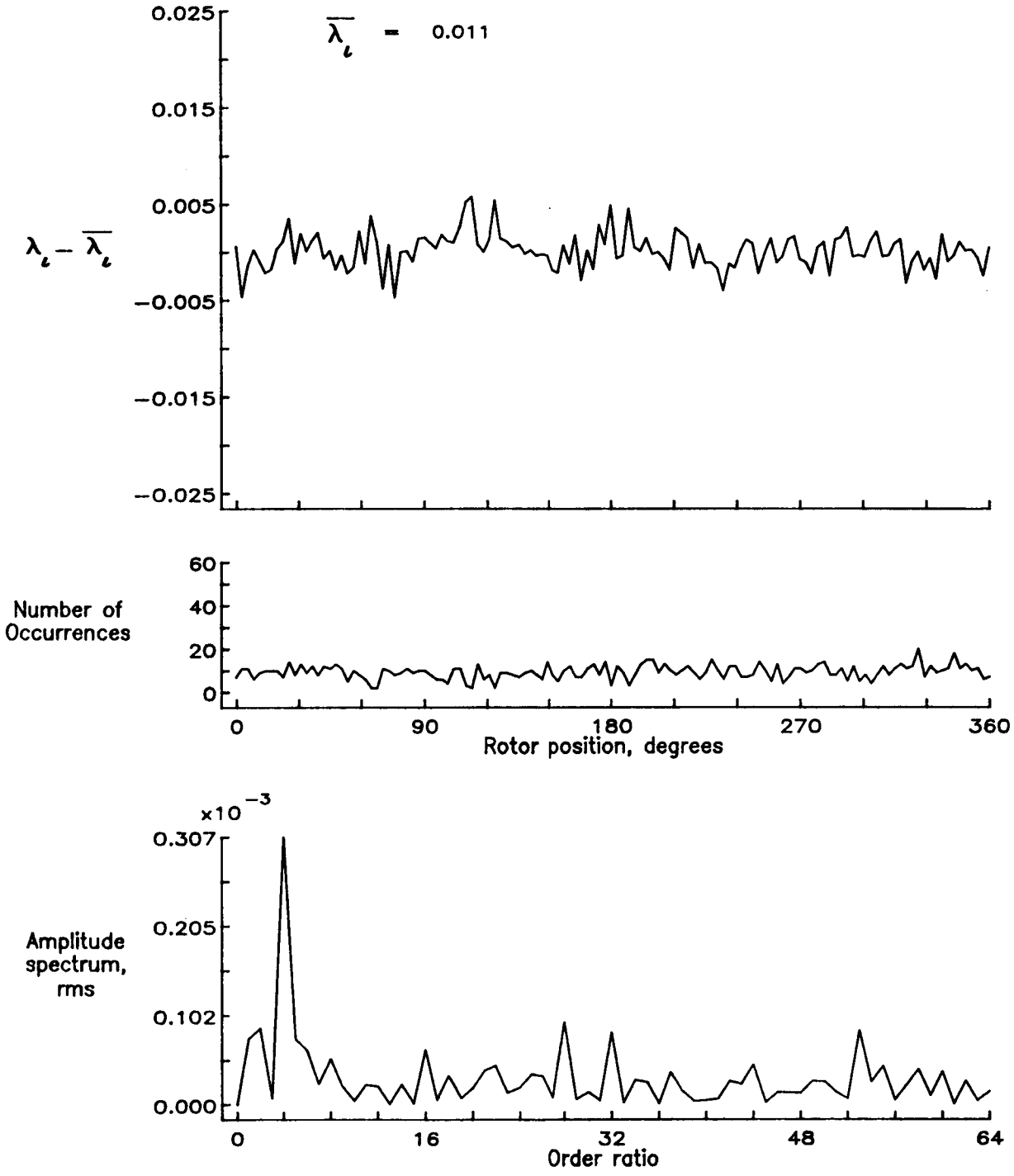


Figure 104.– Concluded.

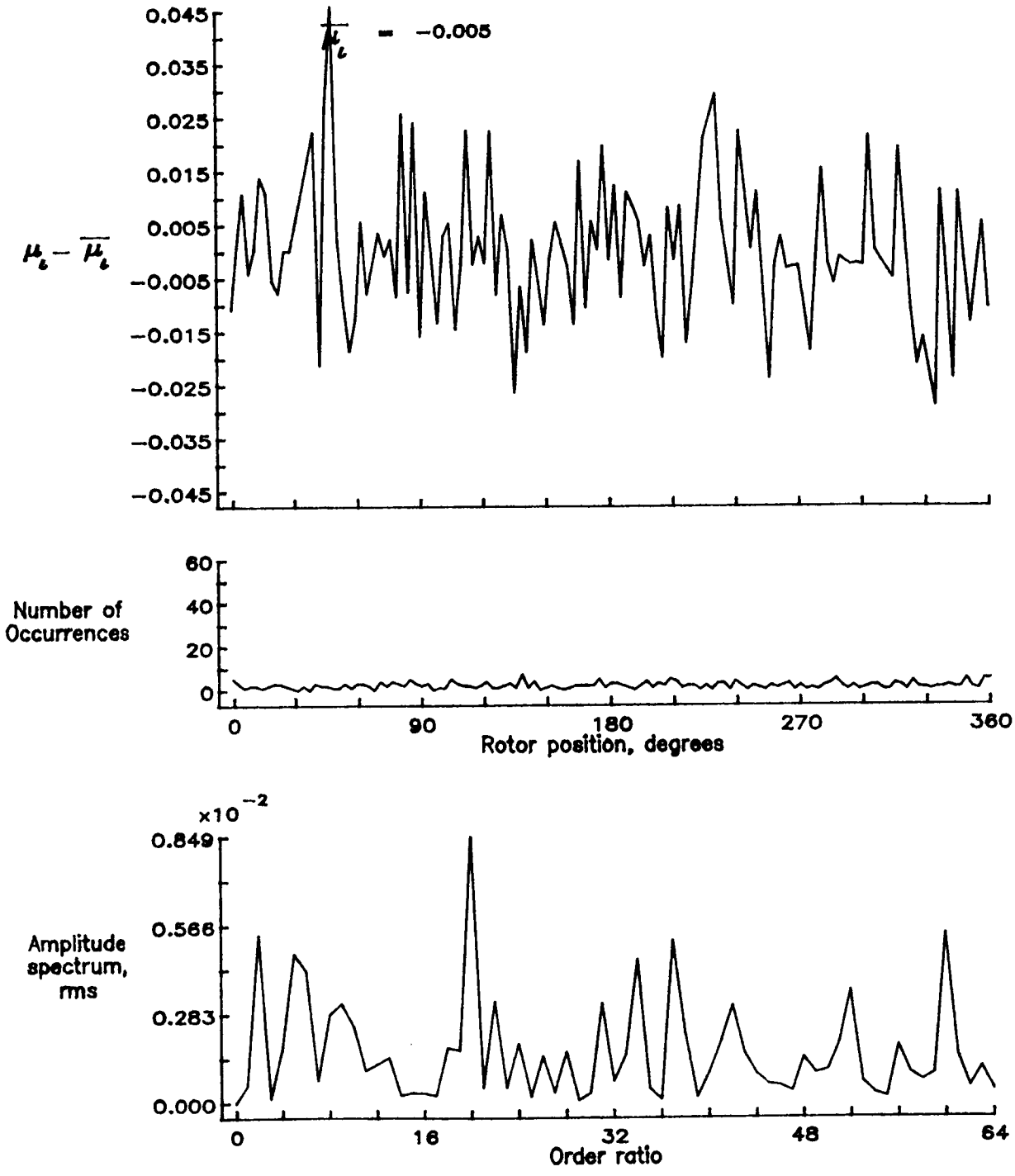


Figure 105.– Induced inflow velocity measured at 180 degrees and r/R of 1.04.

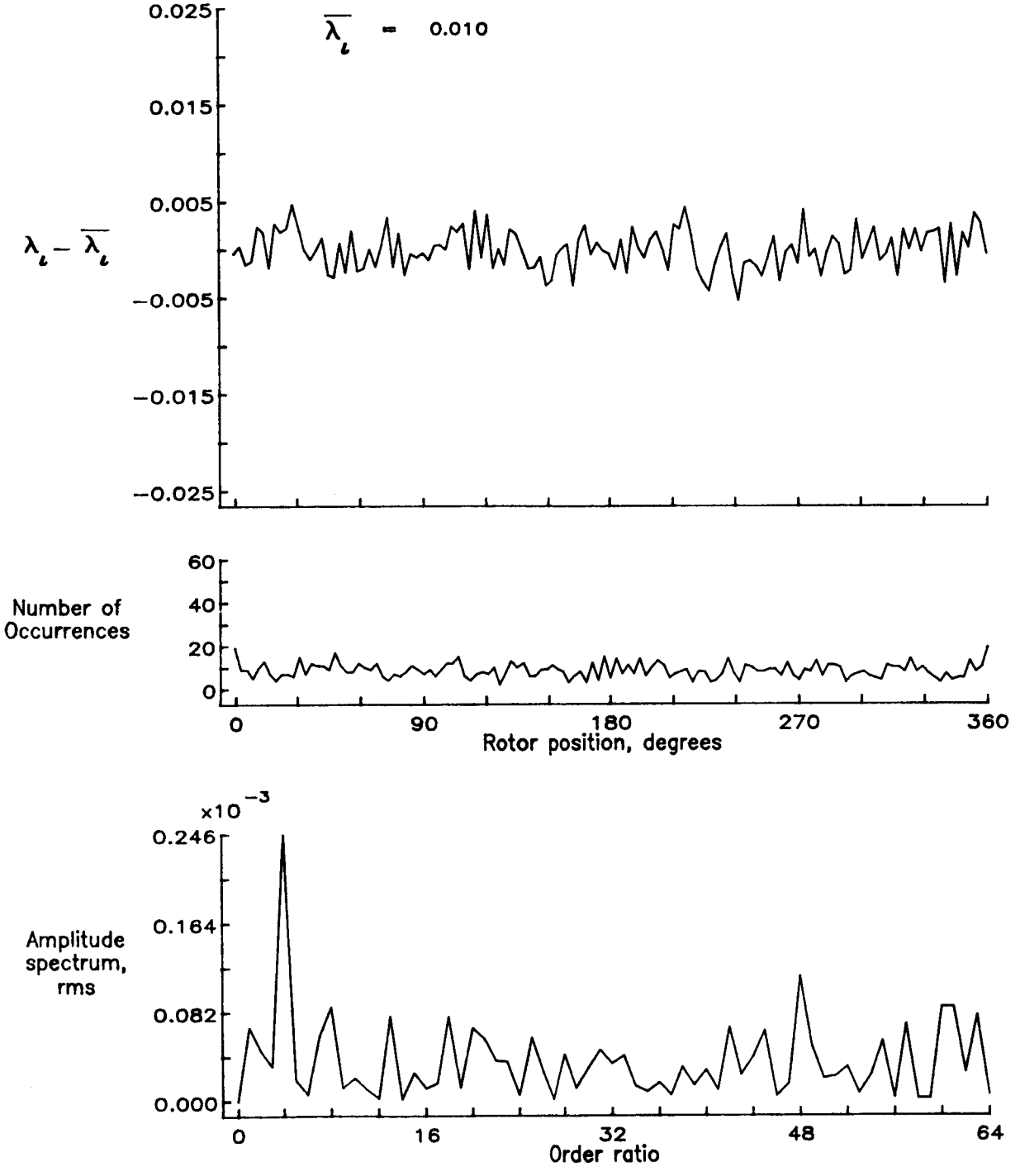


Figure 105.– Concluded.

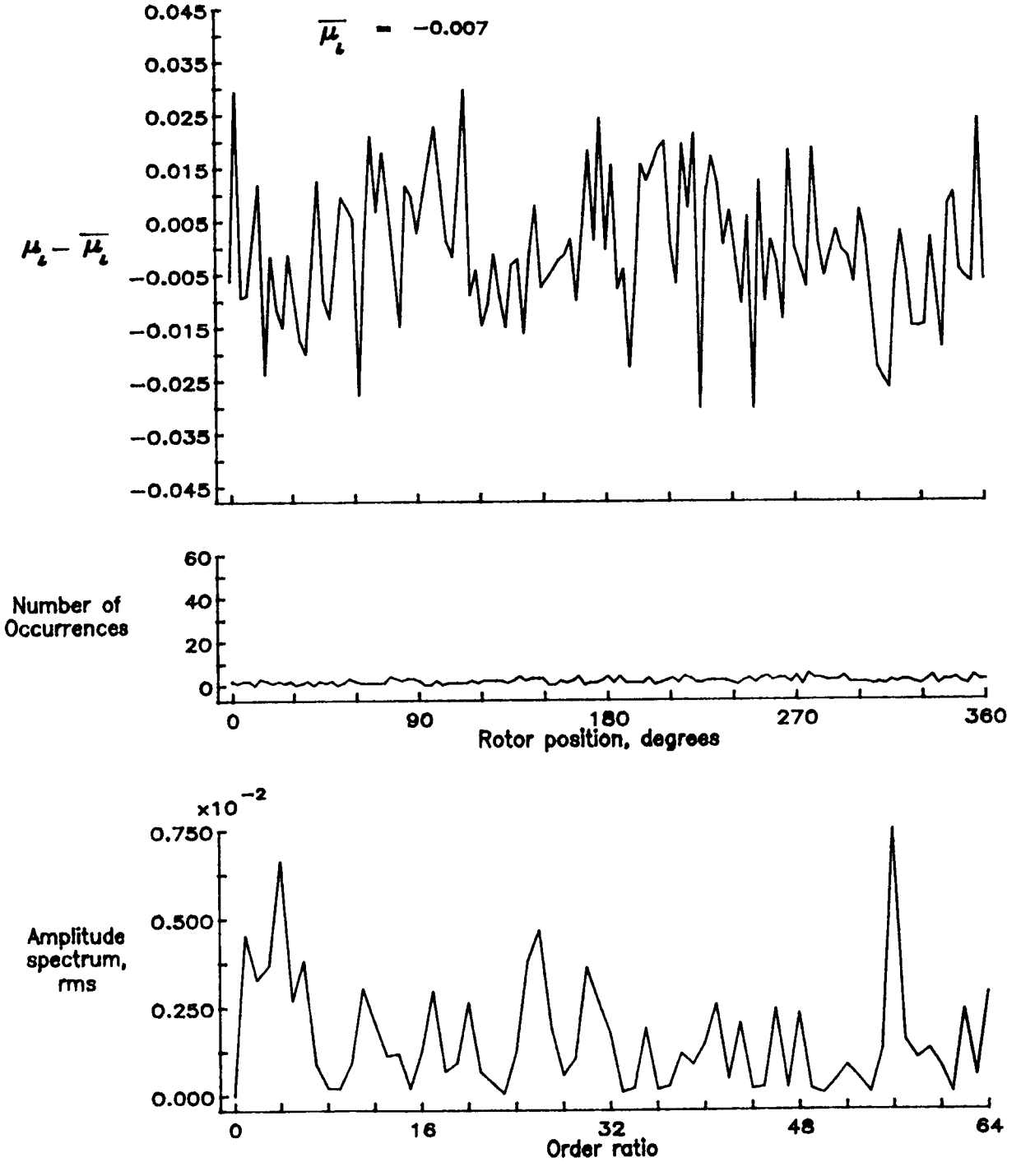


Figure 106.– Induced inflow velocity measured at 180 degrees and r/R of 1.12.

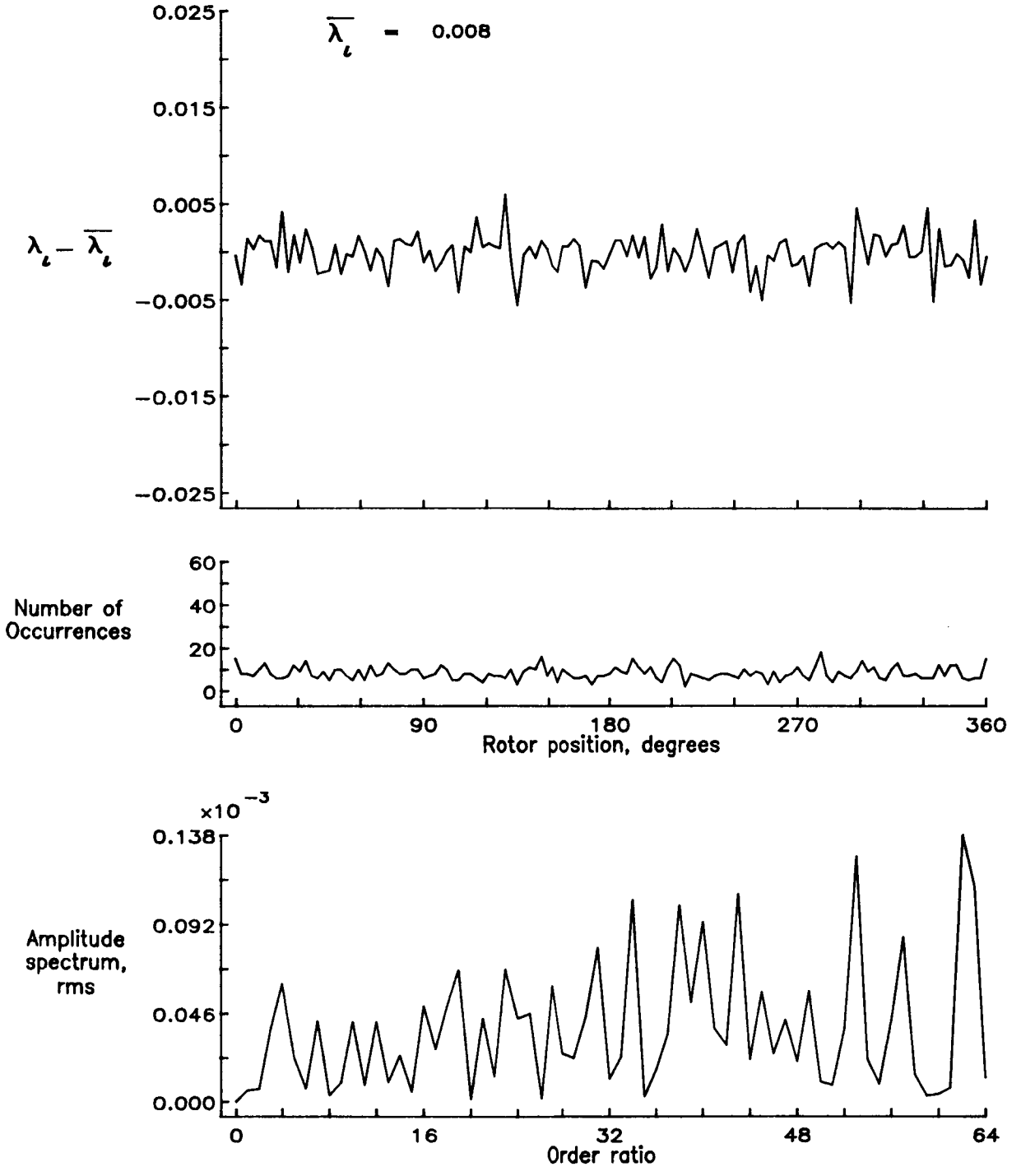


Figure 106.– Concluded.

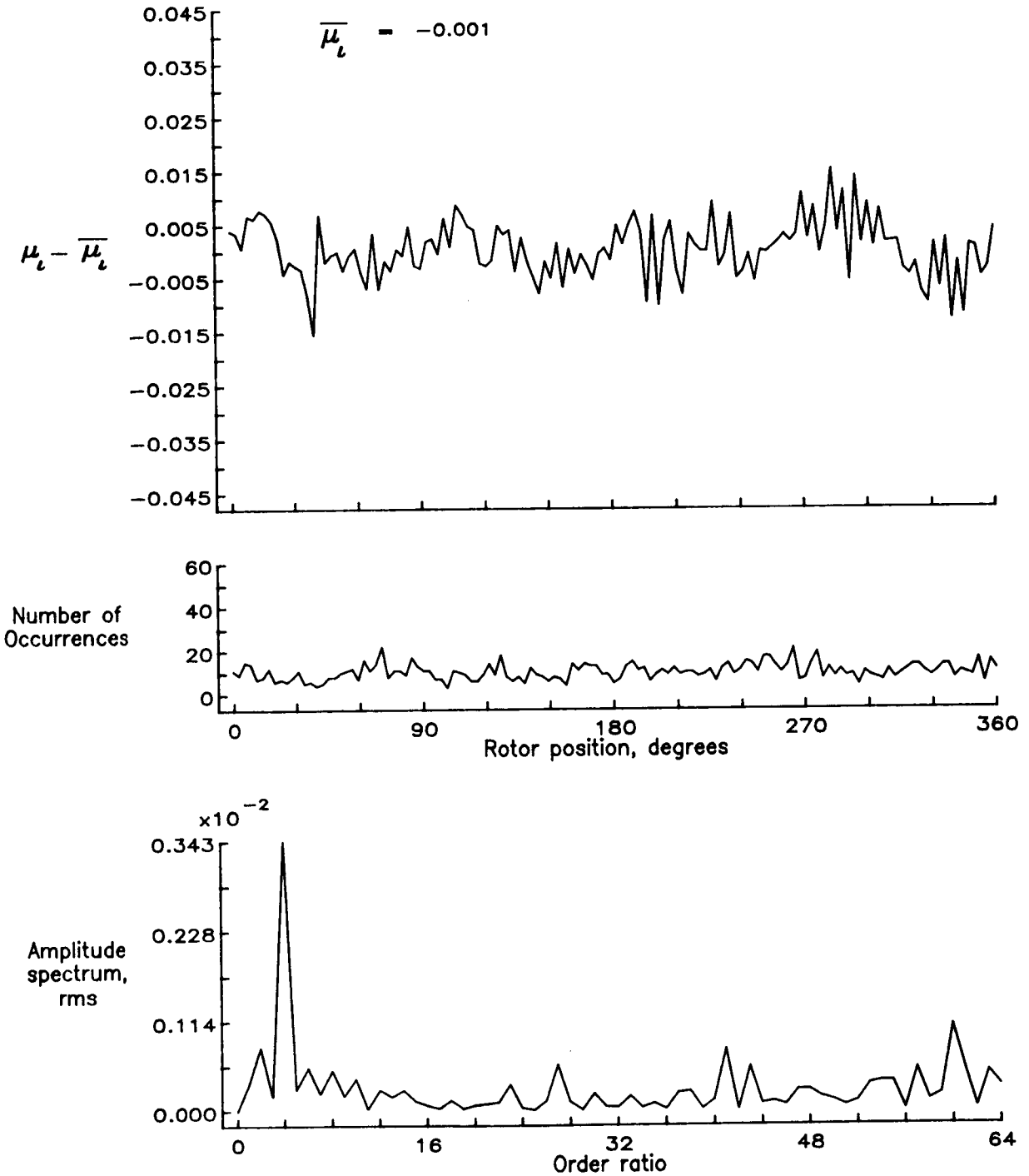


Figure 107.– Induced inflow velocity measured at 210 degrees and r/R of 0.20.

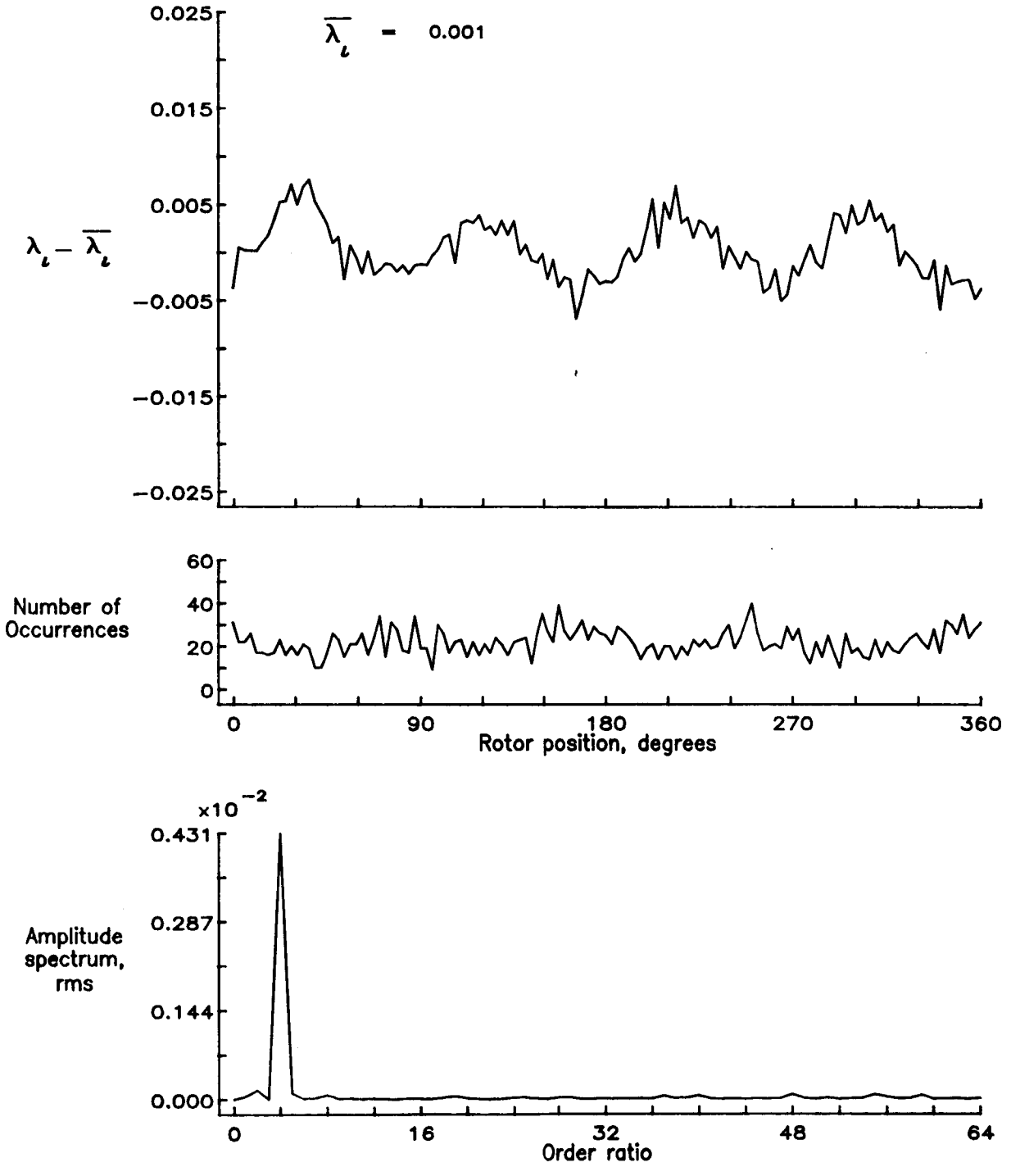


Figure 107.– Concluded.

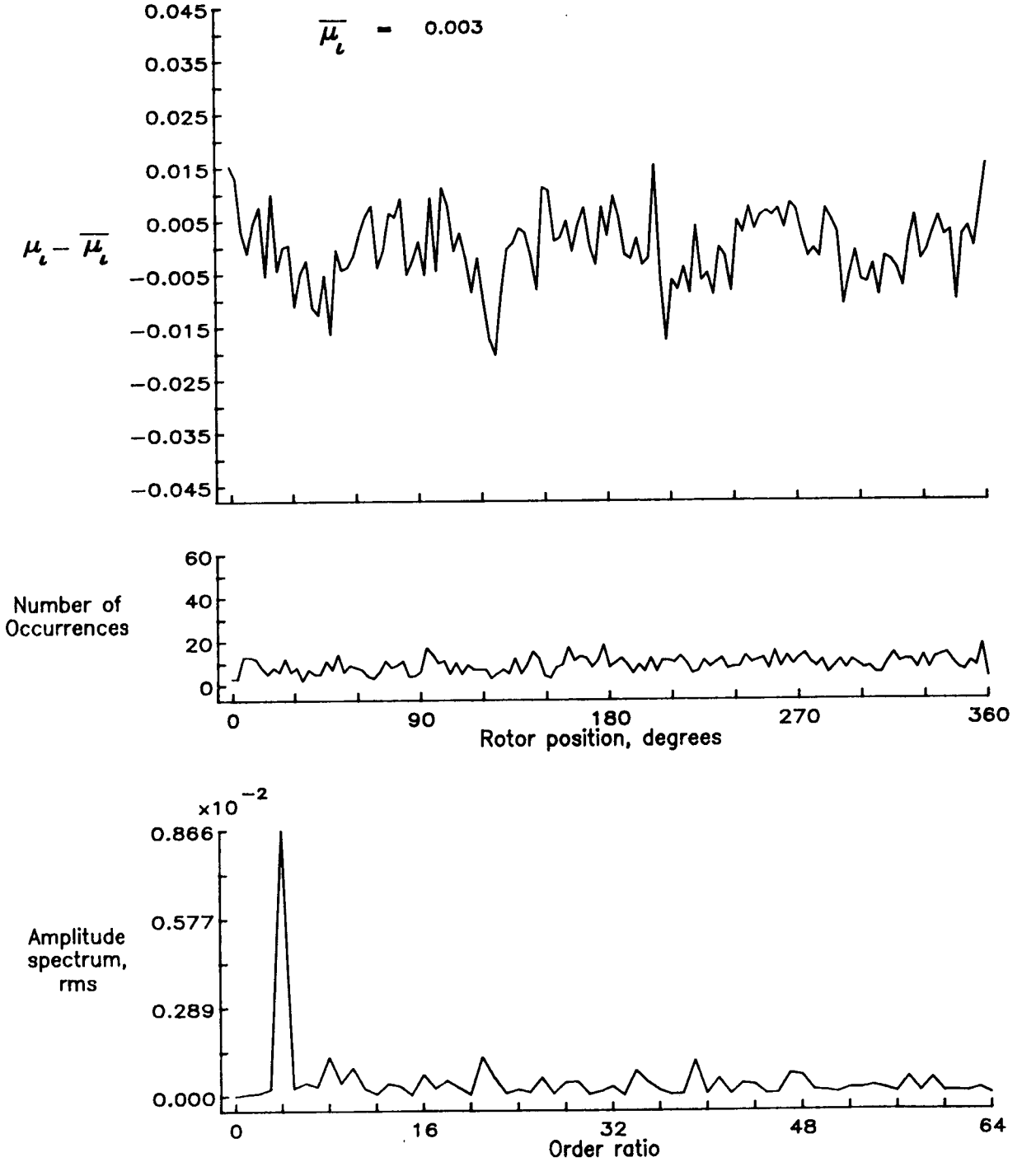


Figure 108.– Induced inflow velocity measured at 210 degrees and r/R of 0.40.

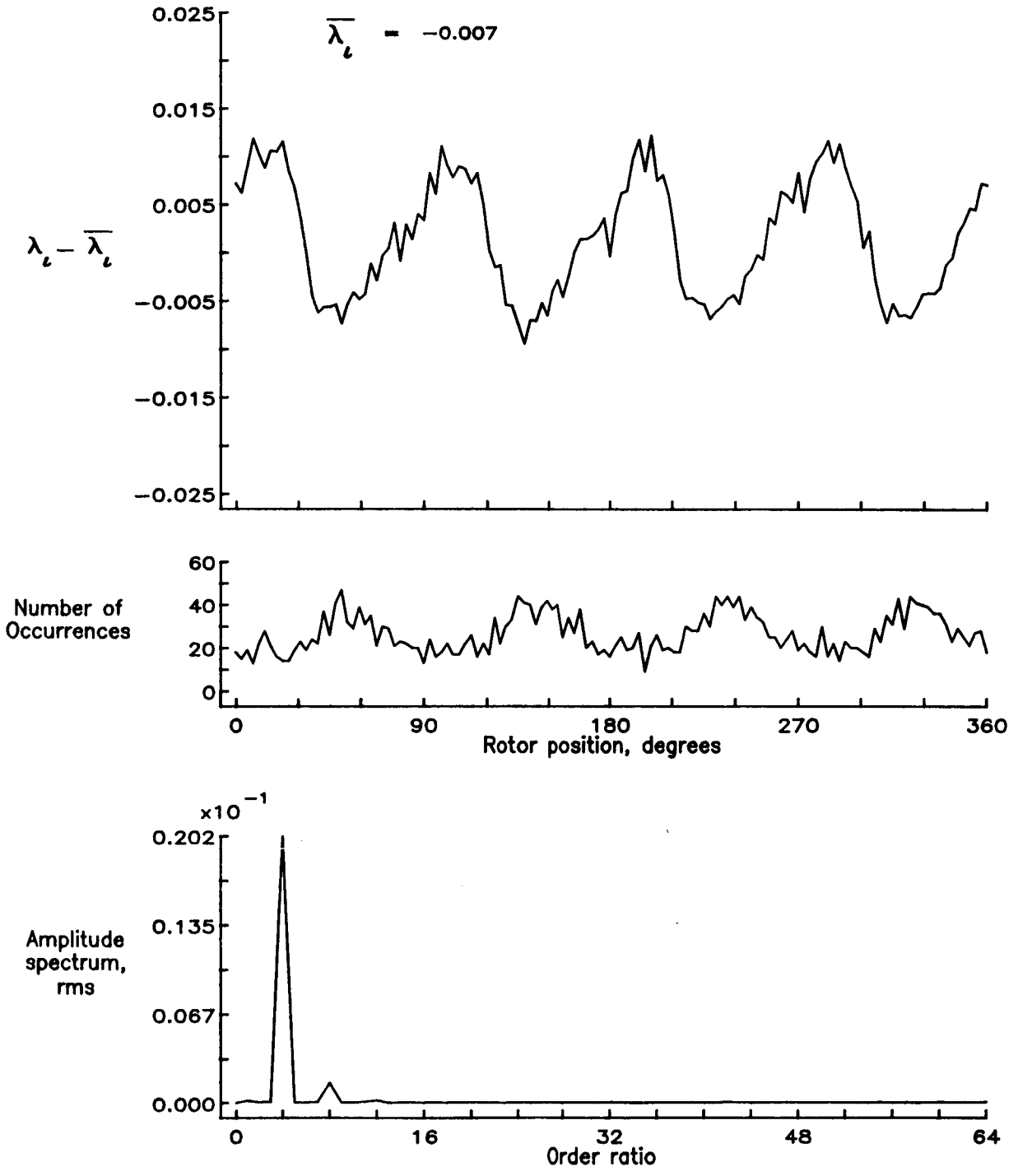


Figure 108.– Concluded.

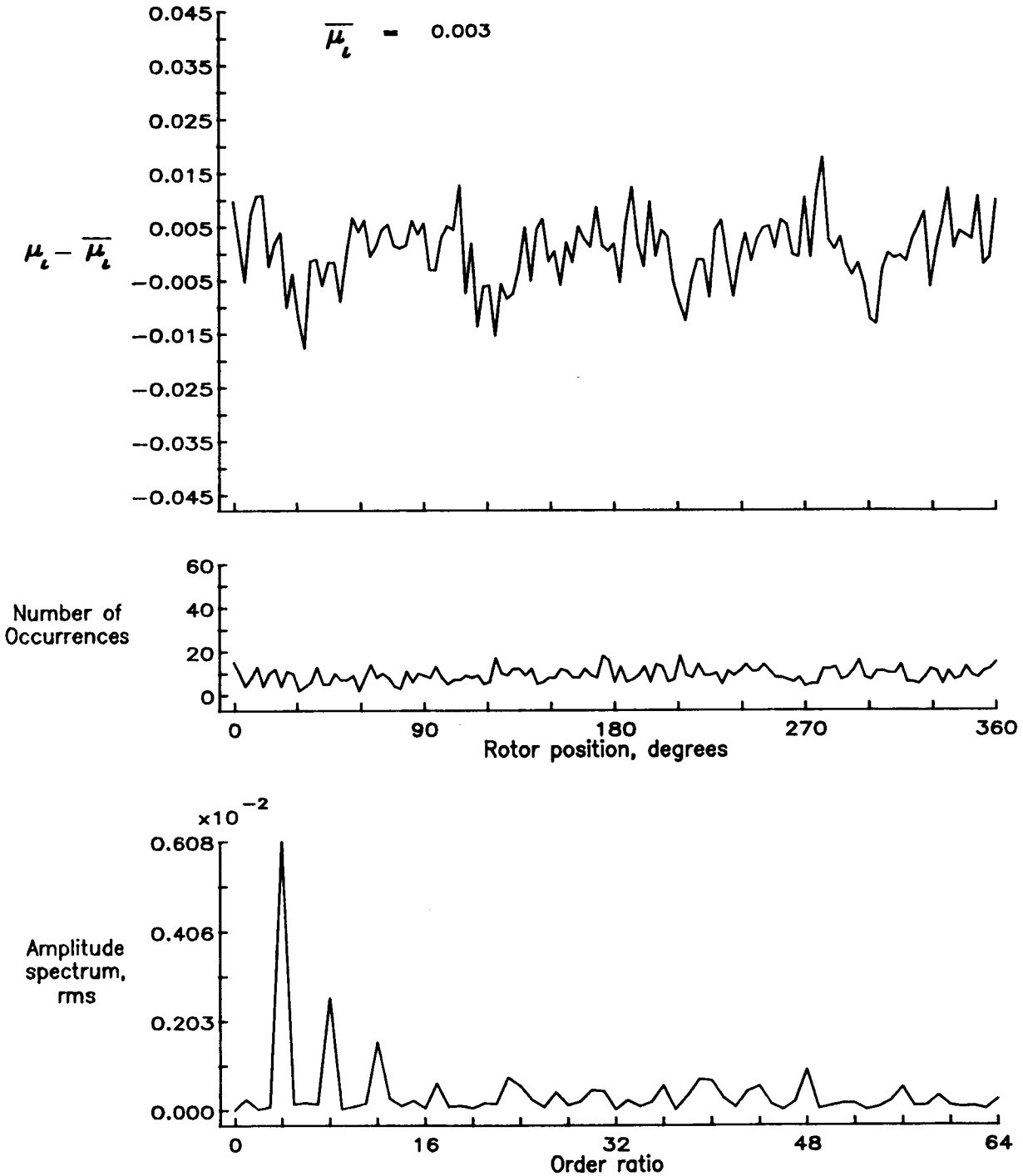


Figure 109.– Induced inflow velocity measured at 210 degrees and r/R of 0.50.

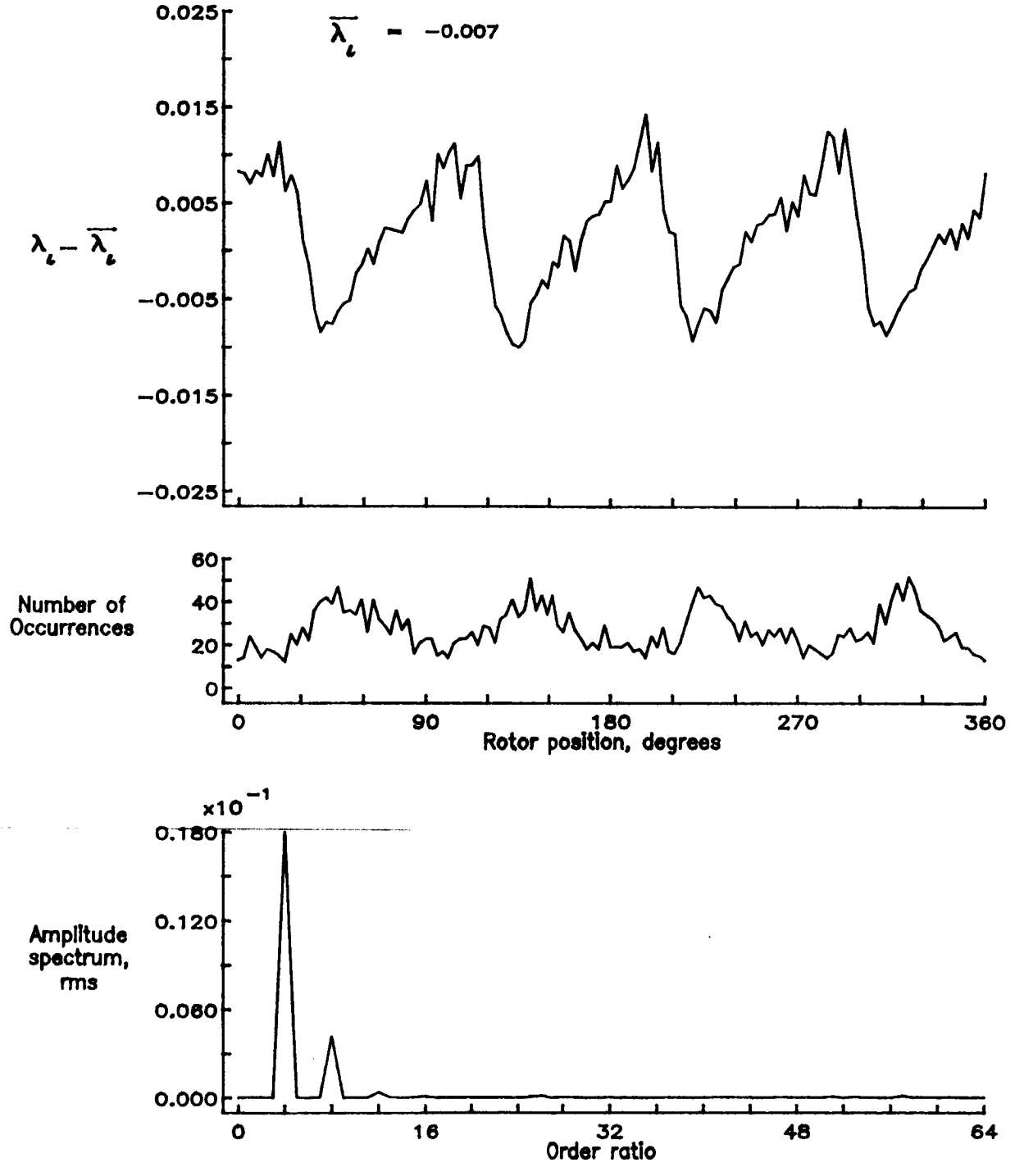


Figure 109.– Concluded.

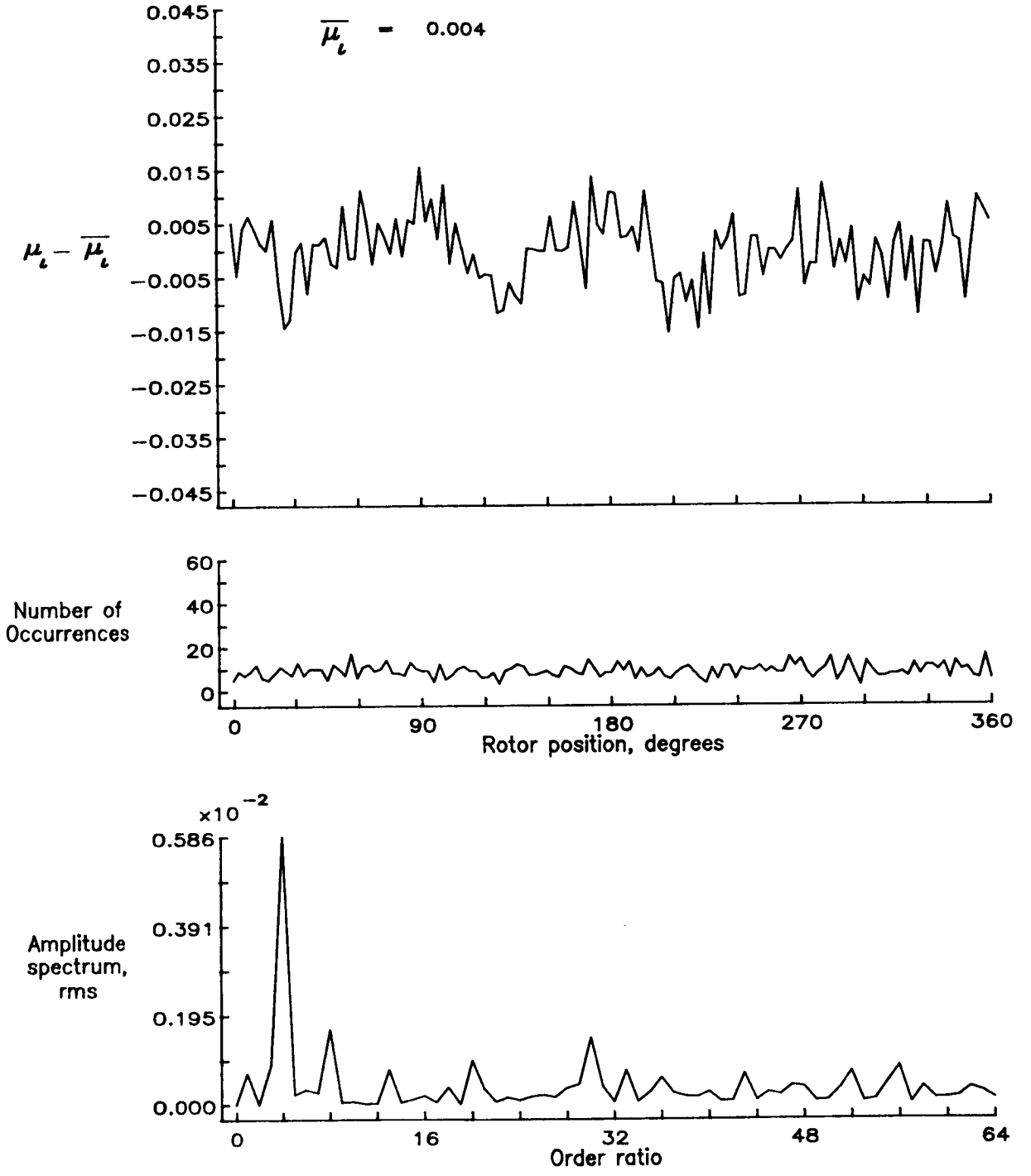


Figure 110.– Induced inflow velocity measured at 210 degrees and r/R of 0.60.

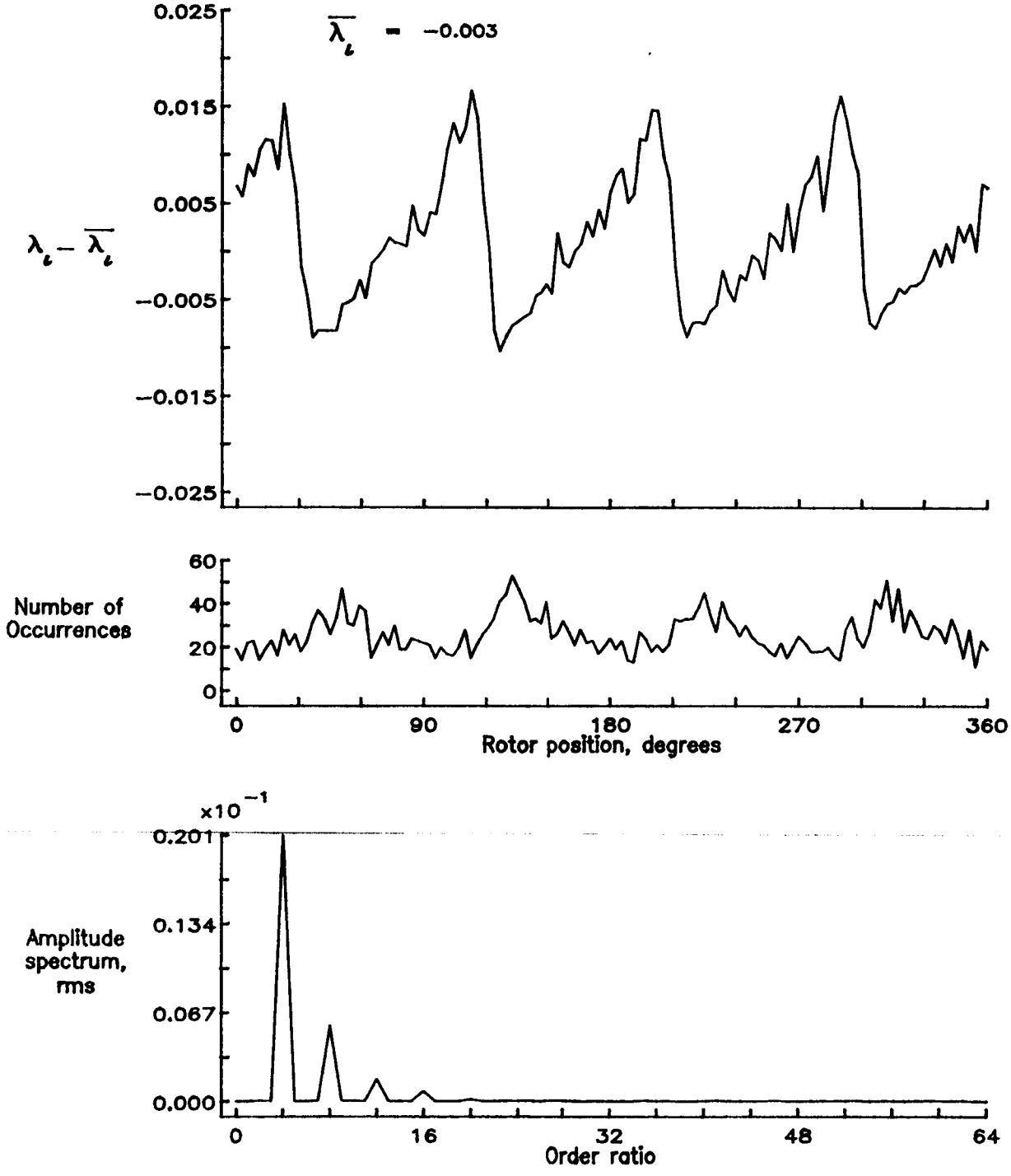


Figure 110.– Concluded.

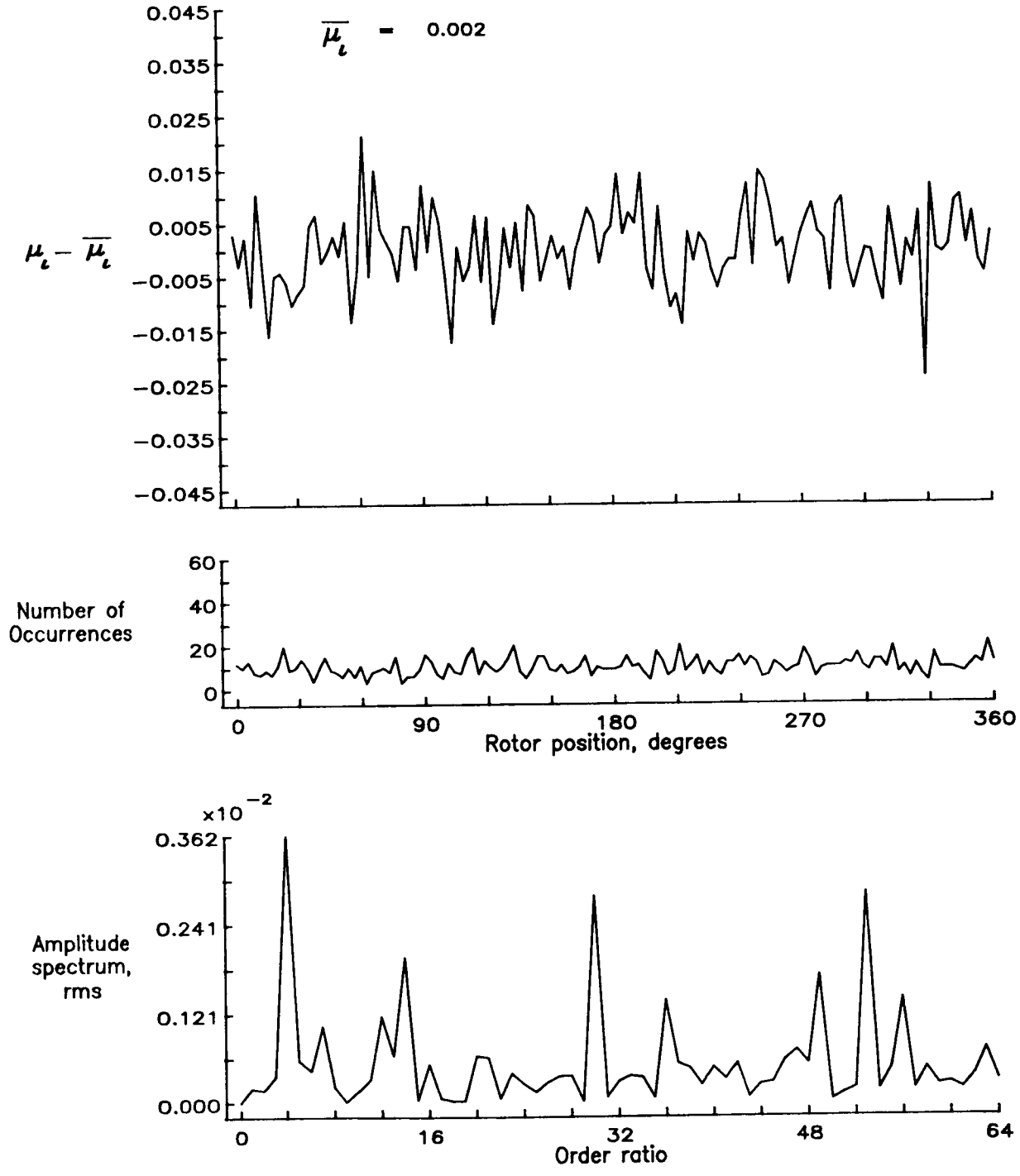


Figure 111.– Induced inflow velocity measured at 210 degrees and r/R of 0.70.

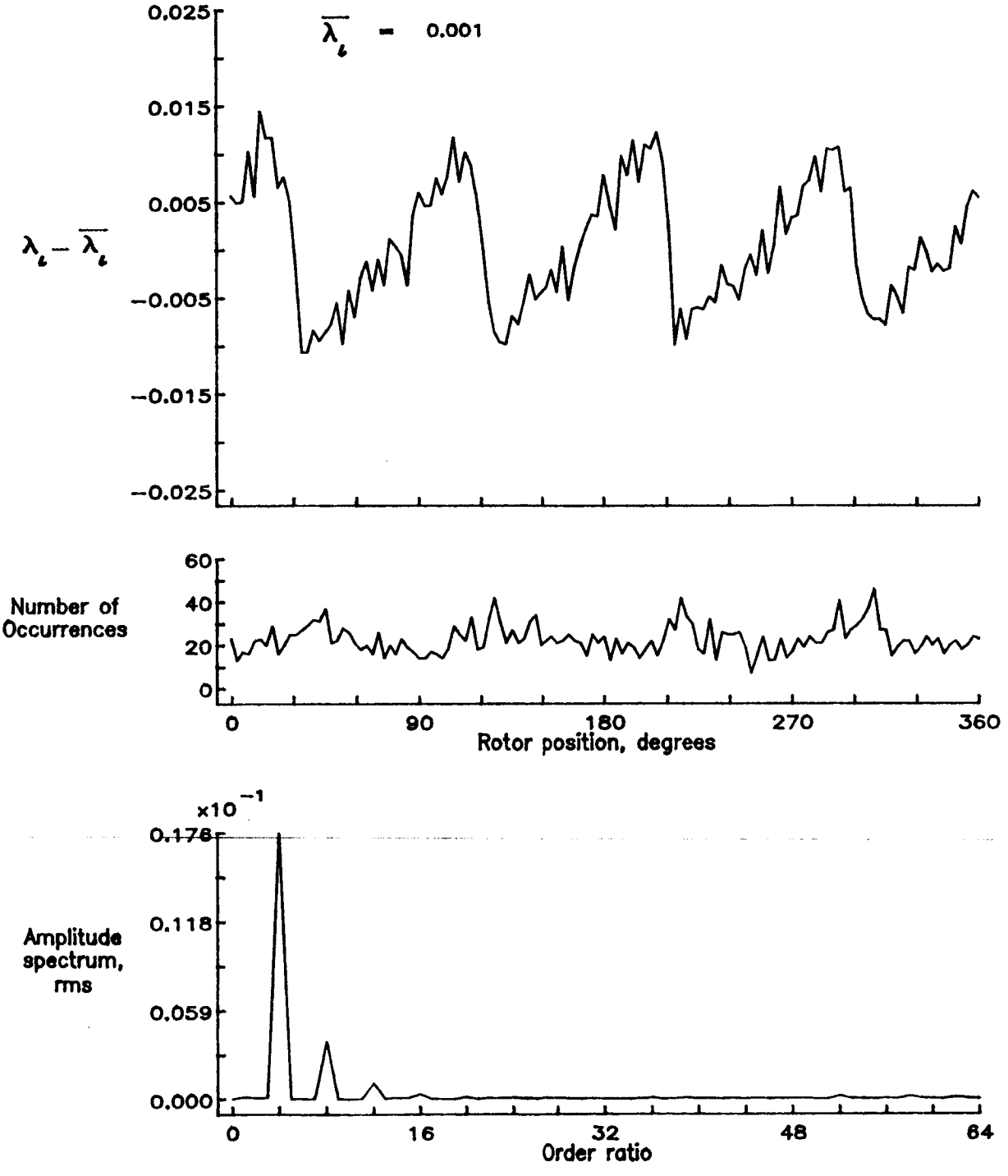


Figure 111.– Concluded.

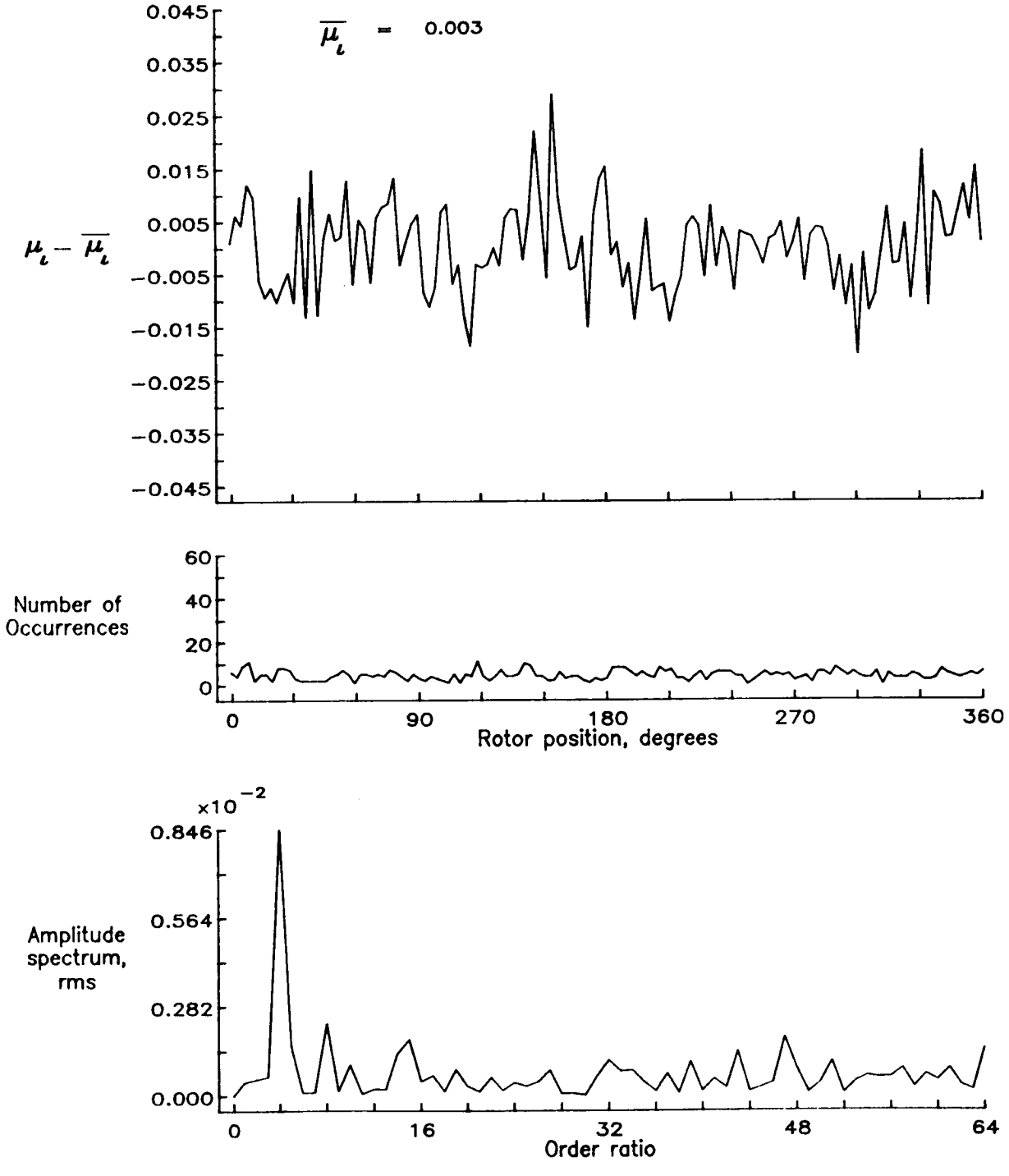


Figure 112.– Induced inflow velocity measured at 210 degrees and r/R of 0.74.

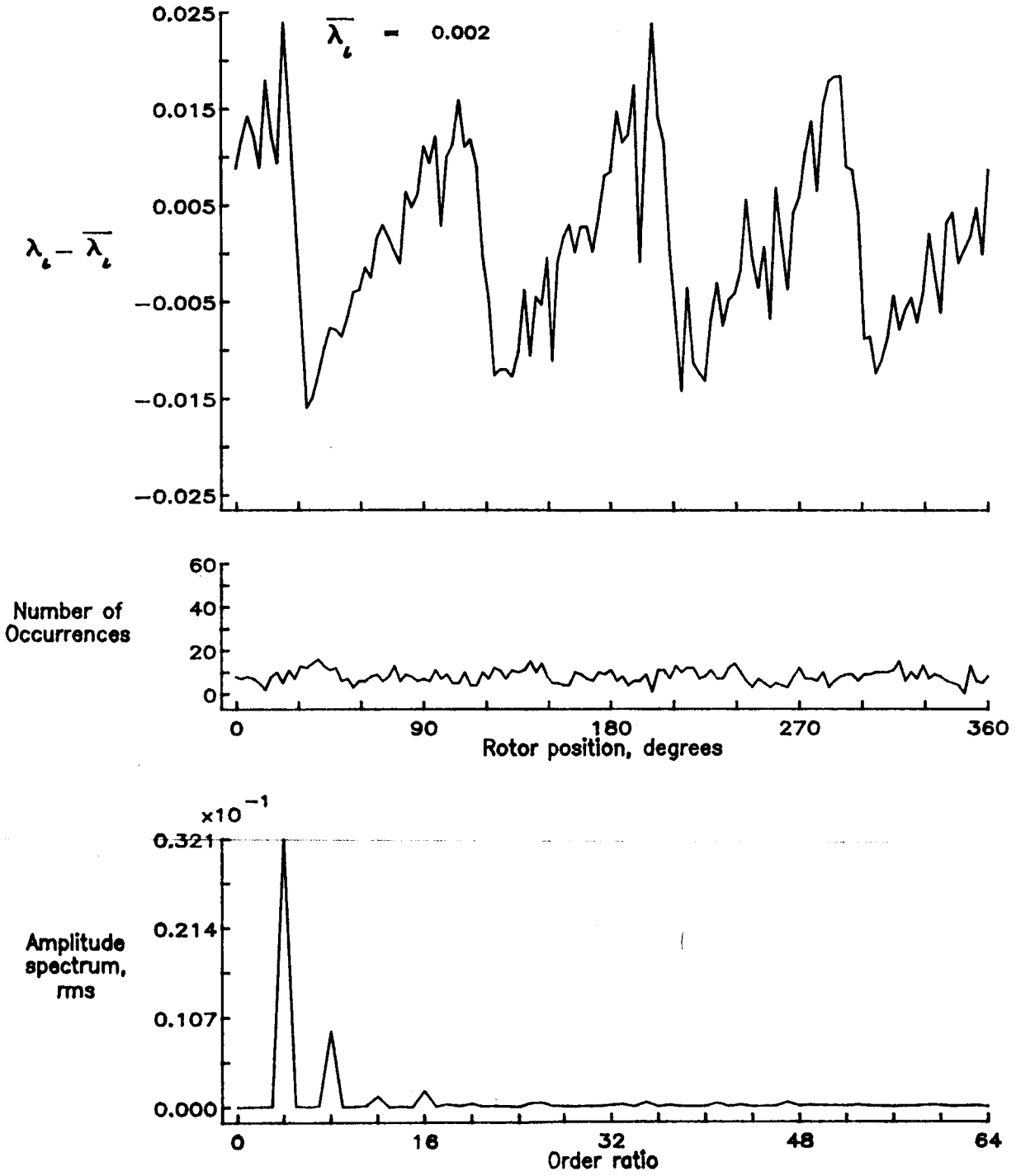


Figure 112.– Concluded.

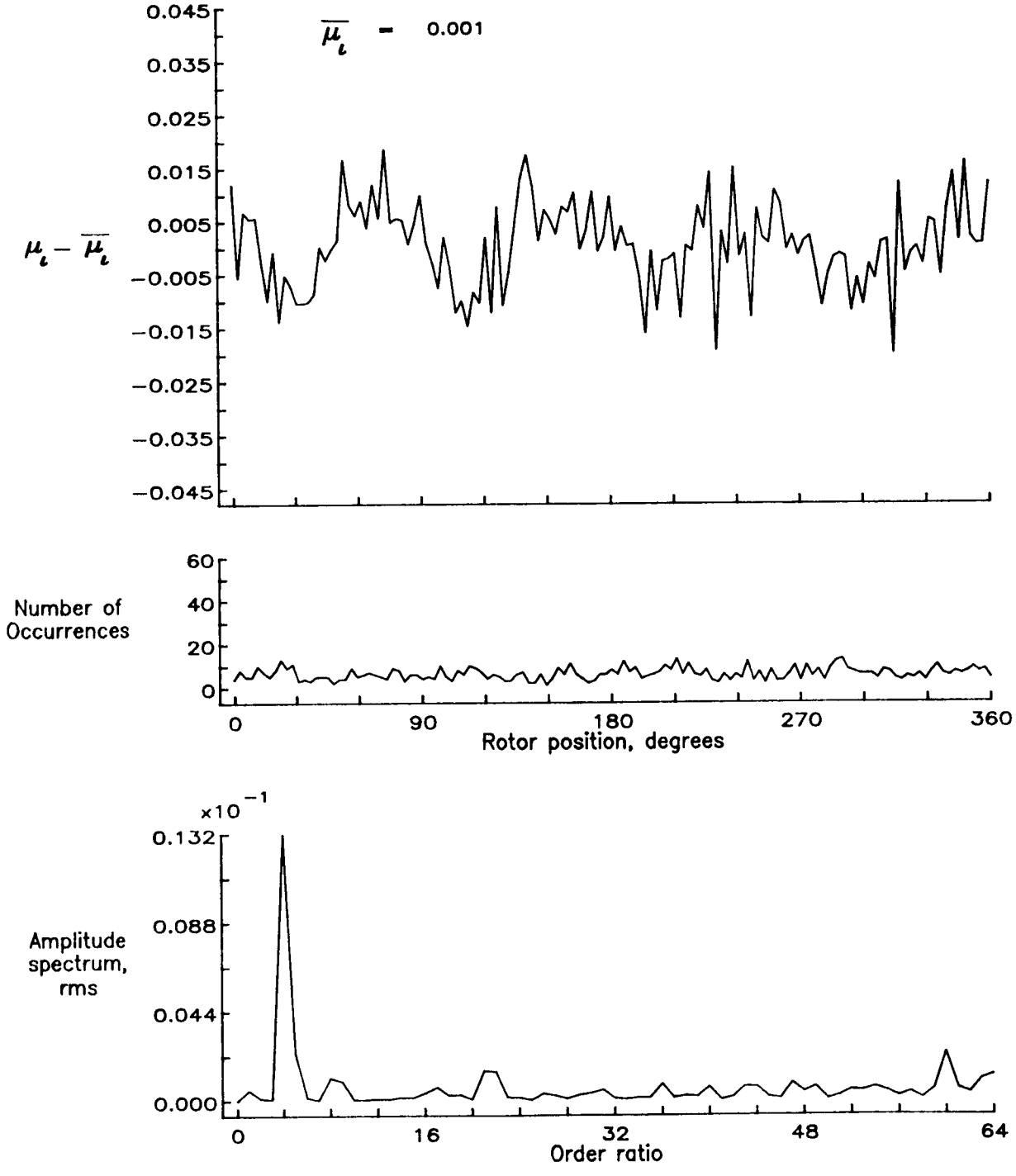


Figure 113.– Induced inflow velocity measured at 210 degrees and r/R of 0.78.

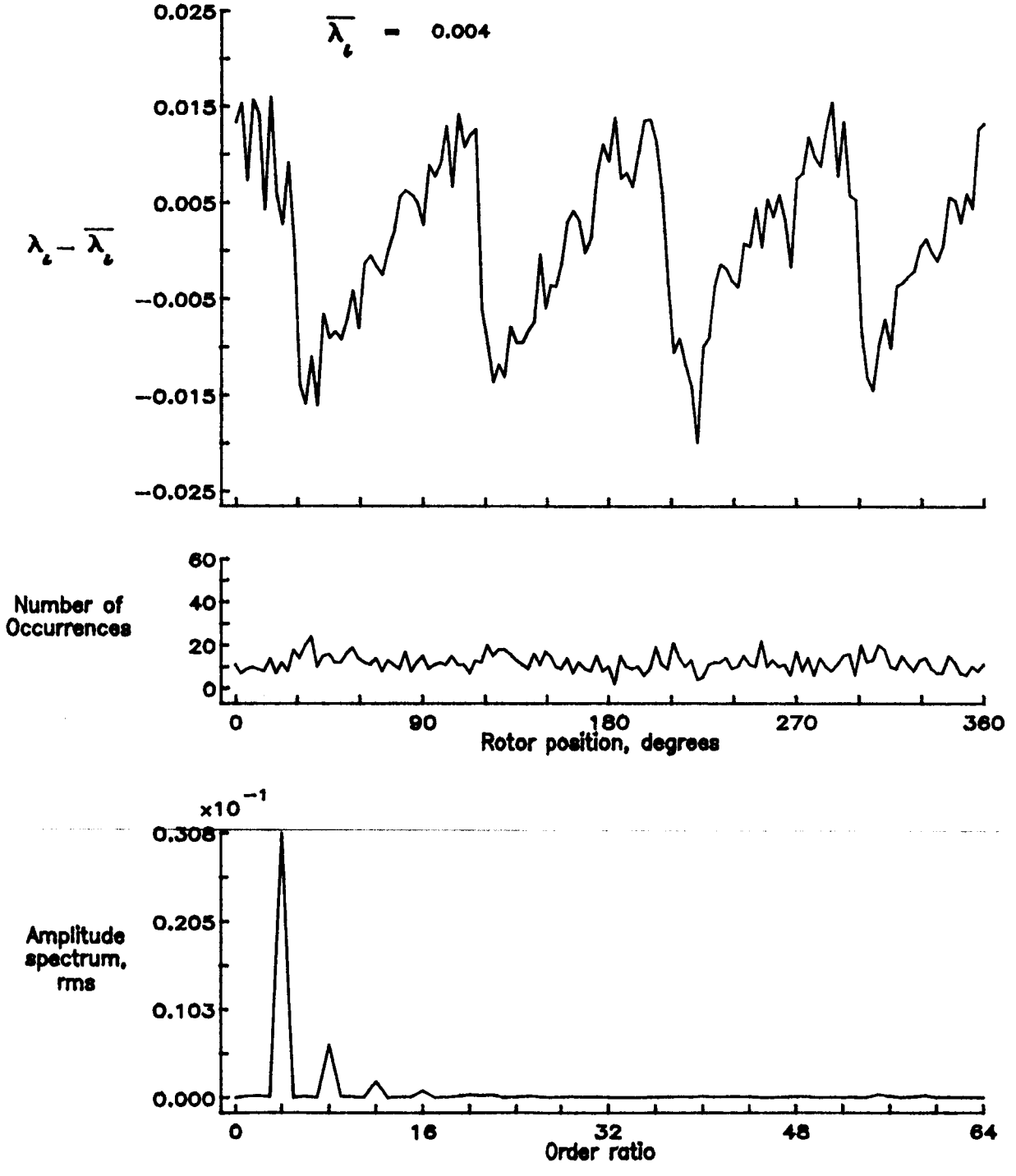


Figure 113.– Concluded.

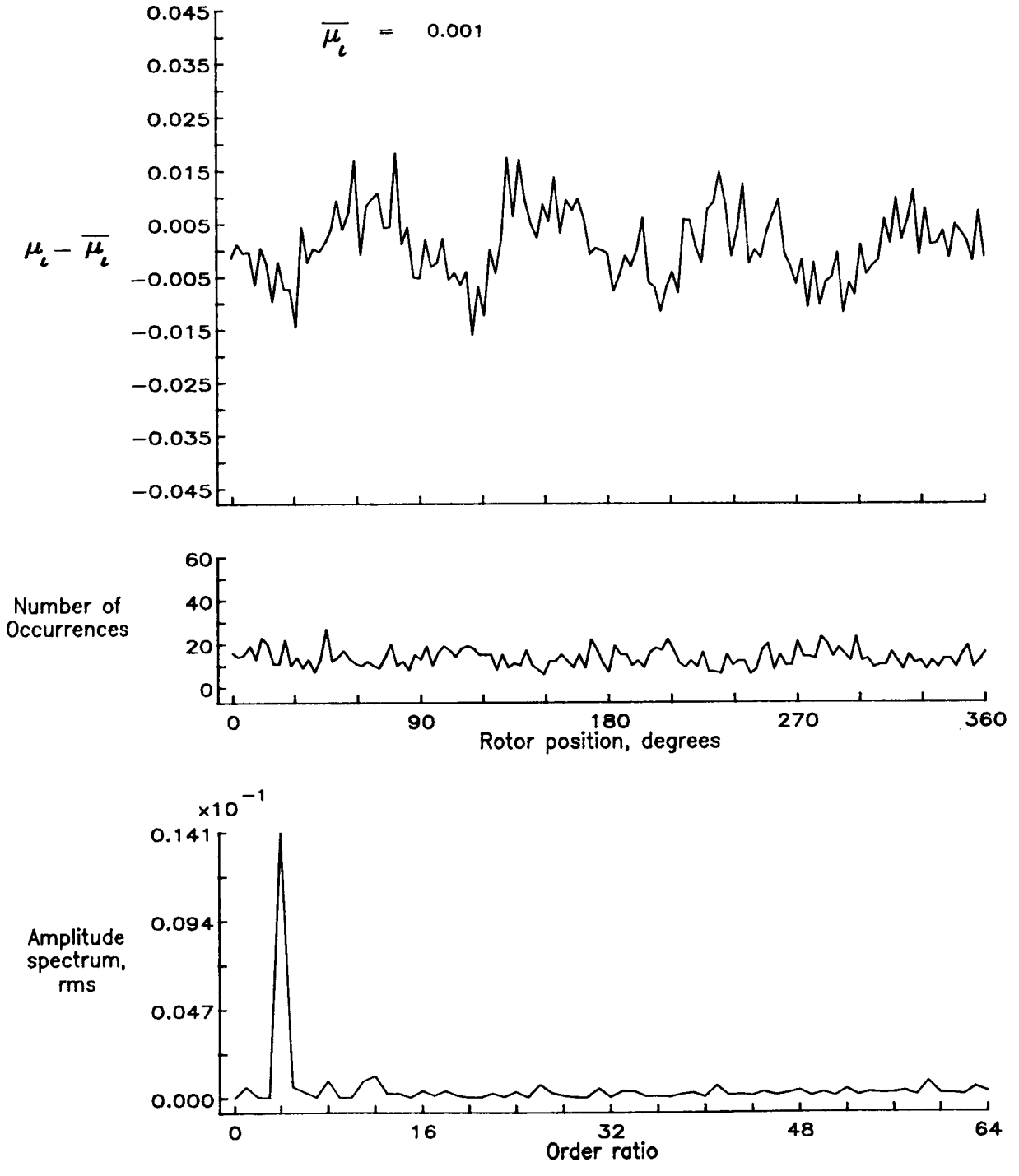


Figure 114.– Induced inflow velocity measured at 210 degrees and r/R of 0.82.

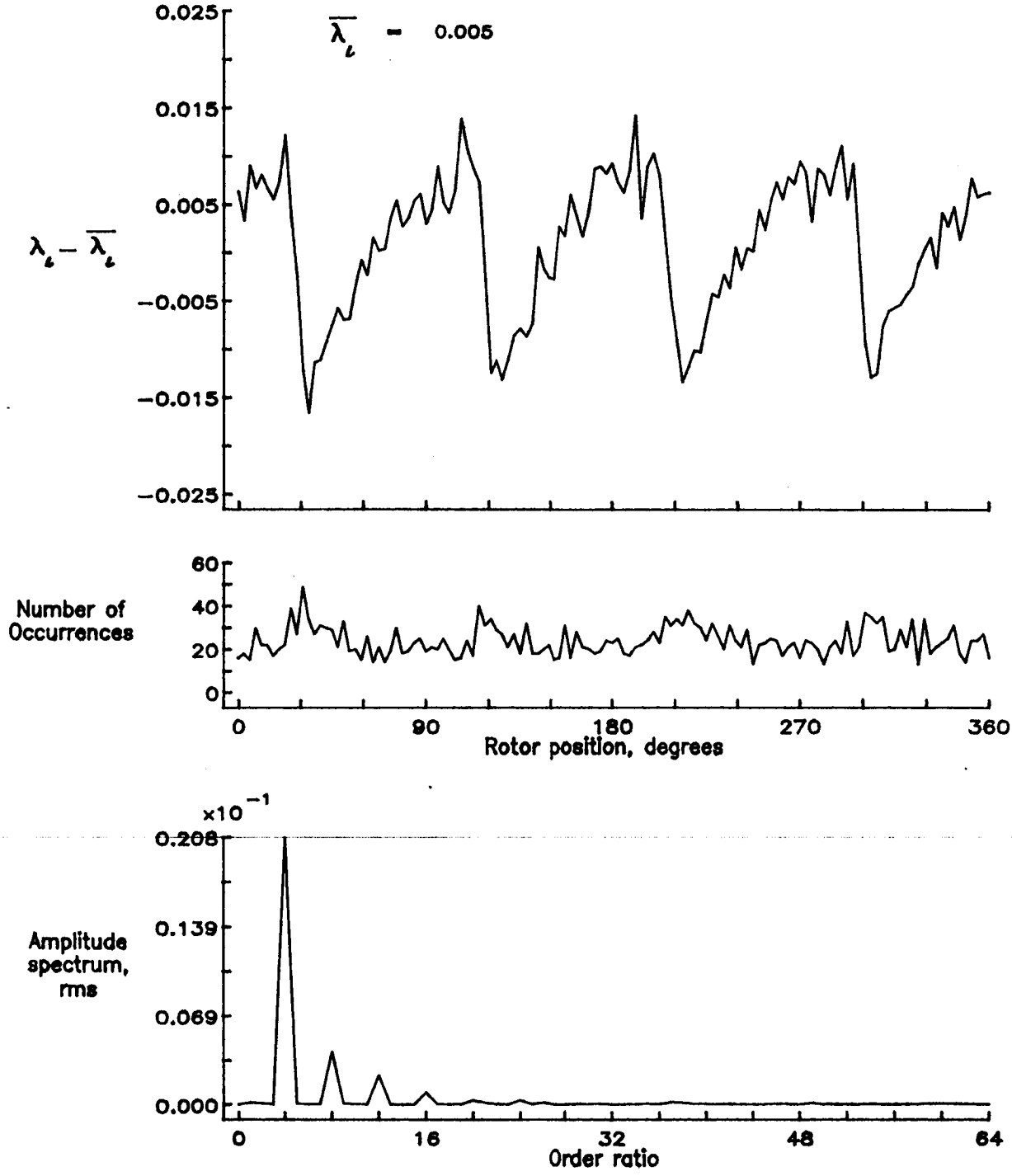


Figure 114.– Concluded.

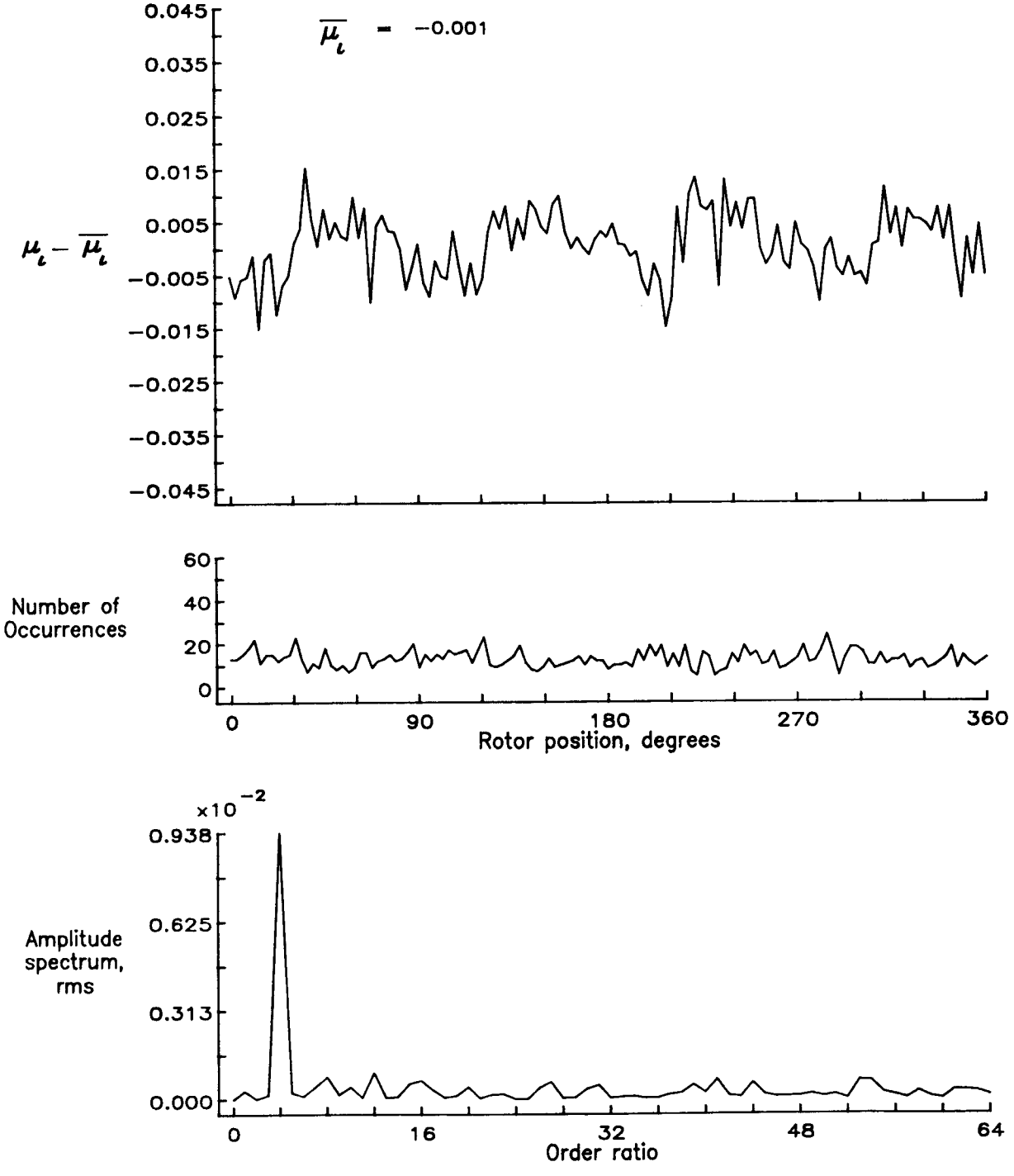


Figure 115.– Induced inflow velocity measured at 210 degrees and r/R of 0.86.

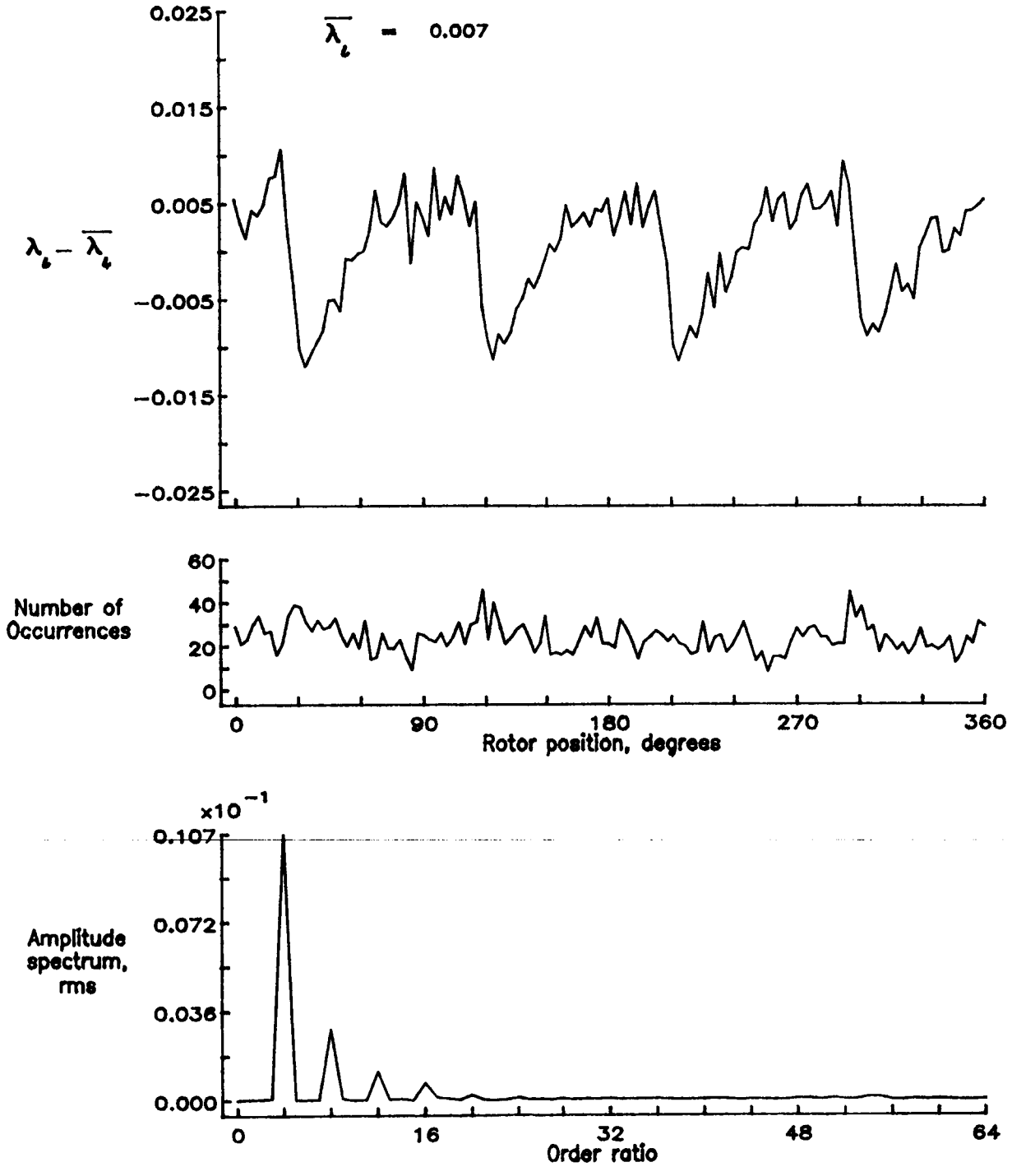


Figure 115.– Concluded.

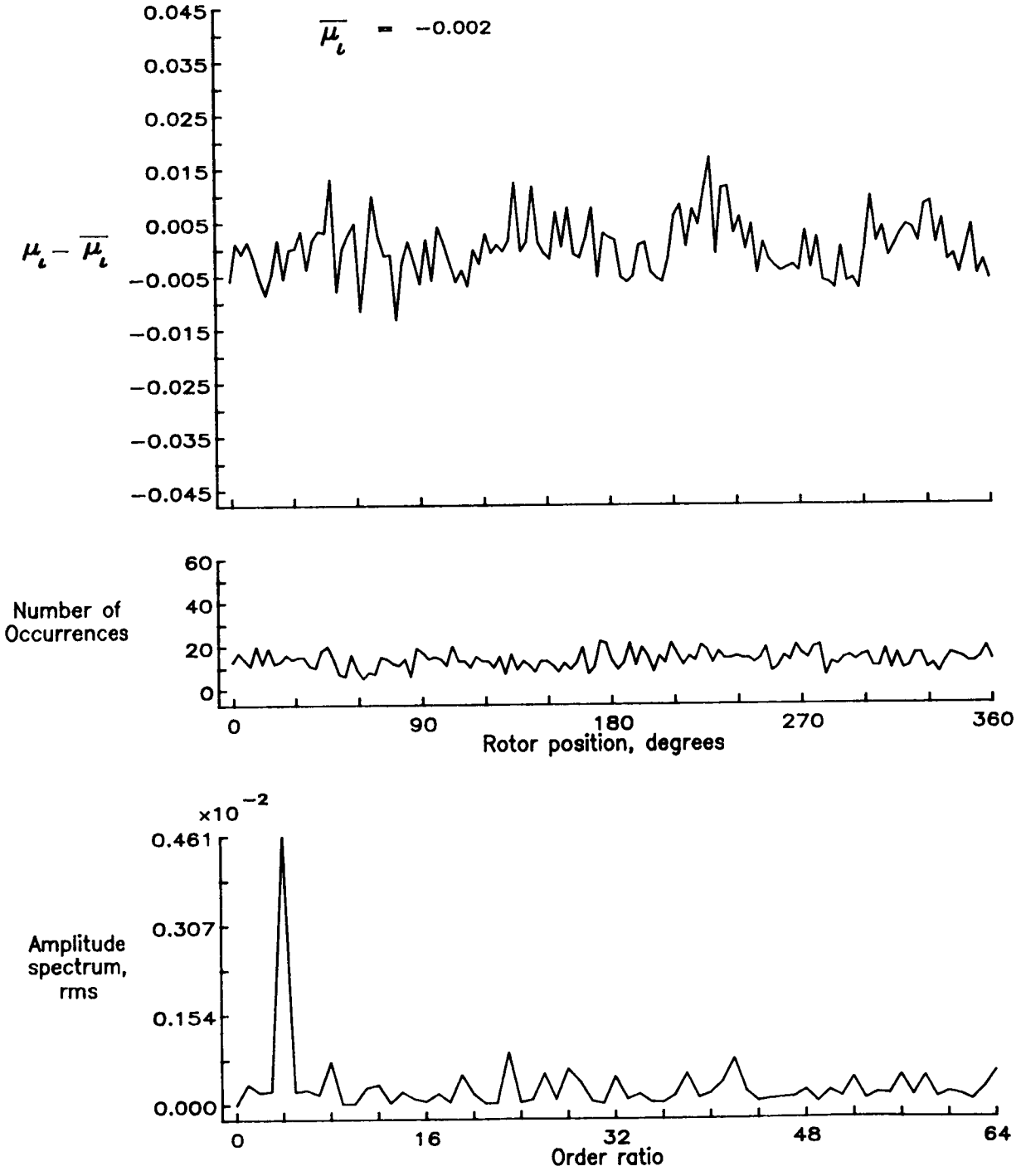


Figure 116.– Induced inflow velocity measured at 210 degrees and r/R of 0.90.

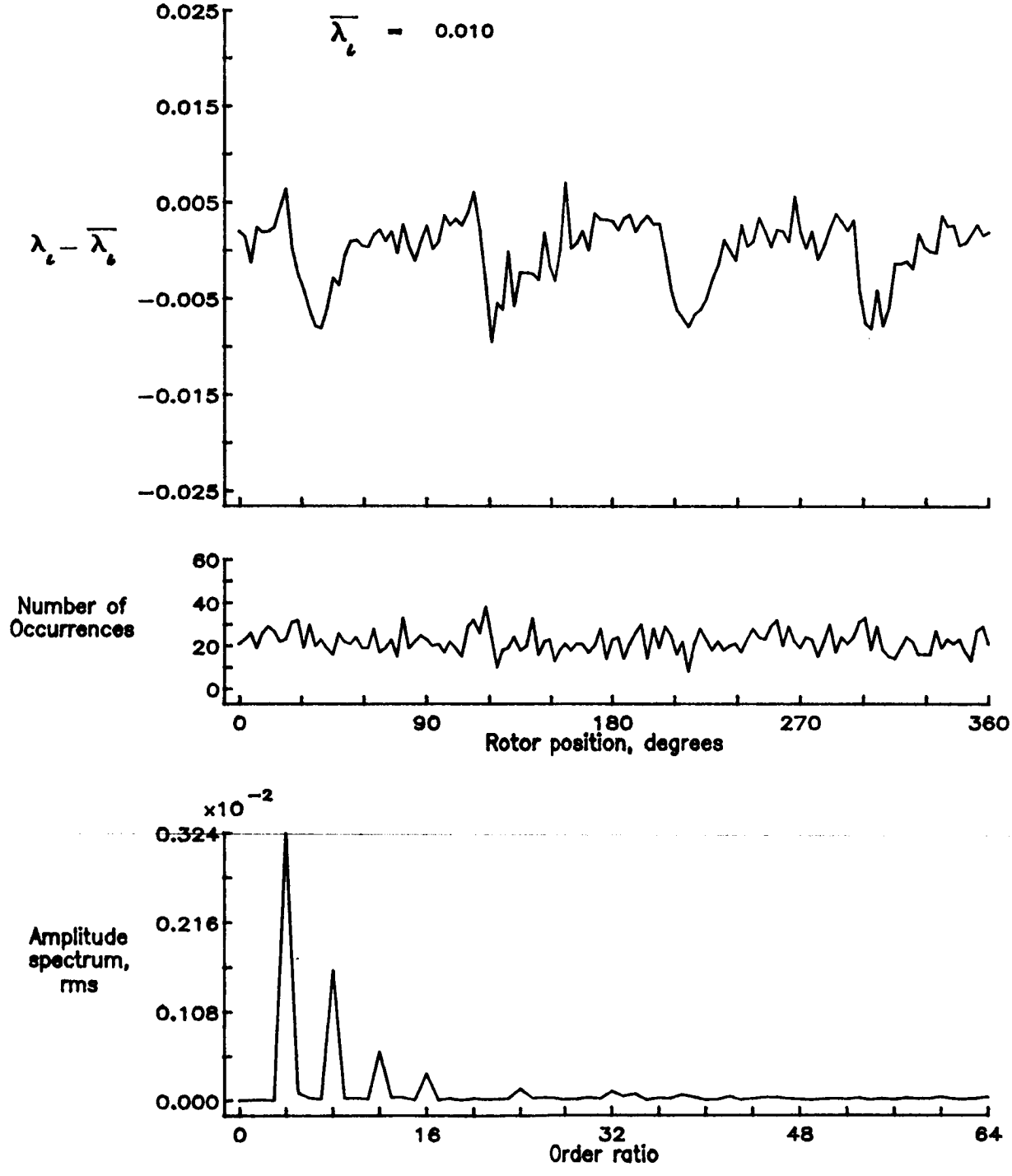


Figure 116.– Concluded.

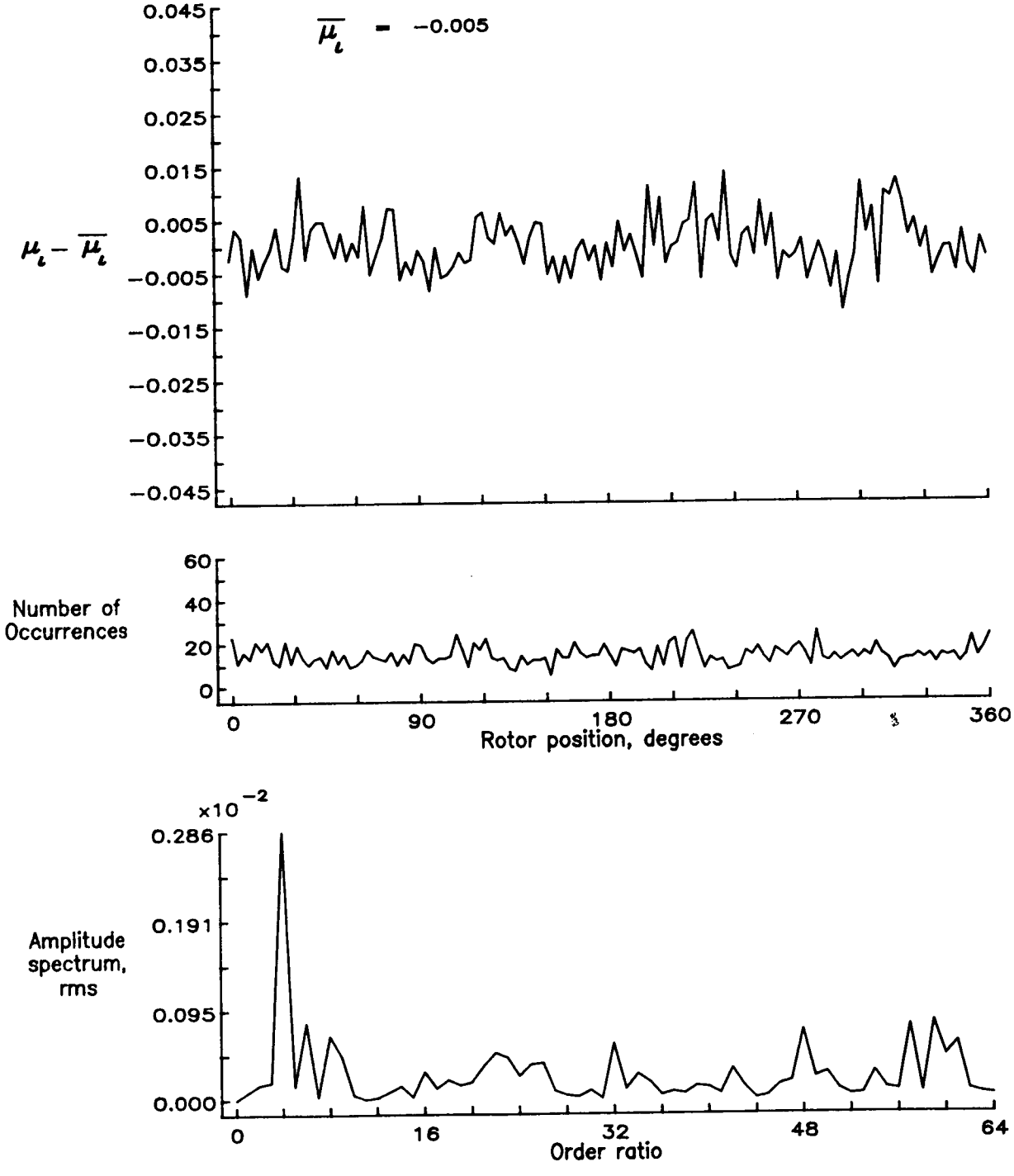


Figure 117.– Induced inflow velocity measured at 210 degrees and r/R of 0.94.

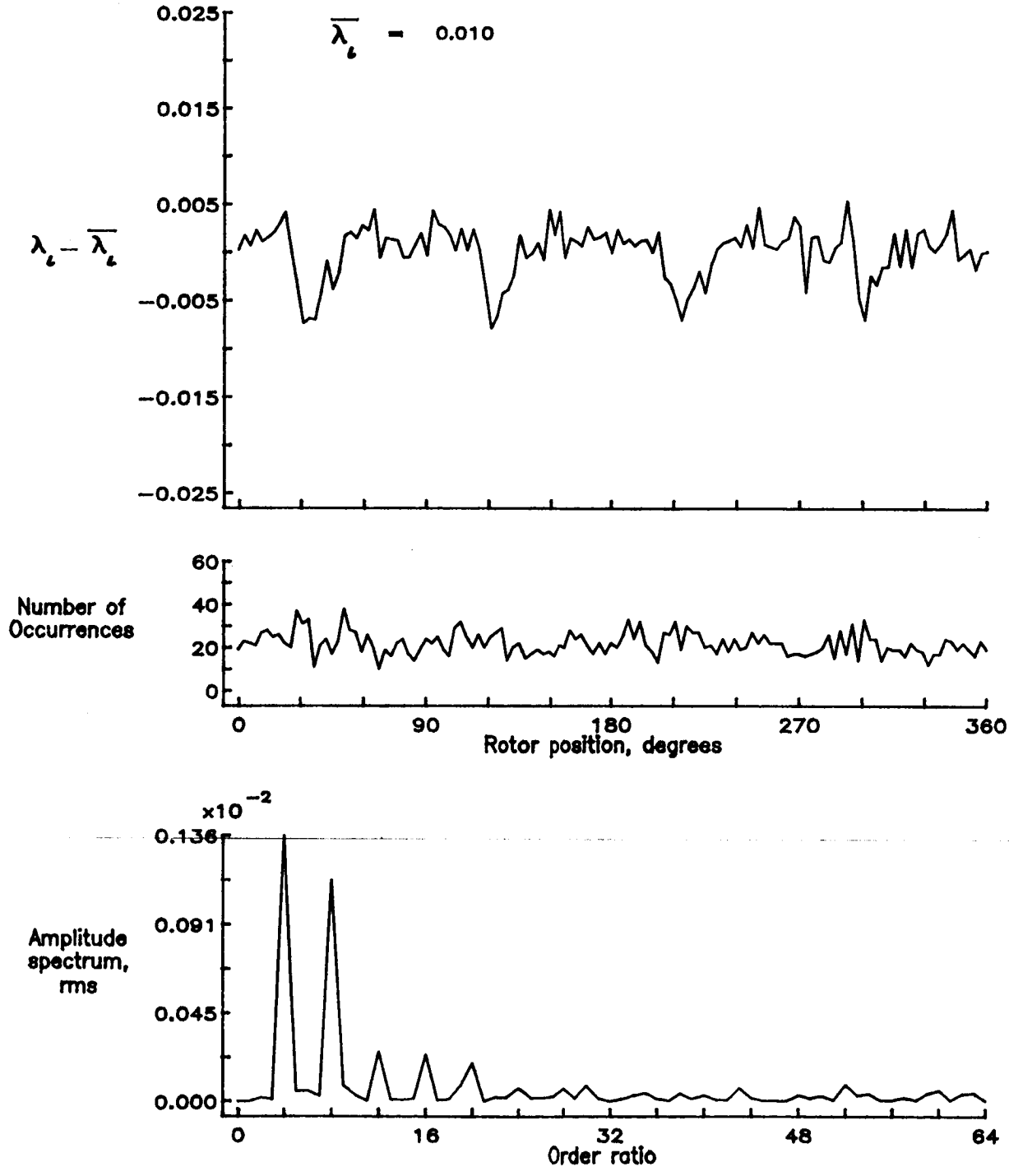


Figure 117.– Concluded.

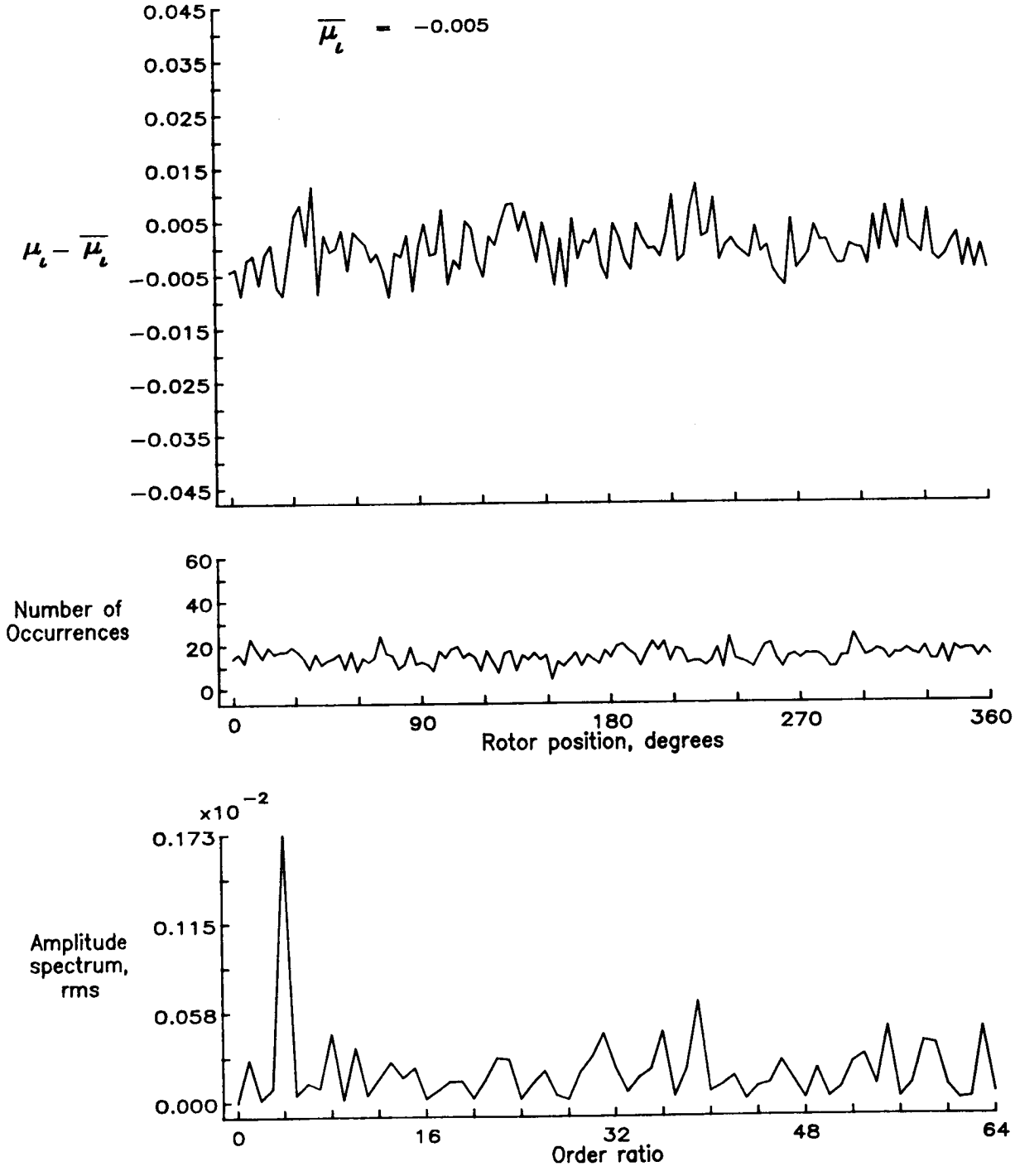


Figure 118.– Induced inflow velocity measured at 210 degrees and r/R of 0.98.

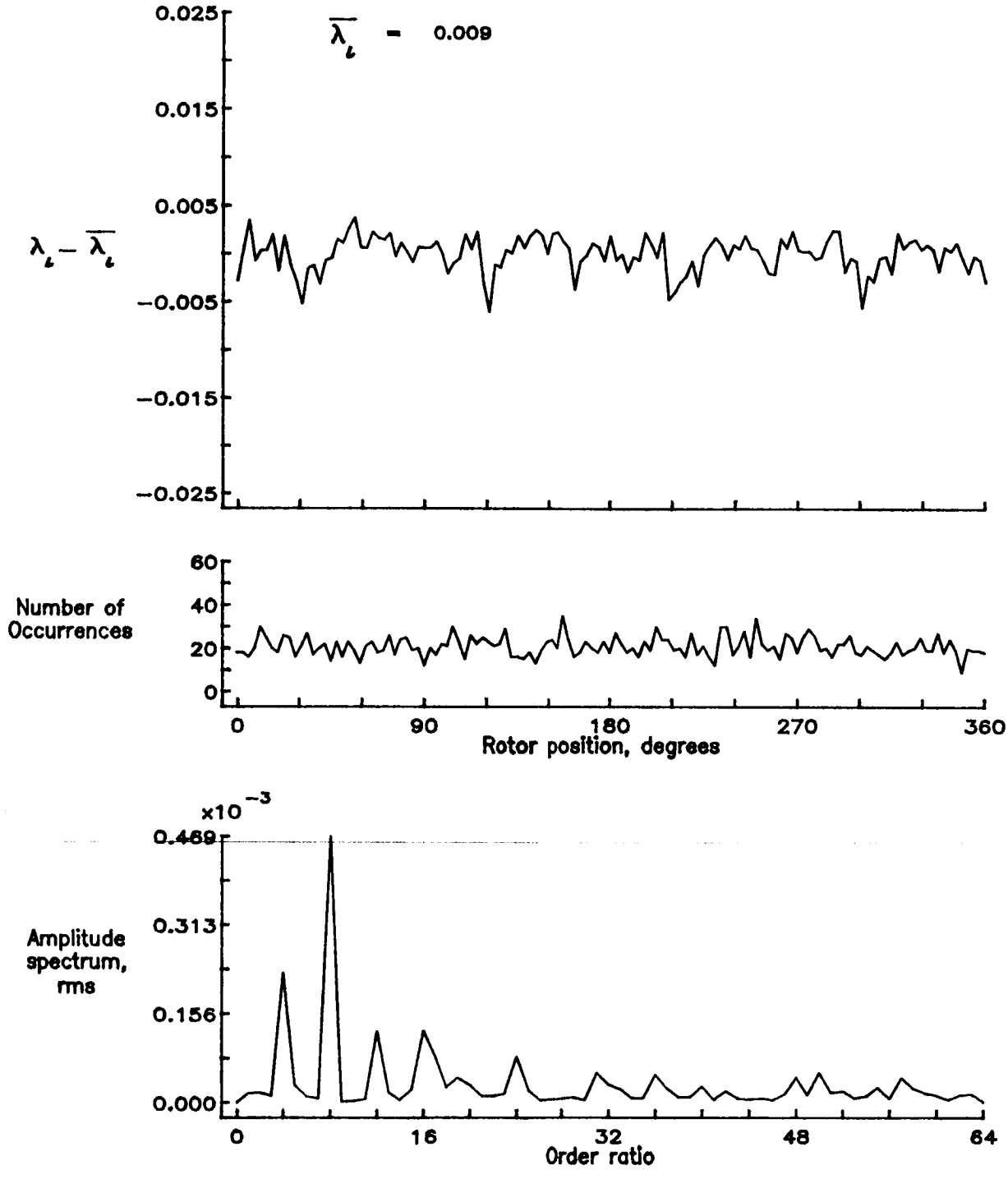


Figure 118.– Concluded.

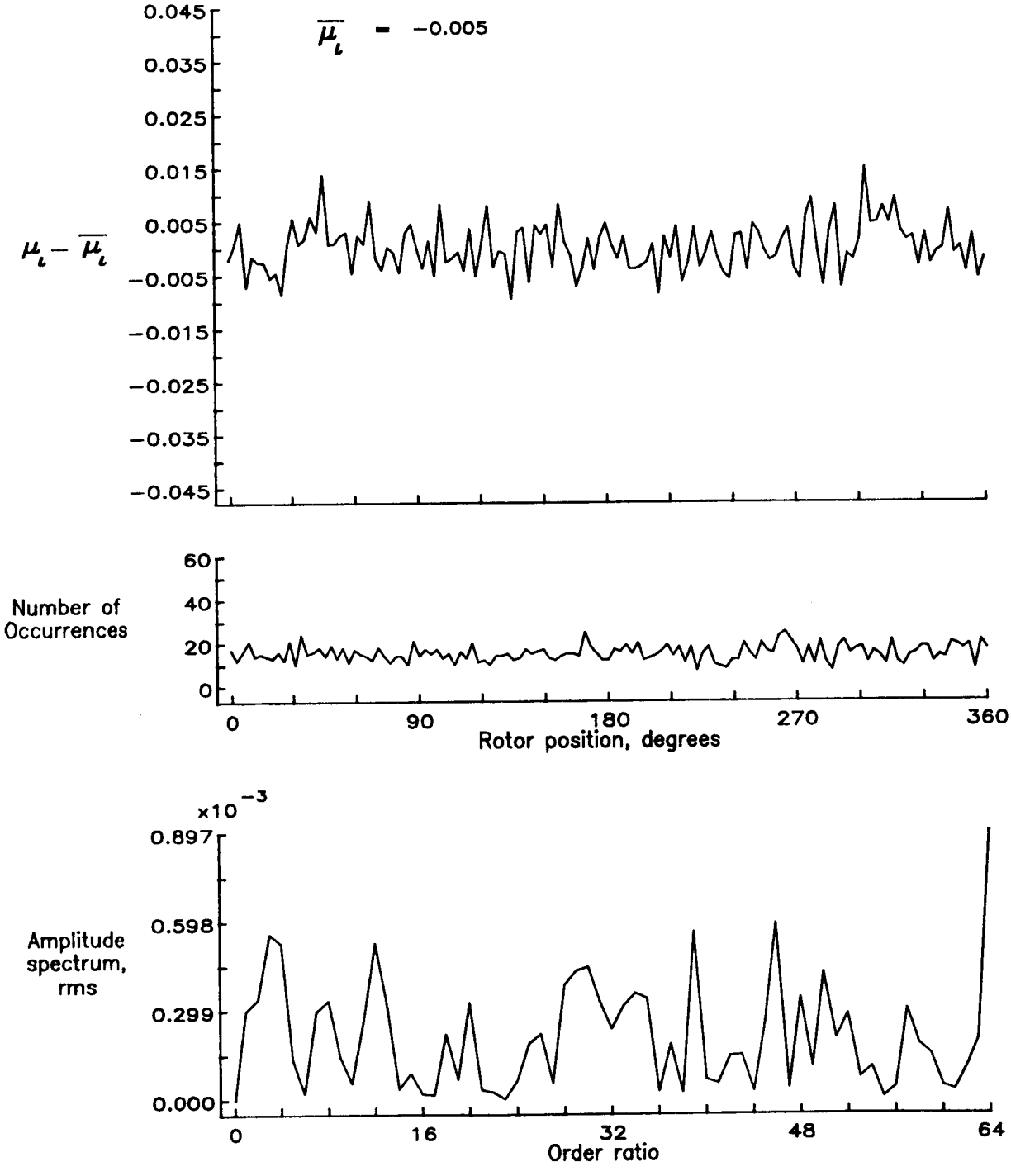


Figure 119.– Induced inflow velocity measured at 210 degrees and r/R of 1.02.

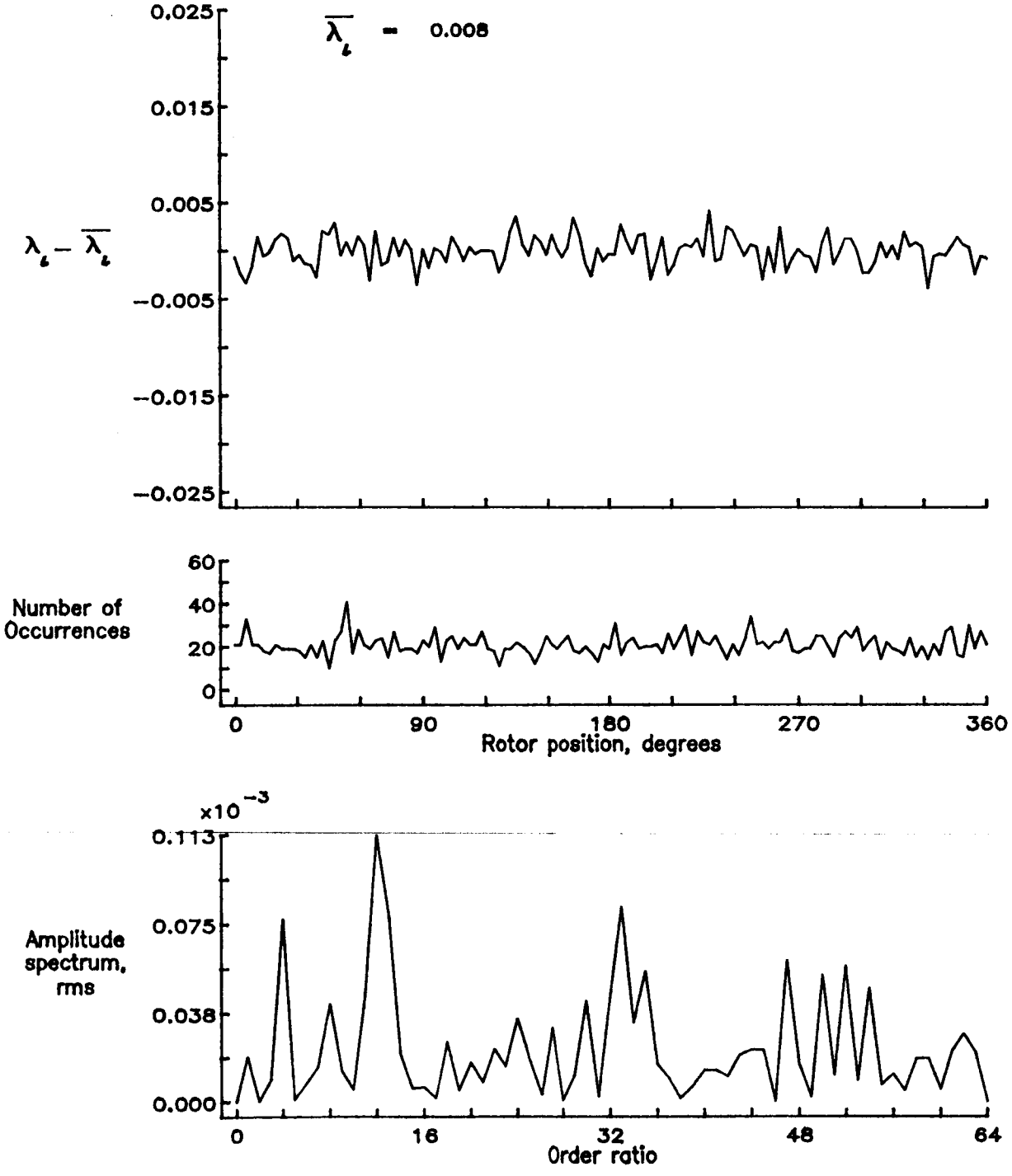


Figure 119.– Concluded.

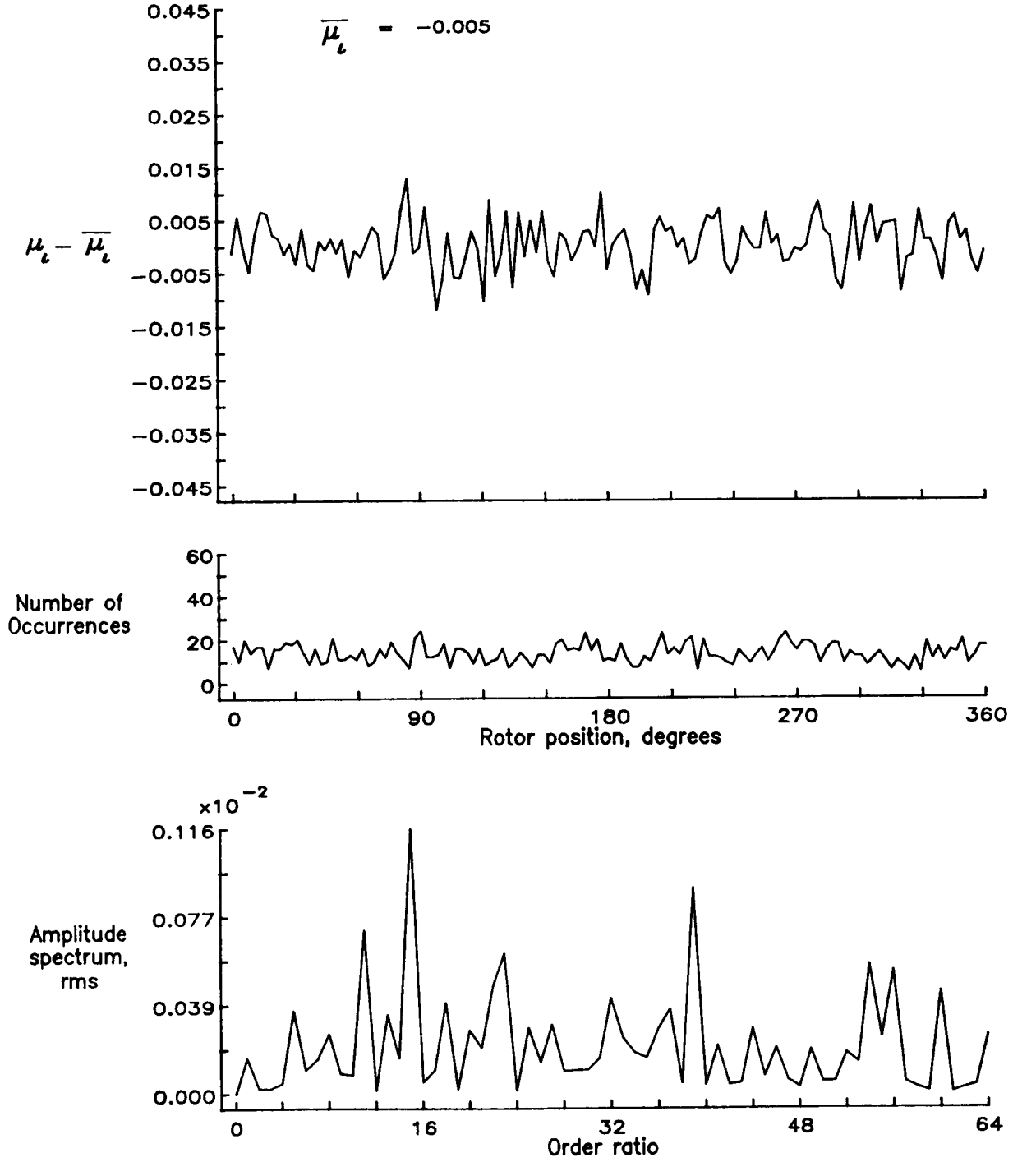


Figure 120.– Induced inflow velocity measured at 210 degrees and r/R of 1.04.

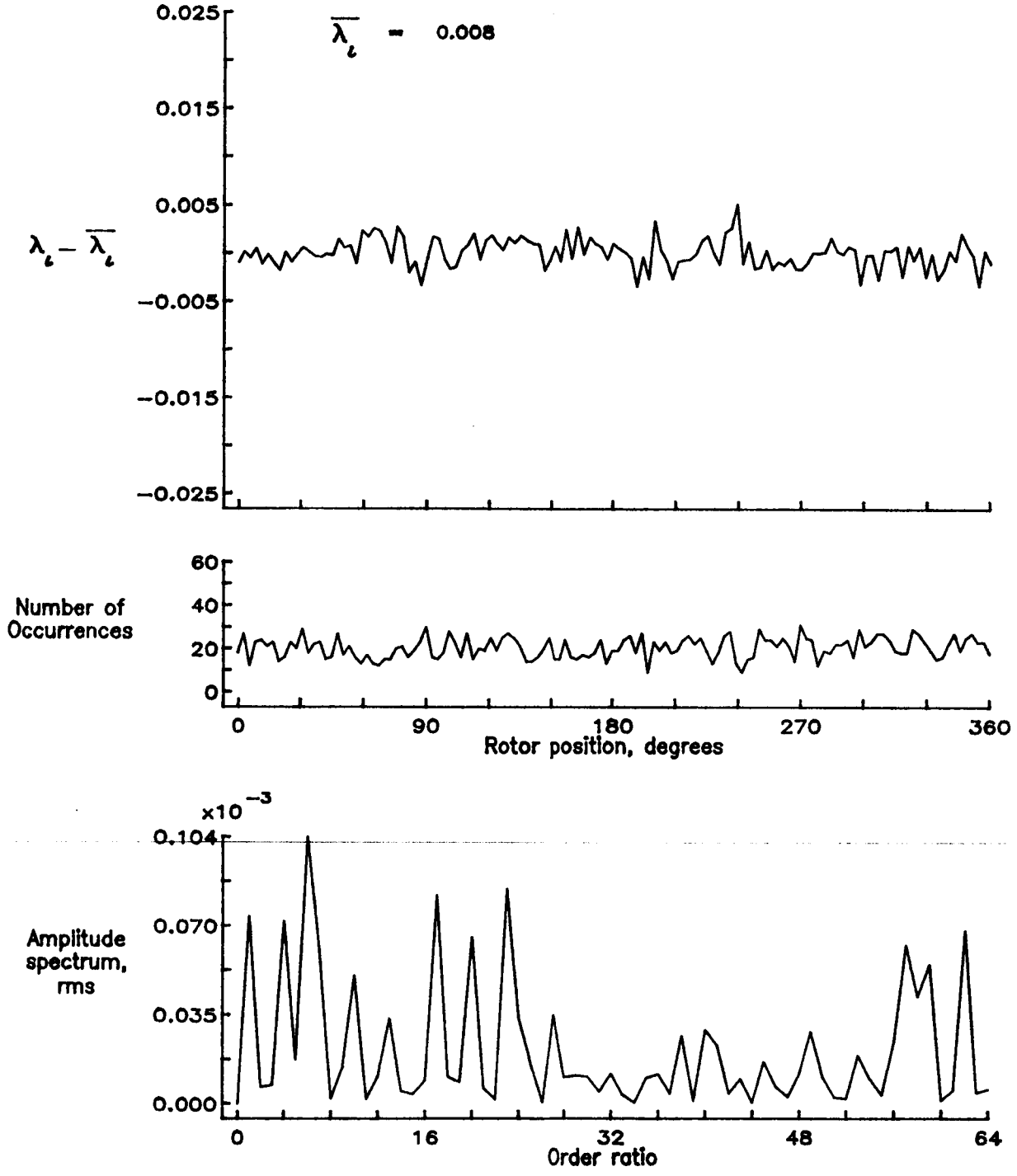


Figure 120.– Concluded.

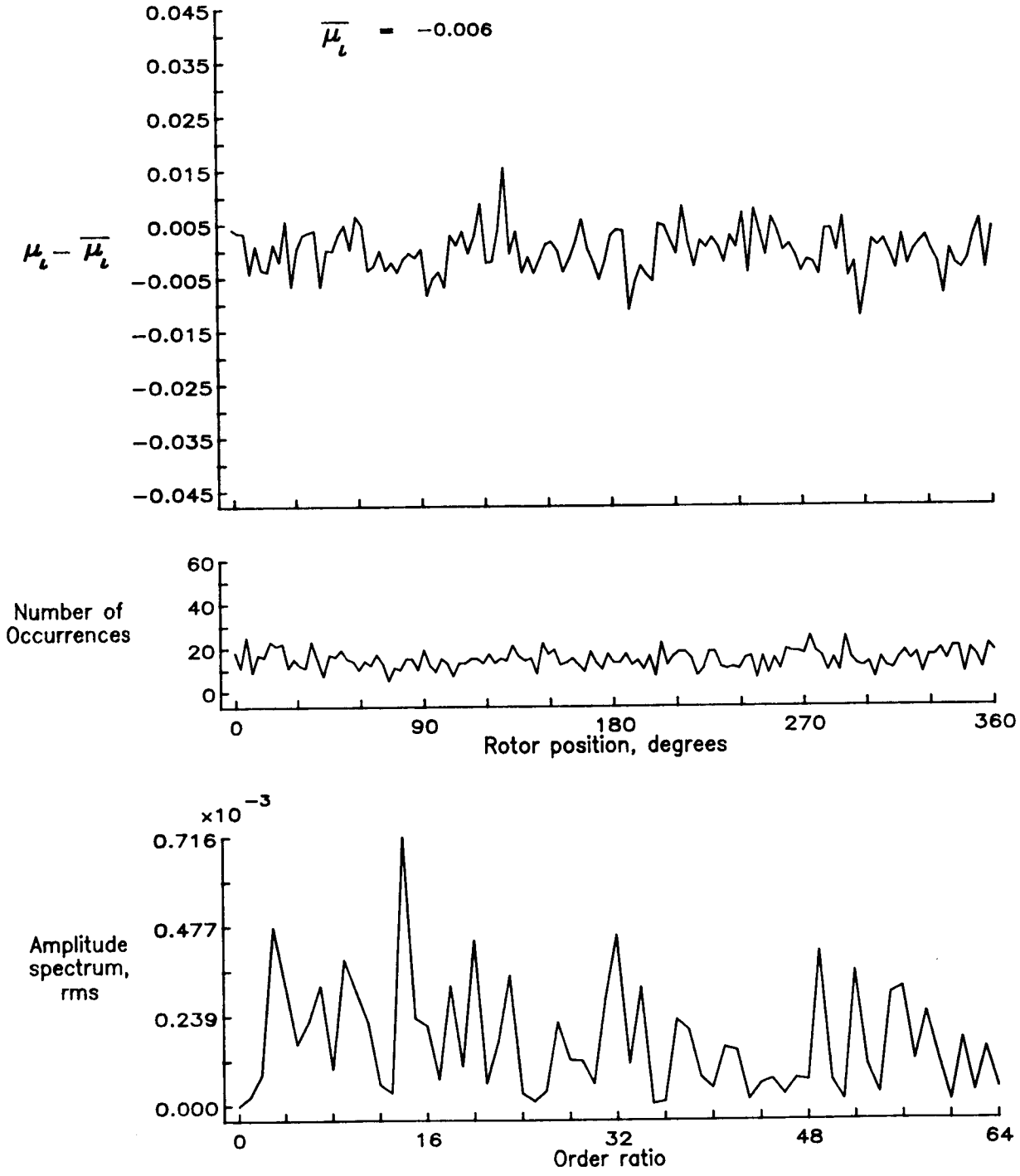


Figure 121.– Induced inflow velocity measured at 210 degrees and r/R of 1.12.

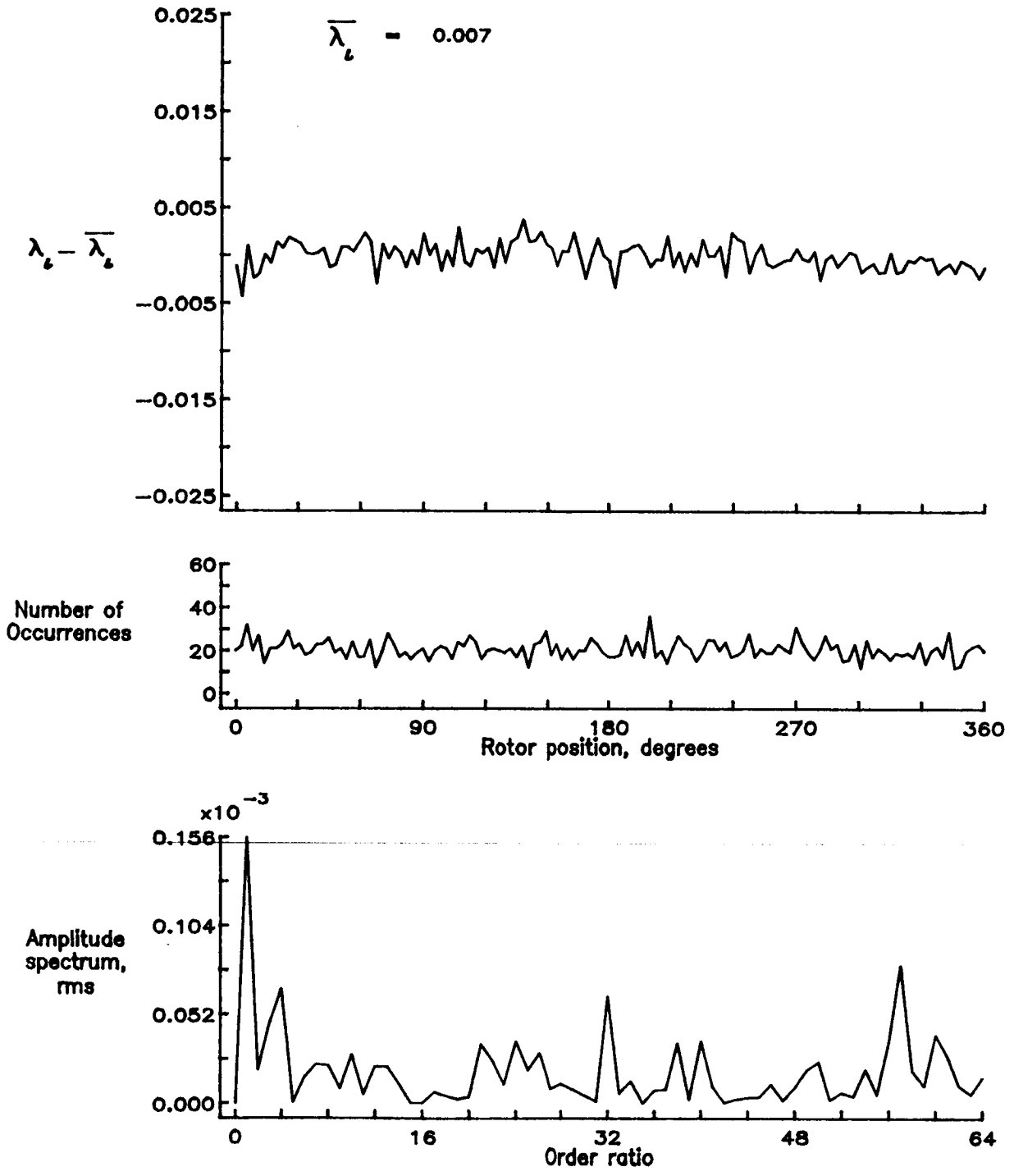


Figure 121.– Concluded.

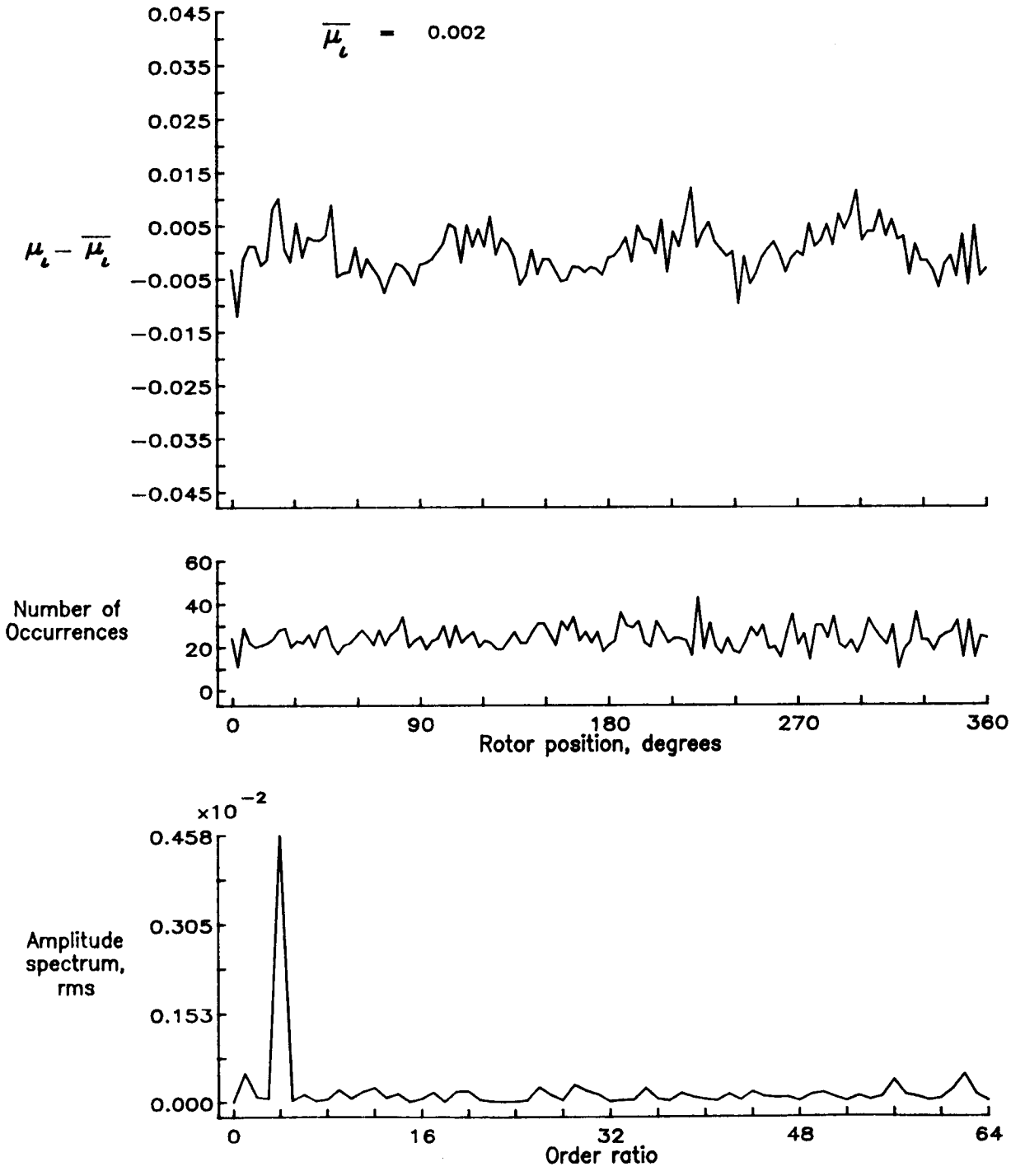


Figure 122.– Induced inflow velocity measured at 240 degrees and r/R of 0.20.

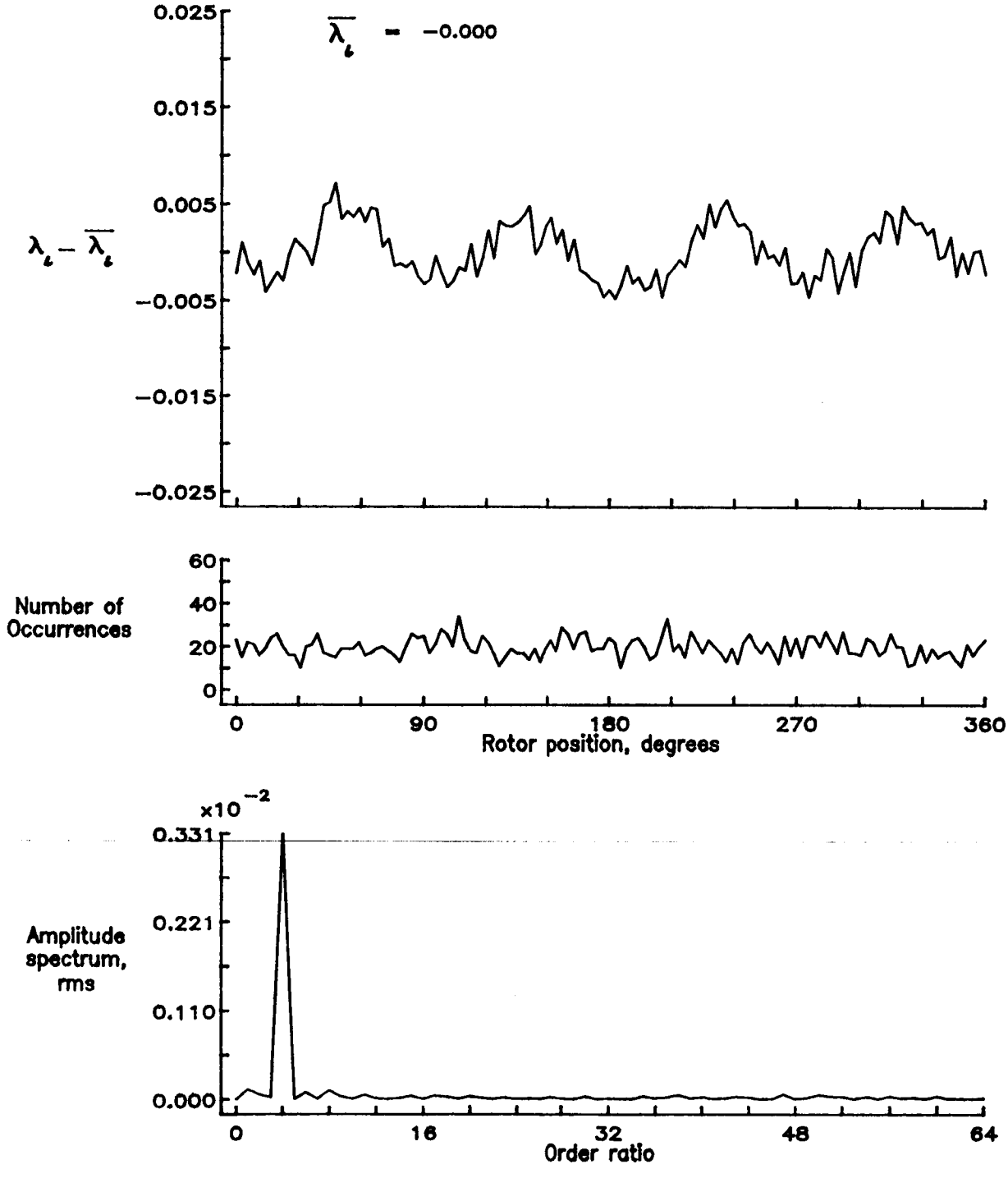


Figure 122.– Concluded.

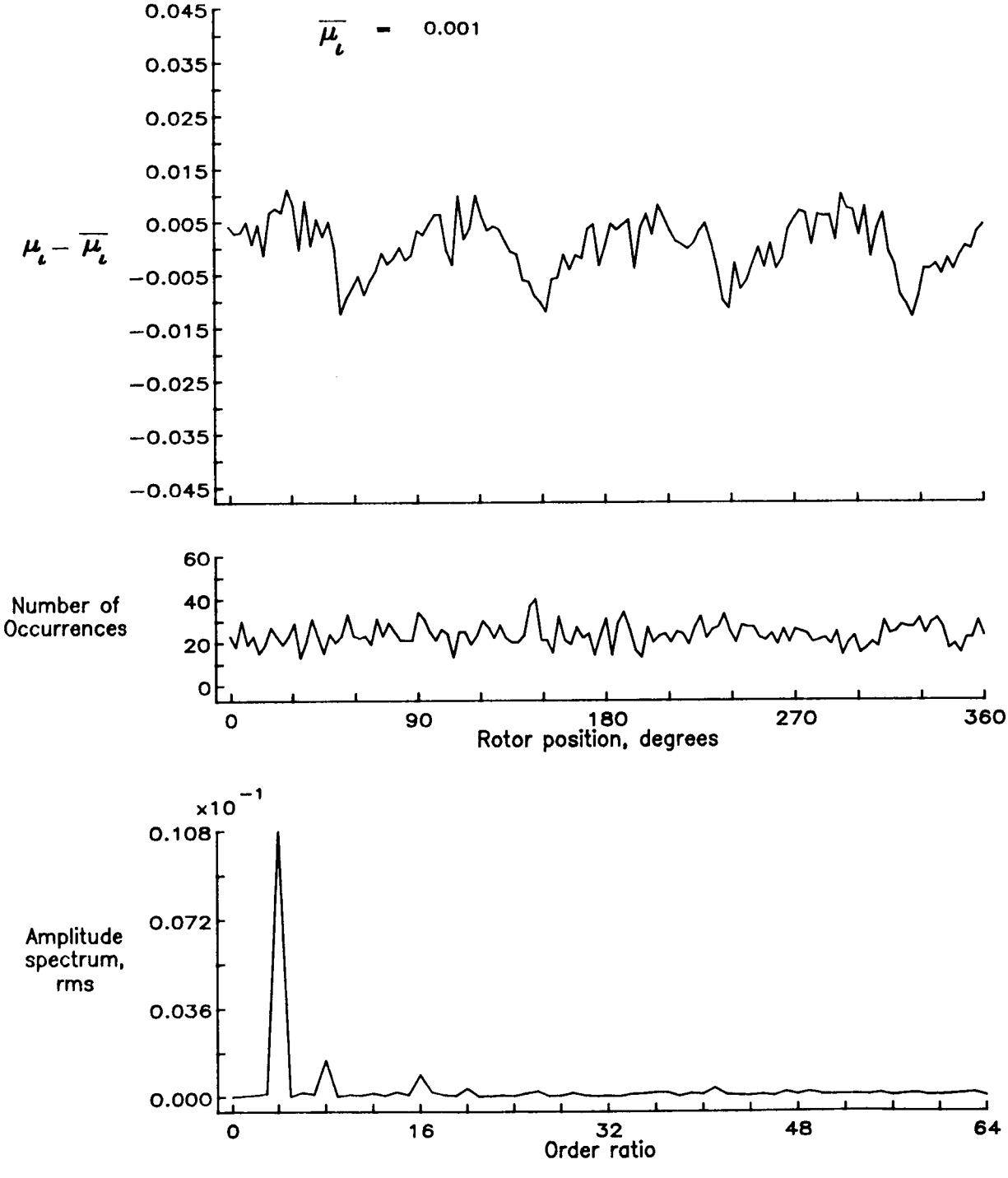


Figure 123.– Induced inflow velocity measured at 240 degrees and r/R of 0.40.

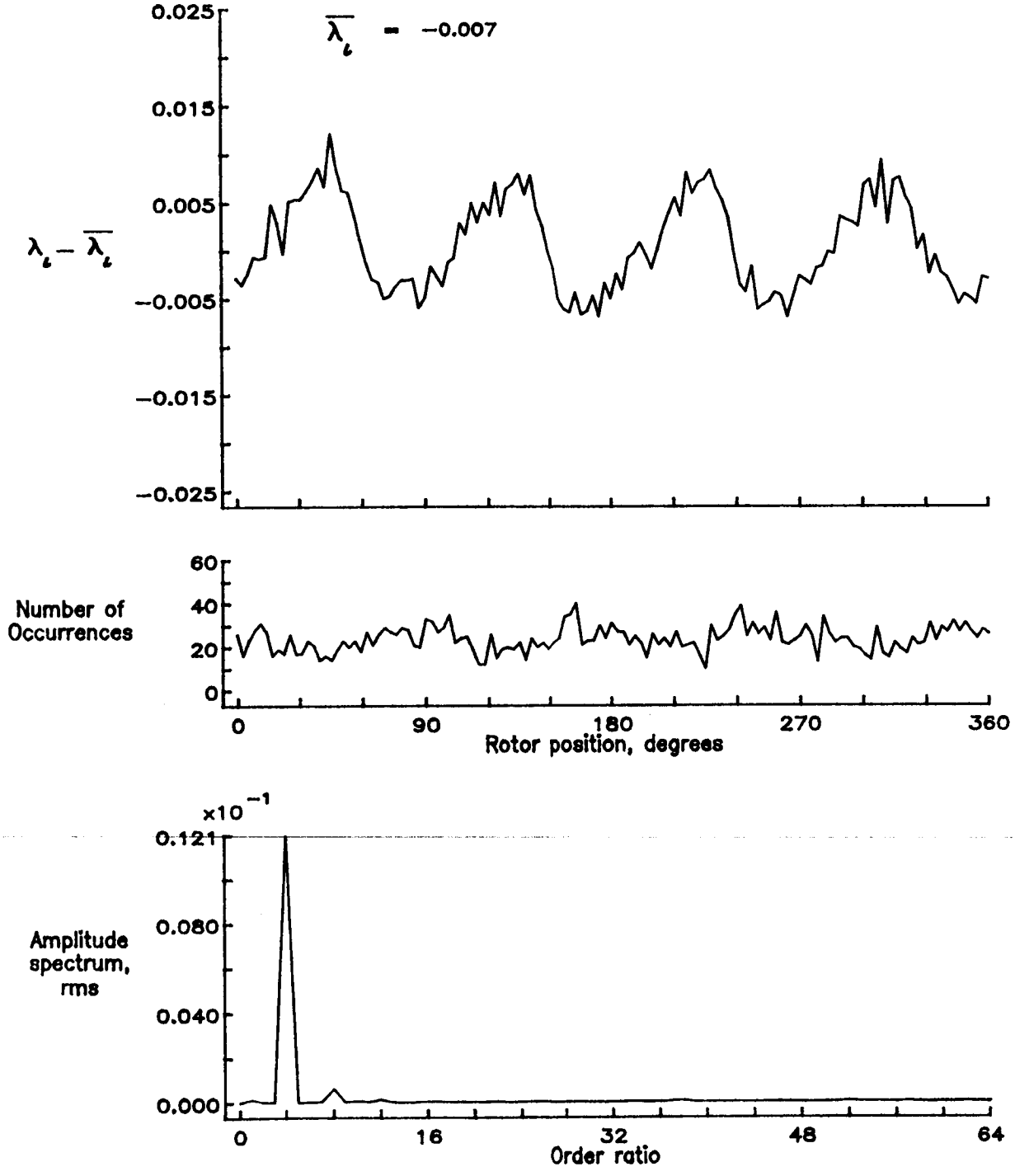


Figure 123.– Concluded.

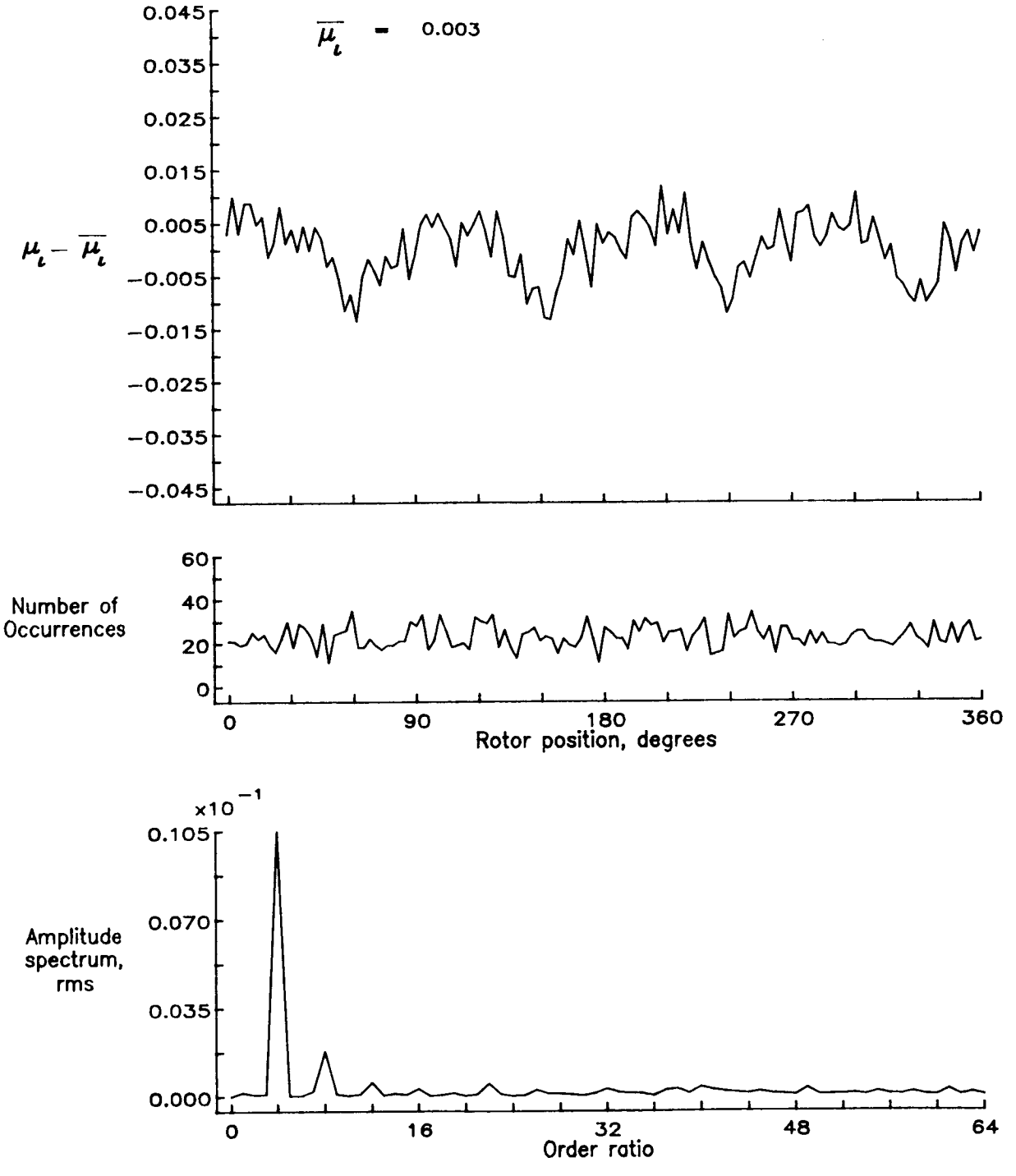


Figure 124.– Induced inflow velocity measured at 240 degrees and r/R of 0.50.

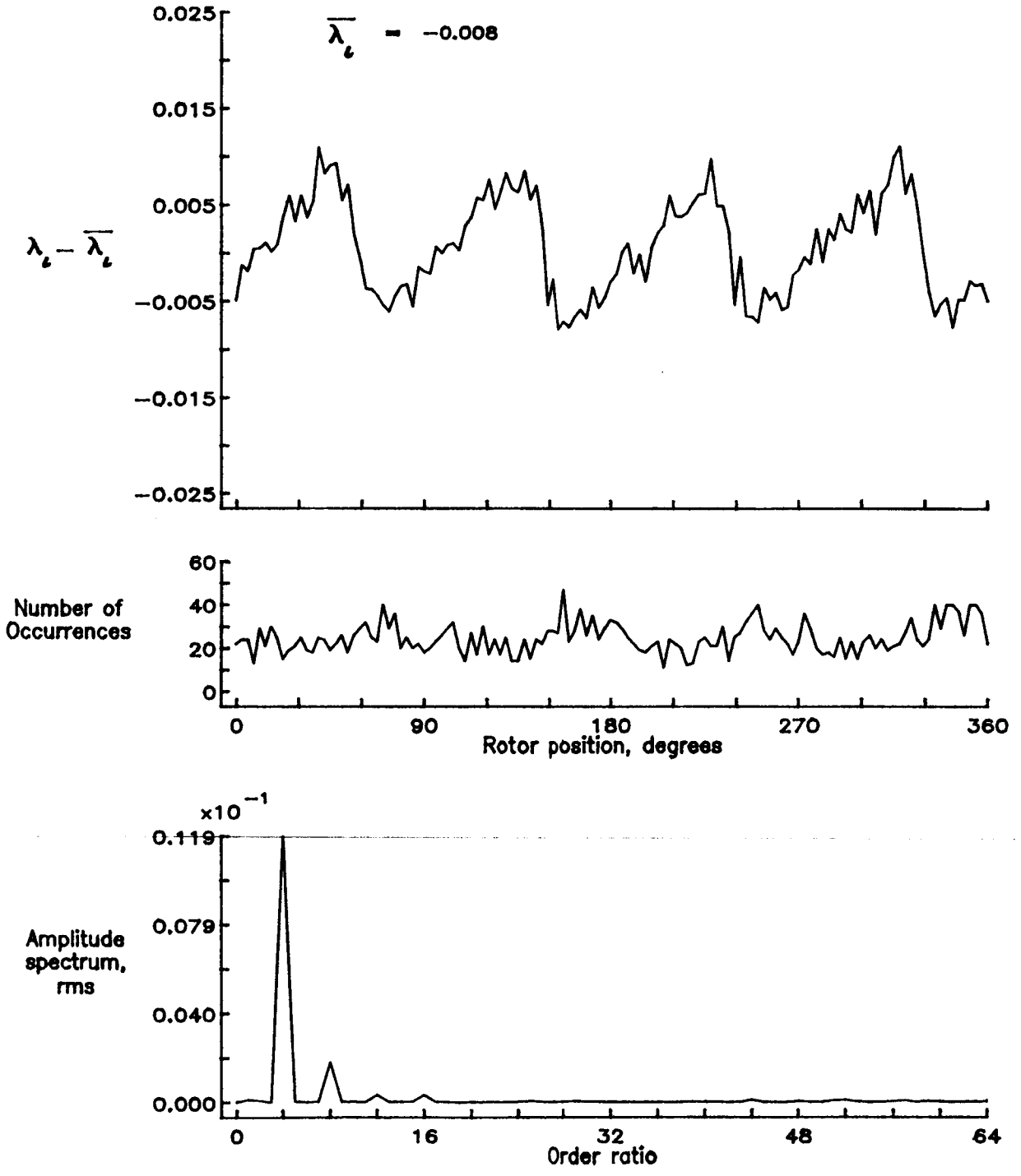


Figure 124.– Concluded.

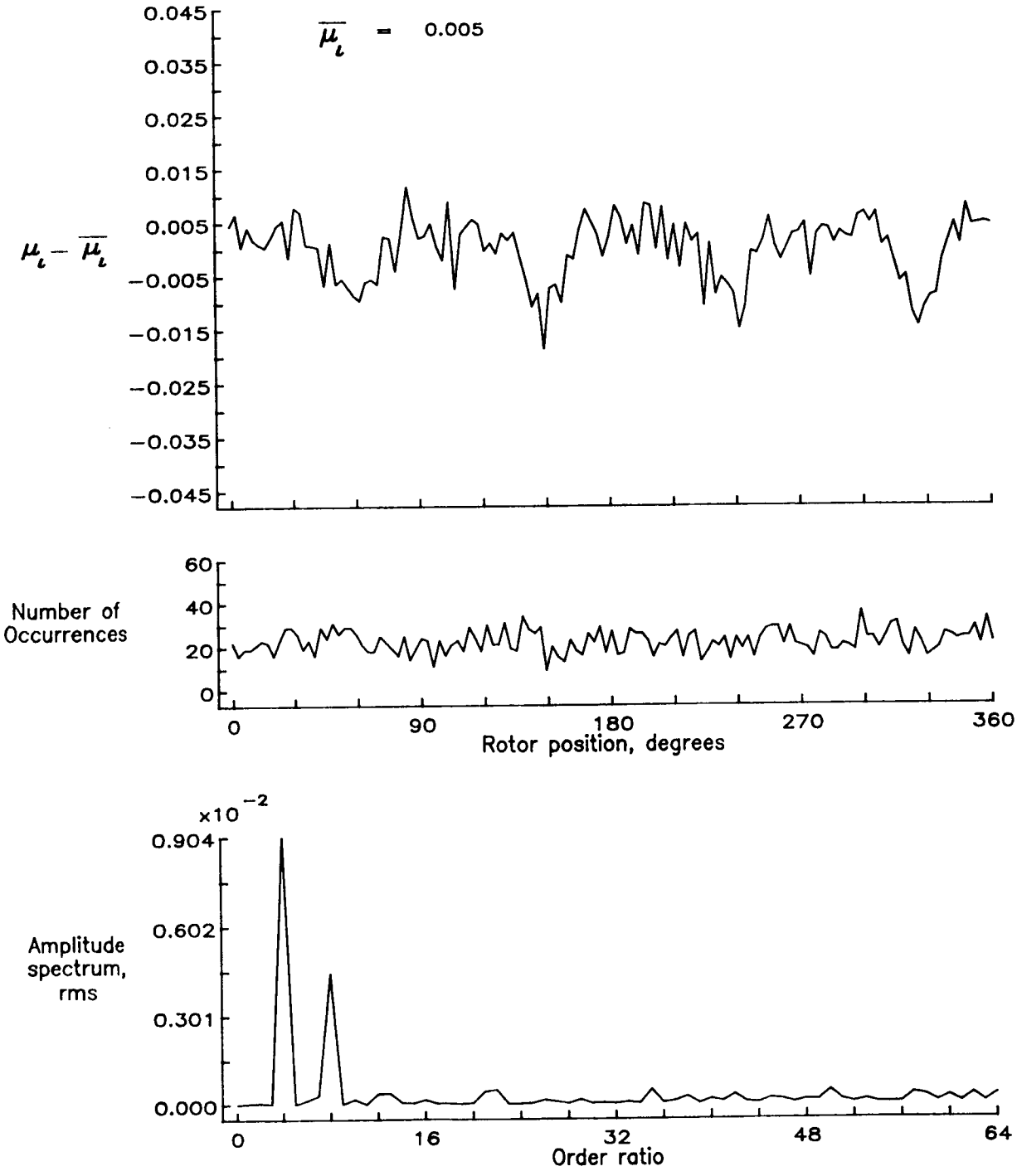


Figure 125.– Induced inflow velocity measured at 240 degrees and r/R of 0.60.

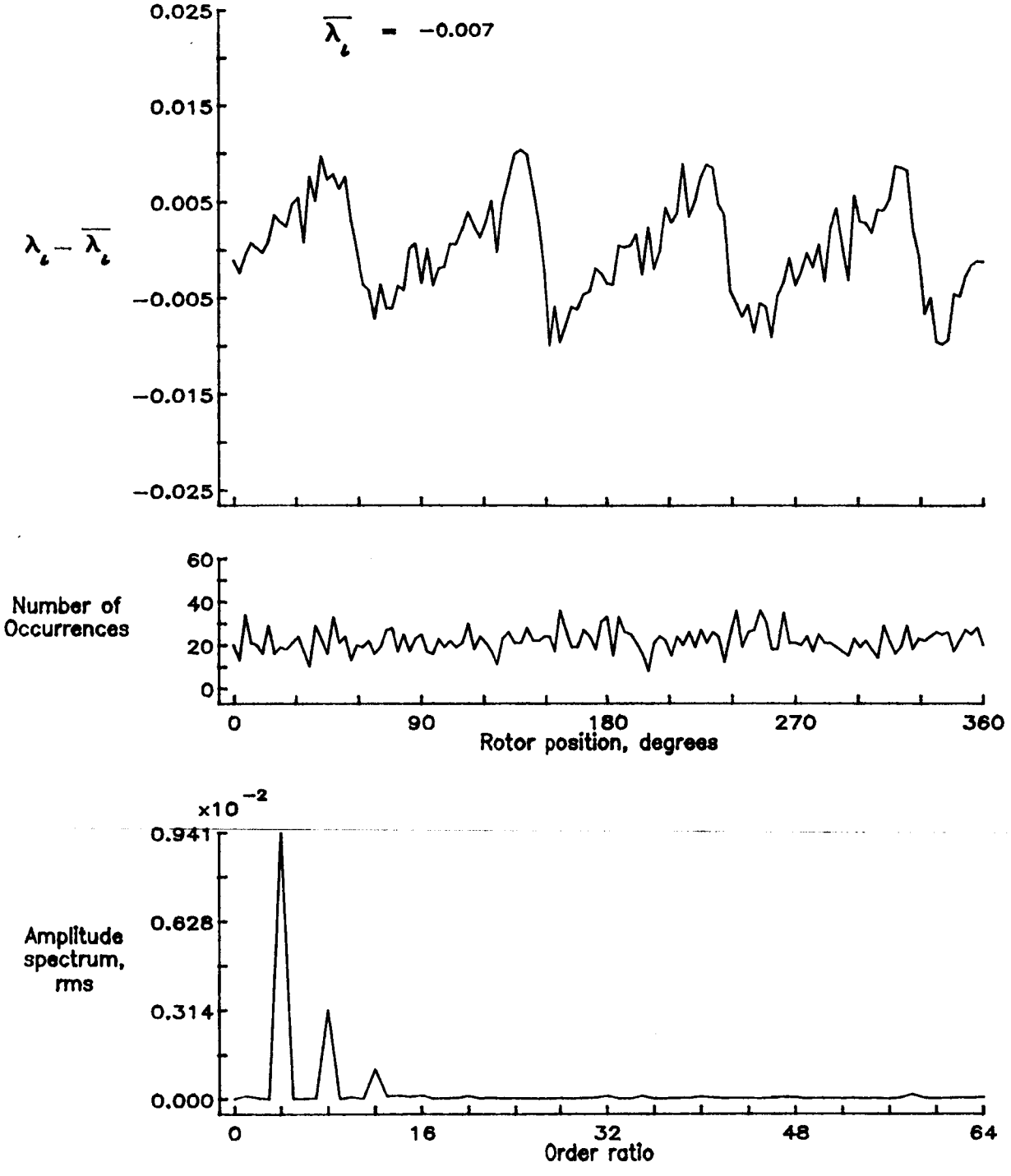


Figure 125.– Concluded.

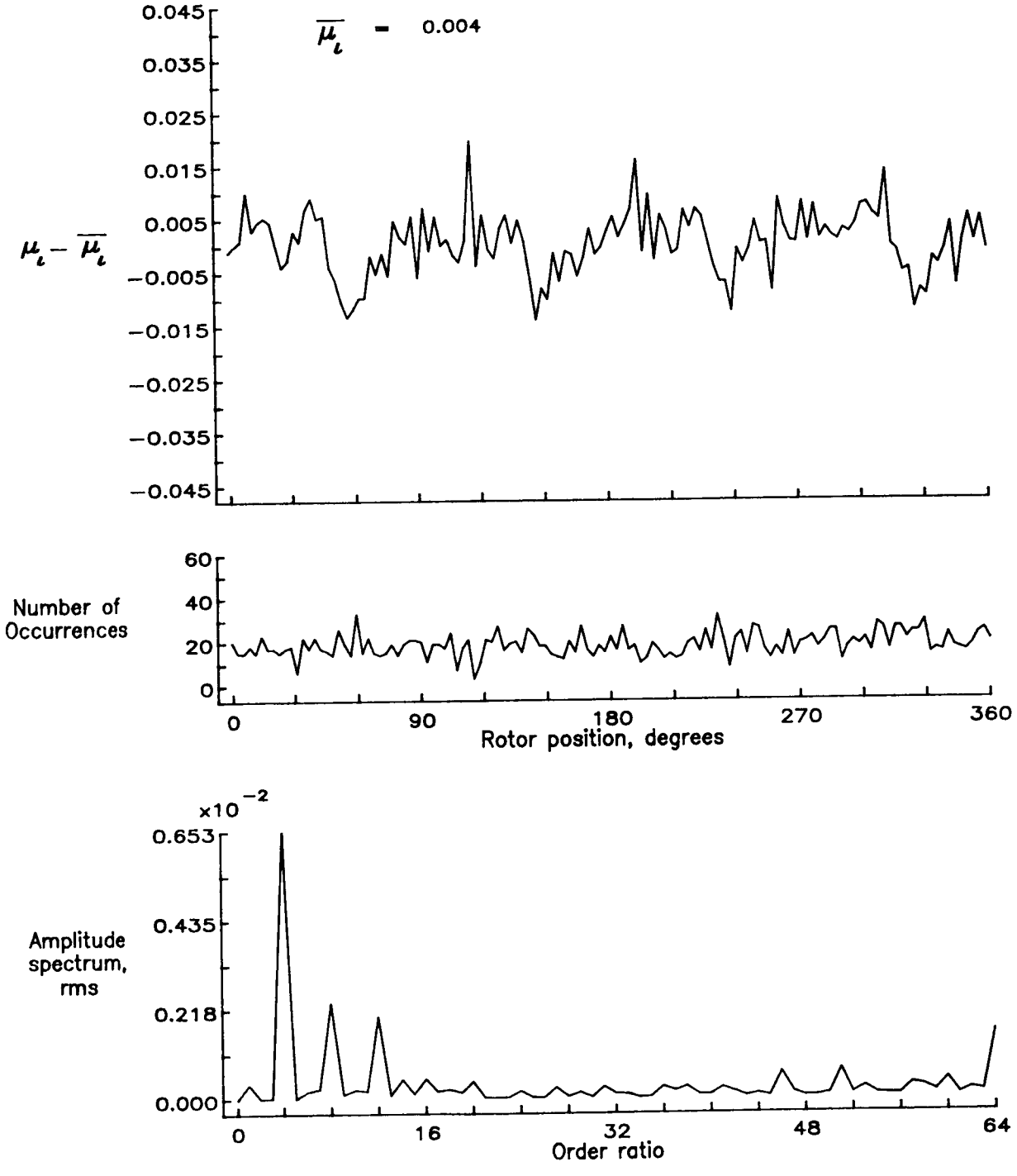


Figure 126.– Induced inflow velocity measured at 240 degrees and r/R of 0.70.

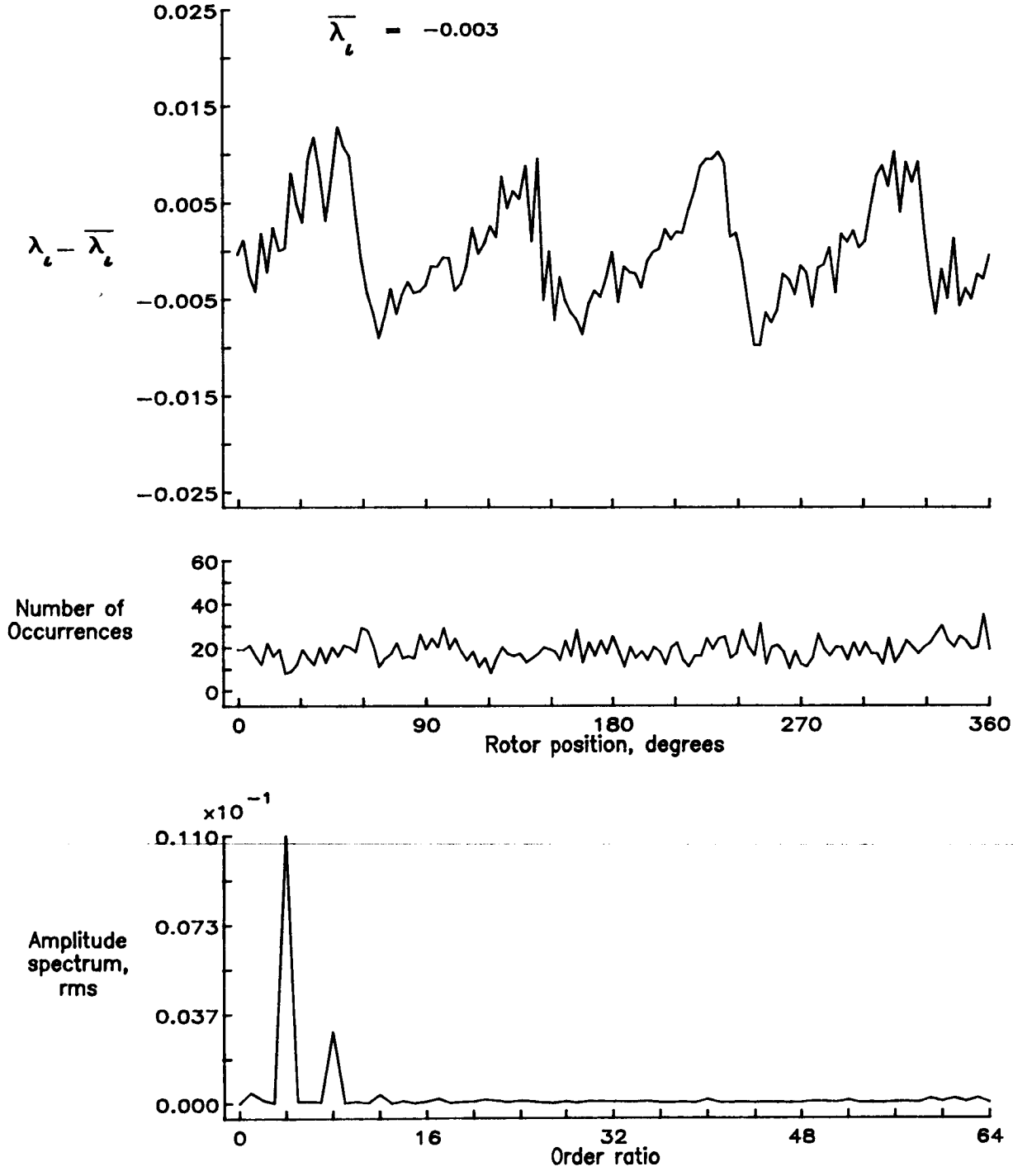


Figure 126.– Concluded.

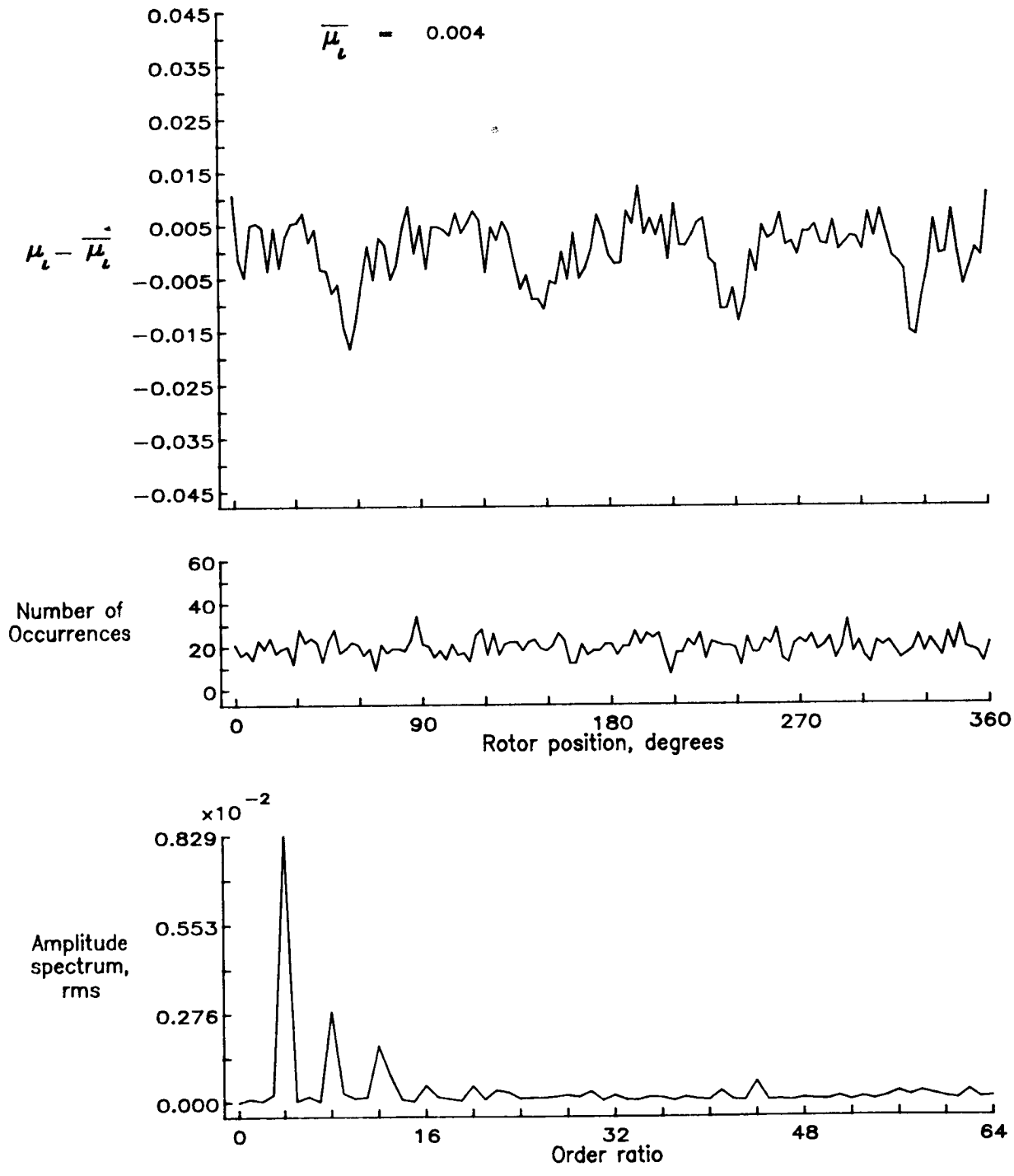


Figure 127.– Induced inflow velocity measured at 240 degrees and r/R of 0.74.

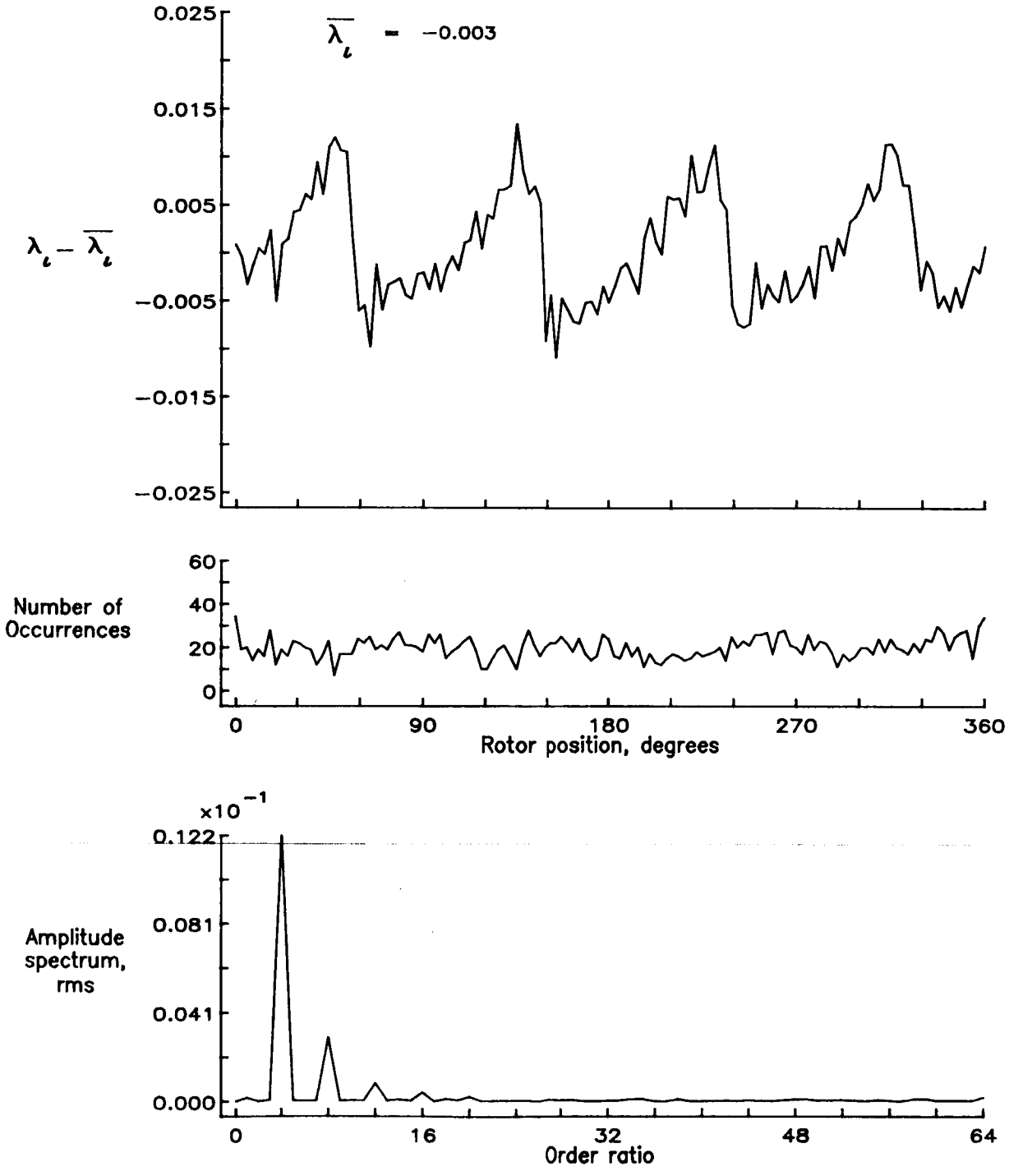


Figure 127.– Concluded.

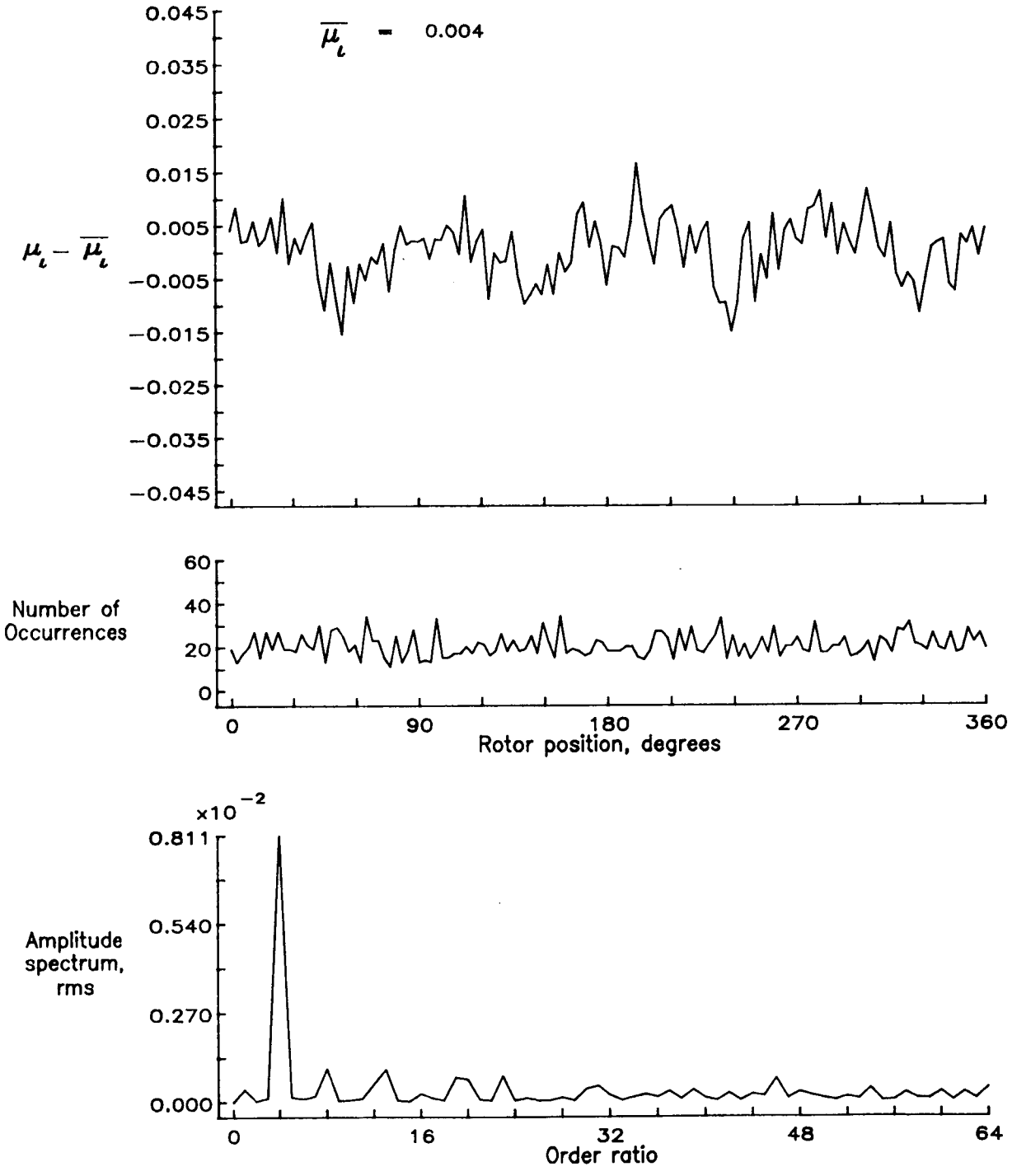


Figure 128.– Induced inflow velocity measured at 240 degrees and r/R of 0.78.

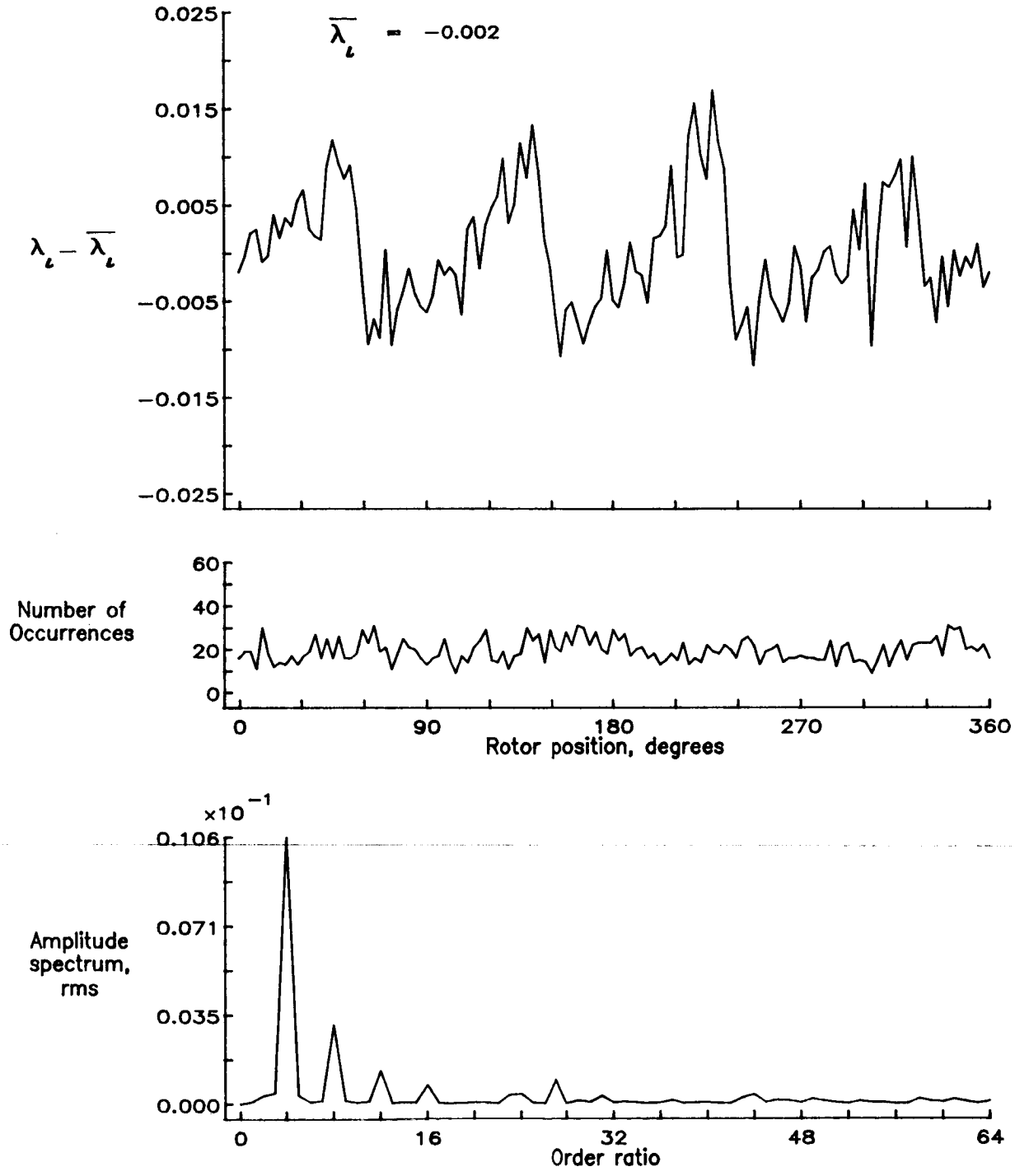


Figure 128.– Concluded.

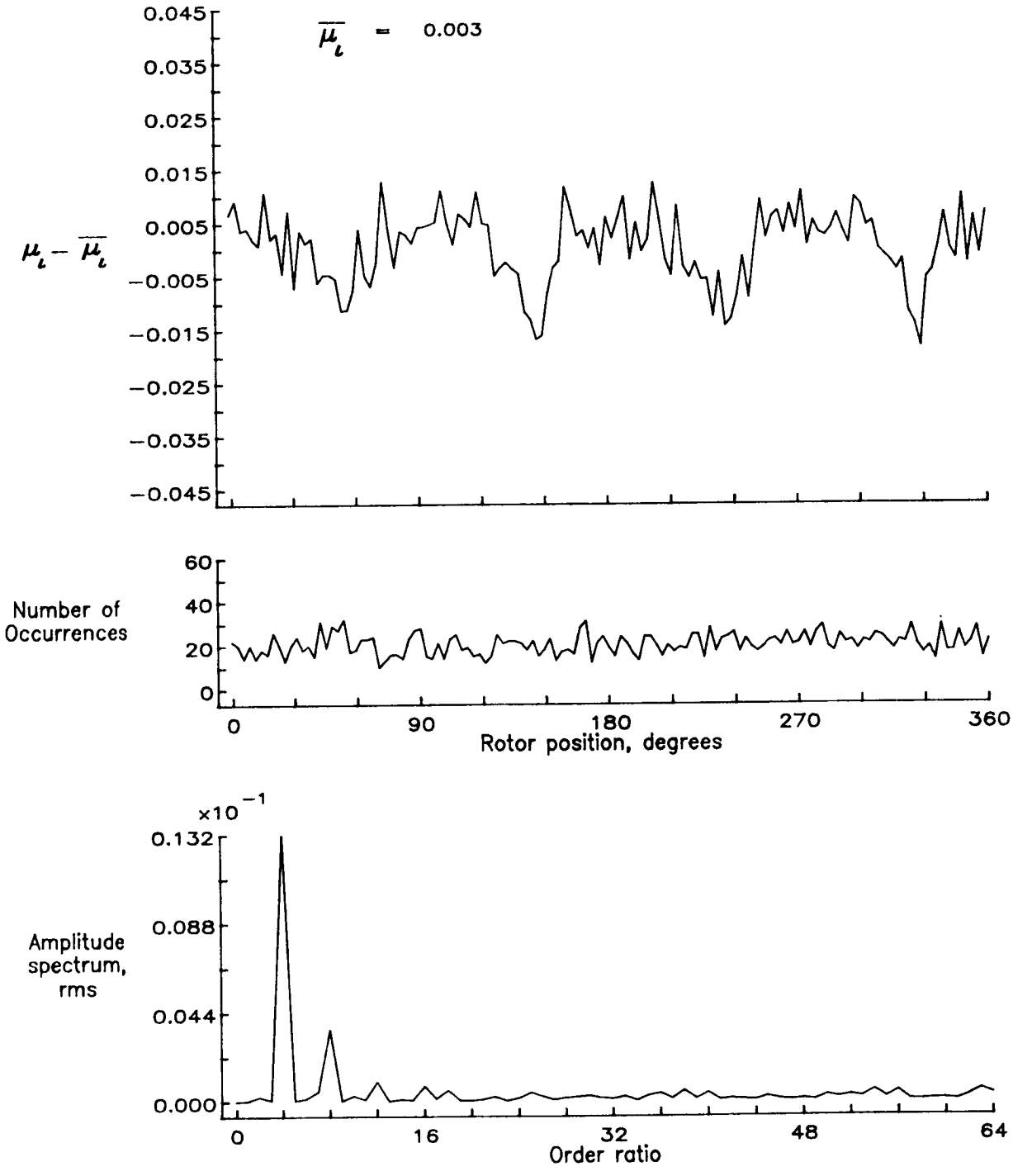


Figure 129.– Induced inflow velocity measured at 240 degrees and r/R of 0.82.

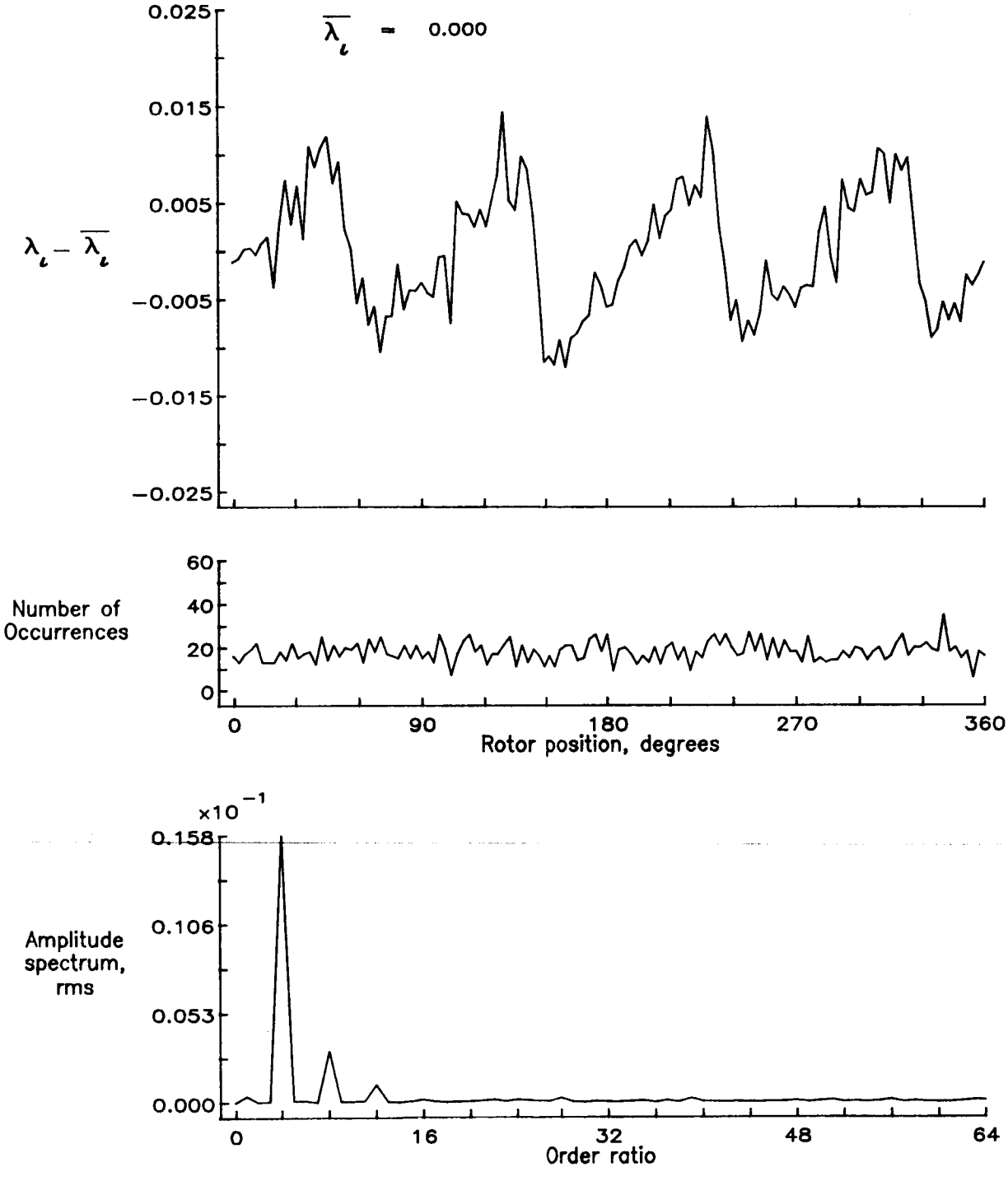


Figure 129.– Concluded.

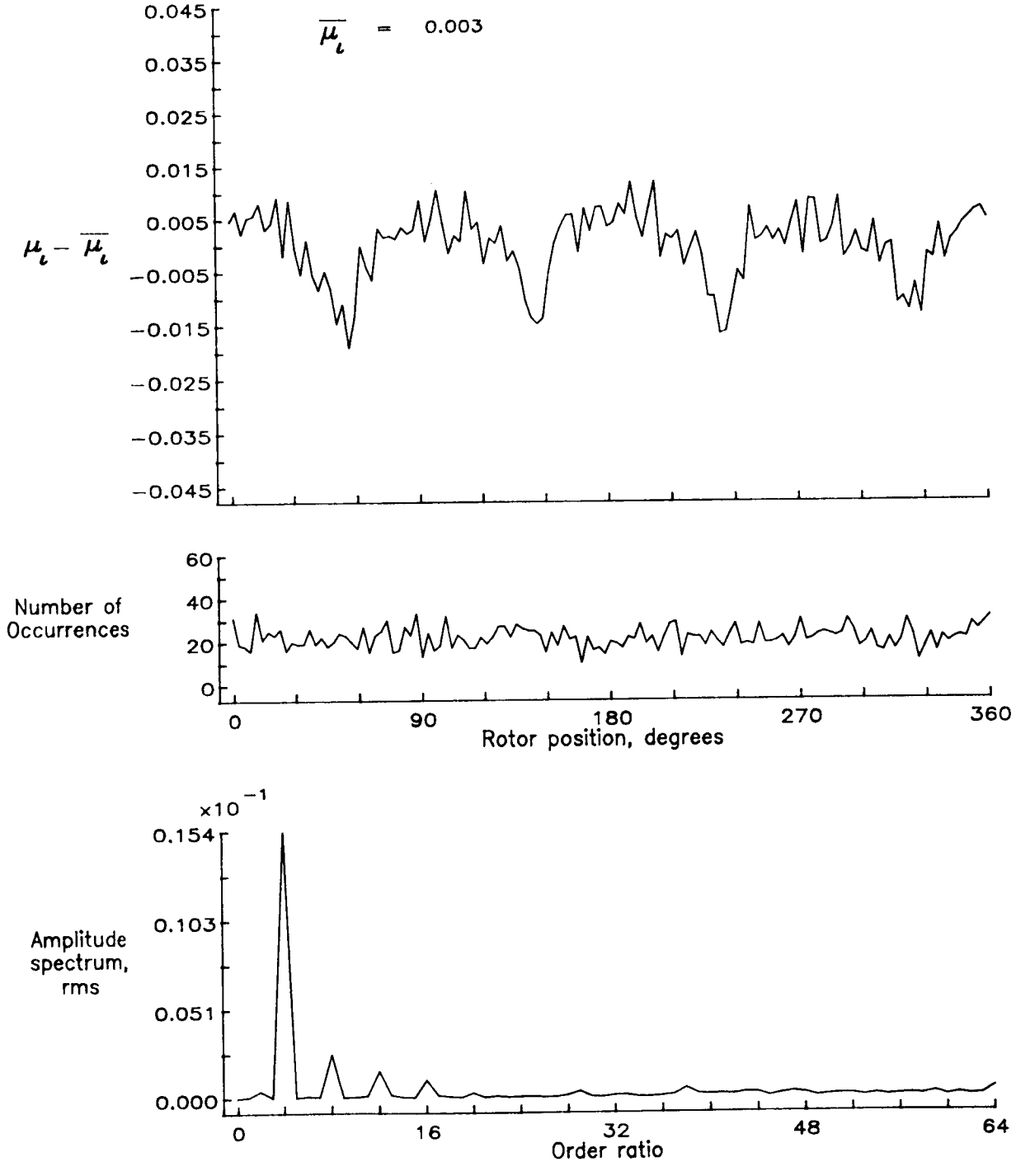


Figure 130.– Induced inflow velocity measured at 240 degrees and r/R of 0.86.

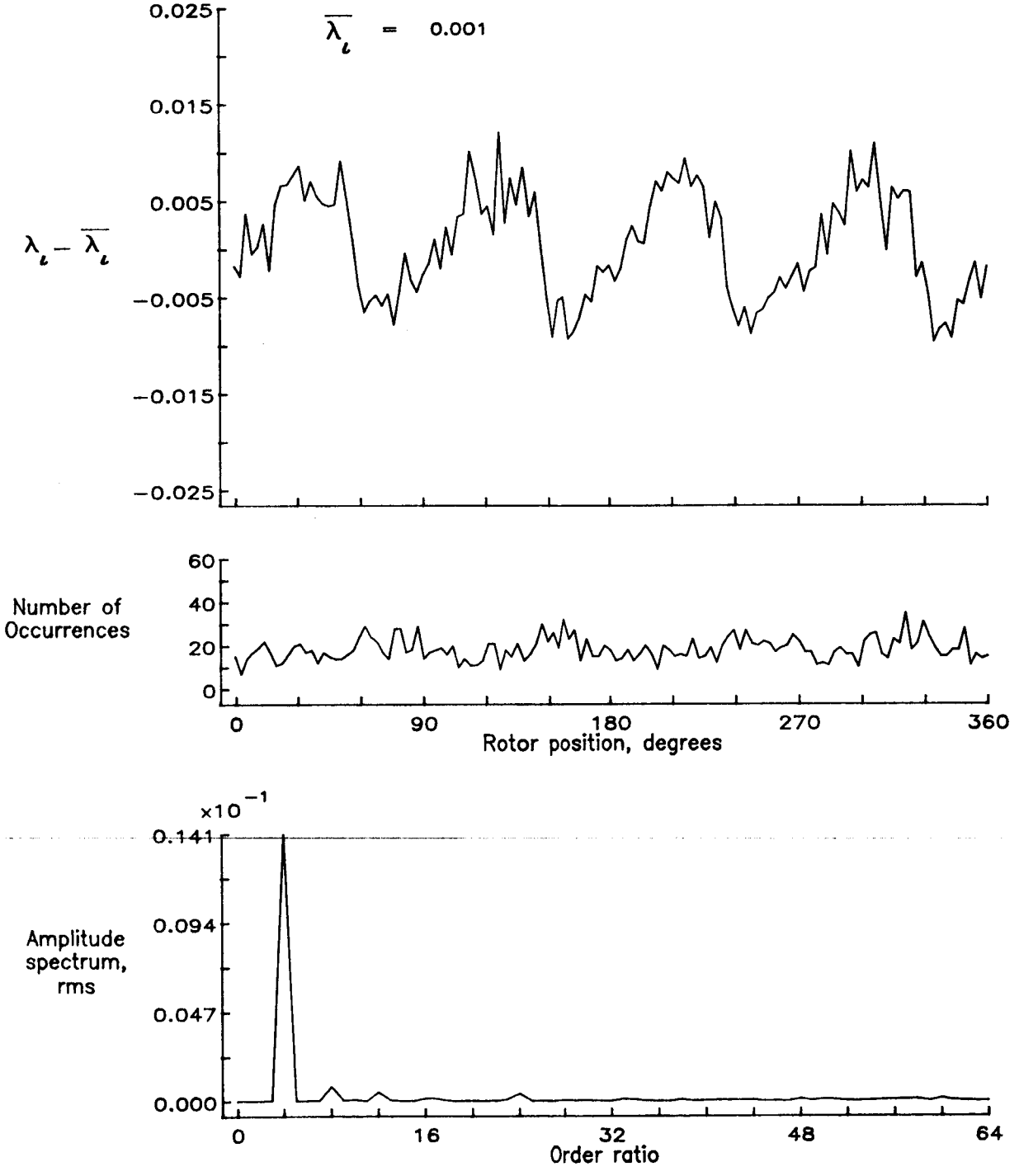


Figure 130.– Concluded.

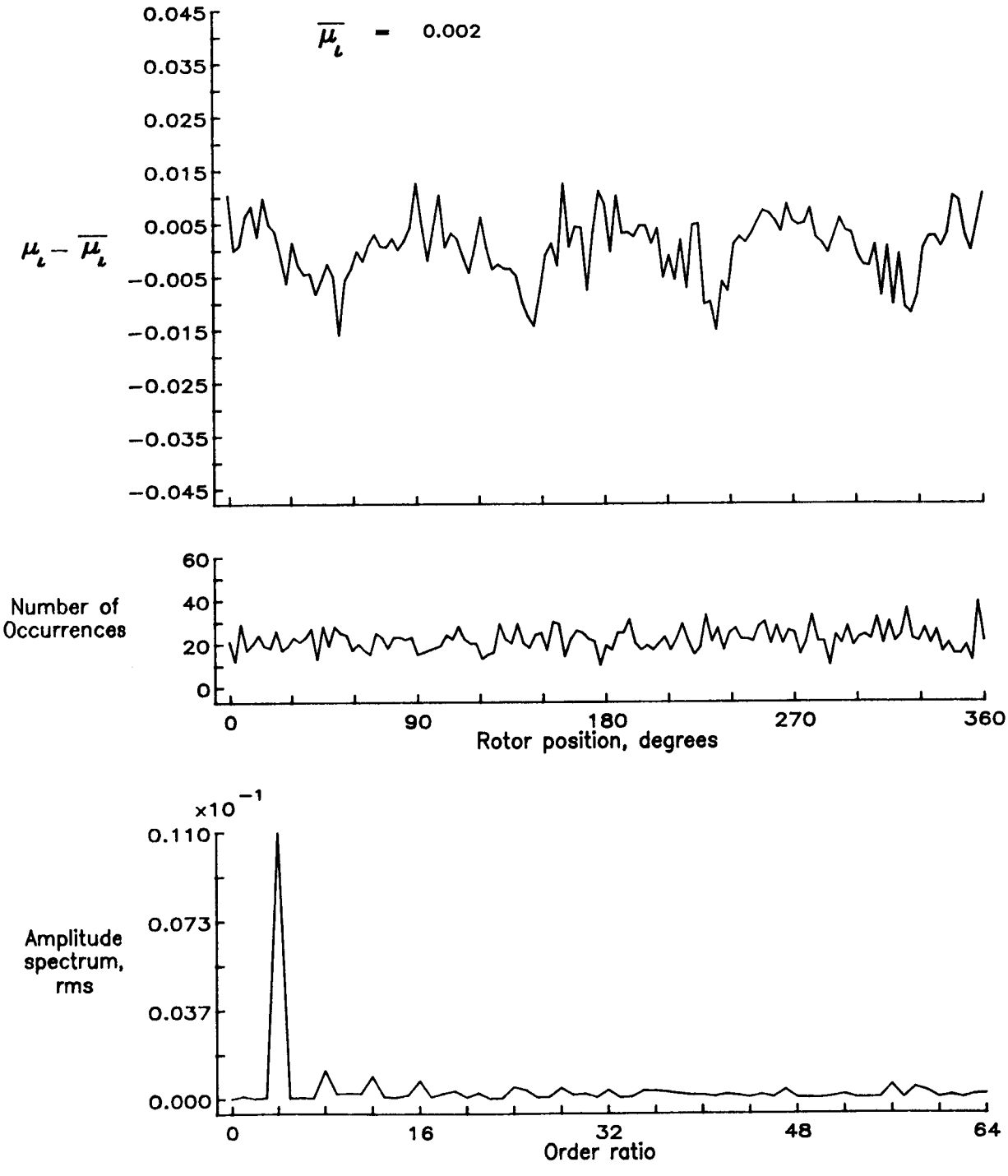


Figure 131.– Induced inflow velocity measured at 240 degrees and r/R of 0.90.

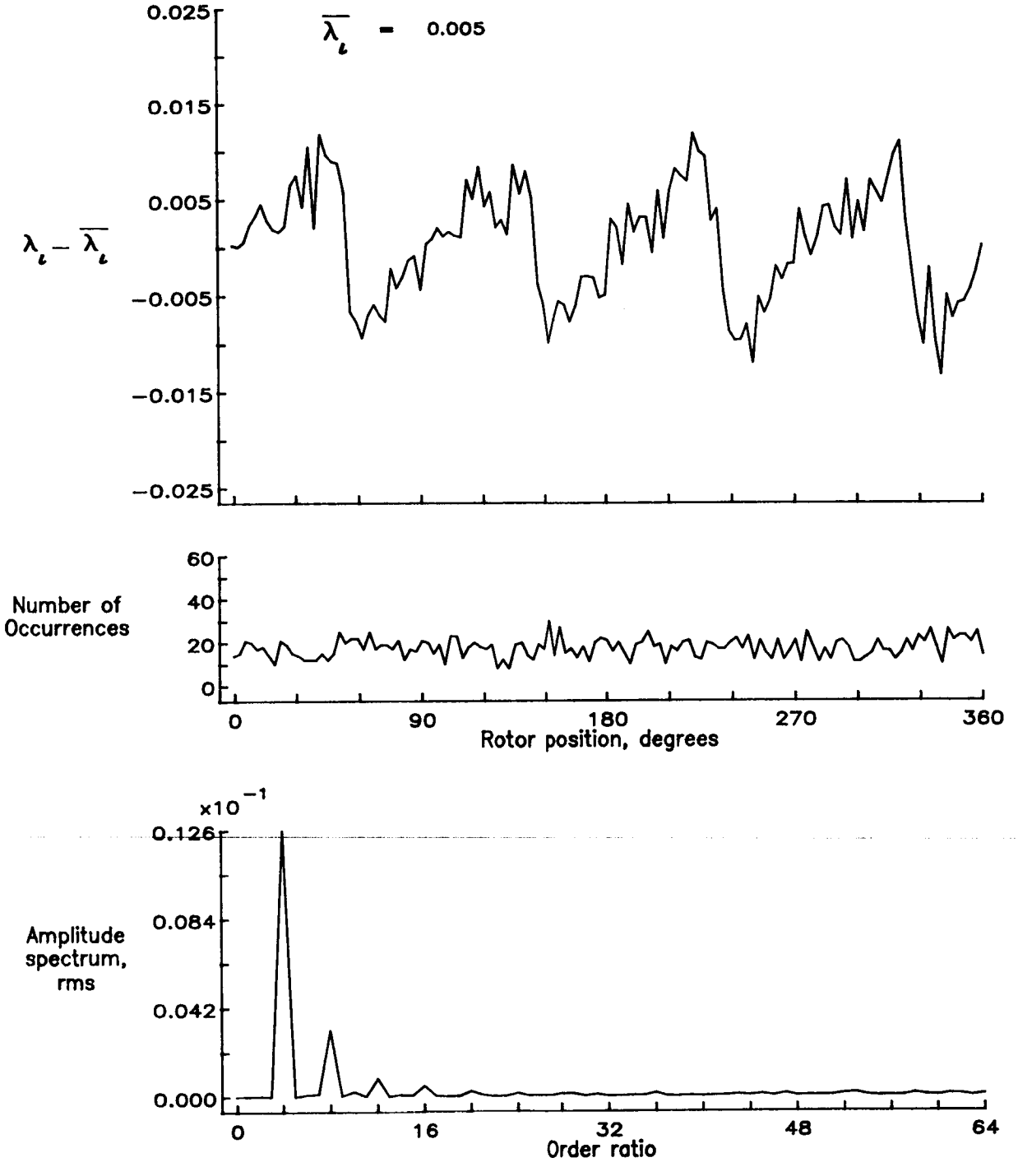


Figure 131.– Concluded.

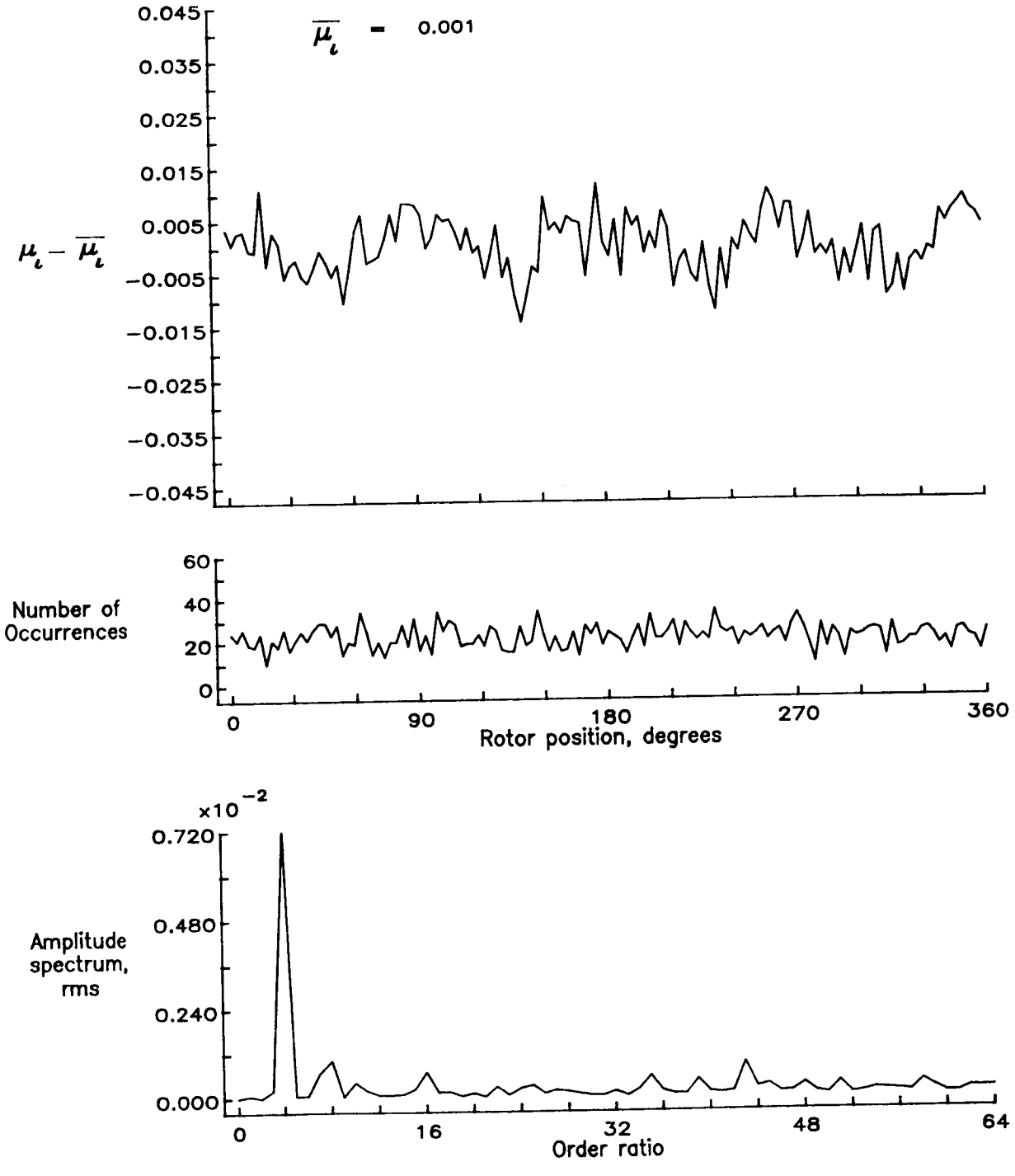


Figure 132.– Induced inflow velocity measured at 240 degrees and r/R of 0.94.

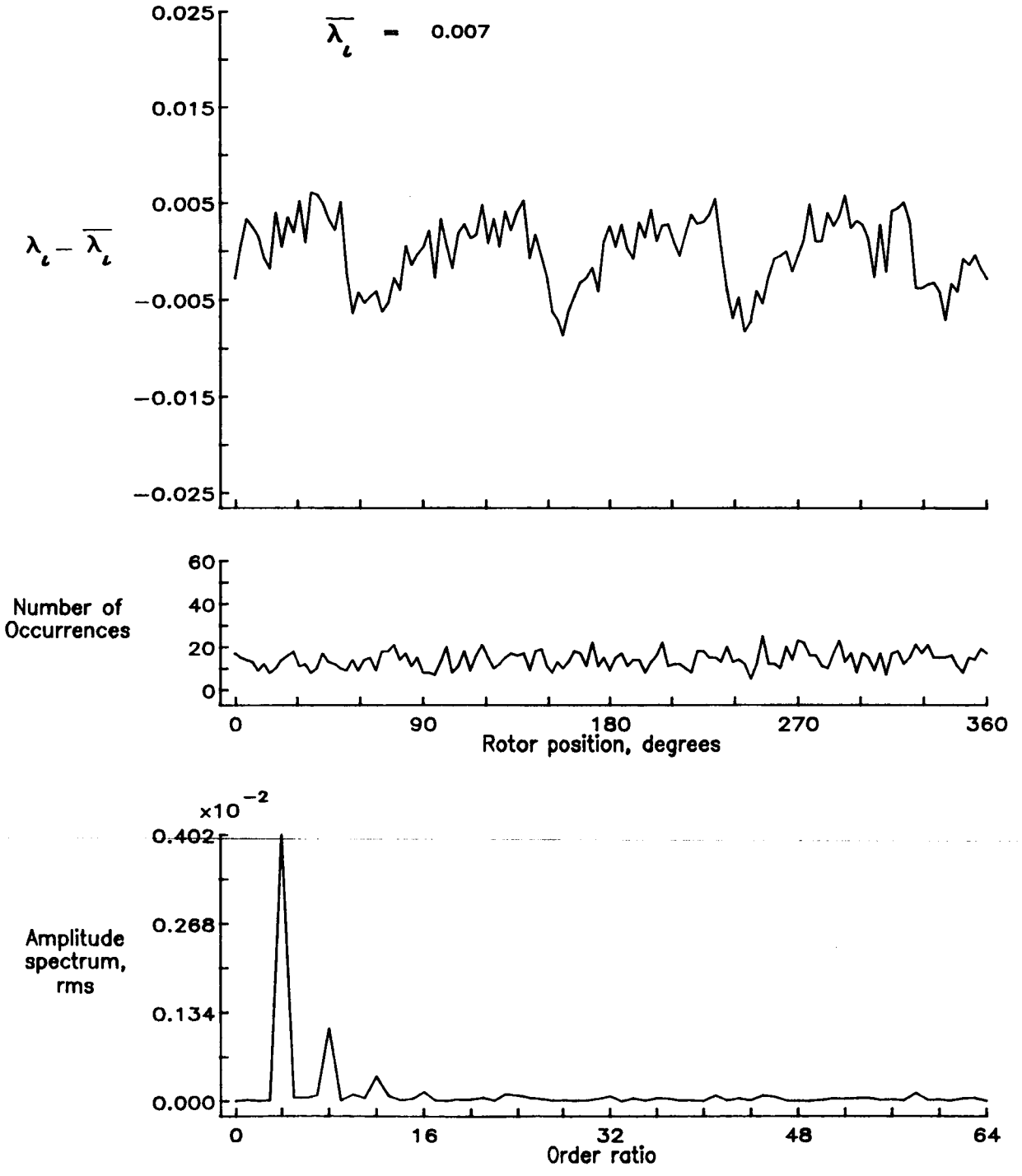


Figure 132.– Concluded.

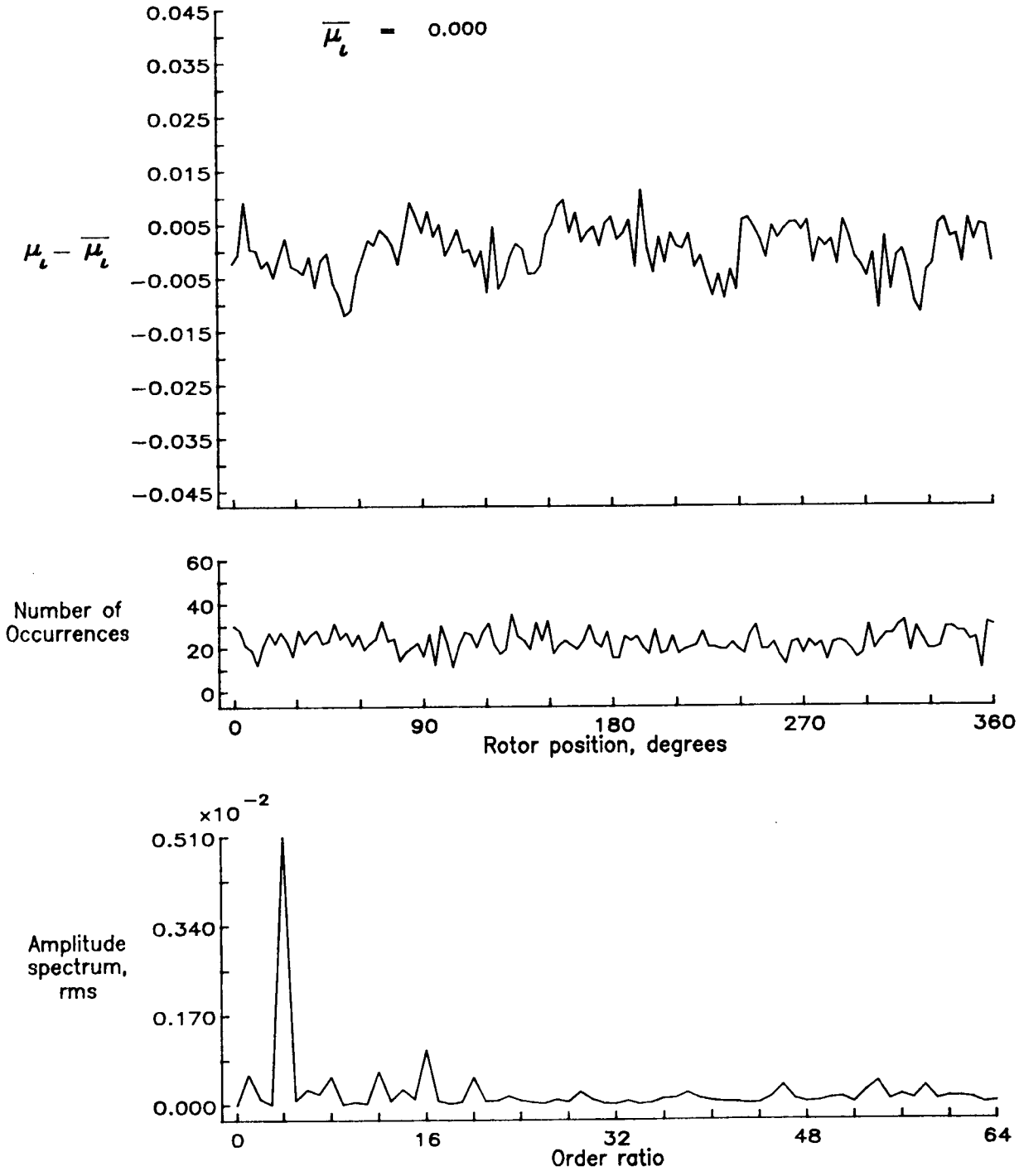


Figure 133.– Induced inflow velocity measured at 240 degrees and r/R of 0.98.

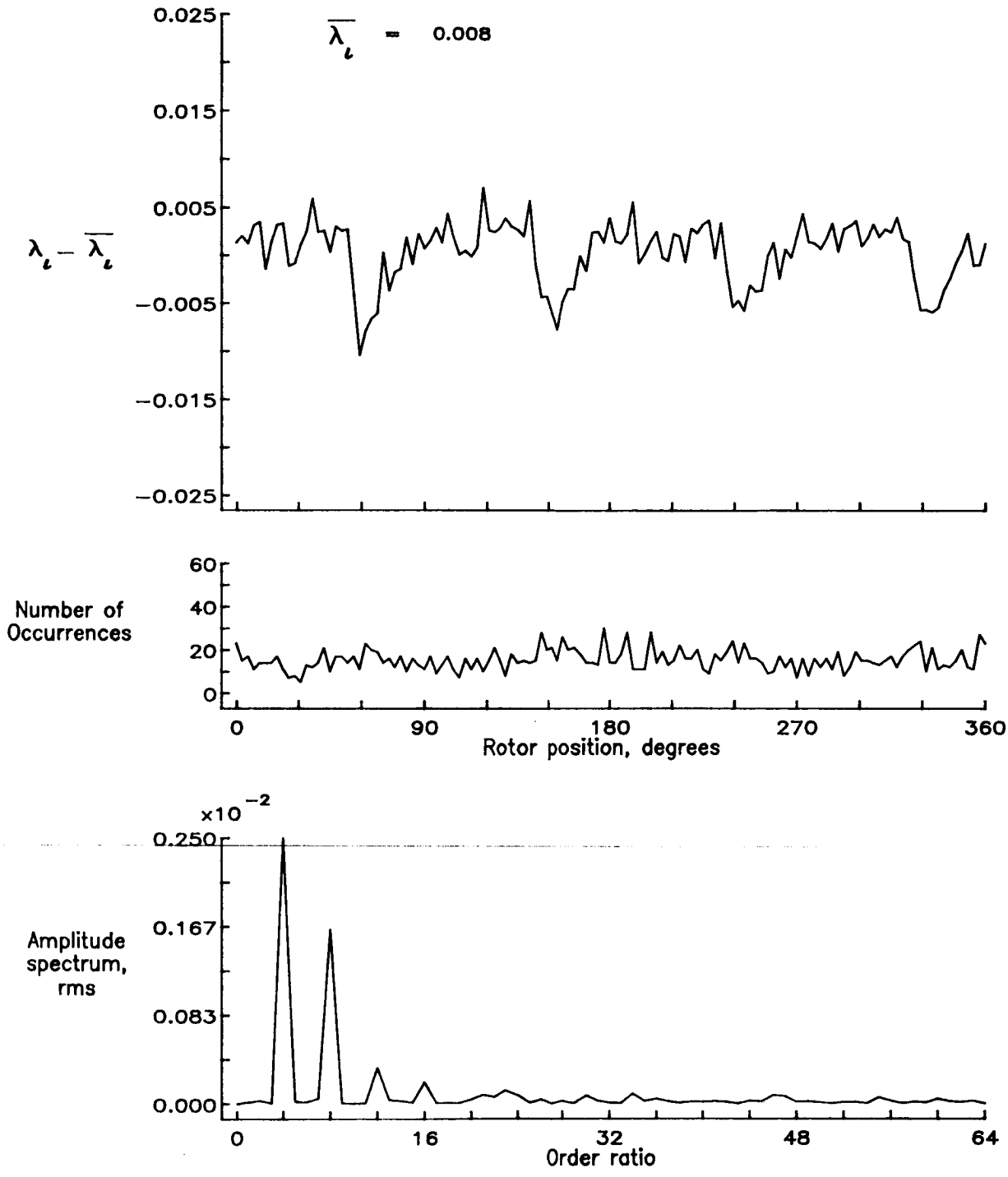


Figure 133.– Concluded.

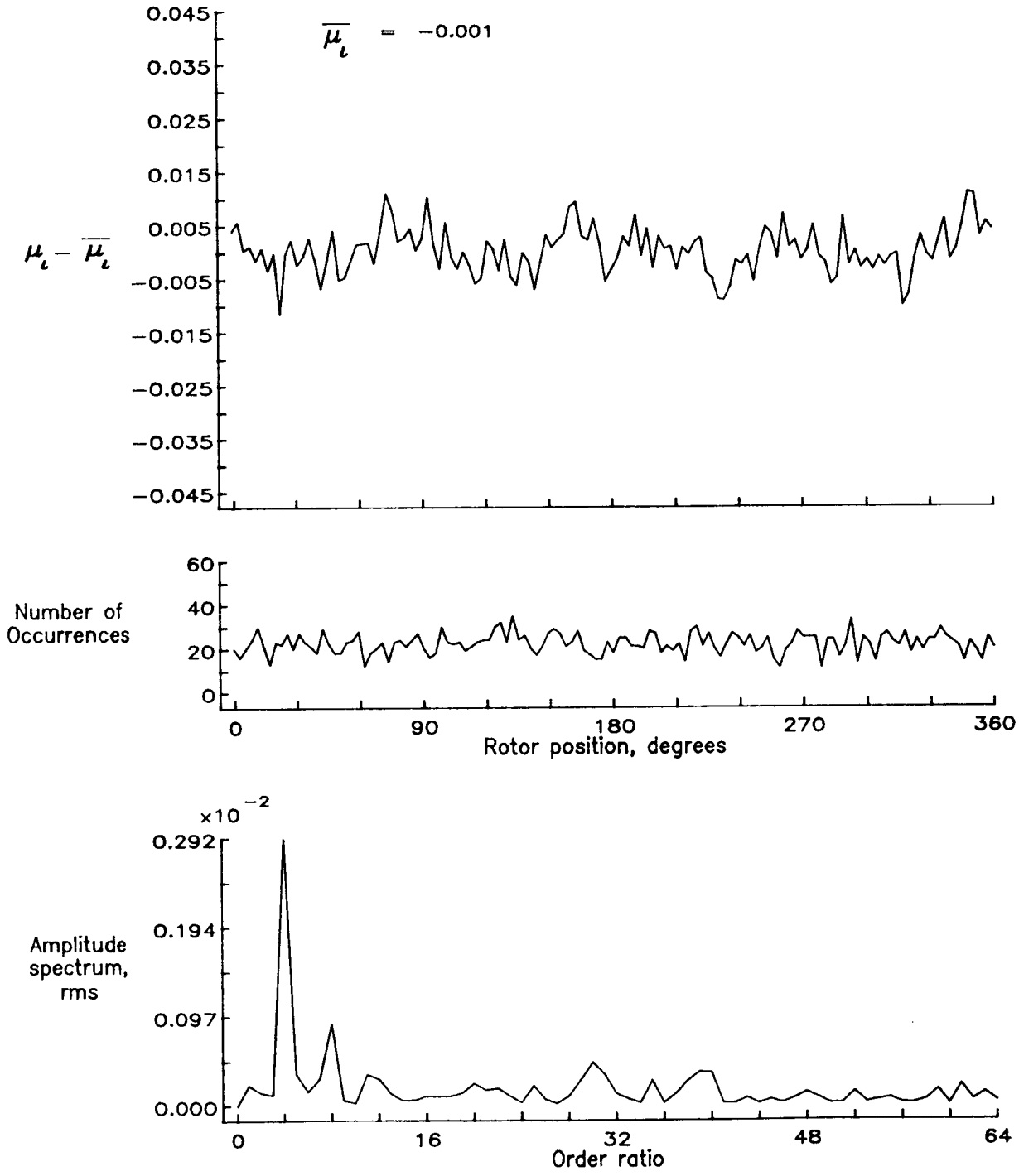


Figure 134.– Induced inflow velocity measured at 240 degrees and r/R of 1.02.

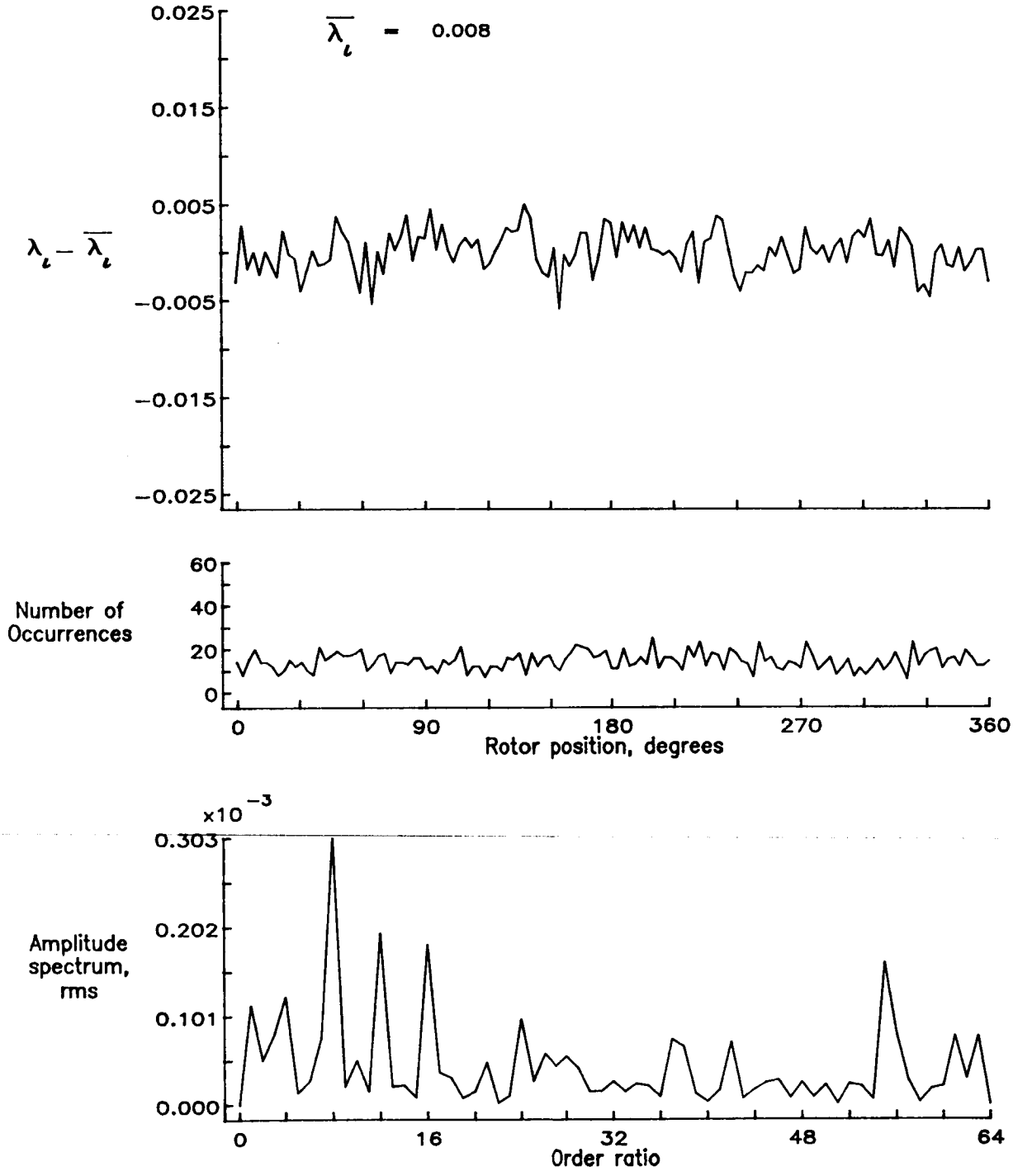


Figure 134.– Concluded.

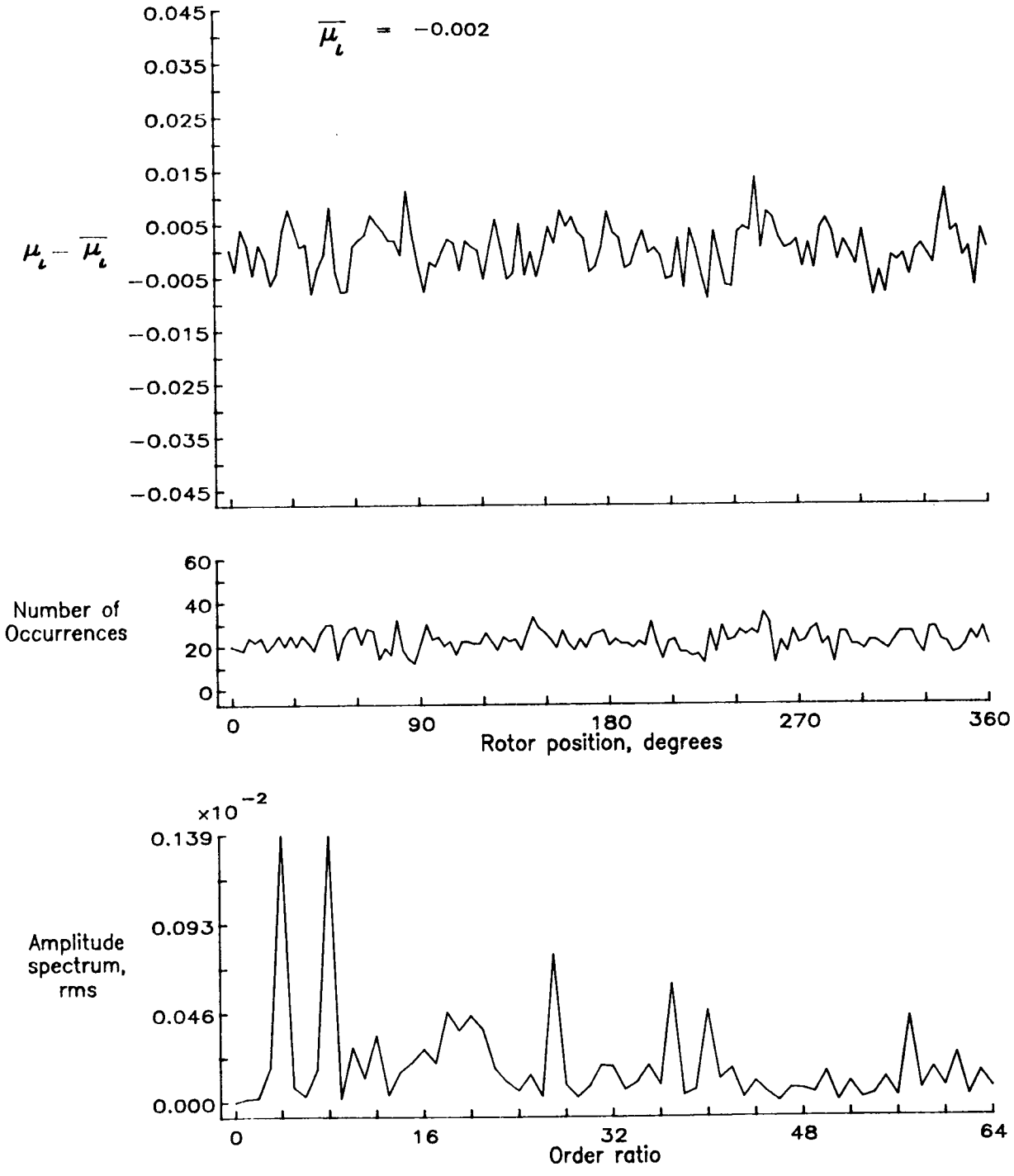


Figure 135.– Induced inflow velocity measured at 240 degrees and r/R of 1.04.

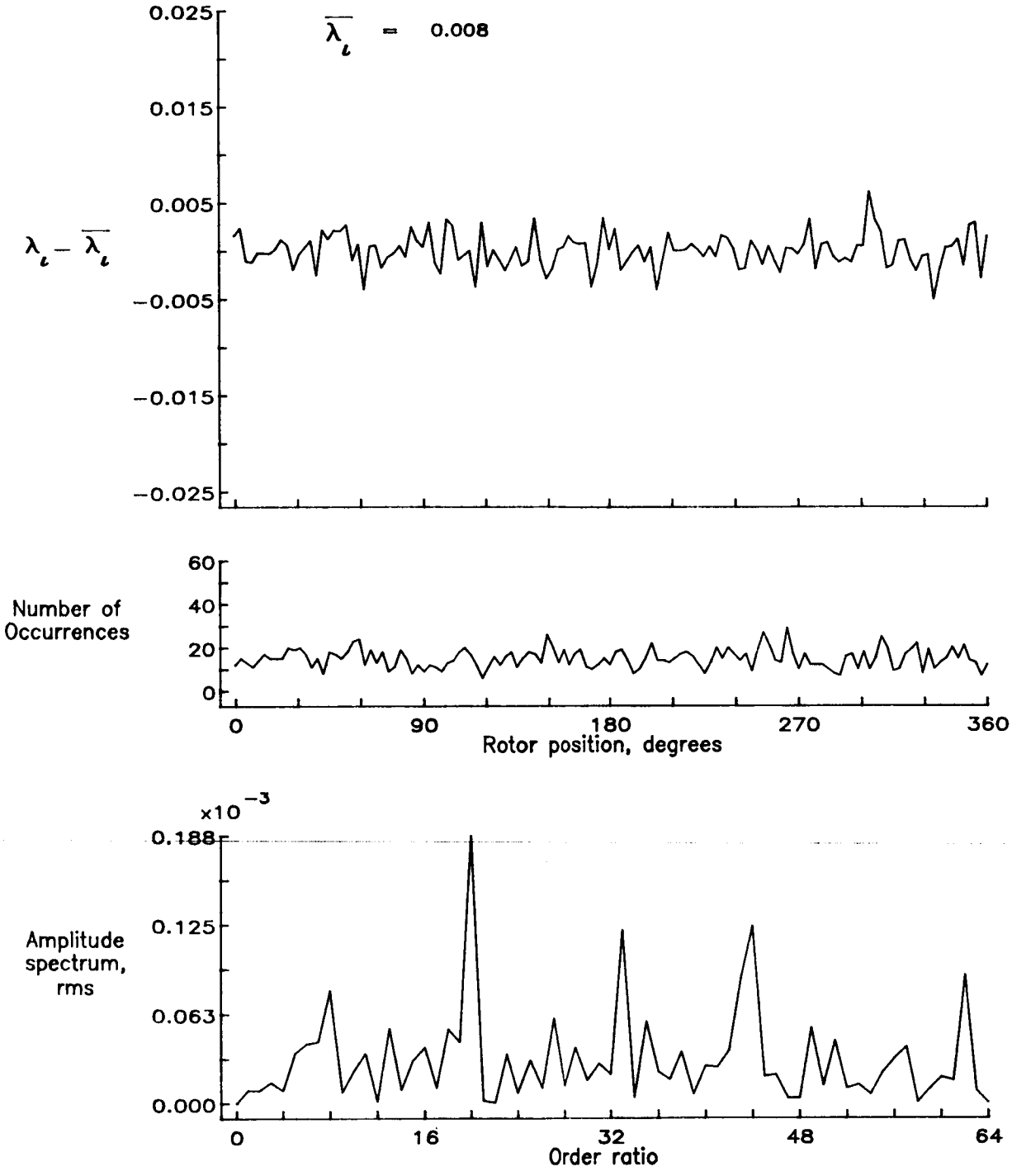


Figure 135.– Concluded.

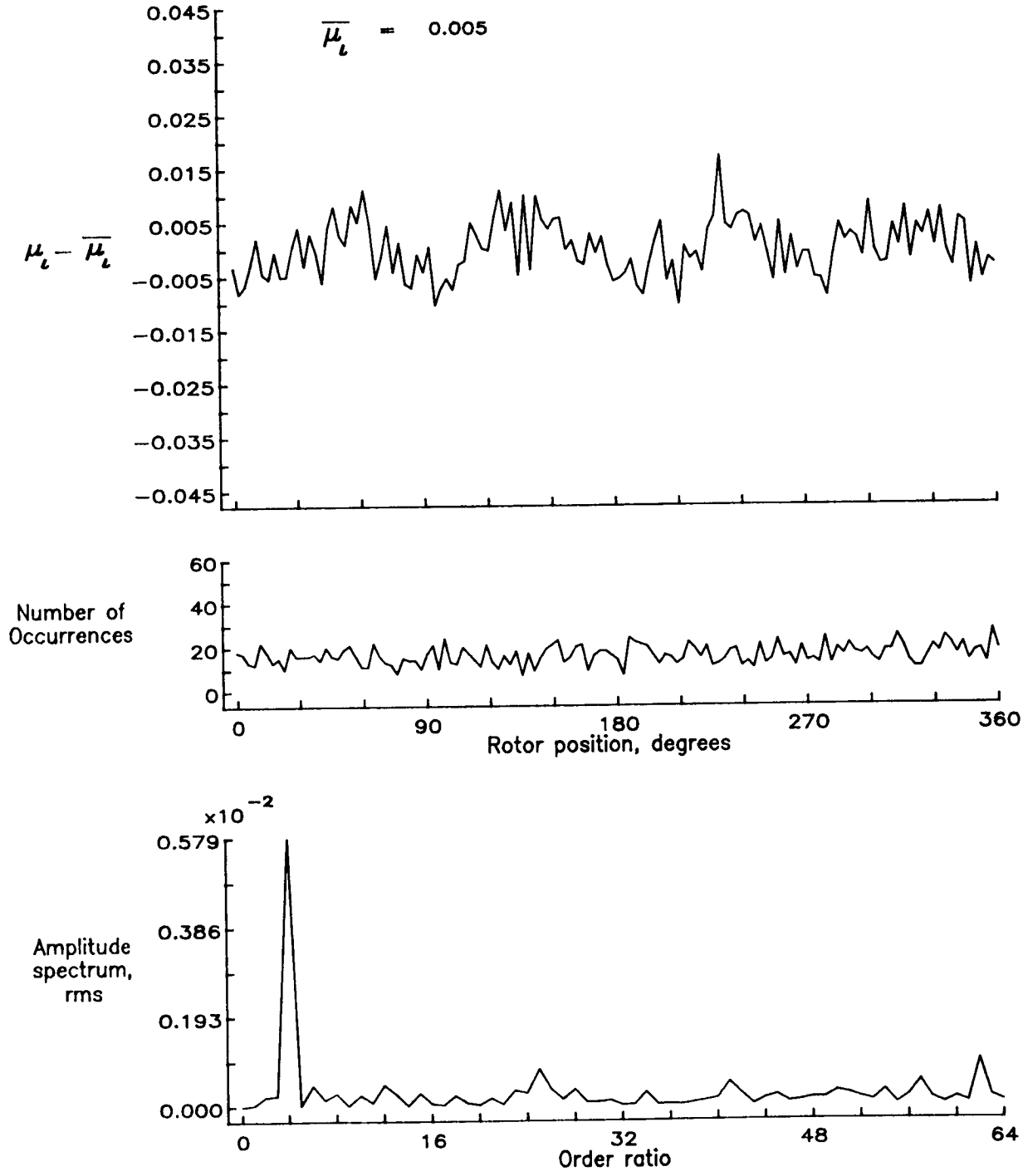


Figure 136.– Induced inflow velocity measured at 270 degrees and r/R of 0.20.

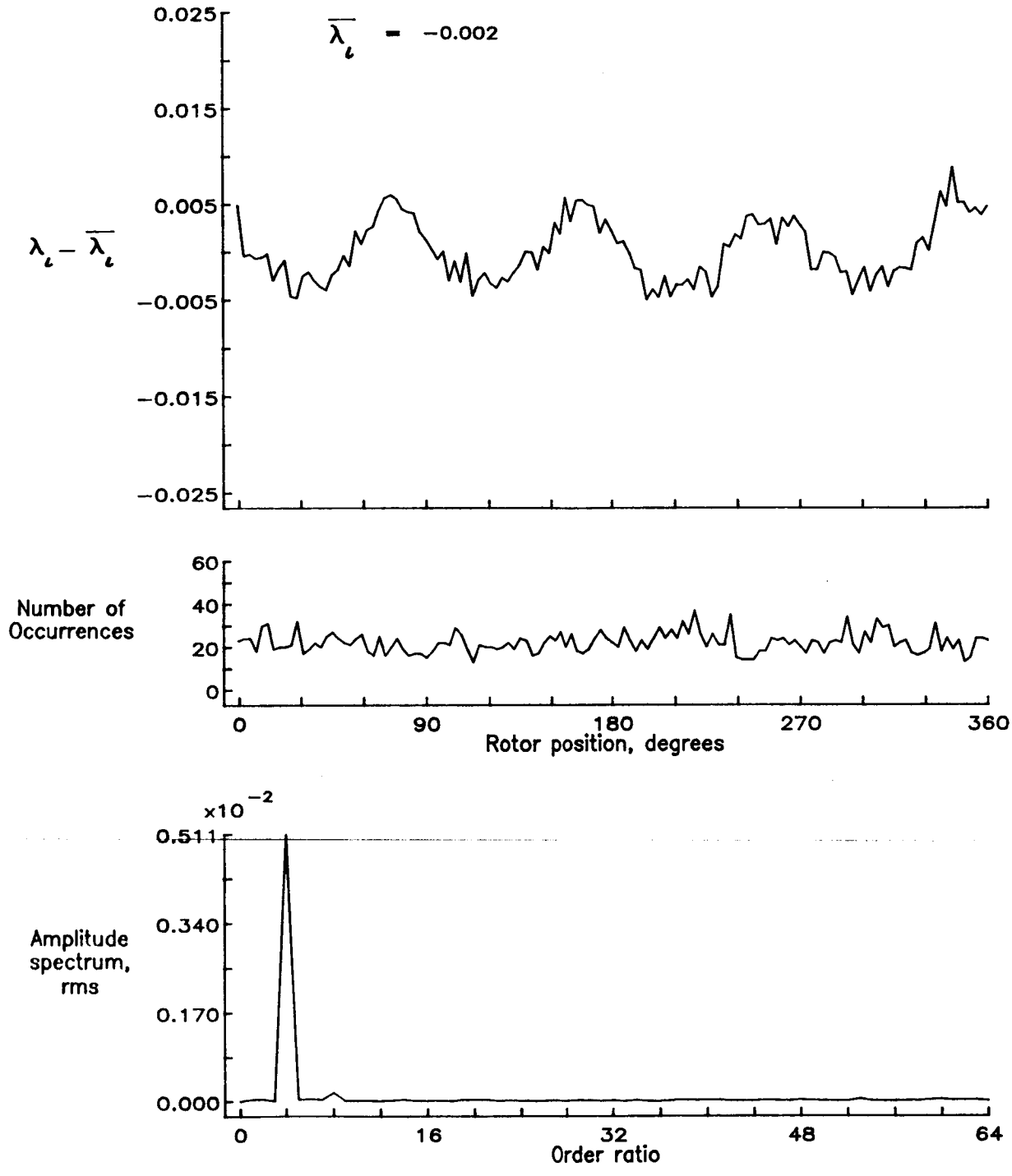


Figure 136.– Concluded.

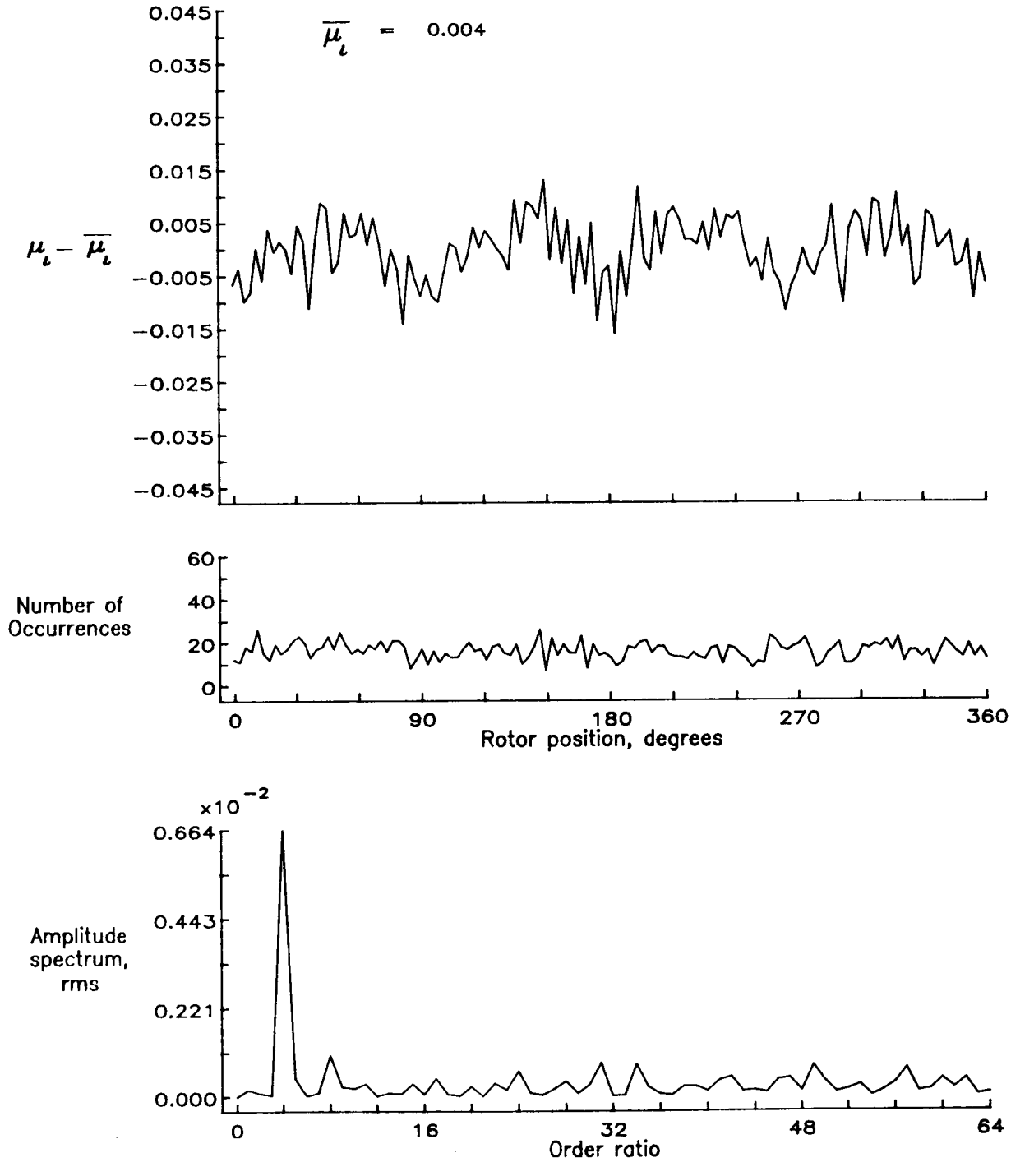


Figure 137.– Induced inflow velocity measured at 270 degrees and r/R of 0.40.

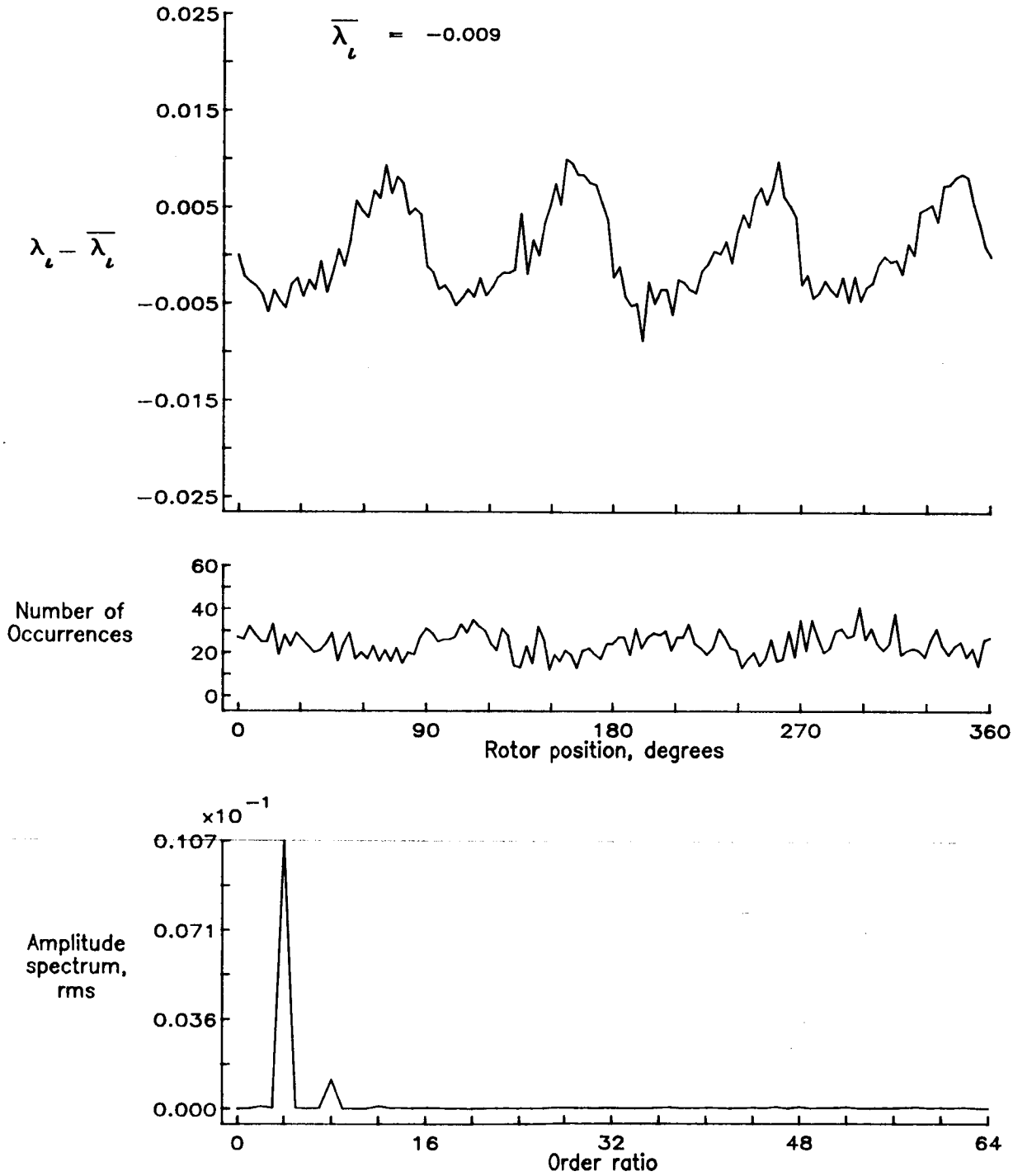


Figure 137.– Concluded.

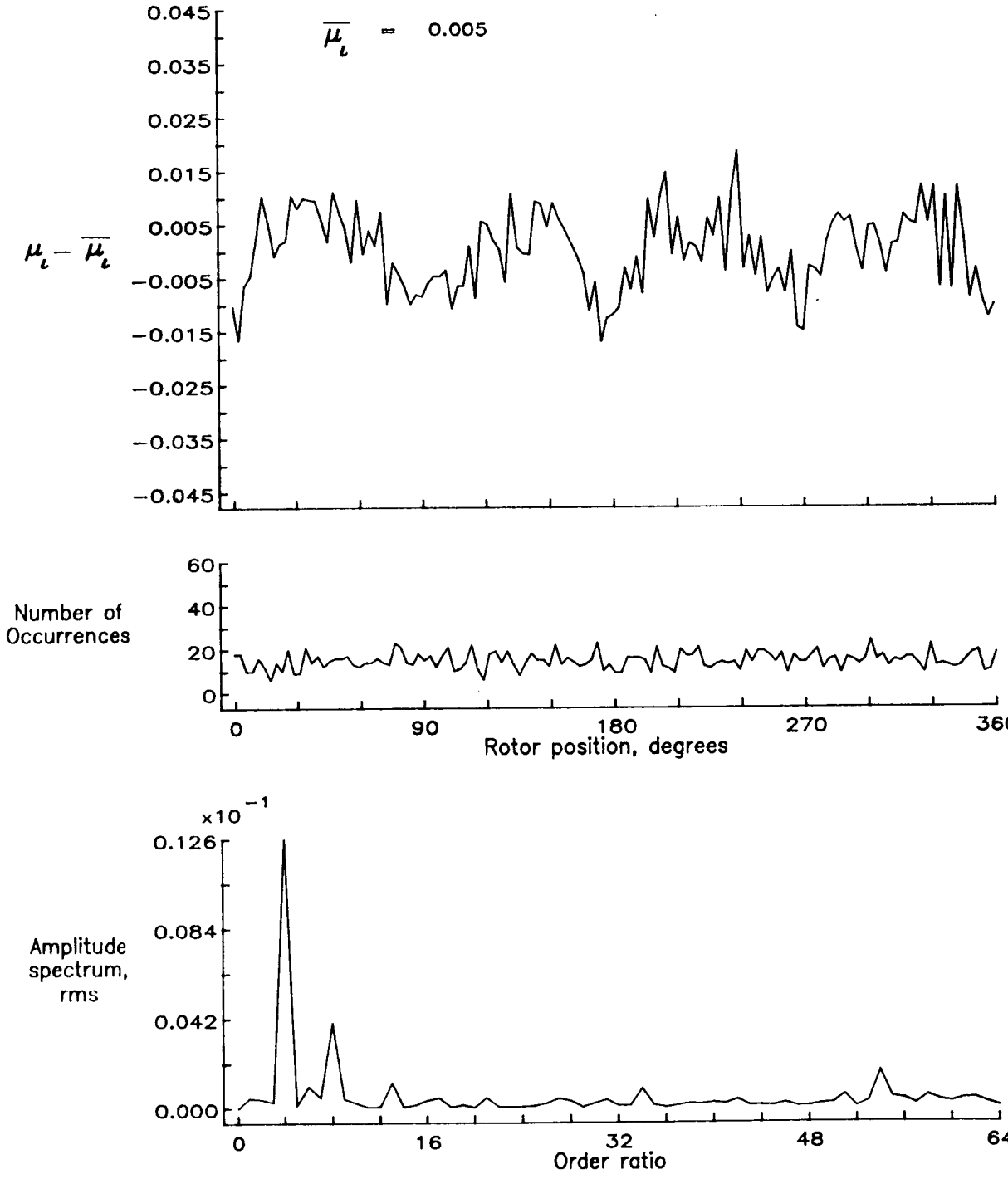


Figure 138.– Induced inflow velocity measured at 270 degrees and r/R of 0.50.

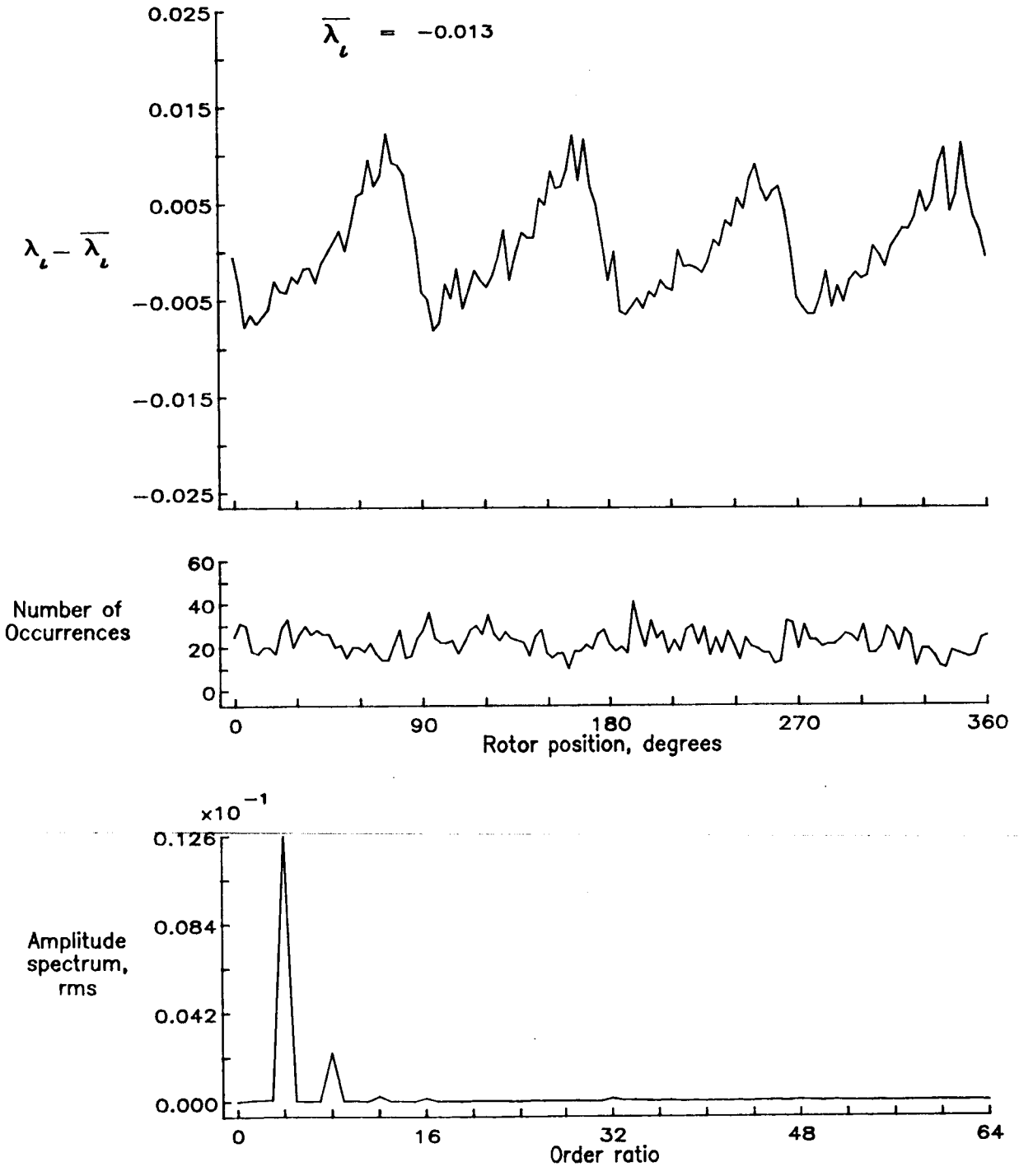


Figure 138.– Concluded.

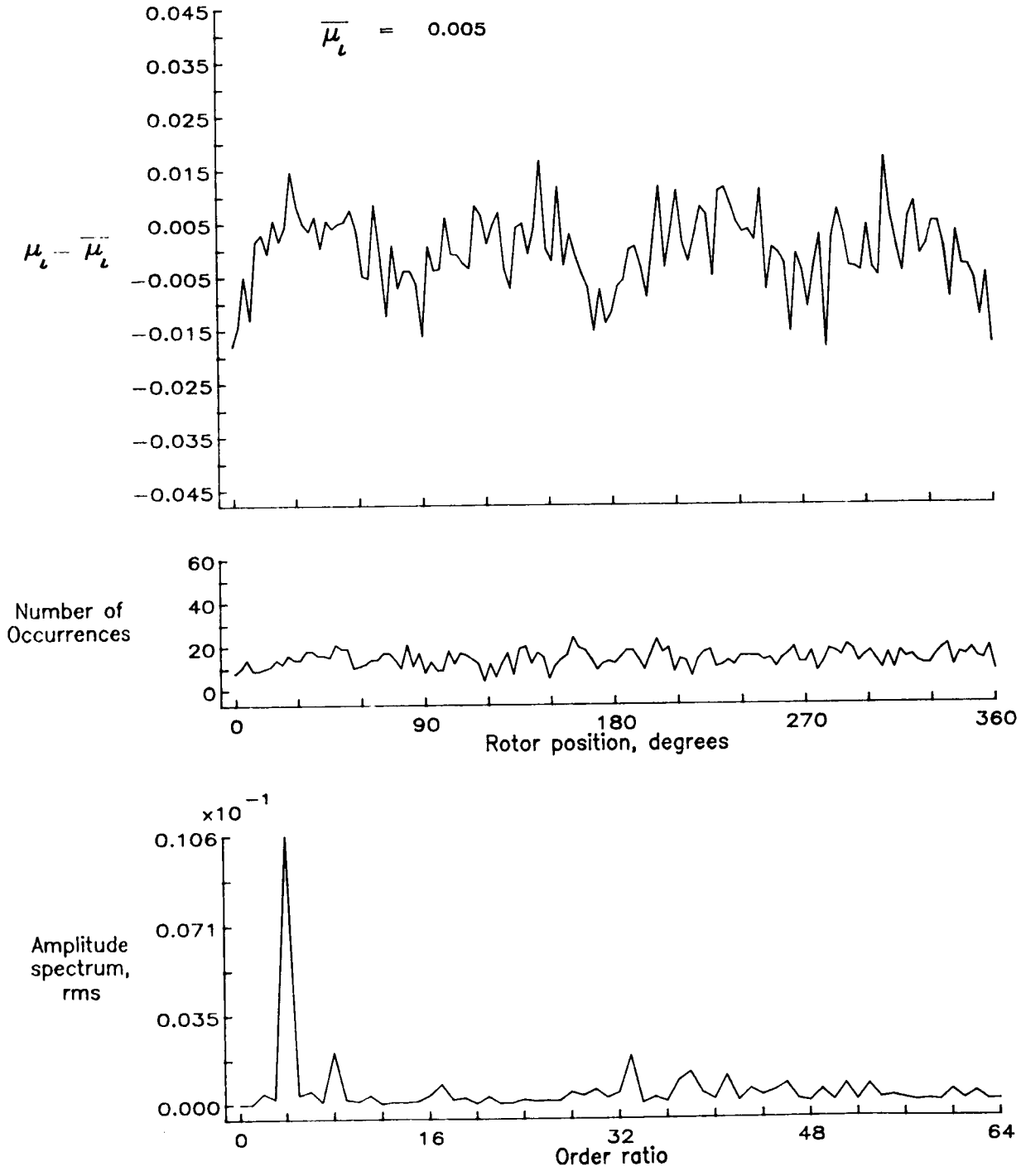


Figure 139.– Induced inflow velocity measured at 270 degrees and r/R of 0.60.

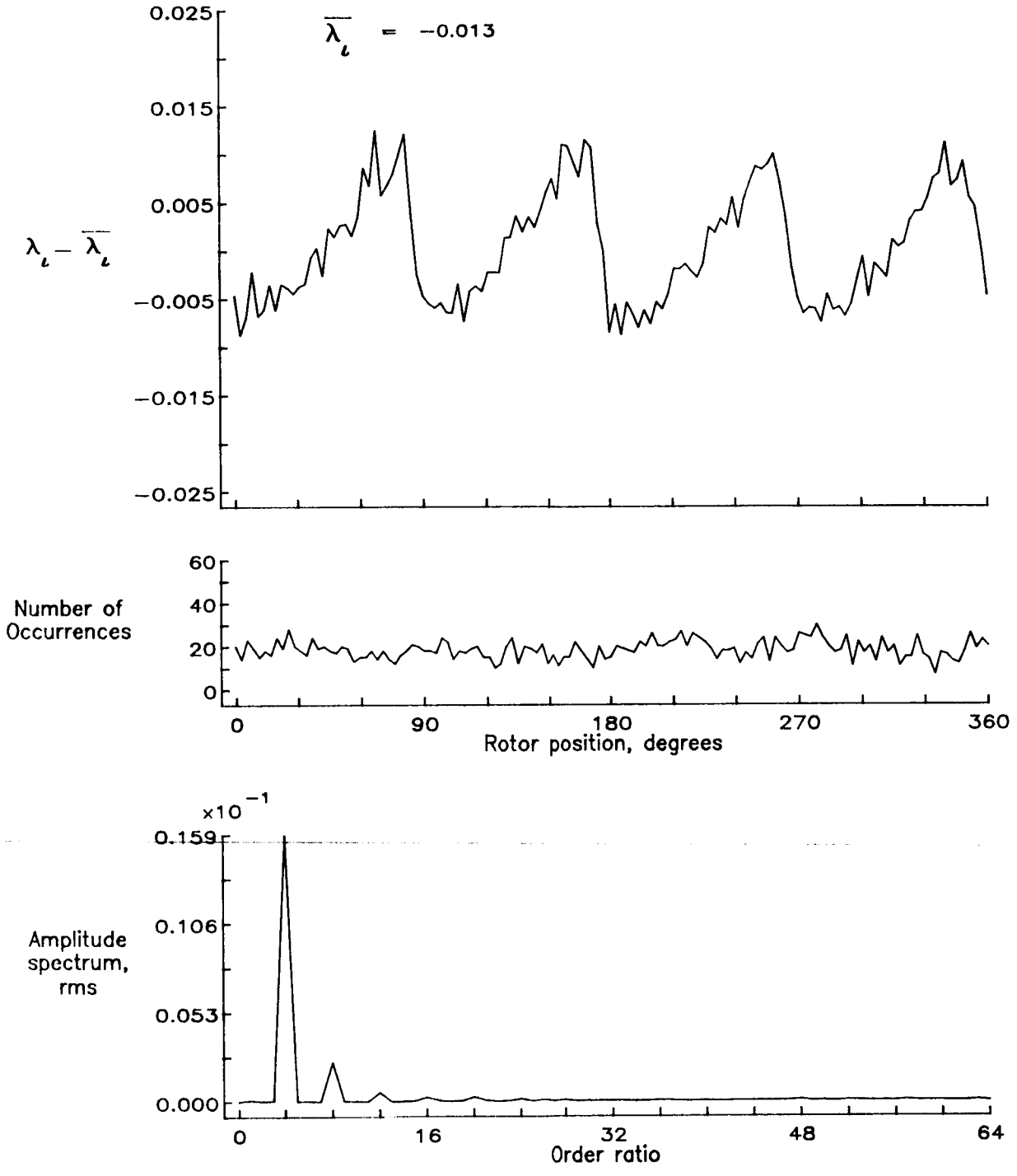


Figure 139.– Concluded.

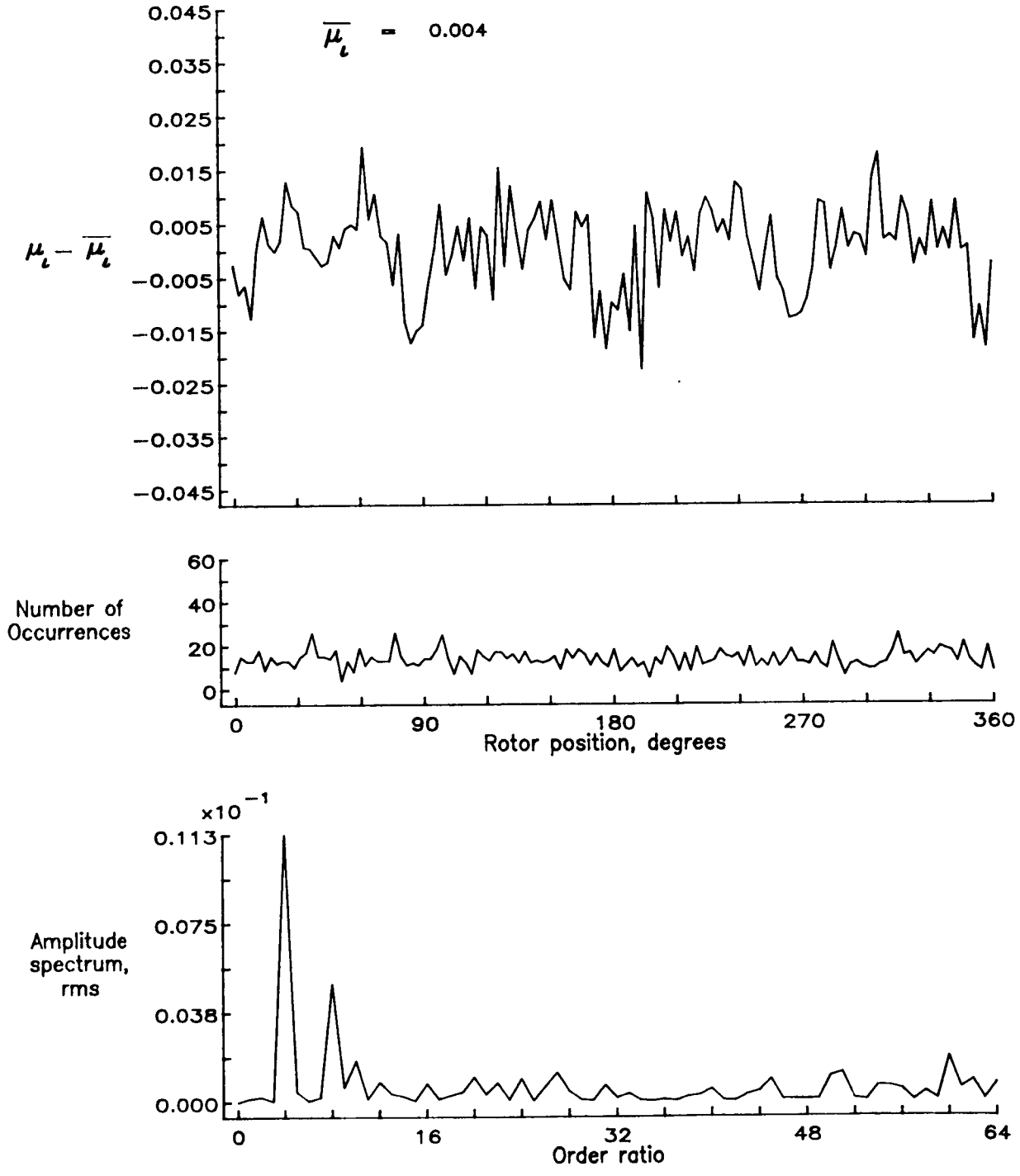


Figure 140.– Induced inflow velocity measured at 270 degrees and r/R of 0.70.

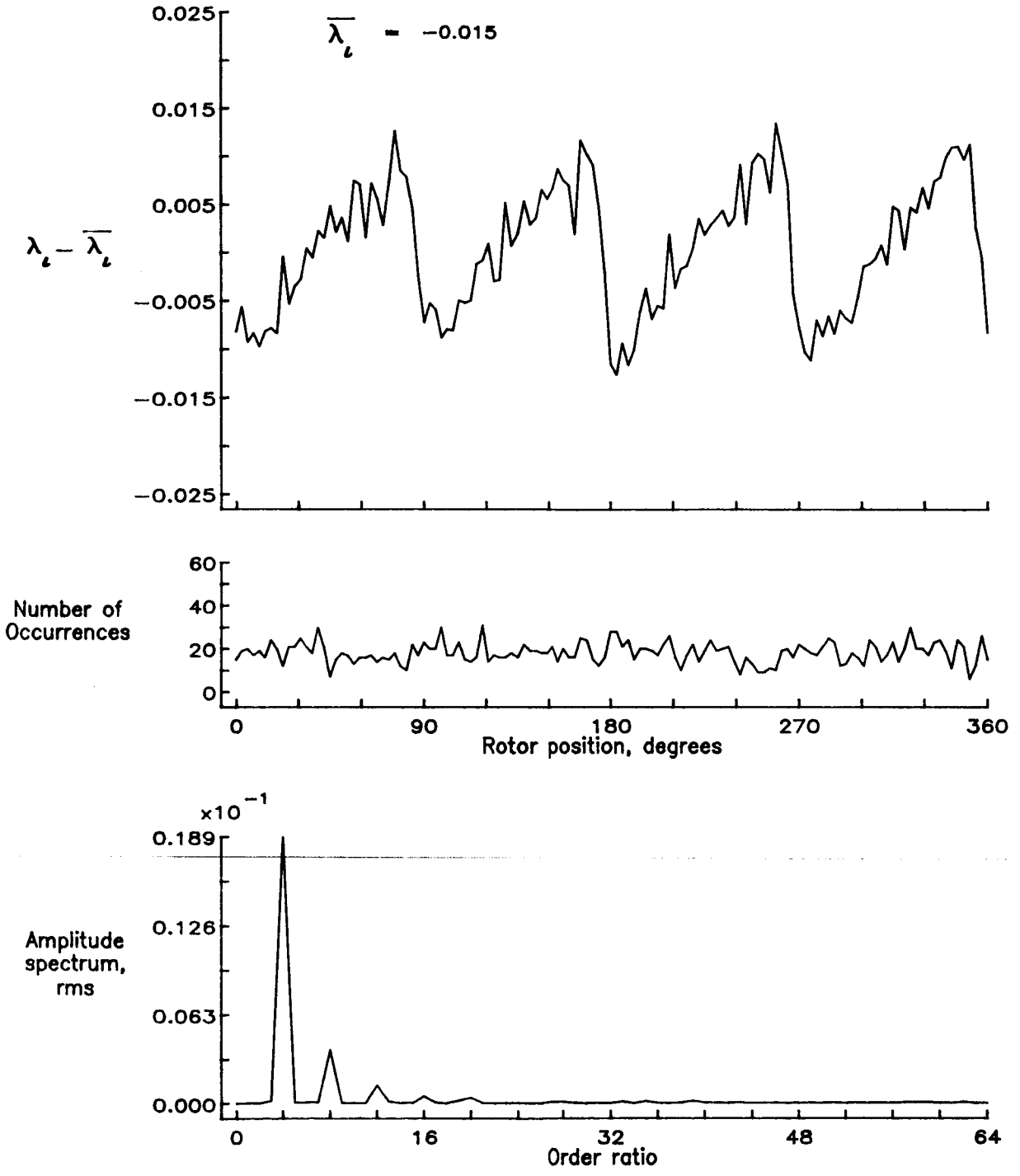


Figure 140.– Concluded.

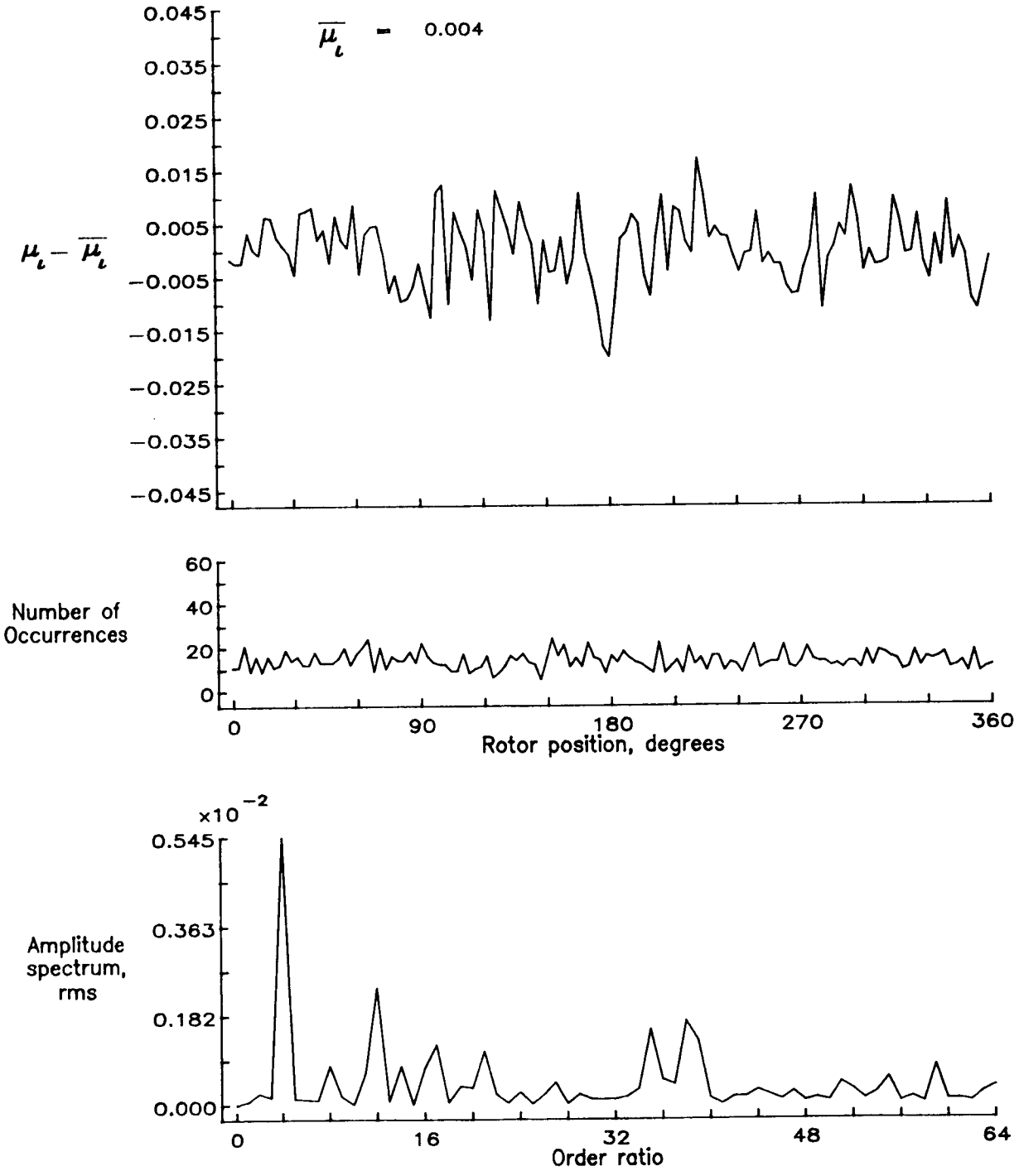


Figure 141.– Induced inflow velocity measured at 270 degrees and r/R of 0.74.

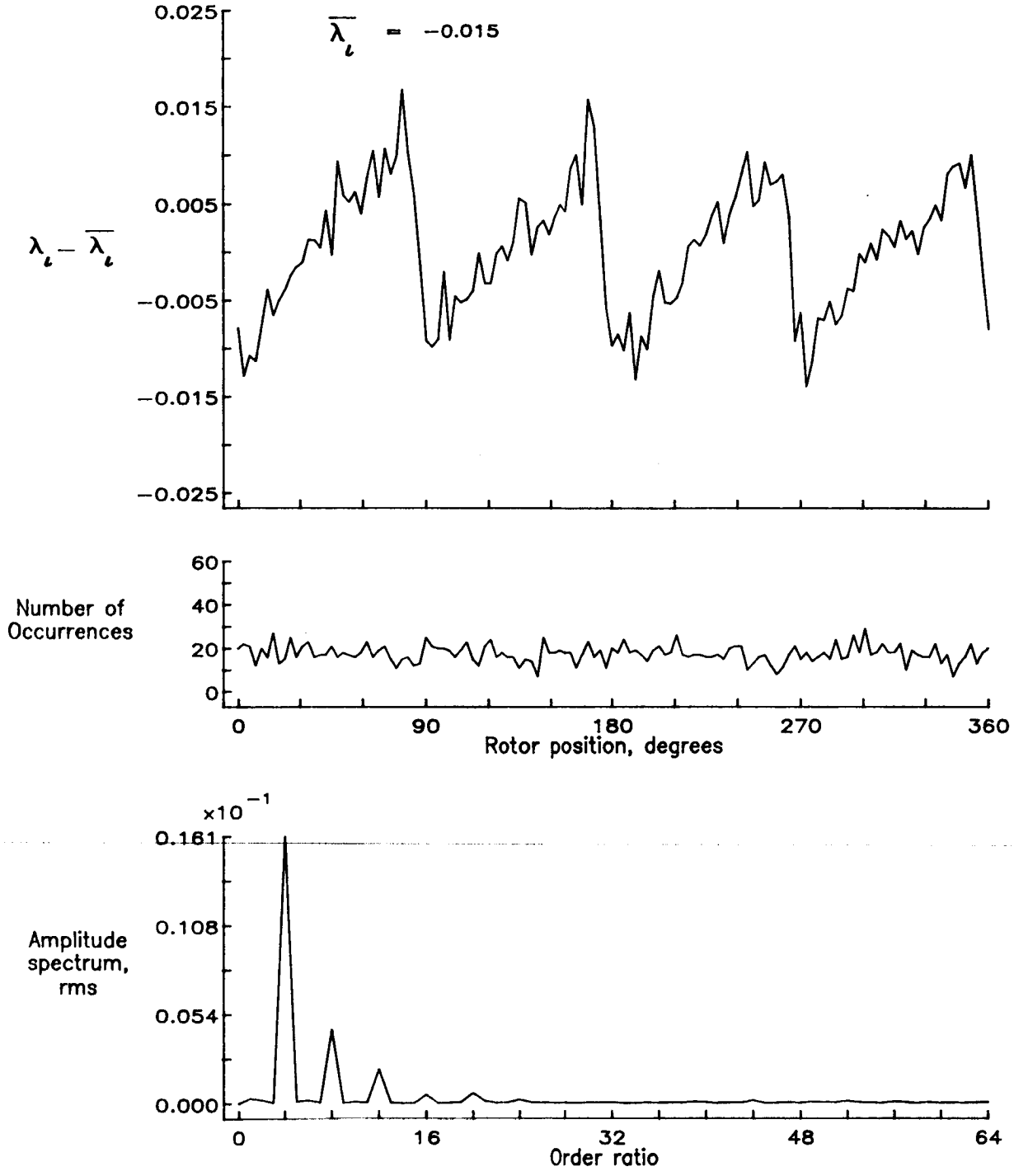


Figure 141.– Concluded.

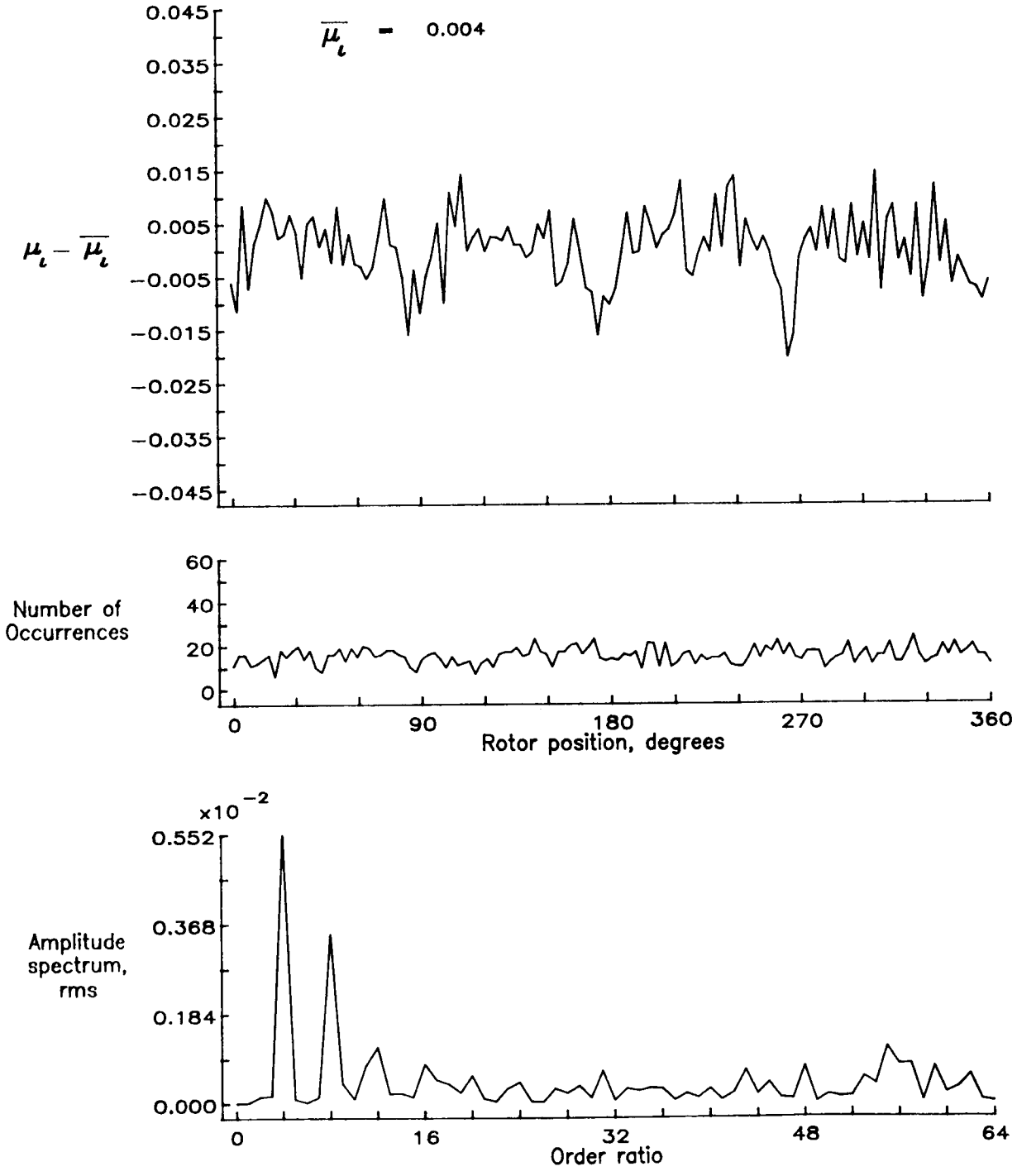


Figure 142.– Induced inflow velocity measured at 270 degrees and r/R of 0.78.

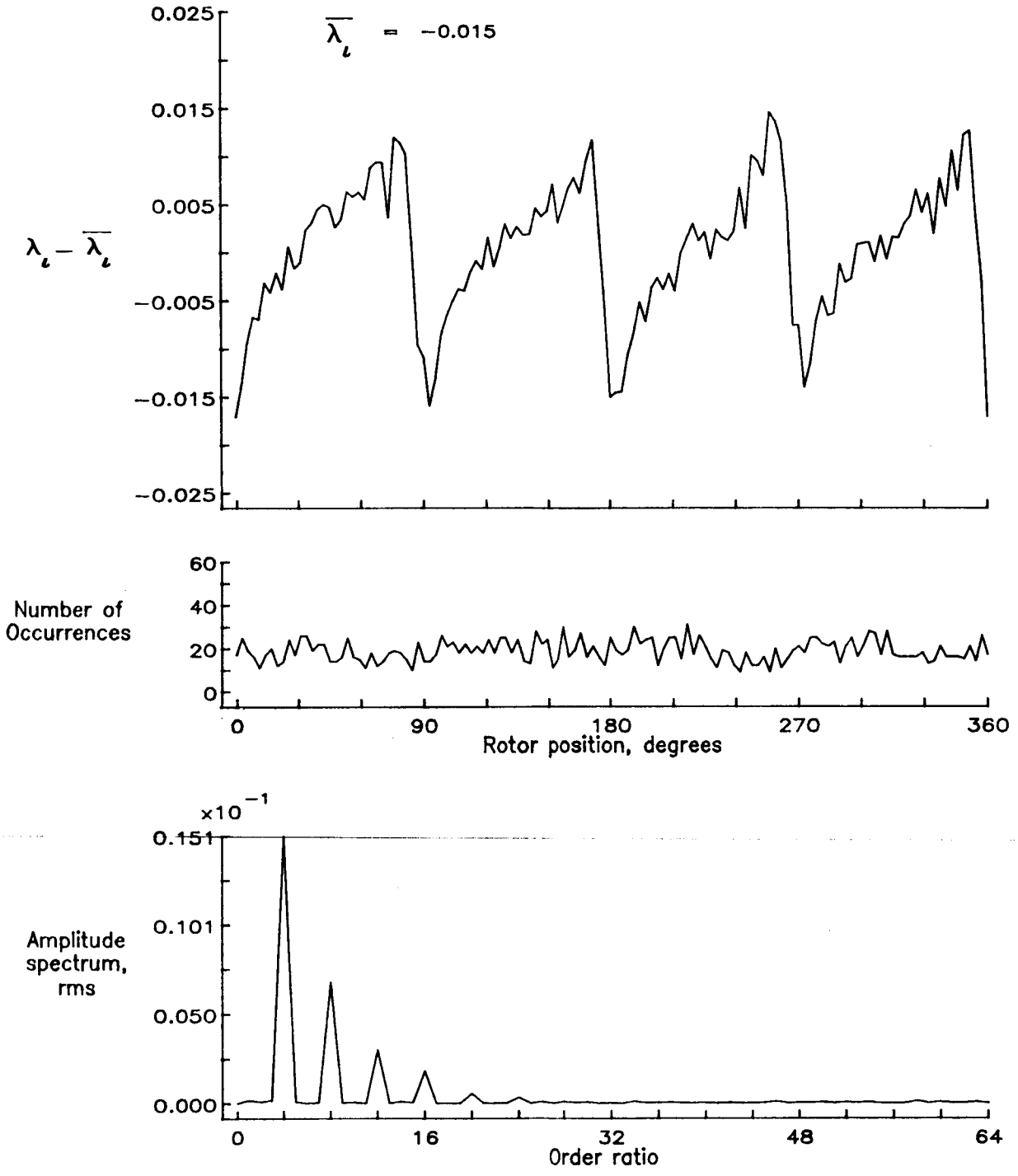


Figure 142.– Concluded.

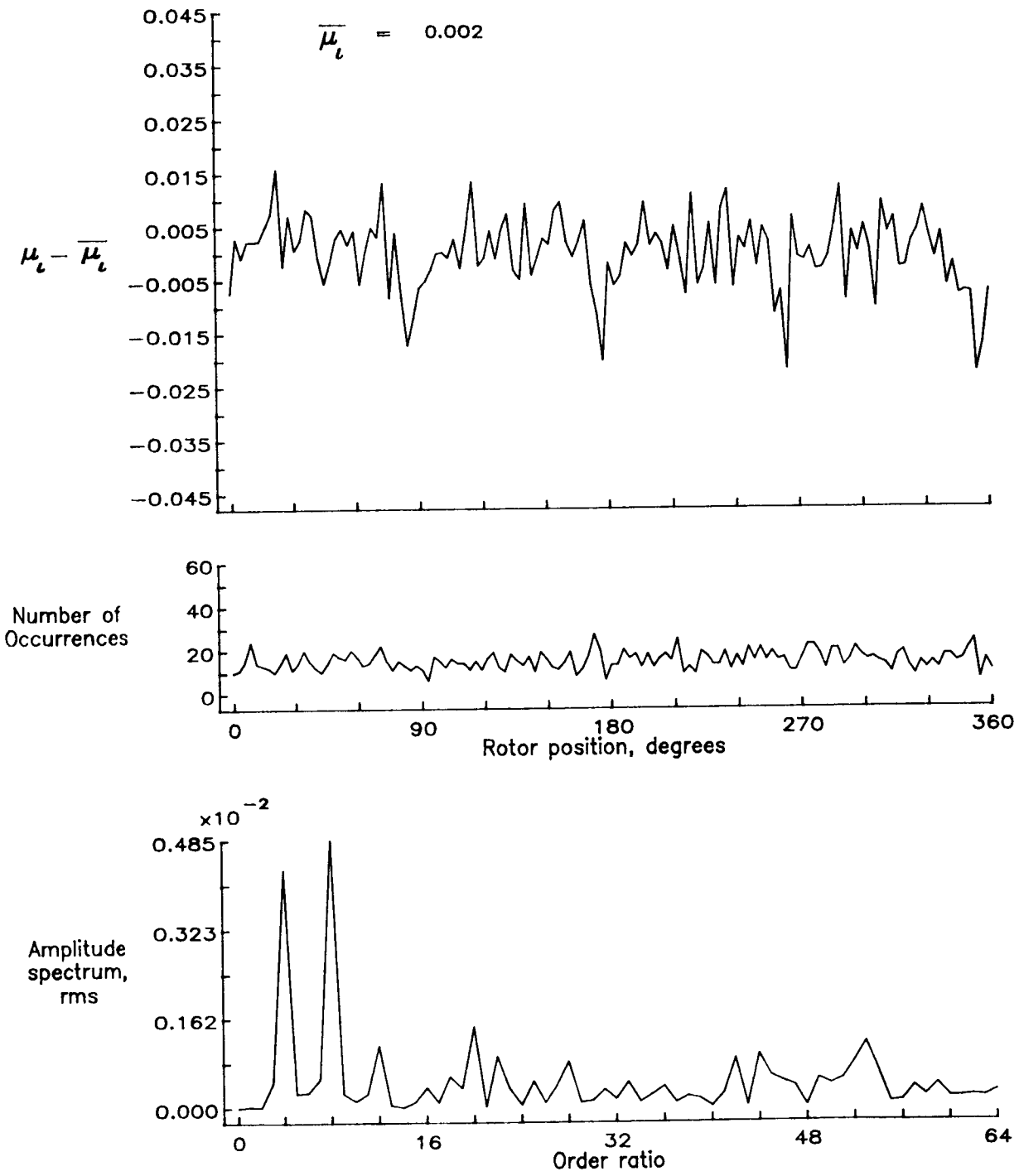


Figure 143.– Induced inflow velocity measured at 270 degrees and r/R of 0.82.

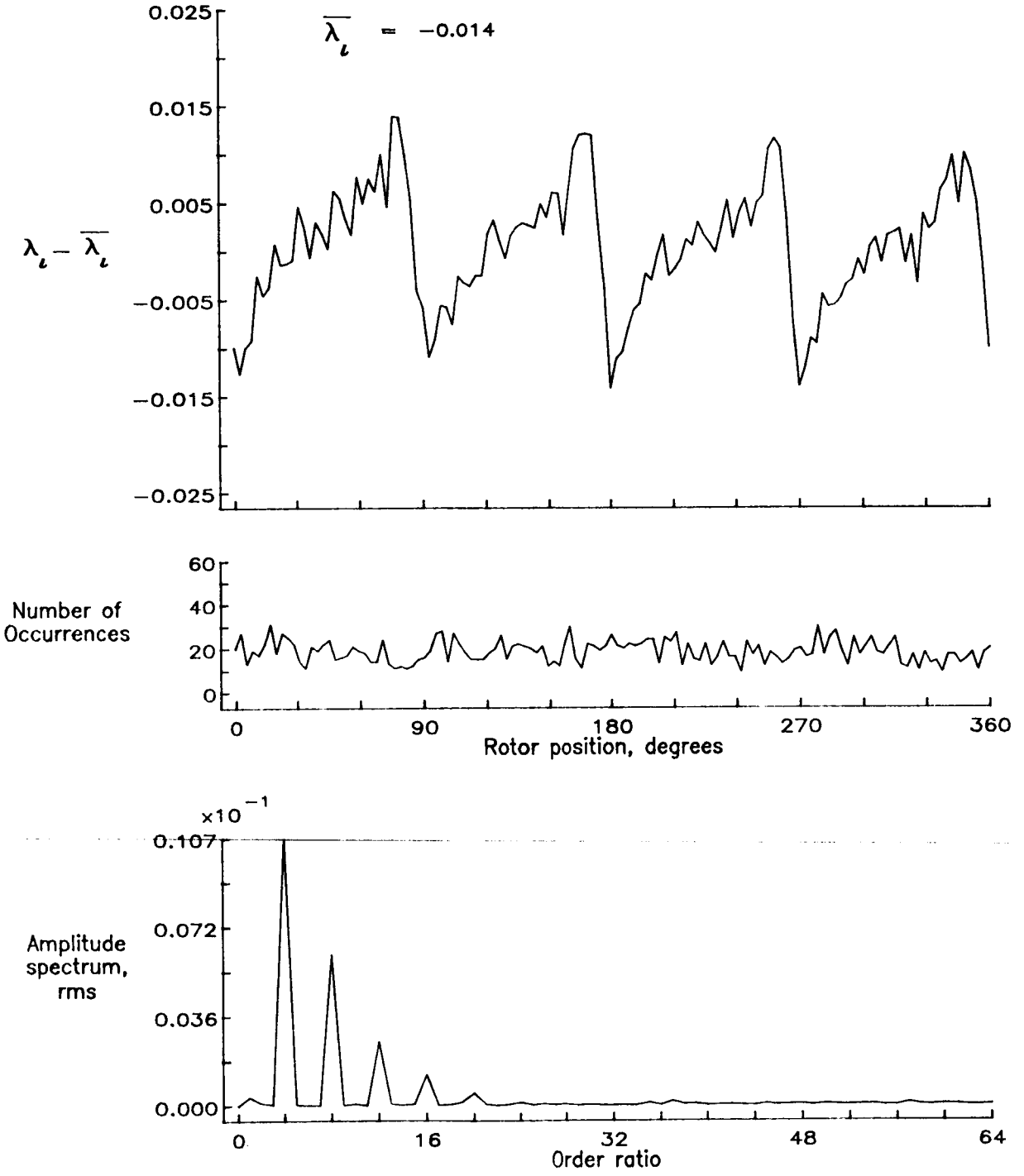


Figure 143.– Concluded.

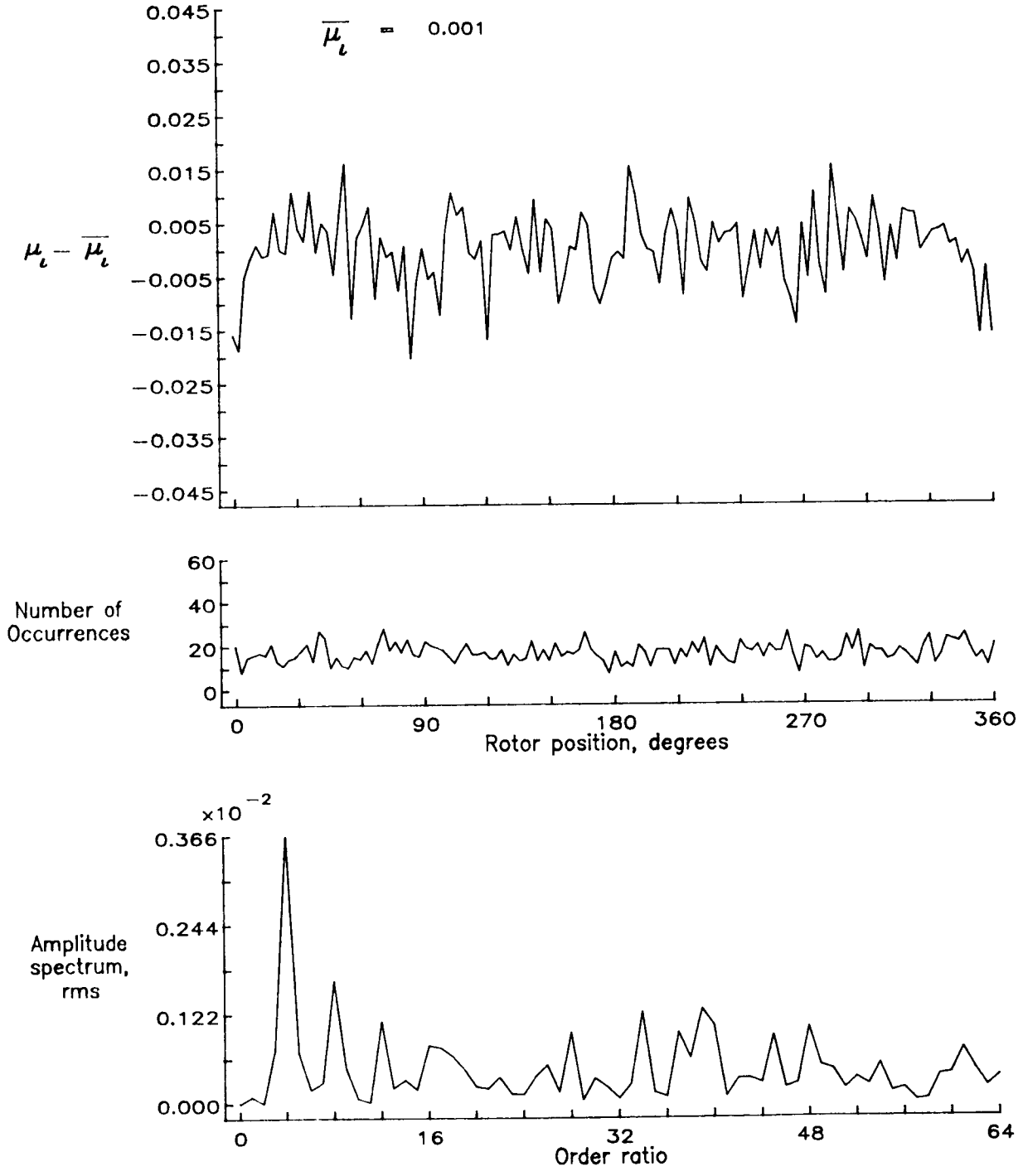


Figure 144.– Induced inflow velocity measured at 270 degrees and r/R of 0.86.

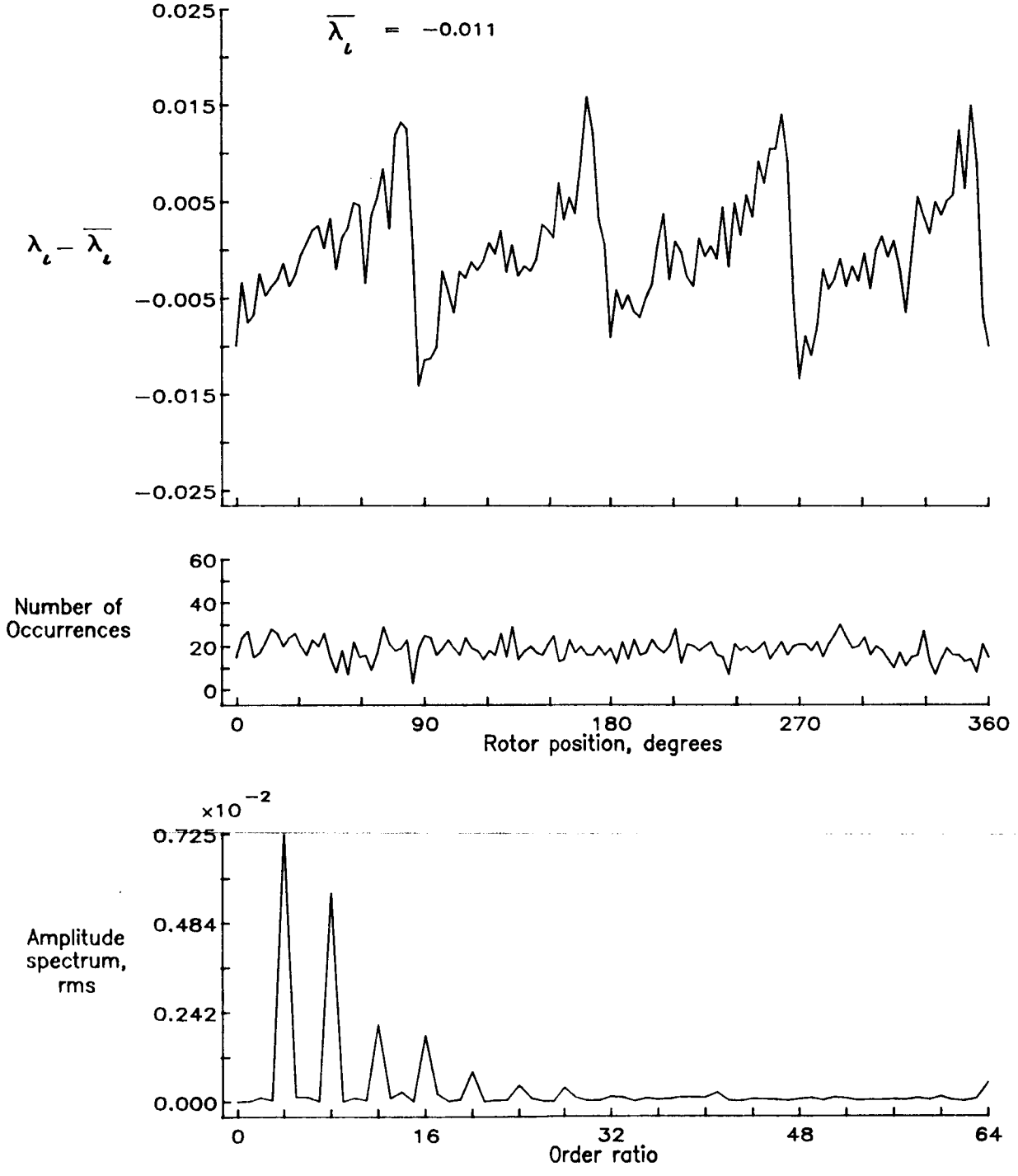


Figure 144.– Concluded.

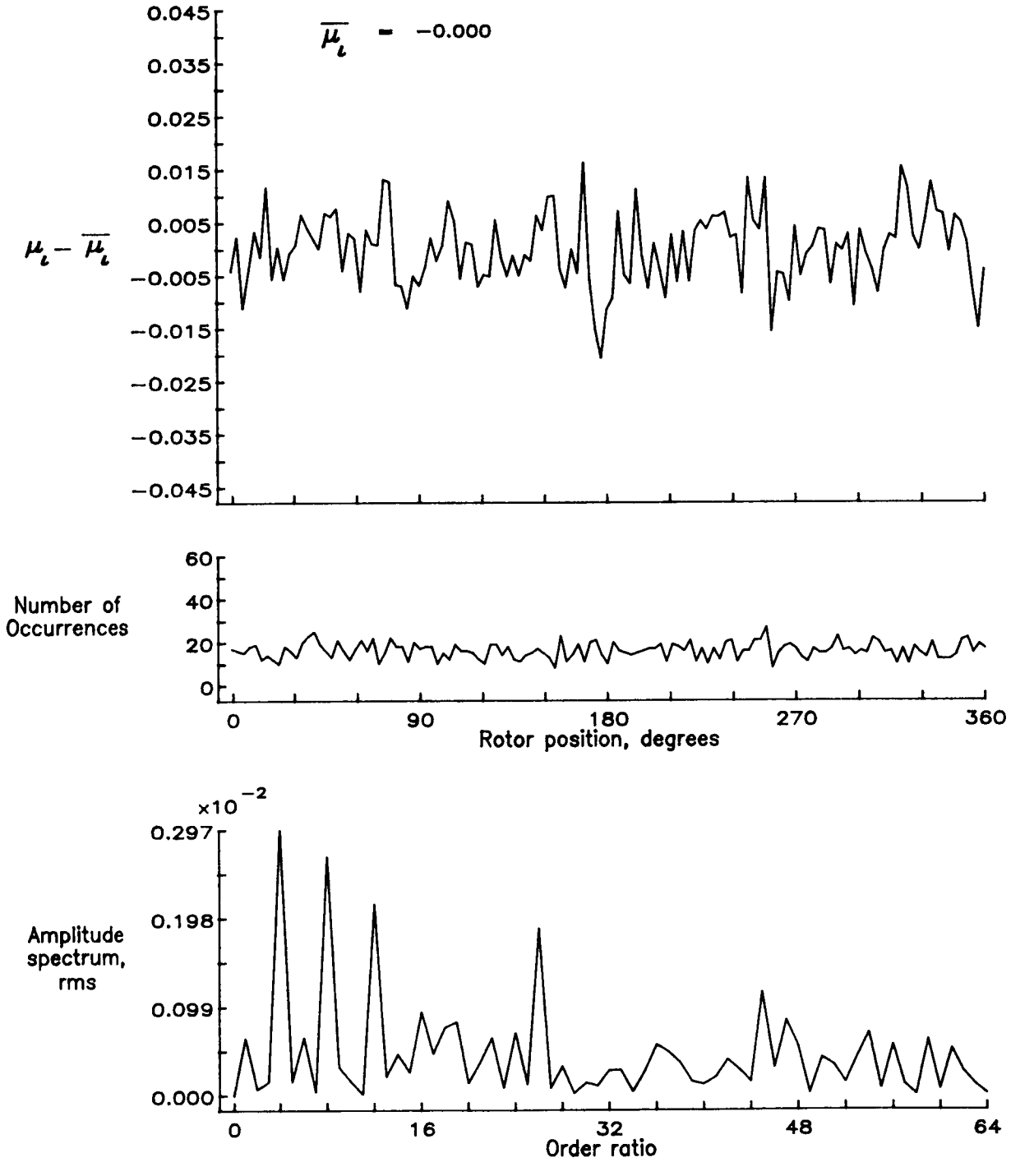


Figure 145.– Induced inflow velocity measured at 270 degrees and r/R of 0.90.

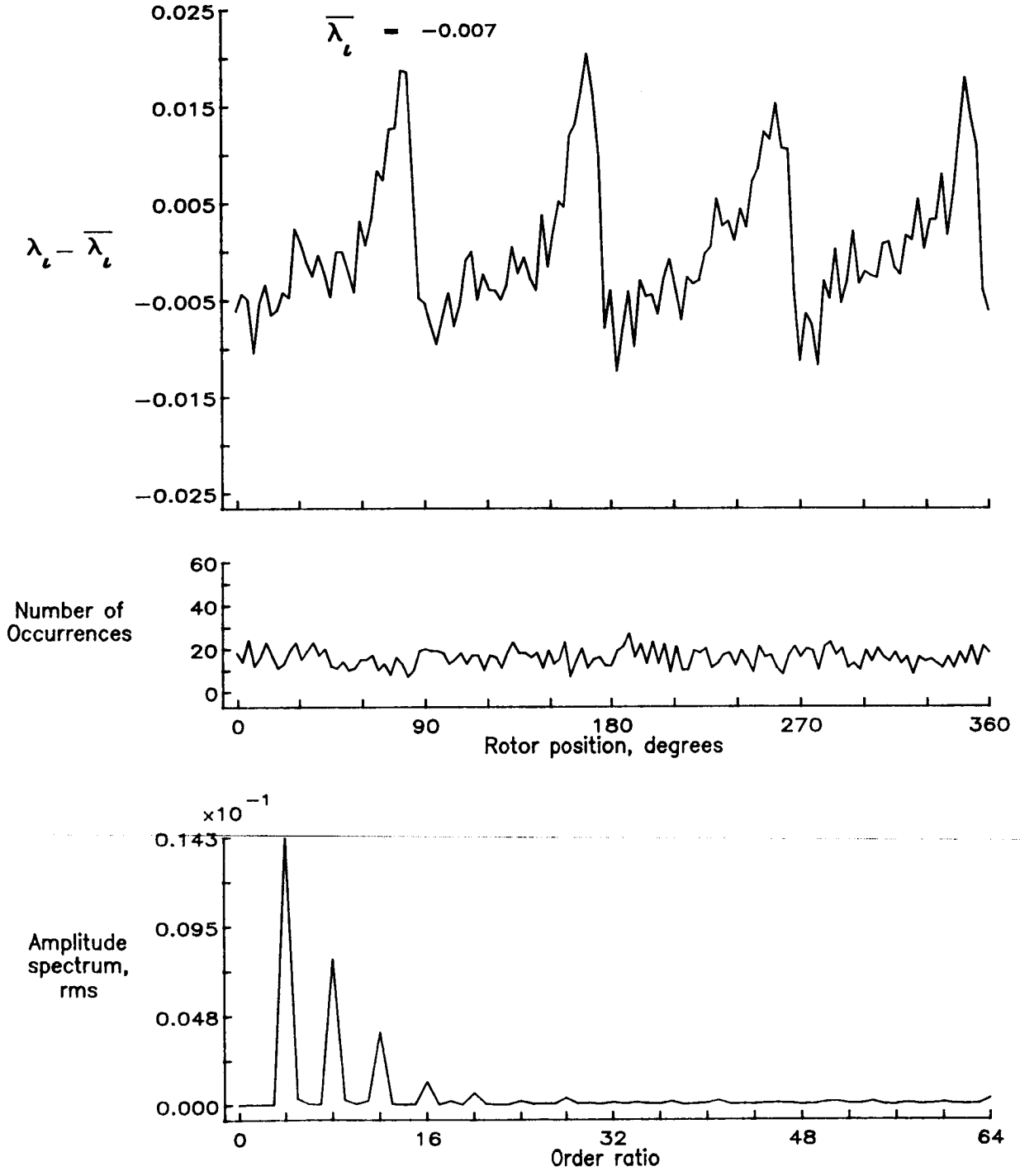


Figure 145.– Concluded.

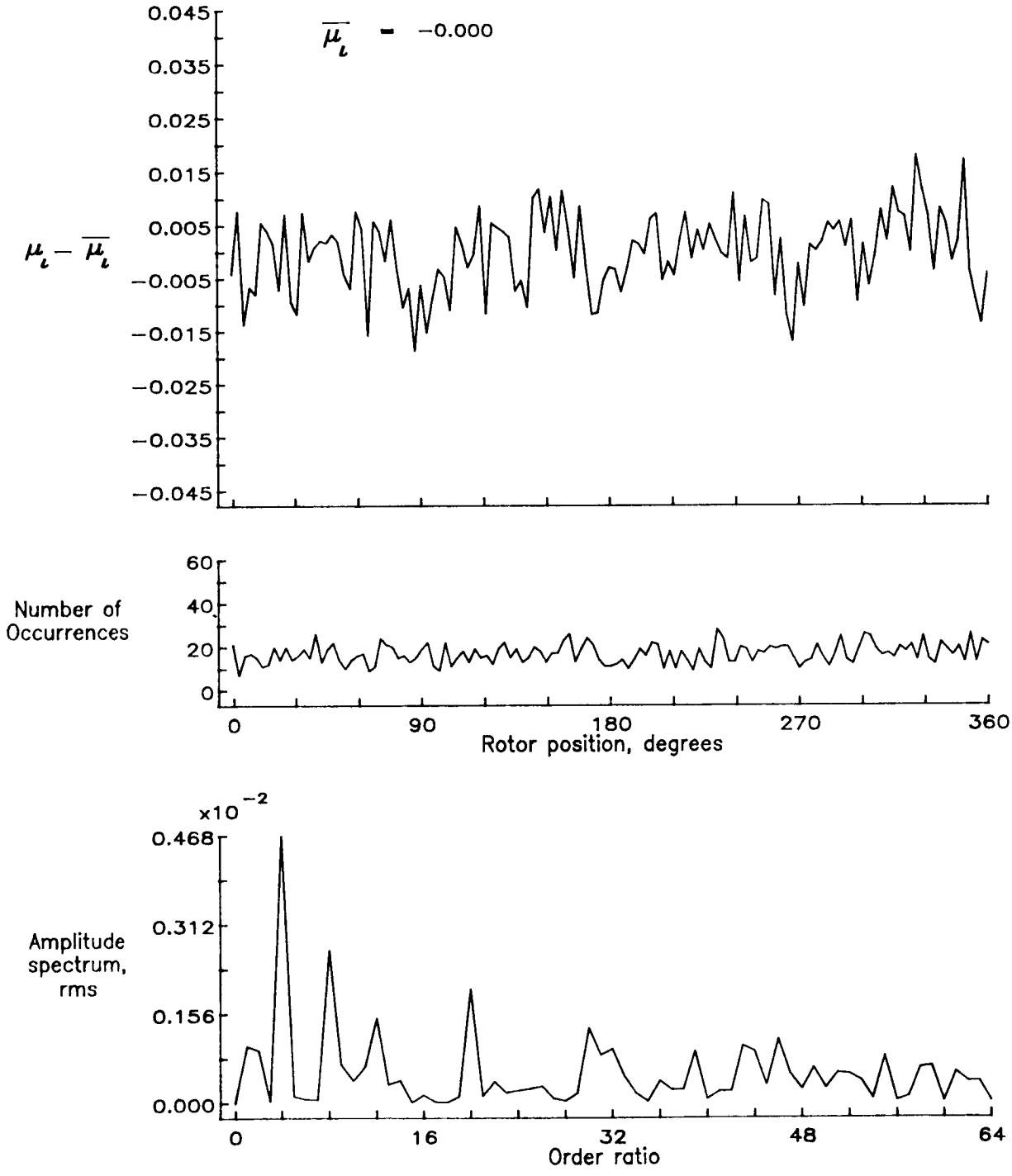


Figure 146.– Induced inflow velocity measured at 270 degrees and r/R of 0.94.

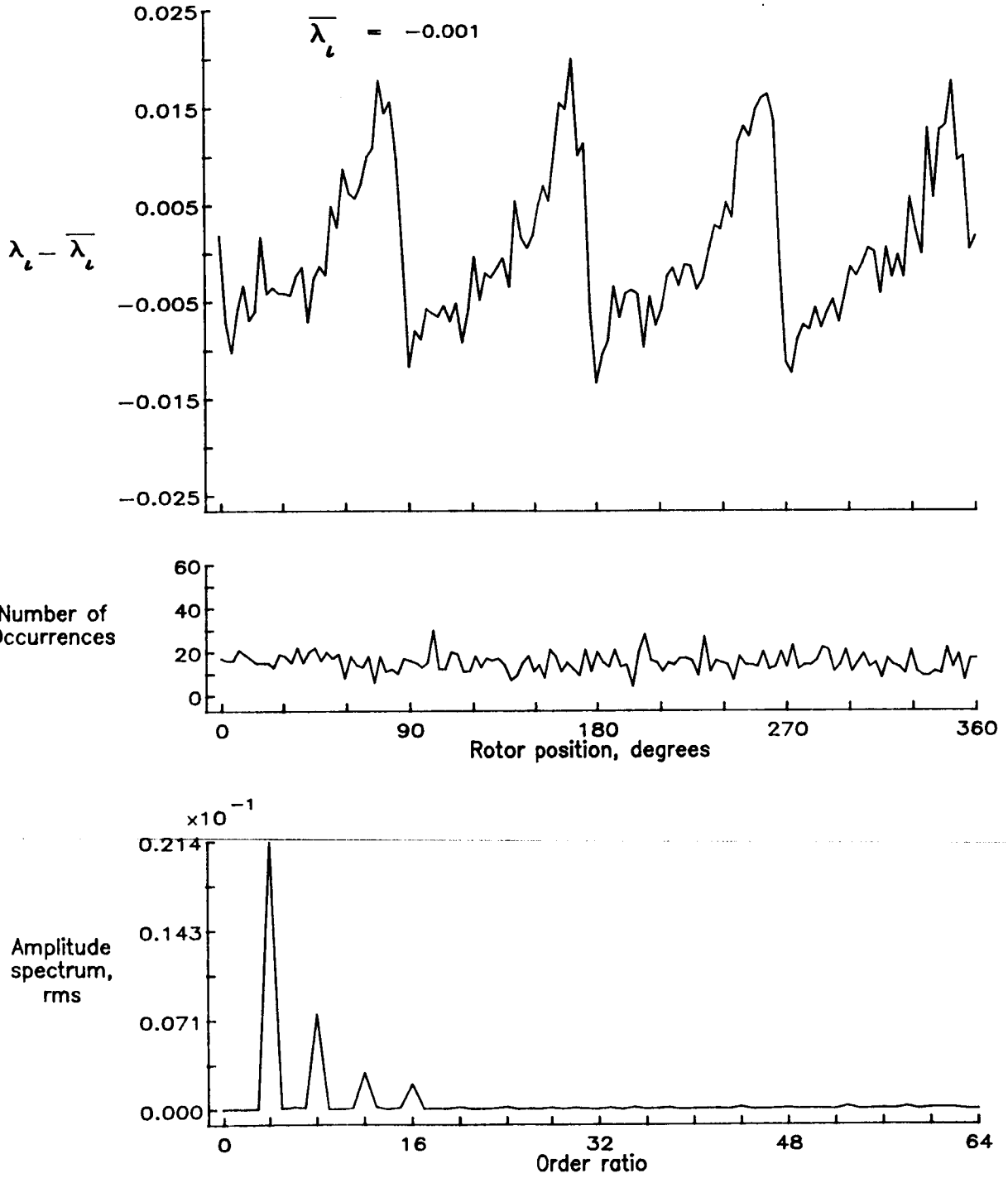


Figure 146.– Concluded.

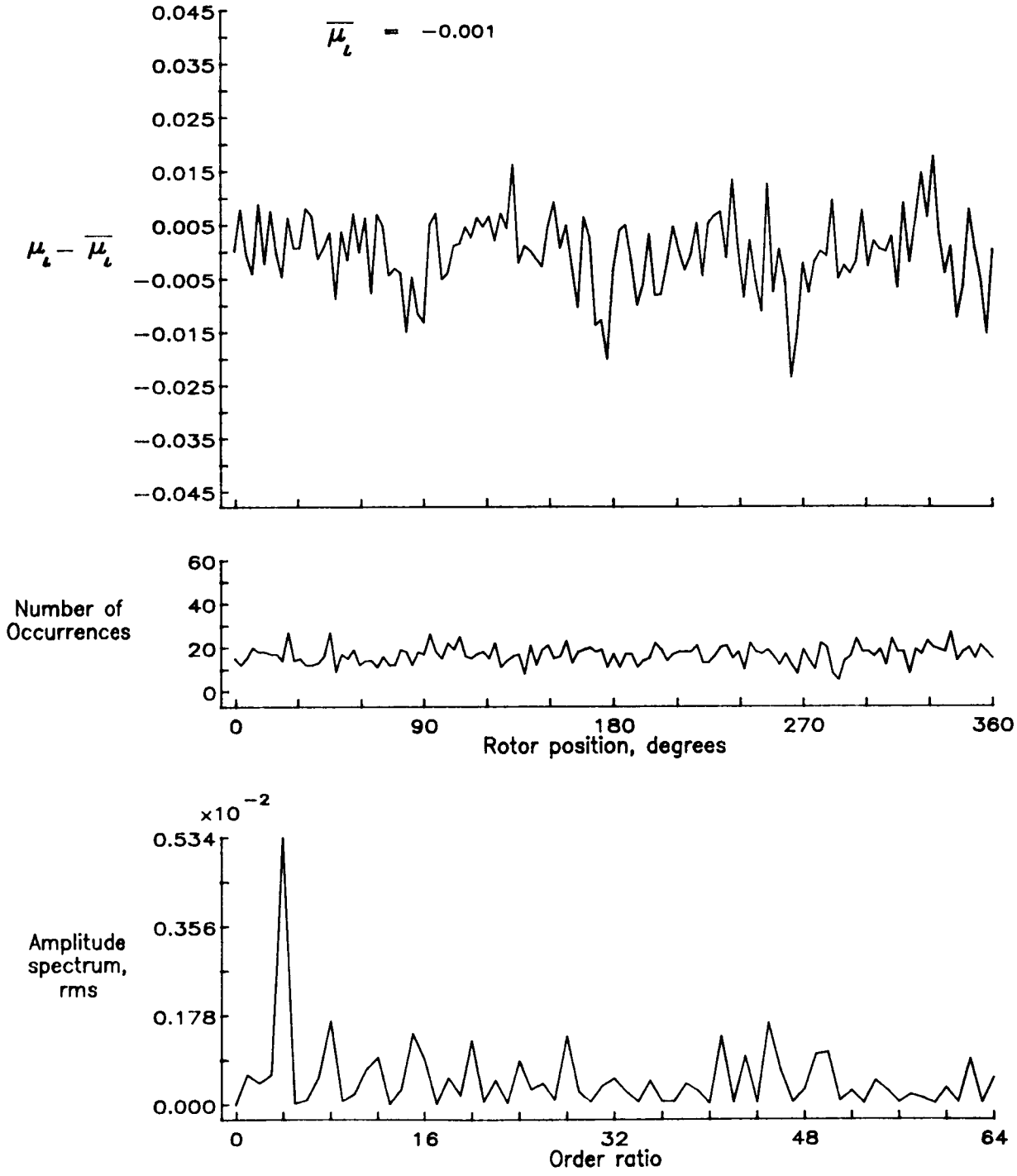


Figure 147.– Induced inflow velocity measured at 270 degrees and r/R of 0.98.

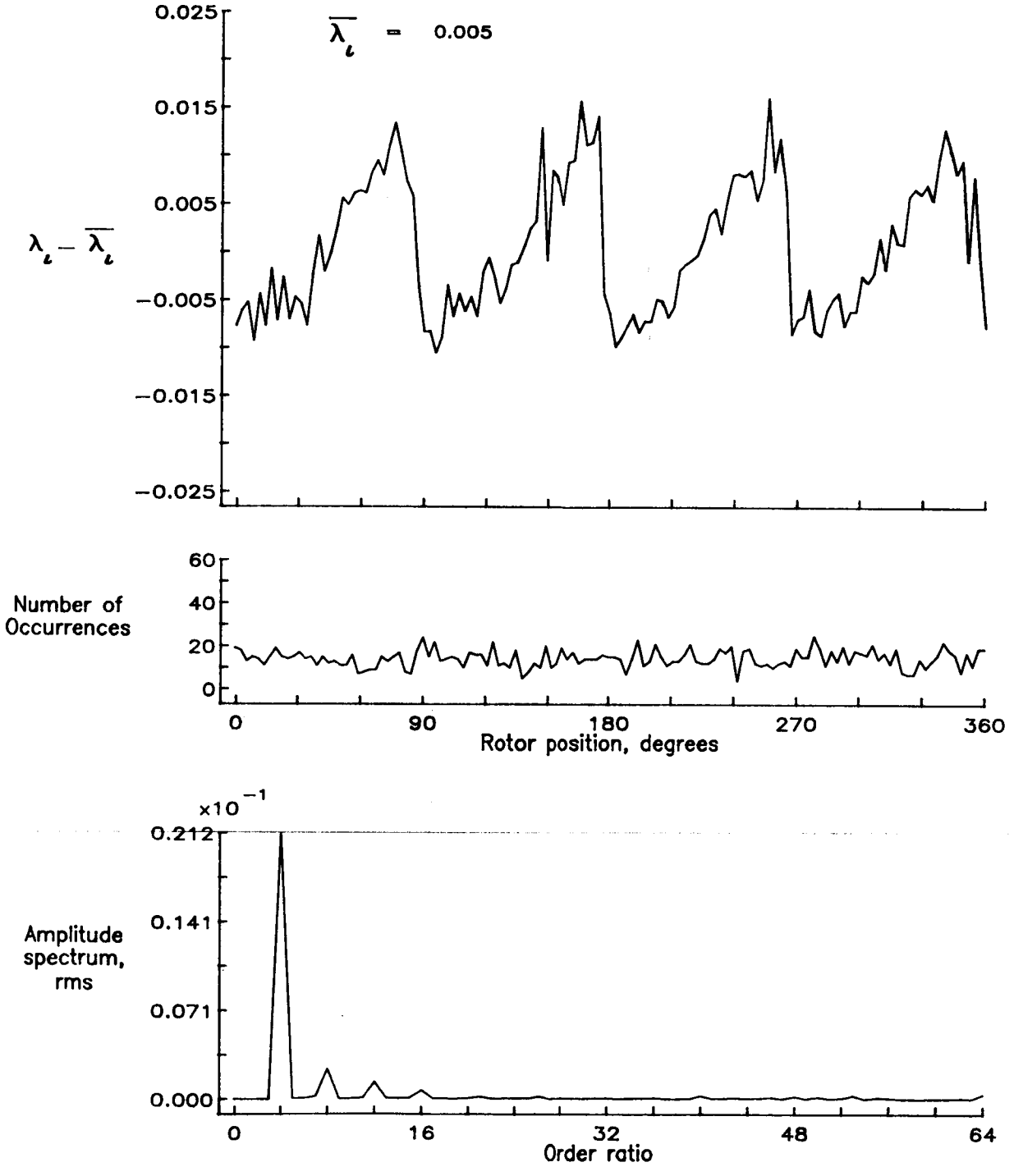


Figure 147.– Concluded.

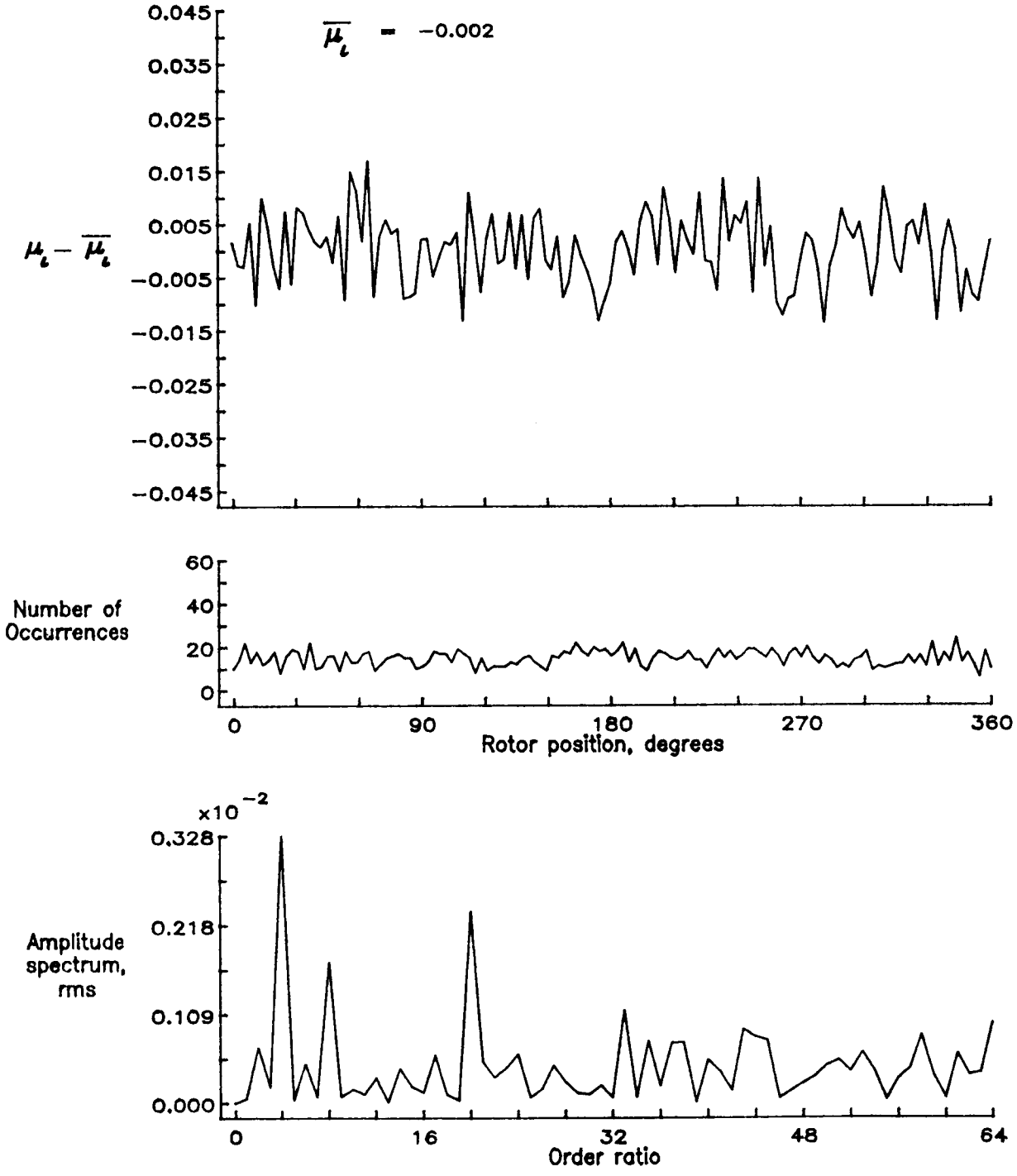


Figure 148.– Induced inflow velocity measured at 270 degrees and r/R of 1.02.

C-4

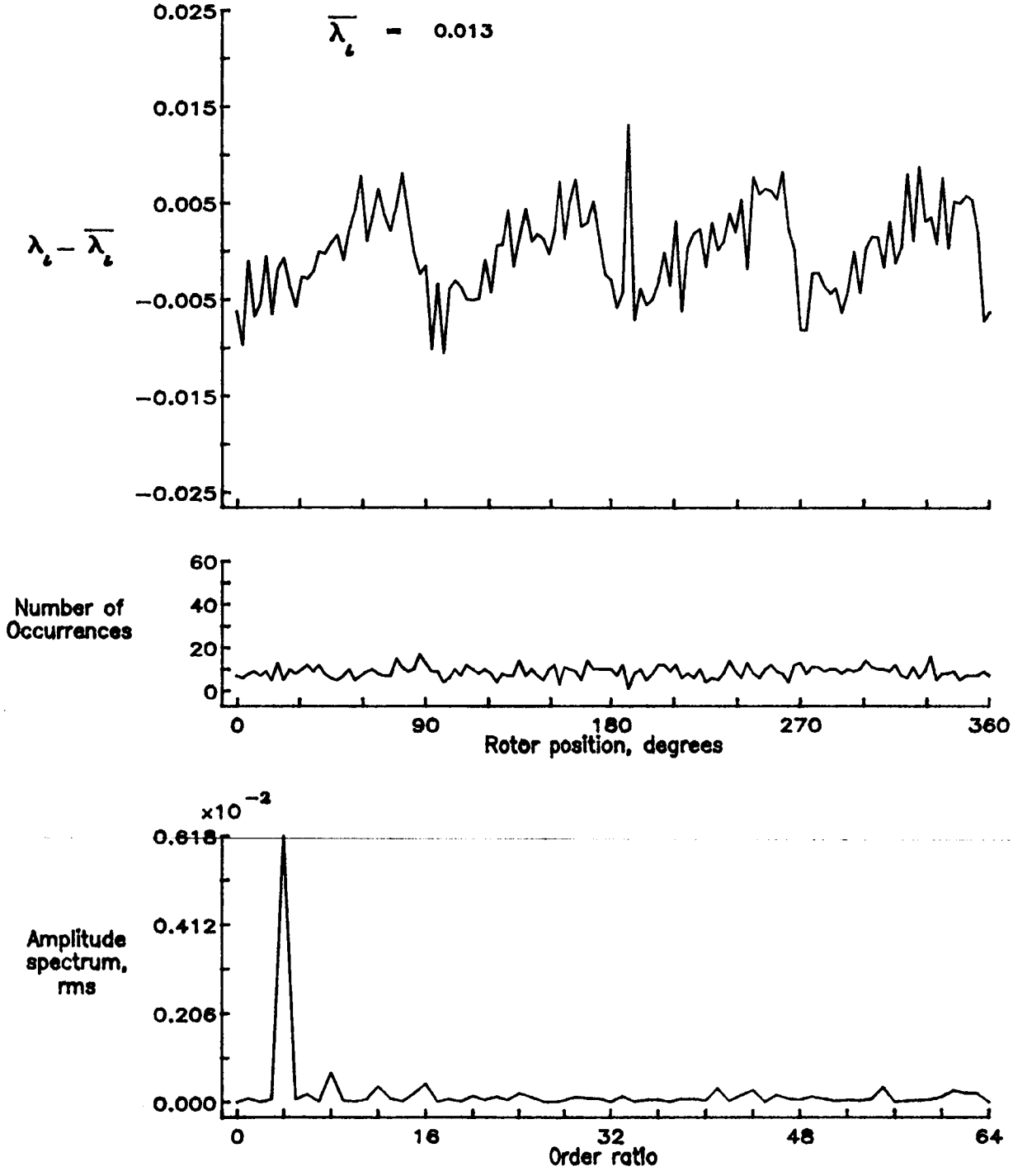


Figure 148.– Concluded.

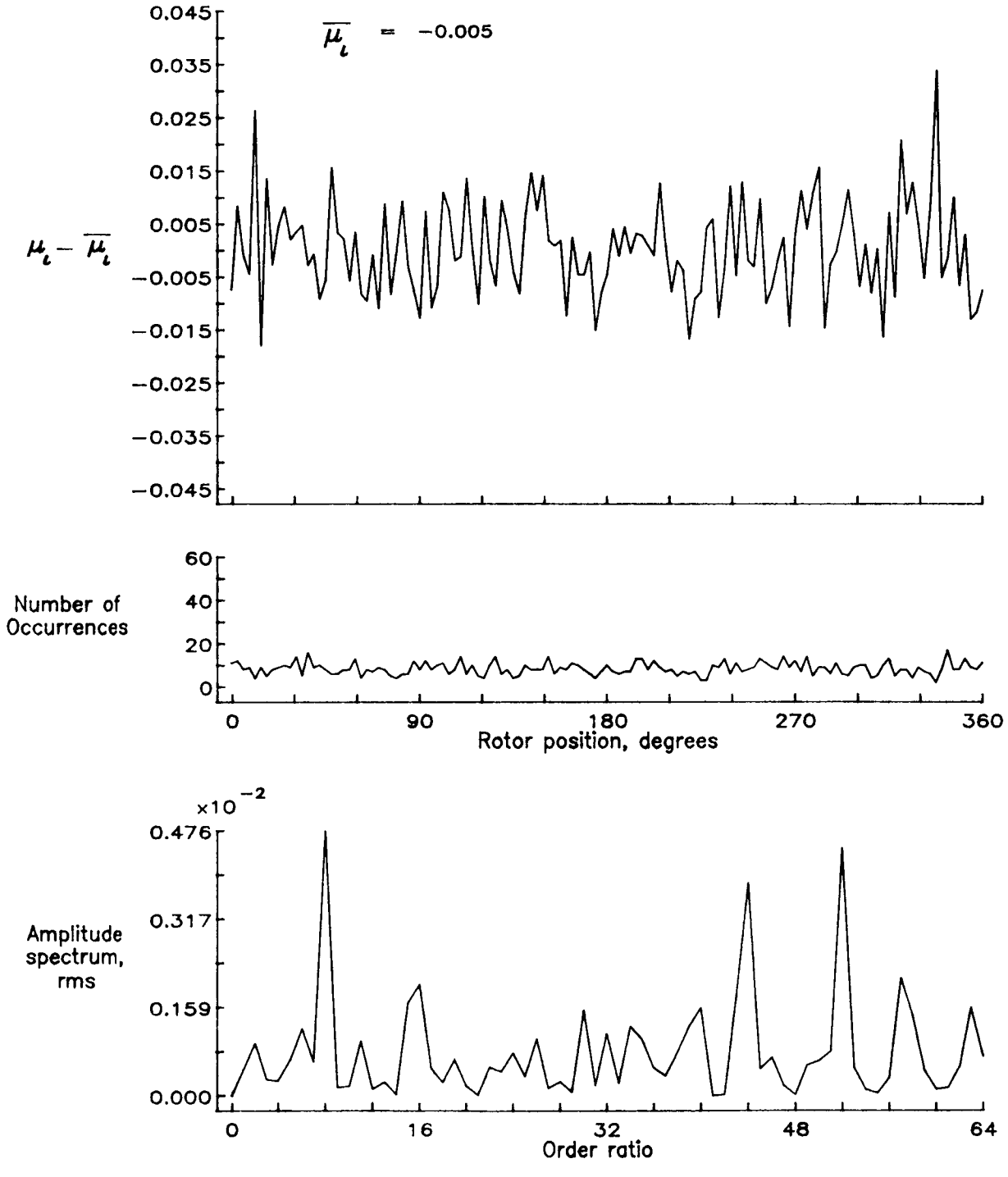


Figure 149.– Induced inflow velocity measured at 270 degrees and r/R of 1.04.

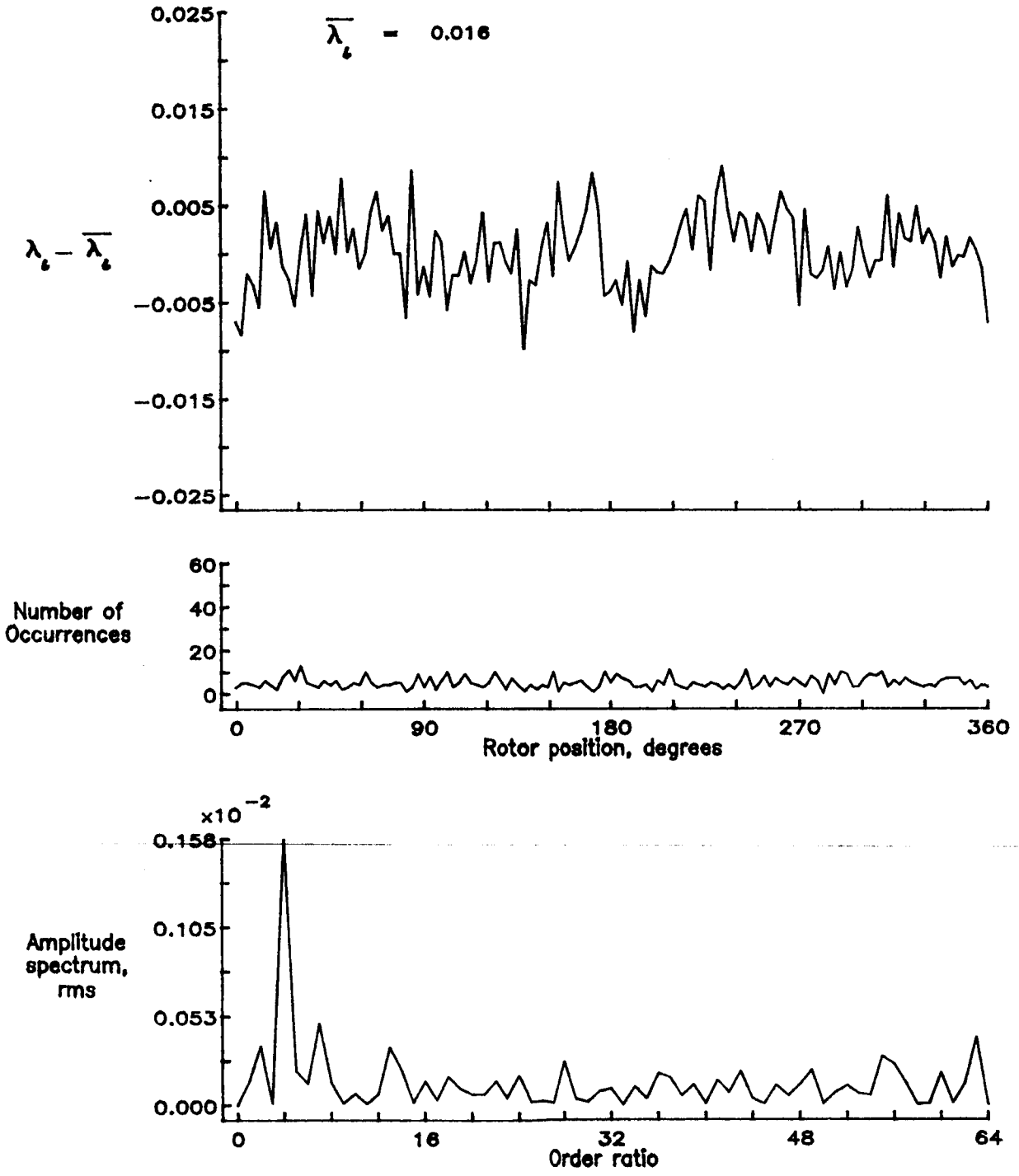


Figure 149.– Concluded.

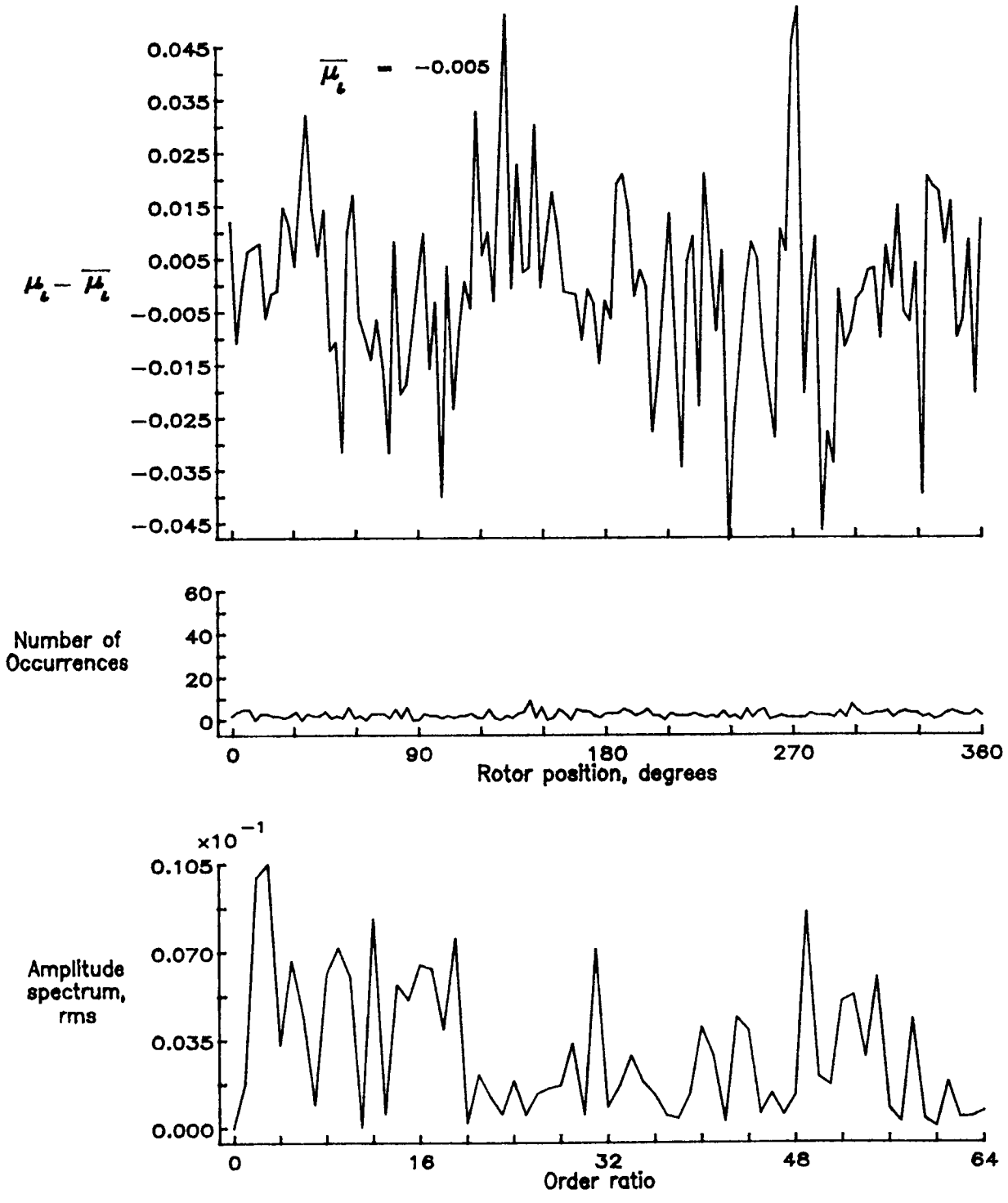


Figure 150.– Induced inflow velocity measured at 270 degrees and r/R of 1.12.

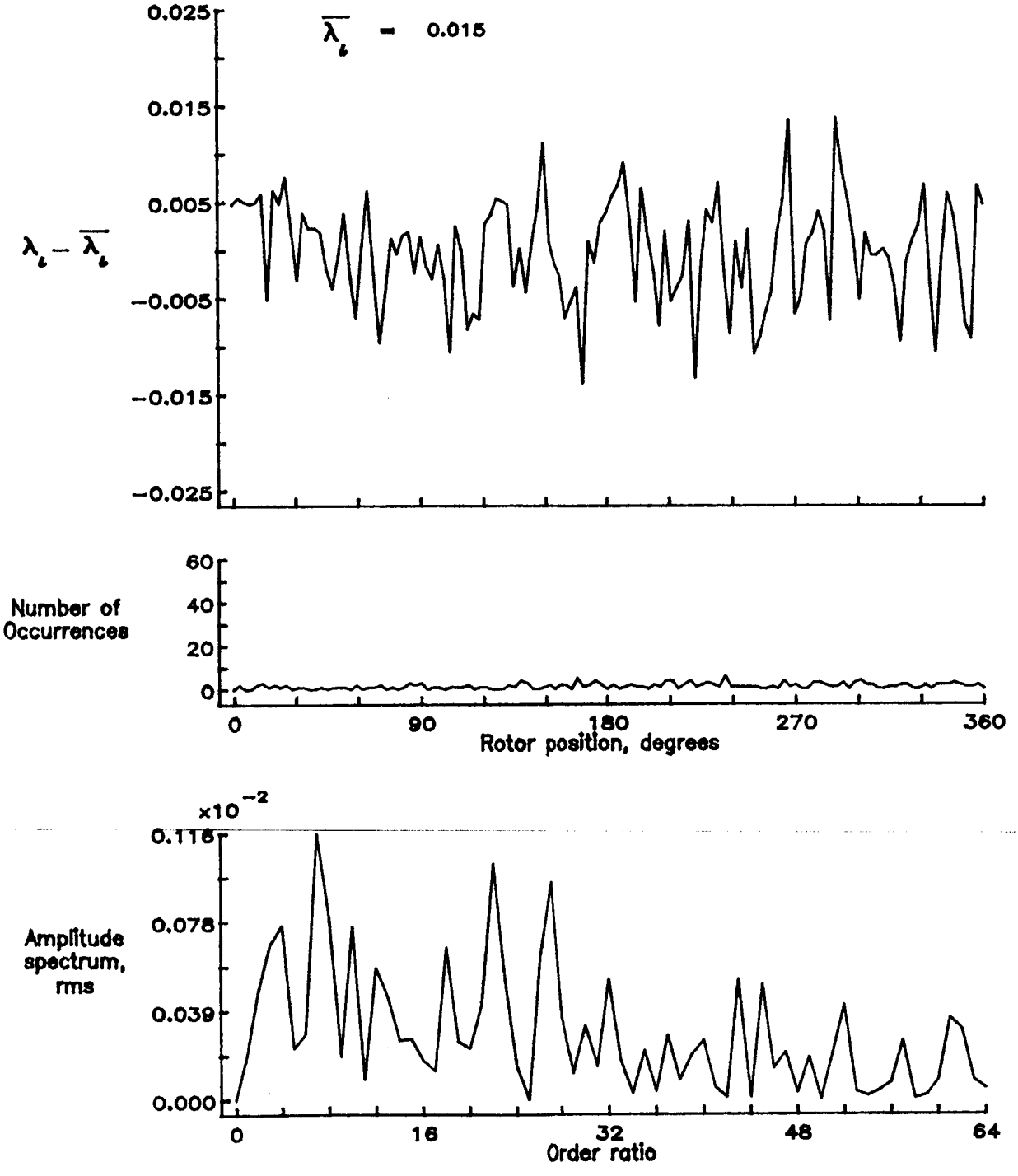


Figure 150.– Concluded.

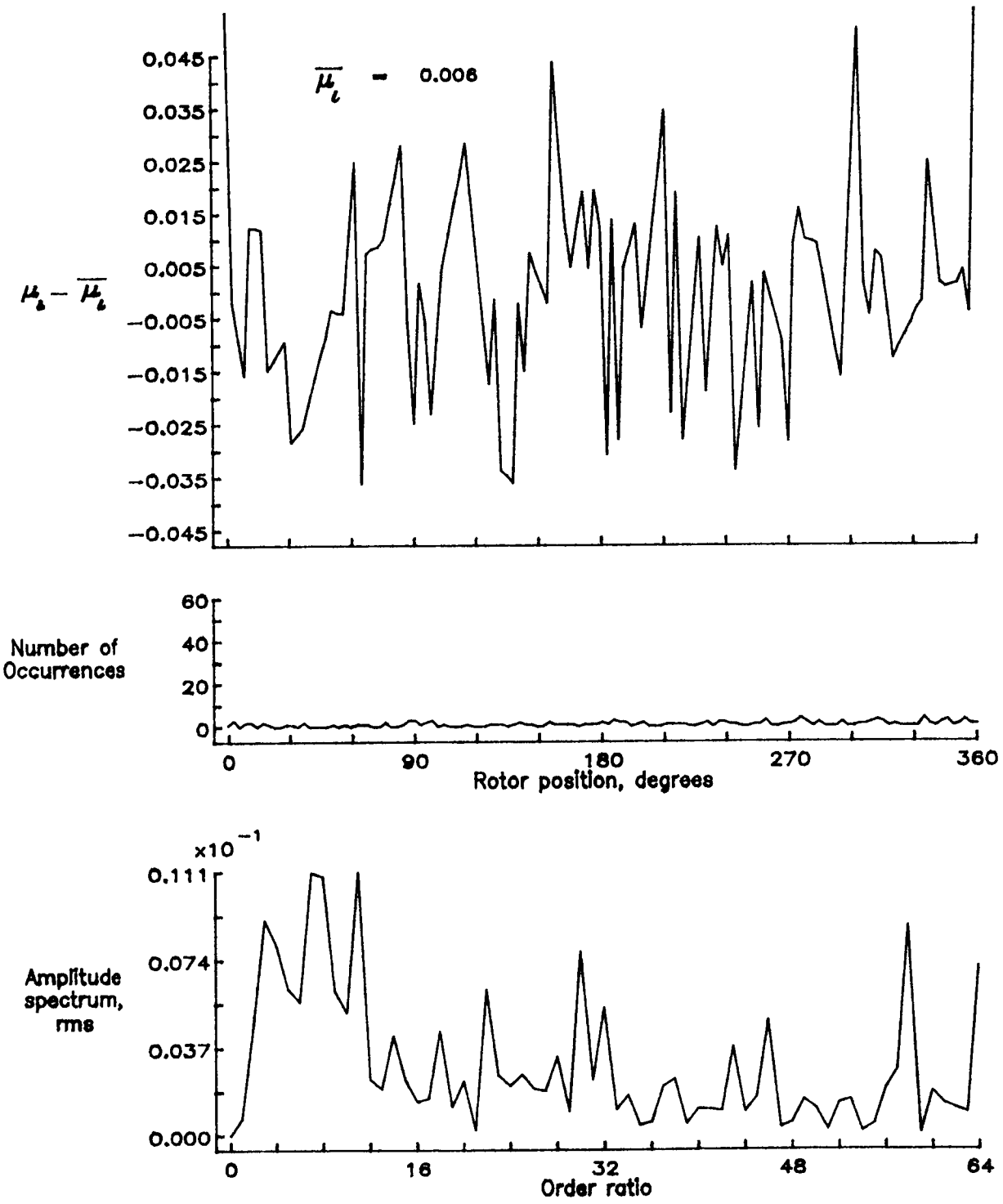


Figure 151.– Induced inflow velocity measured at 300 degrees and r/R of 0.20.

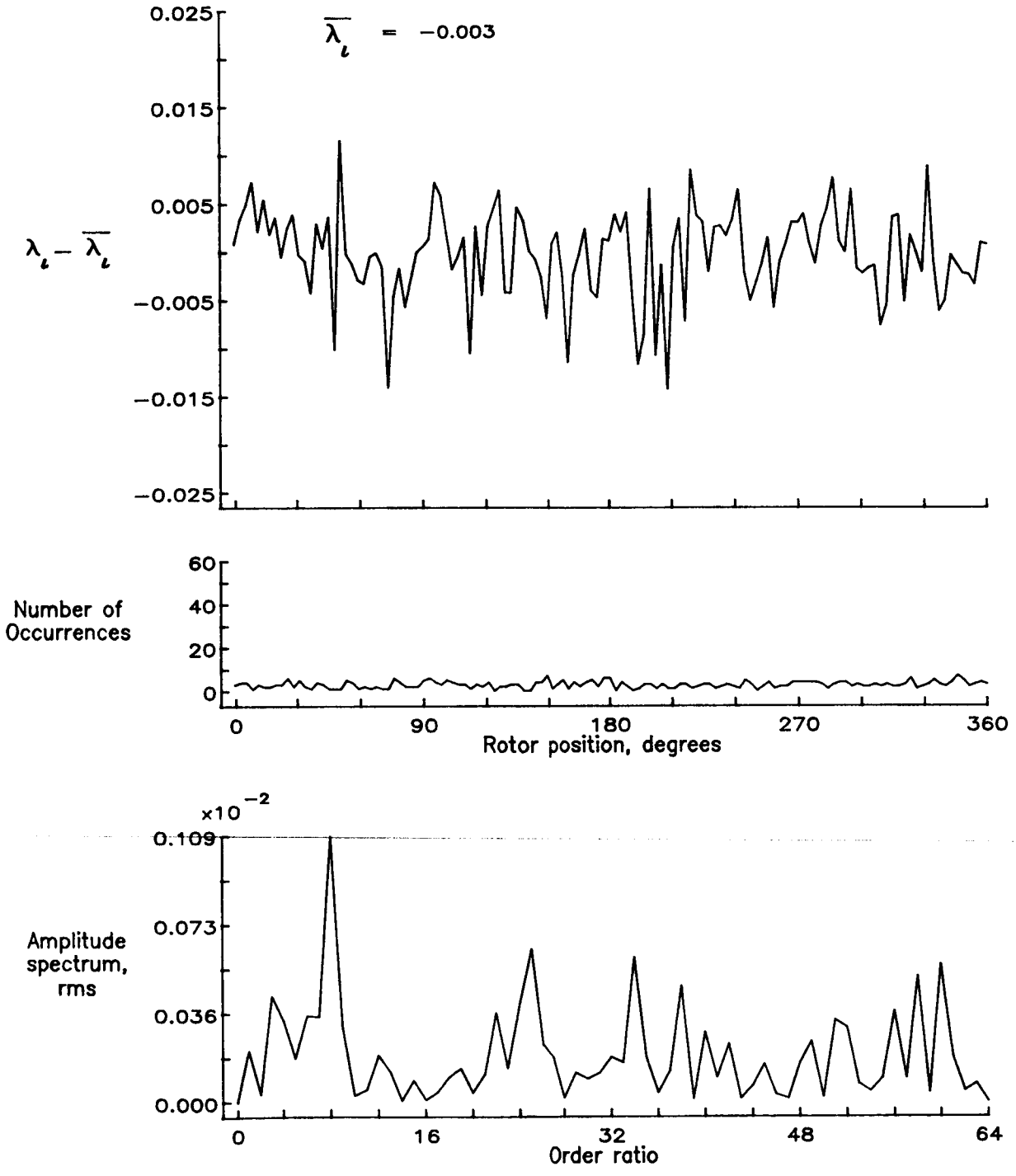


Figure 151.– Concluded.

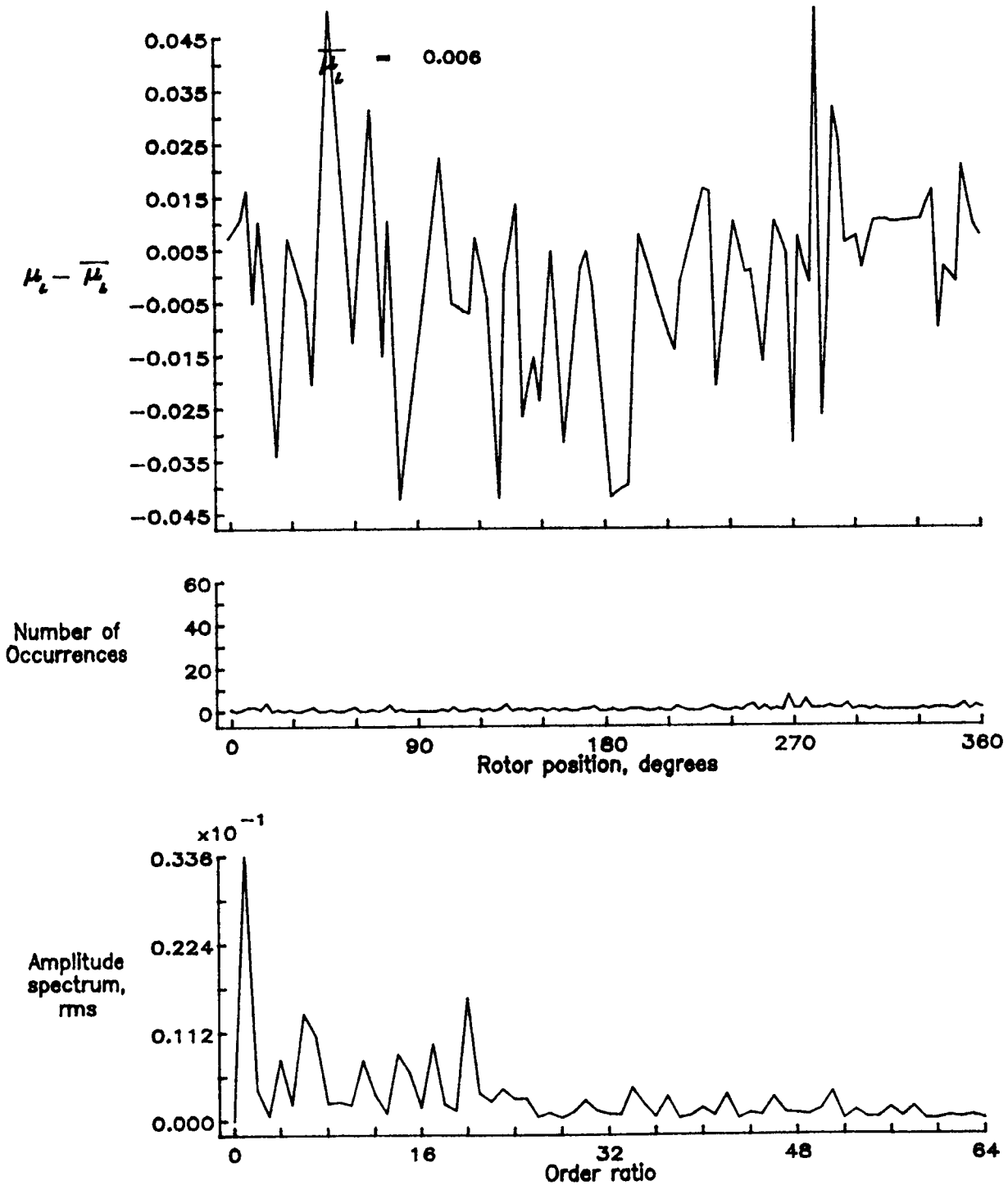


Figure 152.– Induced inflow velocity measured at 300 degrees and r/R of 0.40.

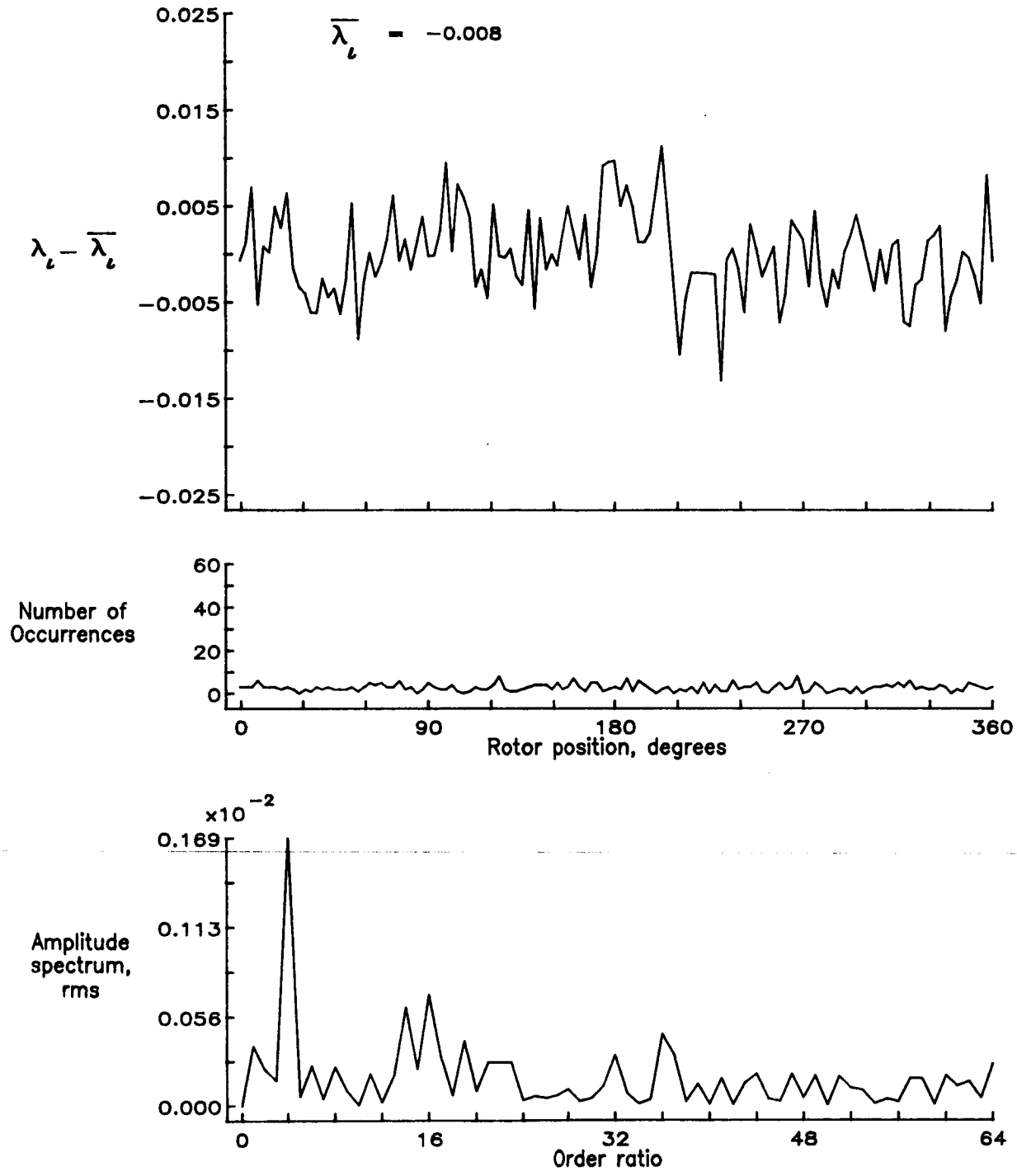


Figure 152.– Concluded.

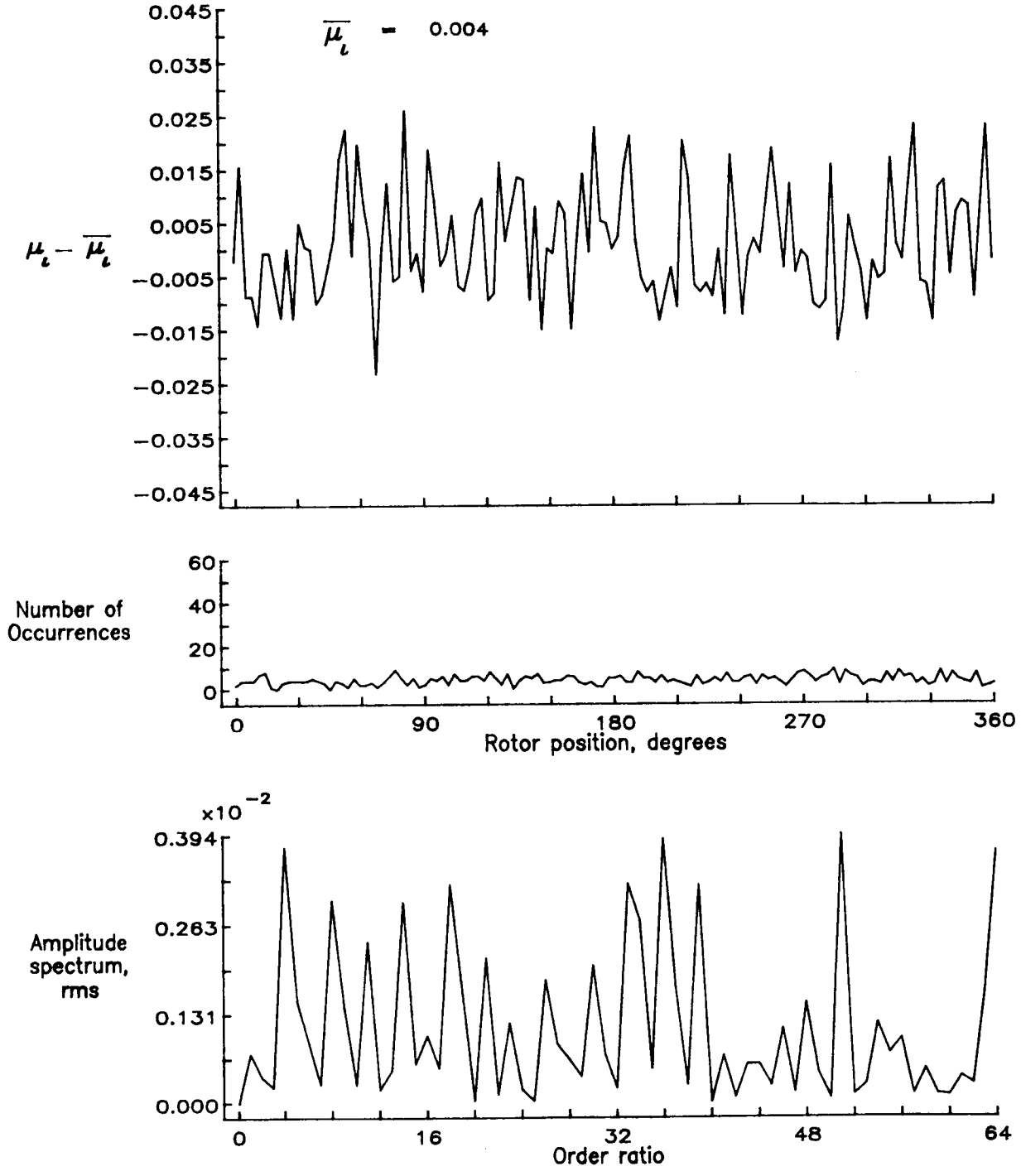


Figure 153.– Induced inflow velocity measured at 300 degrees and r/R of 0.50.

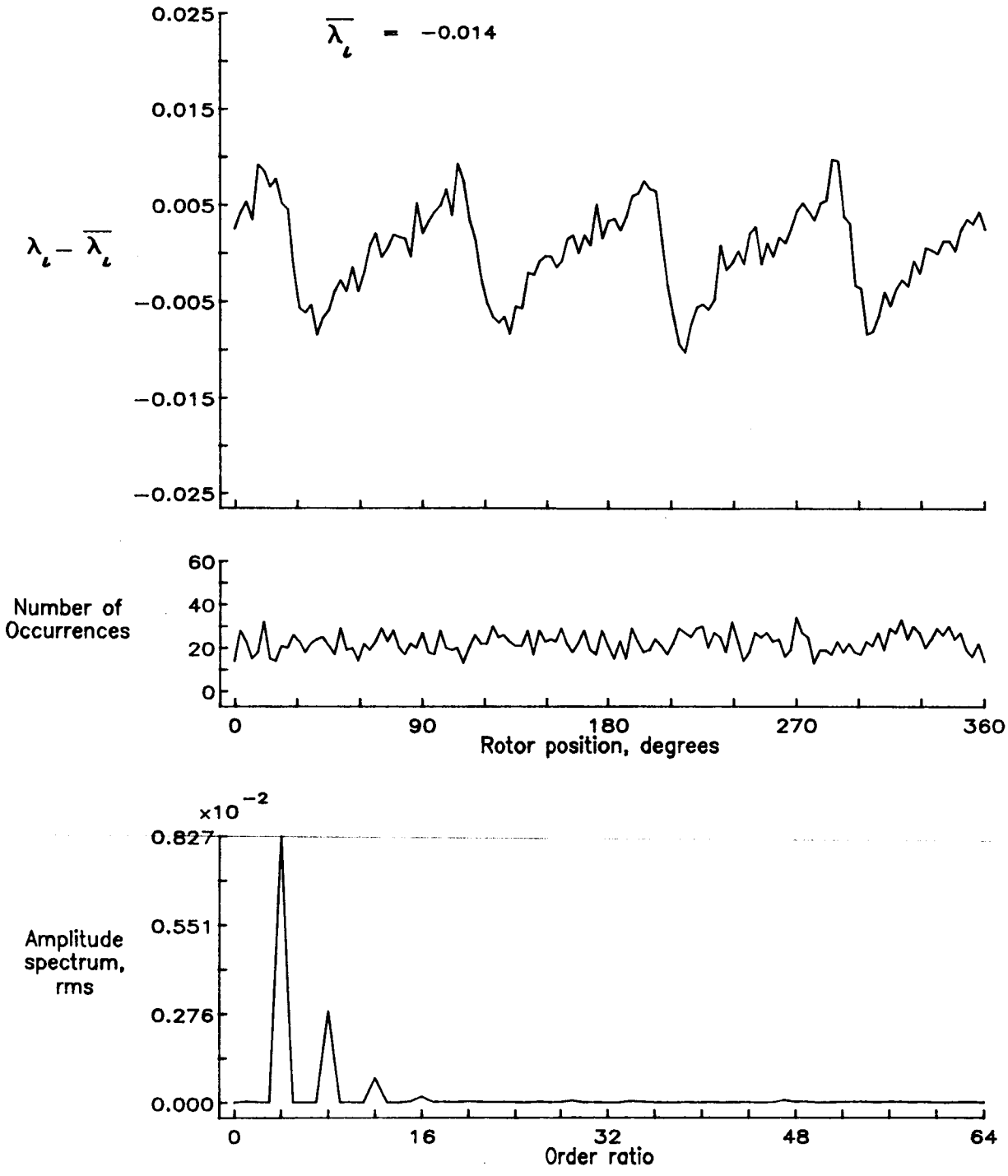


Figure 153.– Concluded.

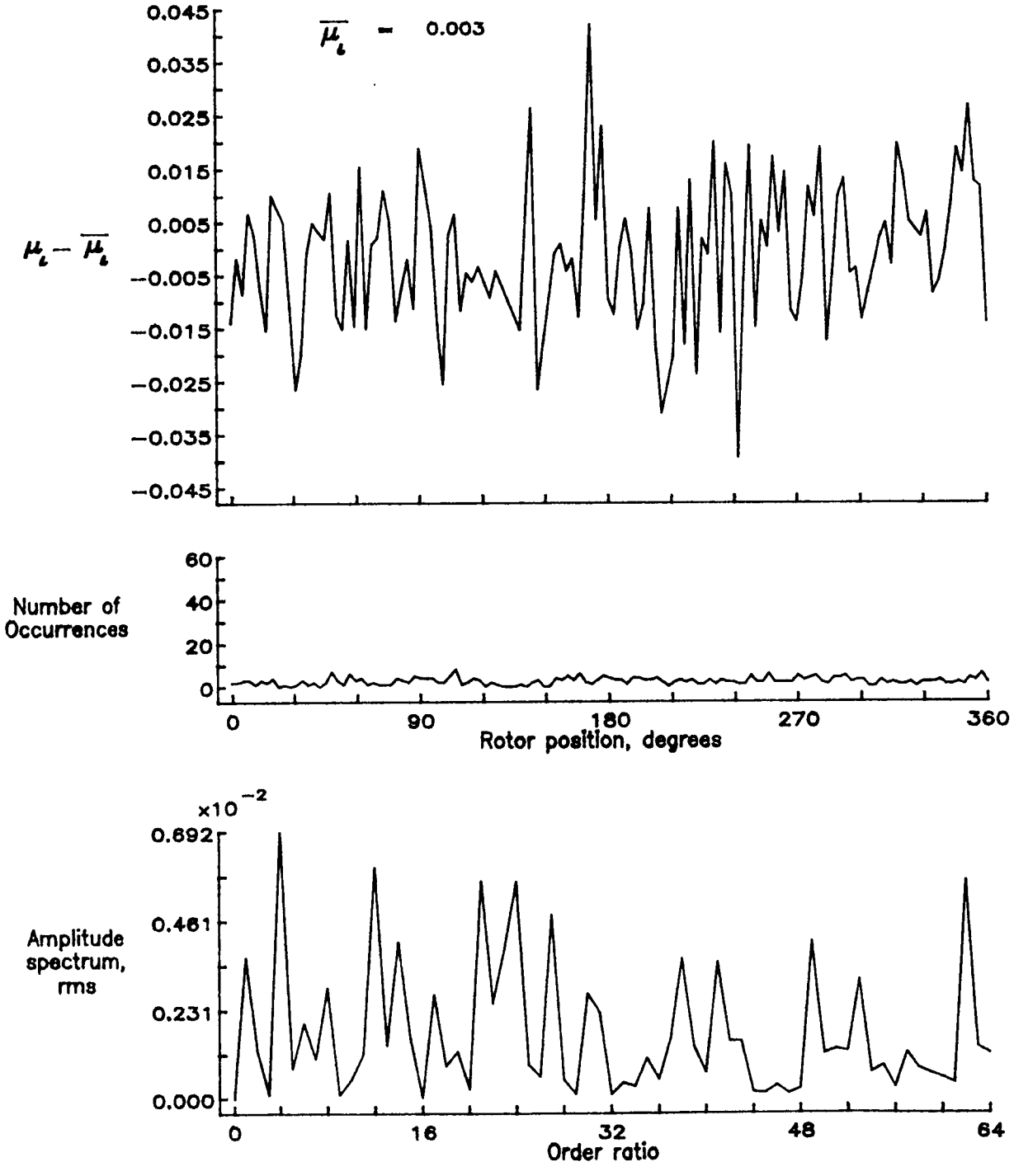


Figure 154.– Induced inflow velocity measured at 300 degrees and r/R of 0.60.

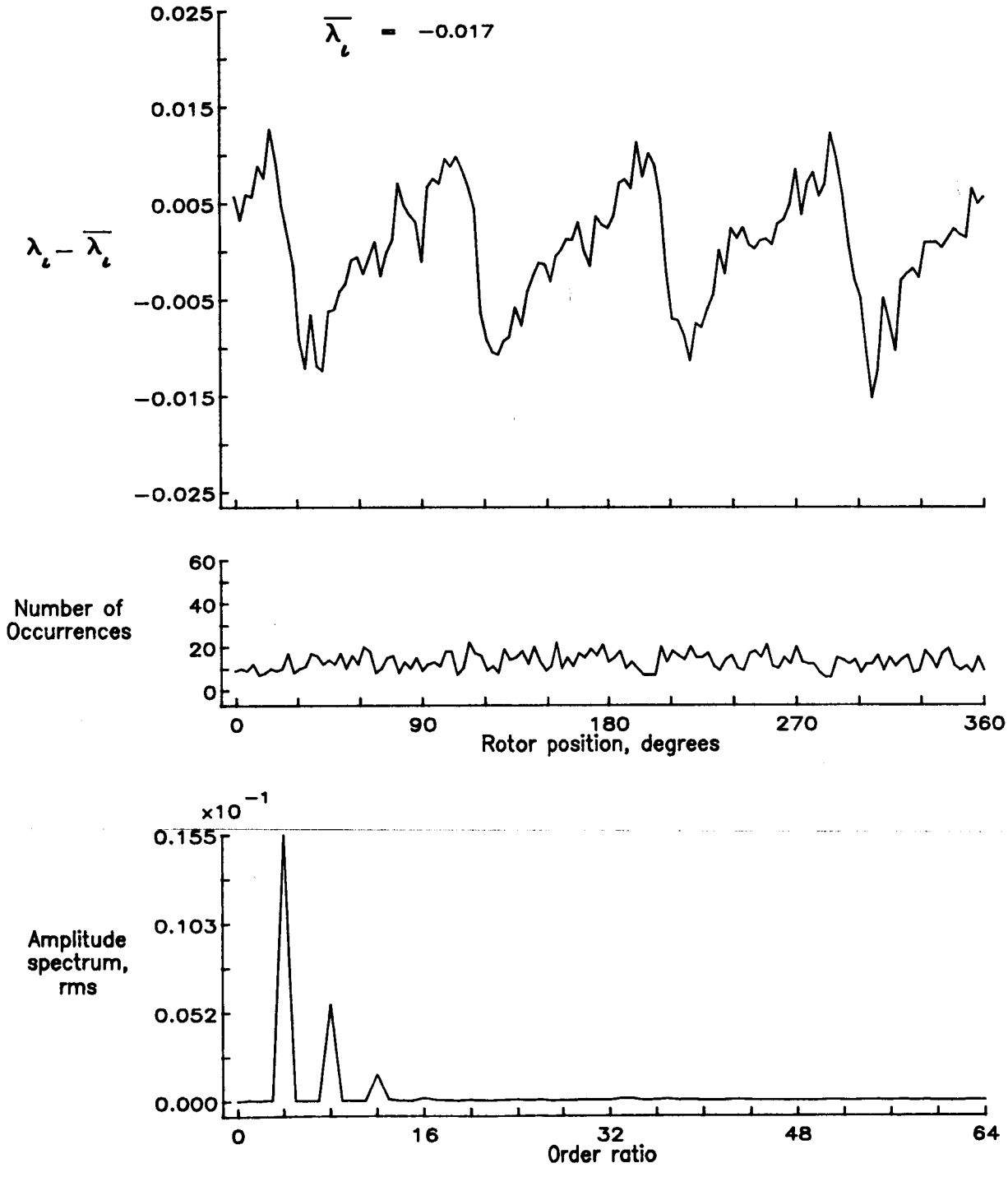


Figure 154.– Concluded.

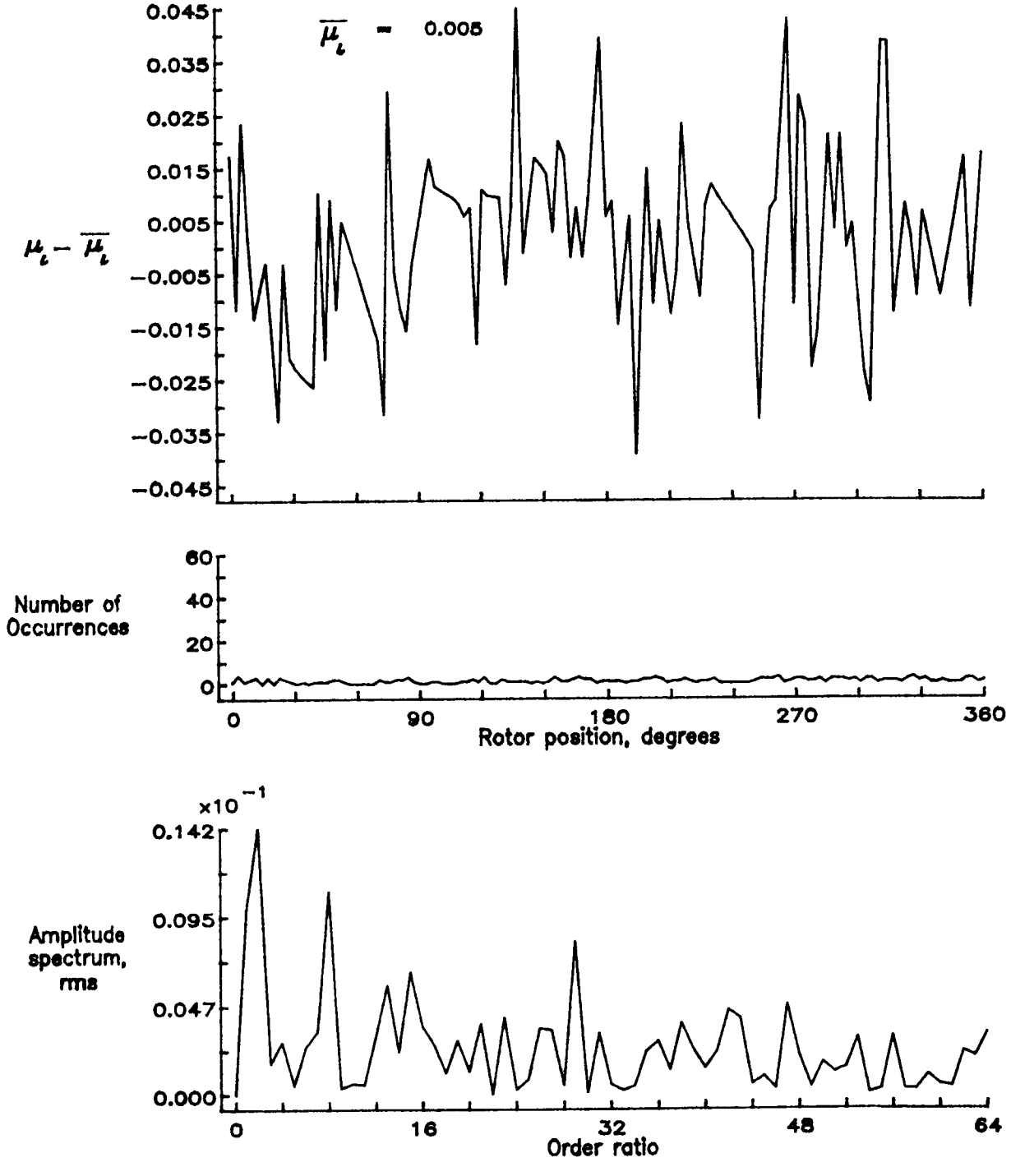


Figure 155.– Induced inflow velocity measured at 300 degrees and r/R of 0.70.

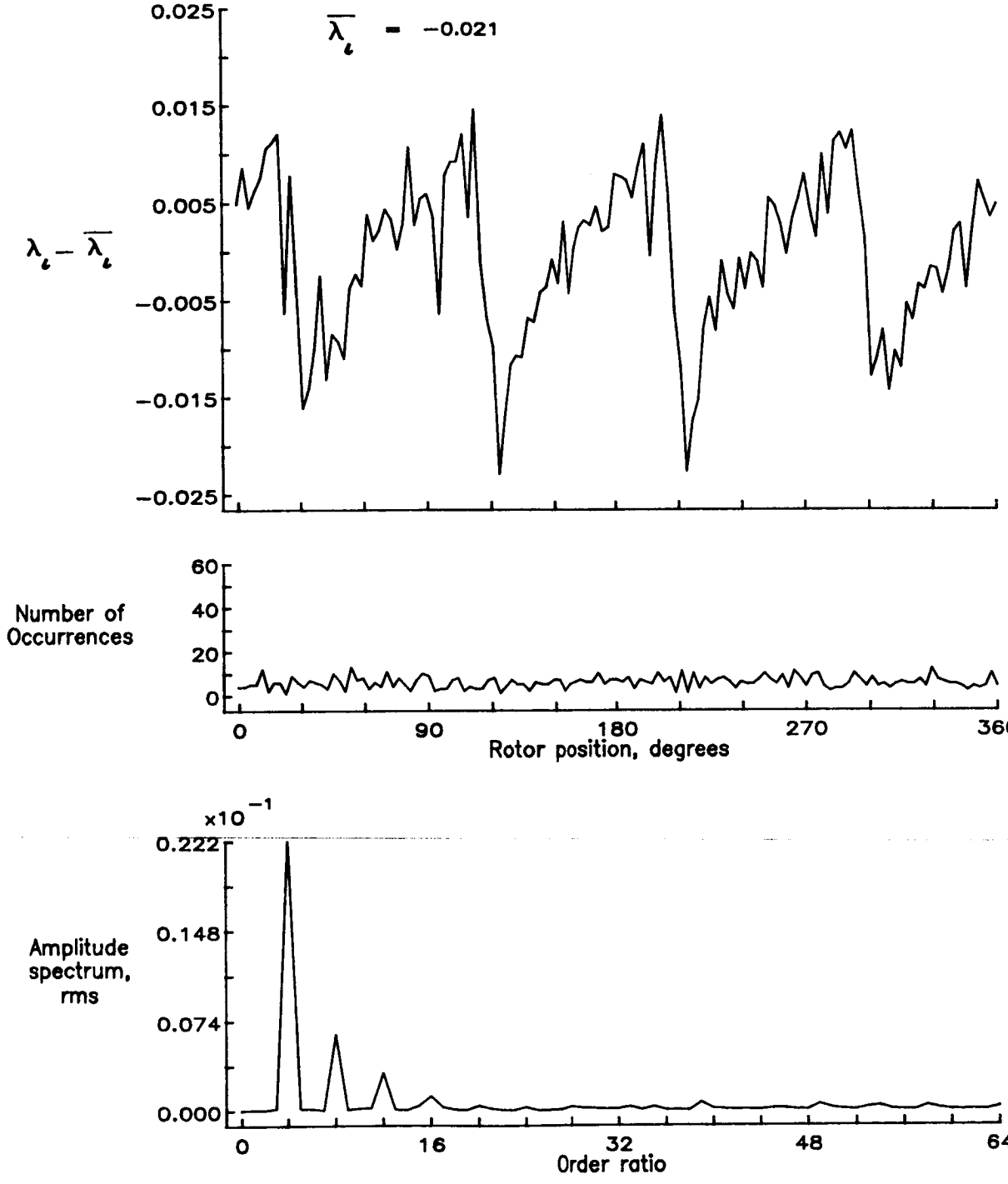


Figure 155.– Concluded.

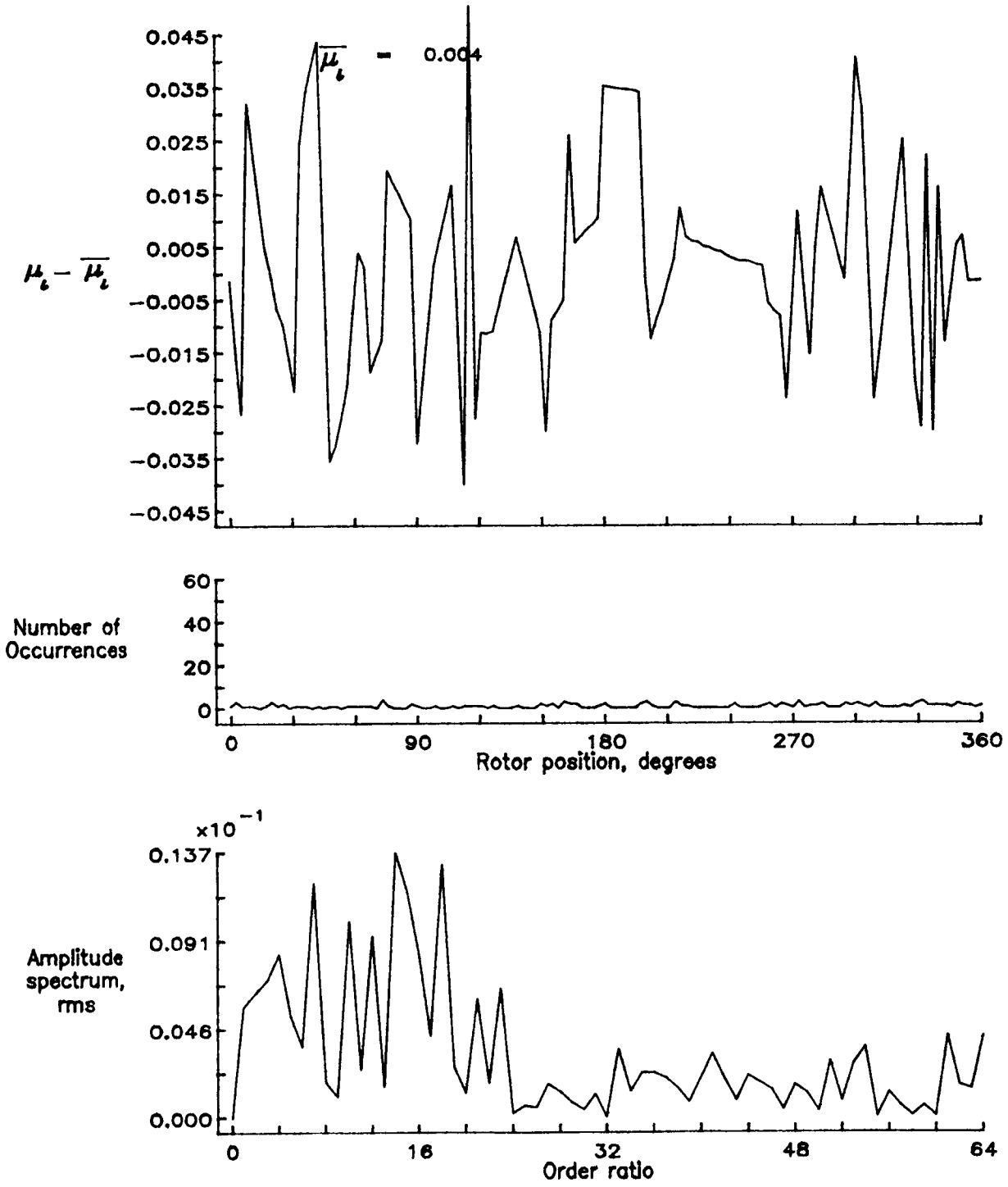


Figure 156.– Induced inflow velocity measured at 300 degrees and r/R of 0.74.

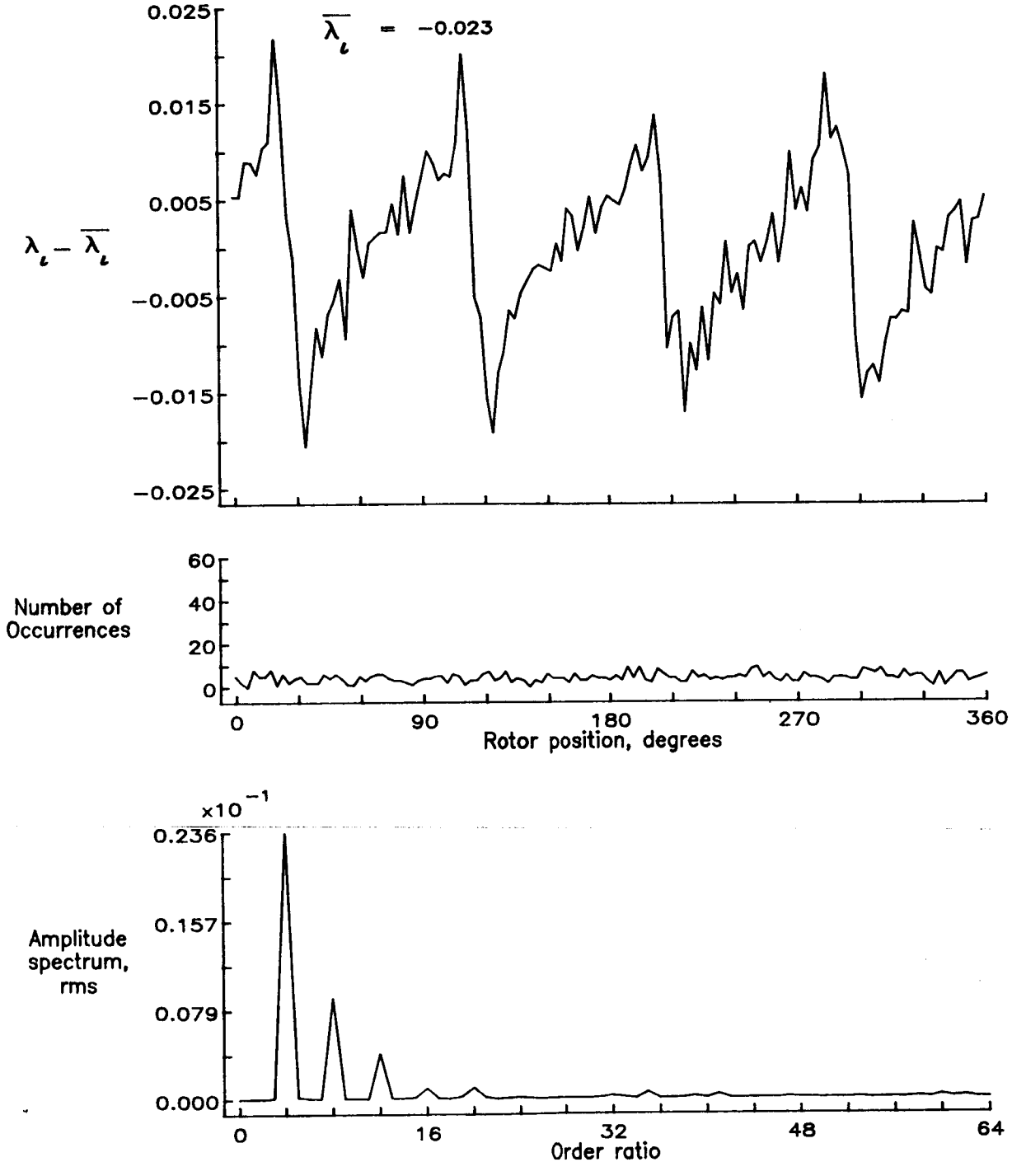


Figure 156.– Concluded.

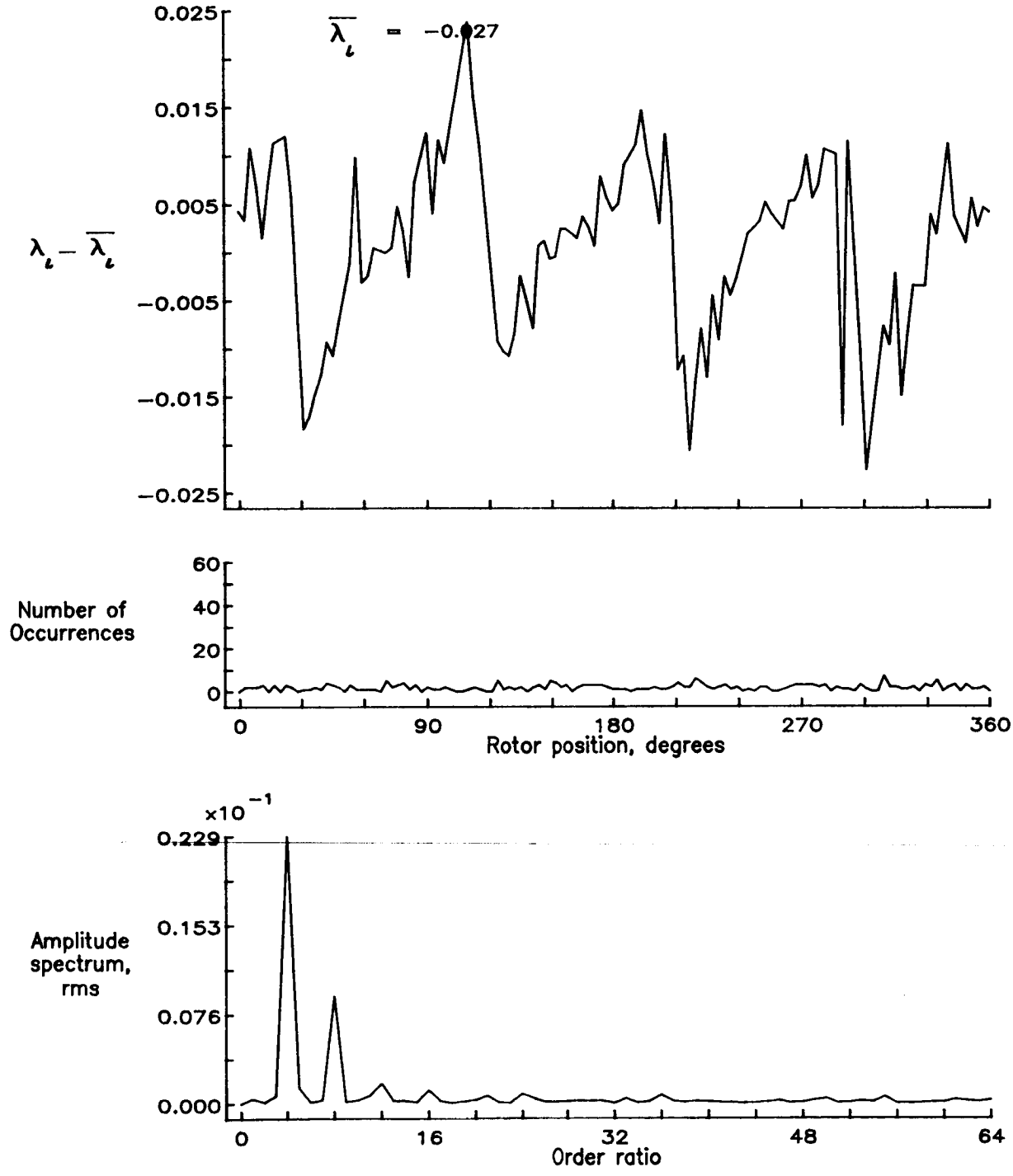


Figure 157.– Induced inflow velocity measured at 300 degrees and r/R of 0.78.

PRECEDING PAGE BLANK NOT FILMED

PAGE 312 INTENTIONALLY BLANK

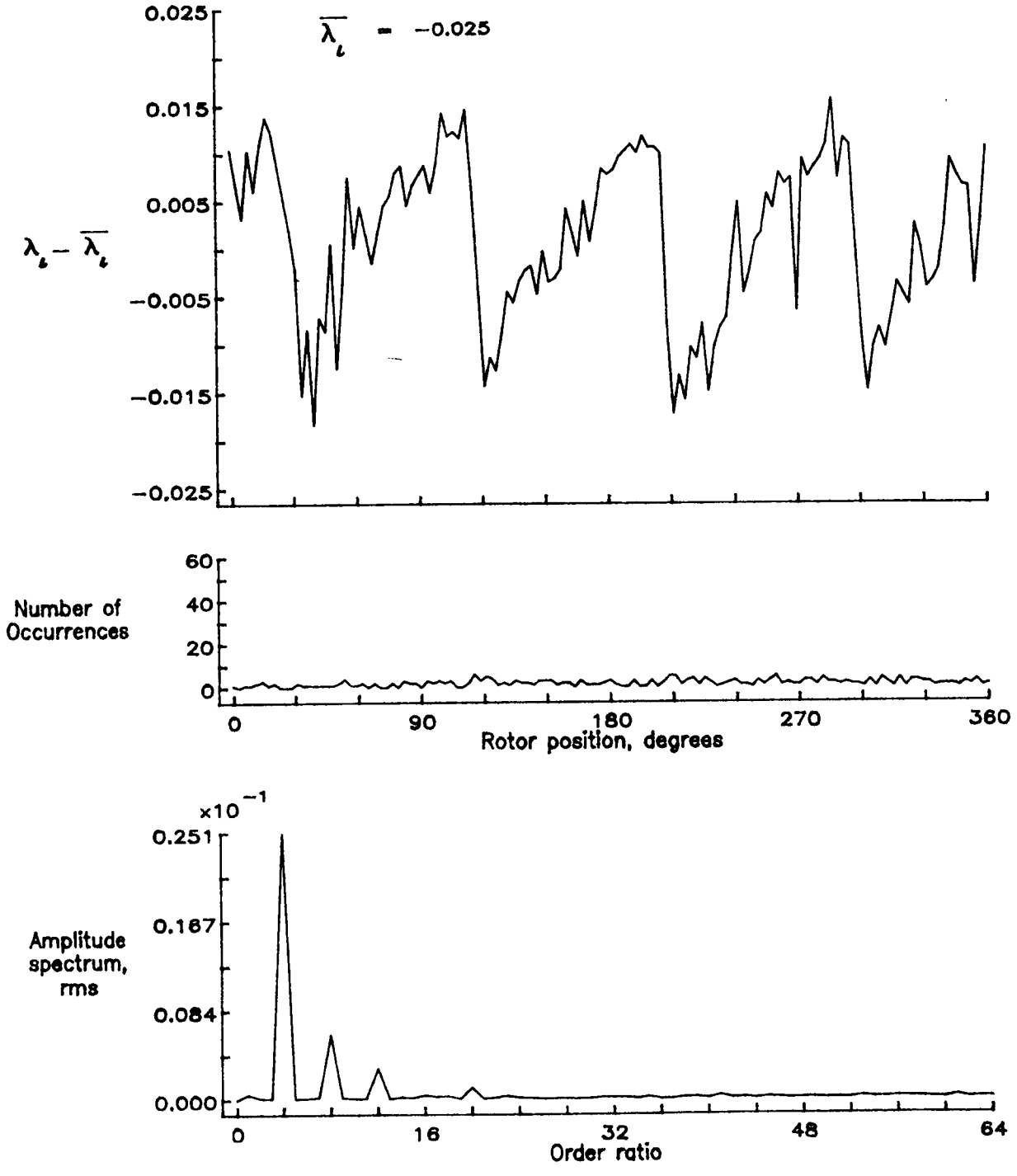


Figure 158.– Induced inflow velocity measured at 300 degrees and r/R of 0.82.

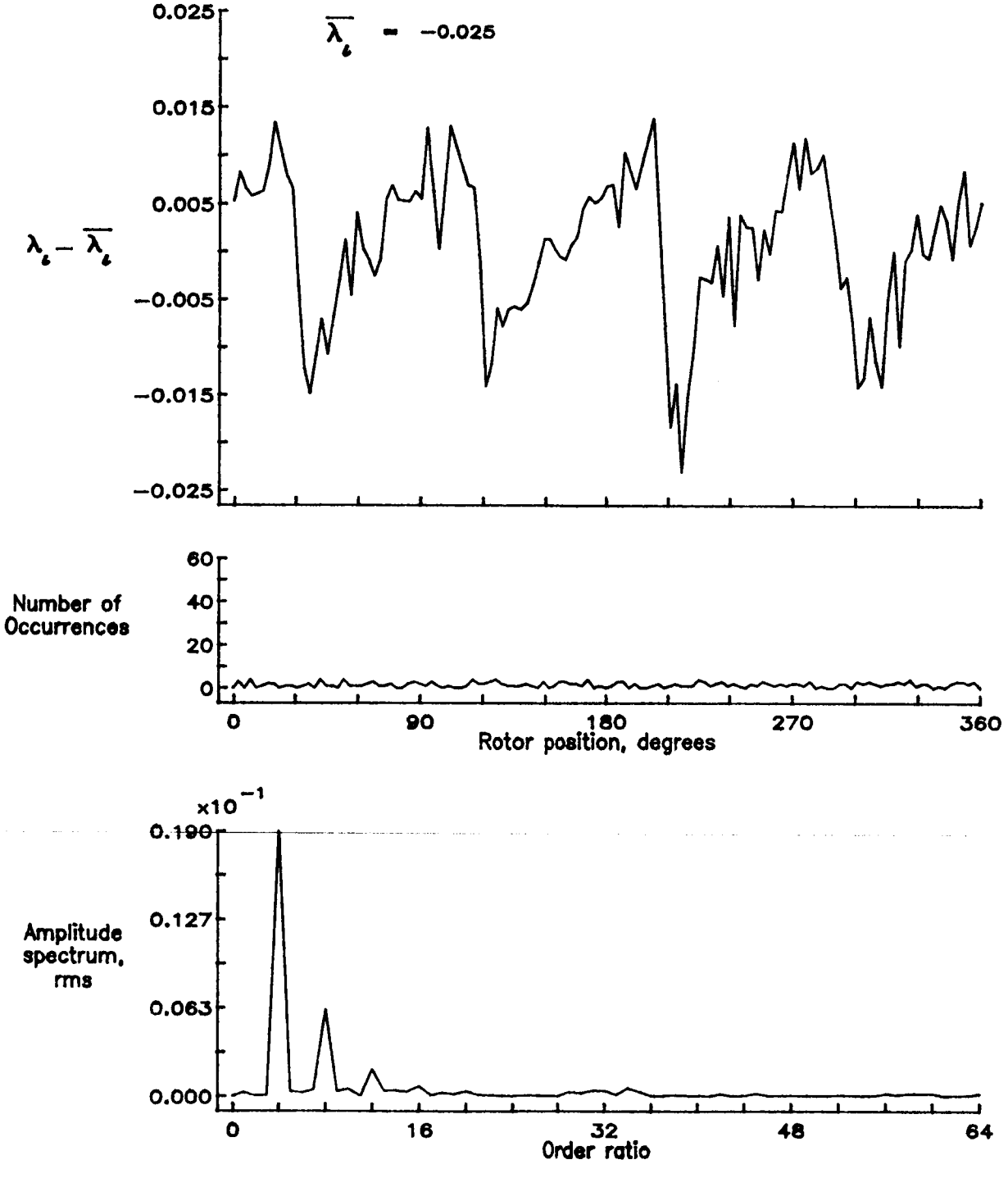


Figure 159.– Induced inflow velocity measured at 300 degrees and r/R of 0.86.

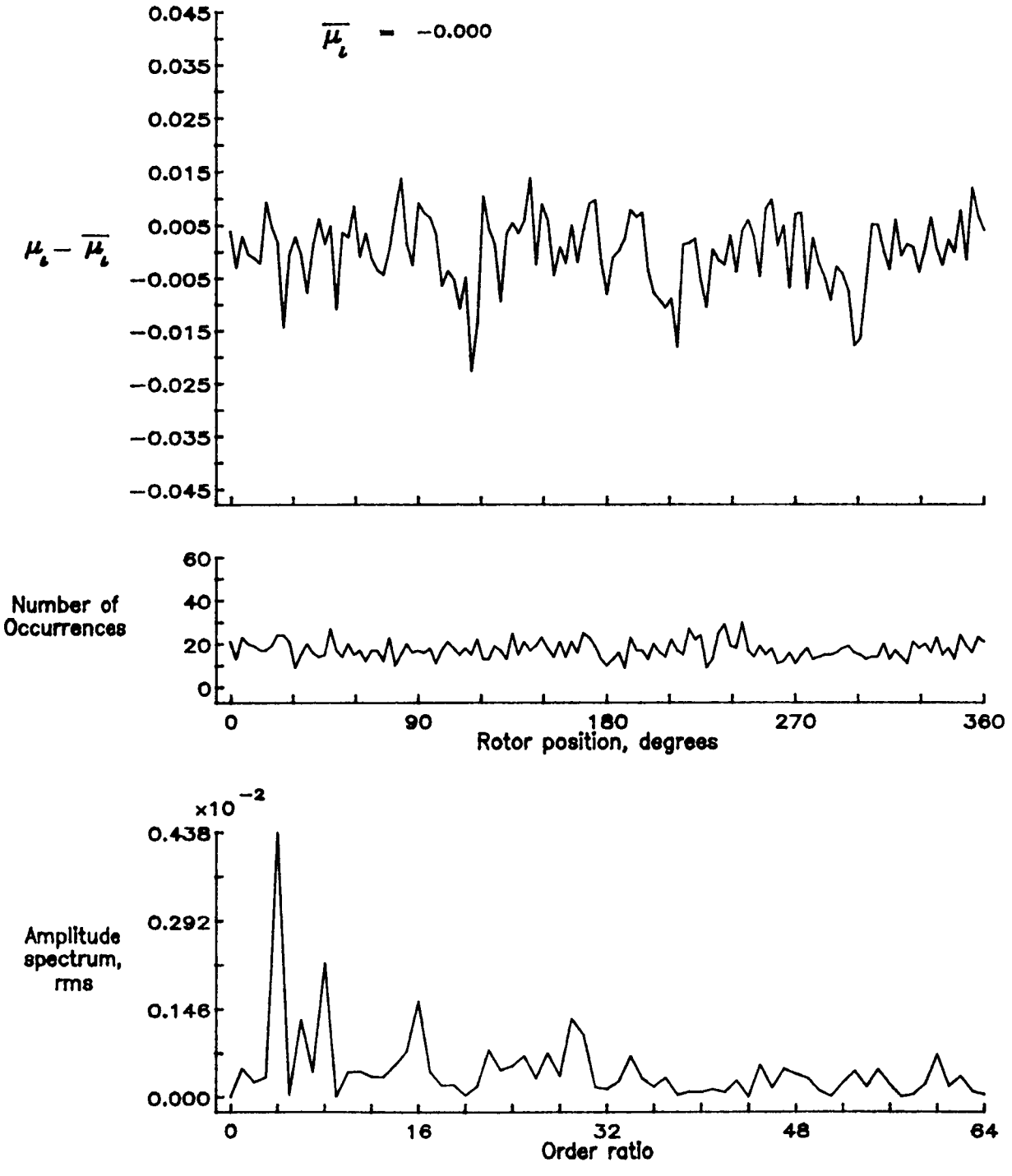


Figure 160.– Induced inflow velocity measured at 300 degrees and r/R of 0.90.

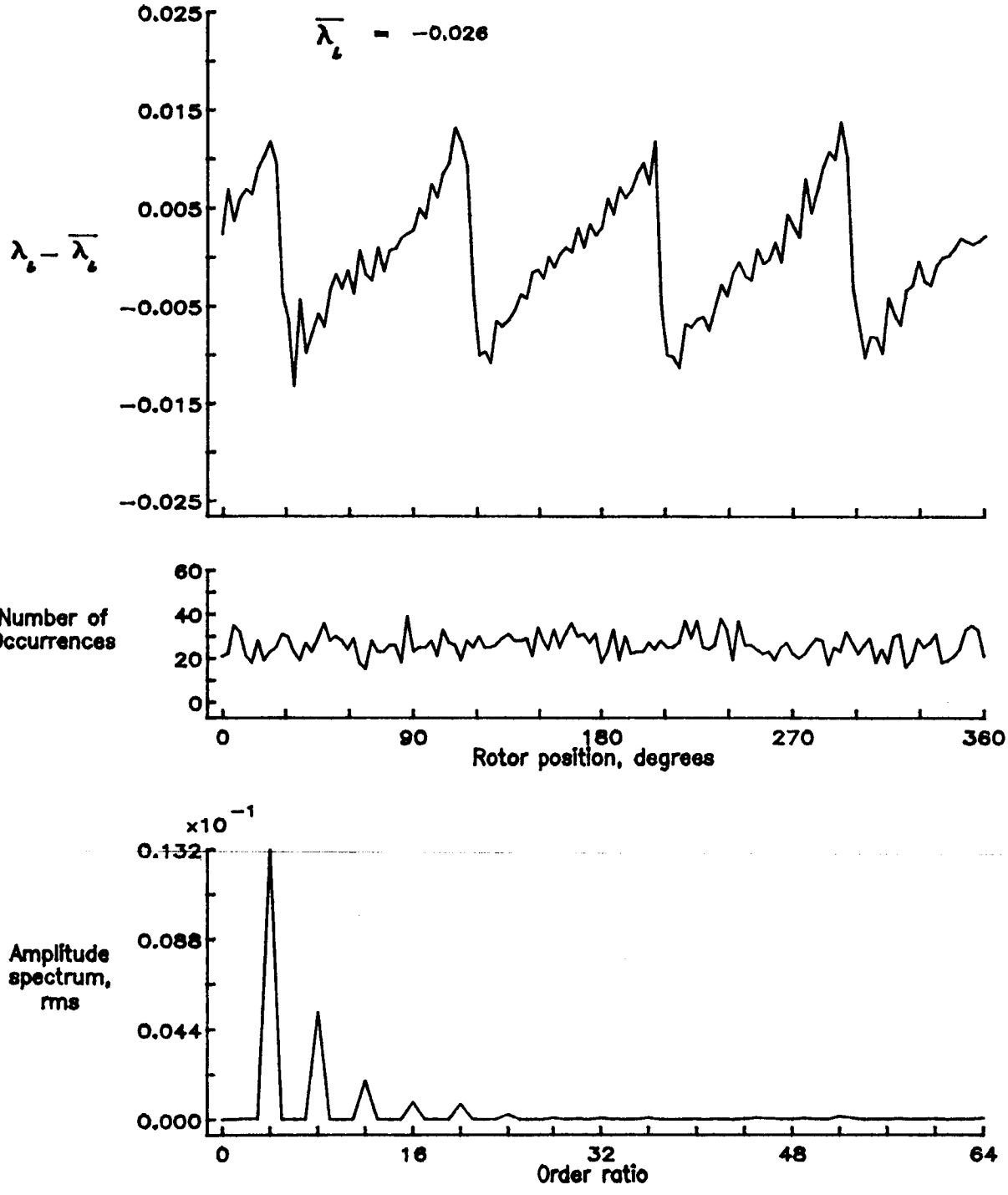


Figure 160.– Concluded.

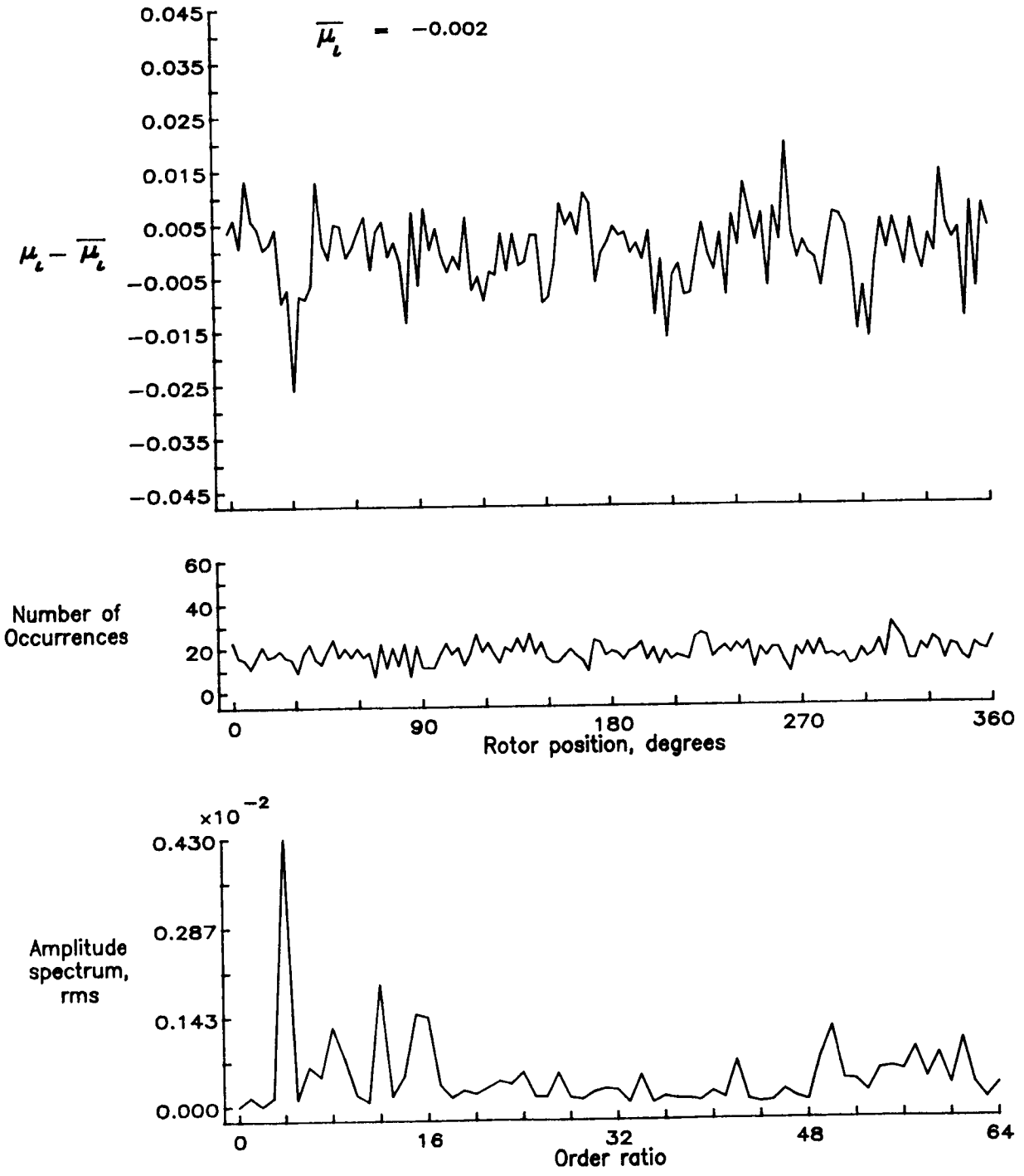


Figure 161.– Induced inflow velocity measured at 300 degrees and r/R of 0.94.

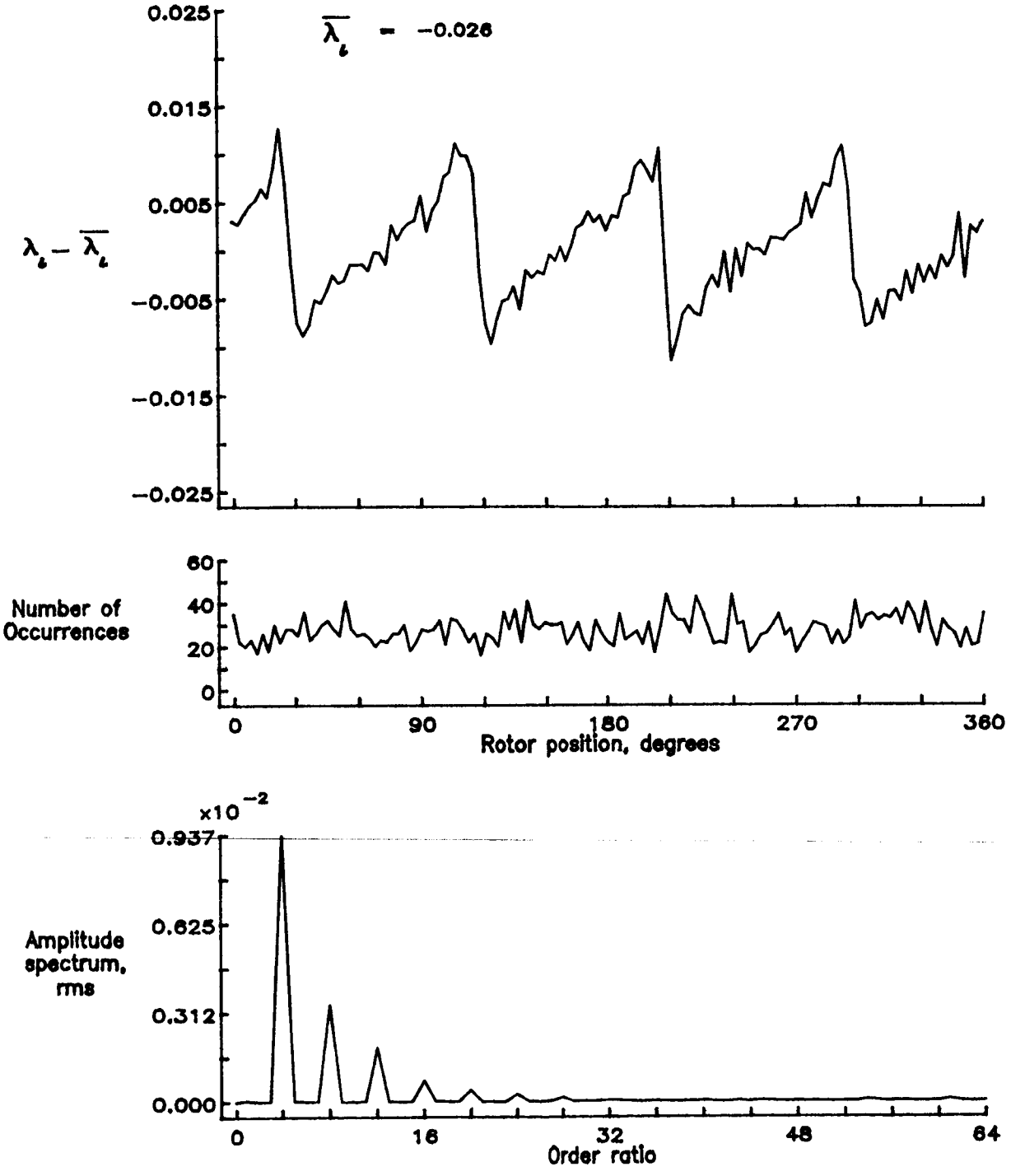


Figure 161.– Concluded.

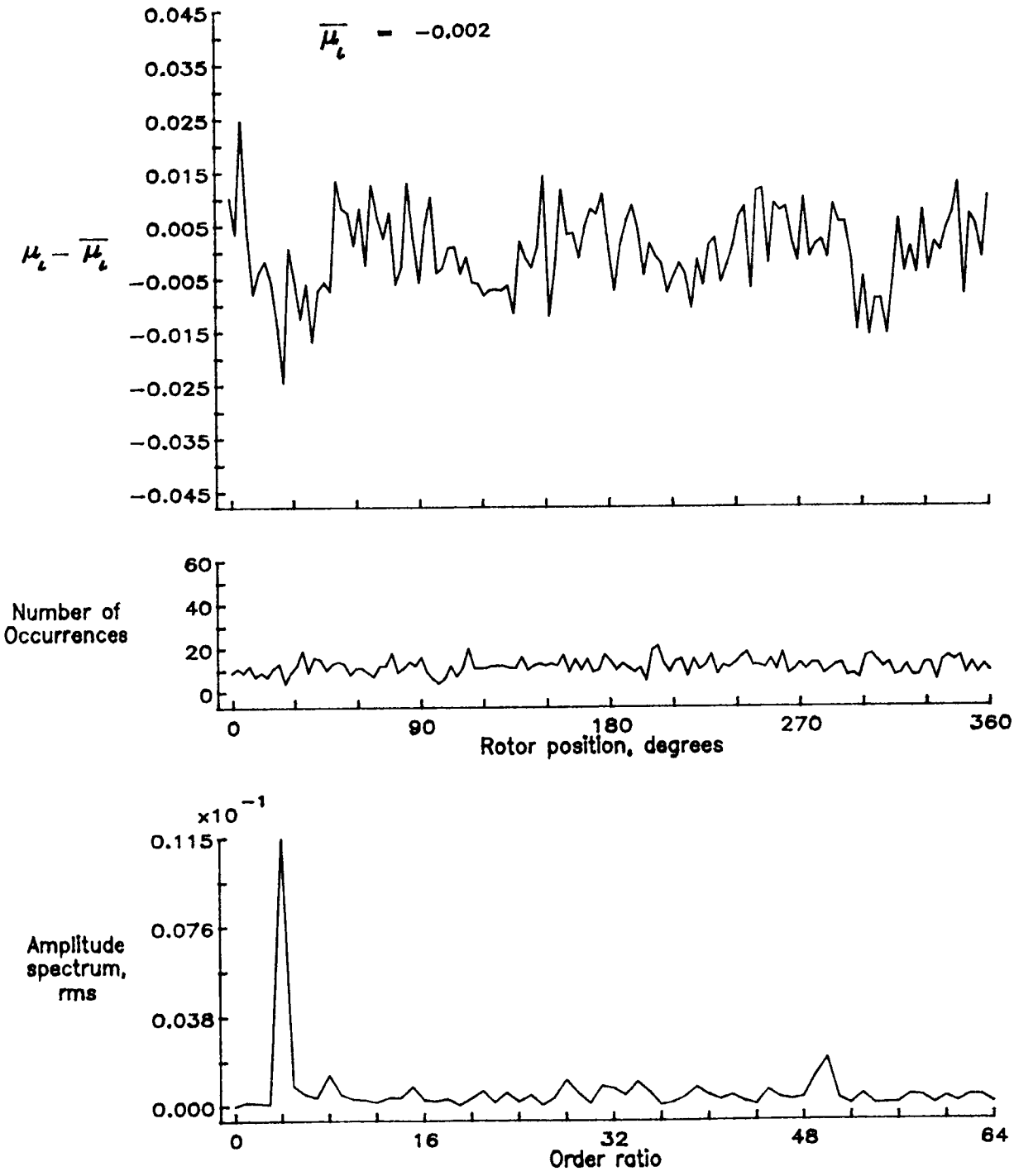


Figure 162.– Induced inflow velocity measured at 300 degrees and r/R of 0.98.

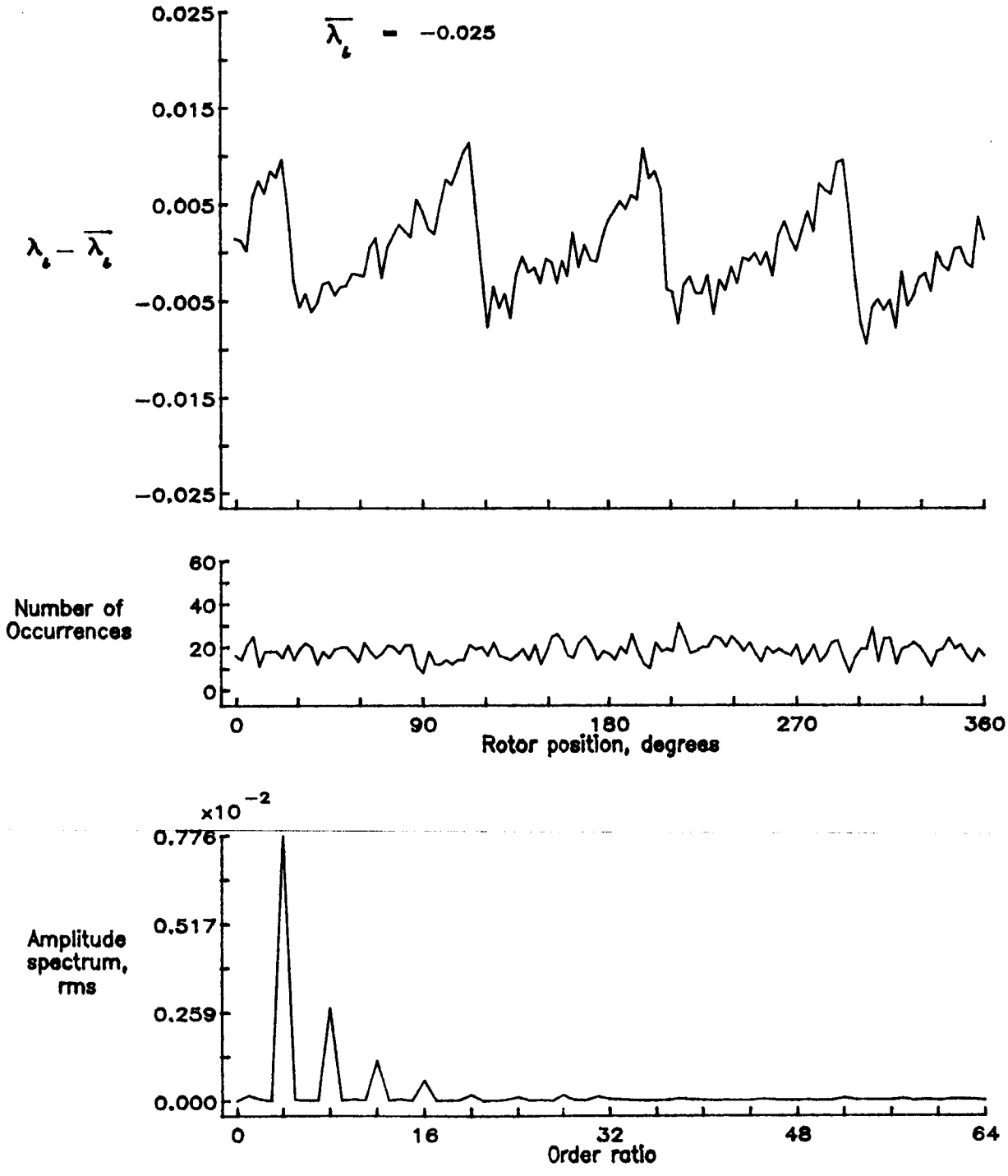


Figure 162.– Concluded.

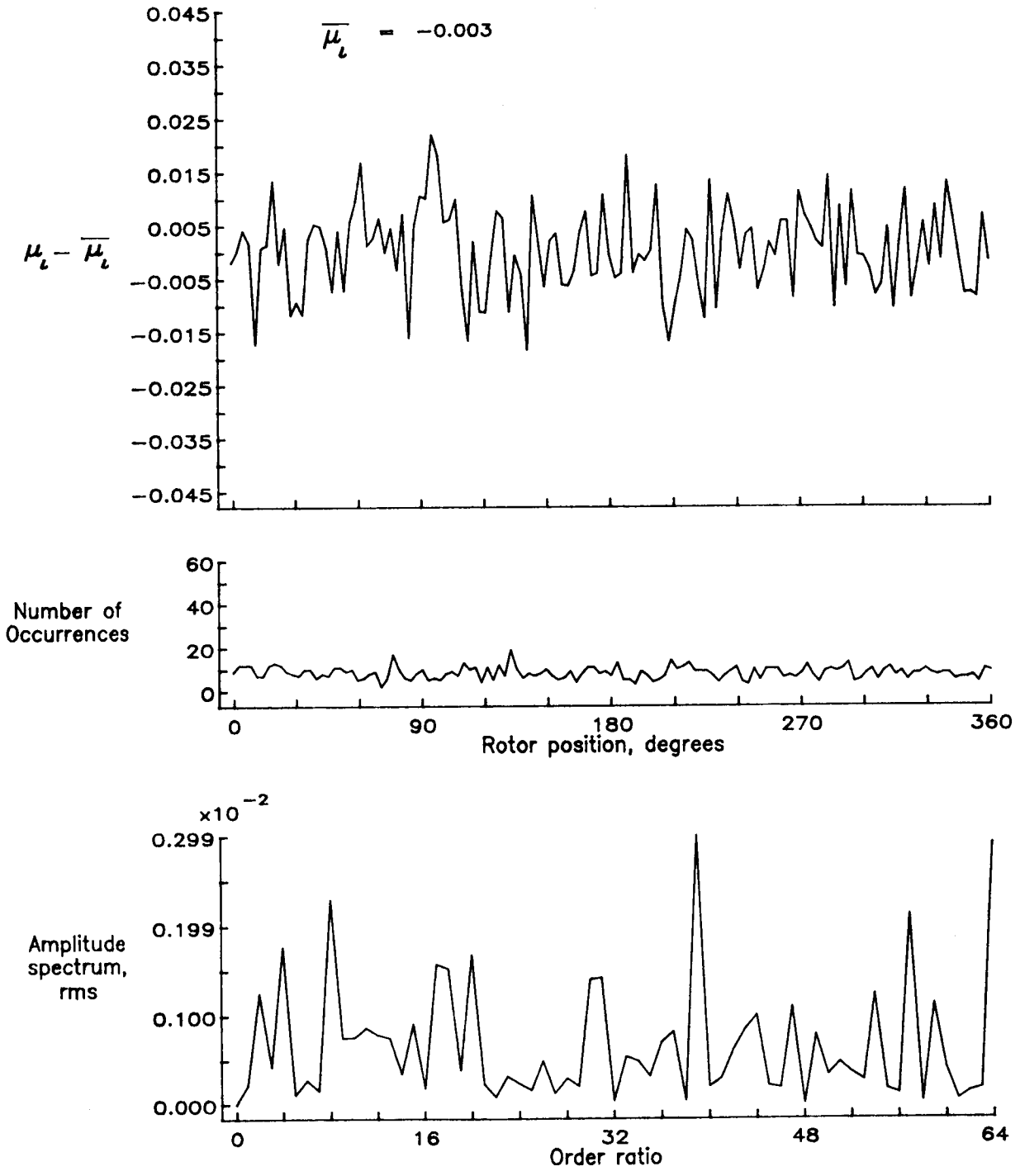


Figure 163.– Induced inflow velocity measured at 300 degrees and r/R of 1.02.

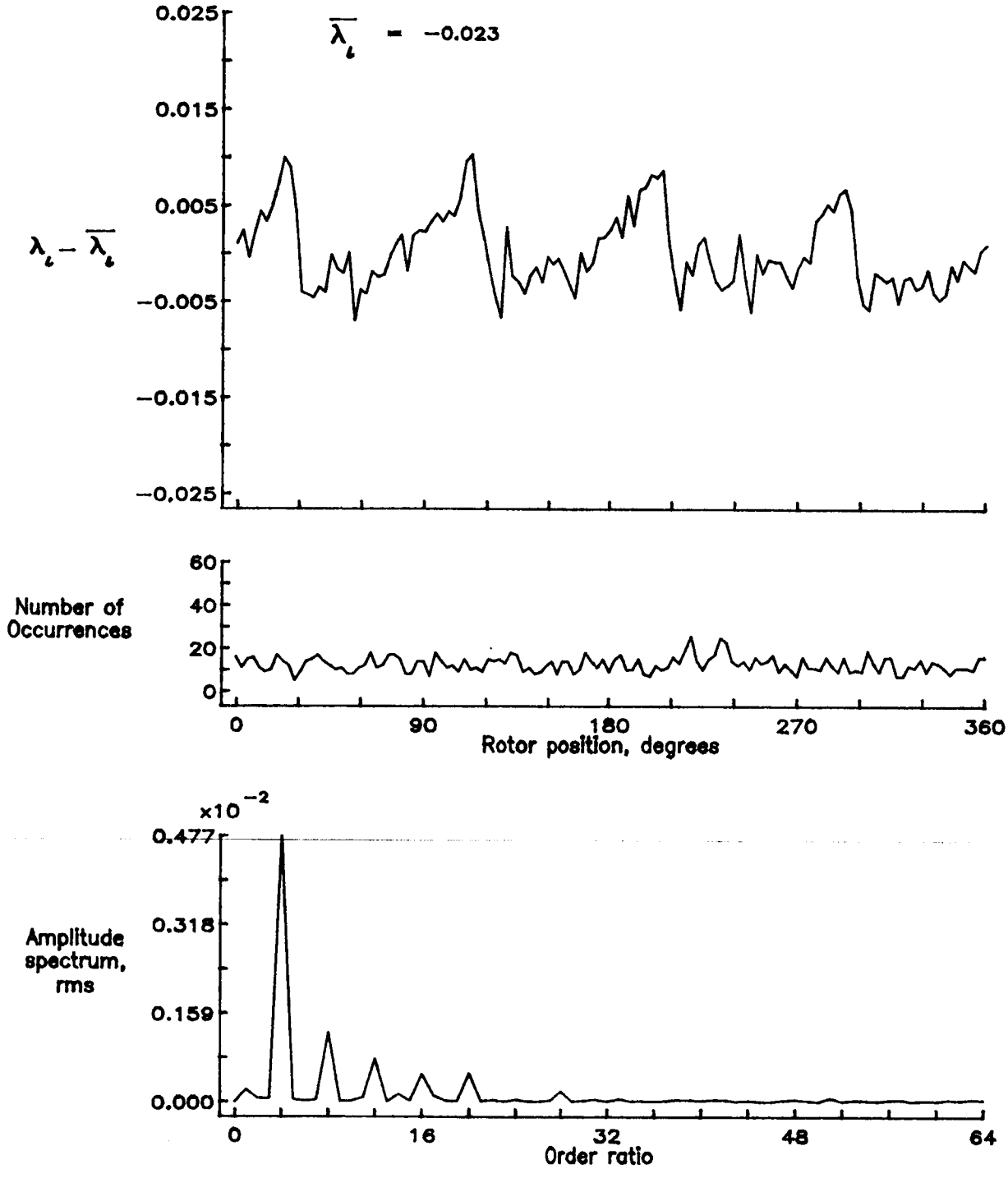


Figure 163.– Concluded.

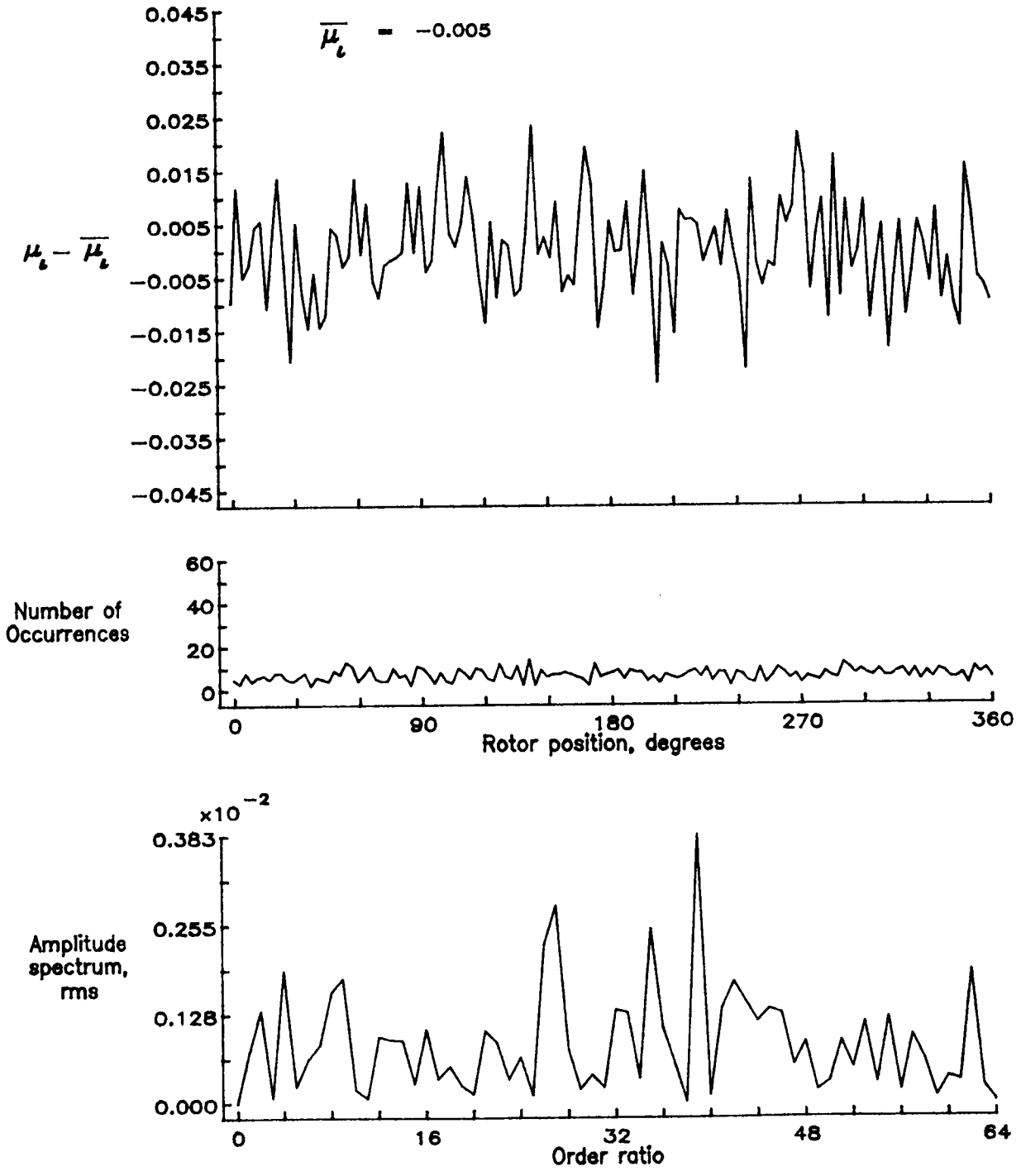


Figure 164.– Induced inflow velocity measured at 300 degrees and r/R of 1.04.

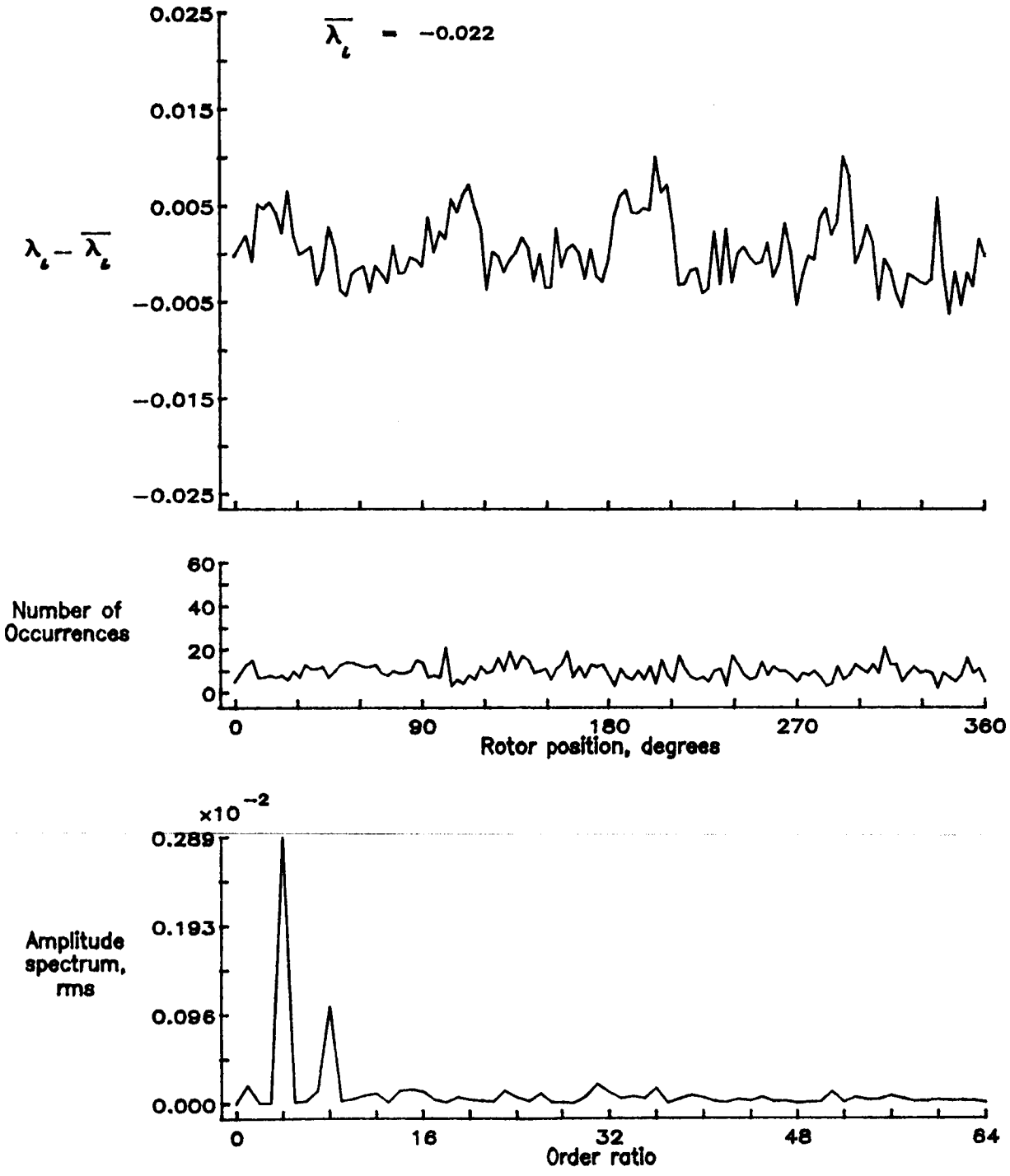


Figure 164.– Concluded.

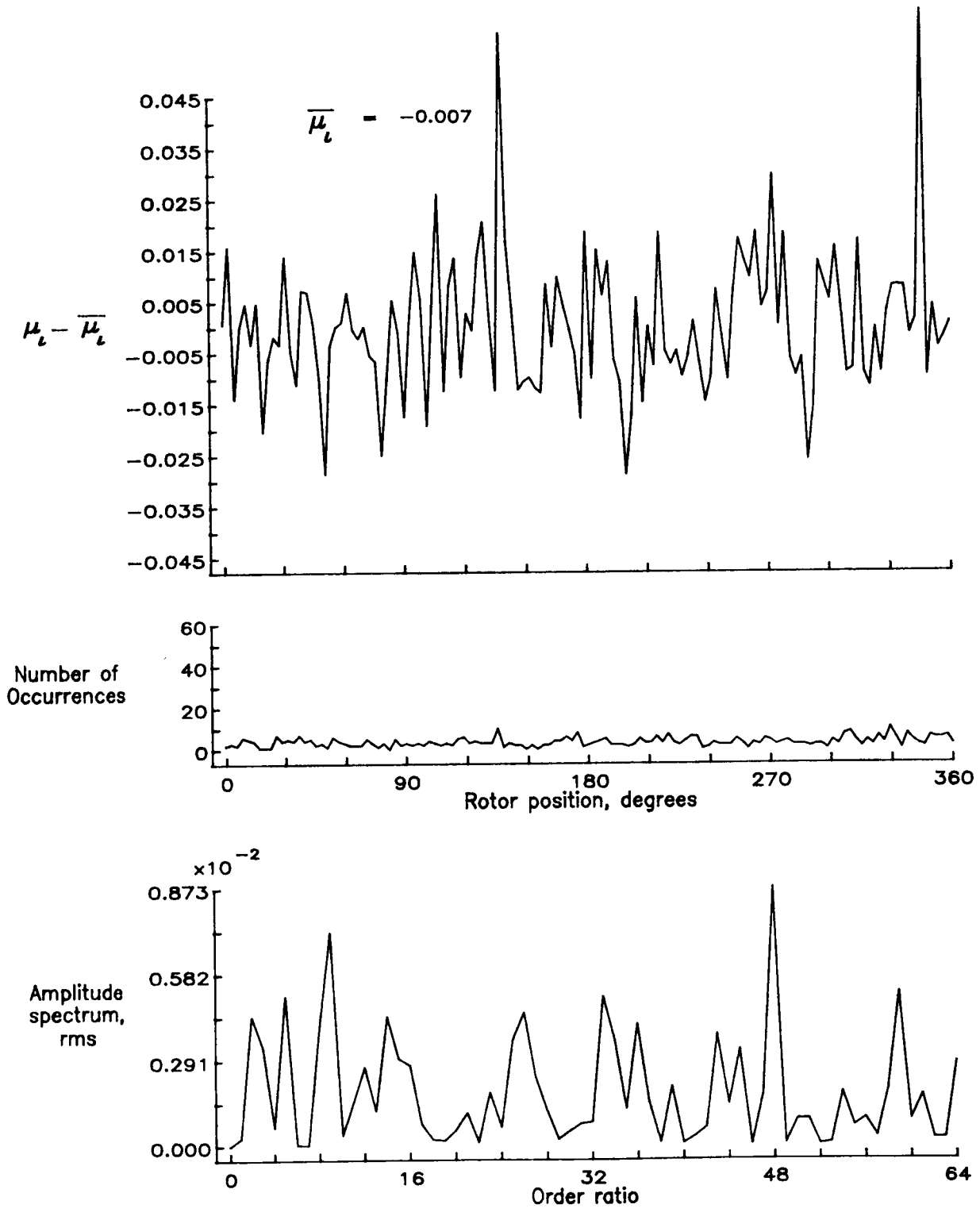


Figure 165.– Induced inflow velocity measured at 300 degrees and r/R of 1.10.

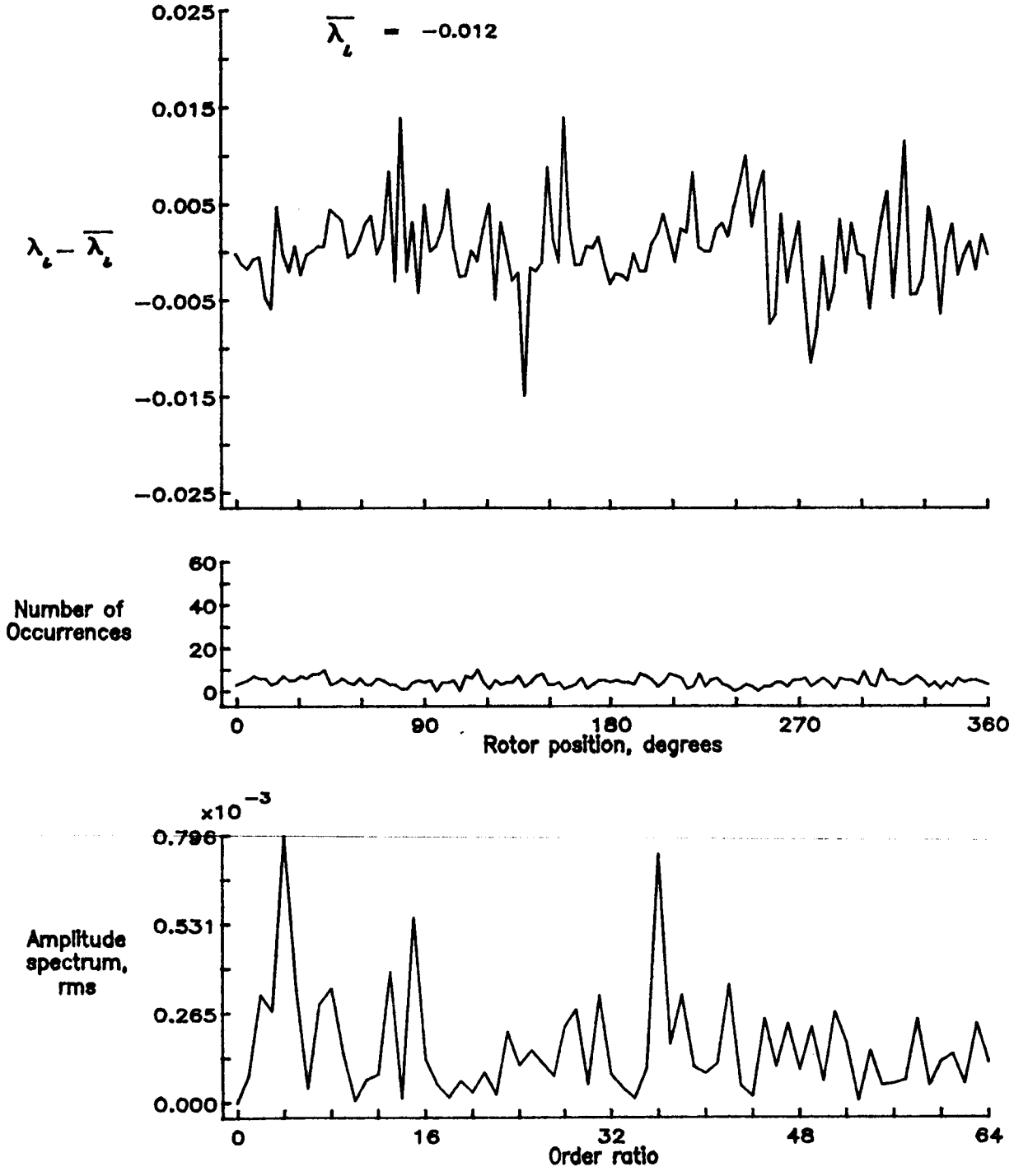


Figure 165.– Concluded.

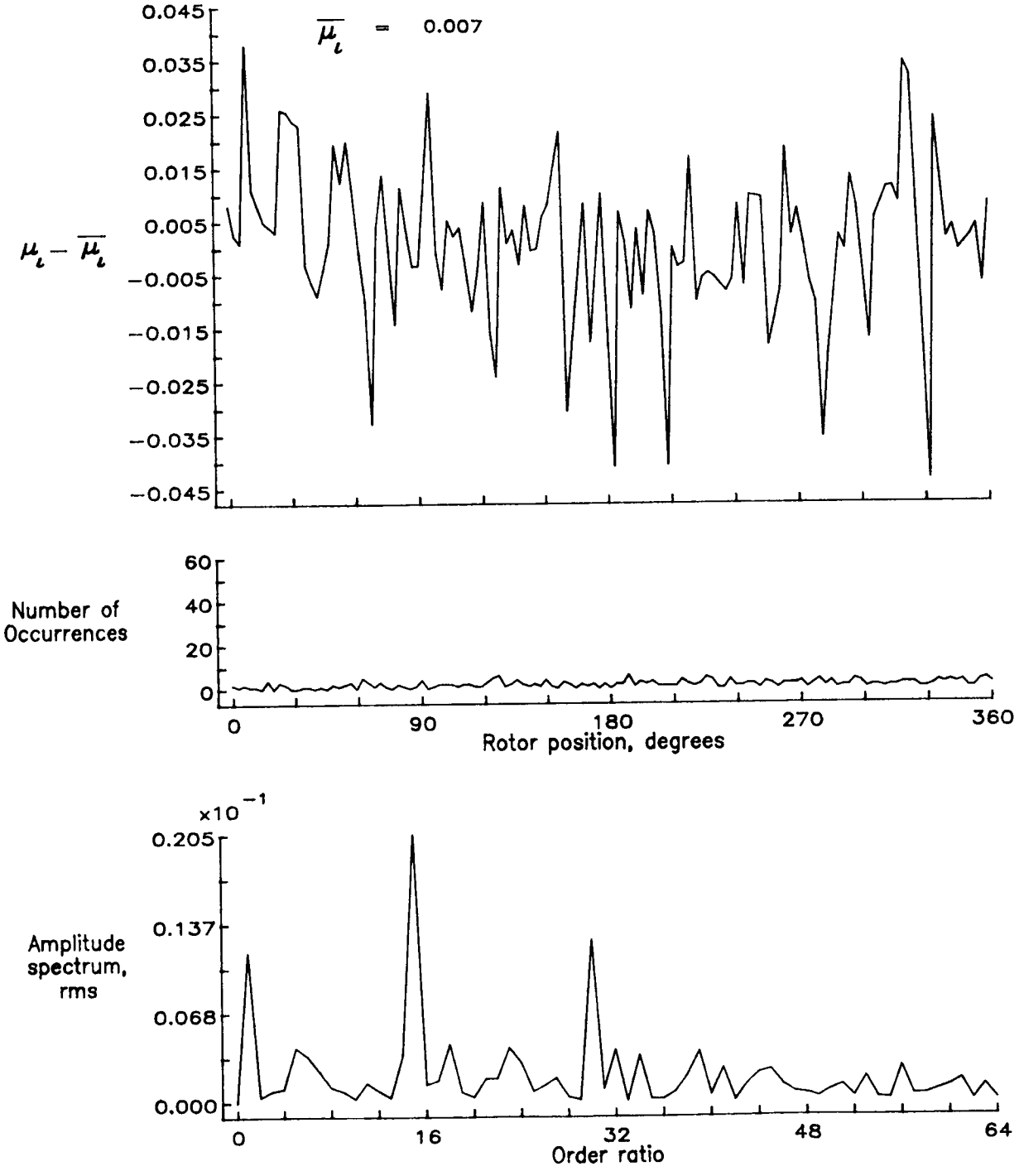


Figure 166.– Induced inflow velocity measured at 330 degrees and r/R of 0.20.

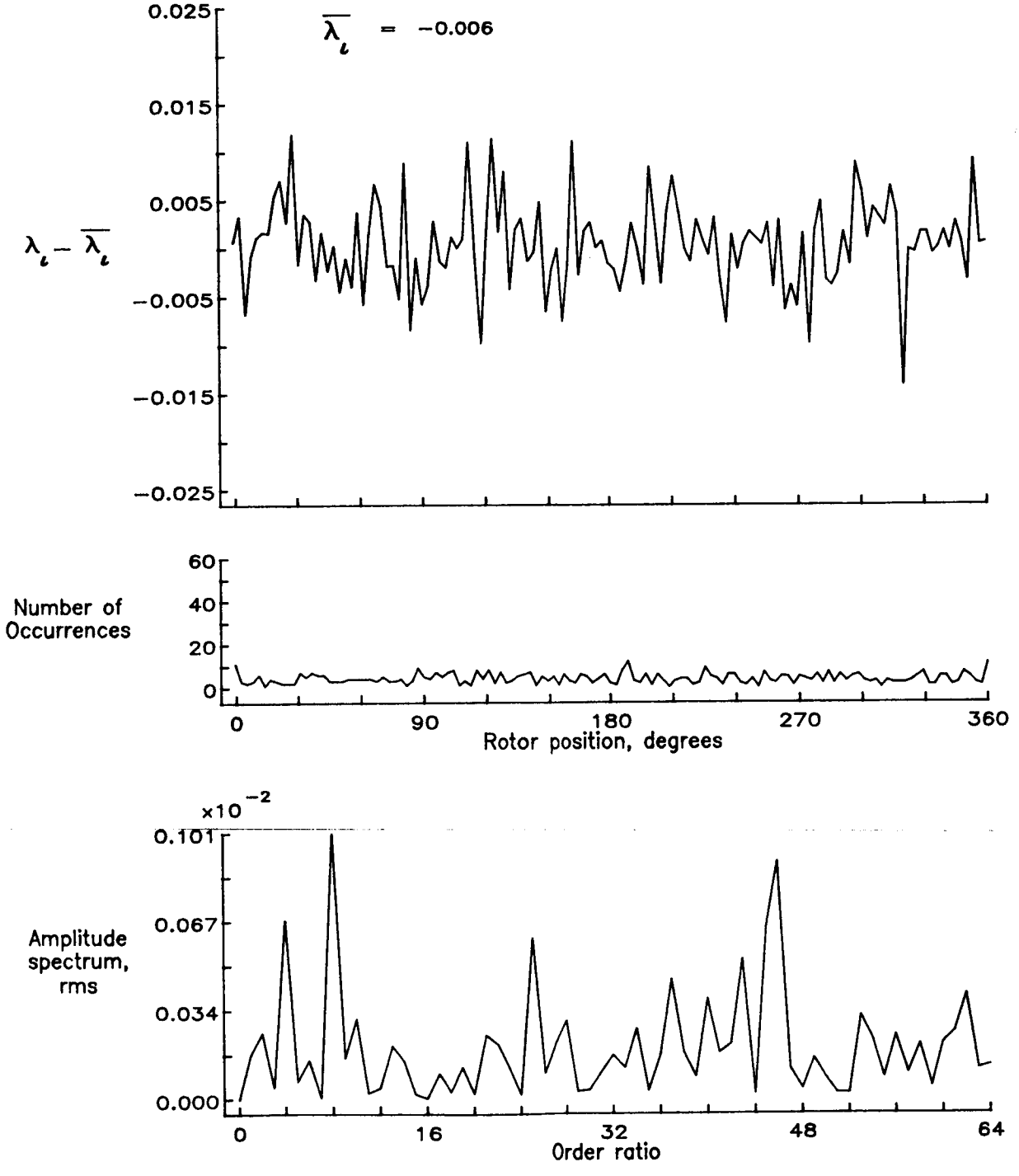


Figure 166.– Concluded.

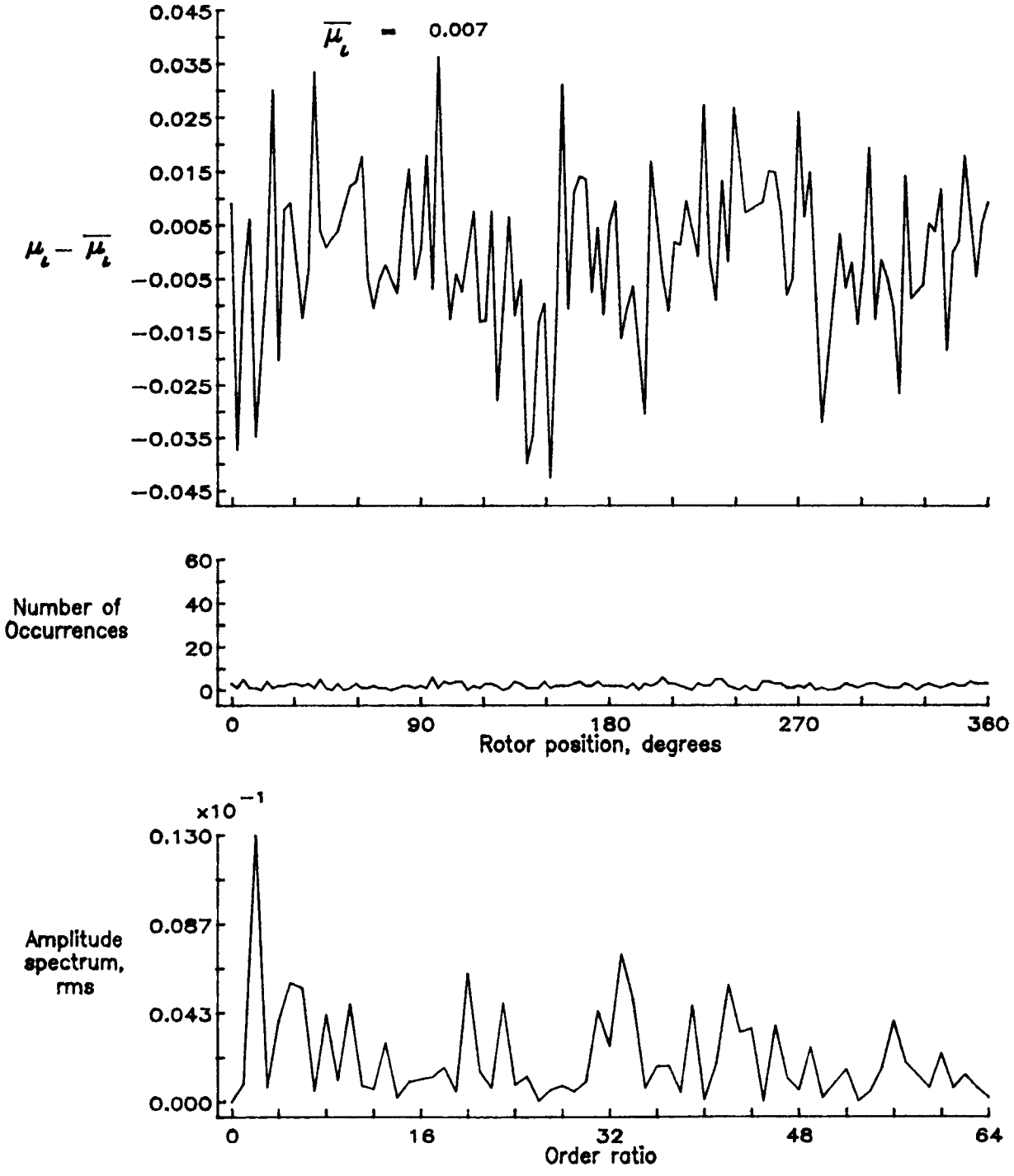


Figure 167.– Induced inflow velocity measured at 330 degrees and r/R of 0.40.

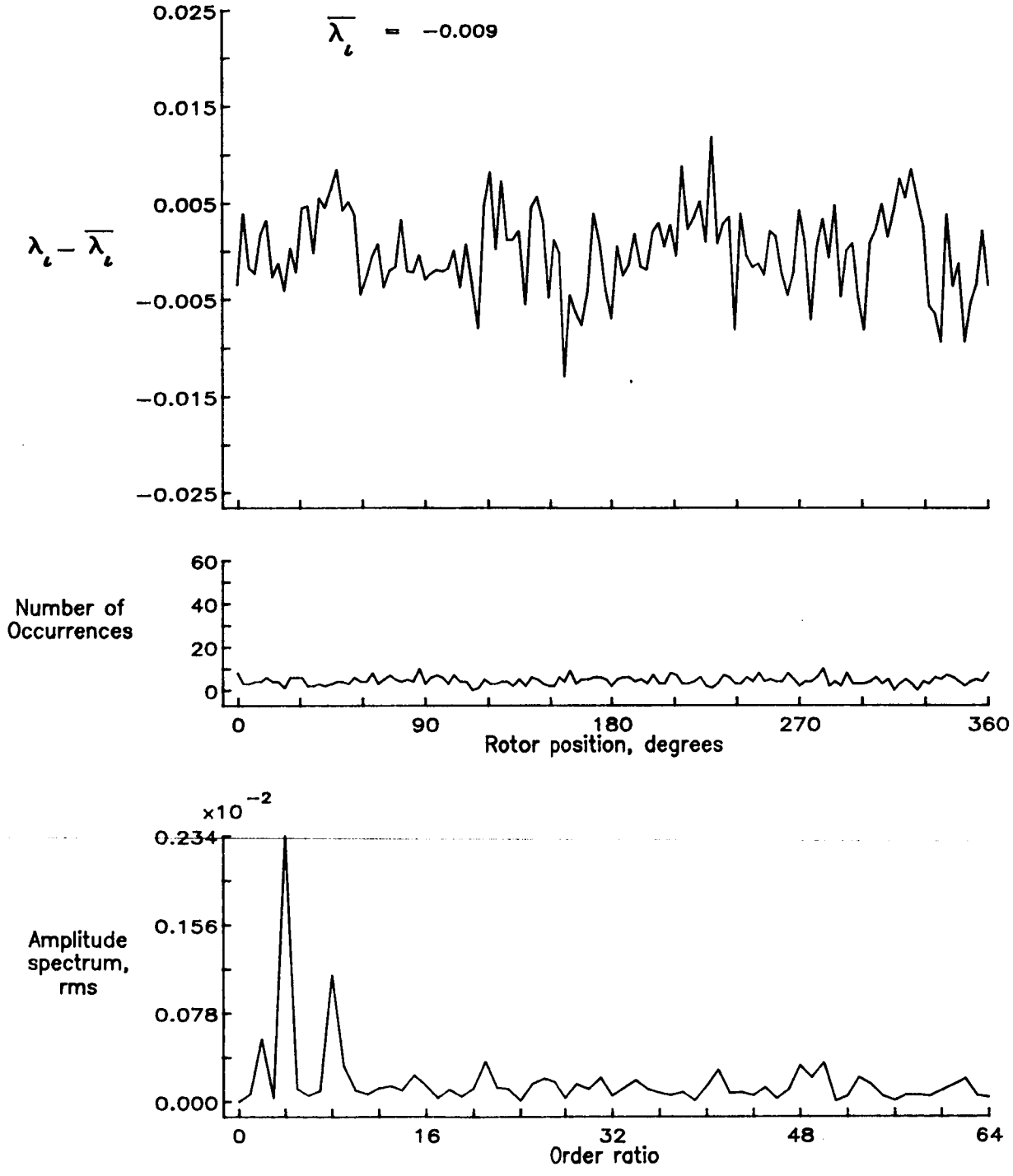


Figure 167.– Concluded.

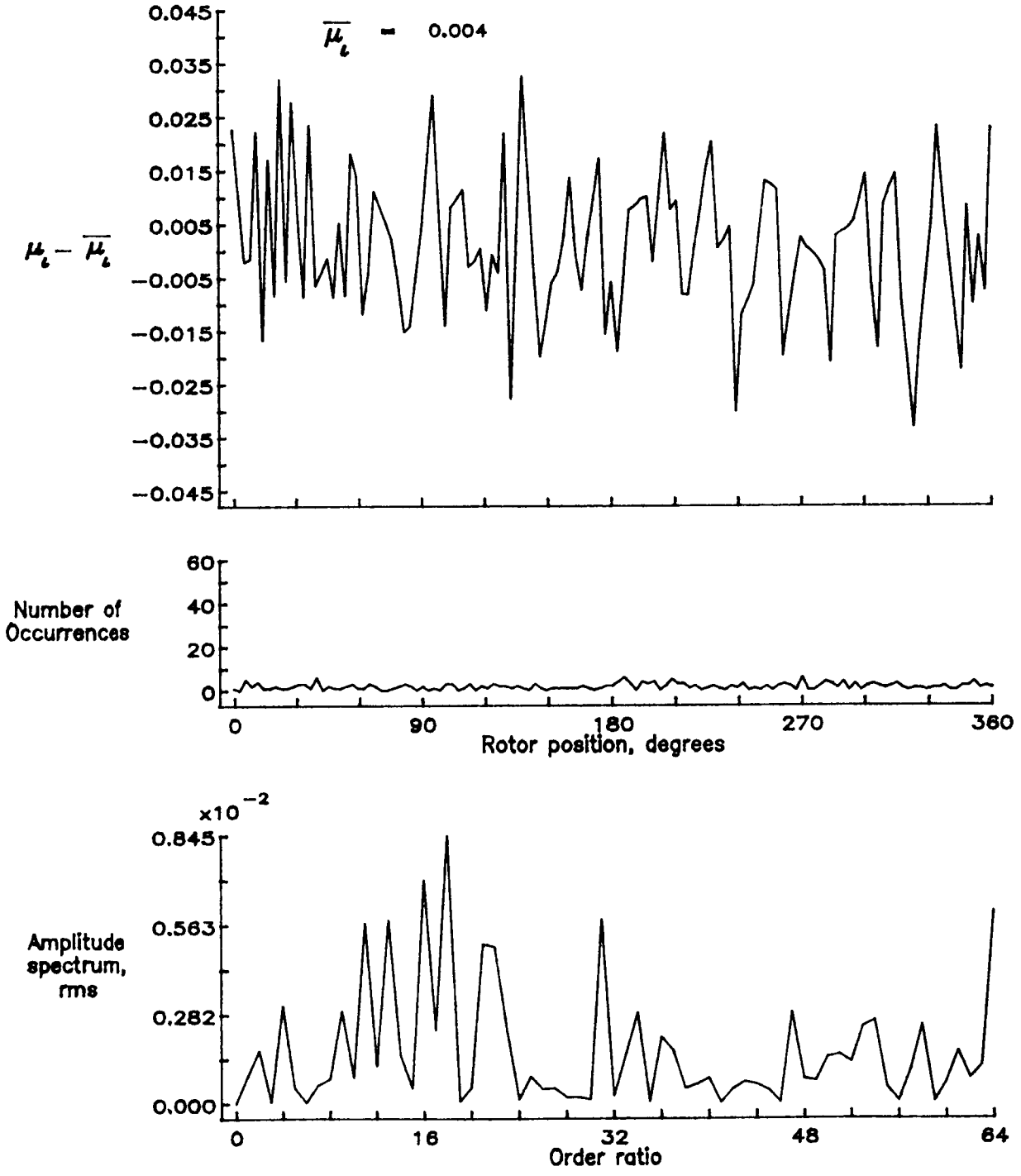


Figure 168.– Induced inflow velocity measured at 330 degrees and r/R of 0.50.

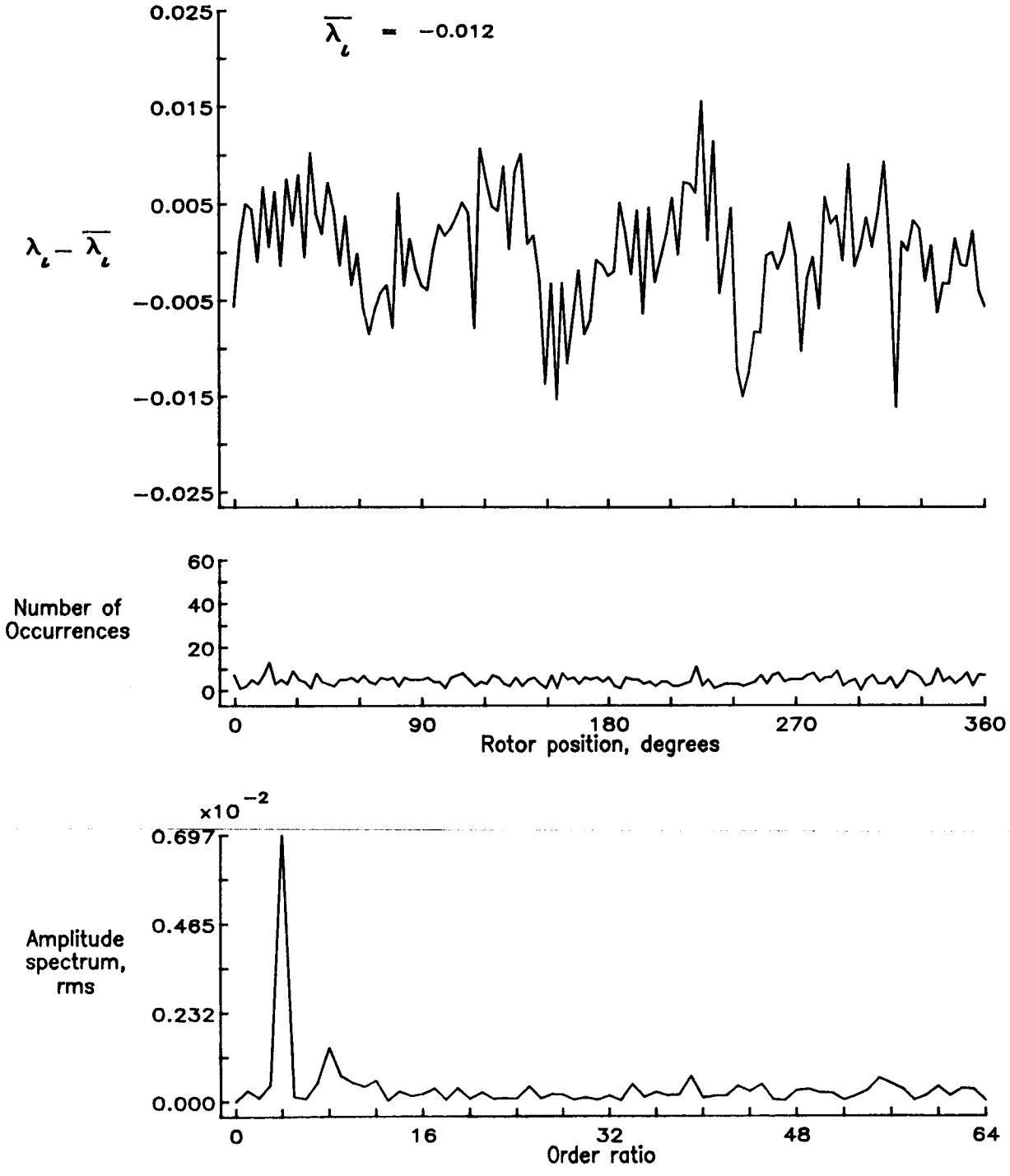


Figure 168.– Concluded.

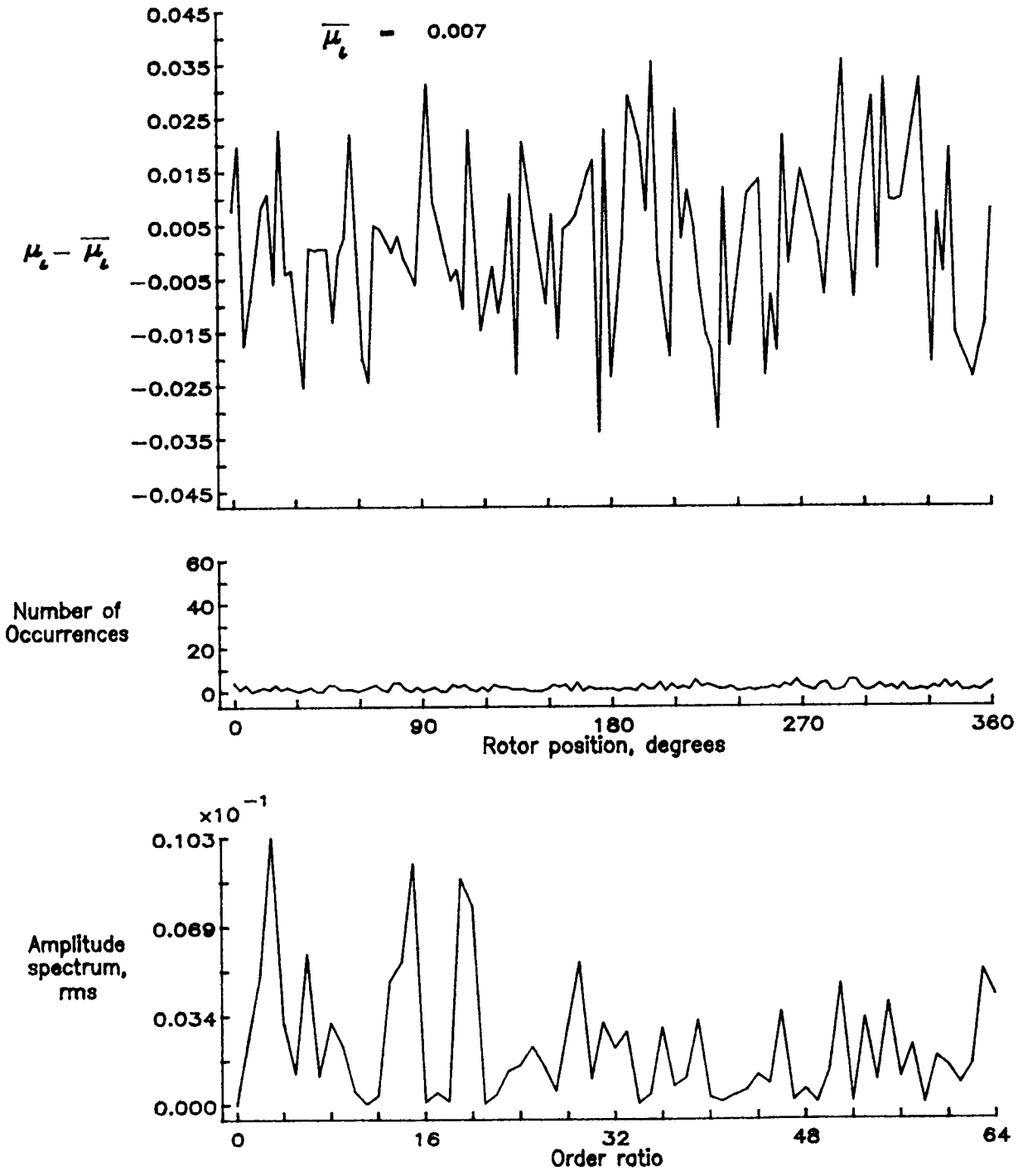


Figure 169.– Induced inflow velocity measured at 330 degrees and r/R of 0.60.

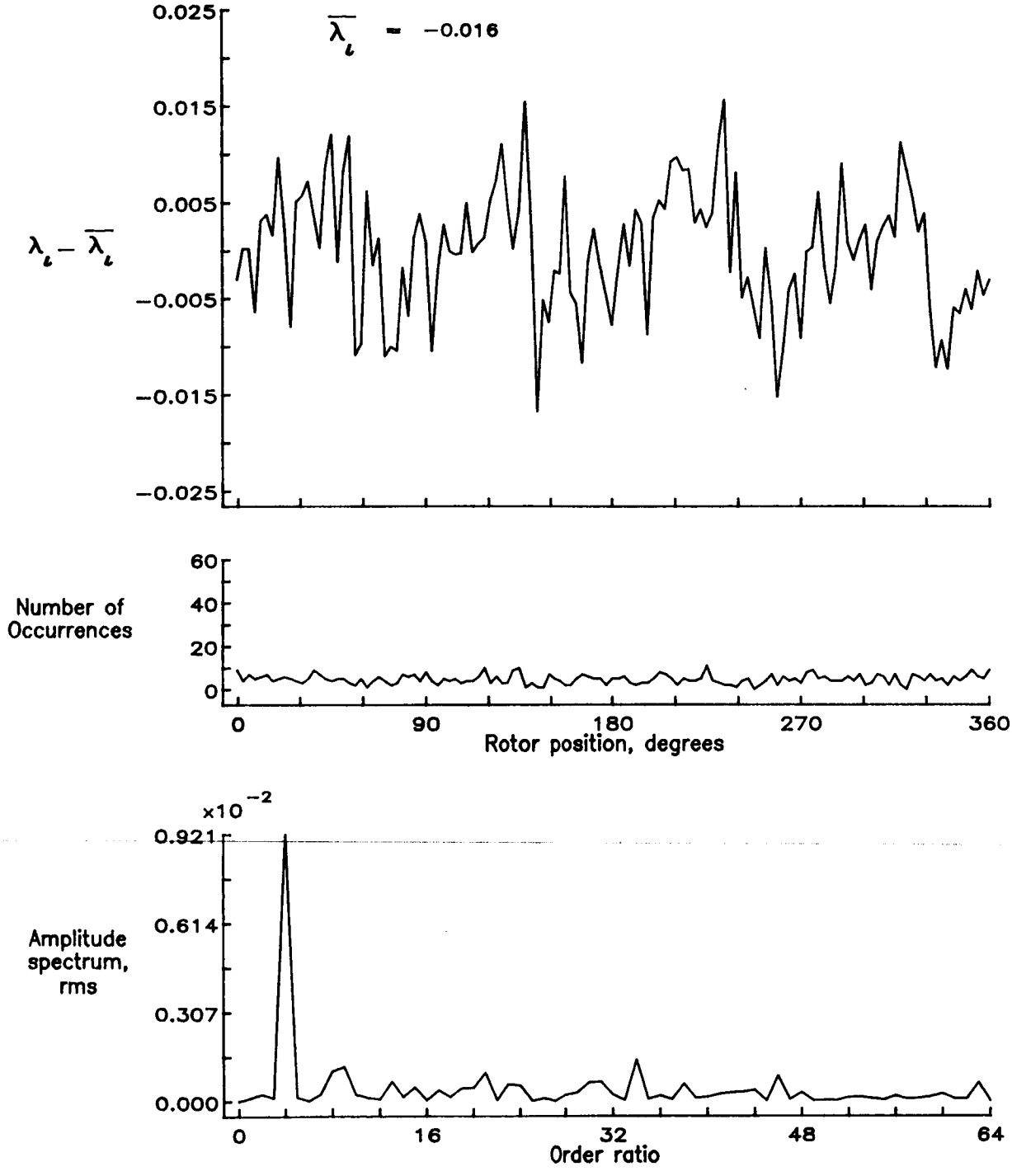


Figure 169.– Concluded.

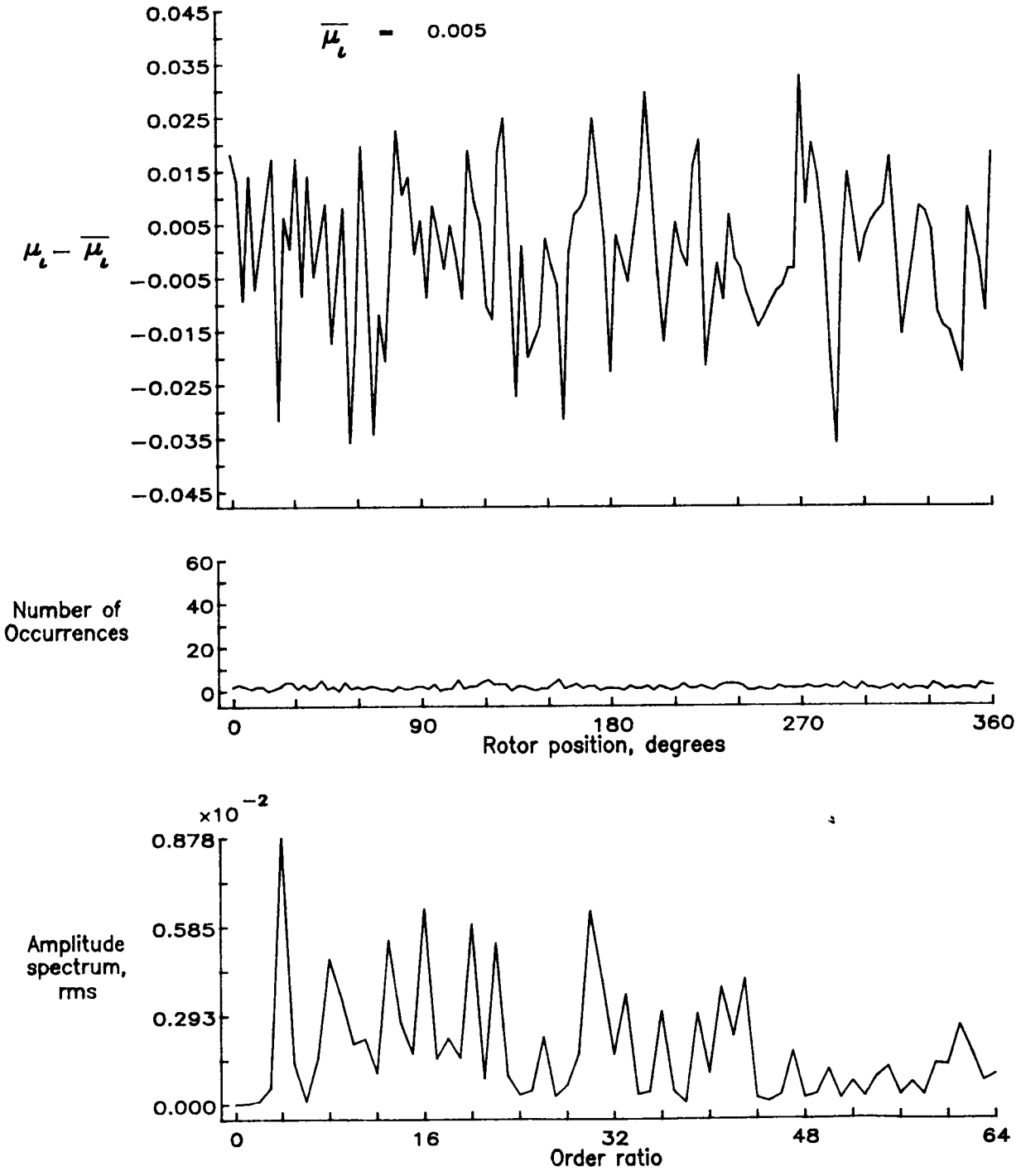


Figure 170.– Induced inflow velocity measured at 330 degrees and r/R of 0.70.

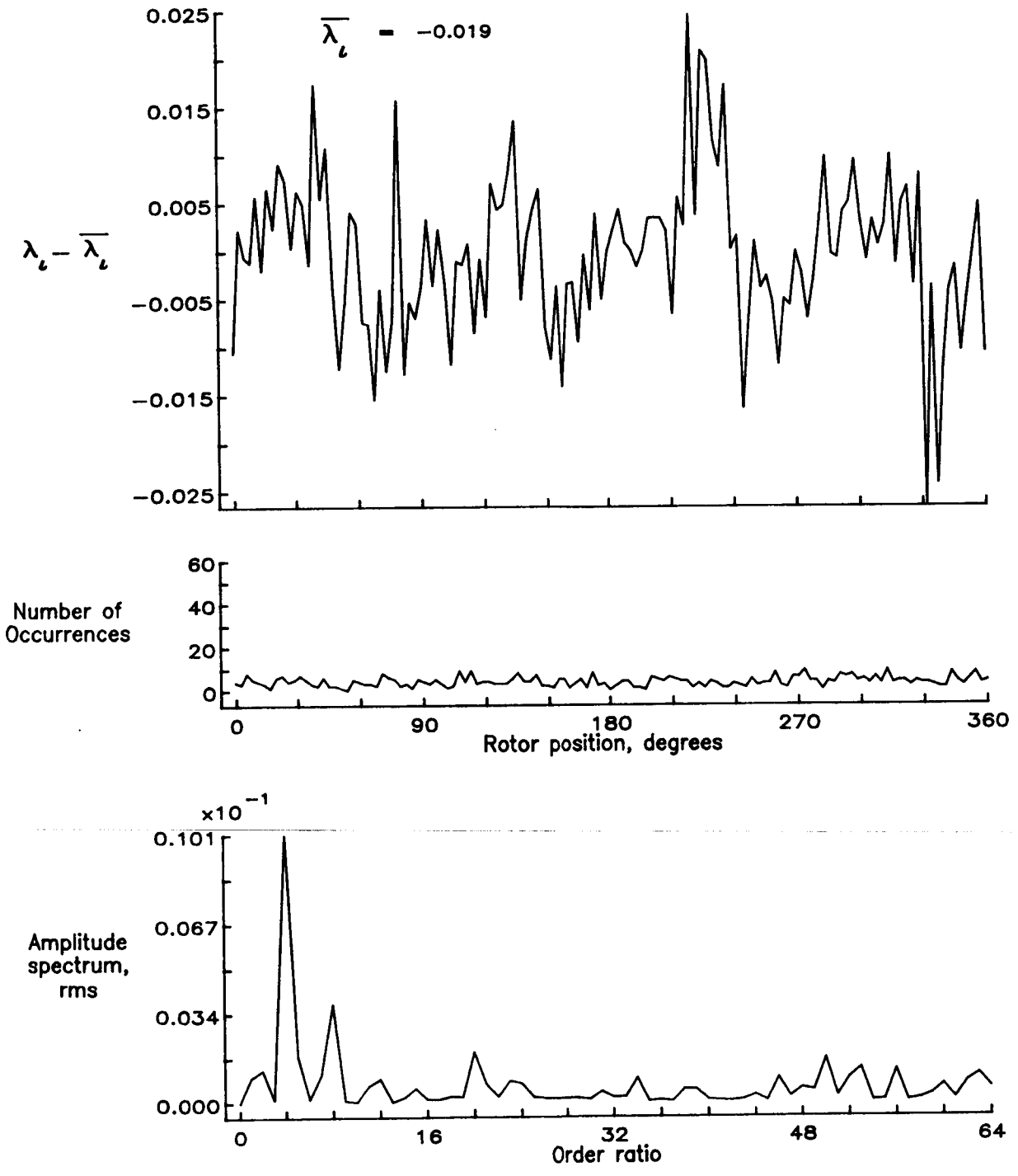


Figure 170.– Concluded.

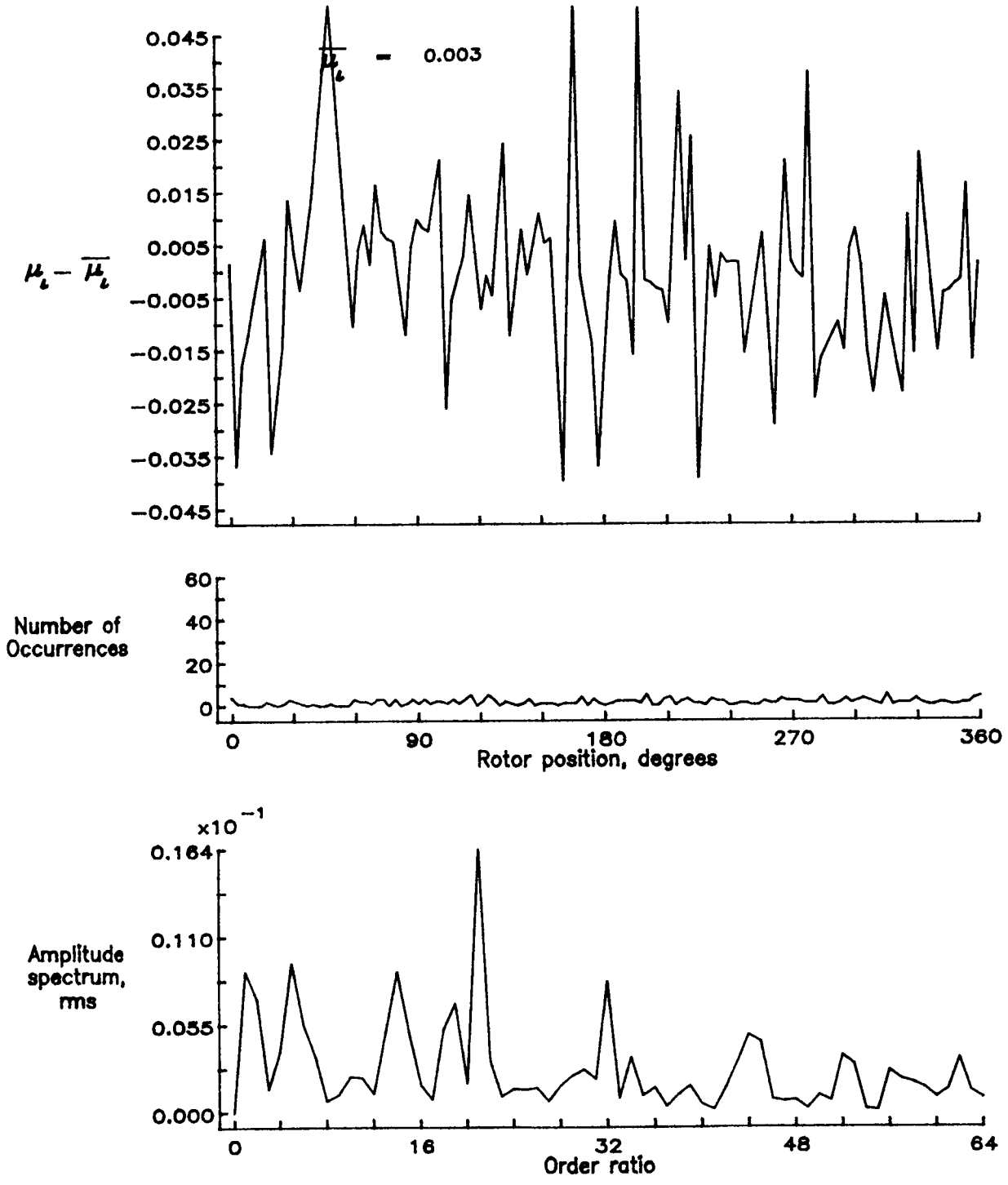


Figure 171.– Induced inflow velocity measured at 330 degrees and r/R of 0.74.

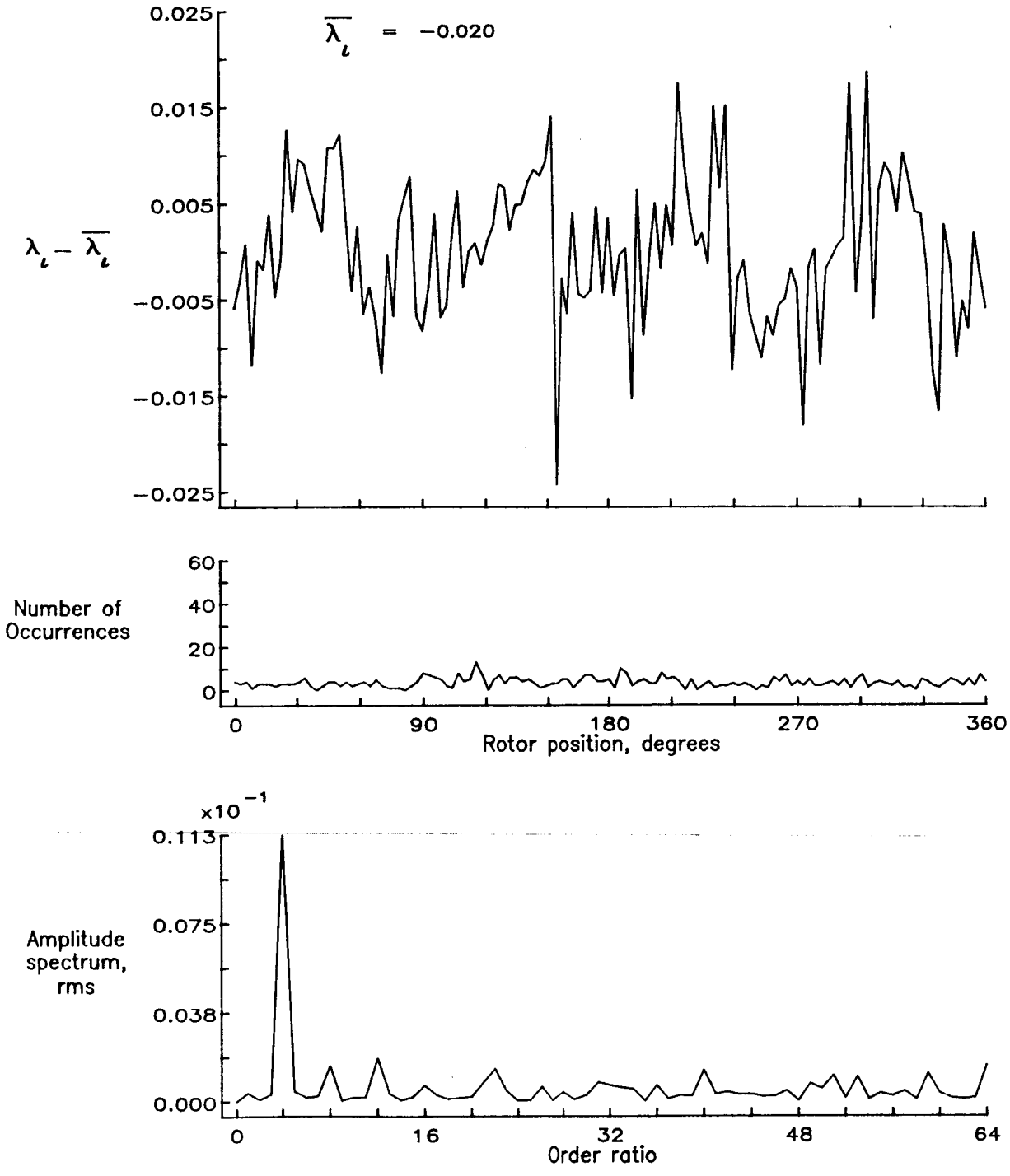


Figure 171.– Concluded.

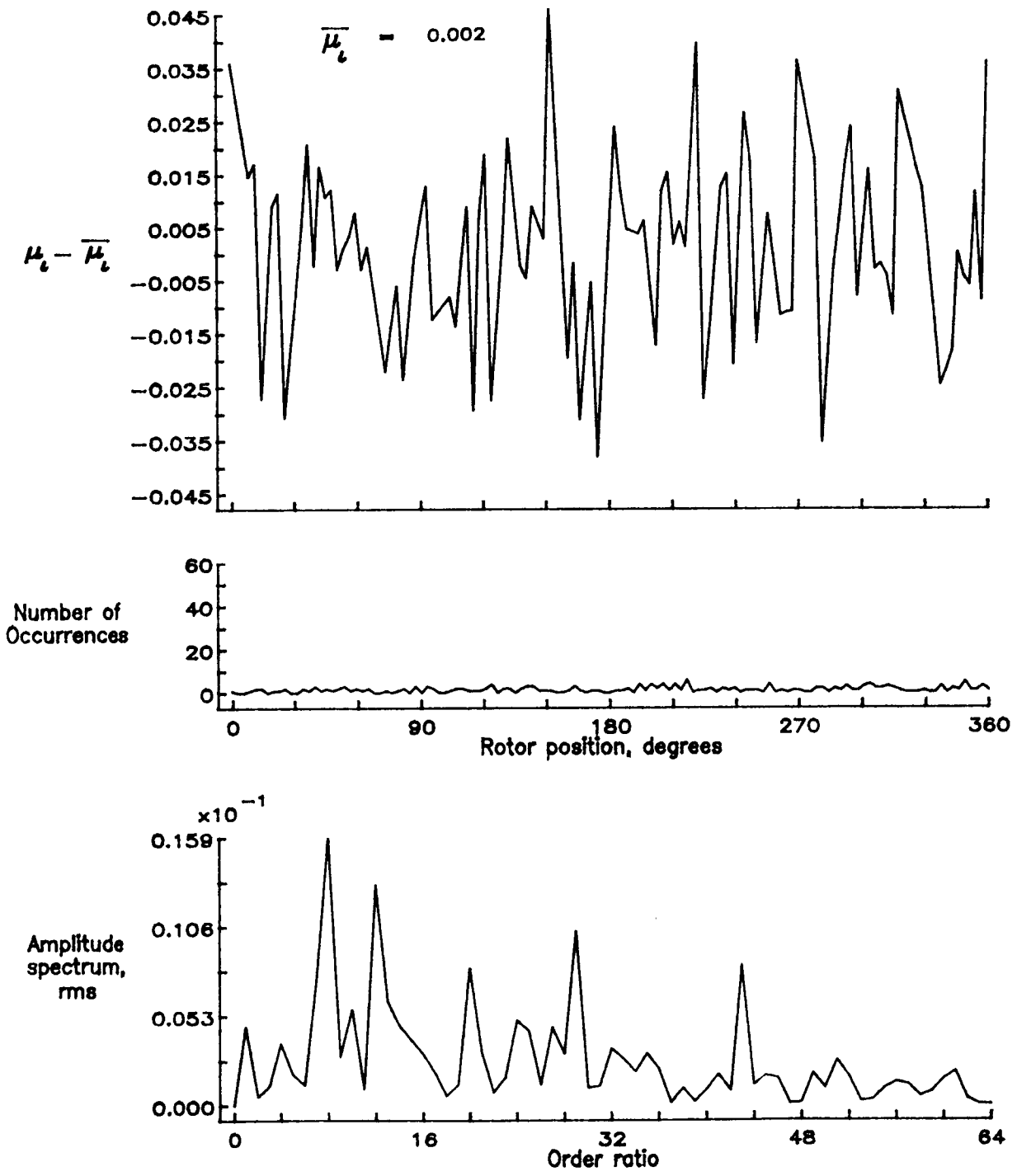


Figure 172.– Induced inflow velocity measured at 330 degrees and r/R of 0.78.

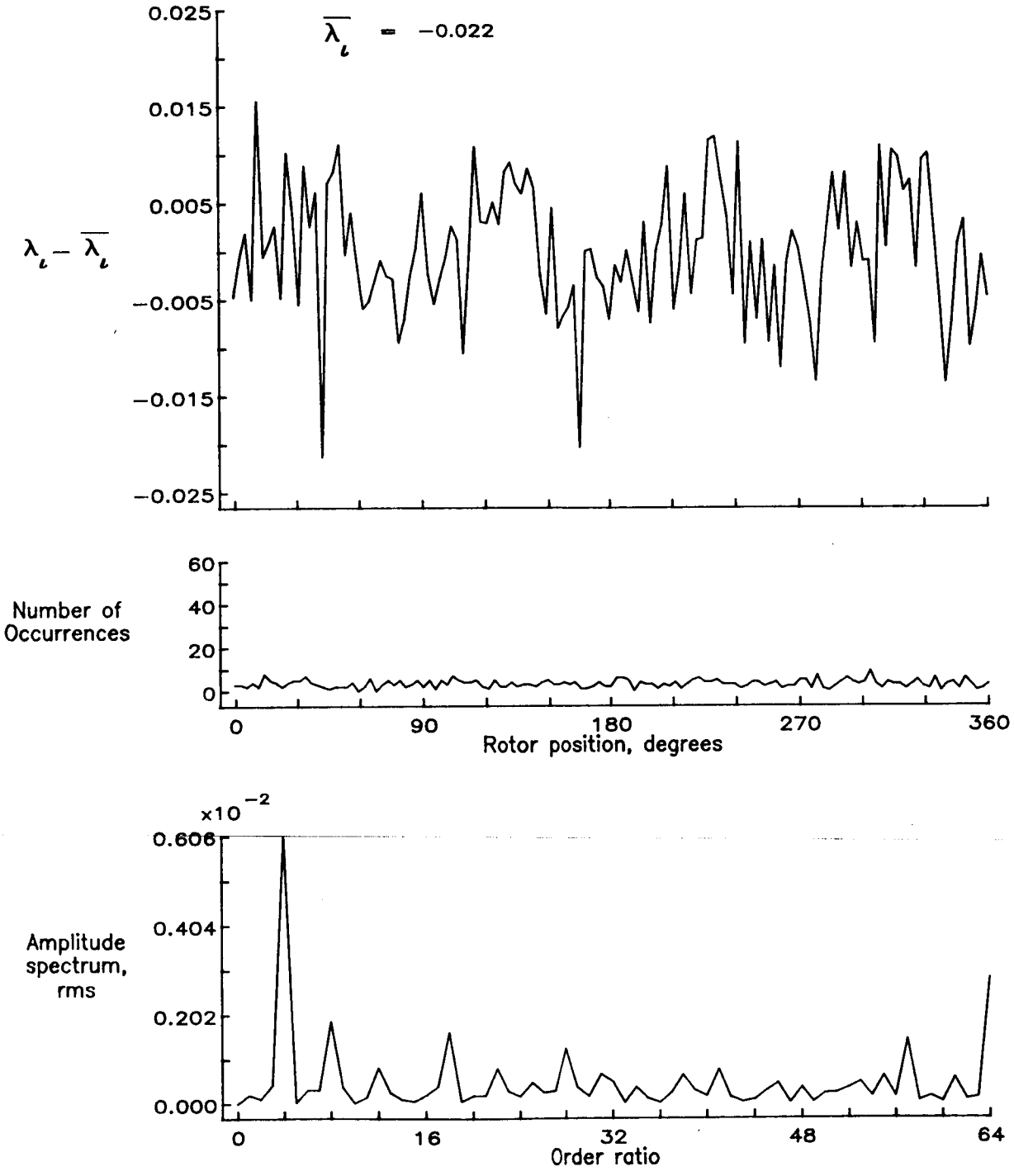


Figure 172.– Concluded.

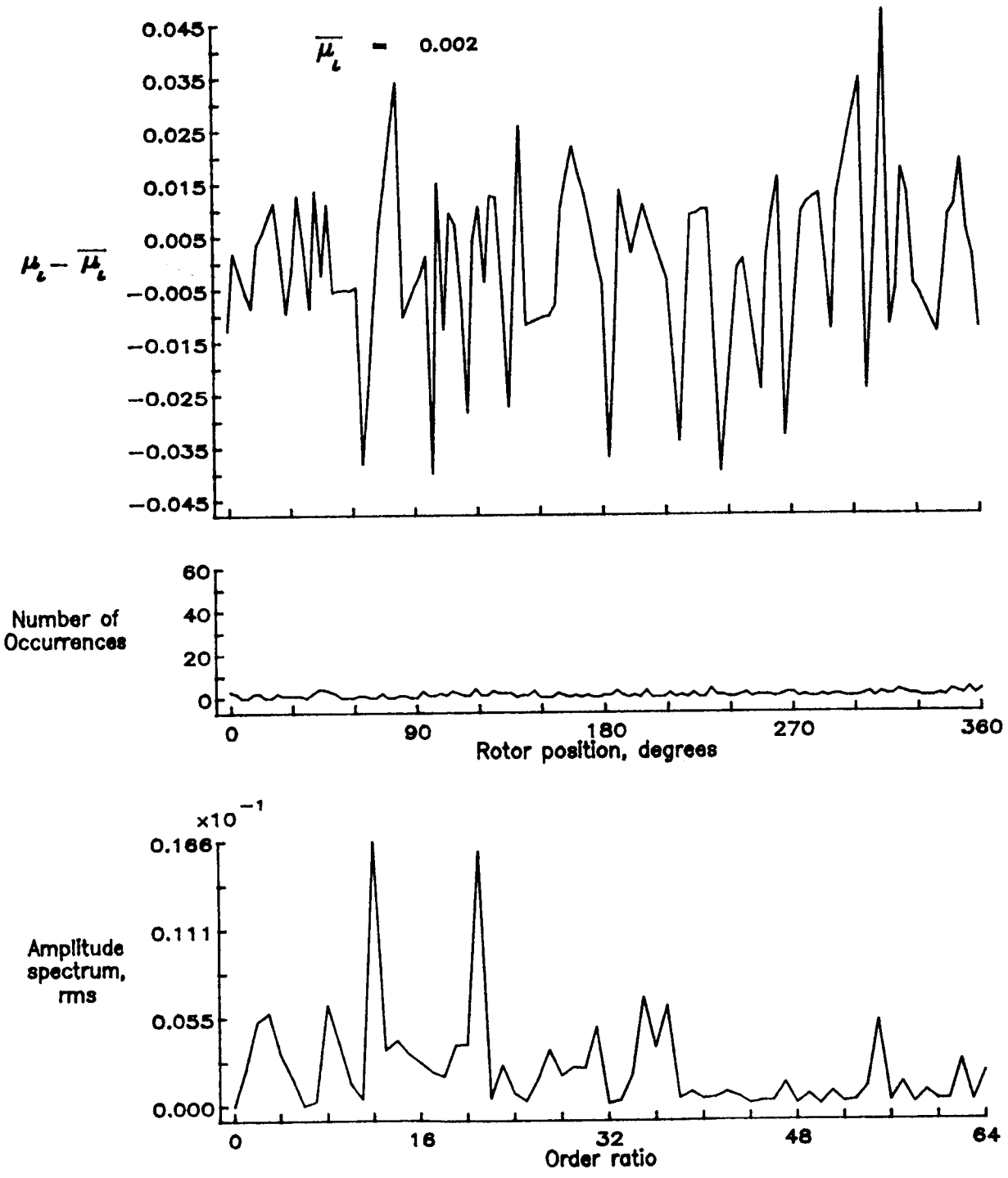


Figure 173.– Induced inflow velocity measured at 330 degrees and r/R of 0.82.

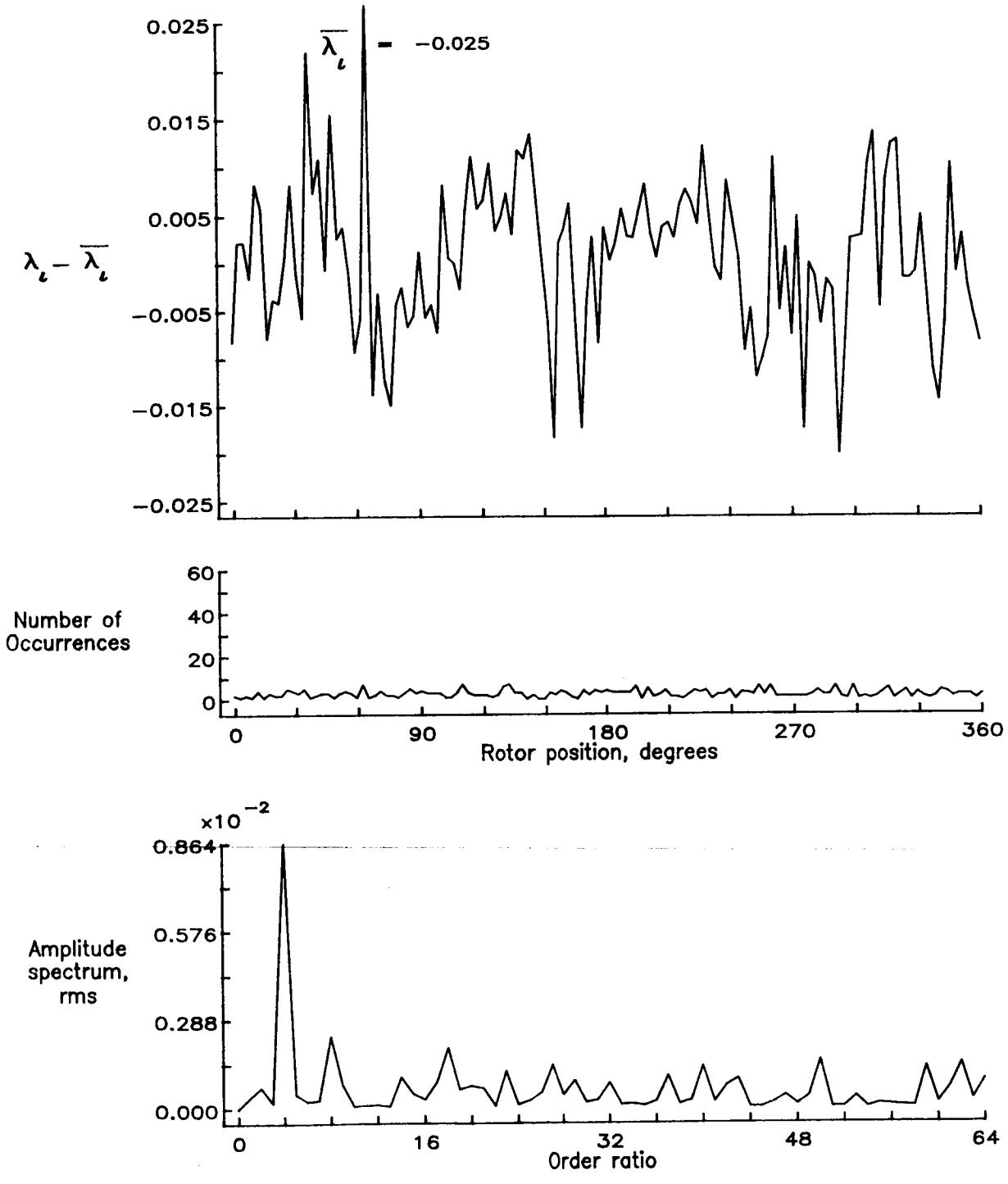


Figure 173.– Concluded.

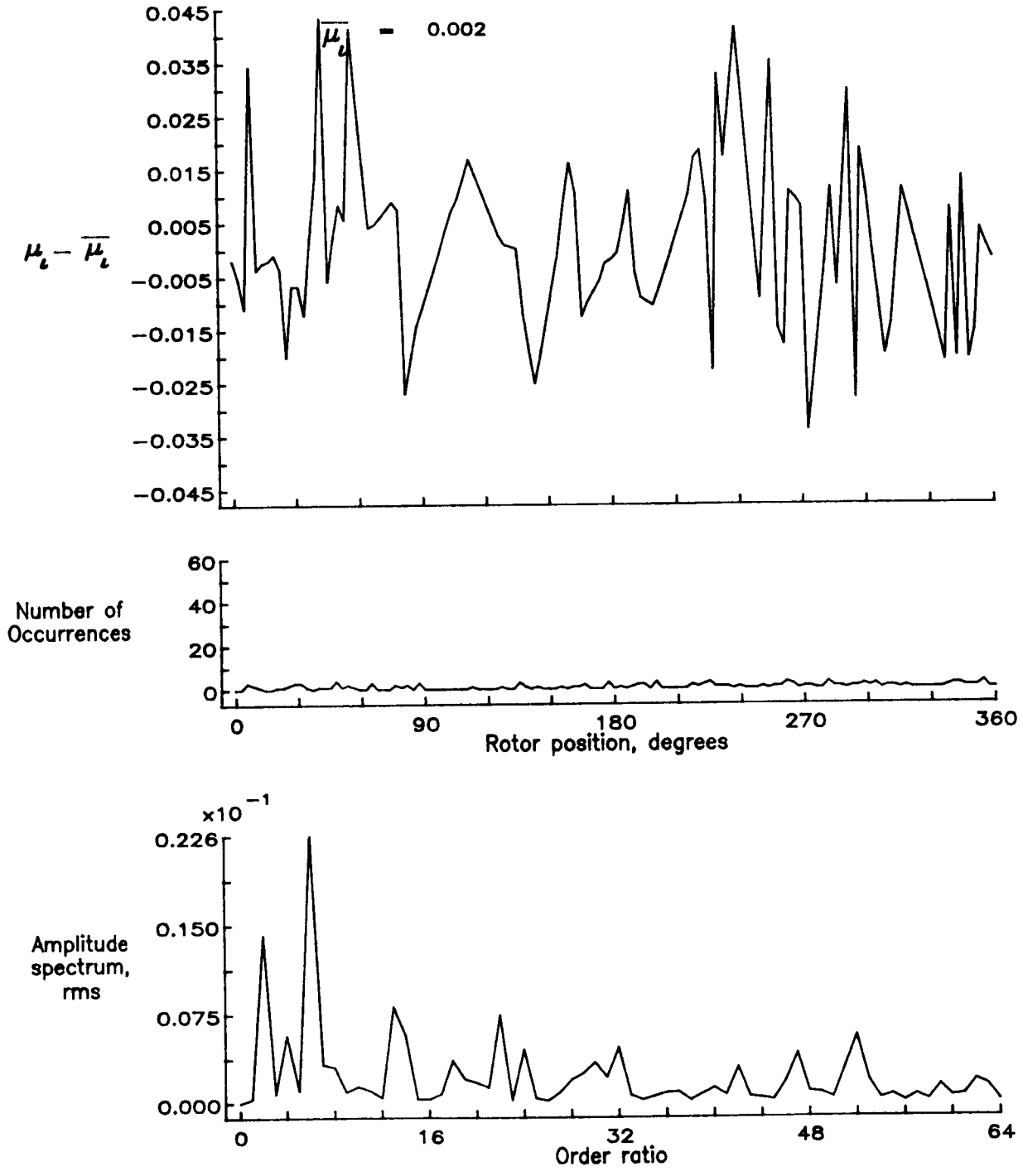


Figure 174.– Induced inflow velocity measured at 330 degrees and r/R of 0.86.

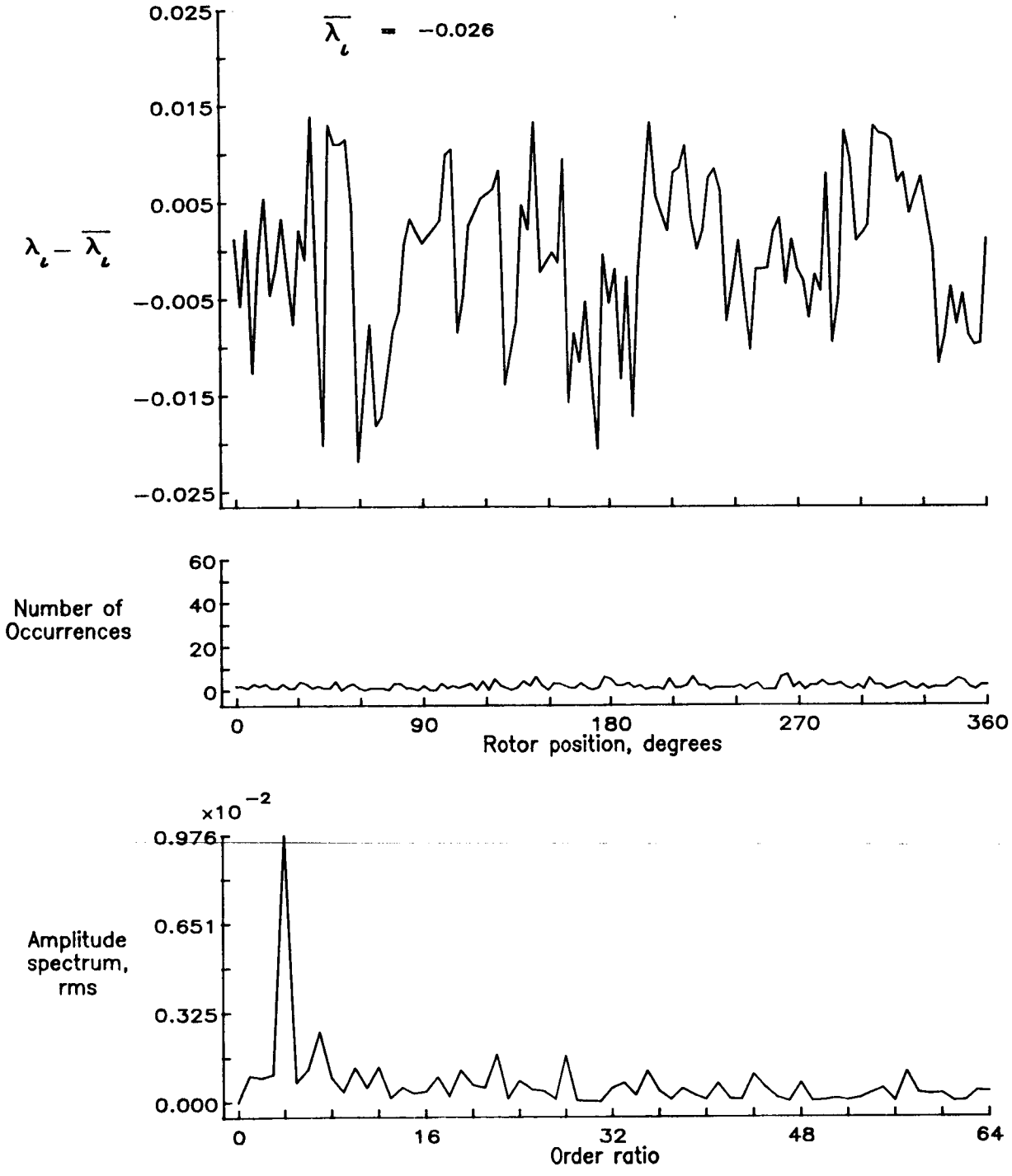


Figure 174.– Concluded.

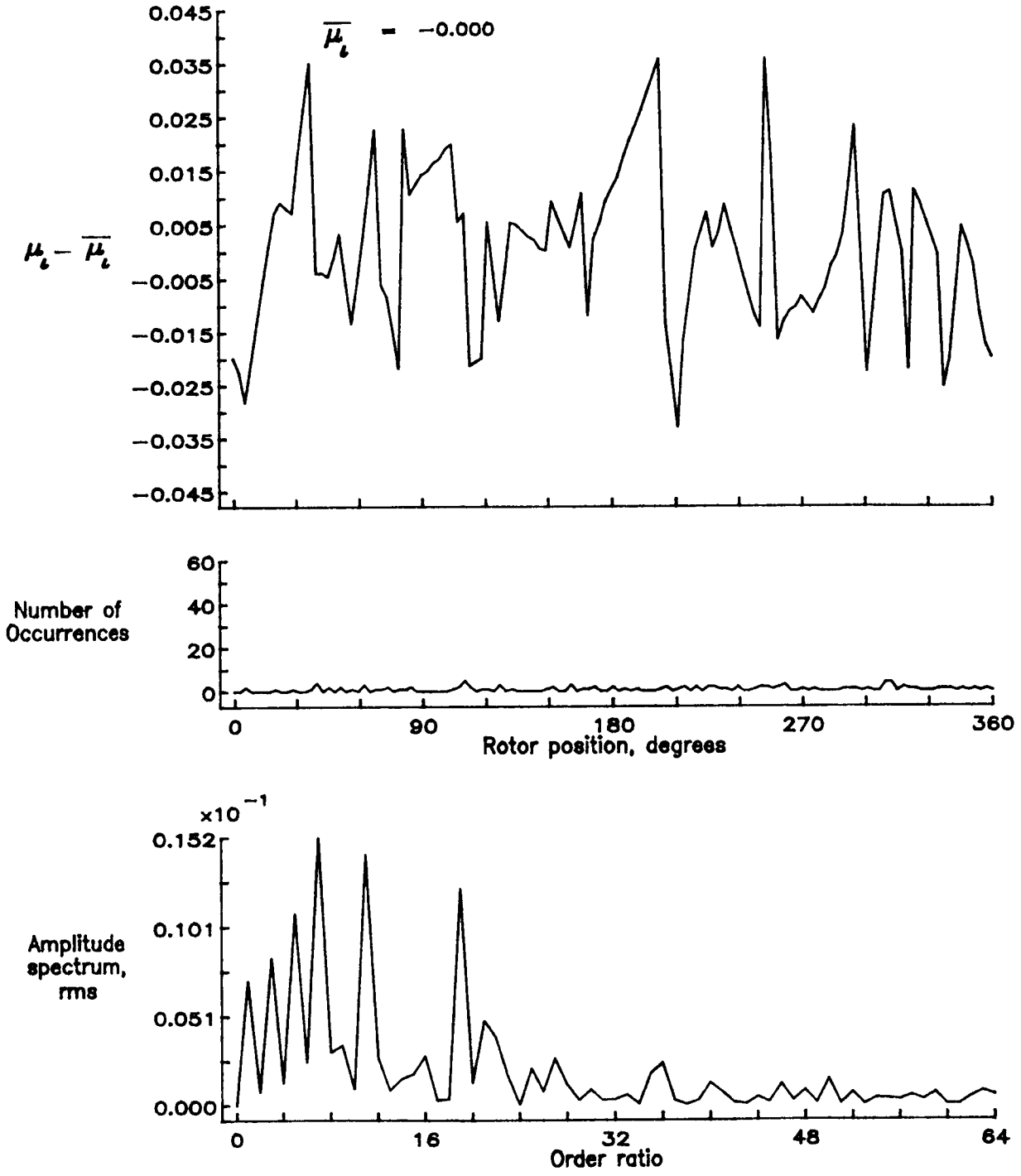


Figure 175.– Induced inflow velocity measured at 330 degrees and r/R of 0.90.

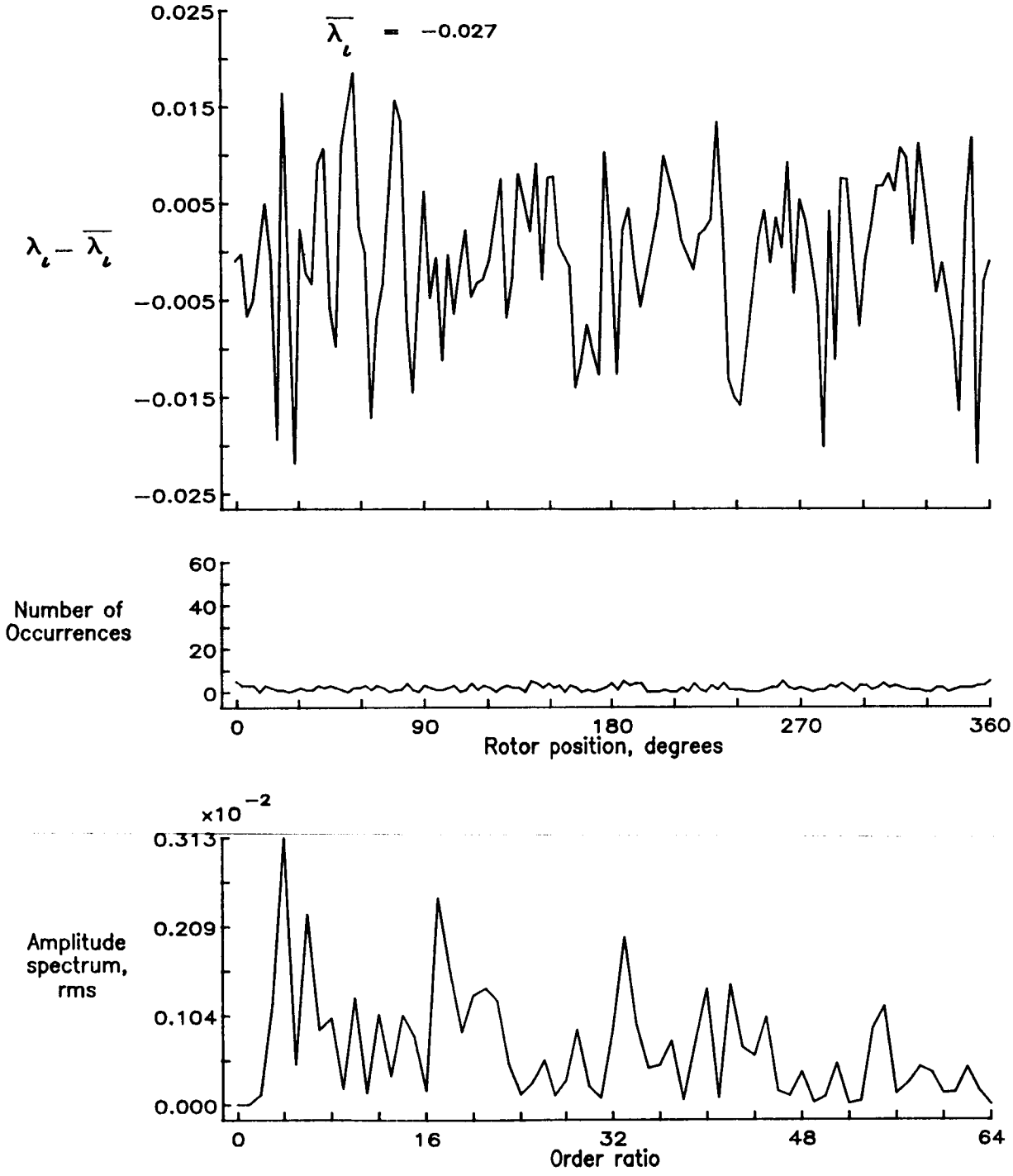


Figure 175.– Concluded.

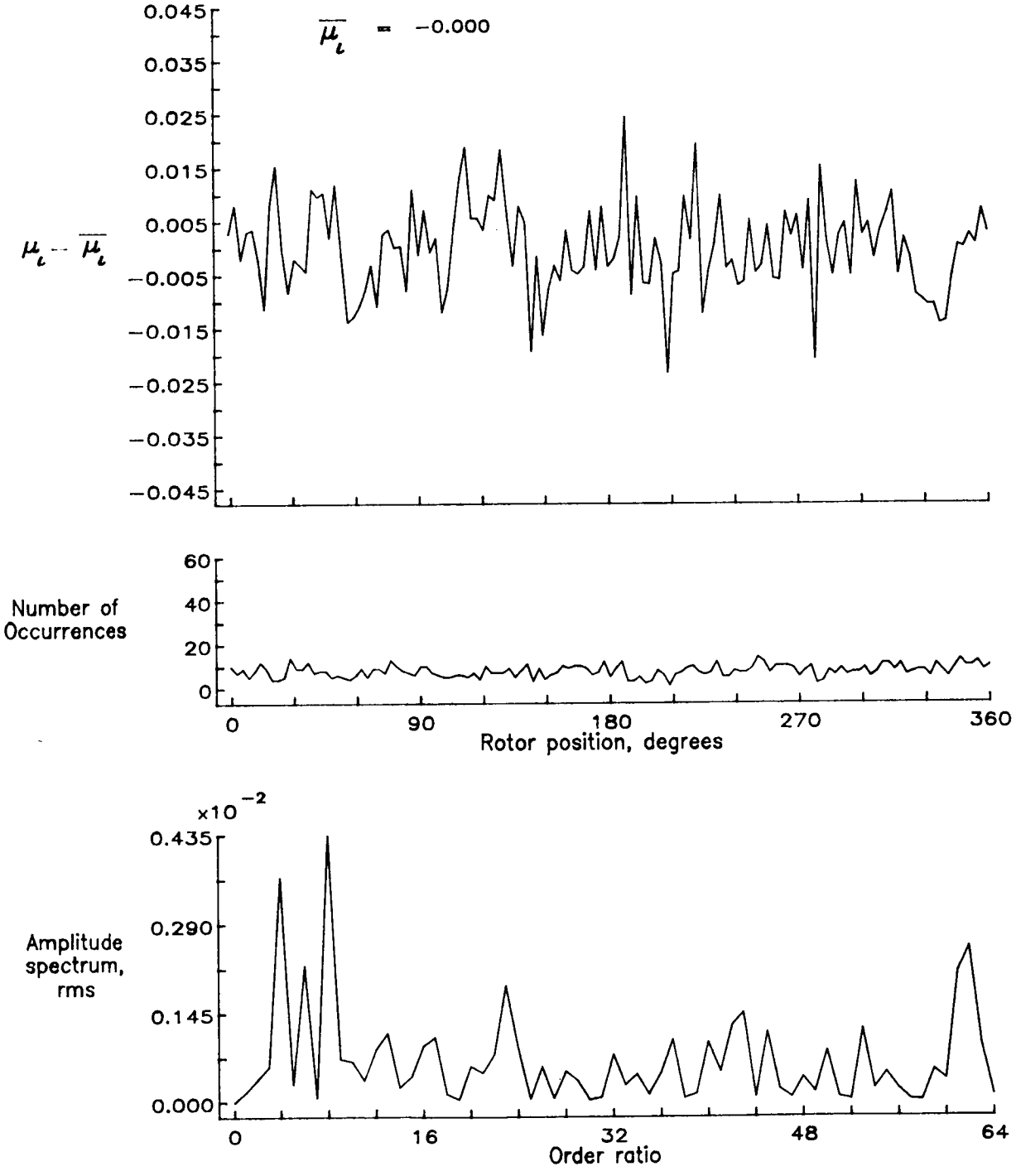


Figure 176.– Induced inflow velocity measured at 330 degrees and r/R of 0.94.

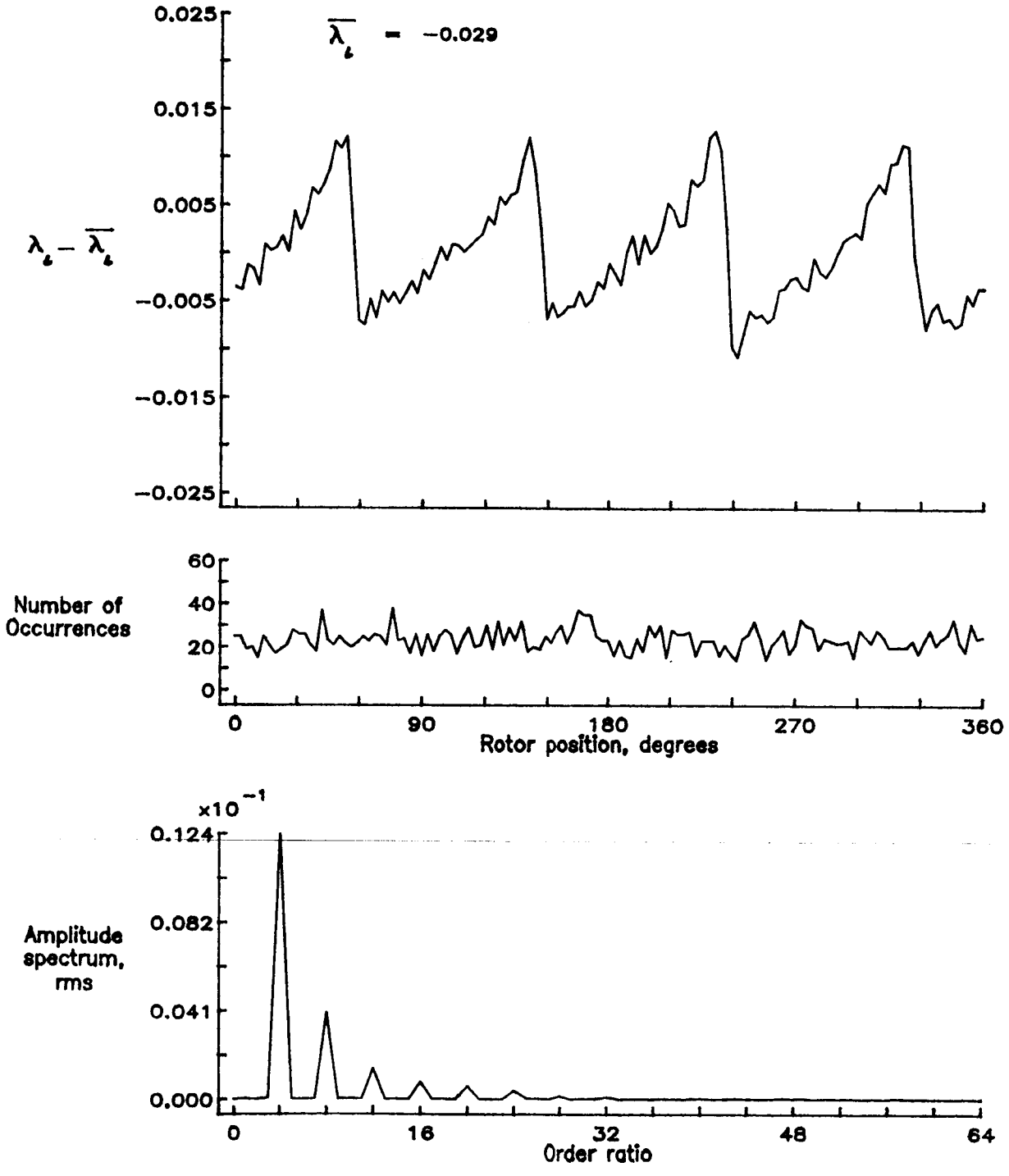


Figure 176.– Concluded.

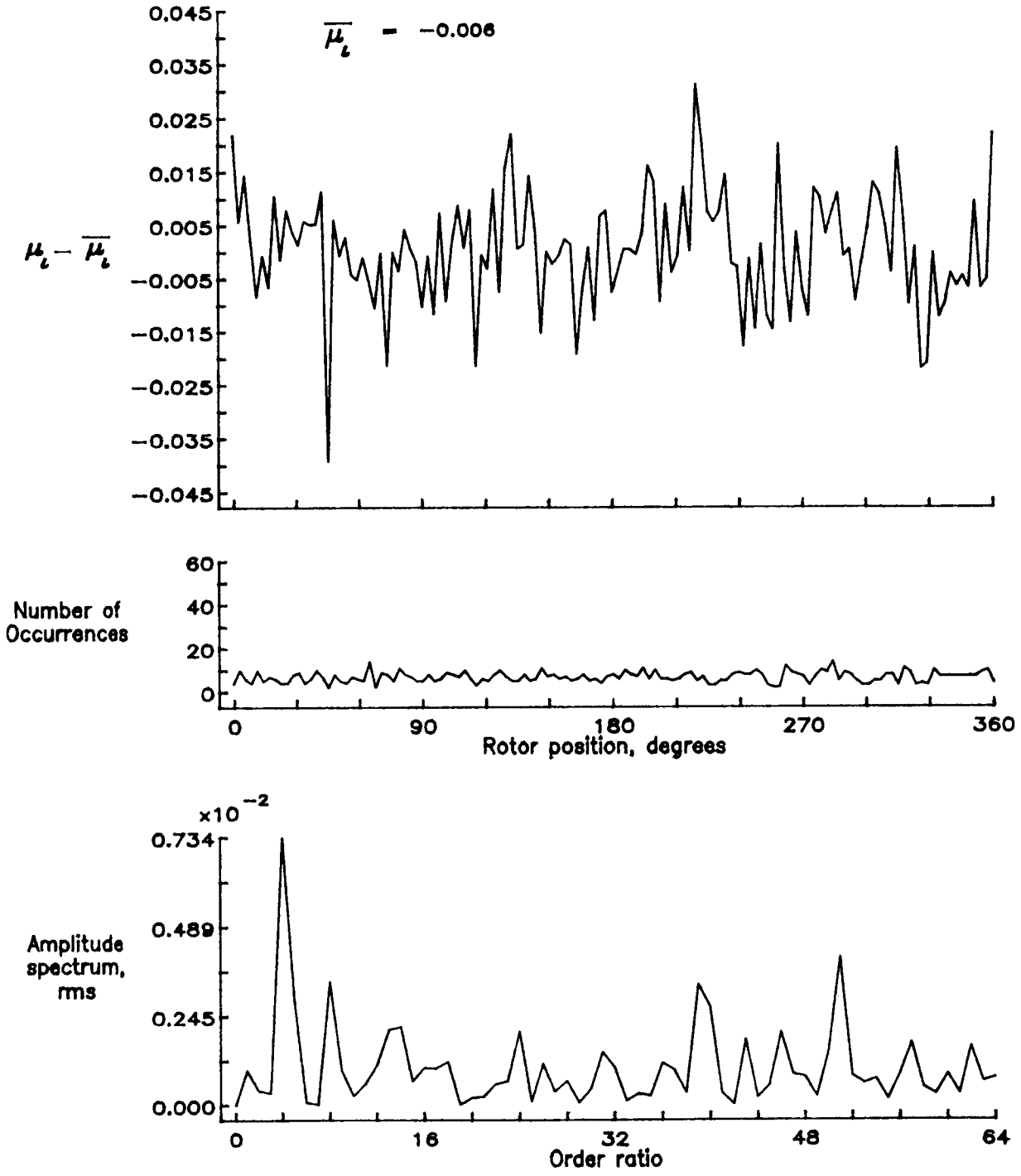


Figure 177.– Induced inflow velocity measured at 330 degrees and r/R of 0.98.

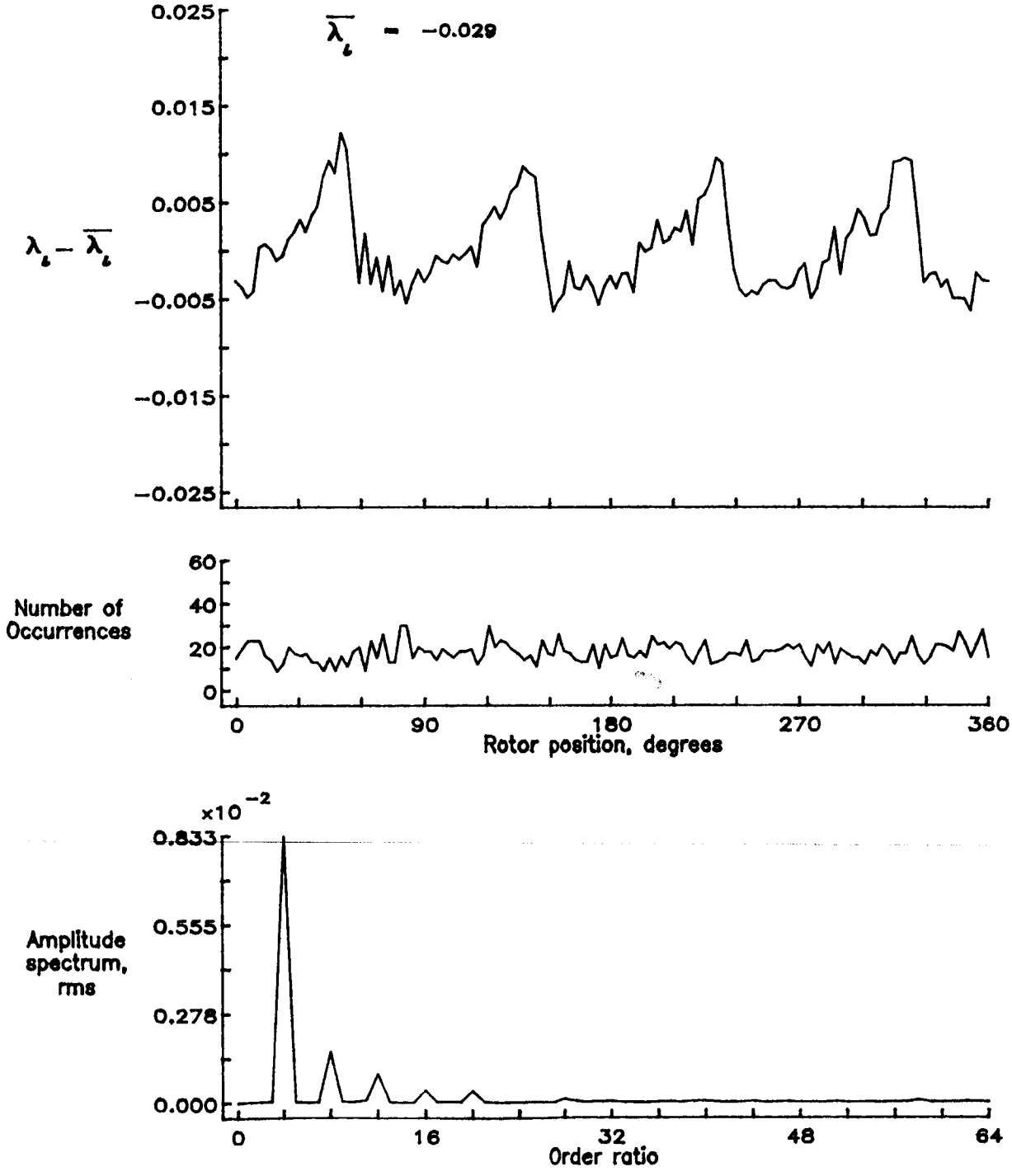


Figure 177.– Concluded.

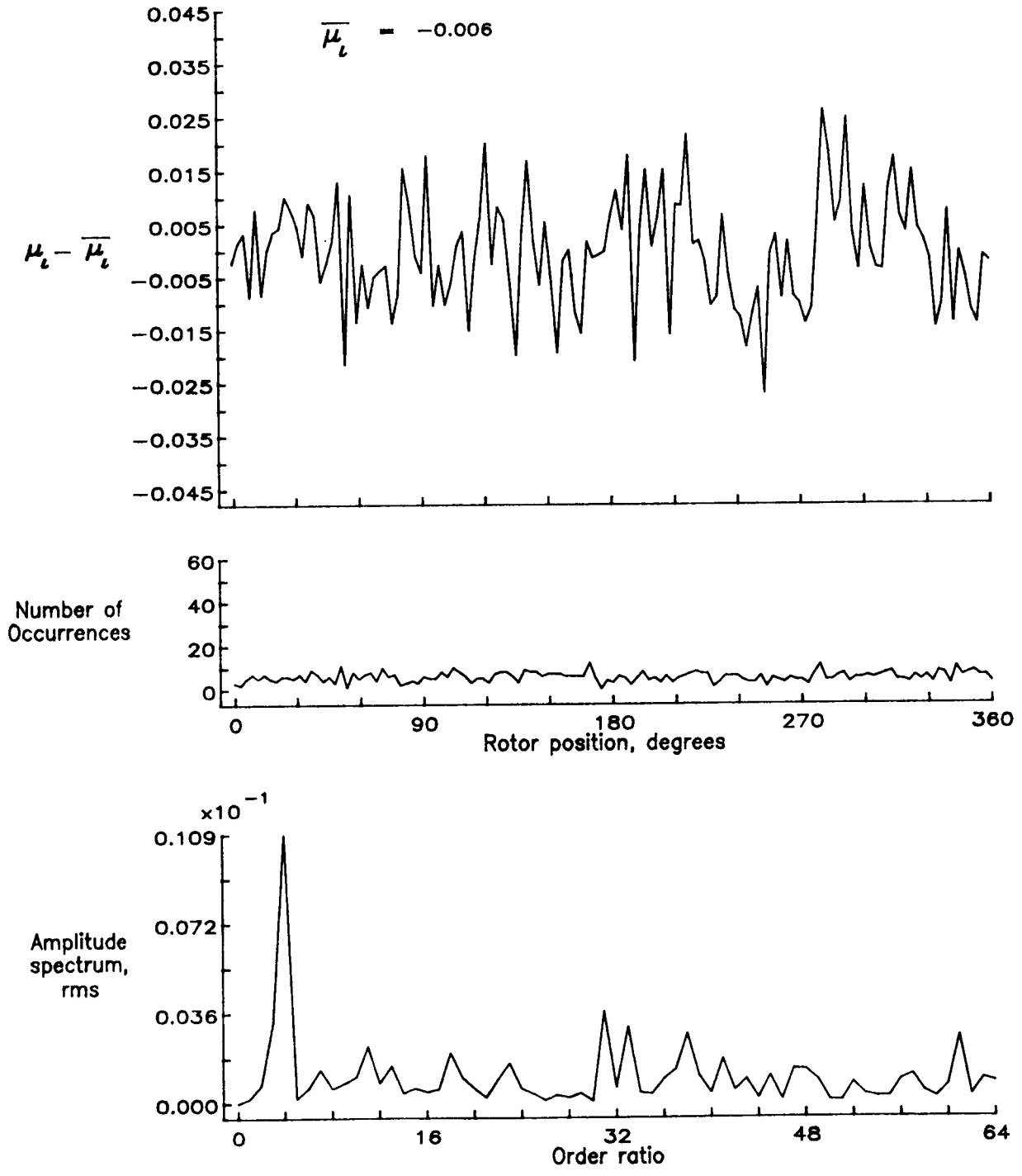


Figure 178.– Induced inflow velocity measured at 330 degrees and r/R of 1.02.

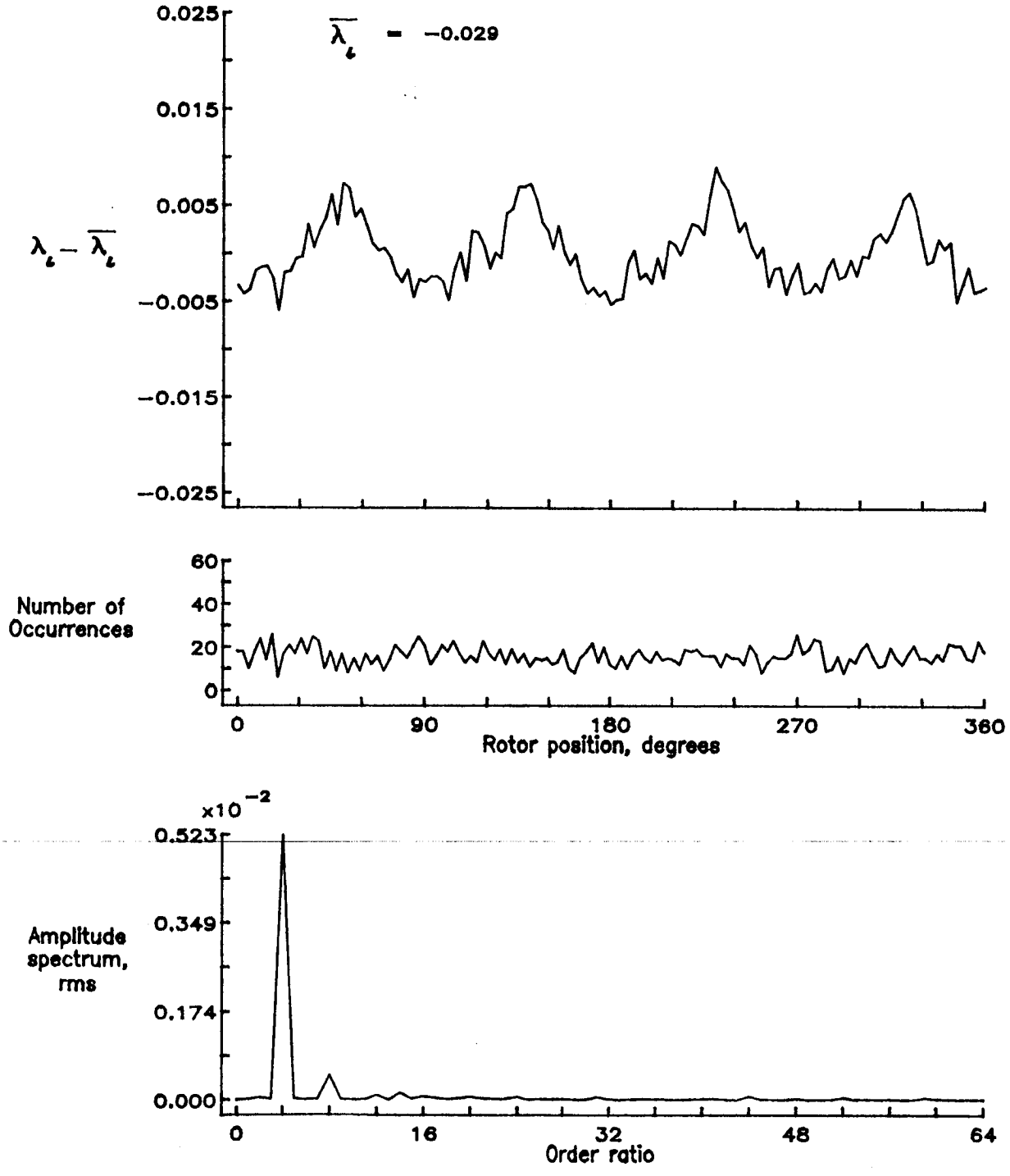


Figure 178.– Concluded.

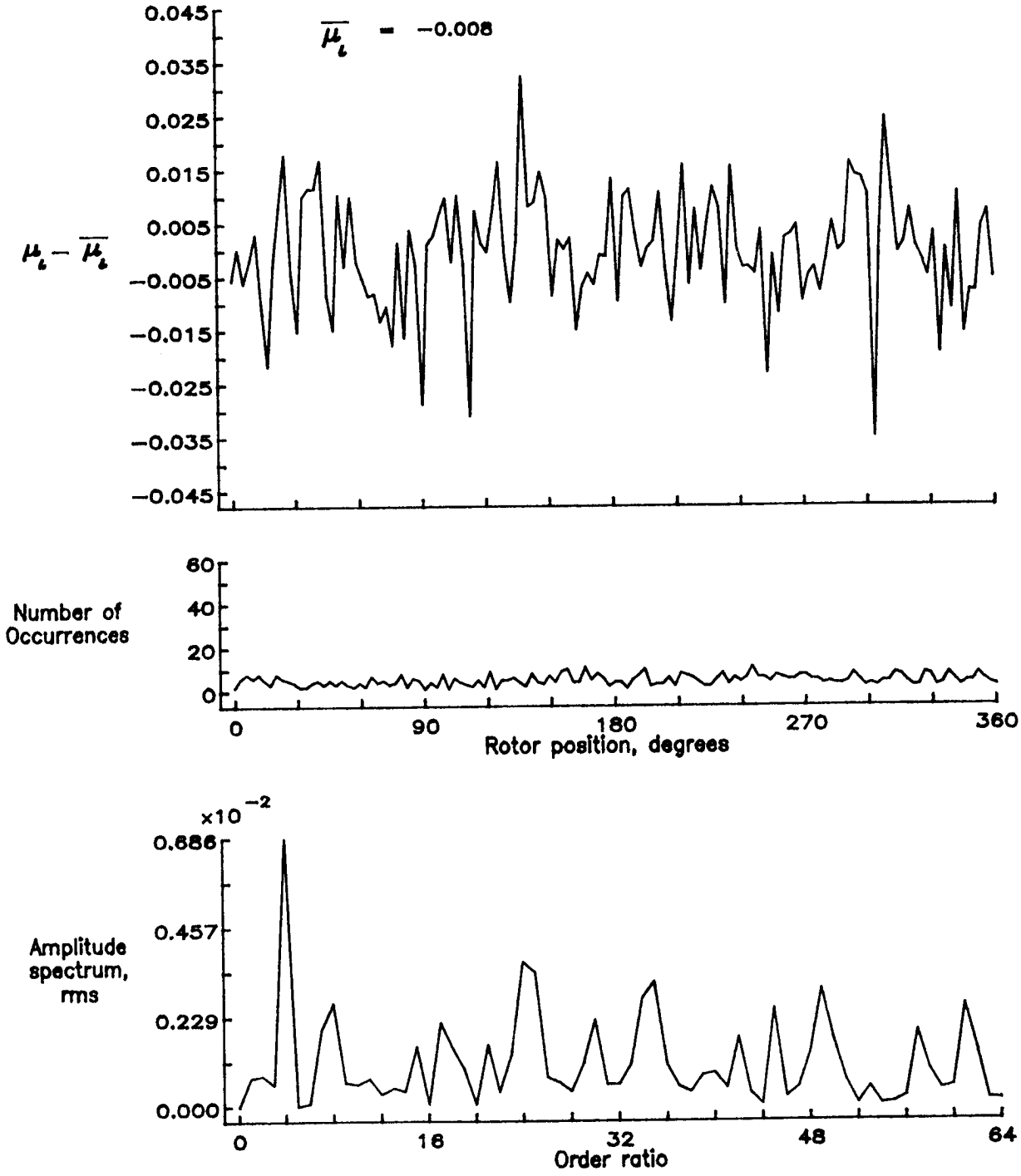


Figure 179.– Induced inflow velocity measured at 330 degrees and r/R of 1.04.

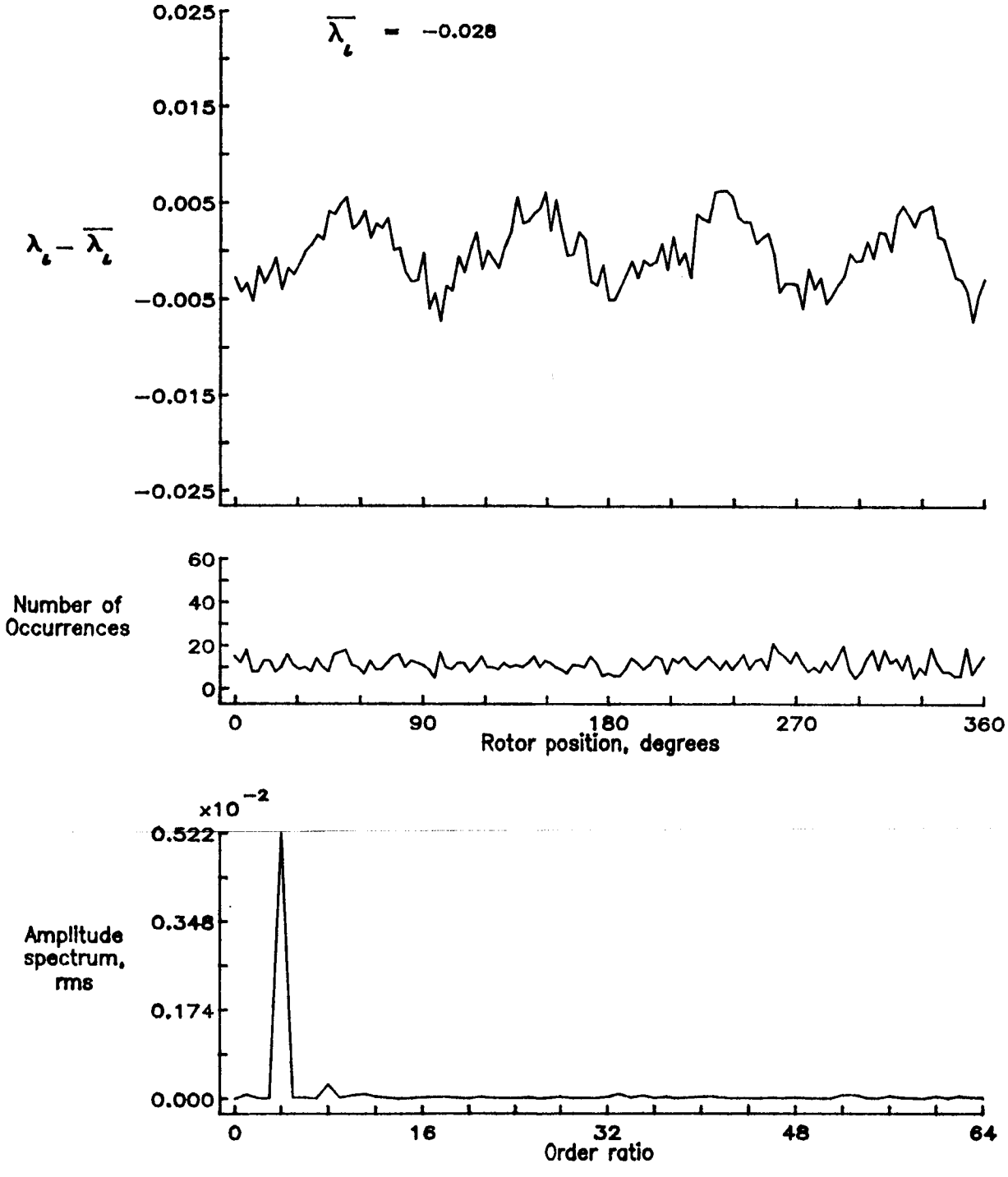


Figure 179.– Concluded.

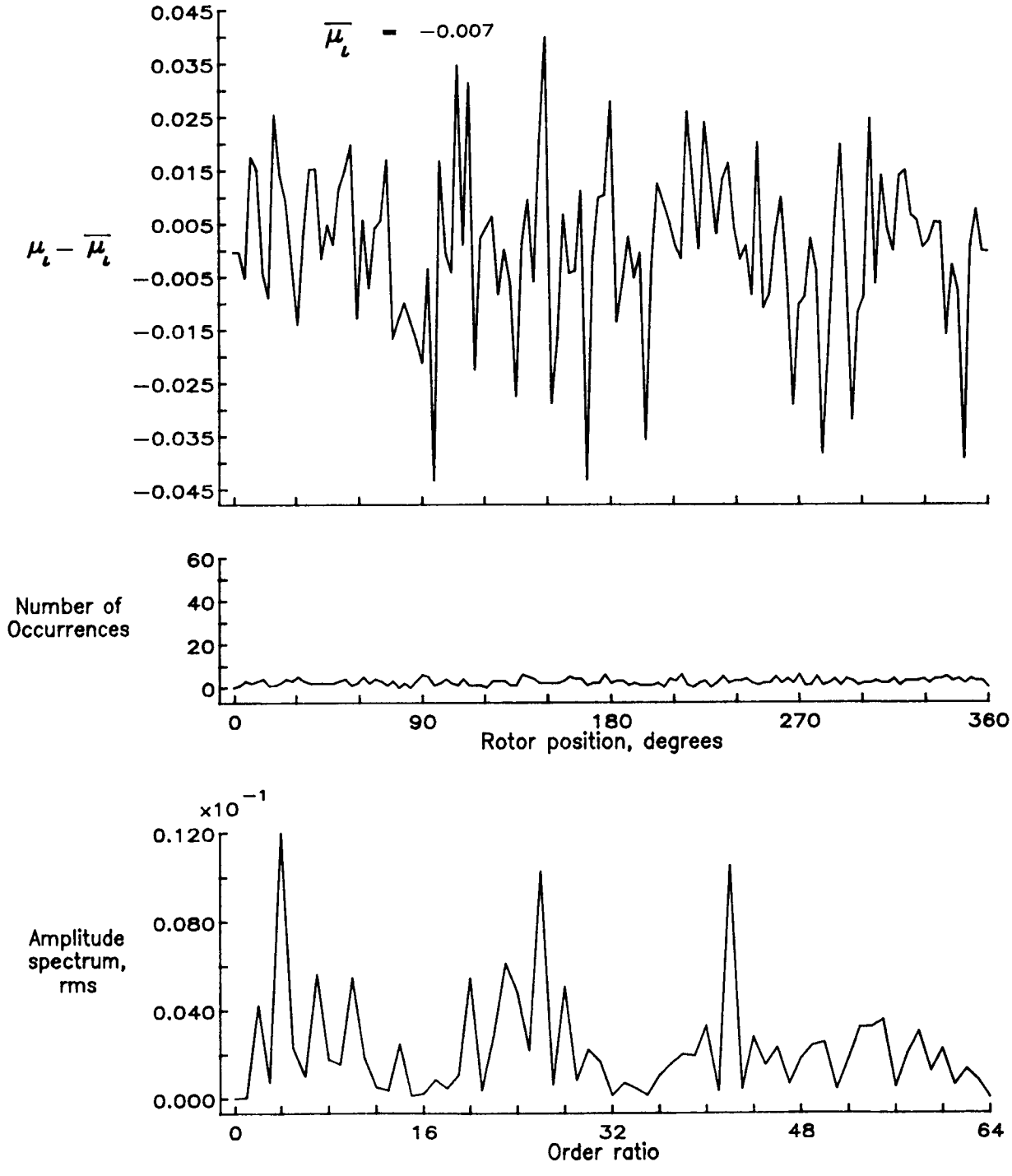


Figure 180.– Induced inflow velocity measured at 330 degrees and r/R of 1.10.

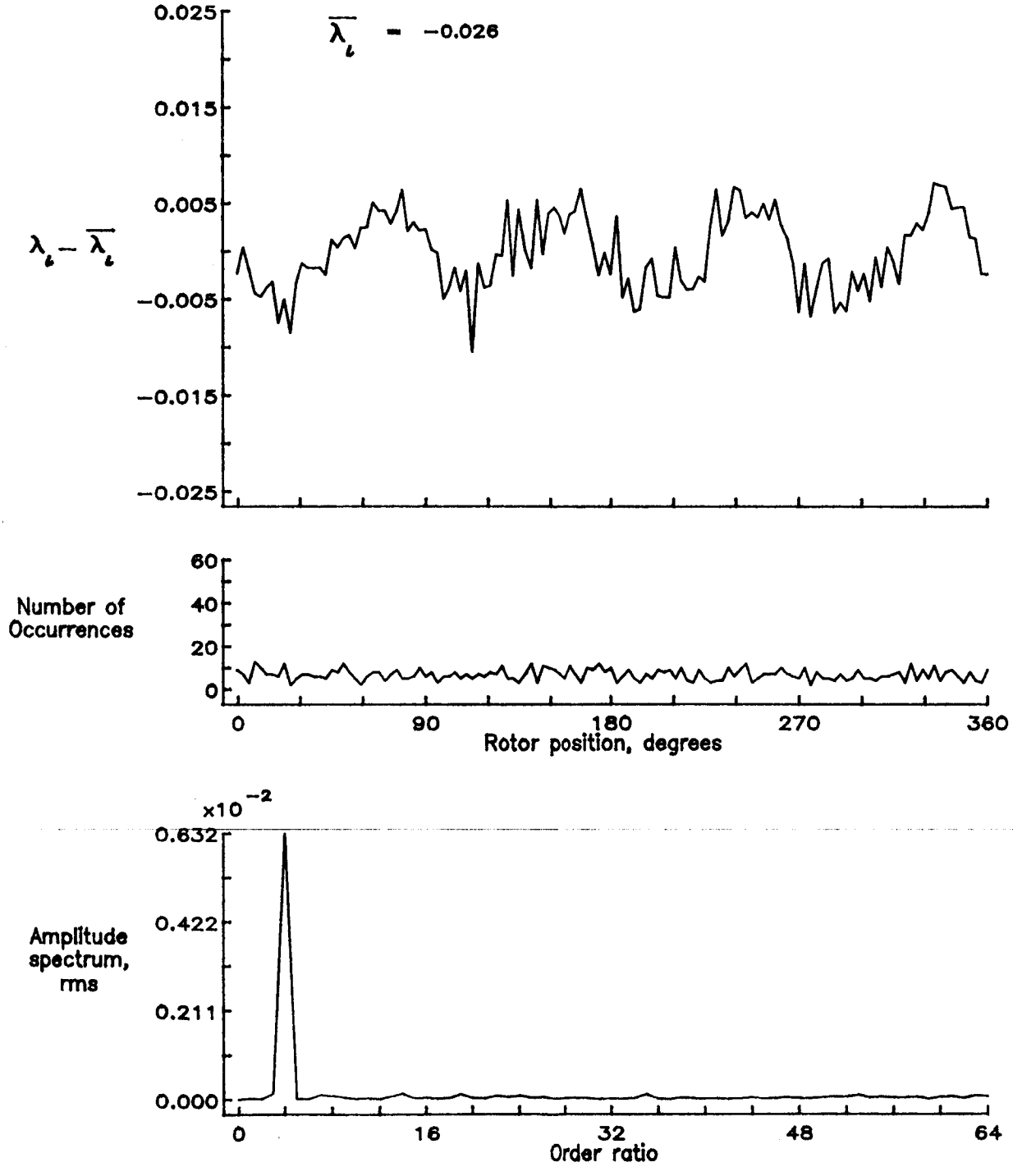


Figure 180.– Concluded.

NASA

Report Documentation Page

1. Report No.	2. Government Accession No.	3. Recipient's Catalog No.
NASA TM-100545 AVSCOM TM 88-B-008		

4. Title and Subtitle

Inflow Measurements Made With A Laser Velocimeter On A Helicopter Model In Forward Flight, Volume V Tapered Planform Blades at an Advance Ratio of 0.23

5. Report Date: April 1988

6. Performing Organization Code:

7. Author(s)

Susan L. Althoff, Joe W. Elliott, and Richard H. Sailey

8. Performing Organization Report No.:

10. Work Unit No.:

9. Performing Organization Name and Address

Aerostructures Directorate
USAARTA-AVSCOM
Langley Research Center
Hampton, VA 23665-5225

11. Contract or Grant No.: 505-61-51-10

13. Type of Report and Period Covered: Technical Memorandum

12. Sponsoring Agency Name and Address

National Aeronautics and Space Administration
Washington, DC 20546-0001 and
US Army Aviation Systems Command
St. Louis, MO 63120-1798

14. Sponsoring Agency Code:

15. Supplementary Notes

Susan L. Althoff and Joe W. Elliott: Aerostructures Directorate, USAARTA-AVSCOM, Langley Research Center, Hampton, VA
Richard H. Sailey: Planning Research Corporation, Hampton, VA

16. Abstract

An experimental investigation was conducted in the 14- by 22-Foot Subsonic Tunnel at NASA Langley Research Center to measure the inflow into a scale model helicopter rotor in forward flight ($\mu_\infty = 0.23$). The measurements were made with a two-component Laser Velocimeter (LV) one chord above the plane formed by the path of the blade tips. A conditional sampling technique was employed to determine the position of the rotor at the time that each velocity measurement was made so that the azimuthal fluctuations in velocity could be determined. Measurements were made at a total of 168 separate locations in order to clearly define the inflow character. This data is presented herein without analysis. In order to increase the availability of the resulting data, both the mean and azimuthally dependent values are included as part of this report on two 5.25 inch floppy disks in Microsoft Corporation MS-DOS format.

17. Key Words (Suggested by Author(s))	18. Distribution Statement
Rotor model Inflow Laser Velocimetry	Unclassified - Unlimited Subject Category 02

19. Security Classif. (of this report)	20. Security Classif. (of this page)	21. No. of pages	22. Price
Unclassified	Unclassified	358	

NASA FORM 1626 OCT 86